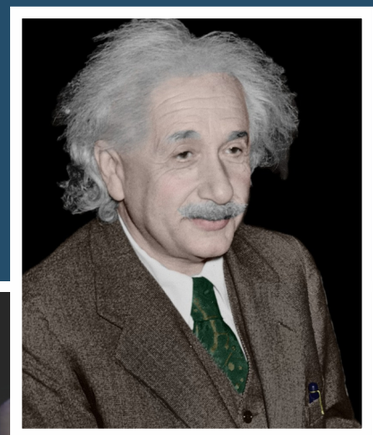

2015
Proceedings of the Int. Conf. Relativ. Astrophys.
M. Sharif (Editor)

Proceedings of the

International Conference on Relativistic Astrophysics, 2015

Muhammad Sharif (Editor)

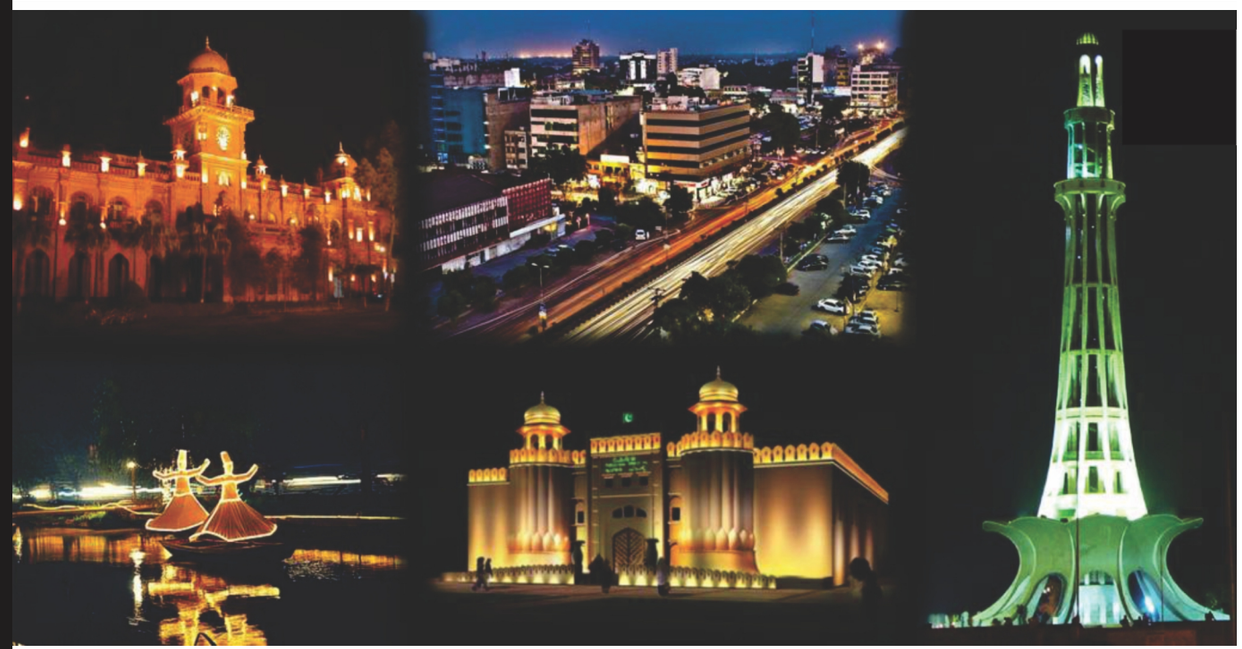

Celebrating 100 Years of Einstein's Theory of General Relativity

Department of Mathematics
University of the Punjab, Lahore-Pakistan

Sponsored by:

Department of Press & Publications
University of the Punjab, Lahore-Pakistan

Published by
Department of Press and Publications
University of the Punjab
Quaid-e-Azam Campus, Lahore-54590
Pakistan

Dr. Manzur Hussain Memorial Library Cataloguing-in-Publication Data
A catalogue for this book is available at Dr. Manzur Hussain Memorial Library.

Cover Image of Punjab University and Lahore-Pakistan.

International Conference on Relativistic Astrophysics (2015)
Proceedings of the 1^{st} International Conference by Department of Mathematics, University of the Punjab

This conference proceedings is the official record of the International Conference on Relativistic Astrophysics organized by Department of Mathematics, University of the Punjab. It is a collection of research papers which corresponds to the technical presentations given at the conference. Additional content may be included.

Printed in Pakistan by Punjab University Press.
Email: icra.math@pu.edu.pk

ORGANIZING COMMITTEES

Scientific Organizing Committee

Rong-Gen Cai (Chinese Academy of Sciences, China)
Ugur Camci (Akdeniz University, Turkey)
Salvatore Capozziell (University of Naples Federico II, Italy)
Naresh K. Dadhich (IUCAA, India)
Luis Herrera (Central University of Venezuela, Venezuela)
Mustapha Ishak (University of Texas at Dallas, USA)
Philippe Jetzer (University of Zurich, Switzerland)
Malcolm A.H. MacCallum (QMUL, UK)
Shin'ichi Nojiri (Nagoya University, Japan)
Sergei D. Odintsov (ICREA and ICE, Spain)
Asghar Qadir (NUST, Pakistan)
Muhammad Sharif-Chair (University of the Punjab, Pakistan)
Alexei A. Starobinsky (Landau Institute for Theoretical Physics, Russia)

Local Organizing Committee

Aziz Ullah Awan (PU)
M. Zaeem Ul Haq Bhatti-Secretary (PU)
Jameel-Un-Nabi (GIKI)
Asghar Qadir (NUST)
Nauman Raza (PU)
Khalid Saifullah (QAU)
Rabia Saleem (PU)
Ghulam Shabbir (GIKI)
Muhammad Sharif-Chair (PU)
Azad A. Siddiqui (NUST)
Zeeshan Yousaf-Associate Secretary (PU)

List of Participants

S. No.	Name	Affiliation
1	Dr. Ghulam Abbas	COMSATS Sahiwal
2	Mr. Kumail Abbas	University of the Punjab
3	Dr. Syed Zeeshan Abbas	University of Karachi
4	Mr. Zain Ul Abidin	COMSATS Islamabad
5	Mr. Adnan	COMSATS Abbottabad
6	Miss Khadeeja Afzal	National University of Science and Technology
7	Miss Sania Afzal	COMSATS Abbottabad
8	Mr. Mubashar Ahmad	Quaid-i-Azam University
9	Mr. Mushtaq Ahmad	The Islamia University of Bahawalpur
10	Mr. Naseer Ahmad	Jalalabad, Afghanistan
11	Miss Uzaira Ahmad	Bahauddin Zakariya University, Multan
12	Dr. Zahid Ahmad	COMSATS Abbottabad
13	Mr. Farhan Ahmed	Isra University, Hyderabad
14	Mr. Iftikhar Ahmed	COMSATS Lahore
15	Mr. Jamil Ahmed	Quaid-i-Azam University
16	Dr. Maqbool Ahmed	Nusrat Jahan College
17	Dr. Mohammad Akbar	The University of Texas at Dallas, USA
18	Mr. Zauq Akhtar	COMSATS Abbottabad
19	Mr. Muhammad Akram	Quaid-i-Azam University
20	Mr. Azhar Ali	University of the Punjab
21	Mr. Murtaza Ali	The Islamia University of Bahawalpur, Pakistan
22	Mr. Askar Ali	Quaid-i-Azam University
23	Mr. Asif Ali	University of Karachi
24	Mr. Sarfraz Ali	University of Sargodha
25	Mr. Shahbaz Ahmed Alvi	Aligarh Institute of Technology, Karachi
26	Miss Muneeba Alvi	University of the Punjab
27	Mr. Hafiz Muhammad Amir	University of Punjab
28	Dr. Muhammad Jamil Amir	University of Sargodha
29	Mr. Zeeshan Amjad	University of the Punjab
30	Mr. Atif Arif	COMSATS Islamabad
31	Mr. Kashif Arshad	PIEAS, Islamabad
32	Mr. Muhammad Arslan	Quaid-i-Azam University
33	Miss Bushra Ashraf	Quaid-i-Azam University
34	Miss Sidra Ashraf	University of Sargodha, Pakistan
35	Miss Javeria Ayub	National University of Science and Technology
36	Dr. Muhammad Ayub	COMSATS Abbottabad
37	Dr. Muhammad Azam	University of Education, Township Campus, Lahore
38	Mr. Syed Ali Mardan Azmi	University of Management and Technology, Lahore
39	Dr. Kazuharu Bamba	Ochanomizu University, Japan
40	Miss Roqia Bano	Quaid-i-Azam University
41	Miss Binish Batool	University of the Punjab
42	Mr. Muhammad Zaeem Ul Haq Bhatti	University of the Punjab
43	Miss Bushra Bibi	Quaid-i-Azam University
44	Miss Rashida Bibi	National University of Science and Technology
45	Miss Maryam Bibi	Quaid-i-Azam University
46	Prof. Dr. Ugur Camci	Akdeniz University, Turkey
47	Mr. Khalil Ur Rehman Chaudhary	Quaid-i-Azam University
48	Miss Nadia Cheema	Government College University, Lahore
49	Dr. Amanullah Dar	Mirpur University of Science and Technology, Pakistan
50	Prof. Dr. Martin Dominik	SUPA, University of St Andrews, School of Physics & Astronomy, UK
51	Miss Zahida Ehsan	COMSATS Institute of Information Technology, Lahore
52	Mr. Zaffar Elahi	University of the Punjab
53	Dr. Ayub Faridi	University of the Punjab
54	Miss Anum Fatima	Quaid-i-Azam University
55	Dr. Suhail Zaki Farooqui	National University of Science and Technology, PNEC, Karachi
56	Ms. Hafiza Ismat Fatima	University of the Punjab
57	Mr. Usman Alam Gilani	Quaid-i-Azam University
58	Miss Attia Gul	COMSATS Abbottabad

59	Miss Nida Haider	Sargodha
60	Mr. Syed Awais Haider	Quaid-i-Azam University
61	Mr. Ali Jan Hassan	University of Karachi
62	Mr. Muhammad Hassan	University of the Punjab
63	Mr. Sohaib Hassan	Pakistan Institute of Engineering and Applied Sciences, Pakistan
64	Mr. Syed Sibit Hassan	COMSATS Lahore, Pakistan
65	Mr. Abrar Hayat	National University of Sciences and Technology
66	Mr. Saqib Hussain	National University of Science and Technology
67	Dr. Ibrar Hussain	National University of Science and Technology
68	Mr. Shahbaz Hussain	COMSATS Abbottabad
69	Mr. Syed Zaheer Hussain	University of Peshawar
70	Mr. Tahir Hussain	University of Peshawar
71	Miss Sehrish Iftikhar	University of the Punjab
72	Mr. Zafar Iftikhar	Ghulam Ishaq Khan Institute of Engineering Sciences & Technology
73	Miss Saima Ijaz	University of Management and Technology, Lahore
74	Miss Ayesha Ikram	University of the Punjab
75	Mr. Muhammad Ilyas	University of the Punjab
76	Mr. Fawad Inam	University of Engineering and Technology, Faisalabad
77	Prof. Dr. Muhammad Jawed Iqbal	University of Karachi
78	Mr. Ommair Ishaque	University of Karachi
79	Miss Samreen Ismail	University of Engineering and Technology, Peshawar
80	Miss Saima Jabbar	Lahore Garrison University
81	Miss Maryam Jalil	University of Sargodha
82	Dr. Mubasher Jamil	National University of Sciences and Technology
83	Mr. Kamran Javaid	Quaid-i-Azam University
84	Mr. Ahsan Javed	University of the Punjab
85	Mr. Muhammad Aamir Javed	University of the Punjab
86	Dr. Wajiha Javed	University of Education, Township Campus, Lahore
87	Mr. Ahmad Javid	University of the Punjab
88	Dr. Abdul Jawad	COMSATS Lahore
89	Prof. Dr. Philippe Jetzer	University of Zurich, Switzerland
90	Miss Tayyaba Kanwal	University of Sargodha
91	Miss Anam Khalid	University of Karachi
92	Mr. Suleman Khalid	Quaid-i-Azam University
93	Mr. Abdul Qadeer Khan	University of Azad Jamuu & Kashmir, Pakistan
94	Dr. Fazeel Mahmood Khan	Institute of Space Technology Islamabad
95	Mr. Hassam Khan	University of Karachi
96	Mr. Hammad Khan	COMSATS Islamabad
97	Mr. Imran Pervez Khan	COMSATS Islamabad
98	Mr. Irfan Khan	Abbottabad
99	Mr. Muhammad Saleem Khan	University of Karachi
100	Mr. Muhammad Sheharyar Khan	Isra University Hyderabad
101	Mr. Muhammad Shoaib Khan	COMSATS Abbottabad
102	Mr. Noshad Khan	COMSATS Abbottabad
103	Mr. Riaz Khan	Qurtuba University Peshawar
104	Dr. Suhail Khan	University of Peshawar
105	Mr. Yousaf Khan	Allama Iqbal Open University, Islamabad
106	Mr. Zahid Khan	Qurtuba University Peshawar
107	Miss Misbah Khurshid	COMSATS Abbottabad
108	Prof. Dr. Malcolm A. H. MacCallum	Queen Mary University of London, UK
109	Miss Hira Mahmood	University of the Punjab
110	Mr. Muhammad Amir Mahmood	COMSATS Abbottabad
111	Miss Bushra Majeed	National University of Sciences and Technology
112	Miss Mehwish Manzoor	Quaid-i-Azam University
113	Miss Rubab Manzoor	University of Management and Technology, Lahore
114	Miss Samra Maqsood	Quaid-i-Azam University
115	Mr. Muhammad Mazhar	COMSATS, Abbottabad
116	Mr. Ijaz Mehmood	The Islamia University Bahawalpur, Bahawalnagar
117	Mr. Awais Mirza	Institute of Space Technology, Islamabad
118	Mr. Atif Moeen	COMSATS Sahiwal
119	Miss Muqadas Moeen	University of the Punjab
120	Miss Sidra Mohsaneen	University of the Punjab

121	Mr. Muhammad Moosa	COMSATS Islamabad
122	Mr. Muhammad Zubair Ali Moughal	Quaid-i-Azam University
123	Miss Saadia Mumtaz	University of the Punjab
124	Prof. Dr. Jameel-Un-Nabi	Ghulam Ishaq Khan Institute, KPK
125	Miss Maria Naeem	COMSATS Islamabad
126	Miss Zunaira Nasir	University of the Punjab
127	Miss Saira Nawaz	University of the Punjab
128	Miss Iqra Nawazish	University of the Punjab
129	Miss Sumera Naz	University of the Punjab, Pakistan
130	Miss Kanwal Nazir	University of the Punjab
131	Mr. Muhammad Nisar	Quaid-i-Azam University
132	Miss Tayyaba Noreen	University of the Punjab
133	Miss Ifra Noureen	University of Management and Technology, Lahore
134	Ms. Isil Basaran Oz	Akdeniz University, Turkey
135	Miss Wajeeha Pervaiz	National University of Sciences and Technology
136	Miss Atia Tul Qadeer	University of the Punjab
137	Prof. Dr. Asghar Qadir	National University of Sciences and Technology
138	Miss Hafiza Qimrah	Institute of Space Technology Islamabad
139	Mr. Shahid Rafiq	The Islamia University of Bahawalpur
140	Miss Rehana Rahim	Quaid-i-Azam University
141	Mr. Masood Rahman	Quaid-i-Azam University
142	Dr. Muhammad Ramzan	The Islamia University of Bahawalpur
143	Dr. Shamaila Rani	University of Management and Technology, Lahore
144	Mr. Fayyaz ur Rasheed	University of Karachi
145	Miss Madiha Rashid	Quaid-i-Azam University
146	Mr. Khalil Ur Rehman	GCU, Lahore
147	Mr. Umer Rehman	Quaid-i-Azam University
148	Mr. Hafiz Wajahat Ahmed Riaz	University of the Punjab
149	Mr. Rafil Riaz	DHA SUFFA University, Karachi
150	Mr. Muhammad Saad	International Islamic University
151	Mr. Mudassar Sabir	National University of Sciences and Technology
152	Dr. Naeem Sadiq	University of Karachi
153	Miss Sobia Sadiq	University of the Punjab
154	Dr. Khalid Saifullah	Quaid-i-Azam University
155	Mr. Taimoor Salahuddin	Quaid-i-Azam University
156	Miss Wardat Us Salam	University of the Punjab
157	Mr. Muhammad Usman Saleem	University of the Punjab
158	Miss Rabia Saleem	University of the Punjab
159	Miss Sumaira Saleem	University of Peshawar
160	Miss Zakia Sanaullah	Bahauddin Zakariya University, Multan
161	Miss Maria Sattar	Qurtuba University Peshawar
162	Ms. Sadia Sattar	University of Sargodha
163	Mr. Omair Sarfraz	COMSATS Islamabad
164	Miss Kanza Sayyam	Quaid-i-Azam University
165	Miss Tayyaba Shabbir	National University of Sciences and Technology
166	Miss Ammara Shafiq	Quaid-i-Azam University
167	Mr. Nasir Shaheed	Kohat University of Science and Technology
168	Prof. Dr. Ghulam Shabbir	Ghulam Ishaq Khan Institute
169	Mr. Muhammad Ali Shahbaz	Quaid-i-Azam University
170	Mr. Farasat Shamir	FAST University
171	Prof. Dr. Muhammad Sharif	University of the Punjab
172	Dr. Umber Sheikh	National Textile University
173	Mr. Falak Sher	Government College University, Lahore
174	Prof. Dr. Azad A. Siddiqui	National University of Sciences and Technology
175	Miss Rabia Siddiqui	Isra university, Hyderabad
176	Dr. Ramzi Fouad Suleiman	Al Quds University, The Palestinian Authority
177	Miss Hira Tahir	Islamia University Bahawalpur, Bahawalnagar
178	Mr. Shauket Ali Tahir	University of Gujrat
179	Miss Anum Tanveer	Quaid-i-Azam University
180	Miss Hira Tariq	University of the Punjab

181	Miss Habiba Tasadduq	Quaid-i-Azam University
182	Mr. Muhammad Usman	National University of Sciences and Technology
183	Mr. Muhammad Waqas	Quaid-i-Azam University
184	Miss Azka Younas	National University of Science and Technology
185	Miss Bushra Younas	University of Gujrat
186	Mr. Muhammad Yousaf	University of Sargodha
187	Mr. Zeeshan Yousaf	University of the Punjab
188	Dr. Asim Zafar	University of the Punjab
189	Miss Hira Zafar	University of the Punjab
190	Miss Nosheen Zafar	Government College of Science
191	Miss Zuriat Zahra	Bahawalpur
192	Miss Zakia Zainib	University of the Punjab
193	Dr. Muhammad Zubair	COMSATS Institute of Information Technology, Lahore
194	Mr. Umer Zubair	Quaid-i-Azam University


INSTITUTE OF CHEMISTRY

Preface

This volume is devoted to the Proceedings of the International Conference on Relativistic Astrophysics which was aimed to *Celebrate* 100 *Years of Einstein's Theory of General Relativity* developed by Albert Einstein in 1915. This conference was organized by Department of Mathematics, University of the Punjab, Lahore-Pakistan. The venue of the conference was decided as Al-Raazi Hall, Centre for Undergraduate Studies, University of the Punjab. It was the first International Conference on Relativistic Astrophysics organized by Department of Mathematics.

Einstein is probably the most well-known scientific genius. His creative ability allowed him to dream of new physics and create scientific revolutions, including his masterpiece, the theory of general relativity. Nearly 100 years after his masterwork, Einstein continues to inspire younger generations of scientists, philosophers and artists, as they strive to answer the big questions about our place in the cosmos. While people around the globe instantly recognize Einstein's image, many in the public still have not had an occasion to learn some of the astonishing details and amazing implications of his most monumental discovery. Celebrating Einstein draws on the power of Einstein and his ideas to tell the exciting story of relativity and astrophysics to public, to inspire younger generations to dare to dream about exploration, to dare to join in the most daunting question of all: to unravel the mysteries of the universe.

The conference included presentations covering the wide range of research areas in general relativity and gravitation, alternative theories of gravity, relativistic astrophysics and cosmology as advertised initially. The program consisted of Plenary sessions with invited talks and then contributed talks in parallel sessions. There was a special discussion session in which it was suggested by the participants of the Conference to hold such events in the near future and to make a society for relativity in Pakistan. The proceedings of the International Conference on Relativistic Astrophysics appeared through the Punjab University Press.

We are most grateful to all the authors for their work in preparing the manuscripts for this proceedings. The Conference organizers are also very grateful to University of the Punjab for providing excellent facilities to conduct this conference with financial support. Also, we would like to acknowledge the financial support provided by Pakistan Academy of Sciences, The Abdus Salam International Center for Theoretical Physics, International Mathematical Union-Commission for Developing Countries. We would also like to acknowledge all the members of Relativity Group of Department of Mathematics for their unfaltering efforts to

make this meeting a success. Finally, we would like to thank all the participants of ICRA-Pakistan, 2015 for making this conference so vital and energizing. We look forward to organize such events in the near future.

Editor

Muhammad Sharif

Sponsors
University of the Punjab (PU)
Pakistan Academy of Sciences (PAS)
International Center for Theoretical Physics (ICTP)
International Mathematical Union (IMU-CDC)

Table of Contents

Proc. Int. Conf. Relativ. Astrophys.
Pages 01-08, (2015)

Einstein's Blip – One of the Puzzle Stones towards Exploring Ourselves in the Vastness of the Universe

Martin Dominik[a,b,1]

[1]SUPA, University of St Andrews, School of Physics & Astronomy, North Haugh, St Andrews, KY16 9SS, United Kingdom

Abstract Einstein's theory of General Relativity is "a most profound theory of Nature, embracing almost all the phenomena of physics".[1] Particularly, the gravitational bending of light is "a most curious effect",[2] providing us with a unique window to the Universe. The exploitation of this effect is a continuing story of curiosity, scepticism, surprise, and fascination. Short blips that will never be seen again now reveal distant worlds, setting the cosmic context of our little blue planet, and ourselves.

Keywords First keyword · Second keyword · More

1 General Relativity and Optics

Einstein's amazing theory of curved space-time [1–3], whose 100th anniversary we celebrate this year, is built upon a small number of relatively simple fundamental principles, and is the result of a long historical process of refining our view of Nature.

With the advent of Greek philosophy, ancient mystic ideas made way for the central and embracing concept of geometry, going hand in hand with simplicity, symmetry, and beauty. These principles governed the view for several millennia, and are famously reflected in the drawing of the human body by Leonardo da Vinci following the description of the Roman architect Vitruvius [4,5].

A strict demand for causality imposed a revolutionary change, ultimately leading Isaac Newton to base his universal law of gravitation, published in 1687 in his most famous book "Philosophiae Naturalis Principia Mathematica", on the concept of acting (and re-acting) forces [6].

It seems tempting to consider the transition from Newton's theory to Einstein's theory in the framework of mechanics. However, this is not really a story of mechanics, but much more one of optics.

Let us therefore have a look at light, which Newton devoted his second most famous book to. In "Opticks", published in 1704, he discussed many phenomena, based on the assumption that light is composed of small corpuscles [7], but he did not find time to dig deeper into some aspects that he came across, and therefore stated at the end: "And since I have not finished this part of my Design, I shall conclude, with proposing only some Queries in order to a further search to be made by others." Remarkably, straightaway the first of his queries reads: "Do not bodies act upon light at a distance, and by their action bend its rays, and is not this action (ceteris paribus) – i.e. everything else being the same – strongest at the least distance?"

Almost exactly a century later, Johann Georg von Soldner applied Newton's theory to find a light ray grazing near the edge of the Sun to be deflected by 0.84 arcseconds [8]. Moreover, he found that 1) the deflection increases with the mass of the gravitating body, 2) and increases with the proximity of the light ray to the deflector (i.e. just as Newton proposed, the action is strongest at the least distance). However, in 1801, he had to conclude that this effect would not be of any practical relevance. He was also quite unlucky with the timing, having pointed out that "Hopefully, nobody will get concerned that I treat a light ray just as a massive body." But people actually *did* get concerned, as the competing wave theory of light, brought forward by Christiaan Huygens [9] was gaining supporters. Following the diffraction experiments by Thomas Young

[a]e-mail: md35@st-andrews.ac.uk
[b]Royal Society University Research Fellow

[1]A.S. Eddington in "Discussion on the Theory of Relativity", Mon. Not. R. Astron. Soc., 80, 96 (1919)

[2]A. Einstein, "Lens-Like Action of a Star by the Deviation of Light in the Gravitational Field", Sci., 84, 506 (1936)

and Augustin Fresnel [10,11], its victory wiped away Soldner's result by 1820. It should take about another 100 years for this fundamental question being addressed again.

In 1905, Albert Einstein proposed a principle of relativity as well as the constancy of the speed of light [12], regardless of whether emitted from a resting or moving body, based on the theory of electric and magnetic fields and their interaction, as formulated by James Clerk Maxwell [13], while also recognising the failure to demonstrate a motion of the Earth relative to a medium in which light would propagate [14]. These two principles intrinsically link space and time, and form what is now known as "Special Relativity".

Einstein then went on to think about what relativity principles would mean for gravitation. He published thoughts about the influence of gravitation on light first in 1908 [15], but wasn't satisfied with the result, so that he got back to this issue in 1911 [16]. In order to avoid "unnecessary complexity", he still applied the mechanics of Newton and Galilei, and found that a light ray grazing near the surface of the Sun would be deflected by 0.83 arcseconds. This result coincidently is the same as found by Soldner, but was derived on entirely different assumptions. Einstein was very clear about how little technical issues of his treatment would matter in stating: "I would hope that astronomers devoted attention to this question, regardless of whether the presented considerations might lack of proper foundations or even look audacious. Apart from any theory, one has to ask whether with today's means an influence of gravitational fields on the propagation of light can be established."[3]

It was only four years later, in 1915, that the theory of General Relativity was fully developed [1,2]. By identifying gravitation with space-time curvature, we are actually back to a geometrical interpretation, replacing Newton's forces. However, in contrast to the ancient Greek philosophy, the geometric properties are now linked to a cause, namely matter, found on one side of Einstein's gravitational field equations, with space-time curvature being on the other. While it turned out that core assumption made by Einstein in his 1911 paper were not justified, notably the only change in the result from applying General Relativity is that the bending angle is twice as large as suggested earlier [17].

[3]Original quotation (in German): "Es wäre dringend zu wünschen, daß sich Astronomen der hier aufgerollten Frage annähmen, auch wenn die im vorigen gegebenen Überlegungen ungenügend fundiert oder gar abenteuerlich erscheinen sollten. Denn abgesehen von jeder Theorie muß man sich fragen, ob mit den heutigen Mitteln ein Einfluß der Gravitationsfelder auf die Ausbreitung des Lichtes sich konstatieren läßt."

But experimental evidence was not obtained until Einstein's prediction from General Relativity was famously confirmed by two British expeditions to Sobral (in Brazil) and the island of Príncipe, the latter led by the later knighted Arthur Eddington, on the occasion of the total Solar Eclipse of 29 May 1919 [18]. Exactly 90 years later, as part of the activities during the International Year of Astronomy 2009, a memorial plaque was unveiled at the plantation on Príncipe where the observations were carried out [19]. Before embarking on the expedition, Eddington wrote about the three possible outcomes: "The present eclipse expeditions may for the first time demonstrate the weight of light; or they may confirm Einstein's weird theory of non-Euclidian space; or they may lead to a result of yet more far-reaching consequences – no deflection." [20] At the end, it was these measurements that made Einstein and his (not-that weird) theory world-famous. Consequently, after having returned, Eddington led the word in a discussion on the Theory of Relativity held at the Royal Astronomical Society in December 1919, and started off by remarking: "The generalised relativity theory is a most profound theory of Nature, embracing almost all the phenomena of physics." [21]

2 The "gravitational lens" and the microlensing effect

A massive object bending light is commonly referred to as a gravitational lens, but this is actually a misnomer. As illustrated in Fig. 1, if we send a bundle of parallel light rays through a convex lens, these get (more or less) focused in a point, given that the deflection increases with distance from its centre. In contrast, gravitational bending gets stronger the closer one gets to the centre, which is similar to what happens if light passes through the foot of a wine glass [22,23]. Sir Oliver Joseph Lodge remarked already in 1919 that it would be "impermissable to say that the solar gravitational field acts as a lens, for it has no focal length". [24]

Looking through the foot of a wineglass, and watching a billiard ball passing underneath (see Fig. 2), one observes two images, resulting from light passing on one or the other side of its centre. If the ball is directly behind the centre of the wine glass the two images merge into a ring of characteristic size. The same occurs if two stars happen to be almost on a line with the observer. The size of the ring in this case increases with the mass of the star, and is actually proportional to its square root [25]. The angular separation between the images is less than a thousandth of an arcsecond, and thereby to small to be resolved with telescopes.

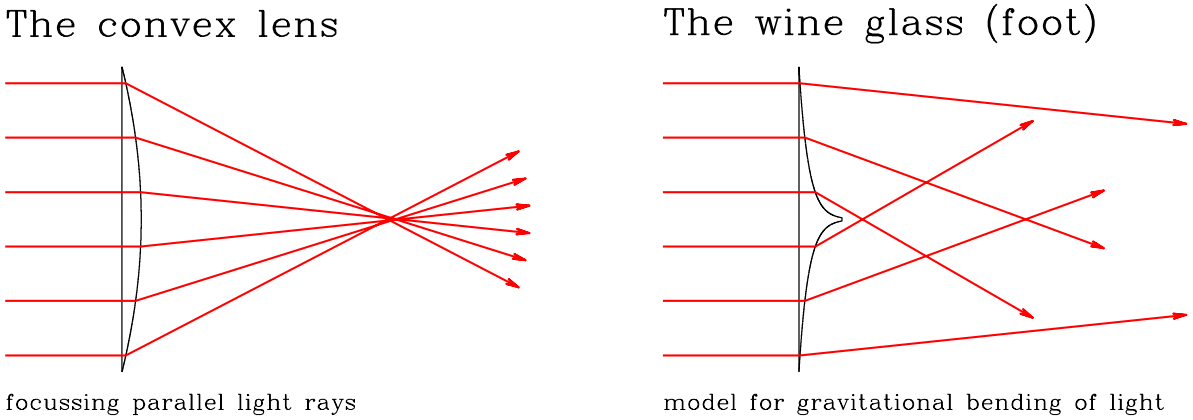

Fig. 1 The optical analogue of gravitational bending of light. The gravitational deflection acts in a similar way on light rays as the foot of a wine glass, rather than a lens, with the deflection being strongest near the centre rather than weakest. Light does *not* not converge in a focus.

Fig. 2 Snapshots of the images of a billiard ball rolling from left to right behind plexiglass shaped in the form of the foot of a wine glass, illustrating the images of a background star arising from the bending of its light due to the gravitation of an intervening foreground star (*demonstration by Phil Yock, University of Auckland, New Zealand*).

While we do not see the images themselves, their distortion leads to a magnification of the observed blob of light that they form, and one calls this effect "gravitational microlensing" [25–28]. The smaller the angular separation between the stars on the sky, the larger the magnification, so that a series of brightness measurements gives us a microlensing light curve that is symmetric with respect to a maximum, which corresponds to the closest angular approach.

Already in 1912, as his notes show, Albert Einstein discussed observable effects of the bending of light due to other stars than the Sun [29]. But despite the fact that the measurements of the gravitational bending of light by the Sun were a great success, Einstein did not believe that this effect would ever become important for other stars. It needed intense persuasion from a third party, namely the Czech engineer and amateur scientist Mandl, to get Einstein to publish the relevant results, finally happening in 1936 [25]. Einstein's conclusion that "There is no great chance of observing this phenomenon" is a politely phrased understatement of his assessment of the relevance of these findings. In his reply to the editor he wrote: "Let me also thank you for your cooperation with the little publication which Mister Mandl squeezed out of me. It is of little value, but it makes the poor guy happy."[4] [29,30]

The chances to observe this effect are in fact not great: just about one in a million! [27,28,31] Only with a further 50 years of advance in technology, the detection of microlensing events could turn into a reality, with the first one being reported in 1993 [32]. A key requirement was massive data processing, impossible still with computer technologies of the 1970s, not talking about 1936, where such a development was beyond imagination. Einstein probable did not even dare to dream about this.

While the chances for this effect to occur for any given star is tiny, there is no shortage of stars on the other hand. The Sun is just one out of around 100 billion in the Milky Way, which itself is just one out of at least 100 billion galaxies in the Universe. But still, as of today, our home, planet Earth, is the only place in the whole Universe which is known to us to harbour life. Should not we live in a usual and maybe rather unspectacular place within a Universe full of Earths? – Or are we indeed unimaginably unique?

[4] Original quotation (in German): "Ich danke Ihnen noch sehr für Ihr Entgegenkommen bei der kleinen Publikation, die Herr Mandl aus mir herauspreßte. Sie ist wenig wert, aber dieser arme Kerl hat seine Freude davon."

3 Planets beyond the Solar System

Until 1995, the only "planets" known were those of the Solar System, which has a clear structure: small rocky inner planets (Mercury, Venus, Earth, and Mars), and giant outer gas planets (Jupiter, Saturn, Uranus, and Neptune). It was widely believed that planetary systems in general should look similar.

But then, 51 Pegasi b, the very first planet orbiting a star other than the Sun that was detected, turned out to have about half the mass of Jupiter, while it is closer to its host star than Mercury is to the Sun [33]. Not at all did this match the expectations, and therefore came as a big surprise, forcing the prevalent theories about planet formation and evolution that described the Solar System all that well into a fundamental revision.

Subsequently, it literally started to rain planets [34]. 150 were reported within 10 years until 2005, a further 150 then within 3 years, the next 150 within just one year [35]. We have now already arrived at more than 2000, and from NASA's Kepler satellite, we even have more than 4000 candidates. These constitute a sample of impressive diversity, most of them being completely different than the planets of the Solar System. Moreover, the planetary systems they reside in, those with up to 7 detected planets having been identified, themselves show a large variety of different structures.

Since stars outshine their planets, it is quite difficult to detect them by means of their emitted or reflected light. The best chances for such a direct detection arise if one has a very nearby star and a large planet in a wide orbit. In 2008, for example, it was possible to find a system with three outer gas giant planets orbiting star HR 8799, for which one could also measure the motion of the planets [36].

If we cannot usually see planets directly, how can we nevertheless find them? An effect that we can exploit is that the planet and its star orbit their common centre of mass. Similar to a hammer and its thrower, the less massive planet speeds around a large orbit while the star only exhibits a tiny periodic wobble. The radial velocity of this wobble can be measured because characteristic lines in the spectrum of the observed star are shifted in wavelength, where this shift is known as the Doppler effect: towards the blue as the star approaches us, and towards the red as it moves away [37,38].

A further opportunity to detect planets was already well-known to occur within the Solar system. If one of the planets Mercury or Venus and the Earth happen to line up with the Sun, an observer on Earth sees the shadow of Mercury or Venus transiting the Sun, and the total light received dips down. Earliest known recorded observations of transits of Mercury or Venus date from 1631 or 1639, respectively, with Johannes Kepler having drawn attention to these opportunities in 1629 [39].

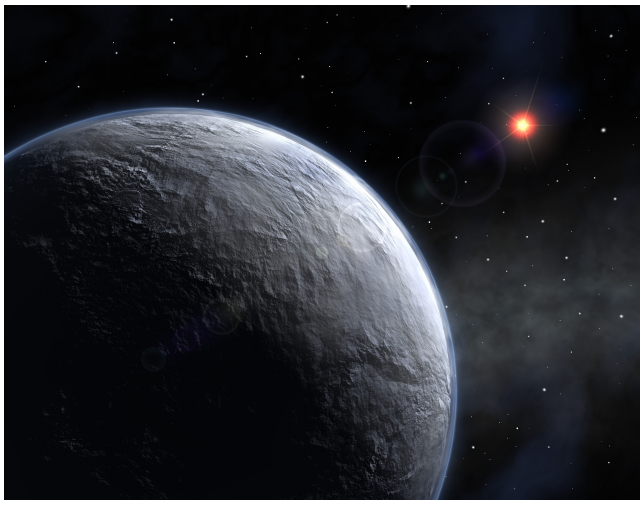

Fig. 3 Artist's impression of OGLE-2005-BLG-390Lb, a five-Earth-mass planet detected by means of gravitational microlensing. It was considered to be the least massive planet known beyond the Solar system when its discovery was announced (January 2006), which moreover provided the first observational hint for Earth-like planets being common in the Universe. It was also recognised as the coldest extrasolar planet ($\sim -220°$C), as well as the most distant one ($\sim 21,500$ light-years) (© *ESO*).

We can therefore identify planets that we do not see by observing their host star. In fact, we can even find planets that we do not see orbiting stars that we do not see either, and this is because planets and stars have mass. This brings us back to gravitation and gravitational microlensing...

Exploiting the gravitational microlensing effect, dedicated surveys are now looking towards the central regions of the Milky Way, and measure the brightness of hundreds of millions of stars, at least daily, and mostly more frequently. This leads to about 100 ongoing events at any time, each of them lasting about a month [40–43].

The 390th event found in 2005 by the OGLE survey [40] in the direction of the Galactic Bulge, systematically named OGLE-2005-BLG-390, hosted a surprise for us. It was monitored with a network of telescopes around the world, forming part of the PLANET and RoboNet microlensing follow-up campaigns [44,45], and providing precise quasi-continuous round-the-clock coverage. While the observed brightening was apparently as expected for a gravitational microlensing event, and OGLE-2005-BLG-390 continued to behave as usual

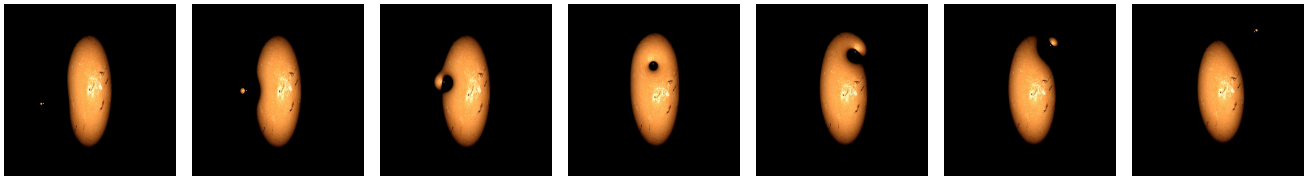

Fig. 4 Planet OGLE-2005-BLG-390Lb (position indicated by blue dot) distorting one of the images of the source star in this microlensing event, resulting in the observed characteric 'blip' in the brightness that lasted about a day and revealed this planet's existence (*simulation by Andrew WIlliams, Perth Observatory, Australia*).

when reaching its peak and then fading back, a small blip, lasting only about a day, caused a lot of excitement, because it turned out to be caused by a planet with just around 5 Earth masses (see Fig. 3), whereas the microlensing efforts mostly aimed at targeting planets of about the mass of Jupiter [44]. Consequently, the discovery of planet "OGLE-2005-BLG-390Lb" gave us a first observational hint that such low-mass planets are common rather than rare in the Universe [46].

The gravitational bending of light by the planet caused a distortion (as illustrated in Fig. 4) of one of the images of the source star that arises from the light bending by the gravitation of the planet's host star (which is the lens star, and *not* the observed source star) [26,47–49]. Given that the distortion increased the image area and thereby the amount of light received, this then gave rise to the observed blip.

The 5 Earth masses of OGLE-2005-BLG-390Lb were far above our sensitivity limit, with a 20 % effect that lasted a whole day. With respect to the mass, we can even go beyond Earth, all way down to the Moon [50,51].

The combination of real-time photometry with fully-automatic data-analysis systems now provides us with the opportunity to publicly disseminate quasi-live information about microlensing events (see Fig. 5) [52]. The search for planets beyond the Solar System is no longer the sole domain of professional astronomers. Enthusiastic amateur astronomers regularly point their 30-40 cm diameter telescopes to ongoing microlensing events [54], becoming eye-level partners in a truly global venture. But one does not even need a telescope for participating in the search for new planets. The citizen science project `Planethunters.org` provides data from NASA's Kepler satellite, and *everybody* can detect planets, while connecting with other "planet hunters" around the world [55].

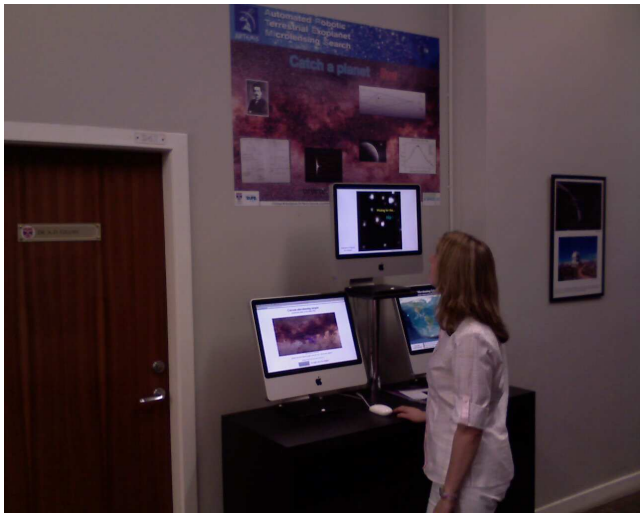

Fig. 5 Microlensing live display, originally conceived for the 2008 Royal Society Summer Science Exhibition [53], in the foyer of the Physics & Astronomy building of the University of St Andrews, providing real-time information and data of ongoing gravitational microlensing events in the Galactic Bulge (*photograph by Martin Dominik © 2008*).

4 Planet Earth and its context

What makes planet Earth so special? While it does not differ that much in size, composition, and temperature from its neighbour planets Venus and Mars, one finds huge differences if one looks at the composition of the planets' atmospheres. In the Earth's atmosphere, we roughly find 4/5 nitrogen and 1/5 oxygen, with 1 % of argon, and a small amount, about 0.03 %, of carbon dioxide as the main constituents. These fractions are by volume of dry air, while spatially and temporally strongly varying amounts of water vapour range from essentially nothing to 4 %. In sharp contrast, our neighbour planets have carbon dioxide/nitrogen atmospheres, with the carbon dioxide fraction exceeding 95%, rather than a nitrogen/oxygen atmosphere [56]. Without the atmospheric fingerprint, how do we know whether we have found a "second Earth" or a "second Venus"?

Amongst all peculiarities of planet Earth, the presence of the Moon is a particularly interesting one. A comparison of satellites within the Solar system shows that the Earth's moon is the largest in relation to the planet it orbits. Some of the Jupiter and Saturn satellites are larger, Ganymede being the largest and most massive one (with about a quarter of the Earth's mass), but Jupiter's radius is about ten times that of the Earth.

Higher organisms are strongly affected by changes to our ecosystem, whereas it is relatively hard to wipe out bacteria. The Moon directly affects the Earth's tides [57], while it has been both suggested and disputed that the Moon stabilises the rotational axis of the Earth [58,59]. Is it just coincidence that the only planet known to harbour life is orbited by a relatively large satellite? [60]

In any case, the respective compositions of Moon and Earth point to a close link in the formation process [61]. The preferred model for this is a giant impact of another body on the Earth, leading to some debris of this collision ending up to form the Moon [62–64]. Such an event could not have left Earth unchanged. And to add to the peculiarities, Earth has a unique elevation profile amongst all bodies in the Solar system, with the ocean floor, the main land mass, and mountains [65]. This is reflected in the fact that 2/3 of its surface is covered by water, not more, and not less. Futhermore, Earth also has a strong plate tectonics activity, which would be hard to explain from a history of just accretion of smaller particles [66].

A giant impact event would be a sound explanation of the dynamics and strong asymmetries that we observe, and would have come with lots of energy, and the flow of material, crucial drivers of chemical reactions. A planet of similar size, mass, and temperature as Earth is likely to be quite different.

Popular pictures of the Solar System show the Sun and the planets, but this is by far not everything. Not only are more than 150 known satellites missing, but also the small bodies, like asteroids and comets, which hold an overwhelming majority [67]. These however are a relevant part of the Solar System if we aim for understanding the role of planet Earth in the Universe.

For stars other than the Sun, we are discussing only the planets so far. Earth mass or Earth size are not the limit, and we must not stop our exploration there, but instead go ever further. – What is beyond?

Ultimately, we are on the search for ourselves. Who are we, and what are we doing here? Understanding all this however requires context: How do we fit into our surroundings and environment? Therefore, our view needs to be widely open rather than restricted. And astronomy is about exactly that: we look far out, in order to be able to look back.

Only because the Heavens and the Earth are governed by the same laws of Nature, this is possible. We now take this for granted, and this concept of cosmic unity was the ever prevalent one in China since ancient times. In Europe however, it was a revolutionary postulate at Tycho Brahe's time, and famously reflected in the pair of enblems over the doors of his castle on the island of Ven: "Despiciendo suspicio – Suspiciendo despicio" ("By looking down, I look up – By looking up, I look down") [68,69].

While our role in the cosmos remains puzzling, we are now given unprecedented opportunities for leaving an era of speculation behind. We now already know that there is no lack of planets. Given our acquired data, a number of more than 100 billion in the Milky Way alone appears to be realistic [70]. However, until now, we have identified a few thousand. Despite of giant leaps forward, from comparing these numbers it becomes obvious that we still know almost nothing.

Even if we once were to find life beyond Earth, it would *not* be the ultimate goal. It would only mark a beginning to advance into territory that we cannot even imagine right now.

All our striving for knowledge, all advance of our society through technology, all descriptions of our existence at the end, are anchored on a quite small number of most fundamental principles that allow us to make sense of our world. These connect the tiniest with the most gigantic, and link every one's existence to the whole of the Universe. Einstein's theory of gravitation provides us with one of the keys for turning observations into understanding. There is much left to explore and discover. Who knows where the road will actually lead us?

References

1. A. Einstein, "Zur allgemeinen Relativitätstheorie", Sitzungsber. preuss. Akad. Wiss., 47, 778-786 (1915)
2. A. Einstein, "Feldgleichungen der Gravitation", Sitzungsber. preuss. Akad. Wiss., 47, 844-847 (1915)
3. A. Einstein, "Grundlage der allgemeinen Relativitätstheorie", Annalen der Physik, 49, 769-822 (1916)
4. [Marcus] Vitruvius [Pollio], "De Architectura", Book III, Chapter I (c. 25 BC)
5. Leonardo da Vinci, "Le proporzioni del corpo umano secondo Vitruvio" (c. 1490). Gallerie dell'Accademia, Venezia, Italy
6. I. Newton, "Philosophiae naturalis principia mathematica". J. Streater for the Royal Society, London (1687)
7. I. Newton, "Opticks: or, a Treatise of the Reflexions, Refractions, Inflexions and Colours of Light. Also Two Treatises of the Species and Magnitude of Curvilinear Figures", S. Smith & B. Walford (Printers to the Royal Society), London (1704)
8. J. Soldner, "Ueber die Ablenkung eines Lichtstrals von seiner geradlinigen Bewegung, durch die Attraktion eines Weltkörpers, an welchem er nahe vorbei geht", Berliner Astron. Jahrb. für das Jahr 1804, 161–172 (1801)
9. C. Huygens, "Traité de la Lumière". Pierre van der Aa, Leiden (1690)
10. T. Young, "The Bakerian Lecture: On the Theory of Light and Colours". Phil. Trans. R. Soc. London, 92, 12–48 (1802)
11. A.-J. Fresnel, "Mémoire Sur la Diffraction de la lumière". Chrochard, Paris (1819)

12. A. Einstein, "Zur Elektrodynamik bewegter Körper", Annalen der Physik, 322, 891–921 (1905)
13. J. Clerk Maxwell, "A Treatise on Electricity and Magnetism". Clarendon Press, Oxford (1873)
14. A. A. Michelson & E. W. Morley, "On the relative motion of the Earth and the luminiferous ether", Am. J. Sci., 34, 333–345 (1887)
15. A. Einstein, "Über das Relativitätsprinzip und die aus demselben gezogenen Folgerungen", Jahrbuch der Radioaktivität und Elektronik, 4, 411–462 (1908)
16. A. Einstein, "Über den Einfluß der Schwerkraft auf die Ausbreitung des Lichtes", Annalen der Physik, 340, 898–908 (1911)
17. A. Einstein, "Erklärung der Perihelionbewegung des Merkur aus der allgemeinen Relativitätstheorie", Sitzungsber. preuss. Akad. Wiss., 47, 831–839 (1915)
18. F.W. Dyson, A.S. Eddington, & C. Davidson, "A Determination of the Deflection of Light by the Sun's Gravitational Field, from Observations Made at the Total Eclipse of May 29, 1919". Phil Trans. R. Soc. A, 220, 291–333 (1920)
19. R. Ellis, P.G. Ferreira, R. Massey, & G. Weszkalny, "90 years on – the 1919 eclipse expedition at Príncipe", Astron. Geophys., 50, 4.12–4.15 (2009)
20. A.S. Eddington, "The total eclipse of 1919 May 29 and the influence of gravitation on light", The Observatory, 42, 119–122 (1919)
21. A.S. Eddington, J.H. Jeans, Sir O. Lodge, Sir J. Larmor, L. Silberstein, F.A. Lindemann, H. Jeffreys, "Discussion on the theory of relativity", Mon. Not. R. Astron. Soc., 80, 96–118 (1919)
22. S. Liebes Jr., "Gravitational Lens Simulator. Am. J. Phys., 37, 103–104 (1969)
23. S. Refsdal & J. Surdej, "Gravitational lenses", Rep. Prog. Phys., 57, 117–185 (1994)
24. O.J. Lodge, "Gravitation and Light", Nat., 104, 354–354 (1919)
25. A. Einstein, "Lens-Like Action of a Star by the Deviation of Light in the Gravitational Field", Sci., 84, 506–507 (1936)
26. K. Chang & S. Refsdal, "Flux variations of QSO 0957+561A, B and image splitting by stars near the light path", Nat., 282, 561–564 (1979)
27. M. Petrou, "Dynamical models of spheroidal systems", PhD thesis, Institute of Astronomy, University of Cambridge (1981)
28. B. Paczyński, "Gravitational microlensing by the galactic halo", Astrophys. J., 304, 1–5 (1986)
29. J. Renn, T. Sauer, & J. Stachel, "The origin of gravitational lensing: A postscript to Einstein's 1936 Science paper", Sci., 275, 184–186 (1979)
30. A. Einstein, Letter to J. Cattell, dated 18 December 1936 (Einstein Archives call no. 65-603)
31. M. Kiraga & B. Paczynski, "Gravitational microlensing of the Galactic bulge stars", Astrophys. J. Lett., 430, L101–L104 (1994)
32. C. Alcock, C.W. Akerlof, R.A. Allsman, T.S. Axelrod, D.P. Bennett, et al., "Possible gravitational microlensing of a star in the Large Magellanic Cloud", Nat., 365, 621–623 (1993)
33. M. Mayor & D. Queloz, "A Jupiter-mass companion to a solar-type star", Nat., 378, 355–359 (1995)
34. A. Vidal-Madjar, "Il pleut des planètes". Hachette Littératures, Paris (1991)
35. F. Roques, J. Schneider, et al., "The Extrasolar Planets Encyclopaedia", `http://exoplanet.eu` (1995–)
36. C. Marois, B. Macintosh, T. Barman, B. Zuckerman, I. Song, J. Patience, D. Lafrenière, & R. Doyon, "Direct Imaging of Multiple Planets Orbiting the Star HR 8799", Sci., 322, 1348–1352 (2008)
37. C. Doppler, "Über das farbige Licht der Doppelsterne und einiger anderer Gestirne des Himmels", Abh. Königl. Böhm. Ges. Wiss., Ser. V, 2, 465–489 (1842/43)
38. G. Kirchhoff & R. Bunsen, "Chemische Analyse durch Spectralbeobachtungen", Annalen der Physik und Chemie, 186, 161–189 (1860)
39. J. Kepler, "De raris mirisque Anni 1631. Phænomenis, Veneris puta & Mercurii in Solem incursu, Admonitio ad Astronomos, rerumque coelestium studiosos". J.-A. Minzelius, Leipzig (1629)
40. A. Udalski, "The Optical Gravitational Lensing Experiment. Real Time Data Analysis Systems in the OGLE-III Survey", Acta Astron., 53, 291–305 (2003)
41. T. Sumi, F. Abe, I.A. Bond, R.J. Dodd, J.B. Hearnshaw, et al., "Microlensing Optical Depth toward the Galactic Bulge from Microlensing Observations in Astrophysics Group Observations during 2000 with Difference Image Analysis", Astrophys. J., 591, 204–227 (2003)
42. Y. Shvartzvald & D. Maoz, "Second-generation microlensing planet surveys: a realistic simulation", Mon. Not. R. Astron. Soc., 419, 3631–3640 (2012)
43. C.B. Henderson, B.S. Gaudi, C. Han, J. Skowron, M.T. Penny, D. Nataf, & A.P. Gould, "Optimal Survey Strategies and Predicted Planet Yields for the Korean Microlensing Telescope Network", Astrophys. J., 794, 52 [29pp] (2014)
44. M. Dominik, M.D. Albrow, J.-P. Beaulieu, J.A.R. Caldwell, D.L. DePoy, et al., "The PLANET microlensing follow-up network: results and prospects for the detection of extra-solar planets", Planet. Space Sci., 50, 299–307 (2002)
45. M. Burgdorf, D.M. Bramich, M. Dominik, M.F. Bode, K.D. Horne, I.A. Steele, N. Rattenbury, & Y. Tsapras, "Exoplanet detection via microlensing with RoboNet-1.0", Planet. Space Sci., 55, 582–588 (2007)
46. J.-P. Beaulieu, D.P. Bennett, P. Fouqué, A. Williams, M. Dominik, et al., "Discovery of a cool planet of 5.5 Earth masses through gravitational microlensing", Nat., 439, 437–440 (2006)
47. S. Mao & B. Paczyński, "Gravitational microlensing by double stars and planetary systems", Astrophys. J. Lett., 374, L37–L40 (1991)
48. A. Gould & A. Loeb, "Discovering planetary systems through gravitational microlenses", Astrophys. J., 396, 104–114 (1992)
49. M. Dominik, "The binary gravitational lens and its extreme cases", Astron. Astrophys., 349, 108–125 (1999)
50. B. Paczyński, "Gravitational Microlensing in the Local Group", Ann. Rev. Astron. Astrophys., 34, 419–460 (1996)
51. M. Dominik, N.J. Rattenbury, A. Allan, S. Mao, D.M. Bramich, M.J. Burgdorf, E. Kerins, Y. Tsapras, & Ł. Wyrzykowski, "An anomaly detector with immediate feedback to hunt for planets of Earth mass and below by microlensing", Mon. Not. R. Astron. Soc., 380, 792–804 (2007)
52. M. Dominik, K. Horne, A. Allan, N.J. Rattenbury, Y. Tsapras, et al., "ARTEMiS (Automated Robotic Terrestrial Exoplanet Microlensing Search): A possible expert-system based cooperative effort to hunt for planets of Earth mass and below", Astron. Nachr., 329, 248–251 (2008)
53. C.A. Haswell, A.J. Norton, M. Dominik, K. Horne, H.R.A. Jones, et al., "Is there anybody out there? Looking for new worlds", Royal Society Summer Science Exhibition, London (2008)
54. A. Udalski, M. Jaroszyński, B. Paczyński, M. Kubiak, M.K. Szymański, et al., "A Jovian-Mass Planet in Microlensing Event OGLE-2005-BLG-071", Astrophys. J. Lett., 628, L109–L112 (2005)

55. M.E. Schwamb, C.J. Lintott, D.A. Fischer, M.J. Giguere, et al., "Planet Hunters: Assessing the Kepler Inventory of Short-period Planets", Astrophys. J., 754, 129 [17 pp] (2012)
56. R.G. Prinn & B. Fegley Jr., "The Atmospheres of Venus, Earth, and Mars: A Critical Comparison", Ann. Rev. Earth and Planet. Sci., 15, 171–212 (1987)
57. D. Webb, "Tides and the evolution of the Earth-Moon system", Geophys. J. R. Astr. Soc., 70, 261–271 (1982)
58. J. Laskar, F. Joutel, & P. Robutel, "Stabilization of the Earth's obliquity by the Moon", Nat. 361, 615–617 (1993)
59. D. Waltham, "Our Large Moon Does Not Stabilize Earth's Axis", EPSC Abstracts, 8, EPSC2013-37 (2013)
60. D. Waltham, "Lucky Planet: Why Earth is Exceptional – and What that Means for Life in the Universe". Icon Books, London (2014)
61. U. Wiechert, A.N. Halliday, D.-C. Lee, G.A. Snyder, L.A. Taylor, & D. Rumble, "Oxygen Isotopes and the Moon-Forming Giant Impact", Sci., 294, 345–348 (2001)
62. R.A. Daly, "Origin of the Moon and Its Topography", Proc. Am. Phil. Soc., 90, 104–119 (1946)
63. W.K. Hartmann & D.R. Davis, "Satellite-sized planetesimals and lunar origin", Icarus, 24, 504514 (1975)
64. A.G.W. Cameron & W.R. Ward, "The origin of the Moon", Lunar Sci., 7, 120–122 (1976)
65. C.R. Perotti & M. Rinaldi, "Mars and Earth topography: a preliminary comparative analysis", Mem. Soc. Astron. It., 82, 334–340 (2011)
66. N.H. Sleep, K.J. Zahnle, & R.E. Lupu, "Terrestrial aftermath of the Moon-forming impact", Phil. Trans. R. Soc. A, 372, 20130172 [26pp] (2014)
67. G. Williams, S. Keys, M. Rodenko, J.L. Galache, & J. Davies, "The International Astronomical Union (IAU) Minor Planet Center – The nerve center of asteroid detection in the Solar System", `http://minorplanetcenter.net` (1947–)
68. T. Brahe, "Astronomiæ instauratæ mechanica". L. Hulsius, Nürnberg (1602)
69. V.E. Thoren & J.R. Christianson (contrib.), "The Lord of Uraniborg – A Biography of Tycho Brahe". Cambridge University Press, Cambridge (1990)
70. A. Cassan, D. Kubas, J.-P. Beaulieu, M. Dominik, K. Horne, et al., "One or more bound planets per Milky Way star from microlensing observations", Nat., 481, 167 (2012)

Proc. Int. Conf. Relativ. Astrophys.
Pages 09-12, (2015)

Validity of Cardy-Verlinde Formula in Non-Commutative Theory of Gravity

G. Abbas[a,1]

[1]Department of Mathematics, COMSATS Institute of Information Technology Sahiwal-57000, Pakistan

Abstract In this paper, we apply the procedure of Stare [1] to a non-commutative black hole obtained by the co-ordinate coherent approch. The Cardy-Verlinde formula is entropy formula of conformal field theory in an arbitrary dimension. It established the relation entropy of conformal filed theory to its total energy and Casimir energy. For this purpose, we have calculated the total energy and Casimir energy of non-commutative Schwarzschild black hole and have shown that entropy of non-commutative Schwarzschild black hole horizon can be expressed in terms of Cardy-Verlinde formula.

Keywords Cardy-Verlinde formula; Casimir Energy; Non-commutative Schwarzschild Black Hole.

PACS 04.70.Bw, 04.70.Dy, 95.35.+d

1 Introduction

Verlinde [2] proved that the entropy of conformal field theory in arbitrary dimension is related to its total energy and Casimir energy, this is known as generalized Verlinde formula (commonly termed as Cardy-Verlinde formula). Recently, it has been investigated that this formula hold well for Reissner-Nordström de-Sitter black hole (BH) [3] and charged Kerr BH [4]. Birmingham and Mokhtari proved the validity of Birmingham and Mokhtari [5] proved the Verlinde formula for Taub-Bolt-Anti-de-Sitter BH. Setare and Jamil [6] discussed the Cardy-Verlinde formula for charged BTZ BH. Many authors [7]-[12] have proved the validity of Cardy-Verlinde for different BHs. The purpose of this paper is to investigate the validity of Cardy-Verlinde entropy formula for NC Schwarzschild BH.

In classical general relativity (GR), the curvature singularity is such a point where physical description of the gravitational field is impossible. This problem can be removed in GR by taking into account the quantum mechanical treatment to the standard formulation of GR. Motivated by such reasoning, some BH solutions in non-commutative (NC) field theory have been derived. In these solutions, curvature singularity at origin is removed by de-Sitter core which is introduced due to NC nature of spacetime [13]. Ansoldi et al. [14] formulated the NC charged BHs solutions, this was extended to rotating non-commutative BHs case by Modesto and Nicollini [15]. Mann and Nicolini [16] have discussed the cosmological production of NC BHs. The first NC version of wormholes solution was investigated by Nicolini and Spallucci [17]. Farook et al. [18] have investigated the higher dimensional wormhole solutions in NC theory of gravity. Motivated by such NC correction to BHs, Sharif and Abbas [19] studied the thin shell collapse in NC Reissner-Nordström geometry. Banerjee and Gangopadhyay [20] derived the Komar energy and Sammar formula for NC Schwarzschild BH.

Motivated by the recent development in NC theory of gravity, we have proved that the entropy of NC Schwarzschild BH horizon can be expressed in terms of Cardy-Verlinde formula. For this purpose, we have used the Setare and Jamil method [6]. The plan of the paper is as follows: In section **2**, we briefly discussed the the thermodynamical relations of NC Schwarzschild BH and Cardy-Verlinde formula and proved that entropy of non-commutative Schwarzschild BH horizon in can be expressed in terms of Cardy-Verlinde formula. Section **3** is devoted to the concluded remarks of the work done.

[a]Email: ghulamabbas@ciitsahiwal.edu.pk

2 Non-Commutative Schwarzschild Black Hole and Cardy-Verlinde formula

According to GR, singularity is such a region of spacetime at which the usual laws of physics break down. This problem can be removed by applying the formulation of NC field theory to GR. For example, the NC BHs are one of the outcomes of string theory. These have such geometric structure in which curvature singularity is recovered by the minimal length introduced by the NC nature of coordinates. Further, all types of NC BHs expose the de-Sitter core due to quantum fluctuations at the center of the manifold.

The NC formulation of GR is one of the long standing problems which has no solution yet. An extensive literature survey [21]-[23], imply that the application of Moyal $\star$-product among the tetrad fields in the gravitational action is a mathematically correct approach but not physically. It is due to the fact that the expansion of $\star$-product in NC parameter is truncated upto a desirable order which causes to destroy the non-local nature of NC theory. This results to face the BH geometry with the same curvature singularities as in GR. Instead of using $\star$-product, one can formulate NC form of GR using the coordinate coherent state approach.

In this approach, the density of point like source in NC spacetime can be governed by a Gaussian distribution by using the relation [13]

$$\rho = \frac{Me^{-\frac{r^2}{4\Theta^2}}}{(4\pi\Theta)^{\frac{3}{2}}}, \tag{1}$$

where M is constant gravitational, Θ is constant having the dimension of length squared. The line element for NC Schwarzschild BH is [13]

$$ds^2 = f(r)dt^2 - \frac{1}{f(r)}dr^2 - r^2(d\theta^2 + \sin^2\theta d\phi^2), \tag{2}$$

where $f(r) = 1 - \frac{4M}{r\sqrt{\pi}}\gamma\left(\frac{3}{2}; \frac{r^2}{4\Theta}\right)$ and γ is lower incomplete gamma function which is defined by

$$\gamma\left(\frac{a}{b}; x\right) = \int_0^x t^{\frac{a}{b}-1}e^{-t}dt. \tag{3}$$

In the commutative limit $\frac{r}{\sqrt{\Theta}} \longrightarrow \infty$, i.e., $\Theta \to 0$, Eq.(2) reduces to conventional Schwarzschild metric. The event horizons of BH can be found by setting $f(r_h) = 0$, which yields

$$r_h = \frac{4M}{\sqrt{\pi}}\gamma\left(\frac{3}{2}; \frac{{r_h}^2}{4\Theta}\right). \tag{4}$$

We take the large radius regime ($\frac{{r_h}^2}{4\Theta} >> 1$) where we can expand the incomplete gamma function to solve r_h by iteration. Keeping the terms upto order $\sqrt{\Theta}e^{\frac{-M^2}{\Theta}}$, we find

$$r_h \simeq 2M\left[1 - \frac{2M}{\sqrt{\pi\Theta}}\left(1 + \frac{\Theta}{2M^2}\right)e^{-M^2/\Theta}\right] \tag{5}$$

Now the Hawking temperature for NC schwarzschild BH upto order $\sqrt{\Theta}e^{\frac{-M^2}{\Theta}}$ is given by

$$T_H = \frac{1}{8\pi M}\left[1 - \frac{4M^3}{\Theta\sqrt{\pi\Theta}}\left(1 - \frac{\Theta}{2M^2} - \frac{\Theta^2}{4M^4}\right)e^{-M^2/\Theta}\right]. \tag{6}$$

The entropy of the NC Schwarzschild BH ($S = A/4 = \pi r_h^2$) upto order $\sqrt{\Theta}e^{\frac{-M^2}{\Theta}}$ is given by

$$S = 4\pi M^2\left[1 - \frac{4M}{\sqrt{\pi\Theta}}\left(1 + \frac{\Theta}{2M^2}\right)\right]e^{-M^2/\Theta}. \tag{7}$$

The generalized form of Cardy formula (also known as Cardy-Verlinde formula) is given by [6]

$$S_{CFT} = \frac{2\pi R}{\sqrt{ab}}\sqrt{E_C(2E - E_c)}, \tag{8}$$

where $a, b > 0$, R is radius of $n+1$ dimensional FRW universe, E_C is the Casimir energy and E is the total energy of underlying field. The definition of Casimir energy is derived by the violation of Euler relation as [7]

$$E_C = n(E + PV - TS - \Phi Q - \Omega J), \tag{9}$$

where the pressure for CFT is $P = \frac{E}{nV}$, J, Q are zero for NC Schwarzschild BH, V is the volume of the system bounded by the apparent horizon. The total energy may be written as sum of extensive part E_E and Casimir energy E_C as

$$E = E_E + \frac{1}{2}E_c, \tag{10}$$

The Casimir energy E_C as well as purely extensive part of energy E_E can be expressed in terms of entropy S and radius R,

$$E_E = \frac{a}{4\pi R}S^{1+\frac{1}{n}}, \tag{11}$$

$$E_C = \frac{b}{2\pi R}S^{1-\frac{1}{n}}. \tag{12}$$

After the work of Witten [24] on the $\mathrm{AdS}_d/\mathrm{CFT}_{d-1}$ correspondence, Savonije and Verlinde [25] proposed that Cardy-Verlinde formula can be derived using the thermodynamical relations of arbitrary BHs in arbitrary dimensions. In this point of view, we shall prove the validity of Cardy-Verlinde formula for NC Schwarzschild BH.

From Eqs.(8) and (10), we get

$$S_{CFT} = \frac{2\pi R}{\sqrt{ab}}\sqrt{2E_E E_c}, \tag{13}$$

Using Eqs.(11) and (12) in above equation,

$$S_{CFT} = S. \tag{14}$$

The Casimir energy given by Eq.(9) for $n = 2$ with Eqs.(6) and (7) takes the following

$$E_C = 3E - 2TS, \tag{15}$$

$$= 3E - M\left[1 - \frac{4M^3}{\Theta\sqrt{\pi\Theta}}\left(1 - \frac{\Theta}{2M^2} - \frac{\Theta^2}{4M^4}\right) \times e^{-M^2/\Theta}\right]\left[1 - \frac{4M}{\sqrt{\pi\Theta}}\left(1 + \frac{\Theta}{2M^2}\right)e^{-M^2/\Theta}\right]. \tag{16}$$

Using above equation in Eq.(10), we get the purely extensive part of total energy as

$$E_E = -\frac{E}{2} + TS \tag{17}$$

$$= -\frac{E}{2} + \frac{M}{2}\left[1 - \frac{4M^3}{\Theta\sqrt{\pi\Theta}}\left(1 - \frac{\Theta}{2M^2} - \frac{\Theta^2}{4M^4}\right) \times e^{-M^2/\Theta}\right]\left[1 - \frac{4M}{\sqrt{\pi\Theta}}\left(1 + \frac{\Theta}{2M^2}\right)e^{-M^2/\Theta}\right]. \tag{18}$$

Further

$$2E - E_C = -E + 2TS \tag{19}$$

$$= -E + M\left[1 - \frac{4M^3}{\Theta\sqrt{\pi\Theta}}\left(1 - \frac{\Theta}{2M^2} - \frac{\Theta^2}{4M^4}\right) \times e^{-M^2/\Theta}\right]\left[1 - \frac{4M}{\sqrt{\pi\Theta}}\left(1 + \frac{\Theta}{2M^2}\right)e^{-M^2/\Theta}\right]. \tag{20}$$

From the comparison of Eqs.(12) and (16), we get

$$R = \frac{bS^{1/2}}{4\pi}\left(\frac{3}{2}E - TS\right)^{-1} \tag{21}$$

$$= \frac{bM}{\sqrt{4\pi}}\left[1 - \frac{4M}{\sqrt{\pi\Theta}}\left(1 + \frac{\Theta}{2M^2}\right)e^{-M^2/\Theta}\right]^{\frac{1}{2}}\left(\frac{3}{2}E - \frac{M}{2}\left[1 - \frac{4M^3}{\Theta\sqrt{\pi\Theta}}\left(1 - \frac{\Theta}{2M^2} - \frac{\Theta^2}{4M^4}\right)e^{-M^2/\Theta}\right] \times \left[1 - \frac{4M}{\sqrt{\pi\Theta}}\left(1 + \frac{\Theta}{2M^2}\right)e^{-M^2/\Theta}\right]\right)^{-1}. \tag{22}$$

Also, the comparison of Eqs.(11) and (18), gives

$$R = \frac{aS^{3/2}}{4\pi}\left(-\frac{1}{2}E + TS\right)^{-1} \tag{23}$$

$$= 4\pi a M^3\left[1 - \frac{4M}{\sqrt{\pi\Theta}}\left(1 + \frac{\Theta}{2M^2}\right)e^{-M^2/\Theta}\right]^{\frac{3}{2}} \tag{24}$$

$$\times \left(-\frac{1}{2}E + \frac{M}{2}\left[1 - \frac{4M^3}{\Theta\sqrt{\pi\Theta}}\left(1 - \frac{\Theta}{2M^2} - \frac{\Theta^2}{4M^4}\right) \times e^{-M^2/\Theta}\right]\left[1 - \frac{4M}{\sqrt{\pi\Theta}}\left(1 + \frac{\Theta}{2M^2}\right)e^{-M^2/\Theta}\right]\right)^{-1}. \tag{25}$$

Taking the product of Eqs.(21) and (23), we get

$$R = \frac{\sqrt{ab}}{4\pi}\frac{S}{\sqrt{\left(-\frac{1}{2}E + TS\right)\left(\frac{3}{2}E - TS\right)}}. \tag{26}$$

Using Eqs.(16), (18) and (26) in Eq.(8), we get

$$S_{CFT} = S. \tag{27}$$

This result shows that the entropy of the NC Schwarzschild BH can be expressed in terms of Cardy-Verlinde formula. As the BH geometric and thermodynamic quantities are evaluated by assuming large-radius approximations. So, the Cardy-Verlinde formula is valid only for large BHs.

3 Out Look

As a prolongation of the research on BH and gravitational collapse [13]-[28] in this paper, we derive the entropy formula in conformal field theory of a $4D$ static spherically symmetric NC Schwarzschild BH. This NC BH solution is obtained by introducing the NC effect through a coordinate coherent state approach, which is in fact the substitution of the point distributions by smeared source throughout a regular region of linear size. We perform the analysis by obtaining entropy and temperature, which show a deviation from their usual relations depending on the NC parameter Θ. We have proved that the entropy of the NC Schwarzschild BH can be expressed in terms of Cardy-Verlinde formula. For this purpose, we have used the approximate of values of incomplete gamma functions upto the term $\sqrt{\Theta}e^{\frac{-M^2}{\Theta}}$. With the same order of approximation the entropy and temperature of NC BH horizons has been calculated. The procedure adopted in this paper has been already used by Stare and Jamil [6,7]. It would be interesting to generalize this work for charged and charged rotating NC BHs. The Cardy-Verlinde formula of charged NC BH [29] is in progress.

References

1. M.R.Setare, Int. J. Mod. Phys. A **21**, (2006) 3007.
2. E.Verlinde, arXiv.: 0008140.
3. M.R.Setare, Mod. Phys. Lett. A **17**, (2002) 2089.
4. M.R.Setare and M.B Altaie, Eur. Phys. J. C **30**, (2003) 273.
5. D.Birmingham and S.Mokhtari, Phys. Lett. B **508**, (2001) 365.
6. M.R.Setare and Jamil, Phys. Lett. B **681**, (2009) 471.
7. M.R.Setare and M.Jamil, Int. J. Theor. Phys. **50**, (2011) 511.
8. M.R.Setare and R.Mansouri, Int. J. Mod. Phys. A **18**, (2003) 4443 .

9. M.R.Setare and E.C.Vagenas, Phys. Rev. D **68**(2003)064014.
10. M.R.Setare and E.C.Vagenas, Int. J. Mod. Phys. A **20**, (2005) 7219.
11. M.R.Setare, Eur. Phys. J. C **33**, (2004) 555.
12. B. Wang, E.Abdalla and R. K. Su, Phys. Lett. B **503**, (2001) 394.
13. P.Nicolini, A.Smailagic and E.Spallucci, Phys. Lett. B **632**, (2006) 547.
14. S.Ansoldi, P.Nicoloni, A.Smailagic and E.Spallucci, Phys. Lett. B **645**, (2007) 261.
15. L.Modesto and P.Nicolini, Phys. Rev. D **82**, (2010) 104035.
16. R.B.Mann and P.Nicoloni, Phys. Rev. D **84**, (2011) 064014.
17. P.Nicolini and E.Spallucci, Class. Quantum Gravity **27**, (2010) 015010.
18. R et al. Farook, Phys. Rev. D **86**, (2012) 106010.
19. M.Sharif and G.Abbas, J. Phys. Soc.Jpn. **81**, (2012) 044002.
20. R.Banerjee and S.Gangopadhyay, Gen.Relativ.Gravit. **43**, (2011) 3201.
21. A.Smailagic and E.Spallucci, J. Phys. A **36**, (2003) L467.
22. A.Smailagic and E.Spallucci, J. Phys. A **36**, (2003) L517.
23. A.Smailagic and E.Spallucci, J. Phys. A **37**, (2004) 1; *Erratum-ibid* 7169.
24. E.Witten, Advances in Theoretical and Math. Phys. **2**, (1998) 505.
25. I.Savonije and E.Verlinde, Phys. Lett. B **507**, (2001) 505.
26. R.Banerjee, S.Gangopadhyay and K.S.Modak, Phys. Lett. B **686**, (2010) 181.
27. R.Banerjee, B.R.Majhi and S.Samanta, Phys. Rev. D **77**, (2008) 124035.
28. R.Banerjee, B.R.Majhi and S.K.Modak, Class. Quant. Gravity **26**, (2009) 085010.
29. G.Abbas, *Cardy-Verlinde Formula of Non-commutative Charged BH* (Work in Progress).

Proc. Int. Conf. Relativ. Astrophys.
Pages 13-17, (2015)

Characteristic Signatures of Radial or Local Acceleration of Electron inside Earth Radiation Belt

Asif Ali Abbasi [a,1], **M. Shahid Qureshi** [2] **and Zahida Ehsan**[3]

[1]Institute of Space and Planetary Astrophysics, University of Karachi, Pakistan
[2]Department of Mathematical Sciences, Institute of Business Administration, Karachi, Pakistan
[3]Department of Physics, COMSATS Institute of Information Technology Lahore, Pakistan and National Center for Physics, Shahdrah Velly, Islamabad

Abstract WRadiation belt science has several enigmatic issues among which is the yet unexplained electron acceleration in the million electron Volt (MeV) energy range. An extensive data set of Relativistic Electron-Proton Tele-scope (REPT) on board the Radiation Belt Storm Probe (RBSP) is studied for the 28 June, 2013 electron acceleration event. Phase space density is first determined for 2.30 MeV particles from measured integral flux and then calculated for the appropriate energy that conserves the first adiabatic invariant. It is shown that the time dependent radial profile of phase space density supports the local acceleration mechanism.

Keywords electron acceleration, phase space density, local peak

1 Introduction

Both experimental and theoretical studies have been carried out to study the earth's radiation environment; however, progress in the radiation belt particle measurement advanced tremendously after the launch of the Van Allen Probes mission (RBSP) (Mauk et al. 2013; Baker et al., 2013). In this regard major studies have done calculation of electron phase space density (PSD) using adiabatic coordinates (e.g., Chen et al., 2007a, 2007b; Tu et al., 2009; Turneret et al. 2012; Morely et al., 2013; Baker et al., 2014) . Radial diffusion - a radical process for radial transport lowers down the gradients, transportation of plasma from high phase space density to the low. In this study of phase space density identification of peaks or gradients is a major setback as the in-situ satellite measurements do not come in terms with the adiabatic invariants. Phase space density is characterized by physically tenor-based measurements than by flux because of the constraints of Liouville's theorem (please provide references). Also its calculations in terms of adiabatic invariants have been mostly based on dynamic geomagnetic storm intervals (Selesnick et al., 1997a, 1997b, 1998, 2000). Studies (Hilmer et al., 2000; McAdams et al., 2001; Reeves et al., 2013 and Boyd et al., 2014) have also reported measurements which clearly distinguish between two types of acceleration including the ones where authors used NASA's Van Allen Radiation Belt Storm Probes.

[a]e-mail: asifhamal@gmail.com

2 Materials, Methods and Apparatus:

REPT consists of a stack of high-performance silicon solid-state detectors in a telescope configuration, a collimation aperture, and a thick case surrounding the detector stack to prevent the sensors from penetrating radiations (Baker et al., 2012).This instruments is pointed perpendicular to the spin axis of the spacecraft and measures high-energy electrons up to 20 MeV with excellent sensitivity and also measures magnetospheric and solar protons to energies well above E=100 MeV. The sublime task for the REPT design is to measure electron intensities in the range $10^2 - 10^6$ particles/cm^2 s sr MeV and energy spectra ratio up to 25 We follow the basic method outlined in (Chen et al. 2005) to calculate the phase space density. Let us write the equation for

$$f_{ch} = \{j_{ch}/ < p^2c^2 > [1.66EXP - 10]\}^*200.3 \qquad (1)$$

where j is the particle flux in 1/cm2sr s keV, E is the particle's kinetic energy in MeV, m0c2 is the electron rest mass in MeV, and the numerical factor is given by

$$< p^2c^2 >= \frac{1}{2}[k_{min}(k_{min}+2m_0c^2)+k_{max}(k_{max}+2m_0c^2)$$

(2)

where the K_{min} and K_{max} are the lower and upper limit of energy channel in MeV, respectively, and m_0c^2 is the rest energy of an electron. "L^*" is defined as the radial distance to the equatorial location where an electron crosses if all external magnetic fields were slowly turned off leaving only an internal dipole field (Roederer 1970), which is related to third adiabatic invariant given as

$$L^* = 2\pi\mu/\phi R_E \tag{3}$$

where "μ" is the earth's magnetic dipole moment, RE is the radius of earth and is the magnetic flux enclosed in the particle drift. The calculation was done with the Tsyganeko field model.

3 Results:

Figure (1) manifests a relativistic electron acceleration event which took place on June 28, 2013. The panels show the Kp index, the disturbance storm time index, the interplanetary magnetic field north-south component and solar wind speed. The interplanetary magnetic field (IMF B_y) feeds on more strongly southward after first 3 hours in genesis of day then fall down slightly after one hour. IMF B_z declines below zero values after 9UT enables reconnection with the earth's magnetic field to transfer energy to magnetosphere.

The REPT instrument electron flux near all pitch angles are shown in figure (2). Flux intensities are color coded based on the color bar at the right vertical column side. The measurements show a very weak flux increase at the beginning of the event and pitch angle annihilated as the event progresses. The most appearance of electrons over the entire range of pitch angles are in boundary of 30 to 150 degrees except between time duration of 08 to 10 UT, as seen in the three panels. Our choice of first adiabatic invariance is determined by the electron instrument energy range.
Figure 3 shows the flux of 2.30 MeV electron fluxes as a function of L shell and time. From the flux measurements, it is clear that there was a increase in the relativistic electron flux between L = 4.0 to 5.0 (We calculate and choose a value of ? 1414 MeV/G). The observed value of electron energy flux is converted to PSD as function of the first adiabatic invariant using equation (1) at equatorially mirroring particle (2nd adiabatic invariance is zero). The results of L* calculation for the space craft corresponding to ? 1414 MeV/G are also shown in figure (4).

The minimum to maximum range of phase space density is plotted in order to look for the characteristics signatures of either radial or local acceleration. The plotted PSD values between time of 08:00 UT 11:00 UT against L* are shown in figure 4. At the onset, there is smooth continuation of the gradients. From 08:43UT, the radiation belt experiences a swift up lift increase in phase space density that goes along for more than an hour till 10:20UT.The analysis identified the development of peaks in electron phase space density, which is a compelling evidence for local electron acceleration.

4 Discussion

The strength of the pitch angle scattering appears to be most intense near the position in L of the maximum of the relativistic electron flux. Our calculated values of phase space density in adiabatic invariance space confirmed that the same characteristic signature of local acceleration was observed in the June 2013 storm that was reported by previous studies of this type especially by Reeves et al., on (OCT: 2012). The time evolution of PSD (L*) show quick formation of the peak and then spreads out. The above results can be expanded to look at the EMFISIS data to observe chorus waves.

Acknowledgements Authors are grateful for suggestions with Drs. Y. Chen and G. D. Reeves, which helped improve the manuscript. CDA web and Dr. D. N. Baker are gratefully acknowledged for providing the data of REPT.

References

1. D.N. Baker et al., Space Sci. Rev., doi:10.1007/s11214-012-9950-9. 2012.
2. D.N. Baker et al., A long-lived relativistic electron storage ring embedded in Earth's outer Van Allen belt. Science, 340(6129), 186-190,doi:10.1126/science.1233518. 2013.
3. D.N., Baker et al., J. Geophys. Res. Lett. :40,1-5, doi:10.1002/grl.50909. 2014.
4. A.J. Boyd et al., J. Geophys. Res. Lett. :41,2275-2281, doi:10.1002/2014GL059626. 2014.
5. Y. Chen, R.H. Friedel, G.D. Reeves, T.E. Cayton, & R. Christensen, Multisatellite determination of the relativistic electron phase space density at geosynchronous orbit: An integrated investigation during geomagnetic storm times, J. Geophys. Res., 112, A11214, doi: 10.1029/2007JA012314. 2007A.
6. R.V. Hilmer & Ginet, Enhancement of equatorial energetic electron fluxes near L=4.2 as a result of high speed solar wind streams,G. P., J. Geophys. Res., 105, 23,311. 2000.

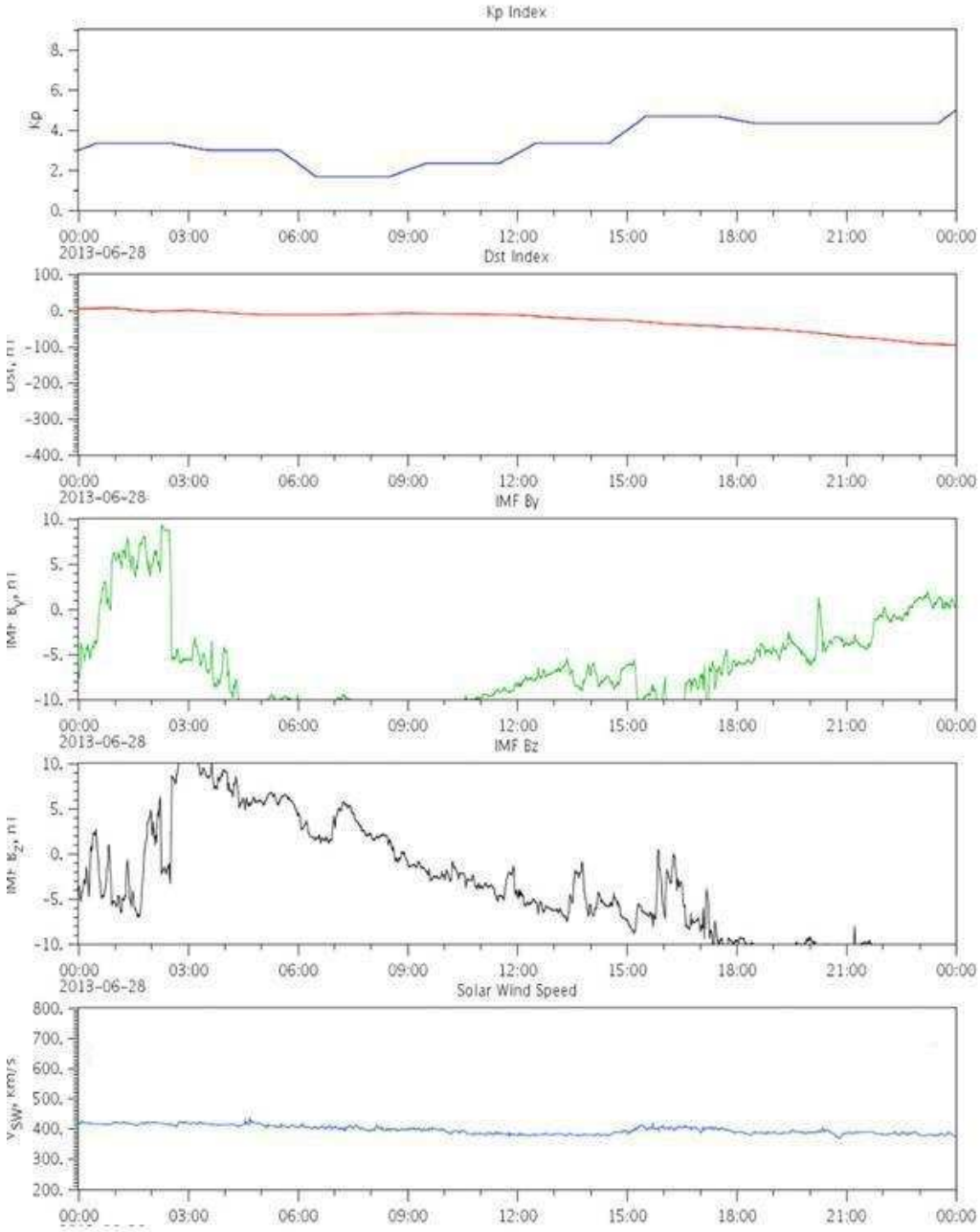

Figure: I. Graph shows Kp index, the disturbance storm time index, the interplanetary magnetic field north south component and solar wind speed on 28 June 2013

7. B.H. Mauk et al, Science objectives and rationale for the radiation belt storm probes mission Space .Sci. Rev., doi:10.1007/s11214-012-9908. . 2013.
8. K.L. McAdams, G.D. Reeves, R.H. Friedel, & T.E. Cayton, Multisatellite comparisons of the radiation belt response to the Geospace Environment Modeling (GEM) magnetic storms, J. Geophys. Res., 106, 10,869. 2001.
9. S.K. Morley et al., , J. Geophys. Res.Lett:40,1-5, doi:10.1002/grl.50909. 2013.
10. G.D. Reeves et al., Electron Acceleration in the Heart of the Van Allen Radiation Belts. Science 341, 991. 2013.
11. J. Roederer, Dynamics of Geomagnetic ally Trapped Radiation, Springer, New York. 1970.
12. R.S. Selesnick & J.B. Blake, A quiescent state of 3 to 8 MeV radiation belt electrons, Geophys. Res. Lett., 24, 1343. 1997A.
13. R.S. Selesnick & J.B. Blake, Dynamics of the outer radiation belt,Geophys. Res.Lett., 24, 1347. 1997B.

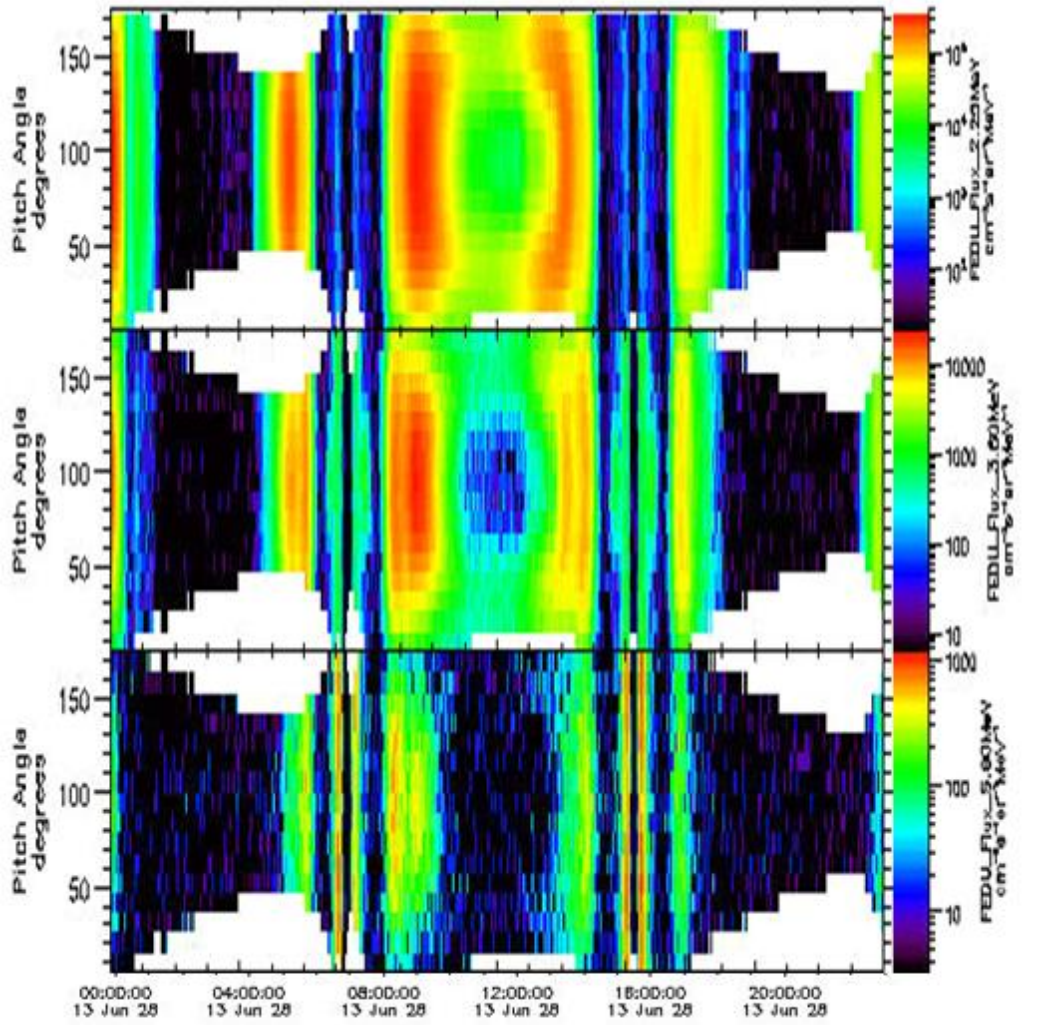

FIGURE 2:FEDU spectrograms by pitch angle at sample energies

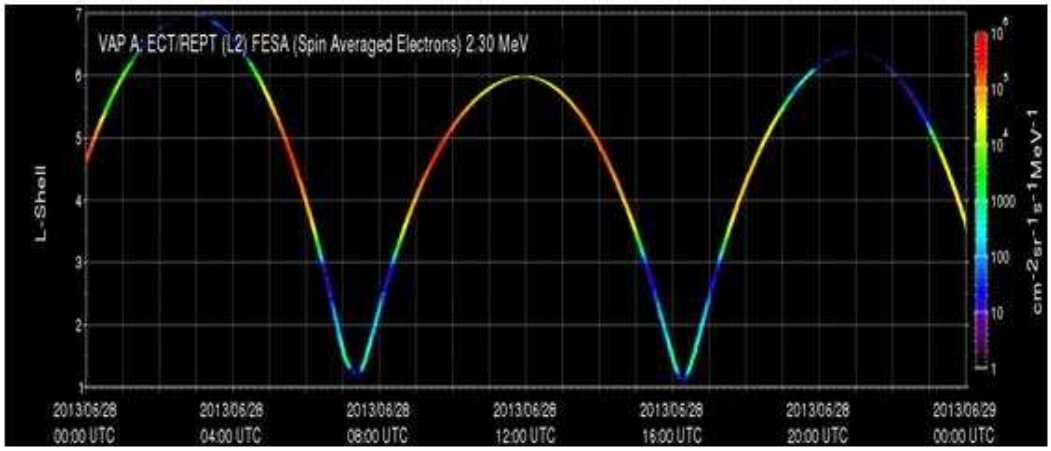

FIGURE:3 FESA for 2.30 MeV energy channel

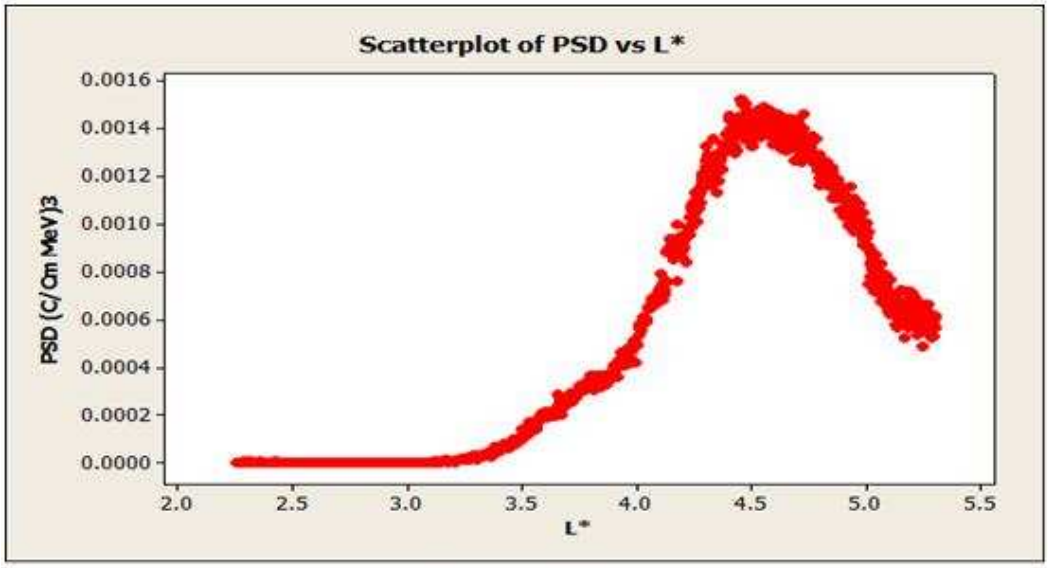

FIGURE 4:Graph between PSD verses L*

14. R.S. Selesnick & J.B. Blake, Radiation belt electron observations following the January 1997 magnetic cloud event, Geophys. Res. Lett., 25, 2553. 1998.
15. Selesnick, R. S.,& Blake, J. B, On the source location of radiation belt relativistic electrons, J. Geophys. Res., 105, 2607. 2000.
16. W. Tu, X. Li, Y. Chen, G.D. Reeves & M. Temerin, Storm dependent radiation belt electron dynamics, J. Geophys. Res., 114, 2156-2202, doi:10.1029/2008JA013480. 2009.
17. D.L. Turner, Y. Shprits, M. Hartinger & V. Angelopoulos, Explaining sudden losses of outer radiation belt electrons during geomagnetic storms. Nat. Phys., 8, 208-212, doi:10.1038/nphys2185. 2012.

Proc. Int. Conf. Relativ. Astrophys.
Pages 18-24, (2015)

Is Discrete the New Continuum?

Maqbool Ahmed[a,1], **Hibatul Shafi**[b,1]

[1]Nusrat Jahan College Rabwah, Chenab Nagar Distt. Chiniot, Pakistan Postal Code 35460

Abstract A glassful of water can be treated as a fluid despite the fact that it is composed of discrete atoms at a smaller scale. Can the same be true about the spacetime that happens "to be" a smooth manifold? Can it be true that the apparent smoothness of a spacetime is an emergent phenomenon and an approximation to an atom-like structure at some smaller scale. One thing to be borne in mind is that "a quantization" of a fluid will not automatically bring out the fact that the underlying structure is actually atomic. Similarly a quantization of the spacetime will, in general, not tell us if the underlying reality is discrete, even if it happened to be so. Discreteness in both cases has to be an independent ingredient of the theory that intends to describe them.

Causal set theory is an attempt to quantize gravity that assumes a discrete fundamental structure. Although a quantum dynamics is still being sought, the theory has a fully developed classical dynamics and has reached a stage in its development where some predictions about cosmology have started to come out. The theory has the potential to resolve the problem of singularities of general relativity and the existence of a fundamental length scale could help cure the problem of infinities in quantum field theory. On top of all this the theory is extremely simple and appealing on philosophical and aesthetic grounds and tends to revolutionize our concepts of space and time. We summarize some of the important aspects of the theory here.

Keywords Causal Set theory · Quantum Gravity · Fundamentally Discrete theories · Partial Orders · Cosmology

[a]e-mail: maqbool72@gmail.com
[b]e-mail: hibatulshafi@hotmail.com

1 Introduction

Despite the fact that there are is no lack of motivation, both on philosophical and physical grounds, to assume an underlying discreteness, a fundamentally discrete theory of spacetime is still lacking. Causal set theory is one such attempt that ventures to describe the fundamental reality as a discrete structure and maintains that a successful theory of "quantum gravity" can only be realized by a quantization of a discrete instead of a continuum structure.

In this paper, after mentioning some of the ideas that motivate a departure from the continuum, we introduce the concept of a causal set, which represents the discrete structure that is assumed to replace the notion of a manifold somewhere around the Planck scale. We then discuss some of the important kinematical results of causal set theory and then mention some ideas on how to recover (the illusion of a) continuum as an approximation. Before we conclude we summarize some of the phenomenological results coming from causal set theory as well.

2 The need for discreteness!

We will not go into the philosophical reasons of why an atomic structure is better than a continuum but will confine ourselves to the arguments coming from known physical theories. Our current understanding of physical phenomena rests on two pillars of modern physics – General Relativity (GR) and Quantum Physics (QP). [1] These immensely successful theories, which have disparate domains, have helped us explain immensely dis-

[1]As the conference, for whose proceedings this paper is but one contribution, was held to commemorate the hundred years of GR and to pay tribute to Einstein, let us remember

parate phenomena ranging from the evolution of the universe to the structure of a proton. Despite this success there are glaring problems that still linger. Most disturbing are the ones that appear in the guise of singularities/infinities. For example, black hole singularities in GR and quantum field theories infinities in particle physics [2]. It is a general belief that these problems can be cured if there is a fundamental cut-off, say, in "length".

There is another set of issues that raises its head when we try to deal with phenomena where both GR and QP are relevant, for example, phenomena in the early universe or close to a black hole singularity. One such issue is of special importance. Let us ask the following question: What happens to the horizon of a black hole when QP is taken into account? QP does not allow the localization of any hypersurface including that of a horizon with infinite precision and consequently we, in general, end up with a "thickened and wrinkled" object [12–14]. If all possible wrinklings are summed over the entropy associated with a black hole diverges. Again a fundamental cut-off might help us evade the problem [3]. Thus it seems imperative, if we want our precious semi-classical results to hold in the statistical analysis of a quantum theory, that a cut-off be present at the fundamental scale. Thus it is no wonder that most quantum gravity theories do incorporate such a fundamental length scale in one way or the other.

3 Causal Set Idea

Causal set theory [1–4] is a program to quantize gravity using a fundamentally discrete structure. That discrete structure is called a causal set, $\mathcal{C}$, which is a partially ordered set with a precedence relation, $\prec$, among some (and not necessarily all) of its elements that satisfies the following properties:

- $x \prec y$ and $y \prec z \Rightarrow x \prec z,\ \forall x, y, z \in \mathcal{C}$
- $x \not\prec x,\ \forall x \in \mathcal{C}$

If one takes the $\prec$ [4] relation to mean the relationship of before and after, then any subset of points of a weakly causal Lorentzian manifold satisfies the above two conditions, where the first property makes $\prec$ a transitive relation and the second excludes the possibility of what are called timelike loops – a condition that characterizes weakly causal Lorentzian manifolds. We add one more condition to ensure discreteness

- cardinality of $\{y | x \prec y \prec z\} < \infty,\ \forall x, z \in \mathcal{C}$.

This is called the condition of local finiterity and basically means that the number of elements of $\mathcal{C}$ in every interval are finite. These three conditions define a causal set.

There are many ways to realize a causal set but a Hasse diagram is the most explicit visually, where the elements of $\mathcal{C}$ are drawn as dots and relations among elements as lines. Only the irreducible relations not implied by transitivity are drawn on the diagram. Figure 1

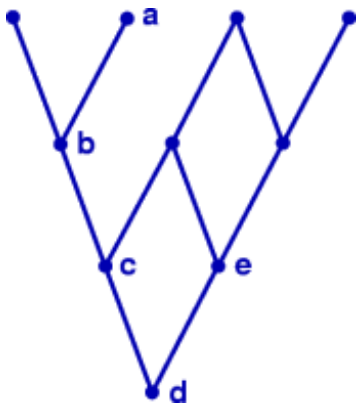

Fig. 1 A ten element causal set. Element d is related to every other element of the set.

shows a ten element causal set. Here elements d and a are related but this relation is implied by transitivity and hence no line is drawn between these two elements. A subset of $\mathcal{C}$ is called a chain/anti-chain if all/none elements in the subset are related. For example, elements a, b, c and d in figure 1 form a chain whereas and elements c and e form an anti-chain.

The above mentioned discrete structure is supposed to replace the notion of a smooth spacetime at the fundamental level. In other words, a spacetime is only an approximation to an underlying reality of discrete spacetime atoms just like the description of a glassful of water as a fluid is an approximation to an underlying reality of discrete atoms that make up that glass of water. It should be intuitively clear that the $\prec$ relationship at the fundamental level becomes the causal relationship of "before and after" at the spacetime level. [5] Where a causal set has just the $\prec$ relationship, a spacetime is intuitively thought to have much more than just its causal relationship. More specifically it has a certain

the immense contributions of Einstein towards the development of both these theories.

[2] The process of renormalization can ameliorate these problems in the case of quantum field theories but they again reappear in naive attempts to quantize gravity.

[3] As it certainly does in the case of causal set theory.

[4] $x \prec y$ is read as x precedes y.

[5] Hence a process of constructing a causal set, essentially creates the notion of time with it.

topology, a differentiable structure and its geometry. It turns out that all this can be recovered from the causal structure of the spacetime. In other words, if all possible relationships of before and after among the elements are given, then this is the most that can be told about a spacetime. In fact, the metric can be recovered from this information up to a conformal factor that in turn can be derived from the density of elements information. This has prompted causal set researchers to coin the slogan *geometry = number + order* [6].

Every causal set has some information about the causal structure. Does it mean that every causal set can generate a spacetime [7]? The answer to this question, unfortunately, is a no. In fact, in some suitable sense the number of causal sets that generate a spacetime is super-exponentially smaller than the ones that do not. The next question is how do we know if a certain causal set can generate a spacetime. The natural answer to this question starts (but does not end) with the observation that the first property such a causal set would posses is that it would be embeddable in that spacetime [8]. We will say more about this question in the next section.

Can any spacetime be produced by an appropriate causal set? The answer is yes and one but has to realize that if one took the spacetime that one wanted to generate and then took a subset of its elements and used its causal structure to induce the $\prec$ relationship, one would have at least "a causal set" that is, by construction, embeddable into that spacetime and hence satisfies the first condition of generating that spacetime. The complete answer to this question can be found in the literature and is beyond the scope of this paper but we will mention this again in the next section when we talk about the concept of sprinkling.

The last answer also clears the question whether we ever have causal sets that are embeddable into spacetimes. Finally, if we are given a causal set, how do we know if it is embeddable into a spacetime. And furthermore as the number of non-spacetime-like causal sets are exponentially more than the one that do generate a spacetime, the related question that how does one "give preference" to the latter over the former type. Again we will not give complete answers but refer the interested reader to the literature. Essentially these are questions which are subjects of current research and are naturally of utmost importance to the causal set community. There are many criteria for checking the embeddibility of a causal set but we will briefly mention just one. It is related to different dimension estimators [9] [7,11] that essentially give the same answer in the case of a spacetime. If we try these estimators on a randomly picked subset of points of that spacetime, it should be obvious that we should again get the same answers for different estimators. Now We can think of this random selection as a causal set (provided it is finite). Hence one way of checking whether a causal set can produce a spacetime would be to try these estimators with that given causal set and we should get the same answer for different estimators if that causal set could produce a spacetime.

As far as the second part of the question is concerned, only dynamics can do that for us. Just like in the case of a particle the dynamics picks out the set of smooth paths which is a set of measure zero in the set of all possible paths, we expect the quantum dynamics of causal sets to prefer causal sets that generate Lorentzian manifolds. Although a quantum dynamics is as yet incomplete, a classical dynamics called the classical sequential growth (CSG) [25] already shows signs that it can prefer causal sets that have many spacetime-like properties despite the fact that it has been proved that it always induces causal sets with structures (on a local level) that cannot be embedded in Minkowski spacetimes. Interested reader should consult [27] for a detailed discussion.

4 Acquiring continuum

Having assumed spacetime discreteness the next step would be to devise a process to go from the fundamental discrete scale to the large scale continuum [10], which should exist as the classical limit in an appropriate sense. Speaking in terms of the sum-over-histories approach one expects that the classical limit should result from the constructive interference of some of the histories, which in this case are causal sets. Of course, the complete theory is as yet not available but if this sum-over-histories is going to give anything like a manifold, we can still talk about the causal sets that will form this classical limit.

[6] Thus all geometrical quantities can be obtained by a simple process of counting (philosophically a very attractive canonical measure). For example, the volume of a region of spacetime is simply the number of elements it contains or $V = l^4 N$.

[7] In the sense that it picks a spacetime that approximates it.

[8] A causal set whose elements are the points of a spacetime and whose relations of $\prec$ are the same as induced by the causal order of that spacetime is said to be embeddable into that spacetime.

[9] like the volume as a function of "height" for an interval or the number of related pair of elements in an interval as fraction of all pairs of elements.

[10] Because, after all, even if the fundamental structure is discrete, the large scale structure is seamlessly described by a continuum

4.1 The concepts of embedding and sprinkling

As already mentioned, a causal set $\mathcal{C}$, is said to be embeddable into a given spacetime if the elements of $\mathcal{C}$ form the spacetime events of that spacetime such that the order in $\mathcal{C}$ matches the causal order of the spacetime. But according to this definition several causal sets could be embedded into a given spacetime. There has to be a way to pick out the (typical) causal set to which that spacetime is an approximation. How do we recognize that (typical) causal set that can be said to generate that particular spacetime? We will only hint at the answer to this question and not go an any great detail here. Interested reader is referred to the references [8–10].

The first thing to notice is that in going from discrete to continuum scale one would expect to take a causal set first and then acquire the corresponding spacetime. But as mentioned earlier, there are exponentially many more non-spacetime-like causal sets and to pick one causal set at random that might be able to generate a spacetime is next to impossible. Quantum dynamics also has not reached a stage where it can help us in this regard. So we take the opposite route and contrary to what should be done, we choose the spacetime first and then choose a large number of spacetime points using Poisson process from that Lorentzian manifold (in a suitable sense). This process is called "sprinkling". The causal order relations of the manifold is used to induce order relations amongst the spacetime points thus chosen via sprinkling and the causal set hence obtained is a called faithfully embeddable causal set (into that spacetime). This causal set can be said to have come from the sprinkling of the Lorentzian manifold with a high probability and hence to approximate that manifold. In other words, this is a typical causal set that will be produced in a sprinkling of the spacetime that it will in turn generate.

One very important consequence of the random nature of sprinkling is that the process is locally Lorentz invariant (LLI). Hence it produces a theory which despite being discrete insofar as its large scale correspondence is concerned is completely LLI. This is such an important point that we should try to explain this idea a bit more clearly.

For theories on a background Minkowski spacetime, Lorentz invariance means that the dynamics should not pick out a preferred frame. For a thoery in which Minkowski spacetime is an approximation to some underlying discrete structure, it means that discreteness may not cause the dynamics to pick a preferred frame. This is achieved due to the random nature of correspondence between the fundamental level and the emergent continnum. It can be shown that if we come up with a rule to assign frames to sprinklings, a Lorentz transformation that connects two sprinklings will in general not connect the frames. Instead of proving this statement it is more instructive to show the Lorentz invariant nature of Poisson sprinkling by the following demonstration.

Fig 2 shows a sprinkling of [11] 4096 spacetime points in a patch of *1+1D* Minkowski spacetime. A small coordinate region in this patch ($0.8 < t < 1$,$0.8 < x < 1$) is selected and magnified in the top right part of the figure. Then a boost of $\beta = 4/5$ is applied on the original patch and the result is shown in the bottom left of the diagram. Again the same coordinate region that is $0.8 < t < 1$ and $0.8 < x < 1$ is selected and magnified in the bottom right as before. It can be seen that the distribution is not identical but we again get another sprinkling with Poisson distribution of the same density which looks "very similar". This shows that the boost does not affect the sprinkling in any way which could connect it to the boost.

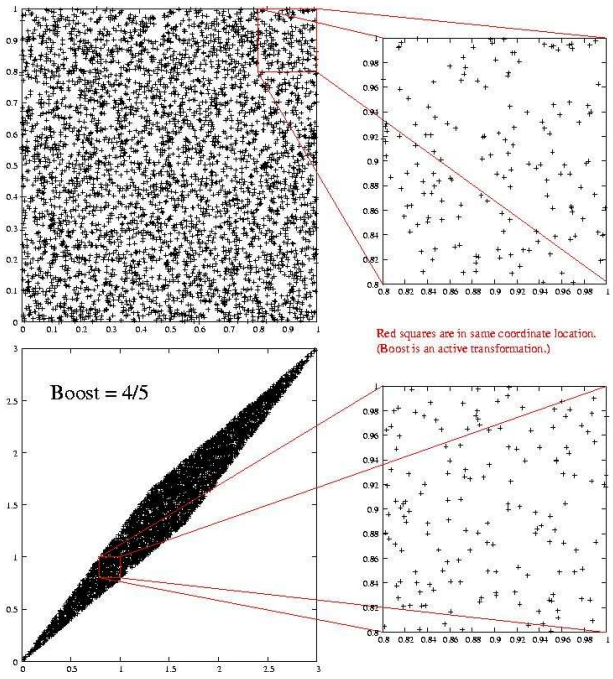

Fig. 2 A demonstration of the Lorentz invariant nature of Poisson sprinkling.

As there seems to be every indication that nature respects Lorentz invariance, this is a very important result. In fact, it will be considered a blow to the causal set program if a violation of the LLI was ever discovered.

[11] Courtesy Rideout.

5 Phenomenology

As must have been felt by the reader, the structure of the causal set theory is particularly simple and, more than that, very clear. As a consequence, it has become possible to make phenomenological models based on this structure even at a relatively early stage of development of the theory. We will discuss only two major developments in this regard.

5.1 Dark energy in Causal Set Theory

Perhaps the most interesting phenomenological prediction that has come out of the causal set theory is about the nature of the so-called dark energy problem. This prediction was made by Rafael Sorkin [18,19], the founder and mainstay of the causal set program, a couple of decades ago when the SN data had not as yet forced a non-zero cosmological constant [17] on the cosmological community. The prediction not only satisfies the observational constraints but also sheds light on the nature of the dark energy. It predicts fluctuation in its magnitude which are quantum in nature. Later on, a model [20] was developed based on the arguments of that predictions that allowed for the evolution of the universe to be studied on a computer with the predicted cosmological term.

In this section we will summarize the arguments that lead to fluctuations in the cosmological term and are described in detail in [18–21]. We start by assuming a relation of the type $\Delta\Lambda\Delta V \sim 1$ [12] that is expected in any theory of quantum gravity provided the two quantities are well defined [13] as they are in causal set theory. This relation is the basis of fluctuation in Λ, which are of the order $\Delta\Lambda \sim 1/\Delta V$ and

$$\Lambda = \langle\Lambda\rangle + \Delta\Lambda. \tag{1}$$

There are reasons to believe that $\langle\Lambda\rangle = 0$ [20], which reduces the above relation to $\Lambda = \Delta\Lambda$. In causal set theory ΔV (and hence $\Delta\Lambda$) is properly defined [14] and is given by $\Delta V = \pm\sqrt{V}$. This leads to

$$\Lambda \sim \pm\frac{1}{\sqrt{V}}. \tag{2}$$

For a rough argument assume that we take V to be the volume of the observable universe then the last equation predicts that the value of

$$|\Lambda| \sim \frac{1}{\sqrt{H^{-4}}} \sim H^2 \sim \rho_{crit}. \tag{3}$$

Here H^{-1} is the Hubble radius of the observable universe and ρ_{crit} is the critical energy density.

The relation 2 assigns a definite meaning to the fluctuations in Λ but if we are to incorporate such a Λ into an evolution of the universe, we still need a model that gives us Λ as a function of time keeping (2) intact. Such a model was developed [20,21] later but instead of mentioning the details of the model we will confine ourselves with just the results. The interested reader will find detailed discussions about the model in the two references mentioned above. The results of computer simulations

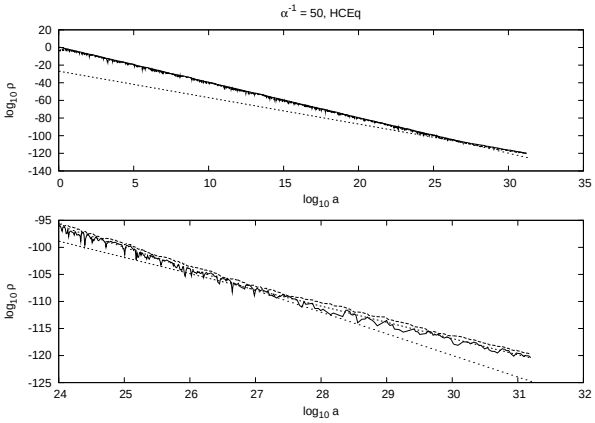

Fig. 3 This is a log-log plot where different energy densities are shown as a function of the size of the universe (in terms of the scale factor). The solid jittery line shows the magnitude of energy density in Λ. This magnitude initially tracks the energy density in radiation (in lightly dotted line) but switches over to tracking matter (in heavy dotted line) when it becomes the dominant component around $loga \sim 27$. The bottom figure expands this crossover region to show the change in tracking more clearly. The total energy density is also plotted as broken jittery line.

show that we get a tracking model in the sense that the magnitude of the energy density in Λ tracks the total energy density as shown in figure 3. Hence the dark energy is not just becoming relevant today; it was always relevant and will always be so. In other words, there is nothing special about the current acceleration in the expansion of the universe. Accelerations, decelerations and even contractions are "natural" phases in the evolution of the universe. This solves "the Why Now?" problem without any fine tuning.

The sign of Λ is of course random, which means that it is, at least in principle, equally likely for Λ to be negative or positive [15] at a particular point in the evolution of the universe. In fact, a recent unpublished

[12] All equations are written in natural units, i.e., $\hbar = 8\pi G = c = 1$. Here V and Λ are the four volume and the cosmological constant respectively.

[13] For example, this relationship comes out very naturally in the uni modular attempts to quantize gravity [22,23].

[14] This is a consequence of the theory being Lorentz invariant.

[15] It is when Λ is small or negative that the universe decelerates and it is when Λ stays negative for a relatively longer period of time that the universe eventually starts to contract [21].

work of one of the authors of this article has shown that it is an almost certainty in the model that Λ will change sign at least once between now and a redshift of 3 [28]. There have been recent indications [26] that Λ might have changed sign at some time between a redshift of 2 and 3. If these are substantiated, causal set theory will be the only fundamental theory to have a natural explanation of negative Λ again without any fine tuning whatsoever. On top of the tracking behavior

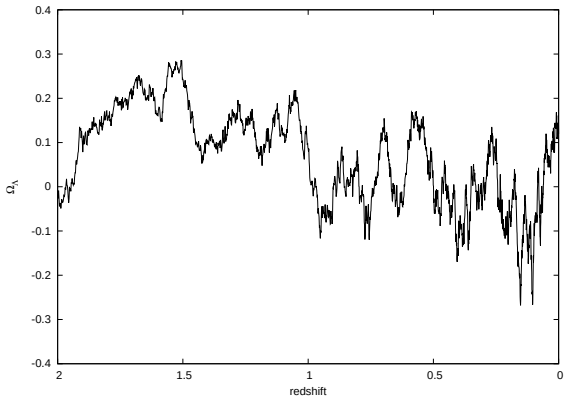

Fig. 4 The value of Ω_Λ fluctuates about zero. These fluctuations show the quantum nature of the cosmological term.

mentioned earlier there are fluctuations in the value of Λ and hence Ω_Λ that allude to the quantum nature of Λ in this model. Figure 4 shows these fluctuations in the value of Ω_Λ in one of the computer simulations.

Let us just mention further that the model is structurally stable and satisfies the constraints on Ω_Λ coming from SN 1a observations with appreciable probability.

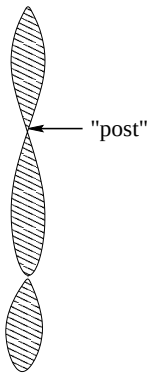

Fig. 5 CSG has parameter space that generates a universe which shows successive cycles of expansion punctuated by one element posts that act like big bang singularities for the new cycle and, of course, big crunch singularities for the old cycle.

5.2 A model of the Early Universe

Classical sequential growth (CSG) dynamics mentioned earlier has a large class of dynamical laws (choices in the parameter space) which generate cyclic universes. These cyclic universes grow to a certain "size" before it contracts back to one element, only to repeat the process all over again (figure 5). These one element junctions are called posts and quite obviously look like big bang (or big crunch) singularities. When the universe immediately after a post was studied [27], it was found that this era looks very much like a de Sitter spacetime with exponential expansion in the "spatial volume". This model of the early universe solves many of the standard cosmology problems, again without any fine tuning. For example, the resulting early universe is homogeneous, which solves the horizon problem and is orders of magnitude bigger than a Planck length when it is just a few Planck times old without the use of any inflaton and/or fine tuning, solving the size problem. There are other very interesting and important phenomenological consequences relating to the black hole entropy [15,16] and the origin of cosmic rays [24] that we have not mentioned here. The interested reader is again advised to consult the references mentioned above.

6 Final Remarks

Causal set theory is an extremely simple and clearly stated attempt at quantizing gravity. Despite being a fundamentally discrete theory it is completely Lorentz invariant. The theory has a well developed classical dynamics, though it still lacks a fully developed quantum version. Still the theory has a lot to say about cosmology and black hole entropy. It predicts quantum fluctuations in the cosmological term, whose magnitude remains of the order of the critical density throughout the history of the universe. It has a model of the early universe that that has the potential to solve many of the standard cosmology puzzles that arise out of the initial conditions. It predicts a finite entropy of the black hole. Taken seriously this discrete theory may just give birth to a very new notion of the continuum.

References

1. R.D. Sorkin, *First Steps with Causal Sets*, (Proceedings of the Ninth Italian Conference of the same name, held Capri, Italy, September, 1990), 68-90, (World Scientific, Singapore), (1991), R. Cianci, R. de Ritis, M. Francaviglia, G. Marmo, C. Rubano, P. Scudellaro (eds.)
2. L. Bombelli, J. Lee, D. Meyer and R.D. Sorkin, *Spacetime as a causal set*, Phys.Rev.Lett. 59:521-524 (1987)

3. R.D. Sorkin,*Causal Sets: Discrete Gravity (Notes for the Valdivia Summer School)*, arXiv:gr-qc/0309009
4. J. Henson *The causal set approach to quantum gravity*, arXiv:gr-qc/0601121
5. G. Brightwell and M. Luczak, *0rder-invariant measures on causal sets*, Annals of Applied Probability 2011, Vol. 21, No. 4, 1493 - 1536, arxiv:0901.0240
6. G. Brightwell and N. Giorgiou, *Continuum limits for causal sequential growth models*, Random Structures and Algorithms, Vol. 36, Issue 2, March 2010
7. D.A. Meyer, *The Dimension of Causal Sets*, PhD thesis (M.I.T., 1988), http://hdl.handle.net/1721.1/14328
8. L. Bombelli and D.A. Meyer, *The Origin of Lorentzian Geometry*, Phys.Lett. A141 (1989) 226-228
9. J. Noldus, *A new topology on the space of Lorentzian metrics on a fixed manifold*, Class. Quantum Grav. 19(2002) 6075-6107, arxiv:1104.1811
10. S. Major, D.P. Rideout and S. Surya, *On Recovering Continuum Topology from a Causal Set*, J.Math.Phys.48: 032501,2007 arxiv.org/abs/gr-qc/0604124
11. D.D. Reid, *Manifold dimension of a causal set: Tests in conformally flat spacetimes*, Phys.Rev. D67 (2003) 024034, arxiv:gr-qc/0207103
12. J.D. Beckenstein, *Do we understand black hole entropy?*, proceedings of the *MG7* meeting, edited by R.T. Jantzen, G. Mac Keiser and R. Ruffini (World Scientific 1996), arxiv:gr-qc/9409015
13. R.D. Sorkin and D. Sudarsky, *Large Fluctuations in the Horizon Area and what they can tell us about Entropy and Quantum Gravity*, Class. Quant. Grav. 16: 3835 - 3857 (1999), arxiv:gr-qc/9902051
14. R.D. Sorkin, *How wrinkled is the surface of a black hole?*, Proceedings of the first Australasian conference on General Relativity and Gravitation (1996), pp 163 - 174, arxiv:gr-qc/9701056
15. D. Dou, *Causal Sets, a Possible Interpretation for the Black Hole Entropy,and Related Topics*, PhD thesis (Trieste, SISSA, 1999), arxiv:gr-qc/0106024
16. R.D Sorkin and D.Dou, *Black-Hole Entropy as Causal Links*, Found. Phy. 33 (2003) 279 - 296, arxiv:gr-qc/0302009
17. S. Weinberg, *The cosmological constant problem,* Rev. Mod. Phys., 61, 1-23, (1989)
18. R.D. Sorkin, *Spacetime and Causal Sets*, in J.C. D'Olivo, E. Nahmad-Achar, M. Rosenbaum, M.P. Ryan, L.F. Urrutia and F. Zertuche (eds.), *Relativity and Gravitation: Classical and Quantum* (Proceedings of the *SILARG VII Conference*, held Cocoyoc, Mexico, December, 1990), pages 150-173 (World Scientific, Singapore, 1991).
19. R.D. Sorkin, *Forks in the Road, on the Way to Quantum Gravity*, talk given at the conference entitled "Directions in General Relativity", held at College Park, Maryland, May, 1993, Int. J. Th. Phys. 36: 2759–2781 (1997), gr-qc/9706002.
20. M. Ahmed, S. Dodelson, P.B. Greene and R.D. Sorkin, *Everpresent Lambda*, Phys.Rev. D69 (2004) 103523, astro-ph/0209274
21. M. Ahmed and R.D. Sorkin, *Everpresent Lambda II, Structural Stability*, Phys.Rev. D87 (2013) 063515, arXiv:1210.2589v3[gr-qc](2012)
22. W.G. Unruh, *"Unimodular theory of canonical quantum gravity"*, Phys. Rev. D40, 1048 (1989).
23. A .Daughton, J. Louko and R.D. Sorkin, *Instantons and unitarity in quantum cosmology with fixed four-volume*, Phys. Rev. D58 084008 (1998), gr-qc/9805101.
24. F.Dowker, J.Henson and R.D. Sorkin, *Quantum Gravity Phenomenology, Lorentz Invariance and Discreteness*, Mod.Phys. Lett. A19(2004) 1829 - 1840, arxiv:gr-qc/0311055
25. D.P. Rideout and R.D. Sorkin, *Classical sequential growth dynamics for causal sets*, Phys. Rev. D61, 024002 (2000), gr-qc/9904062
26. T. Delubac, et. al., *Baryon Acoustic Oscillations in the Lyα forest of BOSS DR11 quasars*, Astronomy and Astrophysics 574, A59(2015), arxiv:1404.1801v1
27. M. Ahmed and D.P. Rideout, *Indications of de Sitter Spacetime from Classical Sequantial Growth Dynamics of Causal Sets*, Phys. Rev. D81, 083528 (2010), arXiv:0909.4771
28. M. Ahmed and R.D. Sorkin, *Is negative Lambda a quantum effect?*, unpublished work, in preparation

Proc. Int. Conf. Relativ. Astrophys.
Pages 26-32, (2015)

Static Axisymmetric Einstein Equations in Vacuum

Symmetry, New Solutions and Ricci Solitons

M M Akbar

Abstract An explicit one-parameter Lie point symmetry of the vacuum Einstein equations with two commuting hypersurface-orthogonal Killing vector fields is presented. The parameter takes values over all of the real line and the action of the group can be effected algebraically on any solution of the system to produce a one-parameter extended family, without having to deal with an associated set of equations that is common in most solution-generation techniques. This enables one to construct new axisymmetric static solutions as well as new cylindrical gravitational wave solutions in four spacetime dimensions, but can equally be applied to higher dimensions, for both Lorentzian and Riemannian signatures. In particular, we obtain the one-parameter family of axially symmetric metrics that generalize the Schwarzschild solution. Exploiting a correspondence between static solutions of Einstein's equations and Ricci solitons (self-similar solutions of the Ricci flow), this also enables us to construct new steady Ricci solitons.

Keywords PDE Symmetry, Exact Solutions, Einstein Equations in Vacuum, Generation Technique, Static Solutions, Ricci Solitons

1 Introduction

The high nonlinearity of the Einstein equations makes it extremely difficult to solve and draw generic physical conclusions about gravity and besets quantization. However, soon after Einstein found his equations, and thought them unsolvable, the first exact solution describing the spacetime around a spherically symmetric massive object was obtained by Schwarzschild. Since then Einstein's equations have been systematically studied for different matter fields subject to various local symmetries, algebraic conditions and other simplifying assumptions, and today we have many exact solutions in four-dimensions that are well-understood ([31], [20], [27]). These solutions provide concrete means to study the nonlinearities of the gravitational field, shed light on more general non-exact solutions, guide numerical study, and play a pivotal role in every quantum gravity program [8]. Their study has brought the physics and mathematics communities together.

The difficulty of directly integrating Einstein's equations has led to many solution-generation techniques in which one obtains a solution, or a family of solutions, from a "seed" solution, of the same system or a different system. Buchdahl in 1954 showed how to obtain a Ricci-flat solution from another in the presence of a hypersurface-orthogonal Killing vector field [9] (more later). Ehlers in 1957 showed how one can obtain a certain one-parameter family starting from any stationary axisymmetric metric [15]. Later in 1972, Geroch showed that one can use the two commuting Killing vector fields of any stationary axisymmetric metric to obtain an infinite parameter family of solutions ([18], [19]). Following the discovery of Tomimatsu-Sato solutions ([32], [33]), stationary axisymmetric systems were vigorously studied, aided by techniques developed in other partial differential equations systems (various Bäcklund and other transformations, inverse-scattering methods [6] etc.). Many sophisticated general results were obtained for stationary axisymmetric systems including the Einstein-Maxwell system (see [24] for a detailed review). It was however generally appreciated that trans-

M M Akbar
Department of Mathematical Sciences
The University of Texas at Dallas
Richardson, TX 75080, USA
Tel.: +1-972-883-6453
Fax: +1-972-883-6622
E-mail: akbar@utdallas.edu

lating those results to obtain explicit solutions, of the same system or otherwise, often involves solving an associated set of equations and performing a good number of mathematical steps. One cannot simply write down a new solution starting from a seed solution.

The impressive work in four-dimensions, and current efforts in obtaining higher-dimensional gravitational solutions modeled on four-dimensional ones, may give the impression that there is little left to explore analytically for the four-dimensional Einstein equations with physically interesting symmetries and simple matter fields, in particular the vacuum. As we will see below, the non-linearities of the Einstein equations still hold surprises even in the very symmetric cases that have been studied for years.

Below we study the vacuum Einstein equations in the presence of two commuting hypersurface-orthogonal Killing vector fields. In Lorentzian four dimensions these are axially-symmetric static solutions and (Einstein-Rosen) cylindrical gravitational waves and can be obtained from one another by a complexification of appropriate coordinates. In particular, we find a one-parameter Lie group that is a symmetry of the system and maps any solution into a one-parameter extended family. In addition, the action of the group can be represented algebraically. This produces, for example, an axially-symmetric family that contains the spherically symmetric Schwarzschild metric as a special case (and is distinct from other generalizations of the latter found in the past).

The two systems – the systems of vacuum static axisymmetric solutions and cylindrical wave solutions – are well-studied systems in relativity (see, for example, [8] for a review). The first gravitational wave solution found by Einstein and Rosen was cylindrical and the cylindrical wave system is among the very first to be quantized. Despite the fact that cylindrical waves cannot describe radiation from an isolated body, they have been used in understanding energy-loss due to gravity, the asymptotic structure of radiative spacetimes, testing the quasilocal mass-energy of Thorn and in cosmic censorship.

This work was initially inspired by our study of the Ricci flow equations, in particular the correspondences between Ricci solitons (self-similar solutions of Ricci flow), the Einstein-scalar field theory and static vacuum solutions of the Einstein equations [2]. The symmetry of the axisymmetric vacuum system that we present here translates to an analogous symmetry for the corresponding steady Ricci solitons which we will discuss at the end. The results obtained are independent of the metric signature, and thus this work will be of interest to mathematicians interested in warped-product Ricci-flat metrics and warped-product Ricci solitons ([7], [28], [29]).

2 The System(s)

Static Vacuum System: It is well know that the general static axially symmetric vacuum solutions of Einstein's equations can be cast in the Weyl coordinates as

$$ds^2 = -e^{2u(\rho,z)}dt^2 + e^{-2u(\rho,z)}\left[e^{2k(\rho,z)}(d\rho^2+dz^2) + \rho^2 d\phi^2\right] \quad (1)$$

where $u(\rho,z)$ and $k(\rho,z)$ satisfy the following three equations:

$$\frac{\partial^2 u}{\partial\rho^2} + \frac{1}{\rho}\frac{\partial u}{\partial\rho} + \frac{\partial^2 u}{\partial z^2} = 0, \quad (2)$$

$$\frac{\partial k}{\partial\rho} = \rho\left[\left(\frac{\partial u}{\partial\rho}\right)^2 - \left(\frac{\partial u}{\partial z}\right)^2\right], \quad (3)$$

$$\frac{\partial k}{\partial z} = 2\rho\frac{\partial u}{\partial\rho}\frac{\partial u}{\partial z}. \quad (4)$$

A solution is a pair (u,k) solving (2)-(4), the first of which is nothing but the axially symmetric Laplace equation in cylindrical coordinates in (an auxiliary) three-dimensional Euclidean space. For any harmonic function $u(z,\rho)$ solving (2), $k(z,\rho)$ is found by integrating (3) and (4), which retain the non-linearities of the Einstein equations. No distinction is made between solutions in which u and/or k differ by constants since they will give rise to the same metric form by mere redefining of coordinates.

Einstein-Rosen Cylindrical Wave System: It can be obtained from (2)-(4) by $z \to it$ and $t \to iz$ and as such we will not separate it for discussion.

3 Symmetries and Generating New Solutions from Old

If (u_1,k_1) and (u_2,k_2) are two solutions, linearity of (2) implies $u = c_1u_1 + c_2u_2$ is a solution of (2). However, non-linearities of (3) and (4) prevent one from obtaining k in terms of the four quantities $\{u_1,u_2,k_1,k_2\}$ by any standard prescription. One has to go through the line integral of (3)-(4) (or some equivalent set of differential equations) starting with $u = c_1u_1 + c_2u_2$, which is nothing short of the basic problem of solving (2)-(4) for a given u.

Given an arbitrary solution (u_0,k_0) can one generate another solution by some simpler means without solving the full set (2)-(4)? Ernst [16] has given

a method in which one can obtain a new solution $(u_0 + \frac{c}{2}(F+G), k_0 + cF - \frac{c^2}{2}\rho^2)$ from a given solution (u_0, k_0) provided the functions F and G satisfy the following (simpler) set of differential equations

$$\nabla F = 2i\nabla u_0, \tag{5}$$

$$\nabla G = 2i\nabla(-u_0 + \ln\rho), \tag{6}$$

where $\nabla = \partial_\rho + i\partial_z$. This method has successfully been applied to various know solutions (see [31]). Ernst himself applied this to obtain a generalization of the C-metric. Kerns and Wild applied this to obtain a one-parameter generalization of the Schwarzschild metric [26]. In all these one solves (5)-(6) starting with the seed solution's u_0, the difficulty of which depends on the functional form of u_0.

Are there further ways to produce new solutions from old, and, if possible, without solving the field equations or any equivalent set of equations? One possible avenue to address this question is to look for symmetries of the system. It is not difficult to see that the transformation

$$(u_0, k_0) \to (\beta u_0, \beta^2 k_0) \tag{7}$$

leaves the system (2)-(4) invariant; in other words, for any arbitrary solution (u_0, k_0) there is a (non-equivalent) solution $(\beta u_0, \beta^2 k_0)$ for $\beta \in (-\infty, \infty)$. A special case of this is $(-u_0, k_0)$. However, this transformation does not mix dependent and independent variables, which is why it was easy to find it by inspection. Below we present a transformation that mixes variables in a nontrivial way.

Theorem 3.1: For $\alpha \in (-\infty, \infty)$, the transformation

$$(u_0, k_0) \to (u_0 + \alpha\ln\rho, k_0 + 2\alpha u_0 + \alpha^2\ln\rho), \tag{8}$$

leaves the system (2)-(4) invariant. In other words, for every static axially symmetric vacuum solutions of the Einstein equations

$$ds^2 = \pm e^{2u_0(\rho,z)}dt^2 + e^{-2u_0(\rho,z)}\left[e^{2k_0(\rho,z)}(d\rho^2 + dz^2) + \rho^2 d\phi^2\right] \tag{9}$$

there exists a one-parameter generalization:

$$ds^2 = \pm e^{2u_0(\rho,z)}\rho^{2\alpha}dt^2 + e^{-2(1-2\alpha)u_0(\rho,z)}\rho^{2\alpha(\alpha-1)} \times \left[e^{2k_0(\rho,z)}(d\rho^2 + dz^2)\right] + e^{-2u_0(\rho,z)}\rho^{2(1-\alpha)}d\phi^2 \tag{10}$$

Proof: By direct substitution into (2)-(4).

With hindsight we would like to note here that symmetry (8) could have been obtained from (5)-(6) with the following complex identifications: $F = 2iu_0$ and $G = 2i(-u_0 + \ln\rho)$ and $c = -i\alpha$. In other words, with these choices for (F, G, c) the Ernst equations can be satisfied identically for any (u_0, k_0) — thus providing a symmetry for the system (2)-(4). It is interesting that this possibility went unnoticed even though (and probably because) (5)-(6) were used to generalize *particular* solutions.

3.1 Group Structure and Solution Space

To appreciate the special nature of our transformation group, let us recall how one can obtain parameter-dependent new solutions from old ones by means of superposition. In general, the role of the Laplace equation (2) is central in characterizing the solutions of the system since k can be obtained by quadrature from it. Thus the vast majority of the literature speaks in terms of "Newtonian gravitational potentials". Given two solutions u_0 and u_1, $u = u_0 + \alpha u_1$ is a solution of (2) and determines k via (3)-(4). The resulting solution (u, k) from (u_0, k_0) will thus involve the parameter α with $\alpha = 0$ being (u_0, k_0). However, it is easy to see that (u, k) thus obtained is specific to u_0 since the new k would in general depend on the functional form and the derivatives of u_0. One can check this by trying out, for example, $u = u_0 + \alpha z$, z being a rather simple harmonic function solving (2). What makes $u = u_0 + \alpha\ln\rho$ special is that one gets an explicit algebraic prescription for k.

We now note that these transformations indeed form a Lie group with parameter α. Denoting the transformation by T_α, it is easy to check closure, $T_{\alpha_2} \circ T_{\alpha_1} = T_{\alpha_1+\alpha_2}$, since successive transformations with α_1 and α_2 take (u_0, k_0) to $(u_0 + (\alpha_1+\alpha_2)\ln\rho, k + 2(\alpha_1+\alpha_2)u_0 + (\alpha_1+\alpha_2)^2\ln\rho)$. The seed metric is the identity with $\alpha = 0$ (in fact any metric within the family can be taken as identity with $\alpha = 0$) and existence of inverse is immediate with $[T_\alpha]^{-1} = T_{-\alpha}$.

Contrasting with the closely-related vacuum stationary system – in which there exists a discrete map producing a new solution from an old one (c.f. Eq (34.37) in [31]) – the existence of the one-parameter Lie group in our case means the whole solution space of axisymmetric static vacuum Einstein system can be divided into equivalent classes which do not intersect under the action of the group. One naturally wonders if there are other explicit transformations that possibly connect these families. This requires a much detailed symmetry analysis of the differential equation system (2)-(4) and is work under progress.

Remark 3.1 Note that, in the Riemannian signature,

the transformation

$$\alpha \to 1-\alpha \tag{11}$$

$$u \to -u \tag{12}$$

only interchanges the role of ϕ and t in (10). These two geometries would therefore be indistinguishable locally.

3.2 Warped Form and Higher Dimensions

Despite the economical way Weyl coordinates express axially symmetric solutions, it does not provide the most natural form for many physically and mathematically important solutions with two commuting hypersurface-orthogonal Killing vector fields. For example, Schwarzschild solutions have a complicated expression when written in the Weyl form ([31]). The simplest, most intuitive, form of a metric with two commuting hypersurface-orthogonal commuting Killing vector fields is its warped-product form with two line fibres [23]

$$ds^2 = g_{11}dx^2 + g_{22}dy^2 + g_{ij}dz^i dz^j, \tag{13}$$

with $i,j = 3,4,..,n-1$, and in which the metric components are only functions of z^i. The theorem above translates as follows for $(n+1)$-dimensions:

Theorem 3.2: For every Ricci-flat metric of the form

$$ds^2 = g_{11}dx^2 + g_{22}dy^2 + g_{ij}dz^i dz^j, \tag{14}$$

where all metric components are functions of z^i,

$$\begin{aligned} ds^2 = {} & (g_{22})^{\gamma}(g_{11})^{\gamma} g_{11}dx^2 + (g_{22})^{-\gamma}(g_{11})^{-\gamma} g_{22}dy^2 \\ & + (g_{22})^{\gamma(\gamma+1)}(g_{11})^{\gamma(\gamma-1)} g_{ij}dz^i dz^j, \end{aligned} \tag{15}$$

is Ricci-flat for $\gamma \in (-\infty, \infty)$.

The proof again is by direct computation of the Ricci tensor. Note that this allows the metric components to assume arbitrary signatures. The slightly elaborate form of the metric components in (15) is deliberate, to make the group structure manifest. If g_{11} and g_{22} have the same sign, the metrics corresponding to γ and $-\gamma$ are locally identical with the role of x and y swapped (cf. (11)-(12)).

3.3 Examples: Solution Extending Schwarzschild and More

We now apply (8) to the Schwarzschild solution and obtain, for $\gamma \in (-\infty, \infty)$,

$$\begin{aligned} ds^2 = {} & -r^{2-2\gamma}(\sin\theta)^{2-2\gamma}\left(1-\frac{2m}{r}\right)^{2-\gamma} dt^2 \\ & + r^{2\gamma^2-2\gamma}(\sin\theta)^{2\gamma^2-2\gamma}\left(1-\frac{2m}{r}\right)^{\gamma^2-3\gamma+1} dr^2 \\ & + r^{2\gamma^2-2\gamma+2}(\sin\theta)^{2\gamma^2-2\gamma}\left(1-\frac{2m}{r}\right)^{\gamma^2-3\gamma+2} d\theta^2 \\ & + r^{2\gamma}(\sin\theta)^{2\gamma}\left(1-\frac{2m}{r}\right)^{\gamma-1} d\phi^2. \end{aligned} \tag{16}$$

This to our knowledge was not found before and is clearly distinct from the generalization of Schwarzschild found by Kerns and Wild [26] using Ernst equations (5)-(6). Once again one can check that (16) is indeed Ricci-flat by direct computation. Note that for $\gamma = 1$ the spacetime symmetry group expands and one gets the codimension-two spherically symmetric Schwarzschild solution. There is obviously a number of ways to write (16), including that the role of t and ϕ can be interchanged with simultaneous signature change etc. With $\gamma \to -\gamma + 1$ (16) can be written such that $\gamma = 0$ is the Schwarzschild metric:

$$\begin{aligned} ds^2 = {} & -r^{2\gamma}(\sin\theta)^{2\gamma}\left(1-\frac{2m}{r}\right)^{\gamma+1} dt^2 \\ & + r^{2\gamma^2-2\gamma}(\sin\theta)^{2\gamma^2-2\gamma}\left(1-\frac{2m}{r}\right)^{\gamma^2+\gamma-1} dr^2 \\ & + r^{2\gamma^2-2\gamma+2}(\sin\theta)^{2\gamma^2-2\gamma}\left(1-\frac{2m}{r}\right)^{\gamma^2+\gamma} d\theta^2 \\ & + r^{2-2\gamma}(\sin\theta)^{2-2\gamma}\left(1-\frac{2m}{r}\right)^{-\gamma} d\phi^2. \end{aligned} \tag{17}$$

Applying this transformation to the flat metric [3]

$$ds^2 = -dt^2 + dx^2 + dy^2 + (ax+by)^2 dz^2, \tag{18}$$

one obtains the following Ricci-flat metric

$$\begin{aligned} ds^2 = {} & -(ax+by)^{2-\gamma}dt^2 + (ax+by)^{-\gamma+\frac{1}{2}\gamma^2}(dx^2+dy^2) \\ & + (ax+by)^{\gamma}dz^2. \end{aligned} \tag{19}$$

Although different from the forms found by Buchdahl (next section), this is also a member of the Kasner class, as one can check.

3.4 Historical Link

As was mentioned in the introduction, it was Hans Buchdahl who pioneered obtaining new solutions from old "without solving the field equations". In 1950's ([10], [11]), just before Ehlers [15], he showed that if a Ricci-flat metric (solution to the vacuum Einstein equation) is "static" in one of its coordinates one can obtain another distinct Ricci-flat metric from it by what he called "reciprocal transformation" that takes the d-dimensional metric

$$ds^2 = g_{ik}(x^j)dx^i dx^k + g_{aa}(x^j)(dx^a)^2 \tag{20}$$

to the following d-dimensional metric

$$ds^2 = (g_{aa})^{2/(d-3)}(x^j)g_{ik}dx^i dx^k + (g_{aa})^{-1}(x^j)(dx^a)^2. \tag{21}$$

Either metric, as Buchdahl termed, is "x^a-static", and it is easy to verify that if (20) is Ricci-flat so is (21), by direct computation. By applying the transformation on (21) one gets back the original metric (20).

In his very first paper [10], Buchdahl applied this transformation on

$$ds^2 = -(dx^2 + dy^2 + dz^2) + x^2 dt^2, \tag{22}$$

and obtained the following Ricci-flat solution, earlier discovered by Joseph [25]

$$ds^2 = -x^4(dx^2 + dy^2 + dz^2) + x^{-2}dt^2. \tag{23}$$

Applying the transformation on the t-static Schwarzschild metric,

$$ds^2 = -\left(1 - \frac{2m}{r}\right) dt^2 + dr^2 \left(1 - \frac{2m}{r}\right)^{-1} + r^2 \left(d\theta^2 + \sin^2\theta d\phi^2\right), \tag{24}$$

Buchdahl obtained

$$ds^2 = -dt^2 \left(1 - \frac{2m}{r}\right)^{-1} + \left(1 - \frac{2m}{r}\right) dr^2 + r^2 \tag{25}$$

$$\times \left(d\theta^2 + \sin^2\theta d\phi^2\right), \tag{26}$$

which, upon the coordinate transformation $R = r - 2m$, is the Schwarzschild metric with mass $-m$. Buchdahl expanded on the implication of this transformation on gravitational energy and showed that this is a special case of how the component of a certain tensorial quantity, related to the Hamiltonian derivative of the Gaussian curvature, changes sign [10]. Buchdahl noted that more general solutions "can be formed by means of a succession of reciprocal transformations, starting with the line element of a flat space". However he did not apply this observation until much later [12], in 1978, when he obtained from the all-positive version of (22), i.e. from the flat space metric

$$ds^2 = (dx^2 + dy^2 + dz^2) + x^2 dt^2, \tag{27}$$

the following Riemannian solution

$$ds^2 = x^{2n(n-1)}(dx^2 + dy^2) + x^{2n}dz^2 + x^{2(n-1)}dt^2 \tag{28}$$

at the $(n-1)$th step of alternately taking the static coordinate x^a to be t and z for the transformation. Although n is an integer, it is easy to see that, as Buchdahl noted, (28) is Ricci-flat for all real n, and also that it can be cast in the Kasner form:

$$ds^2 = dx^2 + x^{2a}dy^2 + x^{2b}dz^2 + x^{2c}dt^2, \tag{29}$$

with

$$a = \frac{n(n-1)}{n^2 - n + 1}, \quad b = \frac{n}{n^2 - n + 1}, \quad c = -\frac{n-1}{n^2 - n + 1},$$

satisfying the algebraic relations $a + b + c = 0$ and $a^2 + b^2 + c^2 = 0$.

As a second set of nontrivial Ricci-flat solutions, Buchdahl obtained from another form of the flat metric

$$ds^2 = dx^2 + dy^2 + y^2 z^2 + x^2 dt^2 \tag{30}$$

the following one-parameter family

$$ds^2 = x^{2n(n-1)}y^{2(n-1)(n-2)}(dx^2 + dy^2) + x^{2n}y^{2(n-1)}dz^2 + x^{-2(n-1)}y^{-2(n-2)}dt^2 \tag{31}$$

which too was known from the work of Harris and Zund [22]. In summary, no new solutions were obtained by this generation technique.

However, in all these what was altogether left out of Buchdahl's consideration is the fact that the Schwarzschild metric has another hypersurface-orthogonal Killing vector field, $\frac{\partial}{\partial\phi}$, which could be used to obtain a different Ricci-flat metric from (24)

$$ds^2 = -r^4 \sin^4\theta \left(1 - \frac{2m}{r}\right) dt^2 + r^4 \sin^4\theta \frac{dr^2}{1 - \frac{2m}{r}} + r^6 \sin^4\theta d\theta^2 + \frac{1}{r^2 \sin^2\theta} d\phi^2. \tag{32}$$

Unlike its t-counterpart (26), (32) is not related to (24) via a coordinate transformation. In addition, alternating between t and ϕ, as he did to arrive at the known solutions (28) and (31), it is conceivable that he could have arrived at our generalized Schwarzschild metric (16) more than fifty years ago and this would have provided him with a genuinely new family of solutions from his transformation.

In addition, and perhaps more importantly, Buchdahl did not look for an explanation why for two static coordinates the discrete exponents produced by alternate transformations work fine for continuous values. Obviously, this question and its answer were hidden in the Lie point symmetry of the vacuum axially symmetric static system (2)-(4) that we addressed here. When written as warped-product with two line fibres — the form used by Buchdahl in all his examples – the parameter-dependent components of the generalized metric (15) appear in identical functional forms for four and higher dimensions, and this can be used to generalize any higher dimensional solutions with two commuting hypersurface-orthogonal Killing vector fields readily.

4 Ricci Flow and Ricci Solitons

Introduced by Richard Hamilton [21] in 1982, Ricci flow has been used to study the interplay between geometry and topology of Riemannian manifolds and has successfully been used to prove the Poincaré Conjecture and Thurston's Geometrization Conjecture (in three dimensions). It is an intrinsic geometric flow in which the

metric $g_{\mu\nu}$ on a manifold M^{n+1} evolves by its Ricci curvature tensor ([13], [14])

$$\frac{\partial g_{\mu\nu}}{\partial \eta} = -2R_{\mu\nu} \tag{33}$$

along the flow parameter η, often referred to as "time". The simplest solutions of the Ricci flow are its fixed points

$$\frac{\partial g_{\mu\nu}}{\partial \eta} = 0, \tag{34}$$

which are the Ricci-flat metrics, $R_{\mu\nu} = 0$. The next simplest are the self-similar solutions in which the metric evolves only by rescalings and diffemorphisms

$$g_{\mu\nu}(\eta) = \sigma(\eta)\psi^*_\eta(g_{\mu\nu}(0)). \tag{35}$$

It is easy to show that (35) implies, and is implied by, the following equation for the initial metric (henceforth $g_{\mu\nu}$)

$$R_{\mu\nu} - \frac{1}{2}\mathcal{L}_X g_{\mu\nu} = \kappa g_{\mu\nu} \tag{36}$$

with $\sigma(\eta) = 1 + 2\kappa\eta$ the scaling and $Y(\eta) = \frac{1}{\sigma(\eta)}X(x)$ the vector generating ψ_η diffeormorphisms.

A Ricci soliton is a manifold-with-metric and a vector field $(M^{n+1}, g_{\mu\nu}, X)$ solving (36). The soliton is called "steady" if $\kappa = 0$, "expander" if $\kappa < 0$, "shrinker" if $\kappa > 0$. A local Ricci soliton is one that solves (36) on an open region that might not cover a complete manifold with the soliton metric. A soliton is called gradient if $X = \nabla f$, where f is a scalar function on M^{n+1}, and thus (36) becomes

$$R_{\mu\nu} - \nabla_\mu\nabla_\nu f = \kappa g_{\mu\nu}. \tag{37}$$

For $X = 0$, or Killing, Ricci solitons (36) are just Einstein metrics. The simplest nontrivial Ricci solition is perhaps the Cigar soliton, which is a steady soliton on $\mathbb{R}^2$:

$$ds^2 = \frac{dx^2 + dy^2}{1 + x^2 + y^2}, \tag{38}$$

with $X = 2\left(x\frac{\partial}{\partial x} + y\frac{\partial}{\partial y}\right)$. It is gradient with $f = x^2 + y^2$. All nontrivial steady gradient solitons are non-compact.

4.1 Ricci Solitons and Static Metrics

It is well-known that ([4], [5], [31]), if

$$ds^2 = \pm e^{2u}dt^2 + e^{-\frac{2u}{n-2}}g_{ij}dx^i dx^j \tag{39}$$

is Ricci-flat in $(n+1)$-dimensions in which $\frac{\partial}{\partial t}$ is a hypersurface-orthogonal Killing vector field – i.e. (39) is static in t – then (u, g_{ij}) solves the Einstein scalar field equations in n-dimensions

$$R_{ij} - \frac{n-1}{n-2}\nabla_i u\nabla_j u = 0\ , \tag{40}$$

$$\Delta u = 0\ . \tag{41}$$

A precise relationship between Ricci solitions and Einstein-scalar field theory with a possible cosmological constant was given in [2] in which every solution of the latter in n-dimensions corresponds to a Ricci soliton in $(n+1)$-dimensions. In the case of zero cosmological constant this means every $(n+1)$-dimensional static vacuum solution (39) can be put in one-to-one correspondence with the following Ricci soliton metric in $(n+1)$-dimensions

$$ds^2 = e^{2\sqrt{\frac{n-1}{n-2}}u}dt^2 + g_{ij}dx^i dx^j \tag{42}$$

with $X := -2\sqrt{\frac{n-1}{n-2}}g^{ij}\nabla_i u\frac{\partial}{\partial x^j}$. Adapting to axisymmetric vacuum solutions in Weyl coordinates we have for every vacuum solution

$$ds^2 = \pm e^{2u(\rho,z)}dt^2 + e^{-2u(\rho,z)}\left[e^{2k(\rho,z)}(d\rho^2 + dz^2) + \rho^2 d\phi^2\right] \tag{43}$$

the following local Ricci soliton

$$ds^2 = \pm e^{2\sqrt{2}u}dt^2 + \left[e^{2k(\rho,z)}(d\rho^2 + dz^2) + \rho^2 d\phi^2\right] \tag{44}$$

with $X = -2\sqrt{2}e^{-2k(\rho,z)}\left(\nabla_\rho u\frac{\partial}{\partial\rho} + \nabla_z u\frac{\partial}{\partial z}\right)$.

Using symmetry (8) of (2)-(4) one thus obtains the following one-parameter family of local Ricci solitons

$$ds^2 = \pm e^{2\sqrt{2}u}\rho^{2\sqrt{2}\alpha}dt^2 + \left[e^{2k(\rho,z)+4\alpha u(\rho,z)}\rho^{2\alpha^2}\ (d\rho^2 + dz^2) + \rho^2 d\phi^2\right] \tag{45}$$

with

$$X = -2\sqrt{2}e^{-2k(\rho,z)+2\alpha u(\rho,z)+\alpha^2\ln\rho} \times \left(\frac{\alpha}{\rho}\frac{\partial}{\partial\rho} + \nabla_\rho u\frac{\partial}{\partial\rho} + \nabla_z u\frac{\partial}{\partial z}\right)$$

for every static axisymmetric vacuum solution (u, k).

5 Conclusion

The primary motivation behind most solution generation techniques has been to advance exact solutions, often starting from a particular solution. We studied (2)-(4) from a symmetry perspective and found a nontrivial exact Lie point symmetry. Being a symmetry of the whole system this can be applied to any solution including non-exact solutions of the system, and thus can guide both analytical and numerical studies. The symmetry applies to arbitrary dimensional vacuum systems with two commuting hypersurface-orthogonal Killing vector fields and can be written in a universal form (15). This form allowed us to generalize the Schwarzschild metric more directly than is possible in the Weyl coordinates. An additional motivation for studying this system comes from outside relativity, following the recent

correspondence between Ricci flow and static metrics [2]. The symmetry in the static system thus generalizes the corresponding Ricci solitons simultaneously.

One would naturally like to understand the properties of the solutions generated by the one-parameter symmetry (like our generalized Schwarzschild above), and find whether they contain new spacetimes or not. However, the stronger message that we believe comes from the existence of explicit symmetries (8), and (7), is that one should continue looking for more Lie transformations, and other possible forms of symmetries of the static system, in order to obtain a clearer picture of the geometry of the solution space under their actions. This requires a detailed and systematic study that falls within the very developed field of symmetry analysis of non-linear partial differential equations [30]. The related stationary system with two commuting vector fields, as we mentioned earlier, has been one of the most rigorously studied systems in relativity and may suggest methods, indicate symmetries, and help us understand the geometry of the solution space in general terms for the static case. Even though the static system is simpler, the connection is far less obvious, and it may not be possible to realize many symmetry transformations explicitly like (8) and one may find the role of different coordinate systems very crucial in the investigation. This is work under progress.

Acknowledgements I would like to thank everyone involved in the organization of the *International Conference on Relativistic Astrophysics*. In particular I would like to thank the Mathematics Department of the University of the Punjab and everyone at The University Club for providing an intellectually stimulating atmosphere and unstinting hospitality. I thank Malcolm MacCallum and Behshid Kasmaie for valuable discussions.

References

1. M. M. Akbar and G. W. Gibbons, "Ricci-flat Metrics with $U(1)$ Action and the Dirichlet Boundary-value Problem in Riemannian Quantum Gravity and Isoperimetric Inequalities," Class. Quant. Grav. **20**, 1787 (2003)
2. M. M. Akbar and E. Woolgar, "Ricci Solitons and Einstein-Scalar Field Theory," Class. Quant. Grav. **26**, 055015 (2009) [arXiv:0808.3126 [gr-qc]].
3. M. M. Akbar, "Pseudo-Riemannian Ricci-flat and Flat Warped Geometries and New Coordinates for the Minkowski Metric" arXiv:1211.1466 [gr-qc]
4. M. T. Anderson, "Scalar Curvature, Metric Degenerations and the Static Vacuum Einstein Equations on 3-manifolds, I", Geom Funct Anal 9 (1999) 855.
5. A. Ashtekar, J.Bičák and B. G. Schmidt, "Asymptotic Structure of Symmetry Reduced General Relativity," Phys. Rev. D **55**, 669 (1997) [gr-qc/9608042].
6. V. Belinski and E. Verdaguer, "Gravitational Solitons," Cambridge, UK: Univ. Pr. (2001) 258 p
7. A. Besse (1986) *Einstein manifolds* (Springer, Berlin)
8. J. Bičák, "The Role of Exact Solutions of Einsteins Equations in the Developments of General Relativity and Astrophysics: Selected Themes, in *Einsteins field equations and their physical implications*, Springer Verlag, Heidelberg, 2000, vol. 540 of *Lecture Notes in Physics.*
9. H. A. Buchdahl, "Reciprocal Static Solutions of the Eqauations $G_{\mu\nu}$," Quart. J. Math. Oxford Ser 2 **5** (1954), 116-19.
10. H. A. Buchdahl, "Reciprocal Static Solutions of the Equations of the Gravitational Field," Austral. J. Phys. **9** (1956), 1318.
11. H. A. Buchdahl, "Reciprocal Static Metrics and Scalar Fields in the General Theory of Relativity," Phys. Rev. **115** (1959) 1325.
12. H. A. Buchdahl, "On Solutions of Einstein's Equations with Scalar Zero-Mass Source," Gen. Rel. Grav. **9**, 59 (1978).
13. B. Chow and D. Knopf, *The Ricci Flow: An Introduction*, Mathematical Surveys and Monographs vol 110 (AMS, Providence, 2004).
14. B. Chow et al, *The Ricci Flow: Techniques and Applications: Geometric Aspects*, Mathematical Surveys and Monographs vol 135 (AMS, Providence, 2007).
15. J. Ehlers, Konstruktionen und Charakterisierungen von Lösungen der Einsteinschen Gravitationsfeldgleichungen, Dissertation, Hamburg, 1957.
16. V. Ernst, "Generalized C-metric," J. Math. Phys. **19**, 489 (1978).
17. "Physical Properties of Some Empty Space-times," Proceedings of the Cambridge Philosophical Society, vol. 53, issue 04, p. 836.
18. R. P. Geroch, "A Method for Generating Solutions of Einstein's Equations," J. Math. Phys. **12**, 918 (1971).
19. R. P. Geroch, "A Method for generating new solutions of Einstein's equation. 2," J. Math. Phys. **13**, 394 (1972).
20. J. B. Griffiths and J. Podolsky, "Exact Space-Times in Einstein's General Relativity,"
21. R. S. Hamilton, "Three-manifolds with Positive Ricci Curvature," J. Differential Geom. **17** (1982), no. 2, 255306.
22. R. A. Harris, J. D. Zund, "A Family of Algebraically General Exact Solutions of Einstein's Source-free Field Equations", Tensor (N.S.) **29** (1975), no. 1, 103106
23. C. He, P. Petersen, W. Wylie "On the classification of warped product Einstein metrics," *Comm. Anal. Geom.* **20** (2012), *no. 2*, 271311.
24. C. Hoenselaers and W. Dietz, "Solutions Of Einstein's Equations: Techniques And Results. Proceedings, International Seminar, Retzbach, F.r. Germany, November 14-18, 1983," Berlin, Germany: Springer (1984) 439 P. (Lecture Notes In Physics, 205)
25. "Physical Properties of Some Empty Space-times," Proceedings of the Cambridge Philosophical Society, vol. 53, issue 04, p. 836.
26. R. M. Kerns, W. J. Wild, "Black Hole in a Gravitational Field," Gen. Rel. Grav. **14**, 1 (1982).
27. M. A. H. MacCallum, "Finding and Using Exact Solutions of the Einstein Equations," AIP Conf. Proc. **841**, 129 (2006) [gr-qc/0601102].
28. B. O'Neill (1983). *Semi-Riemannian Geometry with Applications to Relativity* (Academic Press, New York)
29. P Petersen, *Riemannian geometry* (2^{nd} edition, Springer, 2006) p 159.
30. H. Stephani, "Differential Equations: Their Solutions Using Symmetries," Cambridge, UK: Univ. Pr. (1989) 260 p
31. H. Stephani, D. Kramer, M. A. H. MacCallum, C. Hoenselaers and E. Herlt (2003) *Exact Solutions of Einstein's Field Equations* (Cambridge University Press, UK).

32. A. Tomimatsu and H. Sato, "New Exact Solution for the Gravitational Field of a Spinning Mass," Phys. Rev. Lett. **29**, 1344 (1972).
33. A. Tomimatsu and H. Sato, "Multi-Soliton Solutions of the Einstein Equation and the Tomimatsu-Sato Metric," Prog. Theor. Phys. Suppl. **70**, 215 (1981).

Proc. Int. Conf. Relativ. Astrophys.
Pages 33-38, (2015)

Kinetic Vortices in Non-Maxwellian Plasmas

Kashif Arshad[a,1,2,3]

[1]Pakistan Institute of Engineering and Applied Sciences, P. O. Box Nilore, Islamabad 45650, Pakistan
[2]National Center for Plasma Physics, Shadra Valley Road, Quaid-i-Azam University Islamabad 44000, Pakistan
[3]Department of Physics, Theoretical Physics Group, University of Wah, The Mall, Wah Cantt 47040, Pakistan

Abstract The Kinetic Theory of non-Maxwellian Langmuir modes is developed in the presence of Orbital Angular Momentum. The Laguerre-Gaussian (LG) mode function is applied for the modeling of the non-Maxwellian twisted dielectric function to study the Landau wave-particle interaction in electron plasma system. In the last sention, some numercial results are also presented using appropriate parameters of electron plasma waves.

1 Introduction

The electromagnetic wave consists of polarization and orbital angular mo- mentum (OAM) oriented constitutents of the angular momentum (Berestet- skii et al., 1982). Allen et al.,1992 employed an orthonormal set of Laguerre- Gaussian (LG) functions to study photon orbital angular momentum (OAM) states of laser beams. Some laboratory experiments are setup to develop laser beams, having orbital angular momentum (for example Padgett et al., 1996; Harris 1996; Leach 2002). A few years ago, the eect of orbital angular momen- tum is transferred from quanum optics to various regimes such as radio wave (Thide et al., 2007, Harwit 2004), neutrino physics (Mendonca, 2008), inverse Farady eect (S. Ali, 2010) and plasmas (Mendonca et al. 2009). Recently, the twisted kinetic modes (Mendonca 2012 and Khan 2014) are predicted for the thermally distributed Maxwellian plasmas. But Arshad et al. 2014; 2011; 2010 pointed out the non-thermal behavior of some laboratory and most of the space plasmas. The suitable distribution function to model such plasmas is non-Maxwellian distribution.

[a]e-mail: kashif.arshad.butt@gmail.com

2 Theoretical Model

In this section, the electrostatic kinetic theory is developed for an unmag- netized non-Maxwellian (Kappa distributed) plasmas in the OAM state. The linearized Vlasov equation for the unmagnetized electrostatic plasma can be written as

$$(\partial_t + \mathbf{v}\cdot\partial_r + q_\alpha \mathbf{E}\cdot\partial_p) f_\alpha = 0. \quad (1)$$

This equation is coupled with the Poisson equation $\partial_r^2\phi = 4\pi\Sigma q_\alpha n_\alpha$ where $n_\alpha = \int f_\alpha d^3\mathbf{v}$. Consider the propagation of ion-accoustic wave with slowly varying amplitude propagating along z-axis and evolving as $exp(ikz)$, so that $\partial_r^2\phi = (\partial^2 - k^2 + 2ik\partial_z)\phi$ with transerverse Laplacian operator $\partial_\perp^2 = (1/r)\partial/\partial r(r\partial/\partial r)+(1/r^2)\partial^2/\partial\theta^2$ in cylinderical coordinates. We can assume that the field varies only gradually along the z-axis such that $\partial^2\phi/\partial z^2 << 2k\partial\phi/\partial z$. Under these conditions the waves that are associated with the potential and are having a finite orbital angular momentum satisfy the paraxial equation $(\partial_\perp^2 + 2ik\partial_z)\phi = 0$. Now the solution of Poisson equation $-k^2\phi = 4\pi q_\alpha \int f_\alpha d^3\mathbf{v}$ can be found by the superposition of Laguerre-Gaussian (LG) functions in clyndrical coordinates $\phi(\mathbf{r},t) = \sum \widetilde{\phi}_{pl} F_{pl}(r,t) e^{i\theta}$ e^{ikz-iw}. Here $\widetilde{\phi}_{pl}$ is the mode amplitude, p and l are the radial and angular mode numbers and θ denotes the azimuthal angle. The Laguerre-Gaussian function is defined as $F_{pl}(r,z) = C_{pl} X^{|l|} L_p^{|l|}(X)$ exp(-X/2). Here $X = r^2/w^2(z)$($w(z)$ is the beam waist), C_{pl} $= \sqrt{(l+p!/4\pi p!}$ is the normalization constant and $L_p^{|l|}(X) = \exp(X) d^p/dX^p[X^{l+p}\exp(-X)]$ is the associated Laguerre polynomial. Now we can write the electric field in terms of effective wave number k_{eff}; *i.e.*, $\mathbf{E} = -ik_{eff}\phi$, where $k_{eff} = -\frac{i}{F_{pl}}\partial\mathbf{r}F_{pl}\mathbf{e}_r + \frac{1}{r}\mathbf{e}\theta + (k - \frac{1}{F_{pl}}\partial\mathbf{z}$ $F_{pl})\mathbf{e}_z$. Using Laguerre-Gaussian form of perturbed distribution function $f_\alpha = \sum_{pl} \widetilde{f}_{\alpha pl} F_{pl}(r,t) e^{i\theta} e^{ikz-iw}$ in

the Vlasov equation and inserting the resultant expression in the Poisson equation, we get $1+\chi(\omega)=0$, such that

$$\chi(\omega)=\sum_{e,i}\frac{w_{p\alpha}^2}{k^2}\int\frac{k\partial \mathrm{v}_z f_{\alpha 0}+lq_\theta\partial \mathrm{v}_\theta f_{\alpha 0}}{(\omega-kv_z)-lq\theta v\theta} \tag{2}$$

The three dimensional non-Maxwellian (Kappa) distribution is given by the expression (Ki et al., 2011)

$$f_k=\frac{n_{0\alpha}}{\pi^{3/2}\theta_{\perp\alpha}^2\theta_{||\alpha}}\ \frac{\Gamma(\kappa_\alpha+1)}{\kappa_\alpha^{3/2}\Gamma(\kappa_\alpha-1/2)}\left[1+\frac{v_{||}^2}{\kappa_\alpha\theta_{||\alpha}^2}+\frac{v_\perp^2}{\kappa_\alpha\theta_{\perp\alpha}^2}\right]^{-\kappa-1} \tag{3}$$

where α represents the species under consideration and we have two spices $\alpha=e$ for electrons and $\alpha=i$ ions. $n_{0\alpha}$ is the unperturbed number density of the plasma species, k is the spectral index and $\theta_{(||,\perp)\alpha}=\sqrt{(2\kappa-3)/\kappa v T_{(||,\perp)\alpha}}$ is the Lorentzian thermal velocity such that $vT_{(||,\perp)}\alpha=\sqrt{T_{(||,\perp)\alpha/m_\alpha}}$ is the respectively, with $\kappa>3/2$.

3 Twisted Langmuir Modes

In this section, the twisted Kinetic Theory for the non-Maxwellian high frequency electron plasma is described for the calculation of the dispersion relation and the study of Landau wave-particle interaction. The background number density of the electrons is n_{0e}.It is obvious that due to their very small mass, electrons will behave as Boltzmanen (inertialess) particles while the dynamics of the ions are important due to their large inertia. The dispersion function of the electrons can be expanded under the condition ($\theta_{\|e}\ll v_{ph}=\omega/k$), to get the following dielectric function;

$$\epsilon(k,\omega)=1+\chi_e, \tag{4}$$

such that

$$\chi_e=-\frac{\omega_{pe}^2}{\omega^2}\left[1+\frac{k^2\theta_{\|e}^2}{\omega^2}\ \frac{3k}{(2\kappa-3)}\right]-\frac{l^2q_\theta^2\omega_{pe}^2}{k^2\omega^2}$$

$$\left[1+\frac{l^2q_\theta^2\theta_{\|e}^2}{k^2\omega^2}\ \frac{3\kappa}{(2\kappa-3)}\right]+2i\sqrt{\pi}\frac{\omega\Gamma(\kappa+1)}{\kappa^{3/2}\Gamma(k-1/2)}\ \frac{w_{pe}^2}{l^3\theta_{\|e}^3}$$

$$\left[\left(1+\frac{\omega^2}{\kappa k^2\theta_{\|e}^2}\right)^{-k-1}+\frac{\mu}{k}\left(1+\frac{\omega^2}{\kappa l^2q_\theta^2\theta_{\|e}^2}\right)^{-k-1}\right]. \tag{5}$$

where $\mu=k/lq\theta$. The dielectric function $\epsilon(k,\omega)$ contains real and imaginary parts such that $\epsilon(k,\omega)=Re[\epsilon(k,\omega)]+\mathrm{lm}[\epsilon(k,\omega)]$. Here $\omega=\omega_r+i\gamma$ is the temporal angular frequency of the wave. The expression for ω_r can be obtained by equating the real part of the dielectric function $\epsilon(k,\omega)$ to zero: the yields

$$\omega_r^2=\omega_{pe}^2\frac{(1+\mu^2)}{\mu^2}+\frac{3\kappa k^{2\theta 2}\ \|_e}{(2k-3)}\ \frac{(1+\mu^4)}{\mu^2(1+\mu^2)}. \tag{6}$$

The Landau damping rate γ for the given kappa distributed OAM electron-ion plasma can be computed from the relation ($\gamma=-\mathrm{lm}(\epsilon)/(\partial\mathrm{Re}(\epsilon)/\partial\omega)$). Using the respective values of lm (ϵ) in the expression of γ, we get;

$$\gamma=-\frac{\sqrt{\pi}\omega_r^4\mu^2}{k^3\theta_{\|e}^3}(1+\mu^2)[\gamma_z+\gamma_\theta],$$

where γ_z and γ_θ are presenting the contributions of conventional and twisted damping factor with expressions;

$$\gamma_z=\frac{\Gamma(\kappa+1)}{\kappa^{3/2}\Gamma(\kappa-1/2)}\left(1+\frac{\omega^2}{\kappa k^2\theta_{\|e}^2}\right)^{-\kappa-1} \tag{7}$$

and

$$\gamma_z=\frac{\Gamma(\kappa+1)\mu}{\kappa^{3/2}\Gamma(\kappa-1/2)}\left(1+\frac{\omega^2}{\kappa l^2q_\theta^2\theta_{\|e}^2}\right)^{-\kappa-1} \tag{8}$$

4 Results and Discussion:

In this section, some numerical results of the kappa distributed Langmuir waves with orbital angular momentum, are presented by considering some typical parameters of the electron plasma [12]. In particular, the dimensionless damping rate (γ/ω_{pe}) of the twisted Langmuir waves is analysed against appropriate parameters for the physical interpretation of a given mode.

Fig.01 provides the analysis of wave-particle interaction of non-Maxwellian twisted Langmuir modes in terms of normalized damping rates γ/ω_{pe} . Particularly, we have plotted the normalized damping rates γ/ω_{pe} aganist the normalized wave number $k\lambda D_e$ for different values of Lorentzian spectral index $\kappa=3$, 5, 7(kappa). It can be seen very clearly that the Landau damping pro.les have higher magnitude at small value of spectral index as compare to larger values. This is because of existence of more superthermal particles in the energy spectrum of distribution function. When more particles take energy from the wave, the mode damping increases. So wave damping is larger at $\kappa=3$ in comparison to $\kappa=7$.

The next figure **Fig.02,** shows the normalized damping rates γ/ω_{pe} against the ratio of conventional and twisted wave numbers $\mu=k/lq_\theta$ for different values of Lorentzian spectral index $\kappa=3$, 5, 7(kappa). It is evident from the damping profiles that the wave-particle

interaction is increased corresponding to Lorentzian plasmas (small Lorentzian spectral index) and decreased for the Maxwellian plasmas (large Lorentzian spectral index). The more interaction causes more particles taking energy from wave and vice versa.

The second last figure **Fig.03** describes the three dimensional surface plot of normalized damping rates γ/ω_{pe} against normalized wave number $\kappa\lambda D_e$ and ratio of conventional and twisted wave numbers $\mu = k/lq_\theta$. The steepness of damping rate γ/ω_{pe} surface plot is observed to increase with increasing value normalized wave number $k\lambda D_e$. The more steepness has relevance with more damping on the other hand the increasing value of ratio of conventional and twisted wave numbers $\mu = k/lq_\theta$ is connected to decreasing damping rate.

Finally, **Fig.04** provides the contour damping rates γ/ω_{pe} in terms of ratio of conventional and twisted wave numbers $\mu = k/lq_\theta$ and normalized wave number $k\lambda D_e$. The damping rate γ/ω_{pe} is higher for the smaller μ and larger $k\lambda D_e$.

5 Conclusion:

To conclude, the new kappa distributed dielectric function is derived in the presence of the orbital angular momentum (OAM) state for a non-maxwellian electron plasmas. Twisted kinetic Langmuir modes (kinetic vortices) have been studied viz Landau wave-particle interaction (damping rate). Our findings are general and may be applicable to other space and laboratory plasma systems.

References

1. Ali, S., Davies, J. R., Mendonca, J. T.: Phys. Rev. Lett. 105, 035001(2010).
2. Allen, L., Beijersbergen, M. W., Spreeuw, R. J. C., Woerdman, J. P.: Phys. Rev. A 45, 8185 (1992).
3. Arshad K., Ehsan, Z., Khan S. A., Mahmood, S.: Phys. Plasmas 21, 023704 (2014).
4. Arshad K., Mahmood, S., Mirza, A. M.: Phys. Plasmas 18, 092115 (2011).
5. Arshad K., Mahmood, S. : Phys. Plasmas 17, 124501 (2010).
6. Harris, M., Hill, C. A., Tapster, P. R., Vaughan, J. M.: Phys. Rev. A 49, 3119 (1996).
7. Harwit, M.: Astrophys. J. 597, 1266 (2003).
8. Khan, S. A., Rehman, A., Mendonca, J. T.: Phys. Plasmas 21, 092109 (2014).
9. Ki, Dae-Han, Jung,Y.: Phys. Plasmas 18, 014506 (2011).
10. Leach, J., Padgett, M. J., Barnett, S. M., Franke-Arnold, S., Courtial, J.: Phys. Rev. Lett. 88, 257901 (2002).
11. Mendonca, J. T., Thide, B.: Europhys. Lett. 84, 41001 (2008).
12. Mendonca, J. T., Ali, S., Thide, B.: Phys. Plasmas 16, 112103 (2009).
13. Mendonca, J. T.:Phys. Plasmas 19, 112113 (2012).
14. Padgett, M. J., Arlt, J., Simpson, N. B., Allen, L.: Am. J. Phys. 64, 77(1996).
15. Thide, B., Then, H., Sjoholm, J., Palmer, K., Bergman, J., Carozzi, T. D., Istomin, Ya. N., Ibragimov, N. H., Khamitova, R.: Phys. Rev. Lett. 99, 087701 (2007).
16. V. B. Berestetskii, E. M. Lifshitz, and L. P. Pitaevskii, Quantum Electro- dynamics (Butterworth-Heinemann, Oxford, 1982).

Figure Captions:

– **Fig.1:** The normalized Landau damping rate γ/ω_{pe} of twisted Langmuir modes are plotted against the normalized wave number $k\lambda D_e$ for the different values of kappa i.e., ($\kappa = 3$: Purple Solid line), ($\kappa = 5$: Blue Dashed line) and ($\kappa_e = 7$: Green Dot-Dashed line) for fixed value of temperature $T_e = 3e\mathbf{V}$.

– **Fig.2:** The normalized Landau damping rate γ/ω_{pe} of twisted Langmuir modes are plotted against the ratio of conventional wave number to twisted wave number $\mu = k/lq_\theta$ for the different values of kappa i.e., ($\kappa = 3$: Purple Solid line), ($\kappa = 5$: Blue Dashed line) and ($\kappa_e = 7$: Green Dot-Dashed line) for fixed value of temperature $T_e = 3e\mathbf{V}$.

– **Fig.3:** The three dimensional surface plot of normalized Landau damping rate γ/ω_{pe} of twisted Langmiur modes is drawn against normalized wave number $k\lambda D_e$ and ratio of conventional wave number to twisted wave number $\mu = k/lq_\theta$ for fixed value of temperature $T_e = 3e\mathbf{V}$.

– **Fig.4:** The three dimensional contour plot of normalized Landau damping rate γ/ω_{pe} of twisted Langmuir modes is drawn against normalized wave number $k\lambda D_e$ and ratio of conventional wave number to twisted wave number $\mu = k/lq_\theta$ for fixed value of temperature $T_e = 3e\mathbf{V}$.

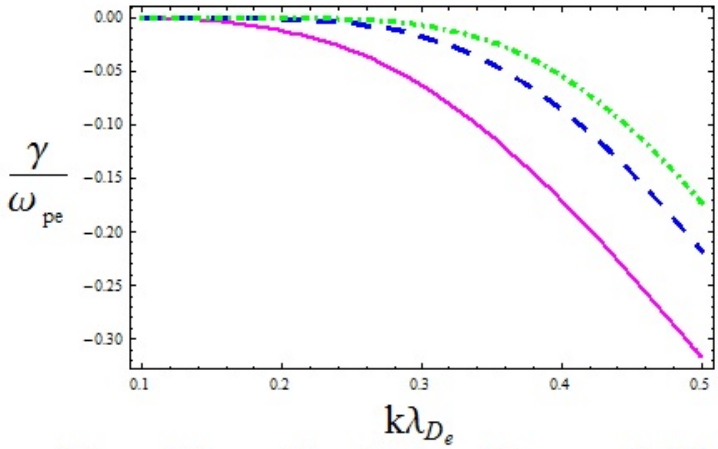

(Non− Maxwellian Twisted Langmuir Modes)

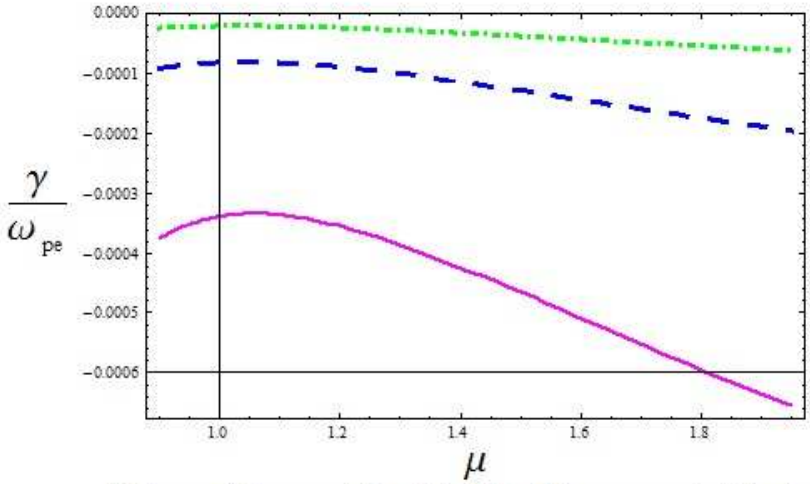

(Non− Maxwellian Twisted Langmuir Modes)

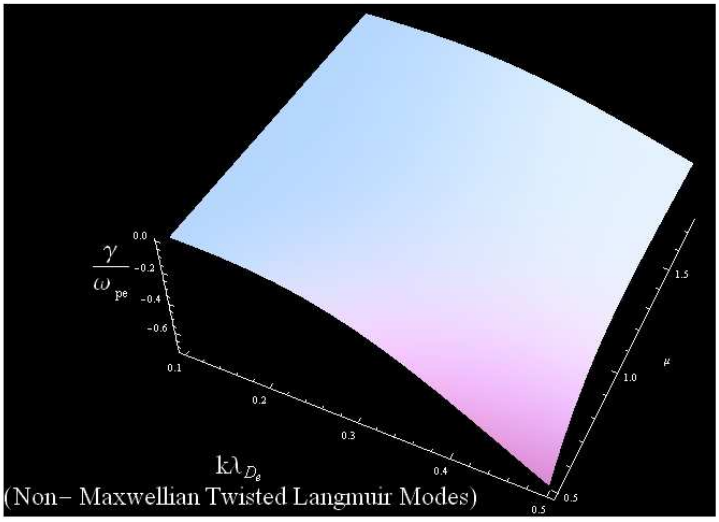
$\frac{\gamma}{\omega_{pe}}$
0.0
-0.2
-0.4
-0.6
0.1
0.2
0.3
0.4
0.5
$k\lambda_{D_e}$
1.5
1.0
μ
(Non– Maxwellian Twisted Langmuir Modes)

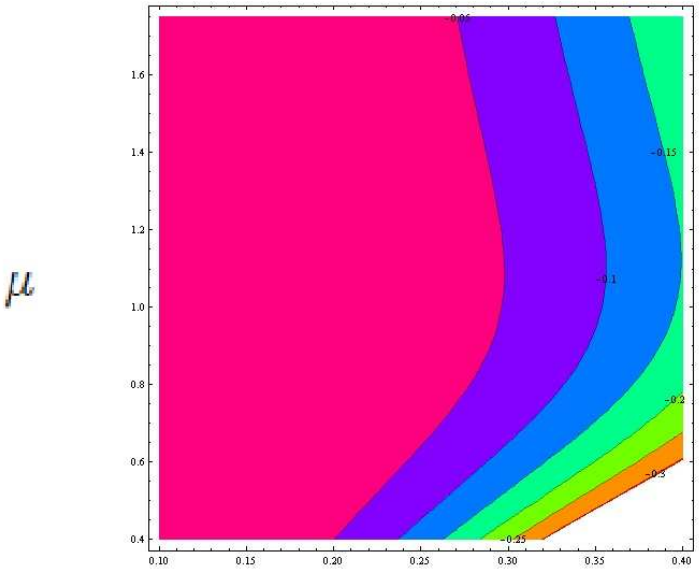
μ
1.6
1.4
1.2
1.0
0.8
0.6
0.4
-0.05
-0.15
-0.1
-0.2
-0.3
-0.25
0.10
0.15
0.20
0.25
0.30
0.35
0.40
$k\lambda_{De}$ (Non-Maxwellian Twisted Langmuir Modes)

Proc. Int. Conf. Relativ. Astrophys.
Pages 39-47, (2015)

Cosmological Issues in $F(T)$ Gravity Theory

Kazuharu Bamba[a,1,2,3]

[1]Leading Graduate School Promotion Center, Ochanomizu University, Tokyo 112-8610, Japan
[2]Department of Physics, Graduate School of Humanities and Sciences, Ochanomizu University, Tokyo 112-8610, Japan
[3]*Present Address: Division of Human Support System, Faculty of Symbiotic Systems Science, Fukushima University, Fukushima 960-1296, Japan*

Abstract We review recent developments on cosmology in extended teleparallel gravity, called "$F(T)$ gravity" with T the torsion scalar in teleparallelism. We explore various cosmological aspects of $F(T)$ gravity including the evolution of the equation of state for the universe, finite-time future singularities, thermodynamics, and four-dimensional effective $F(T)$ gravity theories coming from the higher-dimensional Kaluza-Klein (KK) and Randall-Sundrum (RS) theories.

Keywords Dark energy · Modified theories of gravity · Cosmology · Compactification and four-dimensional models

PACS 95.36.+x · 04.50.Kd · 98.80.-k · 11.25.Mj

1 Introduction

The fact that the current accelerated the cosmic expansion is currently accelerating has been supported by various recent cosmological observations including Type Ia Supernovae (SNe Ia), cosmic microwave background (CMB) radiation, baryon acoustic oscillations (BAO), large scale structure (LSS), and weak lensing effects (see recent results acquired from the Planck satellite [1,2] as well as the Wilkinson Microwave anisotropy probe (WMAP) [3,4]). There exist the following two main procedures to account for the late-time cosmic acceleration: The introducttion of "dark energy" and the extension of gravity, e.g., the so-called $F(R)$ gravity (for recent reviews on dark energy and modified gravity, see, for example, [5] and [6–15], respectively).

As a formulation for gravity, there has been proposed "teleparallelism" where the gravity theory is described by using the Weitzenböck connection (for a recent detailed review, see [16]). This has been considered to be an alternative gravitational theory to general relativity. This gravity theory is written with the torsion scalar T, and not the scalar curvature R defined with the Levi-Civita connection [17–19] as in general relativity. Recently, it has been found that as in $F(R)$ gravity, not only inflation in the early universe [20,21] but also the late-time cosmic acceleration [22–25] can occur in the so-called $F(T)$ gravity, which is an extended version of the original teleparallelism.

In this paper, we review main cosmological consequences in $F(T)$ gravity obtained in Refs. [24–27]. First, we investigate the evolution of the equation of state (EoS) for dark energy [24,25]. We construct an $F(T)$ gravity model in which the crossing of the phantom divide can happen[1]. This phenomenon has been suggested with cosmological observations in Refs. [36–40]. Second, we demonstrate that the finite-time future singularities [41–43] can appear in $F(T)$ gravity [26]. In addition, $F(T)$ gravity models with realizing the finite-time future singularities are reconstructed. We find that the finite-time future singularities can be cured by adding a power-law term T^β with $\beta > 1$, for instance, a T^2 term. The same approach has been used for Loop quantum cosmology [44]. Furthermore, we examine $F(T)$ models in which inflation, the ΛCDM model, Little Rip scenario [45–54], and Pseudo-Rip scenario [55] can be realized. Third, we derive four-dimensional effective $F(T)$ gravity theories from the five-dimensional Kaluza-Klein (KK) [56–58] and Randall-Sundrum (RS) [59,60] models [27]. It is also demonstrated that inflation and the late-time cosmic acceleration can occur in the former four-dimensional effective $F(T)$ gravity theory and the latter RS model, respectively. We use units of $k_{\rm B} = c = \hbar = 1$ and denote the gravitational constant $8\pi G$ by

[a]e-mail: bamba@sss.fukushima-u.ac.jp

[1]In Refs. [28–35], such an $F(R)$ gravity model with the crossing of the phantom divide has been reconstructed.

$\kappa^2 \equiv 8\pi/{M_{\rm Pl}}^2$ with the Planck mass of $M_{\rm Pl} = G^{-1/2} = 1.2 \times 10^{19}$GeV.

The paper is organized as follows. In Sec. II, we consider the cosmological evolution of the EoS for dark energy. In Sec. III, we analyze the finite-time future singularities and reconstruct $F(T)$ gravity models where these finite-time future singularities can appear. We also examine $F(T)$ models to realize various cosmological scenarios. In Sec. IV, we deduce four-dimensional effective $F(T)$ gravity theories from both the KK theories and the RS models. In Sec. V, summary is presented.

2 Cosmological evolutions

In this section, we explain $F(T)$ gravity and examine the cosmological evolutioin of the EoS for dark energy based on the main results in Ref. [24]. The purpose is to construct an $F(T)$ gravity model in which the crossing of the phantom divide can occur as suggested by resent cosmologcal observations.

2.1 Teleparallelism

We first explain the formulation of teleparallelism. The metric is described as $g_{\mu\nu} = \eta_{AB} e^A_\mu e^B_\nu$. Here, η_{AB} is the metric in the Minkowski space-time, $e_A(x^\mu)$ are orthonormal tetrad components ($A = 0, 1, 2, 3$) at points x^μ of the manifold in the tangent space, μ, $\nu = 0, 1, 2, 3$ show coordinate indices on the manifold, ande^μ_A corresponds to the tangent vector of the manifold. The Lagrangian is written with the torsion scalar T. This is different from the case for general relativity, in which the Lagrangian is expressed by using the scalar curvature R. The torsion scalar T is defined as $T \equiv S_\rho{}^{\mu\nu} T^\rho{}_{\mu\nu}$, where $T^\rho{}_{\mu\nu} \equiv e^\rho_A \left(\partial_\mu e^A_\nu - \partial_\nu e^A_\mu\right)$ is the torsion tensor and $S_\rho{}^{\mu\nu} \equiv (1/2)\left(K^{\mu\nu}{}_\rho + \delta^\mu_\rho\, T^{\alpha\nu}{}_\alpha - \delta^\nu_\rho\, T^{\alpha\mu}{}_\alpha\right)$ with $K^{\mu\nu}{}_\rho \equiv -(1/2)\left(T^{\mu\nu}{}_\rho - T^{\nu\mu}{}_\rho - T_\rho{}^{\mu\nu}\right)$ the contorsion tensor.

The Lagrangian of pure teleparallelism is written by the torsion scalar T. This has been extended to an appropriate function of T to realize inflation and the late-time cosmic acceleration. This concept is the same as $F(R)$ gravity, where the Einstein-Hilbert action written by the scalar curvature R is promoted to an appropriate function of R. Accordingly, the action of $F(T)$ gravity is represented as [23] $I = \int d^4x|e| \left[F(T)/\left(2\kappa^2\right) + \mathcal{L}_{\rm M}\right]$ with $|e| = \det\left(e^A_\mu\right) = \sqrt{-g}$ and $\mathcal{L}_{\rm M}$ the matter Lagrangian. If $F(T) = T$, this action is equivalent to that for pure teleparallelism.

We assume the flat Friedmann-Lemaître-Robertson-Walker (FLRW) space-time. The metric is given by $ds^2 = dt^2 - a^2(t) \sum_{i=1,2,3} \left(dx^i\right)^2$. Here, $a(t)$ is the scale factor, and the Hubble parameter reads $H = \dot{a}/a$, where the dot means the time derivative. In the FLRW background, we obtain the expressions of the metric $g_{\mu\nu} = {\rm diag}(1, -a^2, -a^2, -a^2)$, the tetrad components $e^A_\mu = (1, a, a, a)$, and the torsion scalar $T = -6H^2$.

Moreover, in this background, the gravitational field equations are written as $H^2 = \left(\kappa^2/3\right)(\rho_{\rm M} + \rho_{\rm DE})$ and $\dot{H} = -\left(\kappa^2/2\right)(\rho_{\rm M} + P_{\rm M} + \rho_{\rm DE} + P_{\rm DE})$. Here, $\rho_{\rm M}$ and $P_{\rm M}$ are the energy density and pressure for all of the matters, i.e., the perfect fluids, respectively. The continuity equation for the perfect fluid becomes $\dot{\rho}_{\rm M} + 3H(\rho_{\rm M} + P_{\rm M}) = 0$. Furthermore, $\rho_{\rm DE}$ and $P_{\rm DE}$ are the energy density and pressure for the dark energy components, respectively, given by $\rho_{\rm DE} = \left[1/\left(2\kappa^2\right)\right] J_1$ and $P_{\rm DE} = -\left[1/\left(2\kappa^2\right)\right](4J_2 + J_1)$ with $J_1 \equiv -T - F(T) + 2TF'(T)$ and $J_2 \equiv (1 - F'(T) - 2TF''(T))\,\dot{H}$, where the prime denotes the derivative with respect to T as $F'(T) \equiv dF(T)/dT$ and $F''(T) \equiv d^2F(T)/dT^2$. The continuity equation for the dark energy components reads $\dot{\rho}_{\rm DE} + 3H(\rho_{\rm DE} + P_{\rm DE}) = 0$.

2.2 Crossing of the phantom divide

As an $F(T)$ gravity model in which the crossing of the phantom divide can occur, we obtain

$$F(T) = T + \gamma \left\{ T_0 \left(\frac{uT_0}{T}\right)^{-1/2} \ln\left(\frac{uT_0}{T}\right) - T\left[1 - \exp\left(\frac{uT_0}{T}\right)\right]\right\}, \tag{1}$$

$$\gamma \equiv \frac{1 - \Omega^{(0)}_{\rm m}}{2u^{-1/2} + [1 - (1 - 2u)\exp(u)]}, \tag{2}$$

with T_0 the present value of the torsion scalar T and u a constant. In addition, $\Omega^{(0)}_{\rm m} \equiv \rho^{(0)}_{\rm m}/\rho^{(0)}_{\rm crit}$. Here, $\rho^{(0)}_{\rm m}$ is the current energy density of non-relativistic matter, and $\rho^{(0)}_{\rm crit} = 3H_0^2/\kappa^2$ is the current critical density, where H_0 is the Hubble parameter at the present time. The model in Eq. (1) consists of both the logarithmic and exponential terms. The EoS for dark energy is defined as $w_{\rm DE} \equiv P_{\rm DE}/\rho_{\rm DE}$. It is seen that for the model in Eq. (1), the EoS for dark energy $w_{\rm DE}$ evolves from $w_{\rm DE} > -1$ to $w_{\rm DE} < -1$, and thus the crossing of the phantom divide line $w_{\rm DE} = -1$ can happen. We remark that this manner is opposite to the representative behavior for $F(R)$ gravity models.

Furthermore, it can numerically be demonstrated that for the model in Eq. (1), first the density parameter of radiation $\Omega_{\rm r} \equiv \rho_{\rm r}/\rho_{\rm crit}$ dominates, and then the density parameter of non-relativistic matter $\Omega_{\rm m} \equiv \rho_{\rm m}/\rho_{\rm crit}$ is dominant, and eventually the density parameter of dark energy $\Omega_{\rm DE} \equiv \rho_{\rm DE}/\rho_{\rm crit}$ becomes much larger than the density parameters of radiation and

Table 1 Conditions that there exist the finite-time future singularities for H in Eqs. (3) and (4), those for $\rho_{\rm DE}$ and $P_{\rm DE}$, and the evolutions of H and $\dot{H}$ for $t \to t_{\rm s}$.

$q(\neq 0, -1)$ [Type of singularities]	H $(t \to t_{\rm s})$	$\dot{H}$ $(t \to t_{\rm s})$	$\rho_{\rm DE}$	$P_{\rm DE}$
$q \geq 1$ [Type I ("Big Rip")]	$H \to \infty$	$\dot{H} \to \infty$	$J_1 \neq 0$	$J_1 \neq 0$ or $J_2 \neq 0$
$0 < q < 1$ [Type III]	$H \to \infty$	$\dot{H} \to \infty$	$J_1 \neq 0$	$J_1 \neq 0$
$-1 < q < 0$ [Type II ("Sudden")]	$H \to H_{\rm s}$	$\dot{H} \to \infty$		$J_2 \neq 0$
$q < -1$ (q is non-integer) [Type IV]	$H \to H_{\rm s}$	$\dot{H} \to 0$		
		Divergence of higher derivatives of H		

non-relativistic matter around the present time. Here, $\rho_{\rm r}$, $\rho_{\rm m}$, $\rho_{\rm DE}$, and $\rho_{\rm crit} \equiv 3H^2/\kappa^2$ are the energy density of radiation, that of non-relativistic matter, that of dark energy, and the critical density, respectively. Hence, in the model in Eq. (1), the dark energy dominated stage, which follows the radiation dominated stage and the matter dominated stage, can be realized. Moreover, through the statistical analysis with the recent cosmological observational data in terms of SNe Ia, BAO, and the CMB radiation, we derive the observational constraints on the model parameters of the model in Eq. (1). As a result, we find that the model in Eq. (1) can fit the observational data well. In Ref. [61], other $F(T)$ gravity models in which the crossing of the phantom divide can occur have been built up.

3 Finite-time future singularities

In this section, we show that the finite-time future singularities can occur in $F(T)$ gravity by reviewing the consequences in Ref. [26], We also reconstruct $F(T)$ gravity models in which the finite-time future singularities appear.

3.1 Four types of the finite-time future singularities

For the FLRW space-time, the effective EoS is given by [6,7] $w_{\rm eff} \equiv P_{\rm eff}/\rho_{\rm eff} = -1 - 2\dot{H}/\left(3H^2\right)$, where $\rho_{\rm eff} \equiv 3H^2/\kappa^2$ and $P_{\rm eff} \equiv -\left(2\dot{H} + 3H^2\right)/\kappa^2$ are the energy density and pressure of all of the energy components in the universe, respectively. When the dark energy density becomes dominant over the energy density of non-relativistic matters, the following approximation is satisfied: $w_{\rm DE} \approx w_{\rm eff}$. In what follows, we explore such a situation in order to examine the cosmic evolution when there appear the finite-time future singularities at $t = t_{\rm s}$. If $\dot{H} < 0$ (> 0), the universe is in the non-phantom [i.e., quintessence] (phantom) phase with $w_{\rm eff} > -1$ (< -1). For $w_{\rm eff} = -1$, we have $\dot{H} = 0$, namely, the cosmological constant.

The finite-time future singularities are classified into four types [41]. Type I: When $t \to t_{\rm s}$, $a \to \infty$, $\rho_{\rm eff} \to \infty$ and $|P_{\rm eff}| \to \infty$. This types includes the case that $\rho_{\rm eff}$ and $P_{\rm eff}$ become finite values at $t = t_{\rm s}$ [62]. Type II: When $t \to t_{\rm s}$, $a \to a_{\rm s}$, $\rho_{\rm eff} \to \rho_{\rm s}$ and $|P_{\rm eff}| \to \infty$, where $a_{\rm s}(\neq 0)$ and $\rho_{\rm s}$ are constants. Type III: When $t \to t_{\rm s}$, $a \to a_{\rm s}$, $\rho_{\rm eff} \to \infty$ and $|P_{\rm eff}| \to \infty$. Type IV: When $t \to t_{\rm s}$, $a \to a_{\rm s}$, $\rho_{\rm eff} \to 0$, $|P_{\rm eff}| \to 0$. Here, the higher derivatives of H also diverge, and the case that $\rho_{\rm eff}$ and/or $|P_{\rm eff}|$ approach finite values in the limit $t \to t_{\rm s}$ is included. Type I and Type II are known as "Big Rip" [63,64] and "Sudden" [65,66] singularities.

3.2 Conditions for the finite-time future singularities to appear

We suppose that H is described as [67]

$$H \sim \frac{h_{\rm s}}{(t_{\rm s} - t)^q} \ \text{ for } \ q > 0\,, \tag{3}$$

$$H \sim H_{\rm s} + \frac{h_{\rm s}}{(t_{\rm s} - t)^q} \ \text{ for } \ q < -1, \ -1 < q < 0\,, \tag{4}$$

with $h_{\rm s}(> 0)$, $H_{\rm s}(> 0)$, and $q(\neq 0, -1)$ constants. Since the value of H has to be a real number, we examine the range $0 < t < t_{\rm s}$. In Table 1, we summarize the conditions that there exist the finite-time future singularities for H in Eqs. (3) and (4), those for $\rho_{\rm DE}$ and $P_{\rm DE}$, and the evolutions of H and $\dot{H}$ for $t \to t_{\rm s}$.

If H is represented as in Eqs. (3) and (4), we reconstruct $F(T)$ gravity models, in which the finite-time future singularities happen, by using the procedure [68, 69]. It is seen that in the flat FLRW universe, both of two gravitational filed equations can be met when $F(T)$ is given by the following power-law expression: $F(T) = AT^{\alpha}$, where $A(\neq 0)$ and $\alpha(\neq 0)$ are constants. Furthermore, we find a correction term $F_{\rm c}(T)$ curing the finite-time future singularities, given by $F_{\rm c}(T) = BT^{\beta}$ with $B(\neq 0)$ and $\beta(\neq 0)$ constants. It is known that the finite-time future singularities can be removed by the quadratic term (namely, $\beta = 2$) [6,7] for $F(R)$ gravity and non-local gravity [70]. As a result, for $F(T) = AT^{\alpha} + BT^{\beta}$, which is the summation of the original and

Table 2 Conditions that the parameters in a power-law expression for $F(T)$, for which the finite-time future singularities exist, and the forms of a power-low the correction term $F_{\rm c}(T) = BT^{\beta}$ curing the finite-time future singularities.

$q(\neq 0, -1)$ [Type of singularities]	Consequence	$F(T) = AT^{\alpha}$ $(A \neq 0, \alpha \neq 0)$	$F_{\rm c}(T) = BT^{\beta}$ $(B \neq 0, \beta \neq 0)$
$q \geq 1$ [Type I ("Big Rip")]	appears	$\alpha < 0$	$\beta > 1$
$0 < q < 1$ [Type III]	—	$\alpha < 0$	$\beta > 1$
$-1 < q < 0$ [Type II ("Sudden")]	—	$\alpha = 1/2$	$\beta \neq 1/2$
$q < -1$ (q is non-integer) [Type IV]	appears	$\alpha = 1/2$	$\beta \neq 1/2$

Table 3 H and $F(T)$ for which (i) inflation in the early universe, (ii) the ΛCDM model, (iii) Little Rip cosmology and (iv) Pseudo-Rip cosmology can be realized. Here, $h_{\rm inf}$, Λ, $H_{\rm LR}$, ζ, and $H_{\rm PR}$ are constants.

Scenario	H	$F(T)$
(i) Power-law inflation (when $t \to 0$)	$H = h_{\rm inf}/t\,,\ h_{\rm inf}(> 1)$	$F(T) = AT^{\alpha}\,,\ \alpha < 0$ or $\alpha = 1/2$
(ii) ΛCDM model or exponential inflation	$H = \sqrt{\Lambda/3} = \text{constant}\,,\ \Lambda > 0$	$F(T) = T - 2\Lambda\,,\ \Lambda > 0$
(iii) Little Rip scenario (when $t \to \infty$)	$H = H_{\rm LR}\exp(\zeta t)\,,\ H_{\rm LR} > 0$ and $\zeta > 0$	$F(T) = AT^{\alpha}\,,\ \alpha < 0$ or $\alpha = 1/2$
(iv) Pseudo-Rip scenario	$H = H_{\rm PR}\tanh(t/t_0)\,,\quad H_{\rm PR} > 0$	$F(T) = A\sqrt{T}$

correction terms, two gravitational filed equations cannot simultaneously be satisfied. It follows from this fact that the finite-time future singularities can be removed by such a power-law correction term. We show the conditions that the parameters in a power-law expression for $F(T)$, for which the finite-time future singularities exist, and the forms of a power-low the correction term curing the finite-time future singularities in Table 2. From this table, it is clearly seen that Type I and IV singularities can appear.

3.3 Various cosmological scenarios

Moreover, we examine which kinds of the finite-time future singularities occur in each cosmology. If the absolute value of q is large enough, the finite-time future singularities can appear. We also explore $F(T)$ gravity models in which the following cosmological scenarios can be realized: (i) Power-law inflation, (ii) The ΛCDM model, (iii) Little Rip scenario [45–47], and (iv) Pseudo-Rip scenario [55]. The expressions of H and $F(T)$ in the scenarios shown above are presented in Table 3.

In addition, we consider Little Rip scenario, which is a kind of a mild phantom cosmology. The motivation of this scenario is to remove the finite-time future singularities including a Big Rip singularity. In this scenario, the dark energy density grows as the universe evolves, whereas the EoS for dark energy $w_{\rm DE}$ becomes close to $w_{\rm DE} = -1$ from $w_{\rm DE} < -1$. The special feature of this scenario is that at some future time, bound structures are dissolved because an inertial force operating objects becomes large. Such a phenomenon is the so-called Little Rip.

As another related cosmology, we study Pseudo-Rip scenario. With the Hubble parameter, cosmological scenarios can be classified [55]. (i) Power-law inflation: $H(t) \to \infty$ for $t \to 0$. (ii) The ΛCDM model (or Exponential inflation): $H(t) = H(t_0) = \text{constant}$, where t_0 is the current time. (iii) Little Rip scenario: $H(t) \to \infty$ for $t \to \infty$. (iv) Pseudo-Rip scenario (a phantom cosmology approaching de Sitter expansion asymptotically: $H(t) \to H_{\infty} < \infty$ for $t \to \infty$ with $t \geq t_0$ and $H_{\infty}(> 0)$ a constant. For a Big Rip singularity, $H(t) \to \infty,\ \ t \to t_{\rm s}$, as depicted in Table 1.

We note that the EoS parameter $w_{\rm DE}$ for dark energy, the deceleration parameter $q_{\rm dec} \equiv -\ddot{a}/\left(aH^2\right)$, the jerk parameter $j \equiv \dddot{a}/\left(aH^3\right)$ and the snark parameter $s \equiv (j-1)/\left[3\left(q_{\rm dec} - 1/2\right)\right]$ [71,72] are used to observationally constrain the dark energy models. For the ΛCDM model, we have $(w_{\rm DE}, q_{\rm dec}, j, s) = (-1, -1, 1, 0)$. In the flat universe, there have been proposed $w_{\rm DE} = -1.10 \pm 0.14\,(68\%\,\text{CL})$ [3]. By using these parameters, especially, the observational constraints on the models parameters can be derived. For example, with the observational value of $w_{\rm DE}$, the constraints on $H_{\rm LR}$ and $H_{\rm PR}$ shown in Table 3 can be derived. In Little Rip scenario, we obtain $H_{\rm LR} \geq \left[2H_0/\left(3e\right)\right](1/0.24) = 1.50 \times 10^{-42}\,\text{GeV}$, where $H_0 = 2.1h \times 10^{-42}\,\text{GeV}$ [73] with $h = 0.7$ [3,74] is the current Hubble parameter and $e = 2.71828$, and $\chi \equiv H_0/\left(H_{\rm LR}e\right) \leq 0.36$. On the other hand, for Pseudo Rip scenario, we get $H_{\rm PR} \geq (2H_0/3)\left[4/\left(e - e^{-1}\right)^2\right](1/0.24) = 2.96 \times 10^{-42}\,\text{GeV}$ and $\delta \equiv H_0/H_{\rm PR} \leq 0.497196$. Hence, Little Rip scenario with $\chi \ll 1$ and Pseudo Rip scenario with an appropriate value of δ can be compatible with the ΛCDM model.

3.4 Inertial force

In the expanding universe, the relative acceleration between two points separated by a distance l is given by $l\ddot{a}/a$, where a is the scale factor. Suppose that there exists a particle with mass m at each of the points, an observer at one of the masses would measure an inertial force on the other mass. We assume that there are two particles (A) and (B) with its mass m and the distance between them is l. The inertial force $F_{\rm inert}$ on the particle (B), which is measured by an observer at the point of the particle (A), is represented as $F_{\rm inert} = ml\ddot{a}/a = ml\left(\dot{H}+H^2\right)$ [45,47]. In the case of a Big Rip singularity with H in Eq. (3), $F_{\rm inert} \to \infty$ when $t \to t_{\rm s}$. Moreover. for Little Rip scenario with H described in Table 3, $F_{\rm inert} \to \infty$ when $t \to \infty$. Furthermore, in Pseudo-Rip scenario with H presented in Table 3, $F_{\rm inert} \to F^{\rm PR}_{\rm inert\,,\infty} \equiv mlH^2_{\rm PL} < \infty$ when $t \to \infty$. Thus, $F_{\rm inert}$ approaches a finite value asymptotically. This is because $H \to H_{\rm PR}$ and $\dot{H} \to 0$.

If a force $F_{\rm b}$ to bound two particles is smaller than a positive inertial force $F_{\rm inert}(>0)$, the two particle bound system is disintegrated. As an example, we examine the Earth-Sun (ES) system. When $F^{\rm PR}_{\rm inert\,,\infty} > F^{\rm ES}_{\rm b} = GM_\oplus M_\odot/r^2_{\oplus-\odot} = 4.37\times10^{16}\,{\rm GeV}^2$, which is the bound force in the ES system, the ES system is dissociated, so that Pseudo-Rip scenario can be satisfied. Here, we have used the mass of Earth $M_\oplus = 3.357\times10^{51}\,{\rm GeV}$ [73] and that of Sun $M_\odot = 1.116\times10^{57}\,{\rm GeV}$ [73], and we have set $m = M_\oplus$ and $l = r_{\oplus-\odot} = 1{\rm AU} = 7.5812\times10^{26}\,{\rm GeV}^{-1}$ [73] (the Astronomical unit, namely, the distance between Earth and Sun). In this case, we acquire $H_{\rm PR} > \sqrt{GM_\odot/r^3_{\oplus-\odot}} = 1.31\times10^{-31}\,{\rm GeV}$. This is consistent with the observations on the present value of $w_{\rm DE}$ in Pseudo-Rip scenario because this is much stronger than the constraint $H_{\rm PR} \geq 2.96\times10^{-42}\,{\rm GeV}$ given above, which originates from the observations on the value of $w_{\rm DE}$ at the present time.

It is also remarked that in the process of collapse of the star, the time-dependent matter instability can happen not only for $F(R)$ gravity [75,76] but also $F(T)$ gravity.

4 Higher-dimensional theories

In this section, we construct four-dimensional effective $F(T)$ gravity theories from the five-dimensional Kaluza-Klein (KK) [56–58] and Randall-Sundrum (RS) [59,60] theories by following the investigations in Ref. [27].

4.1 Five-dimensional KK theory

First, we derive the effective $F(T)$ gravity theories in the four-dimensional space-time from the KK theory in the five-dimensional space-time. It is supposed that in $F(T)$ gravity, the ordinary procedure of the KK reduction [56–58] can be executed from the five-dimensional space-time to the four-dimensional space-time. In this process, one dimension of space is compacted into a small circle, while the four-dimensional space-time is infinitely extended. The radius of the fifth dimension is set to be around the Planck length so that the KK effects cannot appear. Consequently, the size of the circle is small enough for the phenomena in the quite low energy scale not to be seen. From now on, we concentrate on the gravity sector in the action, and therefore the matter sector is neglected.

The five-dimensional action in $F(T)$ gravity is [77]

$$ {}^{(5)}S = \int d^5x \left|{}^{(5)}e\right| \frac{F({}^{(5)}T)}{2\kappa_5^2}\,, \tag{5}$$

$$ {}^{(5)}T \equiv \frac{1}{4}T^{abc}T_{abc} + \frac{1}{2}T^{abc}T_{cba} - T_{ab}\ {}^{a}T^{cb}\ {}_{c}\,. \tag{6}$$

Here, ${}^{(5)}T$ is the torsion scalar, the Latin indices are $(a,b,\cdots=0,1,2,3,5)$ with "5" the fifth-coordinate component, ${}^{(5)}e = \sqrt{{}^{(5)}g}$ with ${}^{(5)}g$ the determinant of ${}^{(5)}g_{\mu\nu}$, and $\kappa_5^2 \equiv 8\pi G_5 = \left({}^{(5)}M_{\rm Pl}\right)^{-3}$ with G_5 the gravitational constant and $M^{(5)}_{\rm Pl}$ the Planck mass. The superscription "(5)" or the subscription"5" shows the quantities in the five-dimensional space-time. The representation of ${}^{(5)}T$ is equivalent to that of the torsion scalar in the four-dimensional space-time. The five-dimensional metric is given by ${}^{(5)}g_{\mu\nu} = {\rm diag}(g_{\mu\nu}, -\psi^2)$, where ψ is a dimensionless and (spatially) homogeneous scalar field (namely, it only has the time dependence).

The four-dimensional effective action becomes

$$ S^{\rm (eff)}_{\rm KK} = \int d^4x|e|\frac{1}{2\kappa^2}\psi F(T+\psi^{-2}\partial_\mu\psi\partial^\mu\psi)\,, \tag{7}$$

where we have used $e^A_a = {\rm diag}(1,1,1,1,\psi)$ and $\eta_{ab} = {\rm diag}(1,-1,-1,-1,-1)$. In the case that $F(T) = T - 2\Lambda_4$ with $\Lambda_4(>0)$ the positive cosmological constant in the four-dimensional space-time, by defining another scalar field ξ as $\psi \equiv (1/4)\,\xi^2$, we find that the action in Eq. (7) is described as [56]

$$ S^{\rm (eff)}_{\rm KK}|_{F(T)=T-2\Lambda_4} = \int d^4x|e|\frac{1}{\kappa^2}\left[\frac{1}{8}\xi^2 T + \frac{1}{2}\partial_\mu\xi\partial^\mu\xi - \Lambda_4\right]. \tag{8}$$

In the flat FLRW background, from the action in Eq. (8), the gravitational field equations are given by $(1/2)\,\dot{\xi}^2 - (3/4)\,H^2\xi^2 + \Lambda_4 = 0$ and $\dot{\xi}^2 + H\xi\dot{\xi} + (1/2)\,\dot{H}\xi^2 = 0$ [78], and the equation of motion in terms of ξ is written

as $\ddot{\xi} + 3H\dot{\xi} + (3/2)\,H^2\xi = 0$. By using the gravitational field equations, we have $(3/2)\,H^2\xi^2 - 2\Lambda_4 + H\xi\dot{\xi} + (1/2)\,\dot{H}\xi^2 = 0$. Its solution is $H = H_{\rm inf} = \text{constant}(> 0)$, where $H_{\rm inf}$ is the Hubble parameter at the inflationary stage, and $\xi = \xi_1\,(t/\bar{t}) + \xi_2$ with ξ_1 and $\xi_2 (> 0)$ constants, where $\bar{t}$ denotes a time. Thus, when $t \to 0$, inflation with the de Sitter expansion can be realized, where $H_{\rm inf} \approx (2/\xi_2)\,\sqrt{\Lambda_4/3}$, $a \approx \bar{a}\exp\left(H_{\rm inf}t\right)$, and $\xi \approx \xi_2$. Moreover, with the equation of motion in terms of ξ, we acquire $\xi_1 \approx -\,(1/2)\,\xi_2 H_{\rm inf}\bar{t} \approx -\sqrt{\Lambda_4/3}\bar{t}$.

4.2 RS brane-world model

Next, we deduce the effective $F(T)$ gravity theories in the four-dimensional space-time from the RS brane-world model in the five-dimensional space-time. There exist two branes in the RS type-I model [59]: A positive tension brane located at $y = 0$ and a negative one located at $y = u$, where y means the fifth dimension.

The five-dimensional metric is expressed as

$$ds^2 = \exp\left(-2\frac{|y|}{l}\right) g_{\mu\nu}(x)dx^\mu dx^\nu + dy^2\,, \tag{9}$$

where $l = \sqrt{-6/\Lambda_5}$, $\exp\left(-2|y|/l\right)$ is the warp factor, and $\Lambda_5 (< 0)$ is the negative cosmological constant in the bulk. When $u \to \infty$, the RS type-I model is reduced to the RS type-II model [60]. In this model, there is only one positive tension brane in the anti-de Sitter bulk space. In Ref. [79], the gravitational field equation on the brane has been presented for the RS type-II model. It corresponds to the induced equation, i.e., the Gauss-Codazzi equation, on the brane, and it is derived by using the Israel's junction conditions on the brane and the Z_2 symmetry of $y \leftrightarrow -y$. This procedure has recently been considered in teleparallelism [80]. The vector part of the torsion tensor in the bulk is projected on the brane, so that new terms, which do not exist in the curvature gravity, can emerge.

In the flat FLRW background, the Friedmann equation on the brane is given by

$$H^2\frac{dF(T)}{dT} = -\frac{1}{12}\left[F(T) - 4\Lambda - 2\kappa^2\rho_{\rm M} - \left(\frac{\kappa_5^2}{2}\right)^2 \mathcal{I}\rho_{\rm M}^2\right]. \tag{10}$$

Here, $\mathcal{I} \equiv \left(11 - 60w_{\rm M} + 93w_{\rm M}^2\right)/4$ with $w_{\rm M} \equiv P_{\rm M}/\rho_{\rm M}$ the EoS for matter, where $\rho_{\rm M}$ and $P_{\rm M}$ are the energy density and pressure of matter, respectively. In the expression of $\mathcal{I}$, the novel contributions in teleparallelism are included (there are not these terms in the curvature gravity). The effective cosmological constant on the brane reads $\Lambda \equiv \Lambda_5 + \left(\kappa_5^2/2\right)^2\lambda^2$, where $\lambda (> 0)$ is the brane tension and we obtain the relation $G = [1/(3\pi)]\left(\kappa_5^2/2\right)^2\lambda$.

In the following, we consider the situation that the dark energy is dominant and hence the contribution of matter is negligible. If $F(T) = T - 2\Lambda_5$, with $T = -6H^2$, we get a solution of the de Sitter expansion as $H = H_{\rm DE} = \sqrt{\Lambda_5 + \kappa_5^4\lambda^2/6}$ and $a(t) = a_{\rm DE}\exp\left(H_{\rm DE}t\right)$, where $H_{\rm DE}$ and $a_{\rm DE} (> 0)$ are constants. Accordingly, the late-time cosmic acceleration can happen. In addition, when $F(T) = \left(T^2/\bar{M}^2\right) + \eta\Lambda_5$ with $\bar{M}$ a mass scale and η a constant, we find a de Sitter solution with the constant Hubble parameter

$$H = H_{\rm DE} = \left\{\frac{\bar{M}^2}{108}\left[(\eta - 4)\,\Lambda_5 - 4\left(\frac{\kappa_5^2}{2}\right)^2\lambda^2\right]\right\}^{1/4}. \tag{11}$$

In this expression, the content of the 4th root has to be positive. Therefore, we obtain a constraint on η, given by $\eta \geq 4 + \left(\kappa_5^2\lambda^2\right)/\Lambda_5$.

5 Summary

In the present paper, we have stated various cosmological issues as well as theoretical properties in $F(T)$ gravity. First, we have investigated the cosmological evolution of the EoS for dark energy $w_{\rm DE}$. We have constructed an $F(T)$ gravity model consisting of an exponential term and a logarithmic one, in which the crossing of the phantom divide can occur.

Next, we have found that the Type I and IV finite-time future singularities can appear, and reconstructed an $F(T)$ gravity model in which there exist the finite-time future singularities. We have also demonstrated that by adding a power-law term of $T^\beta\,(\beta > 1)$ like T^2, the finite-time future singularities can be cured, similarly to that in $F(R)$ gravity. Furthermore, we have explored $F(T)$ gravity models in which the following cosmological scenario is satisfied: power-law inflation, the ΛCDM model, the Little Rip scenario, and the Pseudo Rip scenario.

Moreover, we have analyzed four-dimensional effective action of $F(T)$ gravity originating from the five-dimensional KK theories and RS models. We have derived the four-dimensional effective action with a coupling of the torsion scalar to a scalar field through the KK reduction to the four-dimensional space-time from the five-dimensional one. We have shown that in this theory, inflation can occur. We have also found that in the RS type-II model with the four-dimensional FLRW brane, $F(T)$ gravity influences on the four-dimensional FLRW brane. We have seen that for this model, the

late-time cosmic acceleration can be realized. Here, inflation or the late-time cosmic acceleration can happen thanks to the torsion effect, and not by the curvature one, so that these KK theories and RS models can be considered to be constructed by not the scalar curvature but the torsion one in teleparallel gravity.

It should be cautioned that there is no local Lorentz invariance in $F(T)$ gravity as indicated in Refs. [81, 82], and this theory is acausal [83–85]. These are the most crucial points for $F(T)$ gravity theory. Thus, these problems have to further be considered seriously.

Finally, we mention a number of other cosmological subjects have been studied in $F(T)$ gravity. As examples, the authors works are raised: Trace-anomaly driven inflation [86], gravitational wave modes [87,88], conformal symmetry [89], thermodynamics [90,91], and the generation of the large-scale magnetic fields [92, 93][2]. It is expected that through such various cosmological investigations in $F(T)$ gravity, the clues to find novel viability conditions for $F(T)$ gravity as an alternative gravity theory to general relativity can be acquired.

Acknowledgements The author sincerely thank the organizers including Professor Dr. Muhammad Sharif (Chair) and Professor Dr. Asar Qadir for their very kind invitation to International Conference on Relativistic Astrophysics held on 10th–14th February, 2015, at Department of Mathematics, University of the Punjab, Lahore, Pakistan, and their quite hearty hospitality very much. Furthermore, he is really grateful to all of the collaborators of our studies in terms of $F(T)$ gravity, especially, all the co-authors of the works in Refs. [24–27]: Professor Chao-Qiang Geng, Dr. Chung-Chi Lee, Dr. Ling-Wei Luo, Professor Ratbay Myrzakulov, Professor Shin'ichi Nojiri, and Professor Sergei D. Odintsov, the results obtained in which are the basis of this paper. The work of the author was partially supported by the JSPS Grant-in-Aid for Young Scientists (B) # 25800136.

References

1. P. A. R. Ade *et al.* [Planck Collaboration], Planck 2015 results. XIII. Cosmological parameters, arXiv:1502.01589 [astro-ph.CO]
2. P. A. R. Ade *et al.* [Planck Collaboration], Planck 2015 results. XIV. Dark energy and modified gravity, arXiv:1502.01590 [astro-ph.CO]
3. E. Komatsu *et al.* [WMAP Collaboration], Seven-Year Wilkinson Microwave Anisotropy Probe (WMAP) Observations: Astrophys. J. Suppl. **192**, 18 (2011)
4. G. Hinshaw *et al.* [WMAP Collaboration], Nine-Year Wilkinson Microwave Anisotropy Probe (WMAP) Observations: Cosmological Parameter Results, Astrophys. J. Suppl. **208**, 19 (2013)

[2] Also in $F(R)$ gravity, trace-anomaly driven inflation [94,95], thermodynamics [31,96–99], and the generation of the large-scale magnetic fields [100,101] have been studied.

5. K. Bamba, S. Capozziello, S. Nojiri and S. D. Odintsov, Dark energy cosmology: the equivalent description via different theoretical models and cosmography tests, Astrophys. Space Sci., **342**, 155 (2012)
6. S. Nojiri and S. D. Odintsov, Unified cosmic history in modified gravity: from F(R) theory to Lorentz non-invariant models, Phys. Rept., **505**, 59 (2011)
7. S. Nojiri and S. D. Odintsov, Introduction to modified gravity and gravitational alternative for dark energy, eConf C, **0602061**, 06 (2006) [Int. J. Geom. Meth. Mod. Phys., **4** 115 (2007)]
8. V. Faraoni and S. Capozziello, Beyond Einstein gravity : A Survey of gravitational theories for cosmology and astrophysics, 467p. Fundamental Theories of Physics, Vol. 170, Springer, Dordrecht (2010)
9. S. Capozziello and M. De Laurentis, Extended Theories of Gravity, Phys. Rept., **509**, 167 (2011)
10. K. Bamba, Equation of State for Dark Energy in Modified Gravity Theories, arXiv:1202.4317 [gr-qc]
11. A. de la Cruz-Dombriz and D. Sáez-Gómez, Black holes, cosmological solutions, future singularities, and their thermodynamical properties in modified gravity theories, Entropy **14**, 1717 (2012)
12. K. Bamba, S. Nojiri and S. D. Odintsov, Modified gravity: walk through accelerating cosmology, arXiv:1302.4831 [gr-qc]
13. K. Bamba and S. D. Odintsov, Universe acceleration in modified gravities: $F(R)$ and $F(T)$ cases, arXiv:1402.7114 [hep-th]
14. A. Joyce, B. Jain, J. Khoury and M. Trodden, Beyond the Cosmological Standard Model, Phys. Rept. **568**, 1 (2015)
15. K. Bamba and S. D. Odintsov, Inflationary cosmology in modified gravity theories, Symmetry **7**, 220 (2015)
16. R. Aldrovandi and J. G. Pereira, Teleparallel Gravity: An Introduction, 214p. Springer, Dordrecht (2013)
17. F. W. Hehl, P. Von Der Heyde, G. D. Kerlick and J. M. Nester, General Relativity With Spin And Torsion: Foundations And Prospects, Rev. Mod. Phys. **48**, 393 (1976)
18. K. Hayashi and T. Shirafuji, New general relativity, Phys. Rev. D **19**, 3524 (1979) [Addendum-ibid. D **24**, 3312 (1981)]
19. E. E. Flanagan and E. Rosenthal, Can Gravity Probe B usefully constrain torsion gravity theories?, Phys. Rev. D **75**, 124016 (2007)
20. R. Ferraro and F. Fiorini, Modified teleparallel gravity: inflation without inflaton, Phys. Rev. D **75**, 084031 (2007)
21. R. Ferraro and F. Fiorini, On Born-Infeld Gravity in Weitzenbock spacetime, Phys. Rev. D **78**, 124019 (2008)
22. G. R. Bengochea and R. Ferraro, Dark torsion as the cosmic speed-up, Phys. Rev. D **79**, 124019 (2009)
23. E. V. Linder, Einstein's Other Gravity and the Acceleration of the Universe, Phys. Rev. D **81**, 127301 (2010) [Erratum-ibid. D **82**, 109902 (2010)]
24. K. Bamba, C. Q. Geng, C. C. Lee and L. W. Luo, Equation of state for dark energy in $f(T)$ gravity, JCAP, **1101**, 021 (2011)
25. K. Bamba, C. Q. Geng and C. C. Lee, Comment on "Einstein's Other Gravity and the Acceleration of the Universe", arXiv:1008.4036 [astro-ph.CO]
26. K. Bamba, R. Myrzakulov, S. Nojiri and S. D. Odintsov, Reconstruction of $f(T)$ gravity: Rip cosmology, finite-time future singularities and thermodynamics, Phys. Rev. D, **85**, 104036 (2012)
27. K. Bamba, S. Nojiri and S. D. Odintsov, Effective $F(T)$ gravity from the higher-dimensional Kaluza-Klein and Randall-Sundrum theories, Phys. Lett. B, **725**, 368 (2013)

28. K. Bamba, C. Q. Geng, S. Nojiri and S. D. Odintsov, Crossing of the phantom divide in modified gravity, Phys. Rev. D **79**, 083014 (2009)
29. K. Bamba, C. Q. Geng, S. Nojiri and S. D. Odintsov, Crossing of Phantom Divide in $F(R)$ Gravity, Mod. Phys. Lett. A **25**, 900 (2010)
30. K. Bamba and C. Q. Geng, Oscillating phantom in $F(R)$ gravity, Prog. Theor. Phys. **122**, 1267 (2009)
31. K. Bamba and C. Q. Geng, Thermodynamics in F(R) gravity with phantom crossing, Phys. Lett. B **679**, 282 (2009)
32. K. Bamba, Finite-time future singularities in modified gravity, arXiv:0904.2655 [gr-qc]
33. K. Bamba, Behavior of F(R) gravity around a crossing of the phantom divide, Open Astron. J. **3**, 13 (2010)
34. K. Bamba, C. Q. Geng and C. C. Lee, Generic feature of future crossing of phantom divide in viable $f(R)$ gravity models, JCAP **1011**, 001 (2010)
35. K. Bamba, C. Q. Geng and C. C. Lee, Phantom crossing in viable $f(R)$ theories, Int. J. Mod. Phys. D **20**, 1339 (2011)
36. U. Alam, V. Sahni and A. A. Starobinsky, The case for dynamical dark energy revisited, JCAP **0406**, 008 (2004)
37. S. Nesseris and L. Perivolaropoulos, Crossing the phantom divide: Theoretical implications and observational status, JCAP **0701**, 018 (2007)
38. P. U. Wu and H. W. Yu, Constraints on a variable dark energy model with recent observations, Phys. Lett. B **643**, 315 (2006)
39. U. Alam, V. Sahni and A. A. Starobinsky, Exploring the Properties of Dark Energy Using Type Ia Supernovae and Other Datasets, JCAP **0702**, 011 (2007)
40. H. K. Jassal, J. S. Bagla and T. Padmanabhan, Understanding the origin of CMB constraints on Dark Energy, Mon. Not. Roy. Astron. Soc. **405**, 2639 (2010)
41. S. Nojiri, S. D. Odintsov and S. Tsujikawa, Properties of singularities in (phantom) dark energy universe, Phys. Rev. D **71**, 063004 (2005)
42. K. Bamba, S. Nojiri and S. D. Odintsov, The Universe future in modified gravity theories: Approaching the finite-time future singularity, JCAP, **0810**, 045 (2008)
43. K. Bamba, S. D. Odintsov, L. Sebastiani and S. Zerbini, Finite-time future singularities in modified Gauss-Bonnet and F(R,G) gravity and singularity avoidance, Eur. Phys. J. C **67**, 295 (2010)
44. K. Bamba, J. de Haro and S. D. Odintsov, Future Singularities and Teleparallelism in Loop Quantum Cosmology, JCAP **1302**, 008 (2013)
45. P. H. Frampton, K. J. Ludwick and R. J. Scherrer, The Little Rip, Phys. Rev. D **84**, 063003 (2011)
46. I. Brevik, E. Elizalde, S. Nojiri and S. D. Odintsov, Viscous Little Rip Cosmology, Phys. Rev. D **84**, 103508 (2011)
47. P. H. Frampton, K. J. Ludwick, S. Nojiri, S. D. Odintsov and R. J. Scherrer, Models for Little Rip Dark Energy, Phys. Lett. B **708**, 204 (2012)
48. A. V. Astashenok, S. Nojiri, S. D. Odintsov and A. V. Yurov, Phantom Cosmology without Big Rip Singularity, Phys. Lett. B **709**, 396 (2012)
49. L. N. Granda and E. Loaiza, Big Rip and Little Rip solutions in scalar model with kinetic and Gauss Bonnet couplings, Int. J. Mod. Phys. D **2**, 1250002 (2012)
50. M. Ivanov and A. V. Toporensky, Stable super-inflating cosmological solutions in f(R)-gravity, Int. J. Mod. Phys. D **21**, 1250051 (2012)
51. Y. Ito, S. Nojiri and S. D. Odintsov, Stability of Accelerating Cosmology in Two Scalar-Tensor Theory: Little Rip versus de Sitter, Entropy **14**, 1578 (2012)
52. M. H. Belkacemi, M. Bouhmadi-Lopez, A. Errahmani and T. Ouali, The holographic induced gravity model with a Ricci dark energy: smoothing the little rip and big rip through Gauss-Bonnet effects?, Phys. Rev. D **85**, 083503 (2012)
53. P. Xi, X. H. Zhai and X. Z. Li, Alternative mechanism of avoiding the big rip or little rip for a scalar phantom field," Phys. Lett. B **706**, 482 (2012)
54. A. N. Makarenko, V. V. Obukhov and I. V. Kirnos, From Big to Little Rip in modified F(R,G) gravity, Astrophys. Space Sci. **343**, 481 (2013)
55. P. H. Frampton, K. J. Ludwick and R. J. Scherrer, Pseudo-rip: Cosmological models intermediate between the cosmological constant and the little rip, Phys. Rev. D **85**, 083001 (2012)
56. Y. Fujii and K. Maeda, The Scalar-Tensor Theory of Gravitation, 240 p. Cambridge University Press, Cambridge (2003)
57. T. Appelquist, A. Chodos and P. G. O. Freund, Modern Kaluza-Klein Theories, Addison-Wesley, Reading (1987)
58. J. M. Overduin and P. S. Wesson, Kaluza-Klein gravity, Phys. Rept., **283**, 303 (1997)
59. L. Randall and R. Sundrum, A Large mass hierarchy from a small extra dimension, Phys. Rev. Lett., **83**, 3370 (1999)
60. L. Randall and R. Sundrum, An Alternative to compactification, Phys. Rev. Lett., **83**, 4690 (1999)
61. P. Wu and H. W. Yu, $f(T)$ models with phantom divide line crossing, Eur. Phys. J. C **71**, 1552 (2011)
62. Y. Shtanov and V. Sahni, Unusual cosmological singularities in brane world models, Class. Quant. Grav. **19**, L101 (2002)
63. R. R. Caldwell, M. Kamionkowski and N. N. Weinberg, Phantom Energy and Cosmic Doomsday, Phys. Rev. Lett. **91**, 071301 (2003)
64. B. McInnes, The dS/CFT correspondence and the big smash, JHEP **0208**, 029 (2002)
65. J. D. Barrow, Sudden Future Singularities, Class. Quant. Grav. **21**, L79 (2004)
66. S. Nojiri and S. D. Odintsov, Quantum escape of sudden future singularity, Phys. Lett. B **595**, 1 (2004)
67. S. Nojiri and S. D. Odintsov, The future evolution and finite-time singularities in $F(R)$-gravity unifying the inflation and cosmic acceleration, Phys. Rev. D **78**, 046006 (2008)
68. S. Nojiri and S. D. Odintsov, Modified f(R) gravity consistent with realistic cosmology: From matter dominated epoch to dark energy universe, Phys. Rev. D **74**, 086005 (2006)
69. S. Nojiri and S. D. Odintsov, Modified gravity and its reconstruction from the universe expansion history, J. Phys. Conf. Ser. **66**, 012005 (2007)
70. K. Bamba, S. Nojiri, S. D. Odintsov and M. Sasaki, Screening of cosmological constant for De Sitter Universe in non-local gravity, phantom-divide crossing and finite-time future singularities, Gen. Rel. Grav. **44**, 1321 (2012)
71. T. Chiba and T. Nakamura, The Luminosity distance, the equation of state, and the geometry of the universe, Prog. Theor. Phys. **100**, 1077 (1998)
72. V. Sahni, T. D. Saini, A. A. Starobinsky and U. Alam, Statefinder: A New geometrical diagnostic of dark energy, JETP Lett. **77**, 201 (2003) [Pisma Zh. Eksp. Teor. Fiz. **77**, 249 (2003)]
73. E. W. Kolb and M. S. Turner, The Early Universe, 600 p. Addison-Wesley, Redwood City, California (1990)
74. W. L. Freedman *et al.* [HST Collaboration], Final Results from the Hubble Space Telescope Key Project to Measure the Hubble Constant, Astrophys. J. **553**, 47 (2001)

75. E. V. Arbuzova and A. D. Dolgov, Explosive phenomena in modified gravity, Phys. Lett. B **700**, 289 (2011)
76. K. Bamba, S. Nojiri and S. D. Odintsov, Time-dependent matter instability and star singularity in $F(R)$ gravity, Phys. Lett. B **698**, 451 (2011)
77. S. Capozziello, P. A. Gonzalez, E. N. Saridakis and Y. Vasquez, Exact charged black-hole solutions in D-dimensional f(T) gravity: torsion vs curvature analysis, JHEP, **1302**, 039 (2013)
78. C. Q. Geng, C. C. Lee, E. N. Saridakis and Y. P. Wu, 'Teleparallel' Dark Energy, Phys. Lett. B, **704**, 384 (2011)
79. T. Shiromizu, K. I. Maeda and M. Sasaki, The Einstein equation on the 3-brane world, Phys. Rev. D, **62**, 024012 (2000)
80. K. Nozari, A. Behboodi and S. Akhshabi, Braneworld Teleparallel Gravity, Phys. Lett. B, **723**, 201 (2013)
81. B. Li, T. P. Sotiriou and J. D. Barrow, $f(T)$ gravity and local Lorentz invariance, Phys. Rev. D **83**, 064035 (2011)
82. T. P. Sotiriou, B. Li and J. D. Barrow, Generalizations of teleparallel gravity and local Lorentz symmetry, Phys. Rev. D **83**, 104030 (2011)
83. P. Chen, K. Izumi, J. M. Nester and Y. C. Ong, Remnant Symmetry, Propagation and Evolution in f(T) Gravity, Phys. Rev. D **91**, 064003 (2015)
84. K. Izumi, J. A. Gu and Y. C. Ong, Acausality and Nonunique Evolution in Generalized Teleparallel Gravity, Phys. Rev. D **89**, 084025 (2014)
85. Y. C. Ong, K. Izumi, J. M. Nester and P. Chen, Problems with Propagation and Time Evolution in f(T) Gravity, Phys. Rev. D **88**, 024019 (2013)
86. K. Bamba, S. Nojiri and S. D. Odintsov, Trace-anomaly driven inflation in $f(T)$ gravity and in minimal massive bigravity, Phys. Lett. B **731**, 257 (2014)
87. K. Izumi and Y. C. Ong, Cosmological Perturbation in f(T) Gravity Revisited, JCAP **1306**, 029 (2013)
88. K. Bamba, S. Capozziello, M. De Laurentis, S. Nojiri and D. Sáez-Gómez, No further gravitational wave modes in $F(T)$ gravity, Phys. Lett. B **727**, 194 (2013)
89. K. Bamba, S. D. Odintsov and D. Sáez-Gómez, Conformal symmetry and accelerating cosmology in teleparallel gravity, Phys. Rev. D **88**, 084042 (2013)
90. K. Bamba and C. Q. Geng, Thermodynamics of cosmological horizons in $f(T)$ gravity, JCAP **1111**, 008 (2011)
91. K. Bamba, M. Jamil, D. Momeni and R. Myrzakulov, Generalized Second Law of Thermodynamics in $f(T)$ Gravity with Entropy Corrections, Astrophys. Space Sci. **344**, 259 (2013)
92. K. Bamba, C. Q. Geng and L. W. Luo, Generation of large-scale magnetic fields from inflation in teleparallelism, JCAP **1210**, 058 (2012)
93. K. Bamba, C. Q. Geng and L. W. Luo, Large-scale magnetic fields from inflation in teleparallel gravity, JPS Conf. Proc. **1**, 013123 (2014)
94. K. Bamba, R. Myrzakulov, S. D. Odintsov and L. Sebastiani, Trace-anomaly driven inflation in modified gravity and the BICEP2 result, Phys. Rev. D **90**, 043505 (2014)
95. K. Bamba, G. Cognola, S. D. Odintsov and S. Zerbini, One-loop modified gravity in a de Sitter universe, quantum-corrected inflation, and its confrontation with the Planck result, Phys. Rev. D **90**, no. 2, 023525 (2014)
96. K. Bamba, C. Q. Geng, S. Nojiri and S. D. Odintsov, Europhys. Lett. **89**, 50003 (2010)
97. K. Bamba, C. Q. Geng and S. Tsujikawa, Equilibrium thermodynamics in modified gravitational theories," Phys. Lett. B **688**, 101 (2010)
98. K. Bamba, C. Q. Geng and S. Tsujikawa, Thermodynamics in Modified Gravity Theories, Int. J. Mod. Phys. D **20**, 1363 (2011)
99. K. Bamba and C. Q. Geng, Thermodynamics in $f(R)$ gravity in the Palatini formalism, JCAP **1006**, 014 (2010)
100. K. Bamba and S. D. Odintsov, Inflation and late-time cosmic acceleration in non-minimal Maxwell-$F(R)$ gravity and the generation of large-scale magnetic fields, JCAP **0804**, 024 (2008)
101. K. Bamba, S. Nojiri and S. D. Odintsov, Inflationary cosmology and the late-time accelerated expansion of the universe in non-minimal Yang-Mills-F(R) gravity and non-minimal vector-F(R) gravity, Phys. Rev. D **77**, 123532 (2008)

Proc. Int. Conf. Relativ. Astrophys.
Pages 48-55, (2015)

Some Inhomogeneity Factors in Self-gravitating Systems

M. Sharif[a,1] **and M. Zaeem Ul Haq Bhatti**[b,1]

[1]Department of Mathematics, University of the Punjab, Quaid-e-Azam Campus, Lahore-54590, Pakistan.

Abstract This paper is aimed to investigate some physical factors which are responsible for energy density inhomogeneity in self-gravitating systems. For this purpose, we take plane symmetric spacetime in the interior which is filled with anisotropic matter in the presence of electromagnetic field. The inhomogeneity factors are explored for some particular cases of dissipative as well as non-dissipative fluids. We found that electromagnetic field increases the energy density inhomogeneity which is due to shear, anisotropy and dissipation.

Keywords Electromagnetic field; Energy density inhomogeneity; Relativistic fluids.

PACS 04.40.Dg; 04.40.Nr.

1 Introduction

Recent observations propose that matter distribution is homogeneous and isotropic at present state of the universe. But the universe was not homogeneous initially and extremely dense in certain areas. Thus, the formation of our universe at very early stages and its exact physical modeling has provoked interest of many researchers. The inhomogeneous mater density is illustrated in many ways like formation of galaxies with different sizes and fluctuation of the local density etc. Abdalla [1] discussed a model describing extremely inhomogeneous matter distribution in a certain range. Herrera [2] studied the stability of homogeneous energy density and identified physical factors responsible for energy density inhomogeneity in self-gravitating spherical star. Sharif and Yousaf discussed evolution of collapsing celestial self-gravitating systems for different viable $f(R)$ models with spherical [3], planar [4] and axial [5] geometries. In recent papers [6], we have investigated the role of different matter variables on the dynamics and inhomogeneity of energy density in plane, spherical and Szekeres symmetry with suitable matter configurations.

The magnetic field is witnessed in compact objects like neutron stars, white dwarfs or magnetized strange quark stars. Rosseland [7] studied the effects of electromagnetic field on the self-gravitating spherically symmetric stars. The general relativistic electromagnetic effects are easily observed through experiments which involve gyroscopic rings [8]. Forder [9] studied the electromagnetic effects through transmission line gyroscopes with certain types of general relativistic fields. It is well-known that Fermi gas under the influence of magnetic field produces pressure anisotropy, sometimes referred as fluid anisotropy [10].

In the last decade, theoretical advances indicate that deviations from perfect fluid models in many systems play a significant role in describing their properties [11, 12]. To analyze the stability of compact objects in the scenario of high red-shift, the role of anisotropic pressure has extensively been studied [13]-[15]. Karmakar *et al.* [16] investigated physical properties of cold compact star by taking anisotropic pressure in Vaidya-Tikekar model [17]. Many phenomena have been classified which yield pressure anisotropy in star models [18]-[21]. The study of general anisotropic configuration has been carried out by different authors [22]-[25].

Gravitational collapse is exceptionally dissipative phenomenon which has significant effects in the dynamics of self-gravitating compact objects. Diffusion (valid in final stages) and streaming out (corresponds to initial stages) are two limiting cases in the collapse scenario. Oppenheimer and Snyder [26] proposed the first mathematical collapsing picture of dust cloud and concluded its final fate as a black hole. Israel and Stewart [27] con-

[a]e-mail: msharif.math@pu.edu.pk
[b]e-mail: mzaeem.math@pu.edu.pk

structed transport equation for heat flux in diffusion approximation. Lake and Hellaby [28] examined the counterpart of Oppenheimer-Snyder problem by providing the end state of radiating collapsing sphere as a naked singularity. Herrera and Santos [29] discussed the dynamics of dissipative collapse by taking spherical star and explored its astrophysical applications. The collapsing phenomenon has also been studied in the context of planar, quasi-spherical and cylindrical symmetries [30]-[36].

Di Prisco *et al.* [37] investigated electromagnetic effects on radiating spherically symmetric collapsing star by coupling dynamical-transport equations. Sharif and Bashir [38] examined the effects of electromagnetic field on the energy density inhomogeneity of spherical star. In recent papers [39]-[41], we have explored dynamics of charged collapsing cylindrical geometry and analyzed its stability using perturbation technique. We have also studied collapse of charged plane and spherically symmetric self-gravitating stars as well as with axial symmetry by taking anisotropic and radiating matter distributions [42]-[46]. Sharif and Yousaf [47]-[50] discussed dynamical properties of adiabatic as well as non-adiabatic collapsing bodies with weak-field approximation in the presence of electromagnetism.

The aim of this paper is to investigate the effects of electromagnetic field with different physical factors on the energy density inhomogeneity in planar symmetry using non-dissipative and dissipative fluids. In non-dissipative case, we discuss dust, locally isotropic and anisotropic matter while in dissipative fluid, a particular case of geodesic dust cloud is considered. The paper is organised in the following format. In the next section, we develop some fundamental variables and field equations in the presence of electromagnetic field. The conservation laws with the evolution equations for the Weyl tensor and a transport equation for heat flux are also formulated. Section **3** is devoted to identify the electromagnetic effects on the emergence of energy density inhomogeneity by considering some particular cases. Section **4** will conclude our results.

2 Fundamental Variables and Field Equations

This section formulates some basic quantities to analyze inhomogeneities in charged self-gravitating planar geometry. The non-static plane symmetric spacetime is

$$ds^2=-A^2dt^2+B^2\left(dx^2+dy^2\right)+C^2dz^2, \tag{1}$$

here $A,\ B$ and C are functions of t and z. The matter distribution inside the plane symmetry is assumed to be imperfect given by

$$T_{\alpha\beta}=(\mu+P_\perp)V_\alpha V_\beta+P_\perp g_{\alpha\beta}+(P_z-P_\perp)\chi_\alpha\chi_\beta+q_\alpha V_\beta +V_\alpha q_\beta+\epsilon l_\alpha l_\beta, \tag{2}$$

where $\mu,\ \epsilon,\ q_\alpha, P_z,\ P_\perp$, and V_α are the energy density, radiation density, heat flux, anisotropic pressures and four velocity, respectively. Also, l^α and χ^α are null four-vector in z-direction and unit four-vector, respectively. These four-vectors in comoving coordinates are chosen such that Eq.(1) satisfies

$$\chi^\alpha=C^{-1}\delta^\alpha_3,\quad q^\alpha=qC^{-1}\delta^\alpha_3,\quad V^\alpha=A^{-1}\delta^\alpha_0, \tag{3}$$

$$l^\alpha=A^{-1}\delta^\alpha_0+C^{-1}\delta^\alpha_3, \tag{4}$$

where q is a function of t and z. These quantities satisfy

$$V^\alpha V_\alpha=-1,\quad \chi^\alpha V_\alpha=0\quad \chi^\alpha\chi_\alpha=1,$$
$$l^\alpha l_\alpha=0,\quad l^\alpha V_\alpha=-1,\quad V^\alpha q_\alpha=0.$$

The energy-momentum tensor of electromagnetic field is [51]

$$S_{\alpha\beta}=\frac{1}{4\pi}\left(F^\gamma_\alpha F_{\beta\gamma}-\frac{1}{4}F^{\gamma\delta}F_{\gamma\delta}g_{\alpha\beta}\right),$$

where $F_{\alpha\beta}=-\phi_{\alpha,\beta}+\phi_{\beta,\alpha}$ is the strength field tensor while the four potential is represented by ϕ_α. This electromagnetic field must obey the Maxwell field equations given as

$$F^{\alpha\beta}_{\ \ ;\beta}=\mu_0 J^\alpha,\quad F_{[\alpha\beta;\gamma]}=0, \tag{5}$$

here $\mu_0=4\pi$ and J_α represent magnetic permeability and four-current, respectively. The four potential and four-current in comoving coordinates are

$$\phi^\alpha=\phi\delta^\alpha_0,\quad J^\alpha=\xi V^\alpha,$$

where $\phi,\ \xi$ indicate the scalar potential and charge density, respectively, both are functions of t and z. Using these in Eq.(5), the non-zero components of the Maxwell field equations lead to

$$\frac{\partial^2\phi}{\partial z^2}-\left(\frac{A'}{A}+\frac{C'}{C}-\frac{2B'}{B}\right)\frac{\partial\phi}{\partial z}=\xi\mu_0AC^2, \tag{6}$$

$$\frac{\partial^2\phi}{\partial t\partial z}-\left(\frac{\dot{A}}{A}+\frac{\dot{C}}{C}-\frac{2\dot{B}}{B}\right)\frac{\partial\phi}{\partial z}=0. \tag{7}$$

Integration of Eq.(6) with respect to z yields

$$\phi'=\frac{\mu_0 s(z)AC}{B^2},\quad \text{where}\quad s(z)=\int_0^z\xi CB^2dz, \tag{8}$$

which identically satisfies Eq.(7). Using this value in the Maxwell field tensor, the non-vanishing components of

Einstein-Maxwell field equations (i.e. $G_{\alpha\beta}=8\pi(T_{\alpha\beta}+S_{\alpha\beta})$) lead to the following set of equations

$$8\pi\tilde{\mu}A^2+\left(\frac{\mu_0 sA}{B^2}\right)^2=\frac{\dot{B}}{B}\left(\frac{2\dot{C}}{C}+\frac{\dot{B}}{B}\right)-\left(\frac{A}{C}\right)^2\times\left[\frac{2B''}{B}-\left(\frac{2C'}{C}-\frac{B'}{B}\right)\frac{B'}{B}\right], \tag{9}$$

$$-8\pi\tilde{q}AC=-2\left(\frac{\dot{B}'}{B}-\frac{A'\dot{B}}{AB}-\frac{B'\dot{C}}{BC}\right), \tag{10}$$

$$8\pi P_{\perp}B^2+\left(\frac{\mu_0 s}{B}\right)^2=-\left(\frac{B}{A}\right)^2\left[\frac{\ddot{B}}{B}-\frac{\ddot{C}}{C}-\frac{\dot{A}}{A}\left(\frac{\dot{B}}{B}+\frac{\dot{C}}{C}\right)+\frac{\dot{B}\dot{C}}{BC}\right]+\left(\frac{B}{C}\right)^2\left[\frac{A''}{A}+\frac{B''}{B}-\frac{A'}{A}\left(\frac{C'}{C}-\frac{B'}{B}\right)-\frac{B'C'}{BC}\right], \tag{11}$$

$$8\pi\tilde{P}_z C^2-\left(\frac{\mu_0 sC}{B^2}\right)^2=\left(\frac{C}{A}\right)^2\left[\frac{2\dot{A}\dot{B}}{AB}-\frac{2\ddot{B}}{B}-\left(\frac{\dot{B}}{B}\right)^2\right]+\left(\frac{B'}{B}\right)^2+\frac{2A'B'}{AB}, \tag{12}$$

here we assume $\tilde{\mu}=\mu+\epsilon$, $\tilde{P}_z=P_z+\epsilon$, $\tilde{q}=q+\epsilon$, while prime and dot stand for z and t differentiations, respectively.

The irrotational fluid distribution is described by three kinematical quantities, i.e., expansion scalar, four-acceleration and shear tensor defined by

$$\Theta=V^{\alpha}_{;\alpha},\quad a_{\alpha}=V_{\alpha;\beta}V^{\beta},$$
$$\sigma_{\alpha\beta}=V_{(\alpha;\beta)}+a_{(\alpha}V_{\beta)}-\frac{1}{3}\Theta h_{\alpha\beta},$$

with $h_{\alpha\beta}=g_{\alpha\beta}+V_{\alpha}V_{\beta}$ as a projection tensor. The non-zero components of these quantities are

$$\Theta=\frac{1}{A}\left(2\frac{\dot{B}}{B}+\frac{\dot{C}}{C}\right),\quad a_3=\frac{A'}{A},\quad a^2=a^{\alpha}a_{\alpha}=\left(\frac{A'}{AC}\right)^2,$$
$$\sigma^2=\frac{1}{2}\sigma_{\alpha\beta}\sigma^{\alpha\beta}=\frac{1}{9}F^2\quad\text{with}\quad F=\frac{1}{A}\left(-\frac{\dot{B}}{B}+\frac{\dot{C}}{C}\right). \tag{13}$$

A relation between heat flux and kinematical quantities is obtained using Eqs.(10) and (13) as follows

$$4\pi\tilde{q}C=\frac{1}{3}(\Theta-F)'-F\frac{B'}{B}.$$

The decomposition of the Weyl tensor ($C_{\alpha\mu\beta\nu}$) into two tensors leads to its electric and magnetic components. Due to symmetry of the problem, the magnetic part does not exist in planar geometry while the electric part is

$$E_{\alpha\beta}=C_{\alpha\mu\beta\nu}V^{\mu}V^{\nu},$$

whose non-vanishing components lead to

$$E_{11}=\frac{1}{3}B^2\varepsilon=E_{22},\quad E_{33}=-\frac{2}{3}C^2\varepsilon,$$

where

$$\varepsilon=-\frac{1}{2A^2}\left[\frac{\dot{B}^2}{B^2}-\frac{\dot{A}\dot{C}}{AC}+\frac{\ddot{C}}{C}+\frac{\dot{A}\dot{B}}{AB}-\frac{\ddot{B}}{B}-\frac{\dot{B}\dot{C}}{BC}\right]-\frac{1}{2C^2}\left[\frac{A'B'}{AB}-\frac{B'^2}{B^2}+\frac{A'C'}{AC}-\frac{B'C'}{BC}-\frac{A''}{A}+\frac{B''}{B}\right]. \tag{14}$$

Alternatively, it can be written by using unit four-vector and projection tensor as

$$E_{\alpha\beta}=\varepsilon(\chi_{\alpha}\chi_{\beta}-\frac{1}{3}h_{\alpha\beta}).$$

The mass function for plane symmetry [52] under the effects of electromagnetic field becomes

$$m(t,z)=\frac{B}{2}\left(\frac{s^2\mu_0^2}{B^2}+\frac{\dot{B}^2}{A^2}-\frac{B'^2}{C^2}\right). \tag{15}$$

We define the proper time derivative as $D_T=\frac{1}{A}\frac{\partial}{\partial t}$ so that the variation of the areal radius known as areal velocity provides $U=D_T B=\frac{\dot{B}}{A}$. Making use of this in the above equation, it follows that

$$E\equiv\frac{B'}{C}=\left[U^2+\frac{s^2\mu_0^2}{B^2}-\frac{2m}{B}\right]^{1/2}.$$

Using Eqs.(9), (11), (12) and (15) in (14), we obtain a relationship between the Weyl tensor and matter variables, i.e., energy density, anisotropic pressure and electric charge as follows

$$\varepsilon=4\tilde{\mu}\pi+\frac{3s^2\mu_0^2}{B^4}-4\pi\Pi-\frac{3m}{B^3}, \tag{16}$$

where $\Pi=P_z-P_{\perp}+\epsilon$. Differentiation of Eq.(15) with z and t and making use of Eqs.(9), (10) and (12), we have

$$m'=4\pi\left(\tilde{\mu}B'+\tilde{q}UC\right)B^2+\frac{s^2\mu_0^2}{B^2}-\frac{ss'\mu_0^2}{B}, \tag{17}$$

$$\dot{m}=-4\pi\left(\tilde{P}_z\dot{B}+\tilde{q}\frac{AB'}{C}\right)B^2. \tag{18}$$

Integrating Eq.(17) with some manipulation, it follows that

$$\frac{3m}{B^3}=4\pi\tilde{\mu}-\frac{4\pi}{B^3}\int_0^z B^3\tilde{\mu}'dz+\frac{4\pi}{B^3}\int_0^z 3B^2UC\tilde{q}dz+\frac{3\mu_0^2}{B^3}\left[\frac{s^2}{2B}+\int_0^z\frac{B's^2}{2B^2}dz\right]. \tag{19}$$

Using above equation in Eq.(16), we obtain

$$\varepsilon=\frac{3\mu_0^2s^2}{2B^4}-4\pi\Pi+\frac{4\pi}{B^3}\int_0^z B^3\tilde{\mu}'dz -\frac{3\mu_0^2}{B^3}\int_0^z\frac{B's^2}{2B^2}dz-\frac{4\pi}{B^3}\int_0^z 3B^2UC\tilde{q}dz. \quad (20)$$

This shows a relation between matter variables and the Weyl tensor.

The contracted Bianchi identities imply the equation of motion for the whole matter distribution, i.e., $T^{\alpha\beta}_{\ \ ;\beta}=0$, yielding

$$\dot{\tilde{\mu}}+\frac{2\dot{B}}{B}(\tilde{\mu}+P_\perp)+\frac{\dot{C}}{C}(\tilde{\mu}+\tilde{P}_z)+\frac{A\tilde{q}'}{C} +2\frac{\tilde{q}A}{C}\left(\frac{A'}{A}+\frac{B'}{B}\right)=0, \quad (21)$$

$$\dot{\tilde{q}}+\tilde{P}_z'\frac{A}{C}+2\tilde{q}\frac{(BC)\dot{}}{BC}+(\tilde{\mu}+\tilde{P}_z)\frac{A'}{A}+2(\tilde{P}_z-P_\perp)\frac{AB'}{CB} -\frac{ss'\mu_0^2}{4\pi B^4C}=0. \quad (22)$$

In addition to the conservation law, our system will strictly rely on two differential equations that will play a major role to construct inhomogeneity factors relating the Weyl tensor to different physical variables. Using the procedure [53], these equations are obtained from Eq.(16) as follows

$$[4\pi(\tilde{\mu}-\Pi)-\varepsilon]'=\frac{3B'}{B}[\varepsilon+4\pi\Pi]+\frac{4s\mu_0^2}{B^4}\left(\frac{sB'}{B}-3s'\right) +12\pi\frac{\dot{B}C}{AB}\tilde{q}, \quad (23)$$

$$[4\pi(\tilde{\mu}-\Pi)-\varepsilon]\dot{}=-12\pi\tilde{q}\frac{B'A}{BC}+3\mu_0^2s^2\frac{\dot{B}}{B^5}-\frac{3\dot{B}}{B} \times(4\pi(\tilde{\mu}+P_\perp)-\varepsilon). \quad (24)$$

In order to investigate the transportation of heat as well as mass and to interpret the action of fluid variables, we use transport equation. The transport equation for dissipative fluids in diffusion approximation ($\tilde{q}=q,\ \epsilon=0$) is represented by second order partial differential equation derived by Muller-Israel-Stewart [54]-[56] as

$$\tau h^{\alpha\beta}V^\gamma q_{\beta;\gamma}=-Kh^{\alpha\beta}(T_{,\beta}+Ta_\beta)-q^\alpha -\frac{1}{2}KT^2\left(\frac{\tau V^\beta}{KT^2}\right)_{;\beta}q^\alpha. \quad (25)$$

Here K, T and τ represent thermal conductivity, temperature and relaxation time (time required for a perturbed system to come spontaneously to its equilibrium state), respectively. The only independent component of Eq.(25) leads to

$$\dot{q}\tau=-\frac{K}{C}(AT)'-qA-\frac{1}{2}T^2qK\left(\frac{\tau}{T^2K}\right)\dot{}-\frac{1}{2}\tau q\Theta.$$

For truncated dissipative theory, i.e., when the last term on the right hand side of Eq.(25) vanishes and hence its non-zero component yields

$$\dot{q}\tau=-\frac{K}{C}(AT)'-qA. \quad (26)$$

This shows that electromagnetic field has no effect on the transportation of heat flux.

3 Inhomogeneities in Matter Configuration

This section explores different factors in the fluid distribution which are responsible for energy density inhomogeneity. We also discuss stability of energy density inhomogeneity for some particular cases.

3.1 Non-Dissipative Charged Dust Cloud

We consider $q=\epsilon=P_\perp=P_z=0$ so that Eq.(22) shows matter configuration to be geodesic, hence we take $A=1$ without loss of any generality. In this scenario, the two equations for the Weyl tensor (23) and (24) become

$$[4\pi\mu-\varepsilon]'=\frac{3B'}{B}\varepsilon+\frac{4s\mu_0^2}{B^4}\left(\frac{sB'}{B}-3s'\right), \quad (27)$$

$$[4\pi\mu-\varepsilon]\dot{}=-\frac{3\dot{B}}{B}(4\pi\mu-\varepsilon)+3\mu_0^2s^2\frac{\dot{B}}{B^5}. \quad (28)$$

For $s=0$, we recover the uncharged case. Equation (27) implies that $\varepsilon=0=s\Leftrightarrow\mu'=0$ which shows inhomogeneity in the energy density not only due to the Weyl tensor but also due to the electromagnetic field. If the Weyl tensor together with electric charge vanishes then it will lead to homogeneous matter distribution. When $\mu'=0$, we obtain

$$\varepsilon=-\frac{1}{B^3}\int_0^z\frac{4s\mu_0^2}{B}\left(\frac{sB'}{B}-3s'\right),$$

where the integration function is evaluated at $\varepsilon(t,0)=0$. This equation indicates that inhomogeneity in density distribution suggest the existence of ε in the presence of electromagnetic field. Making use of the shear scalar (13) and the first conservation law (21) in Eq.(28), it follows that

$$\dot{\varepsilon}+\frac{3\dot{B}}{B}\varepsilon=-4\pi\mu AF-3\mu_0^2s^2\frac{\dot{B}}{B^5}.$$

Integration of the above equation leads to

$$\varepsilon=\frac{3\mu_0^2s^2}{B^4}-\frac{1}{B^3}\int_0^t 4\pi\mu FAB^3dt, \quad (29)$$

here the function of integration is found at $\varepsilon(0,z)=0$. An evolution equation for the Weyl tensor is obtained through Raychaudhuri equation using the kinematical quantities as

$$\varepsilon=\dot{F}+\frac{F^2}{3}+\frac{2}{3}F\Theta. \tag{30}$$

It shows that in the absence of shear scalar, the system will be conformally flat while the conformal flatness does not imply the shear-free case as the Weyl tensor is affected by the electric charge seen from Eq.(29).

3.2 Non-Dissipative Charged Isotropic Fluid

In this case, we take isotropic pressure, i.e., $P_z=P=P_\perp$ by increasing complexity in the previous case. Consequently, the equations for the Weyl tensor given in Eqs.(23) and (24) yield

$$[4\pi\mu-\varepsilon]^{\cdot}=-\frac{3\dot{B}}{B}\left[4\pi(\mu+P)-\varepsilon\right]+3\mu_0^2s^2\frac{\dot{B}}{B^5}, \tag{31}$$

$$[4\pi\mu-\varepsilon]'=\frac{3B'}{B}\varepsilon+\frac{4s\mu_0^2}{B^4}\left(\frac{sB'}{B}-3s'\right). \tag{32}$$

Equation (32) is exactly the same as we obtained in the previous case for charged dissipative dust. As a result, the behavior for inhomogeneity factor will be the same and the Weyl tensor does not vanish in the presence of electromagnetic field. Thus the problem of stability of energy density homogeneity reduces to the stability of conformal flatness which is only possible in the absence of electromagnetic field. Using the shear scalar from Eq.(13) and first equation of motion from Eq.(21) in (31), we obtain

$$\dot{\varepsilon}+\frac{3\dot{B}}{B}\varepsilon=-4\pi AF(P+\mu)-3\mu_0^2s^2\frac{\dot{B}}{B^5}, \tag{33}$$

whose integration leads to

$$\varepsilon=\frac{3\mu_0^2s^2}{B^4}-\frac{1}{B^3}\int_0^t 4\pi AFB^3(P+\mu)dt.$$

In the absence of isotropic pressure, it reduces to Eq.(29) for the dust case. Moreover, the evolution equation through Raychaudhuri equation using kinematical quantities turns out to be

$$\varepsilon=\frac{a'}{C}-\frac{\dot{F}}{A}-\frac{F^2}{3}-a^2-a\frac{B'}{BC}-\frac{2}{3}F\Theta. \tag{34}$$

For zero shear scalar ($F=0$), the solution of Eq.(33) becomes

$$\varepsilon=\frac{3\mu_0^2s^2}{B^4}. \tag{35}$$

It appears that the Weyl tensor does not vanish at any time t. This shows that the conformal flatness is destroyed due to the presence of electromagnetic field as the shear-free condition does not lead to the conformal flatness (as obvious from Eq.(34)) and vice versa, unlike the charged free case. The system will be conformally flat only in the absence of electric charge and shear-free condition.

3.3 Non-Dissipative Anisotropic Fluid

Here we deal with the role of anisotropic pressure on the inhomogeneity in the matter distribution with zero dissipation. We take $q=0=\epsilon$ so that Eqs.(23) and (24) reduce to

$$[4\pi(\mu-\Pi)-\varepsilon]^{\cdot}=3\mu_0^2s^2\frac{\dot{B}}{B^5}-3\frac{\dot{B}}{B}[4\pi(P_\perp+\mu)-\varepsilon], \tag{36}$$

$$[4\pi(\mu-\Pi)-\varepsilon]'=\frac{4s\mu_0^2}{B^4}\left(\frac{sB'}{B}-3s'\right)+3\frac{B'}{B}[\varepsilon+4\pi\Pi]. \tag{37}$$

When we compare with the previous cases, we find that Weyl tensor with electromagnetic effects is not the only quantity responsible for the inhomogeneous matter distribution but anisotropic pressure also plays a key role. In fact, a linear combination of the quantity $\varepsilon+4\pi\Pi+\frac{s^2\mu_0^2}{B^4}$ follows the density inhomogeneity. It can easily be found from Eq.(37) that $\varepsilon+4\pi\Pi=0=s$ yields $\mu'=0$. When we take $\mu'=0$ then Eq.(37) turns out to be

$$\left[-4\pi\Pi+\frac{s^2\mu_0^2}{B^4}-\varepsilon\right]'+3\frac{\dot{B}}{B}\left[-4\pi\Pi+\frac{s^2\mu_0^2}{B^4}-\varepsilon\right]=\frac{s\mu_0^2}{B^4}\times\left(\frac{3sB'}{B}-10s'\right). \tag{38}$$

Making use of Eqs.(13) and (21) in (36), it follows that

$$\left[-4\pi\Pi+\frac{s^2\mu_0^2}{B^4}-\varepsilon\right]^{\cdot}+3\frac{\dot{B}}{B}\left[-4\pi\Pi+\frac{s^2\mu_0^2}{B^4}-\varepsilon\right]=4\pi(P_z+\mu)AF+\frac{2s^2\mu_0^2\dot{B}}{B^5}-8\pi\Pi\frac{\dot{B}}{B}. \tag{39}$$

These represent evolution equations showing the quantity responsible for density inhomogeneity.

Now we relate this quantity to some scalar function which will be identified as an inhomogeneity factor. For this purpose, we define the dual of the Riemann tensor as follows

$$X_{\alpha\beta}=^*R^*_{\alpha\sigma\beta\zeta}V^\sigma V^\zeta=\frac{1}{2}\eta^{\varepsilon\rho}{}_{\alpha\sigma}R^*_{\epsilon\rho\beta\zeta}V^\sigma V^\zeta, \tag{40}$$

where $R^*_{\alpha\beta\sigma\zeta} = \frac{1}{2}\eta_{\varrho\varsigma\sigma\zeta}R^{\varrho\varsigma}{}_{\alpha\beta}$. The tensor $X_{\alpha\beta}$ can be decomposed in its trace free and trace components as

$$X_{\alpha\beta} = X_{TF}\left(\chi_\alpha\chi_\beta - \frac{1}{3}h_{\alpha\beta}\right) + \frac{1}{3}X_T h_{\alpha\beta}. \quad (41)$$

Using Eqs.(4), (9), (11), (12) and (14) in (40) and (41), we find the trace and trace free scalar parts as follows

$$X_T = 8\pi\mu + \frac{\mu_0^2 s^2}{B^4}, \quad X_{TF} = -\varepsilon - 4\pi\Pi + \frac{\mu_0^2 s^2}{B^4}. \quad (42)$$

Substituting the above equation in Eqs.(38) and (39), the evolution equations for density inhomogeneity in terms of scalar X_{TF} turn out to be

$$\dot{X}_{TF} + 3\frac{\dot{B}}{B}X_{TF} = -8\pi\Pi\frac{\dot{B}}{B} + \frac{2s^2\mu_0^2\dot{B}}{B^5} + 4\pi(\mu + P_z)AF,$$
$$X'_{TF} + \frac{3B'}{B}X_{TF} = \frac{s\mu_0^2}{B^4}\left(\frac{3B'}{B} - 10s'\right),$$

which can be integrated to find X_{TF} as follows

$$X_{TF} = \frac{1}{B^3}\int_0^t [4\pi(\mu + P_z)AFB^3 - 8\pi\Pi\frac{\dot{B}}{B^2}]dt + \frac{2s^2\mu_0^2}{B^4},$$
$$X_{TF} = \frac{1}{B^3}\int_0^z \frac{s\mu_0^2}{B}\left(\frac{3B'}{B} - 10s'\right)dz.$$

This indicates that homogeneity of the system is affected by the shear scalar, pressure anisotropy and electromagnetic field. Moreover, electromagnetic field increases the inhomogeneity in the system.

3.4 Dissipative Charged Dust Cloud

Finally, we investigate the effects of dissipating quantities in the inhomogeneity factors for a special case of dust cloud. We take matter distribution along the geodesic by choosing $A = 1$ with $P_\perp = 0 = P_z$. In this scenario, Eqs.(23) and (24) reduce to

$$[4\pi\tilde{\mu} - \varepsilon]^{\cdot} = 3\mu_0^2 s^2\frac{\dot{B}}{B^5} - 12\pi\tilde{q}\frac{B'A}{BC} - 3\frac{\dot{B}}{B}(4\pi\tilde{\mu} - \varepsilon), \quad (43)$$

$$[4\pi\tilde{\mu} - \varepsilon]' = \frac{4s\mu_0^2}{B^4}\left(\frac{sB'}{B} - 3s'\right) + 12\pi\tilde{q}\frac{\dot{B}C}{BA} + 3\frac{B'}{B}\varepsilon. \quad (44)$$

When we take $\tilde{\mu}' = 0$, the inhomogeneity factor from Eq.(44) is defined as

$$\xi \equiv \varepsilon + \frac{12\pi}{B^3}\int_0^z \tilde{q}\dot{B}B^2C dz + \frac{1}{B^3}\int_0^z \frac{4s\mu_0^2}{B}\left(\frac{sB'}{B} - 3s'\right)dz, \quad (45)$$

and consequently $\xi = 0 \Leftrightarrow \tilde{\mu}' = 0$ which shows that the inhomogeneity factor is affected by electric charge.

The evolution equation for ξ can be evaluated by using Eqs.(13) and (21) in (43) as

$$-4\pi\tilde{\mu}F + 4\pi\frac{\tilde{q}B'}{BC} - 3\mu_0^2 s^2\frac{\dot{B}}{B^5} - \frac{3\dot{B}}{B}\xi - 4\pi\frac{\tilde{q}'}{C} = \dot{\xi} - \frac{\dot{\chi}}{B^3},$$

with $\chi = 12\pi\int_0^z \tilde{q}\dot{B}CB^2dz$. The general solution of the above equation yields

$$\xi = \frac{4\pi}{B^3}\int_0^t \left(\tilde{q}\frac{B^2B'}{C} - \tilde{\mu}FB^3 - \tilde{q}'\frac{B^3}{C} - \frac{3\mu_0^2 s^2\dot{B}}{B^2} + \dot{\chi}\right)dt, \quad (46)$$

which indicates the effects of shear, dissipation and electric charge on the inhomogeneity factor of charged dissipative dust fluid.

To analyze the role of these factors, we discuss the shear-free case for which Eq.(13) implies that $B = zC$. Making use of this in Eq.(46), we obtain

$$\xi = \frac{4\pi}{B^3}\int_0^t \left(\tilde{q}zBB' - \tilde{q}'zB^2 - \frac{3\mu_0^2 s^2\dot{B}}{B^2} + \dot{\chi}\right)dt, \quad (47)$$

with $\chi = 12\pi\int_0^z \tilde{q}\frac{\dot{B}B^3}{z}dz$. Now, we study the relaxation effects on the evolution of inhomogeneity factor ξ through transport equation. In the diffusion approximation, i.e., when $\epsilon = 0$, we have $\tilde{q} = q,\ \mu = \tilde{\mu}$, hence Eq.(22) turns out to be

$$\dot{q} + \frac{4q}{3}\Theta - \frac{ss'\mu_0^2}{4\pi B^4 C} = 0.$$

Comparing the above equation with the truncated transport equation (26), we obtain

$$q = \frac{-ss'\mu_0^2\tau}{4\pi B^4 C\left(1 - \frac{4}{3}\Theta\tau\right)} - \frac{KT'}{C\left(1 - \frac{4}{3}\Theta\tau\right)}.$$

Using the shear-free condition, i.e., $B = zC$, it follows that

$$q = \frac{-ss'z\mu_0^2\tau}{4\pi B^5\left(1 - \frac{4}{3}\Theta\tau\right)} - \frac{zKT'}{B\left(1 - \frac{4}{3}\Theta\tau\right)}.$$

Using this value of heat flux in the evolution equation (47), we obtain the inhomogeneity factor in terms of relaxation time τ. Thus, one can analyze the effect of τ with electromagnetic field on the evolution of ξ.

4 Conclusion

In this paper, we have explored the effects of electromagnetic field on the energy density inhomogeneity for non-static plane symmetric spacetime with radiating anisotropic matter configuration. We have formulated a relationship between the fluid parameters and the Weyl

scalar to analyse the effects of electric charge. A couple of equations for conservation laws have been developed from the contracted Bianchi identities and found that one of these equations is affected by electromagnetic field. The evolution equations for the Weyl tensor are developed which indicate different aspects of energy density inhomogeneity. To examine the role played by heat radiation, we have developed a transport equation in diffusion approximation. The main results are summarized as follows.

- For non-dissipative charged dust cloud, it is found that the Weyl tensor is not the only quantity to control energy density inhomogeneity but it also depends on the electric charge. Moreover, the electromagnetic field affects the conformal flatness of the planar geometry. In the absence of shear scalar, we find that the system will be conformally flat as seen from Eq.(30) but the converse is not true due the disturbance of conformal flatness in the presence of electromagnetic field as seen from Eq.(29).
- When the isotropic pressure is included in the charged dust cloud, the effects on the energy density inhomogeneity will remain the same. However, the zero shear scalar does not lead to the conformal flatness and vice versa as indicated in Eqs.(34) and (35). Thus the stability problem of density inhomogeneity is converted to the stability of conformal flatness which is affected by the electromagnetic field.
- In the case of anisotropic pressure, the inhomogeneities in the matter distribution are related to the anisotropic pressure, shear scalar and particularly electric charge. A specific scalar function has been evaluated as an inhomogeneity factor and identified as one of the structure scalars given in Eq.(42).
- For dissipative geodesic dust, the inhomogeneity factor is the combination of geometrical and physical variables with the effects of electromagnetic field and is defined by ξ in Eq.(46). We also show how the relaxation effects on the inhomogeneity of dissipative geometry can be analyzed through the evolution of ξ.

It is worth mentioning that all our results reduce to charge free case when we take $s = 0$.

References

1. E. Abdalla and B.M.H.C. Chirenti: Phys. A **337**(2004)117.
2. L. Herrera: Int. J. Mod. Phys. D. **20**(2011)1689.
3. M. Sharif and Z. Yousaf: Astrophys. Space Sci. **351**(2014)351; **352**(2014)321; ibid. **354**(2014)431; ibid. **354**(2014)471; ibid. **354**(2014)481; **355**(2014)317.
4. M. Sharif and Z. Yousaf: Eur. Phys. J. C **75**(2015)58.
5. M. Sharif and Z. Yousaf: J. Cosmol. Astropart. Phys. **06**(2014)019; Astrophys. Space Sci. **352**(2015)943; Eur. Phys. J. C **75**(2015)194.
6. M. Sharif and M.Z. Bhatti: Mod. Phys. Lett. A **29**(2014)1450094; ibid. 1450129; ibid. 1450165; Phys. Scr. **89**(2014)084004; Int. J. Mod. Phys. D **23**(2014)1450085; ibid. **24**(2015)1550014; Astrophys. Space Sci. **352**(2014)883; ibid. **355**(2015)389; J. Exp. Theor. Phys. **147**(2015)942.
7. S. Rosseland: Mon. Not. R. Astron. Soc. **84**(1924)720.
8. J. Anandan and L. Stodolsky: Phys. Rev. Lett. **50**(1983)1730.
9. P.W. Forder: Class. Quantum Grav. **3**(1986)1125.
10. C.W. Misner and H.S. Zapolsky: Phys. Rev. Lett. **12**(1964)635.
11. M. Ruderman: Ann. Rev. Astron. Astrophys. **10**(1972)427.
12. V. Canuto: Annu. Rev. Astron. Astrophys. **12**(1974)167.
13. M.K. Mak and T. Harko: Proc. R. Soc. London A **459**(2003)393.
14. K. Dev and M. Gleiser: Int. J. Mod. Phys. D **13**(2004)1389.
15. M. Chaisi and S.D. Maharaj: Gen. Relativ. Gravit. **37**(2005)1177.
16. S. Karmakar, S. Mukherjee, R. Sharma and S.D. Maharaj: Pramana-J. Phys. **68**(2007)881.
17. P.C. Vaidya and R. Tikekar: J. Astrophys. Astron. **3**(1982)325.
18. R.F. Sawyer: Phys. Rev. Lett. **29**(1972)382.
19. P.S. Letelier: Phys. Rev. D **22**(1980)807.
20. L. Herrera and N.O. Santos: Phys. Rep. **286**(1997)53.
21. L. Herrera and N.O. Santos: Astrophys. J. **438**(1995)308.
22. H. Heintzmann and W. Hillebrandt: Astron. Astrophys. **38**(1975)51.
23. B.W. Stewart: J. Phys. A **15**(1982)2419.
24. S. Bayin: Phys. Rev. D **26**(1982)1262.
25. M.K. Gokhroo and A.L. Mehra: Gen. Relativ. Gravit. **26**(1994)75.
26. J.R. Oppenheimer and H. Snyder: Phys. Rev. **56**(1939)455.
27. W. Israel and J. Stewart: Phys. Lett. A **58**(1976)213.
28. K. Lake and C. Hellaby: Phys. Rev. D **24**(1981)3019.
29. L. Herrera and N.O. Santos: Phys. Rev. D **70**(2004)084004.
30. K. Nakao and Y. Morisawa: Class. Quantum Gravit. **21**(2004)2101.
31. S. Chakraborty and U. Debnath: Mod. Phys. Lett. A **20**(2005)1451.
32. S. Chakraborty, S. Chakraborty and U. Debnath: Int. J. Mod. Phys. D **16**(2007)833.
33. A. Di Prisco, L. Herrera, M.A.H. MacCallum and N.O. Santos: Phys. Rev. D **80**(2009)064031.
34. M. Sharif and Z. Yousaf: Int. J. Mod. Phys. D **21**(2012)1250095.
35. M. Sharif and Z. Yousaf: Chin. Phys. Lett. **29**(2012)050403; Gen. Relativ. Gravit. **47**(2015)48; Can. J. Phys. **93**(2015)1.
36. M. Sharif and Z. Yousaf: Can. J. Phys. **90**(2012)865; Mon. Not. R. Soc. **440**(2014)3479; Astrophys. Space Sci. **357**(2015)49.
37. A. Di Prisco, L. Herrera, G. Le Denmat, M.A.H. MacCallum and N.O. Santos: Phys. Rev. D **76**(2007)064017.
38. M. Sharif and N. Bashir: Gen. Relativ. Gravit. **44**(2012)1725.
39. M. Sharif and M.Z. Bhatti: Gen. Relativ. Gravit. **44**(2012)2811;

40. M. Sharif and M.Z. Bhatti: J. Cosmol. Astropart. Phys. **10**(2013)056;
41. M. Sharif and M.Z. Bhatti: Phys. Lett. A **378**(2014)469.
42. M. Sharif and M.Z. Bhatti: Mod. Phys. Lett. A **27**(2012)1250141.
43. M. Sharif and M.Z. Bhatti: Astrophys. Space. Sci. **347**(2013)337.
44. M. Sharif and M.Z. Bhatti: Astrophys. Space. Sci. **349**(2014)995.
45. M. Sharif and M.Z. Bhatti: J. Cosmol. Astropart. Phys. **11**(2013)014.
46. M. Sharif and M.Z. Bhatti: Astropart. Phys. **56**(2014)35.
47. M. Sharif and Z. Yousaf: Mon. Not. R. Astron. Soc. **432**(2013)264.
48. M. Sharif and Z. Yousaf: Mon. Not. R. Astron. Soc. **434**(2013)2529.
49. M. Sharif and Z. Yousaf: Phys. Rev. D **88**(2013)024020.
50. M. Sharif and Z. Yousaf: Astropart. Phys. **56**(2014)19.
51. M. Sharif and M.Z. Bhatti: Can. J. Phys. **90**(2012)1233.
52. T. Zannias: Phys. Rev. D **41**(1990)3252.
53. G.F.R. Ellis: Gen. Relativ. Gravit. **41**(2009)581.
54. I. Müller: Z. Physik **198**(1967)329.
55. W. Israel: Ann. Phys. **100**(1976)310.
56. W. Israel and J. Stewart: Ann. Phys. **118**(1979)341.

Proc. Int. Conf. Relativ. Astrophys.
Pages 56-61, (2015)

Noether Gauge Symmetries in Some Gravity Theories

Uğur Camcı [a,1]

[1]Department of Physics, Akdeniz University, Science Faculty, Antalya, Turkey

Abstract Considering the spatially non-flat Friedmann-Lemaitre-Robertson-Walker (FLRW) universe model in the context of $f(R)$ gravity and scalar-tensor gravity theories, it is constructed a point Lagrangian to seek Noether gauge symmetry of that spacetime. For both the $f(R)$ gravity and scalar-tensor gravity theories, we found all possible Noether gauge symmetries of FLRW spacetime which turns out that the existence of Noether symmetries for the considered gravity theories is a powerful tool to find the exact solutions of field equations.

Keywords FLRW spacetime, f(R) theory of gravity, scalar-tensor theory of gravity, Noether gauge symmetry

Keywords First keyword · Second keyword · More

1 Introduction

A cosmological model can be expressed in terms of the configuration space variables which are usually the metric coefficients, matter fields, scalar fields, etc.[1,2]. Therefore, the corresponding configuration space of the cosmological model is a $m-$dimensional Riemannian manifold with coordinates q^i, $i = 1, 2, \ldots, m$, in which it will be constructed a point-like Lagrangian to produce the dynamics of the model.

The cosmological equations can be derived both *from* the field equations of the considered gravity theory *or* deduced by a Lagrangian function $\mathcal{L}(\tau, q^i, \dot{q}^i)$ of the system related to the action $\mathcal{S} = \int \mathcal{L} d\tau$. Here the dot represents the derivative with respect to an affine parameter τ which is the cosmic time t in most of the cosmological models. It is noted that $Q = \{q^i, i = 1, \ldots, m\}$ is the *configuration space* from which it is possible to derive the corresponding *tangent space* $TQ = \{q^i, \dot{q}^i\}$ on which the Lagrangian $\mathcal{L}$ is defined. Taking the variation of $\mathcal{L}$ with respect to the generalized coordinates q^i, the Euler-Lagrange (E-L) equations of motion become

$$\frac{d}{d\tau}\frac{\partial \mathcal{L}}{\partial \dot{q}^i} - \frac{\partial \mathcal{L}}{\partial q^i} = 0. \tag{1}$$

The *energy function* associated with $\mathcal{L}$ is

$$E_{\mathcal{L}} = \dot{q}^k \frac{\partial \mathcal{L}}{\partial \dot{q}^k} - \mathcal{L}, \tag{2}$$

which is also the *Hamiltonian* of the system.

Noether symmetries are associated with differential equations possessing a Lagrangian, and they describe physical features of differential equations in terms of conservation laws admitted by them [3]. From a first order Lagrangian $\mathcal{L} = \mathcal{L}(t, q^k, \dot{q}^k)$, it follows the system of second-order ordinary differential equations (ODEs) of the form

$$\ddot{q}^i = w^i(t, q^k, \dot{q}^k). \tag{3}$$

The strict Noether symmetry approach [4–9] , i.e. Noether symmetry approach without a gauge term, is a kind of symmetry in which the Lie derivative of the Lagrangian that arise from the metric of interest dragging along a vector field $\mathbf{X}$ vanishes, i.e. $\pounds_{\mathbf{X}}\mathcal{L} = 0$. *Noether gauge symmetries* are the generalizations of the strict Noether symmetries as the existence of some extra symmetries is expected [10–17].

A Noether gauge symmetry (*NGS*) generator for ODEs system (3) is given by

$$\mathbf{X} = \xi(t, q^k)\frac{\partial}{\partial t} + \eta^i(t, q^k)\frac{\partial}{\partial q^i}$$

if there exists a gauge function $g(t, q^k)$ and the *Noether symmetry condition*

$$\mathbf{X}^{[1]}\mathcal{L} + \mathcal{L}(D_t\xi) = D_t g \tag{4}$$

[a]e-mail: ucamci@akdeniz.edu.tr

is satisfied, where $D_t = \partial/\partial t + \dot{q}^k \partial/\partial q^k$ is the total derivative operator and $\mathbf{X}^{[1]}$ is the first prolongation of NGS generator $\mathbf{X}$, i.e.

$$\mathbf{X}^{[1]} = \mathbf{X} + \dot{\eta}^k(t, q^\ell, \dot{q}^\ell)\frac{\partial}{\partial \dot{q}^k} \tag{5}$$

where $\dot{\eta}^k(t, q^\ell, \dot{q}^\ell) = D_t\eta^k - \dot{q}^k D_t\xi$. For every NGS, there is a *conserved quantity* (or *a first integral*) of the system of equations (3) given by

$$I = -\xi E_{\mathcal{L}} + \eta^i \frac{\partial \mathcal{L}}{\partial \dot{q}^i} - g. \tag{6}$$

In this work, we aim to give some examples of Noether gauge symmetries of the dynamical Lagrangian $\mathcal{L}$ for the FLRW spacetimes in the following gravity theories.

The action for $f(R)$ theory of gravity in $(1 + n)$-dimensions is

$$\mathcal{S} = \int d^{1+n}x\sqrt{-g}\,[f(R) + \mathcal{L}_m] \tag{7}$$

which gives rise to *field equations*

$$f'(R)R_{\mu\nu} - \frac{1}{2}g_{\mu\nu}f(R) - \nabla_\mu\nabla_\nu f'(R) + g_{\mu\nu}\Box f'(R) = -\frac{1}{2}T^m_{\mu\nu} \tag{8}$$

where $\Box = \nabla^\mu\nabla_\mu$ and $T_{\mu\nu} = -\frac{2}{\sqrt{-g}}\frac{\partial S_m}{\partial g^{\mu\nu}}$.

The action for *scalar-tensor theories of gravity* has the form

$$\mathcal{S} = \int d^4x\sqrt{-g}\times \left[F(\Phi)R - \frac{1}{2}\epsilon g^{\mu\nu}\Phi_\mu\Phi_\nu - U(\Phi) + \mathcal{L}_m\right] \tag{9}$$

where we set $8\pi G = 1$ and $\epsilon = \pm 1$ for standard scalar and phantom fields, respectively, and $\Phi_\mu \equiv \partial_\mu\Phi$. The *field equations* of this theory are

$$F(\Phi)G_{\mu\nu} = -\frac{1}{2}\left(T^m_{\mu\nu} + T^\Phi_{\mu\nu}\right) - g_{\mu\nu}\Box F(\Phi) + F(\Phi)_{;\mu\nu} \tag{10}$$

where $T^\Phi_{\mu\nu} = \Phi_\mu\Phi_\nu - \frac{1}{2}g_{\mu\nu}\Phi_\alpha\Phi^\alpha - g_{\mu\nu}U(\Phi)$ is the energy-momentum tensor of a scalar field. The *Klein-Gordon equation* following from the Bianchi identity $G^{\mu\nu}_{\ \ \nu} = 0$ is $\Box\Phi + RF'(\Phi) - U'(\Phi) = 0$.

Introducing a geometric procedure for two-dimensional systems, Tsamparlis and Paliathanasis [12] have connected the Noether gauge symmetries of classical Lagrangian to the collineations of the second order tensor, so-called *kinetic metric tensor* σ_{ij}, which is defined by the kinematic part of the Lagrangian. The most of the applications of Noether theorem to the extending theories of gravity are concerned with the following standard form of the Lagrangian

$$\mathcal{L} = T - V = \frac{1}{2}\sigma_{ij}(q^k)\dot{q}^i\dot{q}^j - V(q^k), \tag{11}$$

where T is the kinetic energy with a *kinetic metric*

$$ds^2_\sigma = \sigma_{ij}dq^i dq^j$$

of the configuration space, the indices $i, j, k, ...$ run over the dimension of this space and $V(q^k)$ is the potential energy function.

For the form of Lagrangian (11), we obtain the first prolongation of the NGS generator $\mathbf{X}$ as

$$\mathbf{X}^{[1]}\mathcal{L} = -\eta^k V_{,k} + \sigma_{ij}\eta^i_{,t}\dot{q}^j + \frac{1}{2}\left(\pounds_\eta\sigma_{ij} - 2\xi_{,t}\sigma_{ij}\right)\dot{q}^i\dot{q}^j - \xi_{,k}\sigma_{ij}\dot{q}^i\dot{q}^j\dot{q}^k \tag{12}$$

where $\pounds_\eta$ is the Lie derivative operator along $\eta = \eta^k\partial/\partial q^k$. Putting (12) into (4) together with $D_t\xi = \xi_{,t} + \xi_{,k}\dot{q}^k$ and $D_t g = g_{,t} + g_{,k}\dot{q}^k$, the Noether symmetry condition (4) becomes

$$\xi_{,i} = 0, \qquad \sigma_{ij}\eta^j_{,t} - g_{,i} = 0, \tag{13}$$

$$\pounds_\eta\sigma_{ij} = (\xi_{,t})\sigma_{ij}, \tag{14}$$

$$\eta^k V_{,k} + V\xi_{,t} + g_{,t} = 0. \tag{15}$$

The above conditions explicitly yields the geometrical character of the NGS. Here, $\xi_{,i} = 0$ implies $\xi = \xi(t)$, and Eq. (14) means that η is a *Homothetic vector* (HV) field when $\xi(t) \neq 0$.

2 Noether Gauge Symmetries in $f(R)$ Theory of Gravity

The Ricci scalar of $(1 + n)$-dimensional FLRW metric is

$$R = 2n\frac{\ddot{a}}{a} + n(n-1)\frac{(\dot{a}^2 + k)}{a^2}, \tag{16}$$

where $a(t)$ is the cosmological scale factor and $k = 0, \pm 1$. Selecting the suitable Lagrange multiplier and integrating by parts, the Lagrangian $\mathcal{L}$ becomes canonical. Then the point-like Lagrangian of $(1+n)$-dimensional FLRW metric for $f(R)$ gravity has the form

$$\mathcal{L} = n(n-1)f'a^{n-2}\dot{a}^2 + 2nf''a^{n-1}\dot{a}\dot{R} + a^n(Rf' - f) - kn(n-1)f'a^{n-2} + \rho_{m0}a^{n-3} + \rho_{r0}a^{n-4} \tag{17}$$

where ρ_{m0} and ρ_{r0} represent the standard amount of *dust* and *radiation* fluids. The kinetic metric for $f(R)$ Lagrangian (17) is

$$ds^2_\sigma = 2n(n-1)f'a^{n-2}da^2 + 4nf''a^{n-1}dadR, \tag{18}$$

and the potential has the form

$$V = a^n(f - Rf') + kn(n-1)f'a^{n-2} - \rho_{m0}a^{n-3} - \rho_{r0}a^{n-4}. \tag{19}$$

Under the coordinate transformation

$$u=\sqrt{\frac{8}{n}}a^{n/2},\qquad v=(n-1)f'(R), \tag{20}$$

the kinetic metric (18) becomes

$$ds^2_\sigma = vdu^2+\frac{n\,u}{n-1}dudv, \tag{21}$$

with $n\neq 1$.

For the kinetic metric (21), the geometrical Noether symmetry conditions (13)-(15) obtained above yield

$$\xi_{,u}=0,\quad \xi_{,v}=0,\quad \eta^1_{,v}=0, \tag{22}$$

$$\eta^2+2v\eta^1_{,u}+\frac{n\,u}{n-1}\eta^2_{,u}-v\xi_{,t}=0, \tag{23}$$

$$\frac{1}{u}\eta^1+\eta^1_{,u}+\eta^2_{,v}-\xi_{,t}=0, \tag{24}$$

$$v\eta^1_{,t}+\frac{n\,u}{2(n-1)}\eta^2_{,t}-g_{,u}=0, \tag{25}$$

$$\frac{n\,u}{2(n-1)}\eta^1_{,t}-g_{,v}=0, \tag{26}$$

$$V_{,u}\eta^1+V_{,v}\eta^2+V\xi_{,t}+g_{,t}=0. \tag{27}$$

The general solution of Eqs.(22)-(26):

$$\begin{aligned}
\xi &= K_1(t),\\
\eta^1 &= u\left[c_1+\frac{n}{2(n+1)}\dot{K}_1(t)\right]+u^{-\frac{1}{n}}K_2(t),\\
\eta^2 &= v\left[-2c_1+\frac{1}{n+1}\dot{K}_1-\frac{(n-1)\,u^{-\frac{n+1}{n}}}{n}K_2(t)\right]\\
&\quad +u^{\frac{1-n}{n}}K_3(t),\\
g &= \frac{n\,v}{n-1}\left[\frac{n\,u^2}{4(n+1)}\ddot{K}_1+u^{\frac{1-n}{n}}\dot{K}_2\right]\\
&\quad +\frac{n^2\,u^{\frac{1+n}{n}}}{2(n^2-1)}\dot{K}_3+K_4(t),
\end{aligned} \tag{28}$$

where $K_1(t),...,K_4(t)$ are integration functions and c_1 is an integration constant. Thus, there is only one remaining equation (27) to be solved. This includes the potential function $V(u,v)$ given by (19).

Now we take into account some form of $f(R)$, and give complete solution in the following. For flat ($k=0$) FLRW spacetime, we list our finding of the NGS components and the gauge functions as

– $f(R)=f_0R^{\ell}$, $\rho_{m0}=0$, $\rho_{ro}=0$;

$$\xi=c_1t+c_2,\quad \eta^1=\frac{(2\ell-1)}{2}c_1u,$$
$$\eta^2=2(1-\ell)c_1v,\quad g=c_3.$$

– $n=3$, $f(R)=f_0R^{\frac{7}{8}}$, $\rho_{m0}=0$, $\rho_{ro}=0$;

$$\xi=c_1\frac{t^2}{2}+c_2t+c_3,\quad \eta^1=\frac{3u}{8}(c_1t+c_2),$$
$$\eta^2=\frac{v}{4}(c_1t+c_2),\quad g=\frac{9}{32}c_1u^2v+c_4.$$

– $f(R)=f_0R^{\frac{2n}{n+1}}$, $\rho_{m0}=0$, $\rho_{ro}=0$;

$$\xi=c_1t+c_2,\quad \eta^1=\frac{(3n-1)}{2(n+1)}c_1u+(c_3t+c_4)u^{-\frac{1}{n}},$$
$$\eta^2=\frac{2(1-n)}{(1+n)}c_1v+\frac{(1-n)}{n}(c_3t+c_4)\frac{u^{-\frac{1+n}{n}}}{v},$$
$$g=\frac{n}{2(n-1)}c_3u^{\frac{n-1}{n}}v+c_5.$$

We note that Vakili [8] found only the Noether symmetry coming from the parameter c_4.

– $f(R)=(f_0R+f_1)^{\frac{2n}{n+1}}$, $\rho_{m0}=0$, $\rho_{ro}=0$;

$$\xi=c_1,\quad \eta^1=u^{-\frac{1}{n}}\left[c_2\sin(\alpha t)+c_3\cos(\alpha t)\right],$$
$$\eta^2=\frac{(1-n)}{n}u^{-\frac{(1+n)}{n}}v\left[c_2\sin(\alpha t)+c_3\cos(\alpha t)\right],$$
$$g=\frac{n\alpha}{2\sqrt{(n-1)}}u^{-\frac{(1+n)}{n}}v\left[c_2\cos(\alpha t)-c_3\sin(\alpha t)\right]+c_4,$$

where $\alpha=\frac{1}{2}\sqrt{\frac{(n+1)f_1}{nf_0}}$ and $f_1/f_0>0$. As far as we know, the above NGSs are new solutions.

– $f(R)=(f_0R-\Lambda)^{\frac{2n}{n+1}}$, $\rho_{m0}=0$, $\rho_{ro}=0$;

$$\xi=c_1,\quad \eta^1=u^{-\frac{1}{n}}\left[c_2e^{\beta t}+c_3e^{-\beta t}\right],$$
$$\eta^2=\frac{(1-n)}{n}u^{-\frac{(1+n)}{n}}v\left[c_2e^{\beta t}+c_3e^{-\beta t}\right],$$
$$g=\frac{n\beta}{2\sqrt{(n-1)}}u^{-\frac{(1+n)}{n}}v\left[c_2e^{\beta t}-c_3e^{-\beta t}\right]+c_4,$$

where $\beta=\frac{1}{2}\sqrt{\frac{\Lambda(n+1)}{f_0n}}$ and $\Lambda/f_0>0$.

– $n=3$, $f(R)=(f_0R+f_1)^{\frac{7}{8}}$, $\rho_{r0}=0$, $\rho_{mo}\neq 0$;

$$\xi=c_1+c_2\sin(\alpha t)+c_3\cos(\alpha t),$$
$$\eta^1=\frac{3\alpha}{8}u\left[c_2\cos(\alpha t)-c_3\sin(\alpha t)\right],$$
$$\eta^2=\frac{\alpha}{4}v\left[c_2\cos(\alpha t)-c_3\sin(\alpha t)\right],$$
$$g=\left(\rho_{m0}-\frac{9\alpha^2}{32}u^2v\right)\left[c_2\sin(\alpha t)+c_3\cos(\alpha t)\right]+c_4,$$

where $\alpha=2\sqrt{\frac{f_1}{3f_0}}$. The above NGSs are also new solutions.

– $n=3$, $f(R)=(f_0R-\Lambda)^{\frac{7}{8}}$, $\rho_{r0}=0$, $\rho_{mo}\neq 0$;

$$\xi=c_1+c_2e^{\alpha t}+c_3e^{-\alpha t},$$
$$\eta^1=\frac{3\alpha}{8}u\left[c_2e^{\alpha t}-c_3e^{-\alpha t}\right],\quad \eta^2=\frac{\alpha}{4}v\left[c_2e^{\alpha t}-c_3e^{-\alpha t}\right],$$
$$g=\left(\rho_{m0}+\frac{9\alpha^2}{32}u^2v\right)\left[c_2e^{\alpha t}+c_3e^{-\alpha t}\right]+c_4,$$

where $\alpha=2\sqrt{\frac{\Lambda}{3f_0}}$.

For non-flat ($k \neq 0$) FLRW spacetime, we obtained the NGS components and the gauge functions which are found by $n = 3$ only as

– $n = 3,\ f(R) = f_0 R^{\frac{3}{2}}, \rho_{r0} = 0,\ \rho_{mo} \neq 0;$

$$\xi = c_1 t + c_2,\ \eta^1 = u^{-\frac{1}{3}} \left[c_1 \left(u^{\frac{4}{3}} - \frac{4k}{3^{2/3}} t^2 \right) + c_3 t + c_4 \right],$$

$$\eta^2 = u^{-\frac{4}{3}} v \left[c_1 \left(\frac{8k}{3^{5/3}} t^2 - u^{\frac{4}{3}} \right) - \frac{2}{3}(c_3 t + c_4) \right],$$

$$g = c_1 \left(\rho_{m0} - 2k(3u^2)^{\frac{1}{3}} v \right) t + \frac{3}{4} c_3 u^{\frac{2}{3}} v + c_5.$$

– $n = 3,\ f(R) = (f_0 R + f_1)^{\frac{3}{2}},\ \rho_{r0} = 0,\ \rho_{mo} \neq 0;$

$$\xi = c_1, \quad \eta^1 = u^{-\frac{1}{3}} \left[c_2 \sin(\alpha t) + c_3 \cos(\alpha t) \right],$$

$$\eta^2 = -\frac{2}{3} u^{-\frac{4}{3}} v \left[c_2 \sin(\alpha t) + c_3 \cos(\alpha t) \right],$$

$$g = \frac{3\alpha}{4} u^{\frac{2}{3}} v \left[c_2 \cos(\alpha t) - c_3 \sin(\alpha t) \right] + c_4,$$

where $\alpha = \sqrt{\frac{f_1}{3 f_0}}$ and $f_1/f_0 > 0$. We note also that the above NGSs are new solutions.

– $n = 3,\ f(R) = (f_0 R - \Lambda)^{\frac{3}{2}},\ \rho_{r0} = 0,\ \rho_{mo} \neq 0;$

$$\xi = c_1, \quad \eta^1 = u^{-\frac{1}{3}} \left[c_2 e^{\beta t} + c_3 e^{-\beta t} \right],$$

$$\eta^2 = -\frac{2}{3} u^{-\frac{4}{3}} v \left[c_2 e^{\beta t} + c_3 e^{-\beta t} \right],$$

$$g = \frac{3\beta}{4} u^{\frac{2}{3}} v \left[c_2 e^{\beta t} - c_3 e^{-\beta t} \right] + c_4,$$

where $\beta = \sqrt{\frac{\Lambda}{3 f_0}}$ and $\Lambda/f_0 > 0$.

– $n = 3,\ f(R) = f_0 R^2,\ \rho_{r0} = 0,\ \rho_{mo} \neq 0;$

$$\xi = c_1 t + c_2,\ \eta^1 = \frac{3}{2} c_1 u, \quad \eta^2 = -2 c_1 v,$$

$$g = \rho_{m0} c_1 t + c_3.$$

3 Noether Gauge Symmetries in Scalar-Tensor Gravity

The Lagrangian density of *scalar-tensor theories of gravity* is

$$\mathcal{L} = F(\Phi) R - \frac{1}{2} \epsilon g^{\mu\nu} \Phi_\mu \Phi_\nu - U(\Phi) + \mathcal{L}_m \left[g_{\mu\nu}; \psi_m \right] \quad (29)$$

where $\mathcal{L}_m \left[g_{\mu\nu}; \psi_m \right]$ indicates matter fields approximated by a perfect fluid and $\epsilon = \pm 1$ represents ordinary scalar and phantom fields, respectively.

The Ricci scalar of (1+3)-dimensional FLRW spacetime is given by

$$R = 6 \left(\frac{\ddot{a}}{a} + \frac{\dot{a}^2}{a^2} + \frac{k}{a^2} \right). \quad (30)$$

Thus, the Lagrangian density of scalar-tensor theories of gravity in FLRW background becomes

$$\mathcal{L} = -6F(\Phi) a \dot{a}^2 - 6F'(\Phi) a^2 \dot{a} \dot{\Phi} + \frac{1}{2} \epsilon a^3 \dot{\Phi}^2 + 6kF(\Phi) a - a^3 U(\Phi) - \rho_{m0} a^{-3w} \quad (31)$$

where $w = p/\rho$ is the equation of state parameter and $\rho = \rho_{m0} a^{-3(1+w)}$ is density.

Being $q^i = \{a, \Phi\}$ the configuration space of the system, the problem is 2D and then the *kinetic metric* and the potential are

$$ds^2_\sigma = -12F(\Phi) a da^2 + \epsilon a^3 d\Phi^2 - 12F'(\Phi) a^2 da d\Phi, \quad (32)$$

and

$$V(a, \Phi) = -6kF(\Phi) a + a^3 U(\Phi) + \rho_{m0} a^{-3w}. \quad (33)$$

Now, we impose the quadratic form of $F(\Phi)$, i.e. $F(\Phi) = F_0 \Phi^2$ in scalar-tensor kinetic metric (32) and try to achieve NGSs for some form of $U(\Phi)$.

For the FLRW spacetime the Hessian determinant $W = \Sigma \left| \frac{\partial^2 \mathcal{L}}{\partial \dot{q}^i \partial \dot{q}^j} \right|$ turns out to be

$$W = -12 a^4 (3F'^2 + \epsilon F), \quad (34)$$

which is equivalent to the determinant of the kinetic metric σ_{ij}. There exists two cases depending on the Hessian determinant W vanishes or not.

Case (i): If the Lagrangian (29) is degenerate, then the Hessian determinant W vanishes, so that the function $F(\Phi)$ is given by

$$F = -\frac{\epsilon}{12} \Phi^2. \quad (35)$$

Case (ii): If the Lagrangian (29) is non-degenerate, then the Hessian determinant W do not vanish, and the function $F(\Phi)$ has the form $F = F_0 \Phi^2$, where $F_0 \neq -\epsilon/12$.

For $F(\Phi) = F_0 \Phi^2$, transforming the coordinates (a, Φ) to a new coordinates (u, v) defined as

$$a = \frac{1}{4} u^{\frac{2}{3}} v^2, \qquad \Phi = 4 v^{-2}, \quad (36)$$

the kinetic metric (32) in the new coordinates can be cast in a diagonal form

$$ds^2_\sigma = -\frac{4}{3} F_0 v^2 du^2 + (12F_0 + \epsilon) u^2 dv^2. \quad (37)$$

The potential (33) in the new coordinates becomes

$$V(u, v) = -24kF_0 \frac{u^{\frac{2}{3}}}{v^2} + \frac{1}{64} u^2 v^6 U(v) + \rho_{m0} \left(\frac{1}{4} u^{\frac{2}{3}} v^2 \right)^{-3w}. \quad (38)$$

For the kinetic metric (37) of scalar-tensor gravity theory, the geometrical Noether symmetry conditions (13)-(15) gives

$$\xi_{,u}=0,\quad \xi_{,v}=0, \tag{39}$$
$$\frac{1}{v}\eta^2+\eta^1_{,u}-\frac{1}{2}\xi_{,t}=0, \tag{40}$$
$$(12F_0+\epsilon)\left[\frac{1}{u}\eta^1+\eta^2_{,v}-\frac{1}{2}\xi_{,t}\right]=0, \tag{41}$$
$$-\frac{4}{3}F_0v^2\eta^1_{,v}+(12F_0+\epsilon)u^2\eta^2_{,u}=0, \tag{42}$$
$$\frac{4}{3}F_0v^2\eta^1_{,t}+g_{,u}=0,\ (12F_0+\epsilon)u^2\eta^2_{,t}-g_{,v}=0, \tag{43}$$
$$V_{,u}\eta^1+V_{,v}\eta^2+V\xi_{,t}+g_{,t}=0. \tag{44}$$

In the following, we consider some form of the function $U(v)$, and give the components of NGS generator and gauge function if it is not a constant.

For flat ($k=0$) FLRW spacetime with dust matter, i.e. $w=0$, we obtain

– $U(v)=U_0v^{-\ell}$, i.e. $U(\Phi)\propto\Phi^{\frac{\ell}{2}}$:

$$\xi=c_1t+c_2,\quad \eta^1=\frac{(\ell-8)}{2(\ell-4)}c_1u,\quad \eta^2=\frac{2}{(\ell-4)}c_1v,$$
$$g=-\rho_{m0}c_1t.$$

– $U(v)=U_0v^{-\ell}$ and $F_0=-\frac{\epsilon}{12}$:

$$\xi=c_1t+c_2,\quad \eta^1=\frac{(\ell-8)}{2(\ell-4)}c_1u+c_3u^{\frac{2}{6-\ell}},$$
$$\eta^2=\frac{2}{\ell-4}c_1v+\frac{2}{\ell-6}c_3u^{-1-\frac{2}{\ell-6}}v,\quad g=-c_1\rho_{m0}t.$$

– $U(v)=64U_0v^{-6}, i.e. U(\Phi)\propto\Phi^3$, and $F_0=-\frac{\epsilon}{12}$:

$$\xi=c_1t+c_2,\quad \eta^1=-\frac{c_1}{2U_0u}(U_0u^2+\rho_{m0})-\frac{c_3}{2U_0u},$$
$$\eta^2=\frac{v}{2U_0u^2}\left[c_1(2U_0u^2-\rho_{m0})-c_3\right],\quad g=c_3t.$$

– $U(v)=64U_0v^{-6}+U_1v^{-8}$ and $F_0=-\frac{\epsilon}{12}$:

$$\xi=c_1,\quad \eta^1=-\frac{c_2}{2U_0u},\quad \eta^2=-\frac{c_2v}{2U_0u^2},\quad g=c_2t.$$

– $U(v)=U_0v^{-4}$ and $F_0=-\frac{\epsilon}{12}$, i.e. $U(\Phi)\propto\Phi^2$:

$$\xi=c_1t+c_2,\quad \eta^1=u(c_1\ln u+c_3),$$
$$\eta^2=-v[c_1(\frac{1}{2}+\ln u)+c_3],\quad g=-\rho_{mo}c_1t.$$

– $U(v)=U_0v^{-8}$ and $F_0=-\frac{\epsilon}{12}$:

$$\xi=K_1(t),\quad \eta^1=\frac{c_1}{u},\quad \eta^2=v\left(\frac{1}{2}\dot{K}_1+\frac{c_1}{u^2}\right),$$
$$g=-\rho_{m0}K_1(t).$$

– $U(v)=\frac{16}{7}U_0^2v^{-4}$, $F_0=\frac{1}{6}$ and $\epsilon=-1$:

$$\xi=c_1+c_2e^{U_0t}+c_3e^{-U_0t},$$
$$\eta^1=\frac{9U_0}{14}\left(c_2e^{U_0t}-c_3e^{-U_0t}\right)u+c_4u$$
$$+u^{\frac{\sqrt{2}}{3}}v^{-1+\frac{3}{\sqrt{2}}}\left(c_5e^{U_0\frac{t}{2}}+c_6e^{-U_0\frac{t}{2}}\right)$$
$$+u^{-\frac{\sqrt{2}}{3}}v^{-1-\frac{3}{\sqrt{2}}}\left(c_7e^{U_0\frac{t}{2}}+c_8e^{-U_0\frac{t}{2}}\right)$$
$$\eta^2=-\frac{\sqrt{2}}{3}u^{-1+\frac{\sqrt{2}}{3}}v^{\frac{3}{\sqrt{2}}}\left(c_5e^{U_0\frac{t}{2}}+c_6e^{-U_0\frac{t}{2}}\right)$$
$$+\frac{\sqrt{2}}{3}u^{-1-\frac{\sqrt{2}}{3}}v^{-\frac{3}{\sqrt{2}}}\left(c_7e^{U_0\frac{t}{2}}+c_8e^{-U_0\frac{t}{2}}\right)$$
$$-\frac{U_0\,v}{7}\left(c_2e^{U_0t}-c_3e^{-U_0t}\right)-c_4v,$$

and gauge function:

$$g=\left(\frac{U_0^2}{14}u^2v^2+\rho_{m0}\right)\left[c_2e^{U_0t}+c_3e^{-U_0t}\right]$$
$$-\frac{U_0}{3(\sqrt{2}+3)}u^{1+\frac{\sqrt{2}}{3}}v^{1+\frac{3}{\sqrt{2}}}\left(c_5e^{U_0\frac{t}{2}}-c_6e^{-U_0\frac{t}{2}}\right)$$
$$\frac{U_0}{3(\sqrt{2}-3)}u^{1-\frac{\sqrt{2}}{3}}v^{1-\frac{3}{\sqrt{2}}}\left(c_7e^{U_0\frac{t}{2}}-c_8e^{-U_0\frac{t}{2}}\right).$$

When the equation of state parameter is $w=-1$ (dark energy), we find the NGS components and the gauge functions as

– $U(v)=U_0v^{-\ell}-\rho_{m0}$:

$$\xi=c_1t+c_2,\quad \eta^1=\frac{(\ell-8)}{2(\ell-4)}c_1u,\quad \eta^2=\frac{2}{(\ell-4)}c_1v.$$

– $U(v)=U_0v^{-\ell}-\rho_{m0}$ and $F_0=-\frac{\epsilon}{12}$:

$$\xi=c_1t+c_2,\quad \eta^1=\frac{(\ell-8)}{2(\ell-4)}c_1u+c_3u^{\frac{2}{6-\ell}},$$
$$\eta^2=\frac{2}{\ell-4}c_1v+\frac{2}{\ell-6}c_3u^{-1-\frac{2}{\ell-6}}v.$$

– $U(v)=64U_0v^{-6}-\rho_{m0}$ and $F_0=-\frac{\epsilon}{12}$:

$$\xi=c_1t+c_2,\quad \eta^1=-c_1\frac{u}{2}-\frac{c_3}{2U_0u},$$
$$\eta^2=c_1v-c_3\frac{v}{2U_0u^2},\quad g=c_3t.$$

– $U(v)=64U_0v^{-6}+U_1v^{-8}-\rho_{m0}$ and $F_0=-\frac{\epsilon}{12}$:

$$\xi=c_1,\quad \eta^1=-\frac{c_2}{2U_0u},\quad \eta^2=-\frac{c_2v}{2U_0u^2},\quad g=c_2t.$$

– $U(v)=U_0v^{-4}-\rho_{m0}$ and $F_0=-\frac{\epsilon}{12}$:

$$\xi=c_1t+c_2,\quad \eta^1=u(c_1\ln u+c_3),$$
$$\eta^2=-v[c_1(\frac{1}{2}+\ln u)+c_3].$$

– $U(v)=U_0v^{-8}-\rho_{m0}$ and $F_0=-\frac{\epsilon}{12}$:

$$\xi=K_1(t),\quad \eta^1=\frac{c_1}{u},\quad \eta^2=v\left(\frac{1}{2}\dot{K}_1+\frac{c_1}{u^2}\right).$$

For the non-flat ($k \neq 0$) FLRW metric and dust matter ($w = 0$), it follows that

– $U(v) = 64U_0 v^{-8}$ and $F_0 = -\frac{\epsilon}{12}$:

$$\xi = K_1(t), \quad \eta^1 = \frac{c_1 u^{-\frac{1}{3}}}{\sqrt{U_0 u^{4/3} \pm 2k}},$$
$$\eta^2 = \frac{v}{6(U_0 u^{4/3} \pm 2k)}\Big[3(2k \pm U_0 u^{4/3})\dot{K}_1 + \frac{2c_1(2ku^{-\frac{4}{3}} \pm 3U_0)}{\sqrt{U_0 u^{4/3} \pm 2k}}\Big],$$
$$g = -\rho_{m0} K_1(t).$$

When $k \neq 0$ and the equation of state parameter is $w = -1$ (dark energy), then the same components of NGS for dust matter given above appear, but the function $U(v)$ takes the form $U(v) = 64U_0 v^{-8} - \rho_{m0}$ and the gauge function vanishes.

When $k \neq 0$ and $w = \frac{1}{3}$ (radiation), it is found that

– $U(v) = 64U_0 v^{-8}$ and $F_0 = -\frac{\epsilon}{12}$:

$$\xi = K_1(t), \quad \eta^1 = \frac{c_1 u^{\frac{1}{3}}}{\sqrt{U_0 u^{8/3} + 4\rho_{m0} \pm 2ku^{4/3}}},$$
$$\eta^2 = \frac{3v(2ku^{4/3} \pm 4\rho_{m0} \pm U_0 u^{8/3})\dot{K}_1}{6(U_0 u^{8/3} + 4\rho_{m0} \pm 2ku^{4/3})} + \frac{2c_1 v(2ku^{2/3} \pm 4\rho_{m0} u^{-2/3} \pm 3U_0 u^2)}{\left(U_0 u^{8/3} + 4\rho_{m0} \pm 2ku^{4/3}\right)^{3/2}}.$$

4 Summary and Conclusion

In this study, using the FLRW metric, we derived the Noether gauge symmetries of a canonical Lagrangian for the $f(R)$ gravity and scalar-tensor gravity theories. To get the appropriate equations of motion in the considered theory of gravity, we set up an effective point-like Lagrangian in terms of its configuration space variables and their velocities.

Using this effective Lagrangian, we determined the kinetic metric in the configuration space of dynamical system. Thus we considered the latter kinetic metric in a new appropriate coordinate system and used it to calculate and classify Noether gauge symmetry generators by the the geometrical Noether symmetry conditions. Most of the Noether gauge symmetry generators appeared in the previous section are earlier obtained, but some of them are new ones.

The Noether gauge symmetry approach is capable to construct exact solutions of field equations for any gravity theory by reducing their complexity through the first integral of motion. In order to find out analytical solutions of field equations for the considered gravity theory, one can use the obtained Noether gauge symmetry generators to get the first integrals by the formula (6).

Acknowledgements This work was supported by The Scientific Research Projects Coordination Unit of Akdeniz University (BAP). The author would like to thank The University of Punjab for the financial grant of the successful meeting "International Conference on Relativistic Astrophysics (ICRA)", The University of Punjab, Department of Mathematics, Lahore-Pakistan held in February 10-14, 2015.

References

1. H. Stephani D. Kramer, M. A. H. MacCallum, C. Hoenselaers and E. Herlt, *Exact Solutions of Einstein Field Equations*, Cambridge University Press, Cambridge (2003).
2. G. F. R. Ellis, R. Maartens and M. A. H. MacCallum, *Relativistic Cosmology*, Cambridge Univ. Press, Cambridge (2012).
3. P. J.Olver, *Application of Lie Groups to Differential Equations*, Springer Graduate Text in Mathematics, New York (1986).
4. S. Capozziello and G. Lambiase, Gen. Relativ. Gravit. **32**, 673 (2000)
5. S. Capozziello, A. Stabile, and A. Troisi, Class. Quantum Grav.**24** 2153(2007).
6. U. Camci and Y. Kucukakca, Phys. Rev. D **76**, 084023 (2007)
7. S. Capozziello and A. De Felice, J. Cosmol. Astropart. Phys.**08**, 016 (2008)
8. B. Vakili, Phys.Lett.**B664**, 16-20 (2008)
9. Y. Kucukakca and U. Camci, I. Semiz, Gen. Relativ. Gravit. **44**, 1893 (2012)
10. T. Feroze, F. M. Mahomed and A. Qadir, Nonlinear Dyn. **45**, 65 (2006)
11. M. Tsamparlis and A. Paliathanasis, Gen. Relativ. Gravit.**42**, 2957 (2010)
12. M. Tsamparlis and A. Paliathanasis, J.Phys.A.: Math. and Theor.**44**, 175202 (2011)
13. Y. Kucukakca and U. Camci, Astrophys. Space Sci. **338**, 211 (2012)
14. I. Hussain, M. Jamil and F. M. Mahomed, Astrophys. Space Sci. **337**, 373 (2011)
15. F. Ali and T. Feroze, Int. J. Theor. Phys. **52**, 3329 (2013)
16. U. Camci, J. Cosmol. Astropart. Phys.**07**, 002 (2014)
17. U. Camci and A. Yildirim, Phys. Scr. **89**, 084003 (2014)

Proc. Int. Conf. Relativ. Astrophys.
Pages 62-76, (2015)

Symmetries, Orbits and Isotropy in General Relativity Theory

Graham Hall[a,1]

[1]Institute of Mathematics University of Aberdeen Aberdeen AB24 3UE Scotland, UK

Abstract This paper gives a review of the study of symmetry in Einstein's General Theory of Relativity mainly from the global, geometrical viewpoint. Although concentrating mostly on metric (Killing) symmetry, the techniques described are applicable also to homothetic, affine, conformal and projective symmetry together with the symmetries of the curvature tensor and Weyl's conformal and projective tensors and these are briefly described. A discussion will also be given of Killing orbit and isotropy theory and this will be used to characterise cosmological and plane wave metrics in general relativity. A few brief remarks are given on local symmetry.

1 Introduction

In this section some definitions and general notation will be established. Throughout, (M, g) will denote a space-time, that is, a 4-dimensional, smooth, connected (hence path connected), Hausdorff manifold M carrying a smooth metric g of Lorentz signature and components g_{ab}. The Levi-Civita connection arising from g is denoted ∇ and the associated curvature tensor is denoted *Riem* with components $R^a{}_{bcd}$. The corresponding Ricci tensor is denoted *Ricc* with components $R_{ab} \equiv R^c{}_{acb}$ and the Ricci scalar is $R \equiv R_{ab}g^{ab}$. All geometrical objects on M will be assumed smooth unless the contrary is stated. Einstein's field equations are written

$$R_{ab} - \frac{1}{2}Rg_{ab} = T_{ab} \tag{1}$$

where T is the (tensor type $(0, 2)$) energy-momentum tensor. To ensure maximum generality in the geometry of space-times, (1) will be regarded as a definition of T. Of course, physics must then impose its own conditions on T to ensure that it represents the physical situation in an appropriate way. If $T \equiv 0$ on M, (M, g) is called a *vacuum* space-time. It is also useful at this stage to introduce the (tensor type $(1, 3)$) *Weyl conformal tensor* C with components $C^a{}_{bcd}$. This tensor has the property that if two metrics g and g' on M are *conformally related*, that is, there exists a real valued, nowhere-zero function α on M such that $g' = \alpha g$, their corresponding Weyl conformal tensors are equal. This tensor should not be confused with the (tensor type $(1, 3)$) *Weyl projective tensor* W with components $W^a{}_{bcd}$ and which, unlike the tensor C (which depends on g and ∇), depends only on ∇. The tensor W has the property that any two symmetric connections on M which give rise to the same collection of *unparametrised* geodesic paths have the same tensor W [36,35].

In coordinate representations, square brackets will denote the usual skew-symmetrisation of the enclosed indices and a semi-colon, a comma and the symbol $\mathcal{L}$ will denote a covariant derivative with respect to ∇, a partial derivative and a Lie derivative, respectively. The tangent space to M at $m \in M$ is written T_mM and the 6-dimensional Lie algebra (with the usual matrix commutation as Lie product) of skew-symmetric tensors (2-forms) at m is denoted Λ_mM and its members are usually referred to as *bivectors*. It is convenient in considering the set Λ_mM to identify the tensor types $(1, 1)$, $(0, 2)$ and $(2, 0)$ for bivectors at m because of the natural isomorphisms between them (raising and lowering indices) arising from $g(m)$.

In the study of symmetry, one must first decide exactly what constitutes a "symmetry". In essence one would like to say, somewhat imprecisely it must be admitted, that some geometrical object is the "same" at certain points of the space-time M, given some specification of how these points are related. To try and make this precise first choose some geometrical object, for example, a globally defined smooth tensor field K on M,

[a]e-mail: g.hall@abdn.ac.uk

and suppose that $f : M \to M$ is a (smooth) diffeomorphism, that is, a bijective map which is smooth and has a smooth inverse. One might say that f is a "symmetry" of K if $f^*K = K$, where f^* denotes the "pullback" of f. To understand what this means suppose that U is some coordinate domain of M with coordinates x^a and let $f(U)$ be the (necessarily open) image of U under f. One can put a (smooth) coordinate system y^a on $f(U)$ in a natural way as $y^a = x^a \circ f^{-1}$, that is, for $m \in U$, $f(m)$ gets the same coordinates in the y^a system that m got in the x^a system (see, e.g. [1,2]). The condition $f^*K = K$ is then equivalent to the condition that the components of K are (numerically) the same at m (with coordinates x^a) as they are at $f(m)$ (with coordinates y^a). [It is noted here that one is trying to say, intuitively, that a tensor field exhibits a "symmetry" *with respect to* f if it is the "same" in U and $f(U)$ when the points in U and $f(U)$ are paired off using f, so that f specifies the (pairs of) related points as suggested above. Of course it makes no sense to compare values of K at different points of M and so one must circumvent this problem. What one actually does here is to transform the coordinate chart $(f(U), y^a)$ onto U, pointwise, using f^{-1}, to get the chart (U, x^a) and then to compare the original components of K at $m \in U$ in the x^a system with the components of K at $f(m)$ in the system y^a the latter now regarded as being at m in the system x^a. Thus one only compares tensor component values at the same point and in the same coordinate system and gets a "symmetry" in terms of K and f.]

Such a definition of symmetry suggests that the use of smooth maps in the definition of symmetry may be mathematically useful. One disadvantage of this example is that the map f above is a *global* diffeomorphism and physics consists of local observations. One may try to get round the problem by retaining the above idea but where f is now a *local* diffeomorphism whose domain and range are proper open subsets of M. However, many such maps would be needed in order to deal with all relevant observers, that is, some neighbourhood of each point of M, and handling such a collection becomes cumbersome. One method which physicists and geometers have used to get round this problem is the use of *symmetry vector fields*. This approach retains the advantages of the smooth mapping idea above and at the same time gives rise to a sufficient number of local maps upon which a reasonable mathematical structure naturally imposes itself. However, it still requires the existence of a *global* vector field and this problem will be considered in more detail later. The other problems which must be faced are the choice of geometrical object K and whether, for a tensorial choice of K, one wishes to weaken the condition $f^*K = K$. Since, according to general relativity theory, the gravitational field resides in the geometry on M, the choices g, ∇, *Riem*, C, W, etc, for the geometrical object in question suggest themselves naturally.

2 Symmetry Vector Fields

Let X be any globally defined, smooth vector field on M. One may associate with X a family of local diffeomorphisms on M in the following way. Given $m \in M$, X admits an integral curve $c : I \to M$, where I is some open interval in $\mathbb{R}$ containing 0, which begins at m, that is, $c(0) = m$. From the theory of differential equations, given any $m \in M$ there exists an open neighbourhood U of m and a positive real number ϵ such that for any $m' \in U$ the integral curve of X starting from m' is defined on $(-\epsilon, \epsilon)$ (that is, $c(t)$ is defined for $t \in (-\epsilon, \epsilon)$). Thus each point of U may be "moved" along an integral curve of X by a parameter distance t provided $|t| < \epsilon$. This gives a local smooth diffeomorphism ϕ_t with domain U for each such t (see, e.g. [3,4]). This construction may be applied at any $m \in M$ since X is a *global* vector field and thus a family of local diffeomorphisms is generated by X each of which is called a *local flow* of X. Thus vector fields can supply local diffeomorphisms in some neighbourhood of each $m \in M$. In addition, collections of such vector fields usually turn out to be easier to handle than general collections of local diffeomorphisms. One can now consider the effect of assuming the symmetry condition described in section 1 to apply to *each* local flow of X. Thus, for example, if K is a global tensor field on M one assumes that $\phi_t^* K = K$ for each ϕ_t and this is equivalent to the condition that $\mathcal{L}_X K = 0$ [4]. This latter condition gives rise to a set of differential equations to be solved, given K, for X. Such equations are usually more easily handled than collections of vector fields. Similar comments, suitably modified, usually apply if some geometrical condition other than $\phi_t^* K = K$ is used. As an example, let K be the metric tensor g on M. Then let X be a smooth, global vector field on M each of whose local flows is a *local isometry* for g, that is, each local flow satisfies $\phi_t^* g = g$. In this case each ϕ_t "preserves" the metric g, in the sense of section 1, and this is equivalent to X satisfying $\mathcal{L}_X g = 0$. Then X is called a *Killing vector field*. The collection of all Killing vector fields on M is denoted $K(M)$. Thus each $X \in K(M)$ satisfies the equivalent conditions (*Killing's equations*)

$$(a)\, \mathcal{L}_X g = 0, \qquad (b)\, X_{a;b} + X_{b;a} = 0,$$
$$(c)\, X_{a;b} = F_{ab} \qquad (F_{ab} = -F_{ba}) \tag{2}$$

In these expressions, F is a smooth bivector field on M called the *Killing bivector (field)* (of X). The collection

$K(M)$ has some nice properties; first, if $X, Y \in K(M)$ then it is clear from (2)(b) that if $a, b \in \mathbb{R}$, $aX + bY \in K(M)$ and so $K(M)$ is a vector space over $\mathbb{R}$. Second, if $X, Y \in K(M)$ and if $[\ ]$ denotes the usual Lie bracket of vector fields, the identity $\mathcal{L}_{[X,Y]} = \mathcal{L}_X\mathcal{L}_Y - \mathcal{L}_Y\mathcal{L}_X$ reveals that the vector field $[X, Y]$ is a member of $K(M)$ and so $K(M)$ is a (real) Lie algebra under the Lie bracket operation called the *Killing algebra* of M. An important deduction may be made from (2) by using the Ricci identity on X, $X_{a;bc} - X_{a;cb} = X^d R_{dabc}$, the algebraic identity $R_{a[bcd]} = 0$ and some index manipulation. One finds

$$X_{a;bc} = F_{ab;c} = R_{abcd}X^d \tag{3}$$

Then (2)(c) and (3) reveal a first order differential system on (M, g) for the ten components X_a and F_{ab} of the pair X and F and so, since M is path connected, a global Killing vector field on M is uniquely determined by the values $X(m)$ and $F(m)$ at any $m \in M$ (and vanishes identically on M if $X(m)$ and $F(m)$ vanish at some $m \in M$). This gives the important result that $K(M)$ is finite-dimensional and $\dim K(M) \leq 4$ (for $X(m)) + 6$ (for $F(m)) = 10$. Thus, if a Killing vector field vanishes over some non-empty open subset U of M, F vanishes on U and hence $X(m)$ and $F(m)$ vanish at any $m \in U$. Hence X vanishes identically on M. Thus, metric symmetry on M will be characterised in terms of its Killing (Lie) algebra $K(M)$. [It is here remarked that it does not necessarily follow that a Lie *group* of symmetry transformations on M arises from $K(M)$, as is sometimes claimed, but rather only the Lie algebra $K(M)$. However, there is a well defined Lie group action of this type on M arising from $K(M)$ if (and only if) each member of $K(M)$ is a *complete* vector field [5] (see also [3,1]) but this may not necessarily be the case.]

The assumption of a nontrivial $K(M)$ on a spacetime is an advantage in finding exact solutions and many of the well-known metrics in Einstein's theory were discovered in this way (for full details, see [6]). In the event that $\dim K(M) = 10$, (M, g) is of constant curvature. [The converse is not true; in fact, if (M, g) is of constant curvature, only a "local" 10-dimensional Killing algebra is necessarily admitted in some neighbourhood of each point of M; see section 7.] If $\dim K(M) = 8$, (M, g) is again of constant curvature (and the case $\dim K(M) = 9$ is impossible). The maximum dimension of $K(M)$ that can occur without (M, g) being of constant curvature is 7 (cf, [1]). (Some further remarks on local symmetry can be found in section 7.)

However, there are other types of symmetry which are of interest in both general relativity theory and differential geometry and which are not exactly of the type described in section 1. Let X be a global, smooth vector field on M whose local flows are *local conformal isometries* of g, that is, $\phi_t^* g = \xi g$ for some (smooth) function ξ on the domain of ϕ_t. (In the language of section 1 the pull-back of g under ϕ_t is conformally related to g on U.) This turns out to be equivalent to X satisfying $\mathcal{L}_X g = 2\psi g$ for a (smooth) function $\psi : M \to \mathbb{R}$ (the factor 2 being introduced for later convenience) and X is then called a *conformal vector field* and ψ the *conformal function* of X. It can then be checked that X is a conformal vector field if and only if, in any coordinate domain,

$$X_{a;b} = \psi g_{ab} + F_{ab} \qquad (F_{ab} = -F_{ba}) \tag{4}$$

where F is called the *conformal bivector (field)* (of X). The collection of all conformal vector fields on M is denoted $C(M)$ and a similar argument to that for $K(M)$ shows that $C(M)$ is a (real) Lie algebra under the Lie bracket operation called the *conformal algebra*. An application of the Ricci identity on X and F can be used to derive the (more complicated) analogues of (3) above [42] (cf [1]) and reveal that a first order differential system is obtained for the fifteen components X_a, ψ, $\psi_{,a}$ and F_{ab} associated with X and so $C(M)$ is finite-dimensional with $\dim C(M) \leq 15$. If $\dim C(M) = 15$, (M, g) is conformally flat (that is, the Weyl conformal tensor vanishes on M) whilst if (M, g) is conformally flat, a "local" 15-dimensional conformal algebra arises about each point of M. In fact, if $\dim C(M) \geq 8$, (M, g) is conformally flat [1]. Also, a similar argument to that given in the Killing case shows that if a conformal vector field vanishes over some non-empty open subset of M it vanishes on M. It is also clear that a Killing vector field is necessarily conformal with zero conformal function and so $K(M)$ is a subalgebra of $C(M)$. A special subset of $C(M)$ is defined by those members of $C(M)$ for which the function ψ is constant on M and such vector fields are called *homothetic*. The collection of all homothetic vector fields is denoted by $H(M)$ and is easily checked to be a (real) Lie algebra under the Lie bracket operation and is thus a subalgebra of $C(M)$ called the *homothetic algebra*. (and $\dim H(M) \leq 11$). If $X \in H(M)$ satisfies (4) with the (constant) ψ non-zero it is called *proper* homothetic and if $\psi = 0$ it is Killing. The vector fields in $C(M) \setminus H(M)$ are called *proper* conformal. It is remarked that the collections of *proper* conformal and *proper* homothetic vector fields are not Lie algebras or even vector spaces since they do not contain the zero vector field on M. If (M, g) is vacuum and *non-flat* (the latter term meaning that *Riem* does not vanish over any non-empty open subset of M) and admits a proper conformal vector field then it is essentially a pp-wave [44,1] and $\dim C(M) \leq \dim H(M) + 1$

[1]. A recent study of further techniques in conformal symmetry can be found in [43].

If X is a Killing vector field on M and if $m \in M$ is such that $X(m) \neq 0$ then there exists a coordinate neighbourhood U of m on which X does not vanish and has components given by $X^1 = 1$ and with all other components zero (this is true for any vector field X [3]) and then, since X is Killing, the metric components g_{ab} are independent of x^1 (that is, x^1 is an *ignorable coordinate* of g on U). Conversely, if m admits a coordinate neighbourhood U on which the components g_{ab} are independent of the coordinate x^1, then the vector field X on U given by $X^1 = 1$ and with all other components zero is a Killing vector field *on* U. These results are easily checked from (2) and reflect the basic concept of a symmetry given in section 1. [One should compare this with the idea of an ignorable coordinate in elementary Lagrangian mechanics.] There are corresponding results for homothetic and conformal vector fields [1]. One should note the *local* nature of the Killing vector X (on U) in the second part of this result; such a Killing vector field may not be extendible to the whole of M (see section 7). It is easily checked that if g and g' are conformally related metrics on M, X is a conformal vector field on (M, g) if and only if it is a conformal vector field on (M, g') and so the conformal algebras of g and g' coincide.

For a well-known example of some of these symmetries consider the *plane wave* metric given in a global coordinate system u, v, x, y by

$$ds^2 = Hdu^2 + 2dudv + dx^2 + dy^2 \tag{5}$$

where $H(x, y, u) = a(u)x^2 + b(u)y^2 + c(u)xy$ for functions a, b and c. Here there is a Killing algebra of dimension 5, 6 or 7 (depending on the choice of a, b and c in H), one of which is $\partial/\partial v$ (since v is an ignorable coordinate of the metric (5) [34,6]). Also the vector field with components $(0, 2cv, cx, cy)$, for some non-zero constant c, is a proper homothetic vector field (see, e.g.[1]). This metric may also admit proper conformal vector fields (again depending on H).

Another type of symmetry concerns the connection ∇. This is again different from the general type of symmetry suggested in section 1 and arises as follows from global vector fields on M. The connection ∇ determines the geodesic structure of space-time and importance thus focuses on those vector fields whose local flows are *projective*, that is, they preserve the (unparametrised) geodesics of ∇. Thus if whenever $c : I \to M$ is such a geodesic curve in M with respect to ∇, so also is $\phi_t \circ c : I \to M$ for each local flow ϕ_t of a smooth, global vector field X, X is called *projective*. There is a distinction to be drawn here between those local flows which are *affine*, that is, they preserve geodesics *and* their affine parameters and those which are projective and preserve geodesics but not necessarily the affine parameter. If, whenever c is an affinely parametrised geodesic with respect to ∇, so also is $\phi_t \circ c$ for each local flow of X, X is called *affine*. Again one can show that the collection $A(M)$ of all affine vector fields on M and the collection $P(M)$ of all projective vector fields on M are finite-dimensional (real) Lie algebras under the Lie bracket and that $A(M)$ is a subalgebra of $P(M)$ (cf, [1]). If $X \in P(M) \setminus A(M)$ it is called *proper projective*. If an affine or projective vector field vanishes over some non-empty open subset of M it vanishes on M. It is also true that $H(M)$ is a subalgebra of $A(M)$ and if $X \in A(M) \setminus H(M)$ it is called *proper affine*. Again it is remarked that the collections of proper affine vector fields and proper projective vector fields are not Lie algebras or even vector spaces. If X is projective, then a global 1-form χ (the *projective 1-form*) exists on M such that X and χ satisfy, in any coordinate system, the equations (which are the analogues of (2c) and (3))

$$X_{a;b} = \frac{1}{2}h_{ab} + F_{ab} \qquad \mathcal{L}_X g \equiv h \qquad h_{ab} = h_{ba}$$
$$F_{ab} = -F_{ba} \tag{6}$$

where F is the *projective bivector (field) (of* X*)* and where

$$h_{ab;c} = 2g_{ab}\chi_c + g_{ac}\chi_b + g_{bc}\chi_a. \tag{7}$$

The vector field X is affine if and only if $\chi \equiv 0$ on M, homothetic if and only if $h_{ab} = cg_{ab}$ on M for some constant c ($\Rightarrow \chi \equiv 0$ on M) and Killing if and only if $h \equiv 0$ on M ($\Rightarrow \chi \equiv 0$ on M). As an example, consider the metric g given in a global coordinate system $x^0, ..., x^3 = t, v, x, y$, with $v > 0$ by [10,1]

$$ds^2 = -dt^2 + dv^2 + v^2 q_{\alpha\beta}dx^\alpha dx^\beta \tag{8}$$

where Greek letters take the values $2, 3$ and where the $q_{\alpha\beta}$ are independent of t and v and are chosen so that the metric g is not flat. Then the vector field with components $(t^2, vt, 0, 0)$ is proper projective, $(t, 0, 0, 0)$ is proper affine and $(t, v, 0, 0)$ is proper homothetic. A *non-flat, vacuum* space-time cannot admit a proper projective vector field [10,1]. The existence of a *proper* affine vector field on any space-time is a statement that its *holonomy group* has "reduced" [11,1] as is the case in (8). As another example, $u\partial/\partial v$ is proper affine for the metric (5).

Now consider the situation when, in the language of the first paragraph of section 2, one chooses for K the tensor *Riem*. Here one experiences some differences to those results given in the previous paragraphs. A

global, smooth vector field X on M is called a *curvature collineation* if it satisfies $\mathcal{L}_X Riem = 0$ (and recall that $Riem$ has components $R^a{}_{bcd}$). The collection of all curvature collineations is a vector space denoted $CC(M)$. Since the local flows of affine vector fields preserve the connection it follows that any affine vector field is a curvature collineation and that $A(M)$ is a subalgebra of $CC(M)$. For the set $CC(M)$ one cannot achieve a nice closed differential system such as is found for Killing, conformal, etc, vector fields and, as a consequence, $CC(M)$ may not be finite-dimensional. Also the direct integration of the equation $\mathcal{L}_X Riem = 0$ is complicated. Thus the study of such symmetries is rather difficult and is mostly restricted to special cases (see e.g., [12,13,9,14–16]). Fortunately, there is a result which, at least, saves the trouble of such an integration in the "generic" case. There is, in fact, an acceptable topological definition of a "generic situation" for space-times [8] and should (M, g) satisfy it, the tensor $Riem$ on M uniquely determines the Levi-Civita connection from which it arises and the corresponding metric up to a constant conformal factor [7,1]. Then if this is the case on M, suppose $X \in CC(M)$ with local flow ϕ_t with domain U and range $V = \phi_t(U)$. If g is the metric of M restricted to U with curvature tensor $Riem$ and if g' is the metric on M restricted to V with curvature tensor $Riem'$ then $\phi_t^* Riem' = Riem$ since $X \in CC(M)$. But $\phi_t^* g'$ is a metric on U with curvature $\phi_t^* Riem' (= Riem)$ and so g and $\phi_t^* g'$ are metrics on U with the same curvature tensor and hence from the above result $\phi_t^* g' = cg$ for c constant. This is true for all such local flows and so X is homothetic on M. Thus in this generic case, $CC(M) = H(M)$ and $CC(M)$ is finite-dimensional [7,1]. If the generic condition fails, $CC(M)$ may not be finite-dimensional. To see this consider the following metric in a global coordinate system $(x^0, x^1, x^2, x^3) \equiv (t, x^\alpha)$ with $t \in \mathbb{R}$, Greek letters running from 1 to 3 and given by

$$ds^2 = -dt^2 + h_{\alpha\beta} dx^\alpha dx^\beta \tag{9}$$

Here the $h_{\alpha\beta}$ depend only on the coordinates x^α. In this case, $X \equiv \partial/\partial t$ is a *covariantly constant* vector field ($\nabla X = 0$) on M and from (2) is thus Killing. It can then be checked that if $f(t)$ is any globally defined smooth function on M, $f(t)X$ is in $CC(M)$ for all such choices of f. This follows from the equation $\mathcal{L}_X Riem = 0$ after noting that, from the Ricci identity for X, $R^a{}_{bcd} X^d = 0$ and so a component $R^a{}_{bcd}$ of $Riem$ is zero if at least one of the indices a, b, c, d is 0. Thus X, $tX ... t^n X ...$ are independent members of $CC(M)$ for all positive integers n and hence $CC(M)$ is not finite-dimensional. The choice of the *smooth* function f given by $f(t) = 0$ if $t \leq 0$ and $f(t) = e^{-\frac{1}{t}}$ if $t > 0$ also reveals that a *non-trivial* member of $CC(M)$ may vanish over a non-empty open subset of M. This example also shows that a member X of $CC(M)$ is not necessarily uniquely determined by its value together with those of any number of its covariant derivatives at some $m \in M$ (just compare it with the zero vector field in $CC(M)$). Another example of a situation when $CC(M)$ is infinite-dimensional is the metric (5) since it admits a covariantly constant vector field [9]. There is another problem concerning the set $CC(M)$. First it is remarked that if $X \in A(M)$ and is C^2 then it is necessarily smooth (C^∞) and if $X \in C(M)$ or $X \in P(M)$ and is C^3 then it is necessarily smooth [1]. However, any degree of differentiability can be achieved for members of $CC(M)$ as is easily seen by choosing the function f above associated with (9) to be C^r (but not C^{r+1}) for $r \geq 1$. Thus in this case, in order to make $CC(M)$ a Lie algebra, one should, perhaps, insist that each member of $CC(M)$ is smooth (otherwise, $[X, Y]$ may not even be differentiable). However, *generically*, as explained above, $CC(M) = H(M)$ and is hence a Lie algebra.

Another case of interest is when one chooses for K the Weyl conformal tensor C. Call a smooth, global vector field X a *Weyl conformal collineation* if it satisfies $\mathcal{L}_X C = 0$ and denote the set of all such vector fields by $WC(M)$. It is easy to check by a consideration of the associated local flows that $C(M)$ is a subalgebra of $WC(M)$. Again similar problems arise here as for $CC(M)$, that is, $WC(M)$ may be infinite-dimensional. However, as in the case of $CC(M)$, there is a convenient result which states that "generically" (as in the case of $Riem$), the Weyl tensor C uniquely determines the conformal class of the metric g from which it came and then, by a similar argument to that for $Riem$, it can be shown that, *generically*, if $X \in WC(M)$, then $X \in C(M)$ (hence $WC(M)$ equals $C(M)$ and is finite-dimensional). In this case, the generic condition may be stated in terms of the Petrov type of C on (M, g) [1]. The remarks made above on differentiability, etc, regarding $CC(M)$ also apply to $WC(M)$. Some further details can be found in [32]. [Interestingly, $WC(M)$ can be infinite-dimensional for M of any dimension ≥ 4 (this latter restriction ensuring that C is well-defined and not necessarily identically zero) and g of any signature, except $\dim M = 4$ with g positive definite; in this latter case $WC(M) = C(M)$ and is finite-dimensional [37].] It is also remarked here that for the Weyl projective tensor W and for any dimension of $M \geq 3$ (to ensure that W is well-defined and not necessarily identically zero), the vector space $WP(M)$ of all global, smooth vector fields X on M satisfying $\mathcal{L}_X W = 0$ (whose members are called *Weyl projective collineations*

and which contains $CC(M)$ as a subalgebra) may be infinite-dimensional (and is if $CC(M)$ is). A consideration of local flows shows that $P(M)$ is a subalgebra of $WP(M)$. The remarks made above on dimension and differentiability, etc, regarding $CC(M)$ also apply to $WP(M)$. Further details can be found in [38].

Another problem which has been studied is that of symmetries of the Ricci tensor *Ricc*, that is, those (global, smooth) vector fields X on M satisfying $\mathcal{L}_X Ricc = 0$ (Ricci collineations). Here, the lack of any shortcut in any generic situation is a drawback and the calculations are complicated and restricted to special cases. The Lie algebra of Ricci collineations contains $CC(M)$ as a subalgebra. Yet another study concerns the so-called "matter collineations", that is, those (global, smooth) vector fields X on M satisfying $\mathcal{L}_X T = 0$ where T is the (tensor type $(0,2)$) energy-momentum tensor. One extra problem which arises in this latter case is that of whether one studies the symmetries of T_{ab}, $T^a{}_b$ or T^{ab}, the results being different, in general. Progress on these problems seems to be difficult [17–22]. However, if *Ricc* has a non-degenerate matrix R_{ab} of components at each $m \in M$, the collection of Ricci collineations is a finite-dimensional Lie algebra, being the Killing algebra of the metric *Ricc* on M. The remarks made on dimension and differentiability, etc, regarding $CC(M)$ above, also apply to Ricci and matter collineations.

3 Orbit Geometry

First consider $K(M)$, assumed non-trivial, and let $m \in M$. Construct the linear mapping of vector spaces $f : K(M) \to T_mM$ which maps the global Killing vector field $X \in K(M)$ into its value $X(m)$ at m, $X \to X(m)$. Let I_m denote the kernel of this map; $I_m \equiv \{X \in K(M) : X(m) = 0\}$ and let Δ_m denote its range; $\Delta_m \equiv \{X(m) : X \in K(M)\}$ so that Δ_m is a subspace of T_mM. Then from elementary linear algebra, $\dim K(M) = \dim I_m + \dim \Delta_m$ at any $m \in M$. Although $\dim K(M)$ is fixed by (M, g), $\dim I_m$ and $\dim \Delta_m$ may vary with m but must do so consistently with their sum equalling $\dim K(M)$. (A consequence of the possible variability of $\dim \Delta_m$ over M shows that the map $m \to \Delta_m$ may not be a distribution in the sense of Frobenius and is sometimes called a *generalised distribution.* However, in dealing with the *finite-dimensional* symmetry algebras, $K(M), H(M), C(M), A(M)$ and $P(M)$, this does not cause any major problems [28] (and see, e.g.[1])). Now from the fact that if $X \in K(M)$ the conditions $X(m) = 0$ and $F(m) = 0$ (where F is the Killing bivector of X) imply that $X \equiv 0$ on M, it is clear that the subspace of $\Lambda_m M$ given by $\{F(m) : F$ is the Killing bivector of some $X \in I_m\}$ is isomorphic to I_m under the mapping $X \to F(m)$ for $X \in I_m$. This representation of I_m as a subspace of $\Lambda_m M$ is then easily checked to be a Lie algebra under matrix commutation and is Lie-isomorphic to a subalgebra of the Lie algebra of the Lorentz group (the bivector representation of the latter being well known; see, e.g., [24]). The Lie algebra I_m is called the *isotropy algebra* of $K(M)$ at m and, if non-trivial, gives a description of the symmetry resulting from $K(M)$ in the tensor spaces at m. To see this let X be a non-trivial member of I_m. Then $X(m) = 0$ and any local flow ϕ_t of X fixes the point m, $\phi_t(m) = m$. If $v \in T_mM$, choose a smooth curve $c : (-\epsilon, \epsilon) \to M$ for $0 < \epsilon \in \mathbb{R}$ so that $c(0) = m$ and v is tangent to c at m. Then the curve $\phi_t \circ c$ through m has tangent vector equal to the "pushforward", $\phi_{t*}(v)$, of v, using ϕ_t, at m (see, e.g. [1] section 4.10). In this intuitive sense, ϕ_{t*} "drags" T_mM round as directed by the symmetries ϕ_t associated with X. (This idea will be useful later in sections 5 and 6.)

The subspaces Δ_m can be interpreted in the following way. Through each $m \in M$ there is a connected submanifold, denoted O_m and called the *orbit* associated with $K(M)$ through m. The tangent space to O_m at $m' \in O_m$ equals $\Delta_{m'}$ and so one sees that $\dim \Delta_m$ $(= \dim O_m)$ and hence $\dim I_m$ is constant over any such O_m. As m ranges over M the dimension of O_m may change. The orbit O_m may be interpreted using the integral curves of the members of $K(M)$. In fact, if $k \in \mathbb{N}$ let $X_1, ..., X_k \in K(M)$ and let $\phi^1_{t_1}, ..., \phi^k_{t_k}$ be the local flows associated with them for appropriate values of $t_1, ..., t_k$. Consider the set of all local diffeomorphisms on M (where defined) of the form

$$m' \to \phi^1_{t_1}(...\phi^k_{t_k}(m')...)) \qquad m' \in M \tag{10}$$

for each choice of $k \in \mathbb{N}$, $X_1, ..., X_k \in K(M)$ and admissible $(t_1, ..., t_k) \in \mathbb{R}^k$. One can define an equivalence relation $\sim$ on M by $m_1 \sim m_2$ $(m_1, m_2 \in M)$ if and only if some map of the form (10) maps m_1 to m_2. The equivalence classes arising from $\sim$ are exactly the *orbits* associated with $K(M)$ and so the particular orbit O_m consists of those points that m is mapped to under the local flows applied successively, as in (10). If $\dim \Delta_m = 4$ for each $m \in M$ then, since M is connected, there is a single $4-$dimensional orbit associated with $K(M)$ and $K(M)$ is called *transitive* (and (M, g) is called *homogeneous*). The submanifolds O_m may have some unpleasant properties [1,23] but are sufficiently nice for most purposes. More details on their mathematical structure may be found in [25–28,1,23]. They are extremely useful for constructing natural coordinate systems and exact solutions of Einstein's field equations (1) if the space-time in question admits a non-trivial Killing algebra $K(M)$. It is also noted for later use that

if O is any orbit and $\phi_t : O \to O$ any local flow of some member of $K(M)$, then $\phi_t : O \to O$ is smooth and the pushforward map ϕ_{t*} is an isomorphism of the tangent space T_mO to O at $m \in O$ onto the tangent space $T_{\phi_t(m)}O$ to O at $\phi_t(m)$.

It is useful at this point to recall that a 1-dimensional subspace of T_mM is called a spacelike (respectively, timelike or null) *direction* if any spanning member of it is spacelike, (respectively, timelike or null). Then, with regard to the Lorentz inner product $g(m)$ on T_mM, a 2-dimensional subspace (a *2-space*) $U \subset T_mM$ is called *spacelike* if each of its non-zero members is spacelike, *null* if it contains a unique null direction and *timelike* if it contains exactly two distinct null directions. The classification of 3-dimensional subspaces is similar, the definitions for spacelike and null being identical to those in the 2-dimensional case. A 3-dimensional subspace (a 3-*space*) is called *timelike* if it contains at least two (and hence infinitely many) distinct null directions. It follows for either dimension that a subspace is timelike if and only if it contains a timelike member. Now $F \in \Lambda_m M$ has, on account of its skew-symmetry, even (matrix) rank. If this rank is 2, F is called *simple* and it may be written as $F^{ab} = p^a q^b - q^a p^b$ for $p, q \in T_mM$. In this case F uniquely determines the 2-space in T_mM spanned by p and q and this 2-space is called the *blade* of F. Then F is called *spacelike, timelike* or *null* if this blade is, respectively, spacelike, timelike or null. In this case, F (or its blade) is sometimes denoted $p \wedge q$. If F has rank 4 it is called *non-simple* and it can then be shown that F uniquely determines an orthogonal pair of 2-spaces at m, one spacelike and one timelike, and which are collectively called the *canonical pair of blades* of F [33]. It is noted here for later use that any bivector F at m has a *finite* (non-zero) number of null eigendirections at m, one if $F(m)$ is null and two if $F(m)$ is spacelike, timelike or non-simple.

Again considering the Lie algebra $K(M)$, if $m \in M$ and $\dim\Delta(m) = 0$, the orbit through m is the singleton subset $\{m\}$. If $\dim\Delta(m) > 0$ the orbit through m is a connected submanifold of M and at each such m, $\Delta(m)$ coincides with the subspace of T_mM tangent to the orbit through m. An orbit is called *proper* if its dimension is 1, 2 or 3. The *nature* of a proper orbit O_m through $m \in M$ is the type (timelike, spacelike or null) of any of the subspaces $\Delta(m')$ for any $m' \in O_m$ since, by the definition of $K(M)$, this nature is easily checked to be independent of $m' \in O_m$.

If $X \in K(M)$ is not trivial and $X(m) = 0$ then m is a *zero* of X and a *fixed point* ($\phi_t(m) = m$) of any associated local flow ϕ_t of X. The Killing bivector of X, evaluated at m, then makes a non-trivial contribution to the isotropy algebra I_m. If, in addition, the Killing bivector of X is non-simple at m, then m is an isolated zero of X. If, however, the Killing bivector is simple at m there exists an open neighbourhood U of m such that the collection of zeros of X *in* U is a 2-dimensional submanifold of U and hence of M. [1]. If I_m is non-trivial, there are consequences for the various tensors derived from g at m. For example, the energy-momentum (or the Ricci) tensor will inherit eigenvalue degeneracies and the Petrov type is seriously restricted at any zero m of X, being either type **N** or **0** if $F(m)$ is null and type **D** or **0** if $F(m)$ is either non-simple, spacelike or timelike. It is true that if O_m is an orbit of $K(M)$ with $\dim O_m \geq 1$ and $\dim K(M) > \dim O_m$, any point $m' \in O_m$ is a zero of some non-trivial $X \in K(M)$. To see this let $\dim K(M) = n > 1$ and let $X_1, ..., X_n$ be a basis for $K(M)$. Then $X_1(m'), ..., X_n(m')$ are *dependent* members of T_m since they lie in Δ_m and $n > \dim\Delta_m$. Thus there exists $a_1, ..., a_n \in \mathbb{R}$ not all zero such that $\sum_{i=1}^n a_i X_i(m') = 0$. Now define the (global) vector field $X = \sum_{i=1}^n a_i X_i$ which is clearly a non-zero member of $K(M)$ (since $X_1, ..., X_n$ are independent in $K(M)$) and satisfies $X(m') = 0$. So m' is a zero of X. One can extend the study of orbits and isotropies to the finite-dimensional Lie algebras $H(M)$, $C(M)$, $A(M)$ and $P(M)$. For details of some of these see [1,29].

As an example consider the exterior Schwarzschild solution. Here all Killing orbits are 3-dimensional and timelike and given by a constant value of r in the usual coordinates of that solution. For *generic* FRWL cosmological solutions (see section 5), all orbits are 3-dimensional and spacelike and given by a constant value of cosmic time. The Einstein static metric has a single 4-dimensional orbit and is homogeneous. For the metric (5) the orbits can be 3-dimensional and null (and given by u =constant) or 4-dimensional (the homogeneous case). In each of these examples the orbits are of constant dimension over M but this need not be the case. For example, consider the metric g given in global coordinates t, x, y, z on the manifold $\mathbb{R}^4$ by

$$ds^2 = -dt^2 + e^{x^2+y^2+z^2}(dx^2 + dy^2 + dz^2) \qquad (11)$$

For this metric $\dim K(M) = 4$, with $K(M)$ being spanned by the global, Killing vector fields with components $(1, 0, 0, 0)$, $(0, 0, z, -y)$, $(0, y, -x, 0)$ and $(0, z, 0, -x)$. Then (M, g) has a 1-dimensional timelike orbit given by $x = y = z = 0$ with all other orbits being 3-dimensional and timelike.

4 Orbit Structure

An orbit O of $K(M)$ is called *dimensionally stable* [1, 23] if for each $m \in O$ there exists an open neigh-

bourhood U of m such that any orbit through any point of U has the same dimension as O. It turns out that any 3-dimensional spacelike or timelike orbit is dimensionally stable as is any 4-dimensional orbit. Connected regions containing only dimensionally stable orbits may be expected to give pleasant results along the lines of those for a Frobenius type distribution. Examples of pairs (M, g) and $K(M)$ admitting orbits which are not dimensionally stable can be easily constructed. (In fact, the 1-dimensional timelike orbit in (11) is not dimensionally stable; but the other orbits are.) The "generic" FRWL models in relativistic cosmology have space sections (submanifolds of constant cosmic time) which are 3-dimensional, spacelike, dimensionally stable orbits whereas the extended Schwarzschild metric has 3-dimensional, dimensionally stable orbits whose nature may be spacelike, timelike or null. Non-homogeneous plane wave metrics have 3-dimensional, null, dimensionally stable orbits (see section 6). If $K(M)$ is not trivial, one may *disjointly* decompose M as $M = M_s \cup M_{ns}$ where M_s (respectively, M_{ns}) denotes the union of all dimensionally stable (respectively, not dimensionally stable) orbits of $K(M)$. The subset $V_k \equiv \{m \in M : \dim\Delta_m = k\}$, for $1 \leq k \leq 4$, is the union of all the $k-$dimensional orbits of $K(M)$ and $\mathrm{int}V_k$ is the union of all the dimensionally stable orbits of $K(M)$ of dimension k where "int" denotes the interior in the manifold topology on M. Thus M_s is open in M. Since $K(M) \neq \{0\}$ and each $X \in K(M)$ must vanish on V_0, $\mathrm{int}V_0 = \emptyset$.

If O is a proper non-null orbit then, as a submanifold, it inherits an induced metric h from the global metric g and each member of $K(M)$ gives rise in a natural way to a vector field on O which can be shown to be a Killing vector field in O for the metric h. This construction gives a map $K(M) \to K(O)$ which is a Lie algebra homomorphism and which need not be surjective but, if $\dim O = 3$, is injective. The possible lack of injectiveness follows because of the possibility of a non-trivial member $X \in K(M)$ becoming identically zero on the orbit (see, e.g., the metric (11) and the 1-dimensional orbit described there). But, from the results on the zeros of X, this cannot occur for (non-null) orbits of dimension 3 and any orbit of dimension 4 [1, 23]. This is important since some arguments in relativity theory involve the inducing of independent members of $K(M)$ into an orbit and the assumption that such orbit vector fields are *independent* there. This is true for 3-dimensional non-null orbits (and 4-dimensional orbits) but not necessarily true otherwise.

One would also like a relation between the existence of orbits of a certain dimension and the dimension of $K(M)$. This is provided in the following result.

Theorem 1 [1,23]

Let (M, g) be a space-time with Killing algebra $K(M)$. Then the following hold.

(i) If there exists a 3-dimensional null orbit, $3 \leq dimK(M) \leq 7$. If, however, there exists a dimensionally stable, 3-dimensional, null orbit or any non-null, 3-dimensional orbit, $3 \leq dimK(M) \leq 6$.

(ii) If there exists a 2-dimensional, null orbit, $2 \leq dimK(M) \leq 5$ and if there exists a 2-dimensional, non-null orbit, $2 \leq dimK(M) \leq 4$. If there exists any 2-dimensional, dimensionally stable orbit, $2 \leq dimK(M) \leq 3$.

(iii) If there exists a 1-dimensional, null orbit, $1 \leq dimK(M) \leq 5$ and if there exists a 1-dimensional, non-null orbit, $1 \leq dimK(M) \leq 4$. If there exists any 1-dimensional, dimensionally stable orbit, $\dim K(M) = 1$.

It is not to be understood that all possibilities contained within the inequalities for $\dim K(M)$ can actually exist but many of them can and examples are available [1,23]. One corollary of this theorem is that $\dim K(M) = 9$ is impossible since, if it were possible, theorem 1 shows that all orbits would be 4-dimensional and so, if O is any such orbit and $m \in O$, $\dim I_m = \dim K(M) - \dim O = 5$. But the Lorentz algebra has no 5-dimensional subalgebras and a contradiction is obtained. One can similarly show from theorem 1 that if $\dim K(M) = 8$ all orbits are 4-dimensional and so for each $m \in M$ $\dim I_m = 4$. It then turns out that (M, g) is a conformally flat Einstein space and hence is of constant curvature. Thus, *locally*, a 10-dimensional Lie algebra of Killing vector fields exists.

The final two sections of this paper will give a simple application of some of these latter results to the study of cosmology and to the theory of plane waves in general relativity. The first of these presents a simple rigorous and global, geometrical view of cosmology using only the concept of isotropy derived from astronomical observations. The second provides a similar discussion of plane waves using the idea of wave surface isotropy. The consequences are, of course, not new but it is believed that the methods and techniques employed have some interesting novelty value. The idea is to derive the cosmological and plane wave metrics from a single, physically reasonable, geometrical assumption. One useful piece of information which will be required is the subalgebra structure of the Lie algebra L of the Lorentz group in the bivector representation and this is given in table 1. In this table (l, n, x, y) denotes a null tetrad, (x, y, z, t) a pseudo-orthonormal tetrad and $0 \neq \omega \in \mathbb{R}$. The notation is taken from [24] and the trivial subalgebra, R_1, is omitted.

Table 1 Lorentz Subalgebras

Type	Dimension	Basis	Type	Dimension	Basis
R_2	1	$l \wedge n$	R_9	3	$l \wedge n$, $l \wedge x$, $l \wedge y$
R_3	1	$l \wedge x$	R_{10}	3	$l \wedge n$, $l \wedge x$, $n \wedge x$
R_4	1	$x \wedge y$	R_{11}	3	$l \wedge x$, $l \wedge y$, $x \wedge y$
R_5	1	$l \wedge n + \omega x \wedge y$	R_{12}	3	$l \wedge x$, $l \wedge y$, $l \wedge n + \omega(x \wedge y)$
R_6	2	$l \wedge n$, $l \wedge x$	R_{13}	3	$x \wedge y$, $y \wedge z$, $x \wedge z$
R_7	2	$l \wedge n$, $x \wedge y$	R_{14}	4	$l \wedge n$, $l \wedge x$, $l \wedge y$, $x \wedge y$
R_8	2	$l \wedge x$, $l \wedge y$	R_{15}	6	L

5 Cosmological Space-Times

The observation in cosmology referred to as *isotropy* is, roughly speaking, that at any space-time event $m \in M$ there exists an observer for whom "all directions at m are equivalent". This can only be taken to refer to information arriving at m from the boundary or the inside of the past null cone at m and, since most cosmological information arrives in the form of photons, this isotropy will be taken to refer to the indistinguishability of future pointing null directions at m. The concept of *homogeneity* in cosmology (used here in its traditional sense and not as in section 3) is more elusive since it refers to the indistinguishability of events occurring at the "same time" and thus requires the existence of some cosmological time to have already been established. However, only the isotropy described above will be required here. So let a space-time (M, g) be called *cosmological* if it admits a global Killing algebra $K(M)$ such that for each $m \in M$ the collection of (pushforward) isomorphisms ϕ_{t*} arising from all members of I_m acts *transitively* on null directions (that is, given any two null directions at m, some ϕ_{t*} in this collection maps one of them to the other). Thus one tries to mimic this physical, cosmological isotropy using the property of the maps ϕ_{t*} described at the end of the first paragraph in section 3.

Lemma 1

If (M, g) is a cosmological space-time then either;

(i) I_m is isomorphic to the Lie algebra $o(3)$ *at each* $m \in M$, or

(ii) I_m is isomorphic to L *at each* $m \in M$ and, in this case, (M, g) is of constant curvature.

If (M, g) is a cosmological space-time then it is conformally flat.

Proof

Since (M, g) is cosmological the collection of isomorphisms, ϕ_{t*}, arising from all members of I_m cannot *fix* any *null* direction at any $m \in M$. Thus the bivectors in the representation of I_m cannot have a common null eigendirection (cf [1]). A simple inspection of the possible subalgebras of L in table 1 then shows that I_m is isomorphic to either R_{13} ($\approx o(3)$) or to $R_{15}(\approx L)$. (The possibility R_{10} is out since, then, y is fixed in the null tetrad l, n, x, y of table 1 and any null direction orthogonal to y stays orthogonal to y under the maps ϕ_{t*}, contradicting transitivity.) If there exists $m \in M$ with orbit O_m through m such that I_m is isomorphic to $o(3)$) then $\dim K(M) = \dim O_m + \dim I_m \leq 4 + 3 = 7$. If however, there exists $m \in M$ with orbit O_m through m such that I_m is isomorphic to L, $\dim K(M) \geq \dim I_m = 6$ and so, from theorem 1, $\dim O_m \geq 3$ and then $\dim K(M) \geq 6 + 3 = 9$. This contradiction shows that either I_m is isomorphic to $o(3)$ *at each* $m \in M$ or I_m is isomorphic to L *at each* $m \in M$. Since $\dim K(M) = 9$ is impossible it follows that in the latter case, $\dim K(M) = 10$ and (M, g) has constant curvature. The fact that $\dim I_m \geq 3$ at each $m \in M$ shows that the Weyl conformal tensor vanishes everywhere on M [34].□

The consequences of the cosmological assumption in lemma 1 have now become detached from the observer mentioned at the beginning of this section, being a purely geometrical statement on $K(M)$. However, the initial intuitive idea means that the maps ϕ_{t*} arising from I_m should preserve the (timelike) direction of the special observer (intuitively, the universe should turn about him, isotropically, without his need for a change of direction or speed, as would be the case for any other timelike direction at m). If $I_m \approx o(3)$, the collection of all bivectors $F(m) \in I_m$ admits a unique common timelike eigendirection (see table 1) and so there is a unique timelike direction at m which is fixed by all the ϕ_{t*} arising from I_m (the "axis" of I_m). This distinguishes the (unique) special observer's world line for this possibility of I_m. If $I_m \approx L$, then I_m is transitive on timelike directions and the above uniqueness is lost. The general smoothness assumptions together with the assumption that the cosmological symmetries are a consequence of a smooth Killing action will be seen to show that these timelike directions can be spanned locally by smooth unit timelike vector fields on M.

Lemma 2

Suppose that (M, g) is cosmological. Then any orbit of $K(M)$ has dimension 3 or 4 and (M, g) consists of either a single 4-dimensional orbit or each of its orbits is

3-dimensional and spacelike. All orbits are dimensionally stable. In detail then, either;

(i) I_m is isomorphic to L for each $m \in M$, in which case, (M, g) has constant curvature, dim $K(M) = 10$ and $K(M)$ has a single 4-dimensional orbit, *or*

(ii) I_m is isomorphic to $o(3)$ for each $m \in M$ and if (M, g) is non-flat then either $K(M)$ has a single 4-dimensional orbit ($\Rightarrow$ dim$K(M) = 7$) or each orbit of $K(M)$ is 3-dimensional and spacelike ($\Rightarrow$dim$K(M) = 6$).

Proof.

Let O be a 1-dimensional (respectively, a 2-dimensional) *dimensionally stable* orbit of $K(M)$. Whatever the dimension (3 or 6) of the isotropy on M, if $m \in O$, dim$K(M) \geq 3 + 1 = 4$ (respectively, dim$K(M) \geq 3 + 2 = 5$) contradicting theorem 1. So no such dimensionally stable orbits can exist. So let $k \equiv \{\max \text{dim}O : O \text{ an orbit of } K(M)\}$. Then there exists an orbit O' with dim$O' = k$ and by an application of the rank theorem to the distribution Δ the orbit O' is dimensionally stable. The previous argument shows that dim$O' \geq 3$ and so dim$K(M) \geq 3 + 3 = 6$. Further appeal to theorem 1 shows that every orbit of $K(M)$, dimensionally stable or not, has dimension 3 or 4. If a null 3-dimensional orbit O exists and $m \in O$ it follows ([1], section 10.5) that the tangent space T_mO is mapped into itself by the isomorphisms arising from I_m and so the unique null direction at m tangent to O must be fixed by these isomorphisms contradicting the cosmological assumption. If a timelike orbit O exists then, for $m \in O$ a consideration of I_m reveals a fixed spacelike vector $p \in T_mM$. A similar argument to that which ruled out the possibility of the R_{10} case in the proof of lemma 1 shows the impossibility of transitivity on null directions. So any 3-dimensional orbit is spacelike (and dimensionally stable). Then if M is decomposed as $M = M_3 \cup M_4$ where M_3 (respectively, M_4) denotes the union of the all the 3-dimensional (respectively, 4-dimensional) orbits of $K(M)$ then M_4 is open (by the rank theorem) and M_3 is open since it consists of (spacelike) dimensionally stable orbits. Since M is connected either M_3 or M_4 is empty and so $M = M_3$ or $M = M_4$. Finally, if the conditions of (i) hold then, for any $m \in M$ and orbit O through m, dim$K(M)$ =dimI_m+dim$O \geq 6 + 3 = 9$ and hence dim$K(M) = 10$. So dim$O = 4$ and O is the only orbit. Part (ii) follows immediately. □

The metrics in lemma 2(i), in local coordinates, give the de Sitter (positive constant curvature), anti-de Sitter (negative constant curvature) and Minkowski (zero curvature) metrics.

For the metrics in lemma 2(ii) some further analysis is required. The existence of a single (4−dimensional) $K(M)$ orbit together with the conformally flat and non-flat conditions mean that *Ricc* cannot vanish at any point of M. Further, each Ricci eigenvalue (and hence the Ricci scalar, R) is constant on M and that the algebraic Segre type of the Ricci tensor is the same at each $m \in M$. The fact that I_m is isomorphic to $o(3)$ for each $m \in M$ forces this Segre type to be either $\{1, (111)\}$ at each $m \in M$ or $\{(1111)\}$ at each $m \in M$. [1,6]. In the latter case $Ricc = \frac{R}{4}g$ and (M, g) is a conformally flat (lemma 1) Einstein space and hence has constant curvature. [This does not contradict the fact that dim$K(M) = 7$; it simply means that no global, 10-dimensional Killing algebra exists on M but that a *local* 10-dimensional Killing algebra exists in some neighbourhood of each $m \in M$.] In the former case one has constant Segre type $\{1, (111)\}$ for *Ricc* on M and so the two Ricci eigenvalues are distinct constants. The constancy of this Segre type shows [39] that the timelike eigendirection of *Ricc* at each $m \in M$ gives rise to a smooth distribution D on M (but there may not be a smooth *global* (timelike) vector field on M spanning it). However, there is a local smooth (unit timelike) vector field, say u, spanning it in some neighbourhood of any point of $m \in M$ and in such a (connected, coordinate) neighbourhood U one has $R_{ab} = \alpha g_{ab} - \beta u_a u_b$ for constants α and β with $\beta \neq 0$. Since (M, g) is conformally flat the Bianchi identity gives

$$R_{ab;c} - R_{ac;b} = 0 \tag{12}$$

For $X \in K(M)$, $\mathcal{L}_X Ricc = 0$, and so $\mathcal{L}_X(u_a u_b) = 0$ from which it easily follows that $\mathcal{L}_X u_a = \lambda u_a$ for some (smooth) function λ on U. A back substitution then gives $\lambda = 0$ and so $\mathcal{L}_X u_a = 0$ on U. Since $X \in K(M)$, the corresponding local flow maps ϕ_t then satisfy $\phi_{t*}u = u$ and so $\phi_{t*}(\nabla u) = \nabla u$ where ∇ is the Levi-Civita connection from g. In coordinates this is $\mathcal{L}_X(u_{a;b}) = 0$ and so if F is the bivector on U defined by $F_{ab} = u_{[a;b]}$, $\mathcal{L}_X F = 0$ ($\Leftrightarrow \phi_{t*}F = F$). If this last equation is applied at m with $X \in I_m$ and $F(m) \neq 0$, the fact that the maps ϕ_{t*} are transitive on null directions at m contradicts the known result (section 3) that $F(m)$, has a finite, non-zero number of null eigendirections. It follows that $F(m) = 0$ and since this holds at each $m \in U$, $u_{a;b} = u_{b;a}$ on U. Now apply the isotropy at each such m this time to the symmetric tensor $u_{a;b}$ to get $u_{a;b} = \rho g_{ab} + \sigma u_a u_b$ on U for smooth functions ρ and σ [1,6] (which are actually constant on U since $\mathcal{L}_X(u_{a;b}) = 0$ and since there is a single 4-dimensional orbit for $K(M)$, but this fact is not needed). Since $u^a u_a$ is constant, $u^a u_{a;b} = 0$ and so $\rho = \sigma$. Thus $u_{a;b} = \rho(g_{ab} + u_a u_b)$ on U. A substitution of this into (12) reveals that $\rho = 0$ and so $u_{a;b} = 0$ on

U. Then one may choose U and a function $t : U \to \mathbb{R}$ so that $u_a = t_{,a} (\equiv t_a)$.

Since there is a single 4-dimensional orbit for $K(M)$ one may choose (U and) six members $X_i \in K(M)$ $(1 \leq i \leq 6)$ and six smooth associated functions $\mu^i \equiv X_i^a t_a$ such that (a) $X_1(m')$, $X_2(m')$ and $X_3(m')$ are independent members of $T_{m'}M$ for each $m' \in U$, (b) $\mu^1(m) = \mu^2(m) = \mu^3(m) = 0$ and (c) X_4, X_5 and X_6 are independent members of I_m (and hence of $K(M)$) and so $X_4(m) = X_5(m) = X_6(m) = 0$. It follows that the vector fields X_i $((1 \leq i \leq 6))$ are independent members of $K(M)$. [To see this suppose $Z \equiv \sum_1^6 \nu_i X_i = 0$ on M $(\nu_i \in \mathbb{R})$. Then $Z(m) = 0 \Rightarrow \nu_1 = \nu_2 = \nu_3 = 0$ (from (a) and (c)) and so $Z = \sum_4^6 \nu_i X_i = 0$ on M from which it follows from (c) that $\nu_4 = \nu_5 = \nu_6 = 0$.] Now the Ricci identity for u gives $R^a{}_{bcd} u^d = 0$ where $R^a{}_{bcd}$ are the components of the curvature tensor of ∇ on U. So $R_{ab} u^b = 0$ and hence $\alpha = -\beta \neq 0$ and $R_{ab} = \alpha(g_{ab} + u_a u_b)$ on U. Now it follows from (3) that, for any $X \in K(M)$, $X^a{}_{;bc} = F^a{}_{b;c} = R^a{}_{bcd} X^d$ on U. One now easily finds that $\mu^i_{;ab} = R^c{}_{abd} X^d t_c = 0$ and $\mu^i_{,a} t^a = 0$ on U $(1 \leq i \leq 6)$. Thus each covector field $\mu^i_{,a}$ on U is covariantly constant on U and hence, from the Ricci identity, $R^a{}_{bcd} \mu^i_{,a} = 0$ and so $R_a{}^b \mu^i_{,b} = 0$ contradicting the fact that *Ricc* has everywhere rank 3, unless each $\mu^i_{,a}$ is proportional to t_a on U. It follows that μ^i is a function of t only on U and since $\mu^i_{,a} t^a = 0$ on U, $\mu^i_{,a} = 0$ on U. Since U is connected and $\mu^i(m) = 0$ each μ^i vanishes on U and so each X_i is orthogonal to u on U. It follows that for $1 \leq i, j \leq 6$, the Killing vector field $[X_i, X_j]$ is orthogonal to u on U. But, since $K(M)$ is 7-dimensional and transitive and X_i $(1 \leq i \leq 6)$ are independent, a basis for $K(M)$ can be formed from these X_i augmented by another member $Y \in K(M)$ which is nowhere orthogonal to the distribution D on U. On writing $[X_i, X_j]$ out as a *linear combination* of the X_i and Y on M and applying the condition of being orthogonal to u on U one finds that $[X_i, X_j]$ is a linear combination of X_i $(1 \leq i \leq 6)$ on M and so the members X_i $(1 \leq i \leq 6)$ of $K(M)$ constitute a 6-dimensional subalgebra A of $K(M)$ which restricts to a 3-dimensional Frobenius type distribution S on U. Since U is connected, S admits 3−dimensional integral manifolds through each point of U [3] and which are (spacelike and) orthogonal to the distribution D (that is, orthogonal to any spanning member of D) everywhere on U. Now write $M = M_1 \cup M_2$ where M_1 denotes the subset of those points of M at which each member of A is orthogonal to D and $M_2 = M \setminus M_1$. Clearly, by definition, M_2 is open in M and $M_1 \neq \emptyset$. If $m \in M_1$, the subspace $S(m) = \{X(m) : X \in S\}$ of $T_m M$ is 3-dimensional at m since (M, g) is homogeneous. It follows that any $m \in M_1$ admits a neighbourhood such as U above with $U \subset M_1$ and hence M_1 is open in M. Since M is connected and $M_1 \neq \emptyset$, $M = M_1$ and the integral manifolds of S are 3−dimensional, spacelike and orthogonal to D everywhere on M. These integral manifolds with their induced metric from g thus admit (at least six and hence) exactly six induced independent Killing vector fields (section 3) and are thus of constant curvature. Choosing Gauss coordinates based on the level surfaces of t and the (geodesic) vector field u yields, locally, the usual metric for the *Einstein static-type universe*. It is clear that u spans the "axis" of the isotropy at each $m \in U$.

In the case that $\dim K(M) = 6$ and each orbit is 3−dimensional and spacelike then for any $m \in M$ there exists a connected coordinate domain U and $X, Y, Z \in K(M)$ such that $X(m')$, $Y(m')$ and $Z(m')$ are independent members of $T_{m'}M$ for each $m' \in U$. Thus X, Y and Z span the orbits of $K(M)$ on U and a nowhere-zero, smooth, timelike vector field T on U is given by $T^a = \varepsilon^a{}_{bcd} X^b Y^c Z^d$, where ε denotes the alternating tensor. Thus $T^a X_a = T^a Y_a = T^a Z_a = 0$ on U and a differentiation of each of these, using (2) and a subsequent contraction with T^b shows that each integral curve of T is geodesic and orthogonal to the orbit. As in the previous case the orbits of $K(M)$ within U (and with the latter having its induced metric from g) are spaces of constant curvature and Gauss coordinates yield a metric on (if necessary, a reduced) U of the form

$$ds^2 = -dt^2 + h_{\alpha\beta} dx^\alpha dx^\beta \qquad (\alpha, \beta = 1, 2, 3) \tag{13}$$

where t is an affine parameter on the geodesics orthogonal to the orbits and where the Ricci tensor on U takes the form $R_{ab} = \alpha(t) g_{ab} - \beta(t) v_a v_b$ where α and β are functions on U, $v = dt$ $(v_a = t_{,a})$ and α and β are smooth since *Ricc*, g and v are. If the subset $\{m \in M : \beta(m) = 0\}$ of M has non-empty interior then on each component of this interior α is constant and the metric induced on it from g, has constant curvature. If the open subset $V = \{m \in M : \beta(m) \neq 0\}$ of M is non-empty a straightforward argument (see, e.g.,[40]) using the conformally flat Bianchi identity (12) but with the right hand side now given by $\frac{1}{6}(g_{ab} R_{,c} - g_{ac} R_{,b})$ now reveals that each $m \in V$ admits a coordinate neighbourhood on which (13) holds with $h_{\alpha\beta} = f(t) q_{\alpha\beta}$ where the components $q_{\alpha\beta}$ are independent of t. Thus one achieves the standard FRWL metric locally on V. The next theorem now follows.

Theorem 2

Suppose (M, g) is cosmological. Then either

(i) I_m is isomorphic to L at each $m \in M$. In this case (M, g) is of constant curvature, $\dim K(M) = 10$, there is a single 4-dimensional orbit and (M, g) is thus, locally, de Sitter, anti-de Sitter or Minkowski, *or*

(ii) I_m is isomorphic to $o(3)$ at each $m \in M$ *and* $K(M)$ has a single 4-dimensional orbit. In this case $\dim K(M) = 7$ and (M, g) either has constant curvature or is locally of the Einstein static type, or

(iii) I_m is isomorphic to $o(3)$ at each $m \in M$ *and* each orbit is 3-dimensional and spacelike. In this case $\dim K(M) = 6$ and, for each m in the open dense subset $V \cup \text{int}(M \setminus V)$ of M, there exists a connected, open neighbourhood of m whose restricted metric is either of constant curvature or of the usual FRWL type.

The assumption that (M, g) is cosmological also forces "homogeneity" onto (M, g) in the following sense. For theorem 2 parts (i) and (ii), $K(M)$ is transitive on M. If in part (ii) one does not have the constant curvature situation, the orbits associated with the subalgebra A of $K(M)$ define space sections and hence a local cosmic time and spatial homogeneity for (M, g). If the conditions of theorem 2(iii) hold the Killing orbits provide global 3-dimensional, spacelike submanifolds which again form the basis of a local cosmic time and spatial homogeneity.

Thus the definition of (M, g) being "cosmological" leads essentially to the usual cosmological models. Some remarks on the idea of a space-time being *locally cosmological* are given in section 7.

6 Application to Plane Waves

A *plane wave* in general relativity theory is usually taken to be a space-time (M, g) with a global chart u, v, x, y (with some appropriate range for the coordinates u, v, x, y), which is not flat and where the metric takes the form (5) [34] (see also [6]) where H satisfies $H(x, y, u) = a(u)x^2 + b(u)y^2 + c(u)xy$ for smooth functions a, b and c. [One should also mention here the metric given in [41] (see also [6]) which is not contained in (5) but which, perhaps, should be included in this general discussion. It will be commented on later.] For the metric (5), $5 \leq \dim K(M) \leq 7$, and at each $m \in M$, $2 \leq \dim I_m \leq 3$, with I_m containing a subalgebra isomorphic to the 2−dimensional Lie algebra R_8 in table 1. The Weyl tensor is, at any $m \in M$, of Petrov type **N** or **O** and the Ricci tensor is, at any $m \in M$, either zero or of the null fluid type and, if non-zero, its representative null direction $l^a \equiv g^{ab}u_{,b}$ coincides with the repeated principal null direction of the Weyl tensor (if the latter is non-zero) and is covariantly constant. If (5) is a vacuum metric, $5 \leq \dim K(M) \leq 6$, and $\dim I_m = 2$ with I_m isomorphic to R_8. Any 3-dimensional null hypersurfaces of constant u can be interpreted as representing the collection of all world lines of the waves (rays), with tangent vector l which intersect it. If $\dim K(M) = 5$ (and in some cases when it is 6) these hypersurfaces are orbits of $K(M)$; otherwise (M, g) is transitive. [It is remarked that the metric in [41] admits no non-trivial covariantly constant vector field.]

To proceed further let (M, g) be (any) space-time and, for $m \in M$, let $l \in T_mM$ be null. A spacelike 2-space A of T_mM orthogonal to l is called a *wave surface of* l at m [34]. If some observer O passing through m has a worldline with timelike tangent vector T at m and with T orthogonal to each member of A then A is called an *instantaneous wave surface of* l *to* O at m and is uniquely determined by l and T. If $x \wedge y$ is a wave surface of l at m spanned by orthogonal, spacelike vectors $x, y \in T_mM$ the family of *all* wave surfaces of l at m, denoted by $W_m(l)$, can be shown to be in bijective correspondence with the collection $(x + al) \wedge (y + bl)$, for $a, b \in \mathbb{R}$, that is, with the set $\mathbb{R}^2$. Each member of this collection is an instantaneous wave surface of l to some observer at m and any observer at m has its instantaneous wave surface of l of this form. Thus $W_m(l)$ can be regarded as the set containing the original (instantaneous) wave surface of l to a particular observer O at m together with those for all other observers at m related to O by a Lorentz boost at m. This is easily checked using elementary Lorentz transformation theory. The members of $W_m(l)$ are simply those 2-spaces tangent to the level surface of u at m which do not contain $l(m)$.

Returning to the metric (5) and its associated Killing algebra $K(M)$ it can be checked that for each $m \in M$, the isotropy algebra I_m is such that its associated maps ϕ_{t*} are transitive on $W_m(l)$, that is, if $p, q \in T_mM$ span one such wave surface at m, $\phi_{t*}(p)$ and $\phi_{t*}(q)$ can, for appropriate ϕ_t, span any other wave surface at m (see the comments regarding the action of ϕ_{t*} at the end of the first paragraph of section 3). In this sense the instantaneous wave surfaces of l at m to all observers at m are indistinguishable. It is remarked that any member of $W_m(l)$ may be extended to a 2−dimensional submanifold of M to which it is tangent at m. To see this note that one such submanifold W containing m is given by appropriate choices of constant values for u and v in (5). Then choose a coordinate neighbourhood U of m whose coordinates are the restrictions of u, v, x, y to U and on which the appropriate ϕ_t from I_m is defined. Then if W' is the submanifold of U through m with appropriate choices of constant values for u and v in U, $\phi_t(W')$ is the required submanifold. [If the metric (5) is chosen to be *geodesically complete* (as it can be [34]) any affine vector field (and hence each $X \in K(M)$) is *complete* as a vector field [4] and so $K(M)$ gives rise to an effective action of a connected Lie group on M as a Lie transformation group ([5], see also [3,1]). In this case, each local flow ϕ_t is defined on the whole of M

and so an appropriate choice of ϕ_t will map W onto the required submanifold.

Now suppose that a second definition of a plane wave is proposed, that is, a space-time (M, g) which is not flat and which admits a Killing algebra $K(M)$ such that, at each $m \in M$, there is a *unique* null direction spanned by $l' \in T_m M$, called the *wave direction* at m, for which the transformations ϕ_{t*} arising from I_m are *transitive* on $W_m(l')$. Thus the "symmetry" in this second definition arises by assuming the indistinguishability of the instantaneous wave surfaces of l' for all observers at m for each $m \in M$. It follows that if $k \in T_m M$ is *not* proportional to l', I_m cannot fix the *direction* of k. To see this suppose it does and that $k^a l'_a = 0$ at m. Then k is spacelike and lies in some wave surface $S \in W_m(l')$. But then all wave surfaces that I_m can map S into must contain k and since it is easily checked that l' must have a wave surface not containing k a contradiction is obtained. If, on the other hand, $k^a l'_a \neq 0$ at m, $k \wedge l'$ is timelike and the orthogonal complement S of $l' \wedge k$ is spacelike, orthogonal to k and in $W_m(l')$. Then the only wavesurface that I_m can map S into is itself and again a contradiction arises. This completes the proof and reference to table 1 immediately shows that the only possibilities for I_m are R_8, R_9, R_{11}, R_{12} and R_{14} with $l' = l$. This is because R_{15} is transitive on wave surfaces of *all* null directions and the others either fix a non-null direction or two distinct null directions in contradiction to the above result. Hence $\dim I_m \geq 2$. Each of these possibilities is, in fact, transitive on $W_m(l)$ (since R_8 is and all the others contain R_8 as a subalgebra) *and each fixes the null direction* l (since each bivector in their Lie algebras has l as an eigenvector). Hence l is unique in this respect since if any of these subalgebras were transitive on wave surfaces of another null direction the previous argument shows that it could not fix the direction of l.

With (M, g) satisfying this new definition of a plane wave let $M_k = \{m \in M\colon \dim I_m = k\}$ so that $M = M_2 \cup M_3 \cup M_4$ and each $m \in M_2$ has I_m of type R_8, each $m \in M_3$ of type R_9, R_{11} or R_{12} and each $m \in M_4$ of type R_{14}. Since $\dim K(M) = \dim O_m + \dim I_m$, each M_k is a union of orbits of dimension $(\dim K(M) - k)$ and a simple application of the rank theorem shows that M_2 and $M_2 \cup M_3$ are open subsets of M. Now if $\mathrm{int} M_k \neq \emptyset$ the orbit through any point of $\mathrm{int} M_k$ is dimensionally stable. The following lemmas are easily established for this second definition of a plane wave. The proofs are largely similar to those in the cosmological case and only the first is given (theorem 1 is useful in many places here). Always (M, g) will be assumed to satisfy the above (second) definition of a plane wave.

Lemma 3

Suppose M is such that *Riem* does not take the constant curvature form at any $m \in M$ and let O be a dimensionally stable orbit in $K(M)$. Then O is of dimension 3 or 4. If $\dim O = 3$, O is null and the wave direction $l(m)$ is normal to O at each $m \in O$. Whatever the dimension of O, I_m is either type R_8 or R_{11} at each $m \in O$.

Proof

Since O is dimensionally stable, if $\dim O \neq 4$ one must have $\dim O = 3$ (otherwise, one gets $\dim K(M) \leq 3$ and hence $\dim I_m \leq 1$ from theorem 1 and a contradiction). If $m \in O$ one can choose an open neighbourhood U of m and a smooth vector field k on U such that all orbits through U are 3−dimensional and k is everywhere orthogonal to these orbits on U. It follows that $k^a X_a = 0$ on U for any $X \in K(M)$. Choosing X to be a non-trivial member of I_m (so that $X(m) = 0$) a differentiation of $k^a X_a = 0$ and evaluation at m shows that $F_{ab} k^b = 0$ at m for each bivector F in I_m. It follows (table 1) that I_m must be of type R_8 or R_{11} and that the direction spanned by k is unique and null being equal to the wave direction $l(m)$ at m. It follows that O is (3−dimensional and) null. If I_m is of type R_9, R_{12} or R_{14} at some $m \in M$, the previous argument shows that the orbit through m is 4−dimensional and this forces $C = 0$ on O and also O to be an Einstein space ([1] p 302). Thus (M, g) is of constant curvature on O and a contradiction follows. □

Lemma 4

Let O be an orbit in $K(M)$ of dimension 4. Then

(i) $O \subset M_2 \Leftrightarrow \dim K(M) = 6$ and if these hold, $M_4 = \emptyset$ and if $M_3 \neq \emptyset$ it is the union of a (possibly empty) family of 3−dimensional, dimensionally stable null orbits at each point of which I_m is of type R_{11}, together with at least one non-empty, 3−dimensional, null but not dimensionally stable orbit.

(ii) $O \subset M_3 \Leftrightarrow \dim K(M) = 7$ and if these hold, $M_2 = \emptyset$ and $\mathrm{int} M_4 = \emptyset$. Any orbit in M_4 is 3−dimensional, null but not dimensionally stable.

(iii) $O \subset M_4 \Leftrightarrow \dim K(M) = 8$ and if these hold, $M_2 = M_3 = \emptyset$ and $M = M_4$ is of constant curvature.

Lemma 5

Let O be an orbit in $K(M)$ of maximum dimension with $\dim O = 3$. Then O is dimensionally stable and, from lemma 3, is null and $O \subset M_2$ or $O \subset M_3$ and

(i) $O \subset M_2 \Leftrightarrow \dim K(M) = 5$ and if these hold, $\mathrm{int} M_3 = \mathrm{int} M_4 = \emptyset$ and hence any orbit in M_3 or M_4 is of respective dimension 2 or 1 and is not dimensionally stable.

(ii) $O \subset M_3 \Leftrightarrow \dim K(M) = 6$ and if these hold, $M_2 = M_4 = \emptyset$.

Theorem 3

Suppose (M, g) satisfies the above (second) definition of a plane wave, that all orbits are dimensionally stable and that *Riem* nowhere satisfies the constant curvature condition. Then either $M = M_2$ with $\dim K(M) = 5$ (respectively, $\dim K(M) = 6$) *and* all orbits are 3−dimensional and null (respectively, there exists a single 4−dimensional orbit) *and* I_m is of type R_8 for each $m \in M$, *or*, $M = M_3$ with $\dim K(M) = 6$ (respectively, $\dim K(M) = 7$) *and* all orbits are 3−dimensional and null (respectively, there exists a single 4−dimensional orbit) *and* I_m is of type R_{11} for each $m \in M$.

Now suppose, that the conditions of theorem 3 hold. Then at no $m \in M$ can *Ricc* and C vanish together since then *Riem* would satisfy the constant curvature condition at m. Now consider those cases where the orbits are 3−dimensional (and null). If the isotropy is R_8 at each point, *Ricc*, where it does not vanish, is of Segre type $\{(211)\}$ (with null eigenvector l) and C, where it does not vanish, is of Petrov type **N** (with principal null direction spanned by l). If the isotropy is R_{11}, $C = 0$ and *Ricc* is nowhere zero and has Segre type $\{(211)\}$ (with null eigenvector l). Also the null normal to the orbits, l, may be scaled so that $l_{a;b} = l_{b;a}$ on some open neighbourhood U of any $m \in M$, and satisfies $\mathcal{L}_X l = \lambda l$ on U. Since also $X^a l_a$ is zero on U, a differentiation of this and use of the preceeding result shows that $\lambda = 0$ and so $\mathcal{L}_X l = 0$ on U. Thus $\mathcal{L}_X l_{a;b} = 0$ on U. Since $l_{a;b}$ is symmetric, one finds from the isotropy that $l_{a;b} = \alpha g_{ab} + \beta l_a l_b$ for functions α and β on U and a contraction with l^a shows that $\alpha = 0$, that is $l_{a;b} = \beta l_a l_b$. One may now compute $R^a{}_{bcd} l^d$ in two ways; once from the Ricci identity on l and again from the expression for *Riem* and the above algebraic conditions on *Ricc* and C. One finds, after a short calculation, that the Ricci scalar vanishes on U and hence the space-time is either vacuum or a null fluid. It now follows (see, e.g. [6] sections 12.1 and 24.2) that under the conditions of theorem 3, either (M, g) is (locally) a plane wave space-time (with the usual (first) definition given at the beginning of this section) which, at each $m \in M$, either satisfies the vacuum condition or has an energy-momentum tensor of the null fluid type where the null fluid direction is represented, locally, by a covariantly constant null vector field, *or* that it is one of the type **N**, pure radiation (with cosmological constant), homogeneous metrics first given in [41] and for which $\dim K(M) = 6$. Those cases with I_m of type R_{11} are conformally flat (and hence are not vacuum) and those with I_m of type R_8 are such that the Weyl tensor is of Petrov type **N** where it is non-zero. The examples with either $M = M_2$, $\dim K(M) = 6$ and I_m of type R_8 or with $M = M_3$, $\dim K(M) = 7$ and I_m of type R_{11} are homogeneous. *Thus the two definitions of a plane wave considered in this section are essentially equivalent.*

7 Local Symmetry

The concept of a local symmetry can now be discussed. For both mathematical and physical reasons, the idea of a symmetry being represented by a *global* Killing vector field is rather a strong restriction (cf section 1). Let M be a manifold of any dimension admitting a metric g of any signature and let U be some non-empty open subset in M. Suppose X is a smooth vector field on U which satisfies Killing's equations (2) on U. Then X is called a *local Killing vector field for* M (but note that X *may not* be extendible to a global Killing vector field on M and so may not be a member of $K(M)$—— just consider an arbitrary space-time possessing a "flat" proper open subset). One may speak of (M, g) as possessing "local" symmetry if M admits a collection of local Killing vector fields such that for *any* $m \in M$ there exists an open neighbourhood U of m together with a non-trivial local Killing vector field X from this collection defined on U. The set of all Killing vector fields defined on a particular U is then a Lie algebra in the usual way, denoted by $K(U)$. It is clear that if V is an open subset of U, any $X \in K(U)$ restricts to a member of $K(V)$, but that there may be Killing vector fields defined on V that cannot be extended to U. It turns out that if (M, g) possesses "local" symmetry and $m \in M$, there exists an open subset W of m on which the Killing algebra $K(W)$ is "maximal", that is, if $W' \subset W$, $\dim K(W') = \dim K(W)$ and $K(W)$ may be called the *local Killing algebra* at m. The open subset W is called *special* for m and it can be shown that W is then special for any $m' \in W$ [30]. Local Killing algebras occur naturally in mathematics, for example, as mentioned in section 2, a space of constant curvature is characterised as a pair (M, g) with M a (connected, etc) manifold of dimension n and g a metric on M of arbitrary signature such that each $m \in M$ admits a special neighbourhood U with $K(U)$ of maximum dimension $\frac{1}{2}n(n+1)$ (which equals 10 for space-times). Clearly, if (M, g) admits a global Killing algebra of this maximum dimension then the previous local Killing condition is satisfied and (M, g) is of constant curvature but conversely, if (M, g) is of constant curvature, only the local Killing algebras are guaranteed and may not be extendible to M (e.g. consider a 2−dimensional, infinite cylinder in $\mathbb{R}^3$). One may define local conformal, affine, etc, symmetry in an analogous way. It then follows, for example, that (M, g) has vanishing Weyl tensor (so that it is conformally flat) if and only if each

$m \in M$ has a special neighbourhood U with $C(U)$ of maximum dimension $\frac{1}{2}(n+1)(n+2)$ (which equals 15 for space-times).

From the point of view of physics the same conclusion may be arrived at for different reasons. Symmetry in physics is a consequence of observation and experiment and is thus local. Thus if experiment determines something that may be described in terms of Killing symmetry this description is really in terms of *local* Killing symmetry. One question that may be asked concerns the relationship between local and global Killing symmetry. Clearly a global Killing algebra of a certain dimension yields a local Killing algebra of at least that dimension for each $m \in M$. The converse centres around whether one can extend a local Killing vector field or a local Killing algebra on some neighbourhood like U above to a global one on M. An answer to this question is that if the local Killing algebras (that is, on the above special neighbourhoods) all have the same dimension N and if the manifold topology of M is *simply connected* then the global Killing algebra has dimension N [30,31]. In other words any of these local Killing vector fields can be extended to a global one. Thus, for example, in cosmology, if all astronomers are convinced that the universe exhibits local symmetry consistent with the 6-dimensional Killing algebra characteristic of the generic FRWL metrics, and if the universe can be represented by a simply connected manifold, then the universe admits a global 6-dimensional Killing algebra of the FRWL form. Similar results hold for homothetic, affine and conformal symmetry [31].

8 Acknowledgements

The author thanks the organisers (and in particular, Prof. M. Sharif) of The International Conference on Relativistic Astrophysics (ICRA-2015), held at The University of The Punjab in Lahore, Pakistan, in February, 2015, in order to commemorate 100 years of Einstein's General Theory of Relativity, for their help and for the opportunity to deliver the lecture of which this paper is the text.

References

1. G.S Hall, *Symmetries and Curvature Structure in General Relativity*, World Scientific, (2004).
2. K.Yano, *The Theory of Lie Derivatives and its Applications*, North Holland, (1955).
3. F.Brickell and R.S Clark, *Differentiable Manifolds*, Van Nostrand, (1970).
4. S.Kobayashi and k.Nomizu, *Foundations of Differential Geometry*, Vol. 1, Interscience, New York, (1963).
5. Palais R. S., *Mem.Am. Math.Soc*, No 22, (1957).
6. H.Stephani, D.Kramer, M.A.H.MacCallum, C.Hoenselaers and E.Herlt, *Exact Solutions of Einstein's Equations* (Second Edition), Cambridge, (2003).
7. G.S.Hall, *Class. Quan.Grav.* **15**, (1983) 581.
8. A.D.Rendall, *J.Math. Phys.* **29**, (1988), 1569.
9. P.C.Aichelberg, *J. Math. Phys.* **11**, (1970) 2485.
10. G.S.Hall and D.P.Lonie, *Class. Quant. Grav.* **12**, (1995) 1007.
11. G.S.Hall and J.da Costa, *J. Math. Phys.* **29**, (1988) 2465.
12. G.H.Katzin, J.Levine and W.R.Davies, *J. Math. Phys.* **10**, (1969) 617.
13. G.S.Hall and J.da Costa, *J. Math. Phys.* **32**, (1991) 2848-2854.
14. C.D.Collinson and E.L.G.R.Vaz, *Gen.Rel. Grav.* **15**, (1983) 661.
15. E.L.G.R.Vaz and C.D.Collinson,*Gen.Rel. Grav.* **14**, (1982) 5.
16. G.S.Hall and G.Shabbir, *Class. Quant. Grav.* **18**, (2001) 907.
17. M.J.Amir A.H.Bokhari and A.Qadir, *J. Math. Phys.* **35**, (1994) 3005.
18. U.Camci and A.Barnes, *Class. Quant. Grav.* **19**, (2002) 393.
19. M.Sharif and S.Aziz, *Gen.Rel. Grav.* **35**, (2003) 1093.
20. M.Ziad M, *Gen.Rel. Grav.* **35**, (2003) 915.
21. A.Qadir and M.Ziad, *Nu.Cim.* **113B**, (1998) 773.
22. J.Carot, J.da Costa and E.L.G.R.Vaz, *J. Math. Phys.* **35**, (1994) 4832.
23. G.S.Hall, *Class. Quant. Grav.* **20**, (2003) 4067.
24. J.F.Schell, *J. Math. Phys.* **2**, (1961) 202.
25. P.Stefan, *Proc. London. Math.Soc.* **29**, (1974) 699.
26. P.Stefan, *J.London.Math.Soc.* **21**, (1980) 544.
27. H.J.Sussmann,*Trans. Am. Math.Soc.* **180**, (1973) 171.
28. R.Hermann, *Int.Symp. Nonlinear Differential Equations and Nonlinear Mechanics*, New York, Academic Press, (1963), 325.
29. G.S.Hall and M.Patel, *Class. Quant. Grav.* **21**, (2004) 4731.
30. K.Nomizu, *Ann. Math.* **72**, (1960) 105.
31. G.S.Hall, *Class. Quant. Grav.* **6**, (1989) 157.
32. G.S.Hall, D. P.Lonie and A.R.Kashif, *Class. Quant. Grav.* **25**, (2008) 125008.
33. R.K.Sachs, *Proc. Roy.Soc.* **A264**, (1961) 309.
34. J.Ehlers and W.Kundt, in Gravitation; an introduction to current research. ed L.Witten, Wiley, New York, (1962), 49.
35. L.P.Eisenhart, Riemannian Geometry, Princeton, (1966).
36. H.Weyl, Gottinger Nachrichten, (1921), 99.
37. G.S.Hall, *J.Geom. Phys*, **60**, (2010) 1.
38. G.S.Hall, Publications de l'Institut Mathematique **94**, (2013) 55.
39. G. S. Hall and A.D.Rendall, *Int. J. Theor. Phys.* **28**, (1989) 365.
40. G.F.R.Ellis, in General Relativity and Cosmology. Academic Press Inc, New York, (1971), 104.
41. L.Defrise, *Groupes d'isotropie et groupes de stabilite conforme dans les espaces Lorentziens*. Thesis, Universite Libre de Bruxelles. (1969).
42. R.P.Geroch, *Comm. Math. Phys.*, **13**, (1969), 180.
43. B.O.J.Tupper, A.J.Keane and J.Carot, *Class. Quant. Grav.* **29**, (2012) 145016.
44. H.W.Brinkmann, *Math. Ann*, **94**, (1925) 119.

Proc. Int. Conf. Relativ. Astrophys.
Pages 77-85, (2015)

Gravitational Radiation within its Source

L. Herrera[a,1]

[1]Instituto Universitario de Fisica Fundamental, Salamanca, Spain

Abstract We review a recently proposed framework for studying axially symmetric dissipative fluids [1]. Some general results are discussed at the most general level. We then proceed to analyze some particular cases. First, the shear-free case is considered [2]. We shall next discuss the perfect fluid case under the geodesic condition, without impossing ab initio the shear–free condition [3]. Finally a dissipative, geodesic fluid [4], is analyzed in some detail. We conclude by bringing out the attention to some open issues.

Keywords Relativistic fluids · Gravitational radiation

1 INTRODUCTION

The main purpose of the line of work outlined in this conference, is to establish the relationship between gravitational radiation and source properties. Thus, for example, we known that gravitational radiation is an irreversible process, accordingly there must exist an entropy production factor in the equation of state (dissipation) of the source.

Since we are dealing with gravitational radiation, we need to depart from the spherical symmetry. On the other hand, we shall rule out cylindrical symmetry on physical grounds. Thus we are left with axial and reflection symmetry, which as shown in [5] is the highest degree of symmetry of the Bondi metric [6], which do not prevent the emission of gravitational radiation.

We are using the 1+3 formalism [7–9], in a given coordinate system, and we are going to ressort to a set of scalar functions known as Structure Scalars [10], which have been shown to be very useful in the description of self–gravitating systems [11–20].

[a]e-mail: lherrera@usal.es

2 BASIC EQUATIONS, CONVENTIONS AND NOTATION

We shall consider fluid distributions endowed with axial and reflection symmetry, and we shall assume the line element to be of the form:

$$ds^2 = -A^2dt^2 + B^2\left(dr^2 + r^2d\theta^2\right) + C^2d\phi^2 + 2Gd\theta dt, \quad (1)$$

where A, B, C, G are positive functions of t, r and θ, and coordinates are numbered as: $x^0 = t, x^1 = r, x^2 = \theta, x^3 = \phi$.

The energy momentum tensor describes a dissipative fluid distribution and in its canonical form may be written as:

$$T_{\alpha\beta} = (\mu + P)V_\alpha V_\beta + Pg_{\alpha\beta} + \Pi_{\alpha\beta} + q_\alpha V_\beta + q_\beta V_\alpha. \quad (2)$$

with

$$\mu = T_{\alpha\beta}V^\alpha V^\beta, \quad q_\alpha = -\mu V_\alpha - T_{\alpha\beta}V^\beta, \quad (3)$$

$$P = \frac{1}{3}h^{\alpha\beta}T_{\alpha\beta}, \quad \Pi_{\alpha\beta} = h^\mu_\alpha h^\nu_\beta\left(T_{\mu\nu} - Ph_{\mu\nu}\right), \quad (4)$$

$$h_{\mu\nu} = g_{\mu\nu} + V_\nu V_\mu, \quad (5)$$

$$V^\alpha = (\frac{1}{A}, 0, 0, 0); \quad V_\alpha = (-A, 0, \frac{G}{A}, 0). \quad (6)$$

where $\mu, P, \Pi_{\alpha\beta}, q_\alpha, V_\alpha$ denote the energy density , the isotropic pressure, the anisotropic tensor, the dissipative flux and the four velocity respectively.

Next,in order to form an orthogonal tetrad, let us introduce the unit, spacelike vectors $\mathbf{K}, \mathbf{L}, \mathbf{S}$, with components

$$K_\alpha = (0, B, 0, 0); \quad L_\alpha = (0, 0, \frac{\sqrt{A^2B^2r^2 + G^2}}{A}, 0), \quad (7)$$

$$S_\alpha = (0, 0, 0, C), \quad (8)$$

satisfying the following relations:

$$V_\alpha V^\alpha = -K^\alpha K_\alpha = -L^\alpha L_\alpha = -S^\alpha S_\alpha = -1, \quad (9)$$

$$V_\alpha K^\alpha = V^\alpha L_\alpha = V^\alpha S_\alpha = K^\alpha L_\alpha = K^\alpha S_\alpha = S^\alpha L_\alpha = 0. \quad (10)$$

In terms of the above vectors, the anisotropic tensor may be written as

$$\begin{aligned}\Pi_{\alpha\beta} &= \frac{1}{3}(2\Pi_I + \Pi_{II})(K_\alpha K_\beta - \frac{h_{\alpha\beta}}{3}) \\ &+ \frac{1}{3}(2\Pi_{II} + \Pi_I)(L_\alpha L_\beta - \frac{h_{\alpha\beta}}{3}) \\ &+ 2\Pi_{KL} K_{(\alpha} L_{\beta)}, \end{aligned} \quad (11)$$

with

$$\Pi_{KL} = K^\alpha L^\beta T_{\alpha\beta}, \quad , \quad (12)$$

$$\Pi_I = (2K^\alpha K^\beta - L^\alpha L^\beta - S^\alpha S^\beta) T_{\alpha\beta}, \quad (13)$$

$$\Pi_{II} = (2L^\alpha L^\beta - S^\alpha S^\beta - K^\alpha K^\beta) T_{\alpha\beta}. \quad (14)$$

For the heat flux vector we may write

$$q_\mu = q_I K_\mu + q_{II} L_\mu, \quad (15)$$

or

$$q^\mu = (\frac{q_{II} G}{A\sqrt{A^2B^2r^2 + G^2}}, \frac{q_I}{B}, \frac{A q_{II}}{\sqrt{A^2B^2r^2 + G^2}}, 0), \quad (16)$$

$$q_\mu = \left(0, Bq_I, \frac{\sqrt{A^2B^2r^2 + G^2}\, q_{II}}{A}, 0\right). \quad (17)$$

2.1 Kinematical variables

The kinematical variables (the four acceleration, the expansion, the shear tensor and the vorticity) are defined respectively as:

$$\begin{aligned} a_\alpha &= V^\beta V_{\alpha;\beta} = a_I K_\alpha + a_{II} L_\alpha \\ &= \left(0, \frac{A_{,r}}{A}, \frac{G}{A^2}\left[-\frac{A_{,t}}{A} + \frac{G_{,t}}{G}\right] + \frac{A_{,\theta}}{A}, 0\right), \end{aligned} \quad (18)$$

$$\begin{aligned}\Theta &= V^\alpha_{;\alpha} \\ &= \frac{AB^2}{r^2A^2B^2 + G^2}\left[r^2\left(2\frac{B_{,t}}{B} + \frac{C_{,t}}{C}\right)\right. \\ &\left. + \frac{G^2}{A^2B^2}\left(\frac{B_{,t}}{B} - \frac{A_{,t}}{A} + \frac{G_{,t}}{G} + \frac{C_{,t}}{C}\right)\right], \end{aligned} \quad (19)$$

$$\sigma_{\alpha\beta} = V_{(\alpha;\beta)} + a_{(\alpha} V_{\beta)} - \frac{1}{3}\Theta h_{\alpha\beta}, \quad (20)$$

or

$$\begin{aligned}\sigma_{\alpha\beta} &= \frac{1}{3}(2\sigma_I + \sigma_{II})(K_\alpha K_\beta - \frac{1}{3}h_{\alpha\beta}) \\ &+ \frac{1}{3}(2\sigma_{II} + \sigma_I)(L_\alpha L_\beta - \frac{1}{3}h_{\alpha\beta}), \end{aligned} \quad (21)$$

where

$$2\sigma_I + \sigma_{II} = \frac{3}{A}\left(\frac{B_{,t}}{B} - \frac{C_{,t}}{C}\right), \quad (22)$$

$$\begin{aligned}2\sigma_{II} + \sigma_I &= \frac{3}{A^2B^2r^2 + G^2}\left[AB^2r^2\left(\frac{B_{,t}}{B} - \frac{C_{,t}}{C}\right)\right. \\ &\left. + \frac{G^2}{A}\left(-\frac{A_{,t}}{A} + \frac{G_{,t}}{G} - \frac{C_{,t}}{C}\right)\right], \end{aligned} \quad (23)$$

$$\omega_\alpha = \frac{1}{2}\,\eta_{\alpha\beta\mu\nu}\, V^{\beta;\mu}\, V^\nu = \frac{1}{2}\,\eta_{\alpha\beta\mu\nu}\, \Omega^{\beta\mu}\, V^\nu, \quad (24)$$

where $\Omega_{\alpha\beta} = V_{[\alpha;\beta]} + a_{[\alpha}V_{\beta]}$, ω_α and $\eta_{\alpha\beta\mu\nu}$ denote the vorticity tensor, the vorticity vector and the Levi-Civita tensor, respectively;

$$\Omega_{\alpha\beta} = \Omega(L_\alpha K_\beta - L_\beta K_\alpha), \quad (25)$$

$$\omega_\alpha = -\Omega S_\alpha. \quad (26)$$

$$\Omega = \frac{G(\frac{G_{,r}}{G} - \frac{2A_{,r}}{A})}{2B\sqrt{A^2B^2r^2 + G^2}}. \quad (27)$$

Observe that from (27) and regularity conditions at the centre, it follows that: $G = 0 \Leftrightarrow \Omega = 0$.

2.2 The orthogonal splitting of the Riemann Tensor and structure scalars

Using the well kown decomposition of the Riemann tensor in terms of the Weyl tensor, the Ricci tensor and the Ricci scalar, and linking the two later variables with the energy momentum tensor, via the Einstein equations, it can be shown that the Riemann tensor may be written as:

$$R^{\alpha\beta}{}_{\nu\delta} = R^{\alpha\beta}_{(F)\ \nu\delta} + R^{\alpha\beta}_{(Q)\ \nu\delta} + R^{\alpha\beta}_{(E)\ \nu\delta} + R^{\alpha\beta}_{(H)\ \nu\delta}, \quad (28)$$

with

$$R^{\alpha\beta}_{(F)\ \nu\delta} = \frac{16\pi}{3}(\mu + 3P)V^{[\alpha}V_{[\nu}h^{\beta]}_{\delta]} + \frac{16\pi}{3}\mu h^{\alpha}_{[\nu}h^{\beta}_{\delta]}, \quad (29)$$

$$\begin{aligned}R^{\alpha\beta}_{(Q)\ \nu\delta} &= -16\pi V^{[\alpha}h^{\beta]}_{[\nu}q_{\delta]} - 16\pi V_{[\nu}h^{[\alpha}_{\delta]}q^{\beta]} - \\ &-16\pi V^{[\alpha}V_{[\nu}\Pi^{\beta]}_{\delta]} + 16\pi h^{[\alpha}_{[\nu}\Pi^{\beta]}_{\delta]} \end{aligned} \quad (30)$$

$$R^{\alpha\beta}_{(E)\ \nu\delta} = 4V^{[\alpha}V_{[\nu}E^{\beta]}_{\delta]} + 4h^{[\alpha}_{[\nu}E^{\beta]}_{\delta]}, \quad (31)$$

$$R^{\alpha\beta}_{(H)\ \nu\delta} = -2\epsilon^{\alpha\beta\gamma}V_{[\nu}H_{\delta]\gamma} - 2\epsilon_{\nu\delta\gamma}V^{[\alpha}H^{\beta]\gamma}. \quad (32)$$

In the above, $E_{\alpha\beta}, H_{\alpha\beta}$ denote the electric and magnetic parts of the Weyl tensor, respectively, defined as usual by:

$$E_{\alpha\beta} = C_{\alpha\nu\beta\delta}V^\nu V^\delta, \qquad H_{\alpha\beta} = \frac{1}{2}\eta_{\alpha\nu\epsilon\rho}C_{\beta\delta}{}^{\epsilon\rho}V^\nu V^\delta, \quad (33)$$

where $\epsilon_{\alpha\beta\rho} = \eta_{\nu\alpha\beta\rho}V^\nu$.

In our case these tensors may be written in terms of five scalar functions as:

$$E_{\alpha\beta} = \frac{1}{3}(2\mathcal{E}_I + \mathcal{E}_{II})(K_\alpha K_\beta - \frac{1}{3}h_{\alpha\beta}) + \frac{1}{3}(2\mathcal{E}_{II} + \mathcal{E}_I)(L_\alpha L_\beta - \frac{1}{3}h_{\alpha\beta}) + \mathcal{E}_{KL}(K_\alpha L_\beta + K_\beta L_\alpha), \quad (34)$$

$$H_{\alpha\beta} = H_1(S_\alpha K_\beta + S_\beta K_\alpha) + H_2(S_\alpha L_\beta + S_\beta L_\alpha). \quad (35)$$

Let us now introduce the following tensors

$$Y_{\alpha\beta} = R_{\alpha\nu\beta\delta}V^\nu V^\delta, \quad (36)$$

$$X_{\alpha\beta} = \frac{1}{2}\eta_{\alpha\nu}{}^{\epsilon\rho}R^\star_{\epsilon\rho\beta\delta}V^\nu V^\delta, \quad (37)$$

$$Z_{\alpha\beta} = \frac{1}{2}\epsilon_{\alpha\epsilon\rho}R_{\delta\beta}{}^{\epsilon\rho}V^\delta, \quad (38)$$

where $R^\star_{\alpha\beta\nu\delta} = \frac{1}{2}\eta_{\epsilon\rho\nu\delta}R_{\alpha\beta}{}^{\epsilon\rho}$.

Or, using (28)

$$Y_{\alpha\beta} = \frac{1}{3}Y_T h_{\alpha\beta} + \frac{1}{3}(2Y_I + Y_{II})(K_\alpha K_\beta - \frac{1}{3}h_{\alpha\beta}) + \frac{1}{3}(2Y_{II} + Y_I)(L_\alpha L_\beta - \frac{1}{3}h_{\alpha\beta}) + Y_{KL}(K_\alpha L_\beta + K_\beta L_\alpha), \quad (39)$$

with

$$Y_T = 4\pi(\mu + 3P), \quad (40)$$

$$Y_I = \mathcal{E}_I - 4\pi\Pi_I, \quad (41)$$

$$Y_{II} = \mathcal{E}_{II} - 4\pi\Pi_{II}, \quad (42)$$

$$Y_{KL} = \mathcal{E}_{KL} - 4\pi\Pi_{KL}. \quad (43)$$

$$X_{\alpha\beta} = \frac{1}{3}X_T h_{\alpha\beta} + \frac{1}{3}(2X_I + X_{II})(K_\alpha K_\beta - \frac{1}{3}h_{\alpha\beta}) + \frac{1}{3}(2X_{II} + X_I)(L_\alpha L_\beta - \frac{1}{3}h_{\alpha\beta}) + X_{KL}(K_\alpha L_\beta + K_\beta L_\alpha), \quad (44)$$

with

$$X_T = 8\pi\mu, \quad (45)$$

$$X_I = -\mathcal{E}_I - 4\pi\Pi_I, \quad (46)$$

$$X_{II} = -\mathcal{E}_{II} - 4\pi\Pi_{II}, \quad (47)$$

$$X_{KL} = -\mathcal{E}_{KL} - 4\pi\Pi_{KL}. \quad (48)$$

Finally

$$Z_{\alpha\beta} = H_{\alpha\beta} + 4\pi q^\rho \epsilon_{\alpha\beta\rho}. \quad (49)$$

or

$$Z_{\alpha\beta} = Z_I K_\beta S_\alpha + Z_{II}K_\alpha S_\beta + Z_{III}L_\alpha S_\beta + Z_{IV}L_\beta S_\alpha \quad (50)$$

where

$$Z_I = (H_1 - 4\pi q_{II}); \quad Z_{II} = (H_1 + 4\pi q_{II}); \quad Z_{III} = (H_2 - 4\pi q_I); \quad Z_{IV} = (H_2 + 4\pi q_I). \quad (51)$$

Variables:$Y_{T,I,II,KL}, X_{T,I,II,KL}, Z_{I,II,III,IV}$ are the structure scalars of our distribution.

2.3 The super–Poynting vector

An important role in our discussion is played by the super–poynting vector. Indeed, we recall that we define a state of intrinsic gravitational radiation (at any given point), to be one in which the super-Poynting vector does not vanish for any unit timelike vector [21–23]. Then since the vanishing of the magnetic part of the Weyl tensor implies the vanishing of the super-Poynting vector, it is clear that FRW does not produce gravitational radiation. It is also worth recalling that the tight link between the super-Poynting vector and the existence of a state of radiation, is firmly supported by the relationship between the former and the Bondi news function [6,24] (see [25] for a discussion on this point).

Then from the definition of the super-Poynting vector,

$$P_\alpha = \epsilon_{\alpha\beta\gamma}\left(Y^\gamma_\delta Z^{\beta\delta} - X^\gamma_\delta Z^{\delta\beta}\right), \quad (52)$$

we obtain

$$P_\alpha = P_I K_\alpha + P_{II}L_\alpha, \quad (53)$$

with

$$P_I = \frac{H_2}{3}(2Y_{II} + Y_I - 2X_{II} - X_I) + H_1(Y_{KL} - X_{KL}) + \frac{4\pi q_I}{3}\left[2Y_T + 2X_T - X_I - Y_I\right] - 4\pi q_{II}(X_{KL} + Y_{KL}),$$

$$P_{II} = \frac{H_1}{3}(2X_I + X_{II} - Y_{II} - 2Y_I) + H_2(X_{KL} - Y_{KL}) - 4\pi q_I(Y_{KL} + X_{KL}) + \frac{4\pi q_{II}}{3}\left[2Y_T + 2X_T - X_{II} - Y_{II}\right]. \quad (54)$$

Both components have terms not containing heat dissipative contributions. It is reasonable to associate these with gravitational radiation. Also, note that both components have contributions of both components of the heat flux vector.

There is always a non-vanishing component of P^μ, on the plane orthogonal to a unit vector along which there is a non-vanishing component of vorticity (the $\theta-$ r- plane). Inversely, P^μ vanishes along the ϕ-direction since there are no motions along this latter direction, because of the reflection symmetry.

We can identify three different contributions in (54). On the one hand we have contributions from the heat transport process. These are independent of the magnetic part of the Weyl tensor, which explains why they remain in the spherically symmetric limit.

On the other hand we have contributions from the magnetic part of the Weyl tensor. These are of two kinds: a) contributions associated with the propagation of gravitational radiation within the fluid, b) contributions of the flow of super–energy associated with the

vorticity on the plane orthogonal to the direction of propagation of the radiation. Both are intertwined, and it appears to be impossible to disentangle them through two independent scalars.

As mentioned before, both components of the heat flux four-vector, appear in both components of the super–Poynting vector. Observe that this is achieved through the $X_{KL}+Y_{KL}$ terms in (54), or using (43, 48), through Π_{KL}. Thus, Π_{KL} couples the two components of the super–Poynting vector, with the two components of the heat flux vector.

3 THE EQUATIONS

We shall now deploy the whole set of equations for the variables defined so far.

3.1 The heat transport equation

We shall need a transport equation derived from a causal dissipative theory (e.g. the Müller-Israel-Stewart second order phenomenological theory for dissipative fluids [26–29]).

Indeed, the Maxwell-Fourier law for radiation flux leads to a parabolic equation (diffusion equation) which predicts propagation of perturbations with infinite speed (see [30]-[32] and references therein). This simple fact is at the origin of the pathologies [33] found in the approaches of Eckart [34] and Landau [35] for relativistic dissipative processes. To overcome such difficulties, various relativistic theories with non-vanishing relaxation times have been proposed in the past [26–29, 36, 37]. The important point is that all these theories provide a heat transport equation which is not of Maxwell-Fourier type but of Cattaneo type [38], leading thereby to a hyperbolic equation for the propagation of thermal perturbations.

A fundamental parameter in these theories is the relaxation time τ of the corresponding dissipative process. This positive–definite quantity has a distinct physical meaning, namely the time taken by the system to return spontaneously to the steady state (whether of thermodynamic equilibrium or not) after it has been suddenly removed from it. Therefore, when studying transient regimes, i.e., the evolution between two steady–state situations, τ cannot be neglected. In fact, leaving aside that parabolic theories are necessarily non–causal, it is obvious that whenever the time scale of the problem under consideration becomes of the order of (or smaller than) the relaxation time, the latter cannot be ignored, since neglecting the relaxation time amounts -in this situation- to disregarding the whole problem under consideration.

Thus, the transport equation for the heat flux reads [27, 28, 31],

$$\tau h^{\mu}_{\nu} q^{\nu}_{;\beta} V^{\beta} + q^{\mu} = -\kappa h^{\mu\nu}(T_{,\nu} + T a_{\nu}) - \frac{1}{2}\kappa T^2 \left(\frac{\tau V^{\alpha}}{\kappa T^2}\right)_{;\alpha} q^{\mu}, \quad (55)$$

where τ, κ, T denote the relaxation time, the thermal conductivity and the temperature, respectively.

Contracting (55) with L_{μ} we obtain

$$\frac{\tau}{A}\left(q_{II,t} + A q_I \Omega\right) + q_{II} = -\frac{\kappa}{A}\left(\frac{G T_{,t} + A^2 T_{,\theta}}{\sqrt{A^2 B^2 r^2 + G^2}} + A T a_{II}\right) - \frac{\kappa T^2 q_{II}}{2}\left(\frac{\tau V^{\alpha}}{\kappa T^2}\right)_{;\alpha}, \quad (56)$$

where (27), has been used.

On other hand, contracting (55) with K_{μ}, we find

$$\frac{\tau}{A}\left(q_{I,t} - A q_{II} \Omega\right) + q_I = -\frac{\kappa}{B}(T_{,r} + B T a_I) - \frac{\kappa T^2 q_I}{2}\left(\frac{\tau V^{\alpha}}{\kappa T^2}\right)_{;\alpha}. \quad (57)$$

It is worth noting that the two equations above are coupled through the vorticity. This fact entails an interesting thermodynamic consequence. Indeed, let us assume that at some initial time (say $t = 0$) and before it, there is thermodynamic equilibrium in the θ direction, this implies $q_{II} = 0$, and also that the corresponding Tolman's temperature [39] is constant, which in turns implies that the term within the round bracket in the first term on the right of (56) vanishes. Then it follows at once from (56) that:

$$q_{II,t} = -A\Omega q_I, \quad (58)$$

implying that the propagation in time of the vanishing of the meridional flow, is subject to the vanishing of the vorticity and/or the vanishing of heat flow in the r-direction.

Inversely, repeating the same argument for (57) we obtain at the initial time when we assume thermodynamic equilibrium,

$$q_{I,t} = A\Omega q_{II}. \quad (59)$$

Thus, it appears that the vanishing of the radial component of the heat flux vector at some initial time, will propagate in time if only, the vorticity and/or the meridional heat flow vanish.

In other words, time propagation of the thermal equilibrium condition, in either direction r or θ, is assured only in the absence of vorticity. Otherwise, it requires initial thermal equilibrium in both directions.

This result is a clear reminiscence of the von Zeipel's theorem [40].

3.2 The equations for the metric functions, the kinematical variables and the Riemann tensor components.

Let us first recall the decomposition of the covariant derivative of the four–velocity in terms of the kinematical variables given by:

$$V_{\alpha;\beta} = \sigma_{\alpha\beta} + \Omega_{\alpha\beta} - a_\alpha V_\beta + \frac{1}{3}h_{\alpha\beta}\Theta, \tag{60}$$

which entails all the equations (18), (19), (20), (24).

Now, if we regard the above expression as a first order differential equation relating the kinematical variables with first order derivative of the metric functions, and look for its integrability conditions, we find

$$V_{\alpha;\beta;\nu} - V_{\alpha;\nu;\beta} = R^{\mu}_{\alpha\beta\nu}V_\mu. \tag{61}$$

From this last equation the following equations are obtained, by projecting with different combinations of the tetrad vectors:

An evolution equation for the expansion scalar (the Raychaudhuri equation)

$$\Theta_{;\alpha}V^\alpha + \frac{1}{3}\Theta^2 + 2(\sigma^2 - \Omega^2) - a^{\alpha}_{;\alpha} + 4\pi(\mu + 3P) = 0 \tag{62}$$

where $2\sigma^2 = \sigma_{\alpha\beta}\sigma^{\alpha\beta}$.

An equation for the evolution of the shear tensor:

$$\begin{aligned} &h^\mu_\alpha h^\nu_\beta \sigma_{\mu\nu;\delta}V^\delta + \sigma^\mu_\alpha\sigma_{\beta\mu} + \frac{2}{3}\Theta\sigma_{\alpha\beta} \\ &- \frac{1}{3}\left(2\sigma^2 + \Omega^2 - a^\delta_{;\delta}\right)h_{\alpha\beta} + \omega_\alpha\omega_\beta - a_\alpha a_\beta \\ &- h^\mu_{(\alpha}h^\nu_{\beta)}a_{\nu;\mu} + E_{\alpha\beta} - 4\pi\Pi_{\alpha\beta} = 0. \end{aligned} \tag{63}$$

An equation for the evolution of the vorticity tensor:

$$h^\mu_\alpha h^\nu_\beta \Omega_{\mu\nu;\delta}V^\delta + \frac{2}{3}\Theta\Omega_{\alpha\beta} + 2\sigma_{\mu[\alpha}\Omega^\mu{}_{\beta]} - h^\mu_{[\alpha}h^\nu_{\beta]}a_{\mu;\nu} = 0. \tag{64}$$

Two constraint equations relating the kinematical variables and their derivatives with the heat flux vector and the magnetic part of the Weyl tensor:

$$h^\beta_\alpha\left(\frac{2}{3}\Theta_{;\beta} - \sigma^\mu_{\beta;\mu} + \Omega_\beta{}^\mu{}_{;\mu}\right) + (\sigma_{\alpha\beta} + \Omega_{\alpha\beta})\,a^\beta = 8\pi q_\alpha, \tag{65}$$

$$2\omega_{(\alpha}a_{\beta)} + h^\mu_{(\alpha}h_{\beta)\nu}\left(\sigma_{\mu\delta} + \Omega_{\mu\delta}\right)_{;\gamma}\eta^{\nu\kappa\gamma\delta}V_\kappa = H_{\alpha\beta}. \tag{66}$$

3.3 The conservation equations

The conservation law $T^\alpha_{\beta;\alpha} = 0$, leads to the following equations:

$$\begin{aligned} &\mu_{;\alpha}V^\alpha + (\mu + P)\Theta + \frac{1}{9}(2\sigma_I + \sigma_{II})\Pi_I \\ &+\frac{1}{9}(2\sigma_{II} + \sigma_I)\Pi_{II} + q^\alpha_{;\alpha} + q^\alpha a_\alpha = 0, \end{aligned} \tag{67}$$

$$\begin{aligned} &(\mu + P)a_\alpha + h^\beta_\alpha\left(P_{;\beta} + \Pi^\mu_{\beta;\mu} + q_{\beta;\mu}V^\mu\right) \\ &\quad + \left(\frac{4}{3}\Theta h_{\alpha\beta} + \sigma_{\alpha\beta} + \Omega_{\alpha\beta}\right)q^\beta = 0. \end{aligned} \tag{68}$$

3.4 The Bianchi identities

Next, if we regard (61) as a system of differential equations of first order, relating the Riemann tensor components with the kinematical variables and their derivatives, and look for their integrability conditions, we are lead to the Bianchi idenitities, which together with (28), lead to the following set of equations:

An evolution equation for the electric part of the Weyl tensor

$$\begin{aligned} &h^\mu_{(\alpha}h^\nu_{\beta)}E_{\mu\nu;\delta}V^\delta + \Theta E_{\alpha\beta} + h_{\alpha\beta}E_{\mu\nu}\sigma^{\mu\nu} - 3E_{\mu(\alpha}\sigma^\mu_{\beta)} \\ &+ h^\mu_{(\alpha}\eta_{\beta)}{}^{\delta\gamma\kappa}V_\delta H_{\gamma\mu;\kappa} - E_{\delta(\alpha}\Omega_{\beta)}{}^\delta - 2H^\mu_{(\alpha}\eta_{\beta)\delta\kappa\mu}V^\delta a^\kappa = \\ &- 4\pi(\mu + P)\sigma_{\alpha\beta} - \frac{4\pi}{3}\Theta\Pi_{\alpha\beta} - 4\pi h^\mu_{(\alpha}h^\nu_{\beta)}\Pi_{\mu\nu;\delta}V^\delta - 4\pi\sigma_{\mu(\alpha}\Pi^\mu_{\beta)} \\ &- 4\pi\Omega^\mu{}_{(\alpha}\Pi_{\beta)\mu}8\pi a_{(\alpha}q_{\beta)} + \frac{4\pi}{3}\left(\Pi_{\mu\nu}\sigma^{\mu\nu} + a_\mu q^\mu + q^\mu_{;\mu}\right)h_{\alpha\beta} \\ &- 4\pi h^\mu_{(\alpha}h^\nu_{\beta)}q_{\nu;\mu}. \end{aligned} \tag{69}$$

A constraint equation for the spatial derivatives of the electric part of the Weyl tensor

$$\begin{aligned} &h^\mu_\alpha h^{\nu\beta}E_{\mu\nu;\beta} - \eta_\alpha{}^{\delta\nu\kappa}V_\delta\sigma^\gamma_\nu H_{\kappa\gamma} + 3H_{\alpha\beta}\omega^\beta = \frac{8\pi}{3}h^\beta_\alpha\mu_{;\beta} \\ &- 4\pi h^\beta_\alpha h^{\mu\nu}\Pi_{\beta\nu;\mu} - 4\pi\left(\frac{2}{3}\Theta h^\beta_\alpha - \sigma^\beta_\alpha + 3\Omega_\alpha{}^\beta\right)q_\beta, \end{aligned} \tag{70}$$

A constraint equation for the spatial derivatives of the magnetic part of the Weyl tensor

$$\begin{aligned} &\left(\sigma_{\alpha\delta}E^\delta_\beta + 3\Omega_{\alpha\delta}E^\delta_\beta\right)\epsilon_\kappa{}^{\alpha\beta} + a^\nu H_{\nu\kappa} - H^{\nu\delta}{}_{;\delta}h_{\nu\kappa} = \\ &4\pi(\mu + P)\Omega_{\alpha\beta}\epsilon_\kappa{}^{\alpha\beta} \\ &+ 4\pi\left[q_{\alpha;\beta} + \Pi_{\nu\alpha}(\sigma^\nu{}_\beta + \Omega^\nu{}_\beta)\right]\epsilon_\kappa{}^{\alpha\beta}, \end{aligned} \tag{71}$$

An evolution equation for the magnetic part of the Weyl tensor

$$\begin{aligned} &2a_\beta E_{\alpha\kappa}\epsilon_\gamma{}^{\alpha\beta} - E_{\nu\beta;\delta}h^\nu_\kappa\epsilon_\gamma{}^{\delta\beta} + E^\delta_{\beta;\delta}\epsilon_{\gamma\kappa}{}^\beta + \frac{2}{3}\Theta H_{\kappa\gamma} \\ &+ H^\mu_{\nu;\delta}V^\delta h^\nu_\kappa h_{\mu\gamma} - \left(\sigma_{\kappa\delta} + \Omega_{\kappa\delta}\right)H^\delta_\gamma \\ &+ \left(\sigma_{\beta\delta} + \Omega_{\beta\delta}\right)H^\mu_\alpha\epsilon_\kappa{}^\delta{}_\mu\epsilon_\gamma{}^{\alpha\beta} + \frac{1}{3}\Theta H^\mu_\alpha\epsilon_\kappa{}^\delta{}_\mu\epsilon_\gamma{}^\alpha{}_\delta \\ &= \frac{4\pi}{3}\mu_{,\beta}\epsilon_{\gamma\kappa}{}^\beta + 4\pi\Pi_{\alpha\nu;\beta}h^\nu_\kappa\epsilon_\gamma{}^{\alpha\beta} \\ &+ 4\pi\left[q_\kappa\Omega_{\alpha\beta} + q_\alpha(\sigma_{\kappa\beta} + \Omega_{\kappa\beta} + \frac{1}{3}\Theta h_{\kappa\beta})\right]\epsilon_\gamma{}^{\alpha\beta}. \end{aligned} \tag{72}$$

Equations (55), (62)-(72) form the full set of equations for the variables of our problem. However, the following remarks are in order at this point:

– Obviously, not all of these equations are independent, however depending on the problem under consideration, it may be more advantageous to use one subset instead of the other, and therefore here we present them all.

– The scalar equations obtained by projecting the above system, on all possible combinations of tetrad vectors, are deployed in the Appendix B of [1].
– The obtained equations are of first order, unlike the Einstein equations, which are differential equations of second order for the metric functions. This reduction is achieved by enlarging the number of variables and equations.
– In the case of specific modeling, another important question arises, namely: what additional information is required to close the system of equations? It is clear that information about local physical aspects of the source (e.g. equations of state and/or information about energy production) are not included in the set of deployed equations and therefore should be given, in order that metric and matter functions could be solved for in terms of initial data.

4 THE EFFECTIVE INERTIAL MASS DENSITY OF THE DISSIPATIVE FLUID

In classical dynamics the inertial mass is defined as the factor of proportionality between the three-force applied to a particle (a fluid element) and the resulting three-acceleration, according to Newton's second law.

In relativistic dynamics a similar relation only holds (in general) in the instantaneous rest frame (i.r.f.), since the three-acceleration and the force that causes it are not (in general) paralell, except in the i.r.f. (see for example [41]).

We shall derive below, an expression for the effective inertial mass density for our dissipative fluid distribution.

By "effective inertial mass" (e.i.m.) density we mean the factor of proportionality between the applied three-force density and the resulting proper acceleration (i.e., the three-acceleration measured in the i.r.f.).

As we shall see, the obtained expression for the e.i.m. density contains a contribution from dissipative variables which reduces its value with respect to the non-dissipative situation. Such decreasing of e.i.m. density was brought out for the first time in the spherically symmetric self-gravitating case in [42]. Afterwards this effect was also detected in the axially symmetric self-gravitating case [43], for slowly rotating self-gravitating systems [44], and under other many different circumstances [45–50].

It is perhaps worth noticing that the concept of effective inertial mass is familiar in other branches of physics, thus for example the e.i.m. of an electron moving under a given force through a crystal, differs from the value corresponding to an electron moving under the same force in free space, and may even become negative (see [51,52]).

Combining the equations (68) and (55) we obtain

$$
\begin{aligned}
&(\mu+P)\,(1-\alpha)\,a_\alpha = -h^\beta_\alpha \Pi^\mu_{\beta;\mu} - \nabla_\alpha P \\
&-(\sigma_{\alpha\beta}+\Omega_{\alpha\beta})q^\beta + \frac{\kappa}{\tau}\nabla_\alpha T \\
&+\left\{\frac{1}{\tau}+\frac{1}{2}D_t\left[ln(\frac{\tau}{\kappa T^2})\right]-\frac{5}{6}\Theta\right\}q_\alpha, \qquad (73)
\end{aligned}
$$

an expression which takes the desired, "Newtonian", form.

$$\text{Force=e.i.m.} \times \text{acceleration(proper)},$$

where $\nabla_\alpha P \equiv h^\beta_\alpha P_{,\beta}$, $D_t f \equiv f_{,\beta}V^\beta$ and $\alpha = \frac{\kappa T}{\tau(\mu+P)}$.

The factor multiplying the four acceleration vector represents the effective inertial mass density. Thus, the obtained expression for the e.i.m. density contains a contribution from dissipative variables, which reduces its value with respect to the non-dissipative situation.

From the equivalence principle it follows that the "passive" gravitational mass density should be reduced too, by the same factor. This in turn might lead, in some critical cases when such diminishing is significative, to a bouncing of the collapsing object.

It should be observed that causality and stability conditions hindering the system to attain the condition $\alpha = 1$, are obtained on the basis of a linear approximation, whose validity, close to the critical point ($\alpha = 1$), is questionable [53].

At any rate, examples of fluids attaining the critical point and exhibiting reasonble physical properties have been presented elsewhere [54,55].

In order to evaluate α, let us turn back to c.g.s. units. Then, assuming for simplicity $\mu + p \approx 2\mu$, we obtain

$$\frac{\kappa T}{\tau(\mu+p)} \approx \frac{[\kappa][T]}{[\tau][\mu]} \times 10^{-42} \qquad (74)$$

where $[\kappa]$, $[T]$, $[\tau]$, $[\mu]$ denote the numerical values of these quantities in $erg.\,s^{-1}\,cm^{-1}\,K^{-1}$, K, s and $g.\,cm^{-3}$, respectively.

Obviously, this will be a very small quantity (compared to 1), unless conditions for extremely high values of κ and T are attained.

At present we may speculate that α may increase substantially (for a non-negligible values of τ) in a pre-supernovae event

Indeed, at the last stages of massive star evolution, the decreasing of the opacity of the fluid, from very high values preventing the propagation of photons and neutrinos (trapping [56]), to smaller values, gives rise to radiative heat conduction. Under these conditions

both κ and T could be sufficiently large as to imply a substantial increase of α. Indeed, the values suggested in [57] ($[\kappa] \approx 10^{37}$; $[T] \approx 10^{13}$; $[\tau] \approx 10^{-4}$; $[\mu] \approx 10^{12}$) lead to $\alpha \approx 1$. The obvious consequence of which would be to enhance the efficiency of whatever expansion mechanism, of the central core, at place, because of the decreasing of its e.i.m. density. At this point it is worth noticing that the relevance of relaxational effects on gravitational collapse has been often exhibited and stressed (see [58–62], and references therein)

It is also worth noticing that the inflationary equation of state (in the perfect fluid case) $\mu + P = 0$, is, as far as the equation of motion is concerned, equivalent to $\alpha = 1$ in the dissipative case (both imply the vanishing of the e.i.m. density).

Finally, it is worth stressing that it is the first term on the left and the second on the right, in (55) the direct responsible for the decreasing in the e.i.m density. Therefore any hyperbolic dissipative theory yielding a Cattaneo-type equation in the non-relativistic limit, is expected to give a result similar to the one obtained here.

5 SOME PARTICULAR CASES

In what follows we shall consider some particular cases, where some variables (e. g. the shear) are assumed to vanish. We do so, on the one hand for simplicity, and on the other, in order to bring out the role of some specific variables. However, it should be kept in mind that such kinds of "suppressions" may lead to inconsistencies in the set of equations. This is for example the case of "silent" universes [63,64], where dust sources have vanishing magnetic Weyl tensor, and lead to a system of 1+3 constraint equations that do not seem to be integrable in general [65]. In other words for any specific modeling, the possible occurrence of these types of inconsistencies should be carefully considered.

5.1 The shear free case

This case has been analyzed in detail in [2]. Below we summarize the main results obtained under the shear–free condition.

- For a general dissipative and anisotropic (shear free) fluid, vanishing vorticity, is a necessary and sufficient condition for the magnetic part of the Weyl tensor to vanish.
- Vorticity should necessarily appear if the system radiates gravitationally. This further reinforces the well established link between radiation and vorticity.
- In the geodesic (shear–free) case, the vorticity vanishes (and thereof the magnetic part of the Weyl tensor). No gravitational radiation is produced. A similar result is obtained for the cylindrically symmetric case, suggesting a link between the shear of the source and the generation of gravitational radiation.
- In the geodesic (non-dissipative) case, the models do not need to be FRW, however the system relaxes to the FRW spacetime (if $\Theta > 0$). Such tendency does not appear for dissipative fluids.

5.2 The perfect, geodesic fluid

In [3] we have considered the case of perfect and geodesic fluid, without assuming *ab initio* the shear–free condition. As the result of such study we have found that:

- All possible models compatible with the line element (1) and a perfect fluid, are FRW, and accordingly non–radiating (gravitationally). Both, the geodesic and the non–dissipative, conditions, are quite restrictive, when looking for a source of gravitational waves.
- Not only in the case of dust, but also in the absence of dissipation in a perfect fluid, the system is not expected to radiate (gravitationally) due to the reversibility of the equation of state. Indeed, radiation is an irreversible process, this fact emerges at once if absorption is taken into account and/or Sommerfeld type conditions, which eliminate inward traveling waves, are imposed. Therefore, the irreversibility of the process of emission of gravitational waves, must be reflected in the equation of state through an entropy increasing (dissipative) factor.
- Geodesic fluids not belonging to the class considered here (Szekeres) have also been shown not to produce gravitational radiation. This strengthens further the case of the non–radiative character of pure dust distributions.

5.3 The dissipative, geodesic fluid

From the results discussed above, it becomes clear that the simplest fluid distribution which we might expect to be compatible with a gravitational radiation, is a dissipative dust under the geodesic condition. Such a case was analyzed in [4].

The two possible subcases were considered separately, namely: the fluid distribution is assumed, from the beginning, to be vorticity–free, or not.

In the former case, it is shown that the vanishing vorticity implies the vanishing of the heat flux vector, and therefore, as shown in [3], the resulting spacetime is FRW.

In the latter case, it is shown that the enforcement of the regularity conditions at the center, implies the vanishing of the dissipative flux, leading also to a FRW spacetime.

Thus all possible models, sourced by a dissipative geodesic dust fluid, belonging to the family of the line element considered here, do not radiate gravitational waves during their evolution, unless regularity conditions at the center of the distribution are relaxed. Therefore physically acceptable models require the inclusion of, both, dissipative and anisotropic stresses terms, i.e. the geodesic condition must be abandoned. In this case, purely analytical methods are unlikely to be sufficient to arrive at a full description of the source, and one has to resort to numerical methods.

6 OPEN ISSUES

Below we display a partial list of problems which we believe deserve some attention:

- How could one describe the "cracking" (splitting) of the configurations, in the context of this formalism ?
- We do not have an exact solution (written down in closed analytical form) describing gravitational radiation in vacuum, from bounded sources. Accordingly, any specific modeling of a source, and its matching to an exterior, should be done numerically.
- It should be useful to introduce the concept of the mass function, similar to the one existing in the spherically symmetric case. This could be relevant, in particular, in the matching of the source to a specific exterior.
- What is the behaviour of the system in the quasi–static approximation? Would be there gravitational radiation in this case?

References

1. L. Herrera, A. Di Prisco, J. Ibáñez and J. Ospino, *Phys. Rev. D* **89**, 084034, (2014).
2. L. Herrera, A. Di Prisco and J. Ospino, *Phys. Rev. D* **89**,127502, (2014).
3. L. Herrera, A. Di Prisco, J. Ospino and J. Carot *Phys. Rev. D* **91**, 024010, (2015).
4. L. Herrera, A. Di Prisco and J. Ospino, *Phys. Rev. D* **91**, 124015, (2015).
5. A. Di Prisco, L. Herrera, J. Jiménez, V. Galina and J. Ibáñez, *J. Math. Phys.*, **28**, 2692, (1987).
6. H. Bondi, M. G. J. van der Burg and A. W. K. Metzner, *Proc. Roy.Soc. A* **269**, 21 (1962).
7. G. F. R. Ellis and H. van Ellst, *gr–qc/9812046v4* (1998).
8. G. F. R. Ellis *Gen. Rel. Grav.* **41**, 581 (2009).
9. G. F. R. Ellis, R. Maartens and M. A. H. MacCallum, *Relativistic Cosmology* (Cambridge U. P., Cambridge) (2012).
10. L. Herrera, J. Ospino, A. Di Prisco, E. Fuenmayor and O. Troconis, *Phys. Rev. D* **79**, 064025 (2009).
11. L. Herrera, A. Di Prisco and J. Ospino, *Gen. Relativ. Gravit.* **44**, 2645, (2012).
12. L. Herrera, A. Di Prisco, J. Ospino and J. Carot, *Phys. Rev.D* **82**, 024021 (2010).
13. L. Herrera, A. Di Prisco and J. Ospino, *Gen.Relativ. Gravit.* **42**, 1585 (2010).
14. L. Herrera, A. Di Prisco and J. Ibáñez, *Phys. Rev. D* **84**, 064036 (2011).
15. L. Herrera, A. Di Prisco and J. Ibáñez *Phys. Rev. D* **84**, 107501 (2011).
16. M. Sharif and N. Bashir, *Gen. Relativ. Gravit.* **44**, 1725 (2012).
17. M. Sharif and M. Zaeem ul Haq Bhati, *Mod. Phys. Lett. A* **27**, 1250141 (2012).
18. M. Sharif and M. Zaeem ul Haq Bhati, *Gen. Relativ. Gravit.* **44**, 2811 (2012).
19. M. Sharif and Z. Yousaf, *Astr. Space. Sci.* **352**, 321 (2014).
20. M. Sharif and Z. Yousaf, *Astr. Space. Sci.* **354**, 2093 (2014).
21. L. Bel, *Cah. de Phys.* **16**, 59 (1962).
22. A. García-Parrado Gómez Lobo, *Class. Quantum Grav.* **25**, 015006 (2008).
23. A Di Prisco, L. Herrera, M. A. H. MacCallum and N.O. Santos, *Phys. Rev. D* **80**, 064031 (2009).
24. R. Sachs, *Proc. Roy.Soc. A* **270**, 103 (1962).
25. L. Herrera, W. Barreto, J. Carot and A. Di Prisco, *Class. Quantum Grav.*, **24**, 2645, (2007).
26. I. Müller, *Z. Physik* **198**, 329 (1967)
27. W. Israel, *Ann. Phys., NY*, **100**, 310 (1976).
28. W. Israel and J. Stewart, *Phys. Lett. A*, **58**, 213 (1976).
29. W. Israel and J. Stewart, *Ann. Phys.* (NY) **118**, 341, (1979)
30. D. Joseph and L. Preziosi, *Rev. Mod. Phys.* **61**, 41 (1989).
31. R. Maartens, *astro-ph/9609119*.
32. L. Herrera and D. Pavón, *Physica A*, **307**, 121 (2002).
33. W. Hiscock and L. Lindblom, *Ann. Phys.* (NY) **151**, 466 (1983).
34. C. Eckart, *Phys. Rev.* **58**, 919 (1940).
35. L. Landau and E. Lifshitz, *Fluid Mechanics* (Pergamon Press, London) (1959).
36. D. Pavón, D. Jou and J. Casas-Vázquez, *Ann. Inst. H Poincaré* **A36**, 79 (1982).
37. B. Carter, *Journées Relativistes*, ed. M. Cahen, R. Debever and J. Geheniau, (Université Libre de Bruxelles) (1976).
38. C. Cattaneo, *Atti Semin. Mat. Fis. Univ. Modena* **3**, 3 (1948).
39. R Tolman *Phys. Rev.* **35** 904 (1930).
40. R Kippenhahn, A. Weigert, *Stellar Structure and Evolution*, Springer Verlag, Berlin, (1990).
41. W. Rindler, *Essential Relativity, 2nd edition*, (Springer-Verlag, Berlin) (1977) .
42. L. Herrera, A. Di Prisco, J. L. Hernández-Pastora, J. Martín and J. Martínez, *Class. Quantum Grav.*, **14**, 2239 (1997).
43. L. Herrera L, A. Di Prisco and J. Martínez, *Phys. Lett. A*, **243**, 7 (1998).

44. L. Herrera and J. Martínez, *J. Math. Phys*, **39**, 3260 (1998).
45. L. Herrera and N.O. Santos, *Phys. Rev. D* **70**, 084004 (2004).
46. L. Herrera, *Phys. Lett. A*, **300**, 157 (2002).
47. L. Herrera, *Int. J. Mod. Phys. D* **15**, 2197 (2006).
48. M. Sharif, H. Tahir, *Eur.Phys.J.Plus*,**128**,146, (2013).
49. M. Sharif, I. Nawazish, *Astr. Space. Sci.* **351**, 313, (2014).
50. M. Sharif, M. Zaeem Ul Haq Bhatti, *Mod. Phys. Lett. A* **29**,1450165, (2014).
51. M. Jammer, *Concepts of Mass in Contemporary Physics and philosophy*, (Princeton U. P., Princeton) (2000).
52. C. Kittel,*Introduction to Solid State Physics*, (John Wiley and Sons,New York) (1986).
53. L. Herrera and J. Martínez J, *Class. Quantum Grav.*, **14**, 2697 (1997).
54. L. Herrera and J. Martínez ,*Class. Quantum Grav.*, **15**, 407 (1998).
55. L. Herrera and J. Martínez, *Astr. Space Sci.*, **259**, 235 (1998).
56. W. Arnett, *Astrophys. J.*, **218**, 815 (1977).
57. J. Martínez, *Phys. Rev. D*, **53**, 6921 (1996).
58. M. Govender and K. Govinder, *Phys. Lett. A*, **283**,71 (2001).
59. S. Wagh, M. Govender, K. Govinder, S. Maharaj, P. Muktibodh and M. Moodly, *Class.Quantum.Grav.* **18**, 2147 (2001).
60. M. Govender, R. Maartens and S. Maharaj, *Mon. Not. Roy. Ast.Soc.*, **310**, 557 (1999).
61. S. Maharaj and M. Govender, *Pramana J.P.*, **54**, 715 (2000).
62. M. Govender, K. Reddy, S. Maharaj, *Int. J. Mod. Phys. D* **23** ,1450013, (2014).
63. S. Matarrese, O. Pantano and D. Saez, *Phys. Rev.* D **47** 1311 (1993).
64. M. Bruni, S. Matarrese and O. Pantano, *Astrophys. J.* **445** 958 (1995).
65. H. van Ellst, C. Uggla, W. M. Lesame, G. F. R. Ellisand and R. Maartens, *Class Quantum Grav* **14** 1151 (1997).

Proc. Int. Conf. Relativ. Astrophys.
Pages 86-88, (2015)

Connection between Lie Symmetries, Noether Symmetries and Collinations

Ibrar Hussain[a,1]

[1]School of Electrical Engineering and Computer Science, National University of Sciences and Technology, H-12 Campus, Islamabad, Pakistan

Abstract In this note a brief review of the relationship between Lie symmetries, Noether symmetries and spacetime symmetries or collineations is given.

Keywords Lie symmetries; Noether symmetries; Collineations

Noether symmetries or symmetries of Lagrangians (more generally symmetries of actions) and Lie Symmetries or symmetries of the corresponding equations of motion (in general symmetries of differential equations (DEs)) play an important role in finding solutions of DEs [1]. In the case of ordinary differential equations (ODEs) they reduce the order of the ODEs. They can be used to reduce the number of independent variables in the case of partial differential equations (PDEs) [2]. They have also used to linearize nonlinear DEs [3–6]. Between these two type of symmetries the Noether symmetries are more useful than the Lie symmetries (for those problems for which Lagrangian exists) in the sense as they give double reduction of DEs. Another important property of the Noether symmetries is that they yield conservation laws or conserved quantities or first integrals of the Euler-Lagrange equations via the Noether theorem [7].

On the other hand spacetime symmetries or collineations have their own importance in Einstein's the theory of General Relativity (GR) [8]. The Spacetime symmetries e.g. isometries or Killing vectors (KVs), homothetic vectors (HVs), conformal Killing vectors (CKVs) and curvature collineations (CCs) etc have widely used in classification of different spacetimes of GR [9–14]. They have also used for finding exact solutions of the Einstein Field Equations [15]. Here we give the definitions of the Lie symmetries, Noether symmetries and collineations.

[a]E-mail: ibrar.hussain@seecs.nust.edu.pk

Consider a vector field

$$\mathbf{X}=\xi(s,x^{\mu})\frac{\partial}{\partial s}+\eta^{\nu}(s,x^{\mu})\frac{\partial}{\partial x^{\nu}}, \tag{1}$$

where s, the arc length parameter, is the independent variable and x^{μ} are the dependent variables. The first and second prolongations of the above vector field is given by

$$\mathbf{X}^{[1]}=\mathbf{X}+(\eta^{\nu}_{,s}+\eta^{\nu}_{,\mu}\dot{x}^{\mu}-\xi_{,s}\dot{x}^{\nu}-\xi_{,\mu}\dot{x}^{\mu}\dot{x}^{\nu})\frac{\partial}{\partial\dot{x}^{\nu}}, \tag{2}$$

and

$$\mathbf{X}^{[2]}=\mathbf{X}+\eta^{[1]\mu}\frac{\partial}{\partial\dot{x}^{\mu}}+\eta^{[2]\mu}\frac{\partial}{\partial\ddot{x}^{\mu}}. \tag{3}$$

The prolongation coefficients $\eta^{[1]}$ and $\eta^{[2]}$ are defined by

$$\eta^{[1]\mu}=\frac{d\eta^{\mu}}{ds}-\dot{x}^{\mu}\frac{\xi}{ds}, \tag{4}$$

$$\eta^{[2]\mu}=\frac{d\eta^{[1]\mu}}{ds}-\ddot{x}^{\mu}\frac{\xi}{ds}. \tag{5}$$

The vector field $\mathbf{X}$ given in (1) is said to be a Lie symmetry generator of a DE if

$$\mathbf{X}^{[2]}E=0,\quad mod\quad E\equiv 0, \tag{6}$$

where E is a second-order DE. Note that here we restrict the definition of Lie symmetries to the second-order DEs only as they corresponds to the first-order Lagrangians which are physically interesting. More general definition of the Lie symmetries is available in the literature (see for example [16]). Throughout this note "$\cdot$" denotes differentiation with respect to the independent variable s.

The vector field $\mathbf{X}$ given by (1)is a Noether point symmetry generator of the Lagrangian

$$L(s,x^{\mu},\dot{x}^{\mu})=g_{\mu\nu}(x^{\sigma})\dot{x}^{\mu}\dot{x}^{\nu}, \tag{7}$$

if there exists a gauge function, $G(s, x^\mu)$, such that

$$\mathbf{X}^{[1]}L + (D_s\xi)L = D_sG, \tag{8}$$

where

$$D_s = \frac{\partial}{\partial s} + \dot{x}^\mu \frac{\partial}{\partial x^\mu}, \tag{9}$$

is the total derivative operator. The significance of Noether symmetries can be seen from the following Noether's theorem [1].

Theorem: If $\mathbf{X}$ is a Noether point symmetry generator corresponding to a Lagrangian $L(s, x^\mu, \dot{x}^\mu)$ of a second-order ODE $\ddot{x}^\mu = f(s, x, \dot{x}^\mu)$, then

$$I = \xi L + (\eta^\mu - \dot{x}^\mu\xi)\frac{\partial L}{\partial \dot{x}^\mu} - G, \tag{10}$$

is a first integral (the conserved quantity) of the ODE, associated with $\mathbf{X}$.

A vector field $\mathbf{X}$ is said to be a CKV if the condition

$$\pounds_{\mathbf{X}} g_{\mu\nu} = \psi(x^\sigma) g_{\mu\nu}, \tag{11}$$

holds [17]. Where $\psi(x^\sigma)$ is a conformal factor and $\pounds$ denotes the Lie derivative operator. If $\psi_{,\sigma} = 0$, then $\mathbf{X}$ is known as a HV and a KV if $\psi = 0$, where the comma denotes the partial derivative with respect to the spacetime coordinates. In (1), if we replace the metric tensor $g_{\mu\nu}$ with the Riemann curvature tensor $R^\mu_{\ \nu\lambda\sigma}$ and put $\psi = 0$, then the vector field $\mathbf{X}$ is known as a CC. On using the Weyl tensor $C^\mu_{\ \nu\lambda\sigma}$, Ricci tensor $R_{\mu\nu}$ or matter tensor $T_{\mu\nu}$ instead of the Rieman tensor one can get Weyl collineations (WCs) [14], Ricci collineations (RCs) [18] and matter collineations (MCs)[19] respectively. To restrict ourselves to the four dimensional manifold of GR, all the indexes μ, ν, λ and σ run from 0 to 3.

Among all these types of spacetime symmetries the set of KVs is the basic one. This set is always contained in the set of all other types of spacetime symmetries e.g. CKVs, HVs, CCs , WCs, RCs, and MCs (for detail see [17]). The algebra of KVs form a subalgebra of the symmetry algebra of the geodesic equations or Euler-Lagrange equations of the underlying spaces [20]. It is also known that the set of Noether symmetries always contained in the set of the Lie symmetries of the corresponding Euler-Lagrange equations [16].

For the Minkowski spacetime which is flat and hence conformally flat, it is known thatt it admits 15 CKVs [21]. The geodesic Lagrangian for this spacetime admits 17 Noether symmetries which properly contains the 15 CKVs [22]. Since the algebras of KVs and HVs form subalgebra of the CKVs, therefore for the Minkowski spacetime all these three types of spacetime symmetries are contained in the set of 17 Noether symmetries. On the basis of this result, it was conjectured, that the algebra of the CKVs form a subalgebra of the algebra of the symmetry generators of the Lagrangian that minimizes arc length for any spacetime [22]. A counter example of a non-flat cylindrically symmetric static spacetime was constructed for which the set of symmetries of the Lagrangian for the geodesic equations only contain the set of the KVs and not the sets of the HVs and CKVs. Hence the conjecture was proved false [23]. The geodesic Lagrangian depends on the metric tensor $g_{\mu\nu}$ only and and not on its conformal structure, therefore it seems reasonable that the geodesic Lagrangian may only admit the symmetries of the metric tensor i.e. KVs and not the CKVs. Since for conformally flat spacetimes the metric is transformed conformally, therefore, one may expect that the geodesic Lagrangian may admit the CKVs in the case of conformally flat spacetimes. This issue was addressed in [24], and it was shown that the symmetry algebra of the Lagrangian for the geodesic equation in conformally flat spacetimes only contains the algebra of KVs and not of the CKVs.

In the recent years Noether symmetries are used for the classification of different spacetimes in GR. In this regards plane symmetric static [25], and spherically symmetric statics [26], spacetimes have been classified by using their Noether symmetry algebra. Recently the Noether symmetry classification of Bianchi type II spacetimes has been done in [27]. The classification of Bianchi type V spacetimes via their Noether symmetries has been carried out in a very recent work [28]. Noether symmetries and its relation with KVs has been studied in [29]. An investigation of Noether symmetries and isometries of the minimal surface Lagrangian under constant volume in a Riemannian space is given in [30]. Collineations, Lie symmetries and Noether symmetries of geodesic equations have been discussed in [31].

Acknowledgements I am grateful to the organizing committee for financial support and their very kind invitation to the International Conference on Relativistic Astrophysics, $10^{th} - 14^{th}$ February, 2015, at the Department of Mathematics, University of the Punjab, Lahore, Pakistan.

References

1. N.H.Ibragimov, *Elementary Lie Group Analysis and Ordinary Differential Equations*, Wiely, Chichester, 1999.
2. G.Bluman and S.Kumei, *Symmetries and Differential Equations*, Springer-Verlarg, New york, 1989.
3. S.C.Wafo and F.M.Mahomed, *Int. J. Nonlinear Mech.* **36**, (2001) 671.
4. N.H.Ibragimov and S.V. Maleshko, *J. Math. Anal. Applic.* **308**, (2005) 266.
5. F.MMahomed and A.Qadir, *Nonlinear Dyn.* **48**, (2007) 417.

6. A.Qadir, *SIGMA*. **3**, (2007) 103, 7 pages, arXiv.0711.0814.
7. E.Noether, *Nachr. Konig. Gissell. Wissen., Gottingen, Math.-Phys.Kl.* **2**, (1918) 235-257. (English translation in transport theory and statistical physics **1**, (1971)) 186.
8. G.S.Hall, *Symmetries and Curvature Structure in General Relativity*, World Scientific, Singapore, 2004.
9. A.Qadir and M.Ziad, *Nuovo Cimeto*, **B110**, (1995) 277.
10. A.H.Bokhari, A.Qadir, M.S.Ahmed and M.Asghar, *J. Math. Phys.*, **38**, (1997) 3639.
11. M.Ziad, *Nuovo Cimeto*, **B114**, (1999) 683.
12. A.H.Bokhari, A.R.Kashif and A.Qadir, *J. Math. Phys.*, **41**, (2000) 2167.
13. A.H.Bokhari, A.R.Kashif and A.Qadir, *Gen. Rel. Grav.*, **35**, (2003) 1059.
14. I.Hussain, A.Qadir and K.Saifullah, *Int. J. Mod. Phys.*, **D14**, (2005) 1431.
15. D.Kramer, H.Stephani, M.A.H.MacCullum and E.Herlt, *Exact Solutions of Einstein Field Equations*, Cambridge University Press, Cambridge, 1980.
16. P.J.Olver, *Applications of Lie Groups to Differential Equations*, Springer-Verlag, New York, 1993.
17. G.H.Katzin, J.Levine and W.R. Davis, *J. Math. Phys.*, **10**, (1969) 617.
18. U.Camci, I.Yavuz, H.Baysal, I.Tarhan and I.Yilmaz, *Int. J. Mod. Phys.*, **D10**, (2001) 751.
19. U.Camci and M.Sharif, *Class.Quant.Grav.*, **20**, (2003) 2169.
20. T.Feroze, F.M.Mahomed and A.Qadir, *Nonlinear Dyn.*, **45**, (2006) 65.
21. R.Maartens and S.D.Maharaj, *Class. Quant. Grav.*, **3**, (1986) 1005.
22. I.Hussain, F.M.Mahomed and A.Qadir, *Gen. Rel. Grav.*, **41**, (2009) 2399.
23. I.Hussain, *Gen. Rel. Grav.*, **42**, (2010) 1791.
24. T.Feroze and I.Hussain, *J. Geom. and Phys.*, **61**, (2011) 658.
25. F.Ali and T.Feroze, *Int. J. Theo. Phys.* **52**, (2013) 3329.
26. F.Ali and T.Feroze and S.Ali, arXiv:1309.3861.
27. M.R.Tarayrah, H.Azad, A.H.Bokhari and F.D.Zaman, arXiv:1502.02138.
28. S.Ali and I.Hussain, preprint from School of Electrical Engineering and Computer Science, National university of Sciences and Technology, Islamabad.
29. A.H.Bokhari, A.H.Kara, A.R.Kashif and F.D.Zaman, *Int. J. Theo. Phys.*, **45**, (2006) 1029.
30. M.Tsamparlis, A.Paliathanasis and A.Qadir, *Int. J. Geom. Methods Mod. Phys.*, **12**, (2015) 1550003.
31. M.Tsamparlis and A.Paliathanasis, *Gen. Rel. and Grav.*, **42**, (2010) 2957.

Proc. Int. Conf. Relativ. Astrophys.
Pages 89-94, (2015)

Dynamics of Scalar Thin-Shell

M. Sharif [1], **Sehrish Iftikhar** [2]

[1]Department of Mathematics, University of the Punjab, Quaid-e-Azam Campus, Lahore-54590, Pakistan
[2]Department of Mathematics, Lahore College for Women University, Lahore-54000, Pakistan

Abstract In this paper we study the dynamics of scalar field thin-shell. We formulate equation of motion using Israel junction conditions. The corresponding effective potentials and scalar fields are evaluated numerically for massless and massive cases. We conclude that massless scalar shell leads to collapse, expansion and equilibrium while the massive case leads to collapse only.

Keywords Gravitational collapse · Scalar field · Israel thin-shell formalism.

PACS 04.20.-q · 4.40.Dg0 · 04.70.Bw · 75.78.-n

1 Introduction

Scalar fields play a key role in several astrophysical phenomena and have many applications in theoretical physics, cluster dynamics and cosmology. Wheeler [1] found particle like solutions (geons) from classical electromagnetic field coupled to general relativity (GR) which were extended by Brill and Wheeler [2] as well as by Frederick [3]. Bergmann and Leipnik [4] investigated solution of the Einstein field equations in the presence of scalar field for Schwarzschild geometry. Christodoulou [5] examined spherically symmetric scalar collapse and formation of singularities. Choptuik [6] studied spherically symmetric collapse of a massless scalar field minimally coupled with gravity and discussed its solutions numerically.

The study of dynamics of a thin-shell has been the subject of keen interest for many people. Chase [7] examined instability of spherically symmetric charged fluid shell by using equation of state. Boulware [8] investigated time evolution of the charged thin-shell and found that end state of collapse could be a naked singularity if and only if density is negative. Barrabès and Israel [9] studied dynamics of thin-shells traveling at the speed of light. *Núñez* et al. [10] investigated stability and dynamical behavior of a real scalar field for the Schwarzschild BH. Goncalves [11] examined dynamical properties of timelike thin-shell by using Israel formalism and formulated necessary and sufficient condition for the shell crossing. Recently, Sharif and Abbas [12] explored the dynamics of scalar field charged thin-shell and concluded that for both (massless and massive scalar fields) shell can expand to infinity or collapse to zero size forming a curvature singularity or bounce under suitable conditions.

It is well-known that BH solutions (Schwarzschild, Reissner-Nordström (RN), Kerr and Kerr-Newman) contain curvature singularity beyond their event horizons. A comprehensive understanding of BH requires singularity-free solutions. Black holes having the regular centers are called regular or nonsingular BHs. Regular BHs are static and asymptotically flat, satisfying the weak energy condition. Regular BHs are the exact solutions of Einstein's equations for which singularity is avoided in the presence of horizons (the exterior Schwarzschild-like horizon and an interior de-Sitter-like horizon). An important analysis of singularity avoidance has been proposed by Hayward [13]. This BH consists of a compact spacetime region of trapped surfaces, with inner and outer boundaries which join circularly as a single smooth trapping horizon.

The purpose of this paper is to study the dynamical effects of scalar field on magnetically charged thin-shell using Israel thin-shell formalism for Hayward BH. The format of the paper is as follows. In the next section, we derive equation of motion for the thin-shell using Israel formalism. Section **3** investigates the equation of motion for Hayward BH for both massless and massive scalar fields. Final remarks are given in the last section.

[1]msharif.math@pu.edu.pk
[2]sehrish3iftikhar@gmail.com

2 Thin-Shell Formalism and Equation of Motion

Thin-shell formalism [14] has extensively been used to study the dynamics of matter fields, wormholes, collision of shells, interior structure of BHs, bubble dynamics and inflationary scenarios. In this method, surface properties are described in terms of jump of the extrinsic curvature (functions of intrinsic coordinates of the layer) across the boundary layer. This formalism allows to choose four-dimensional coordinates independently on both sides of the boundary layer. The governing equations resulting from this formalism correspond to the equation of motion whose solution can completely describe the dynamics of the shell.

We assume three-dimensional timelike boundary surface Σ, which splits spherically symmetric spacetime into two four-dimensional manifolds N^+ and N^-. The interior and exterior regions are described by a metric of the form

$$ds^2 = F_{\pm}(R)dT^2 - F_{\pm}^{-1}(R)dR^2 - R^2(d\theta^2+\sin^2\theta d\varphi^2), \quad (1)$$

where $F_{\pm}(R) = 1 - \frac{2M_{\pm}R^2}{R^3+2e_{\pm}^2}$ and $M_{\pm}$ and $e_{\pm}$ are the mass and monopole charge of a self-gravitating magnetic field of a non-linear electrodynamics source, respectively. The above metric describes Hayward BH which correspond to the Schwarzschild BH for $e = 0$. Moreover, it is assumed that the interior region contains more mass than the exterior region, i.e., gravitational masses are unequal $M_- \neq M_+$ while charge is uniformly distributed in both regions, i.e., $e = e_- = e_+$. By applying the intrinsic coordinates $(\tau,\ \theta,\ \varphi)$ on the hypersurface (Σ) at $R = R(\tau)$, Eq.(1) becomes

$$(ds)^2_{\pm\Sigma} = \left[F_{\pm}(R) - F_{\pm}^{-1}(R)(\frac{dR}{d\tau})^2(\frac{d\tau}{dT})^2 dT^2\right] - R^2(\tau)(d\theta^2+\sin^2\theta d\varphi^2). \quad (2)$$

Here, it is assumed that $T(\tau)$ is a timelike coordinate, i.e., $g_{00} > 0$. Also, the induced metric on the boundary surface is given as

$$(ds)^2 = d\tau^2 - \alpha^2(\tau)(d\theta^2+\sin^2\theta d\varphi^2). \quad (3)$$

The continuity of first fundamental forms give

$$\left[F_{\pm}(R) - F_{\pm}^{-1}(R)(\frac{dR}{d\tau})^2(\frac{d\tau}{dT})^{\frac{1}{2}}\right] dT = (d\tau)_{\Sigma}, \quad R(\tau) = \alpha(\tau)_{\Sigma}. \quad (4)$$

The outward unit normals $\eta_{\mu}^{\pm}$ in $N^{\pm}$ coordinates are calculated as

$$\eta_{\mu}^{\pm} = (-\dot{R}, \dot{T}, 0, 0), \quad (5)$$

where dot represents differentiation with respect to τ. The surface stress energy-momentum tensor is defined as

$$S_{\mu\nu} = \frac{1}{\kappa}([K_{\mu\nu}] - \gamma_{\mu\nu}[K]), \quad (6)$$

where $\gamma_{\mu\nu}$ denotes the induced metric, κ is the coupling constant and

$$[K_{\mu\nu}] = K^+_{\mu\nu} - K^-_{\mu\nu}, \quad [K] = \gamma^{\mu\nu}[K_{\mu\nu}]. \quad (7)$$

The non-vanishing components of extrinsic curvature are

$$K^{\pm}_{\tau\tau} = \frac{d}{dR}\sqrt{\dot{R}^2+F_{\pm}}, \quad K^{\pm}_{\theta\theta} = -R\sqrt{\dot{R}^2+F_{\pm}}, \quad K^{\pm}_{\varphi\varphi} = \sin^2\theta K^{\pm}_{\theta\theta}. \quad (8)$$

The surface stress energy-momentum tensor for a perfect fluid is

$$S_{\mu\nu} = (\rho+p)u_{\mu}u_{\nu} - p\gamma_{\mu\nu}, \quad (9)$$

where ρ is the energy density, p is the isotropic pressure and $u_{\mu} = \delta^0_{\mu}$ is the velocity of the shell. Using Eqs.(4), (6) and (9), we find

$$\rho = \frac{2}{\kappa R^2}[K_{\theta\theta}], \quad p = \frac{1}{\kappa}([K_{\tau\tau}] - \frac{[K_{\theta\theta}]}{R^2}). \quad (10)$$

Using Eq.(8) in (10), we can obtain the following relations

$$(\omega_+ - \omega_-) + \frac{\kappa}{2}\rho R = 0, \quad (11)$$

$$\frac{d}{dR}(\omega_+ - \omega_-) + \frac{1}{R}(\omega_+ - \omega_-) - \kappa p = 0, \quad (12)$$

where $\omega_{\pm} = \sqrt{\dot{R}^2+F_{\pm}}$.

The above equations lead to the following differential equation

$$\frac{d\rho}{dR} + \frac{2}{R}(\rho+p) = 0, \quad (13)$$

which is equivalent to the energy conservation of the thin-shell

$$\dot{m} + p\dot{A} = 0, \quad (14)$$

where $m = \rho A$ and $A = 4\pi R^2(\tau)$ represent mass and area of the shell, respectively. It is mentioned here that Eq.(13) can be solved using the equation of state $p = \check{k}\rho$ whose solution is

$$\rho = \rho_0\left(\frac{R_0}{R}\right)^{2(\check{k}+1)}, \quad (15)$$

where R_0 represents initial position of the shell at time $\tau = \tau_0$ and ρ_0 denotes matter density of the shell at R_0. Using the above equation, the mass of the shell takes the form

$$m = 4\pi\rho_0\frac{R_0^{2(\check{k}+1)}}{R^{2\check{k}}}. \quad (16)$$

Equation (11) leads to the equation of motion of the shell

$$\dot{R}^2 + V_{eff} = 0, \quad (17)$$

where

$$V_{eff}(R) = \frac{1}{2}(F_+ + F_-) - \frac{(F_+ + F_-)^2}{(\kappa\rho R)^2} - \frac{1}{16}(\kappa\rho R)^2, \quad (18)$$

is the effective potential which describes shell's motion.

3 Analysis of Equation of Motion

Here we study the dynamical behavior of the scalar shell for a family of regular BHs. For this purpose, we first calculate the effective potential and the corresponding velocity of the shell with respect to the stationary observer. We investigate the effect of charge parameter on the dynamics of the shell. In 2006, Hayward [13] found a simple regular BH solution in which e is related to the cosmological constant Λ as $e^2 = \frac{3M}{\Lambda}$ and for the well-defined asymptotic limits, this corresponds to the Schwarzschild BH as $R \to \infty$ while it becomes de Sitter spacetime at the center ($R \to 0$). The corresponding effective potential is

$$V_{eff}(R) = 1 - \left(\frac{2R^3}{R^3+2e^2}\right)^2 \left(\frac{M_+ - M_-}{m}\right)^2 - \frac{(M_+ + M_-)R^2}{(R^3+2e^2)} - \left(\frac{m}{2R}\right)^2. \quad (19)$$

Equation (17) and (19) yield

$$\dot{R} = \pm \left[\left(\frac{2R^3}{R^3+2e^2}\right)^2 \left(\frac{M_+ - M_-}{m}\right)^2 + \frac{(M_+ + M_-)R^2}{R^3+2e^2} + \left(\frac{m}{2R}\right)^2 - 1\right]^{\frac{1}{2}}. \quad (20)$$

Here $-(+)$ correspond to collapse (expansion) of the shell. In Figure **1**, the left graph represents $\dot{R} > 0$ while the right graph shows the behavior of shell's velocity when $\dot{R} < 0$. In the first case, the velocity of the shell decreases positively while increases negatively in the second case. We also see that velocity of charged shell is less than the uncharged in both cases and both curves match for the large radius.

3.1 Dynamics of Scalar Shell

In this section, we study the dynamics of thin-shell with the scalar field. For this purpose, we obtain the energy-momentum tensor for the scalar field by applying a transformation on Eq.(9) given as [15]

$$u_\mu = \frac{\varphi_{,\mu}}{\sqrt{\varphi_{,\nu}\varphi^{,\nu}}}, \quad \rho = \frac{1}{2}[\varphi_{,\nu}\varphi^{,\nu} + 2V(\varphi)],$$
$$p = \frac{1}{2}[\varphi_{,\nu}\varphi^{,\nu} - 2V(\varphi)], \quad (21)$$

where $V(\varphi) = m^2\varphi^2$ is the potential term representing a massive scalar field. In the absence of this term, the scalar field will become massless. From Eqs.(9) and (21), the energy-momentum tensor for the scalar field can be written as

$$S_{\mu\nu} = \nabla_\mu\varphi\nabla_\nu\varphi - \gamma_{\mu\nu}[\frac{1}{2}(\nabla\varphi)^2 - V(\varphi)]. \quad (22)$$

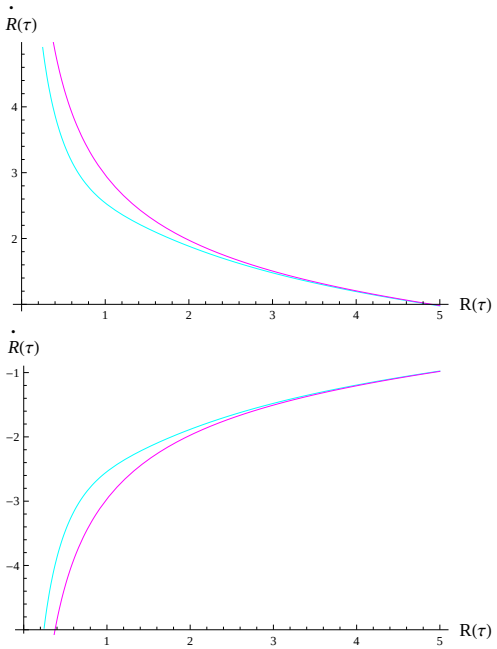

Fig. 1 Plots of $\dot{R}(\tau)$ versus R for Hayward BH

Since the induced metric is a function of τ only, so φ also depends on τ. Thus Eq.(21) takes the form

$$\rho = \frac{1}{2}[\dot{\varphi}^2 + 2V(\varphi)], \quad p = \frac{1}{2}[\dot{\varphi}^2 - 2V(\varphi)]. \quad (23)$$

The total mass of the scalar shell can be written as

$$m = 2\pi R^2[\dot{\varphi} + 2V(\varphi)]. \quad (24)$$

Inserting Eqs.(23) and (24) in (14), we obtain

$$\ddot{\varphi} + \frac{2\dot{R}}{R}\dot{\varphi} + \frac{\partial V}{\partial\varphi} = 0, \quad (25)$$

which is the Klien-Gordon (KG) equation, $\varphi + \frac{\partial V}{\partial\varphi} = 0$, written in shell's coordinate system.

The effective potentials for the Hayward BH in terms of scalar field are obtained as

$$V_{eff}(R) = 1 - \left(\frac{2R^3}{R^3+2e^2}\right)^2 \left(\frac{M_+ - M_-}{2\pi R^2(\dot{\varphi} + 2V(\varphi))}\right)^2 - \frac{(M_+ + M_-)R^2}{(R^3+2e^2)} - [\pi R(\dot{\varphi} + 2V(\varphi))]^2. \quad (26)$$

Now we solve Eqs.(17) and (25) with the help of Eq.(26). These equations cannot be solved analytically, so we solve them numerically, assuming $M_- = 0$, $M_+ = 1$, $R_0 = \rho_0 = \check{k} = 1$, $e = 1$ and $m = 1$ which are shown in Figure **2**. Left graph describes solutions of the KG equation (17). The upper curves represent collapsing while the lower curves show the expanding scalar shell. The scalar field density is increasing in the first case (collapse) while it decays to zero as time increases in the second case (expansion). Right graph shows the behavior of shell's radius is represented where the upper

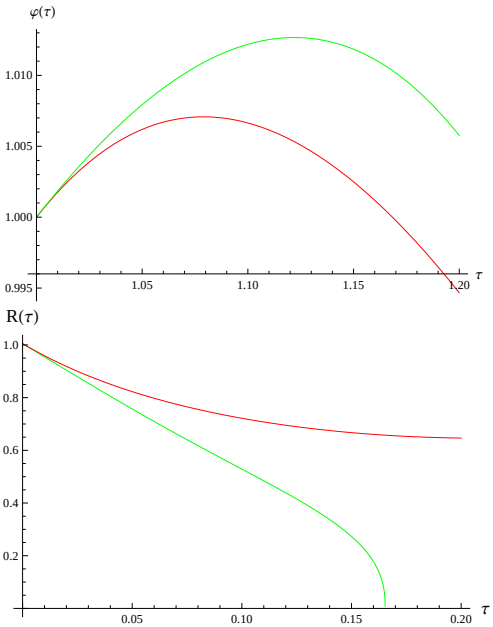

Fig. 2 Plots of the scalar field (left) and shell's radius (right). Green and red curves correspond to collapse and expansion

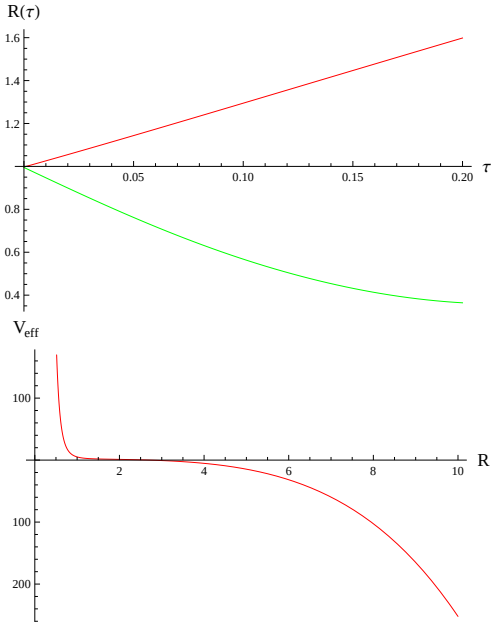

Fig. 3 Behavior of radius (left) and V_{eff} versus R for the massless case (right) for fixed M_- and M_+.

and lower curves represent the expanding and collapsing shell which describe the motion of the shell. The upper curves indicate that the shell expands endlessly and the lower curve shows that the radius is decreasing continuously.

3.1.1 Massless Scalar Shell

Here we investigate dynamics of the shell in the absence of $V(\varphi)$, i.e., the massless scalar field. In this case, KG equation becomes $\ddot{\varphi} + \frac{2\dot{R}}{R}\dot{\varphi} = 0$, and its integration leads to $\dot{\varphi} = \frac{\lambda}{R^2}$, where λ is an integration constant. The corresponding equations of motion become

$$\dot{R}^2 + 1 - \left(\frac{2R^5}{R^3+2e^2}\right)^2 \left(\frac{M_+ - M_-}{2\pi\lambda^2}\right)^2 - \frac{(M_+ + M_-)R^2}{R^3+2e^2} - \left(\frac{\pi\lambda^2}{R^3}\right)^2 = 0. \tag{27}$$

This can be simplified by using the parameters

$$[M] = M_+ - M_-, \quad \bar{M} = \frac{M_+ + M_-}{2}. \tag{28}$$

Inserting these parameters in above equation, we have

$$\dot{R}^2 + V_{eff} = 0, \tag{29}$$

where

$$V_{eff}(R) = 1 - \left(\frac{2R^5}{R^3+2e^2}\right)^2 \left(\frac{[M]}{2\pi\lambda^2}\right)^2 - \frac{(2\bar{M})R^2}{R^3+2e^2} - \left(\frac{\pi\lambda^2}{R^3}\right)^2. \tag{30}$$

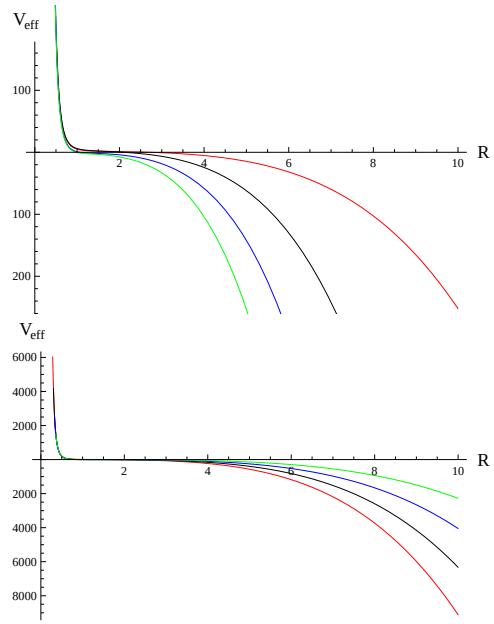

Fig. 4 Behavior of V_{eff} of the massless shell by varying M_+ (left), M_- (right)

In Figures **3**-**5**, we examine numerical results for the massless scalar field using $M_- = 0$, $M_+ = 1$, R_0, $e = 1$ and $\lambda = 1$. In Figure **3** left graph shows that increasing and decreasing shell radius lead to expansion and collapse, respectively. The behavior of the effective potential is presented in the right graph which is divided into two regions. The upper region has a positive potential that leads to expansion. There is a turning (saddle) point where $V_{eff} = 0$, the shell stops for a while and

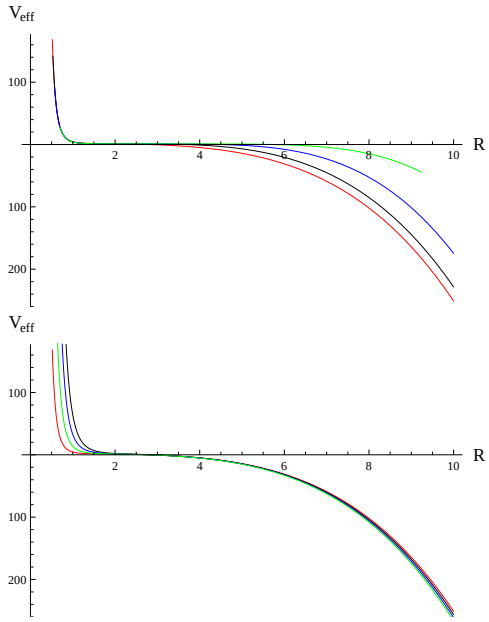

Fig. 5 Behavior of V_{eff} of the massless shell by varying e (left) and λ (right)

then changes its behavior at $R \approx 4$. The effective potential decreases infinitely after these points and becomes negative. This suggests that for large values of R the shell begins to contract continuously. Figures **4** describe behavior of the effective potential by varying M_+ and M_-. The saddle point ($V_{eff} = 0$) separates shell's motion into two regions: the upper (positive) and lower (negative) regions describe expansion and contraction of the shell, respectively. Figures **5** represents the behavior of effective potential by varying charge and λ. Again, the shell depicts three types of motion, expands in the upper region ($V_{eff} > 0$), in equilibrium position ($V_{eff} = 0$) and in the lower region the effective potential diverges negatively which leads the shell to collapse.

3.1.2 Massive Scalar Shell

Here we discuss the case when the thin-shell is composed of a massive scalar field with scalar potential. From Eq.(23), we obtain

$$\dot{\varphi}^2 = \rho + p, \quad V(\varphi) = \frac{1}{2}(p - \rho). \tag{31}$$

We take p as an explicit function of R, i.e., $p = p_0 e^{-\check{k}R}$, where $\check{k}$ and p_0 are constants. Using the value of p in Eq.(13), we find

$$\rho = \frac{\zeta}{R^2} + \frac{2(1+\check{k}R)p_0 e^{-\check{k}R}}{\check{k}^2 R^2}, \tag{32}$$

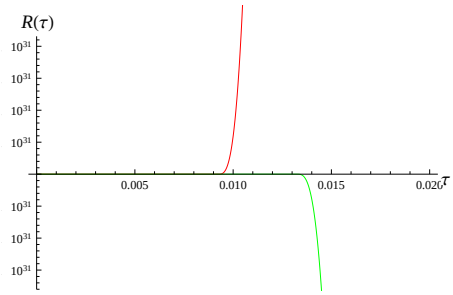

Fig. 6 Plots of the shell radius in massive scalar field.

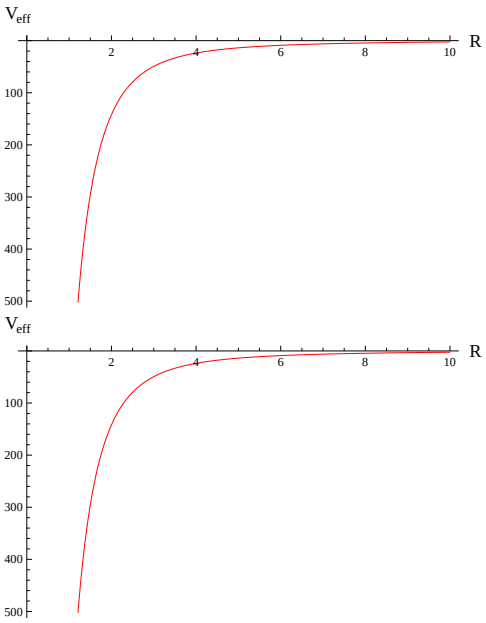

Fig. 7 Behavior of V_{eff} of a massive scalar shell for fixed e (left) and by varying e (right).

where ζ is the constant of integration. Inserting the values of p and ρ in Eq.(31), we obtain

$$V(\varphi) = \frac{\zeta}{2R^2} - \frac{p_0 e^{-\check{k}R}}{2}\left(1 - \frac{2(1+\check{k}R)}{\check{k}^2 R^2}\right), \tag{33}$$

$$\dot{\varphi}^2 = \frac{\zeta}{R^2} + p_0 e^{-\check{k}R}\left(1 + \frac{2(1+\check{k}R)}{\check{k}^2 R^2}\right), \tag{34}$$

which satisfy the KG equation. Using Eqs.(32)-(34) in (26), it follows that

$$V_{eff}(R) = 1 - \left(\frac{2R^3}{R^3+2e^2}\right)^2 \left(\frac{M_+ - M_-}{m}\right)^2 - \frac{(M_+ + M_-)R^2}{(R^3+2e^2)} - \left(\frac{m}{2R}\right)^2, \tag{35}$$

where

$$m = 4\pi R^2 \rho \equiv 4\pi\zeta + \frac{8\pi p_0 e^{-\check{k}R}}{\check{k}^2}(1+\check{k}R). \tag{36}$$

Figures **6** and 7 show the behavior of thin-shell for the massive scalar field for $M_- = 0$, $M_+ = 1$,

$R_0 = p_0 = \check{k} = 1$, $e = 1$ and $\zeta = 3$. Figure **6** describes the nature of the shell radius for the massive scalar field. The upper curve corresponds to constant motion which leads to expansion of the shell with the increasing time. The lower curve follows the same initial configuration leading the shell to collapse. Figures **7** illustrate the behavior of effective potential for the massive scalar field with fixed mass and varying the charge parameter. The effective potential diverges for the initial data. This negative effective potential indicates that the gravitational forces lead the shell to collapse. In the right graph, the effective potential is plotted for different values of charge parameter which shows that the shell collapses for all values of charge.

4 Final Remarks

In this paper, we have examined the dynamics of spherically symmetric scalar thin-shell (both massless and massive scalar fields) by taking Hayward BH for the interior as well as exterior regions. The equation of motion (17) and the KG equation (25) can completely describe the dynamical behavior of the shell. We have discussed solutions of these equations graphically shown in Figures **1** and **2** which represent both collapse and expansion of the shell. It is found that the scalar field increases for the case of collapse while for expansion it shows decreasing behavior for all BHs.

In massless case, the increase or decrease in shell's radius along the proper time represents that the shell expands continuously or collapses. The motion of the shell is determined by the effective potential where the shell is partitioned into two regions by a saddle point ($V_{eff} = 0$) which expands forever in the region $V_{eff} > 0$ while the region with $V_{eff} < 0$ indicates the collapsing shell. For massive scalar field, the behavior of the shell radius shows that it either expands forever or undergoes collapse. The effective potential is always negative for the fixed mass (interior and exterior) with different values of e. These results indicate that the massive scalar shell always collapse to zero size for the considered parameters. We conclude that there are three possibilities in the dynamical evolution of the scalar thin-shell: continuous expansion ($V_{eff} > 0$), stable configuration ($V_{eff} = 0$) and gravitational collapse ($V_{eff} < 0$).

References

1. J.A. Wheeler, Geons, Phys. Rev., **97**, 511 (1955).
2. D.R. Brill and J.A. Wheeler, Interaction of Neutrinos and Gravitational Fields, Phys. Rev., **29**, 465 (1957).
3. J. Frederick and Jr. Ernst, Variational Calculations in Geon Theory, Phys. Rev., **105**, 1662 (1957).
4. O. Bergmann and R. Leipnik, Space-Time Structure of a Static Spherically Symmetric Scalar Field, Phys. Rev., **107**, 1157 (1957).
5. D. Christodoulou, The formation of black holes and singularities in spherically symmetric gravitational collapse, Commun. Pure Appl. Math., **44** 339 (1991).
6. , M.W. Choptuik, Universality and scaling in gravitational collapse of a massless scalar field, Phys. Rev. Lett., **70**, 9 (1993).
7. J.E. Chase, Gravitational instability and collapse of charged fluid shells, Nuovo Cimento B, **67**, 136 (1970).
8. D.G. Boulware, Naked Singularities, Thin Shells and the Reissner-Nordstrm Metric, Phys. Rev. D, **8**, 2363 (1973).
9. C. Barrabès and W. Israel, Thin shells in general relativity and cosmology: The lightlike limit , Phys. Rev. D, **43**, 1129 (1991).
10. D. N*úñ*ez, Oscillating shells: A Model for a variable cosmic object, Astrophys J., **482**, 963 (1997).
11. S.M.C.V. Goncalves, Relativistic shells: Dynamics, horizons, and shell crossing, Phys. Rev. D, **66**, 084021 (2002).
12. M. Sharif and G. Abbas, Expanding and Collapsing Scalar Field Thin Shell, Gen. Relativ. Gravit., **44**, 2353 (2012).
13. S.A. Hayward, Formation and evaporation of nonsingular black holes, Phys. Rev. Lett., **96**, 031103 (2006).
14. W. Israel, Singular hypersurfaces and thin shells in general relativity, Nuovo Cimento B **44**, 1 (1966).
15. D. N*úñ*ez, H. Quevedo and M. Salgado, Dynamics of a spherically symmetric scalar shell, Phys. Rev. D, **58**, 083506 (1998).

Proc. Int. Conf. Relativ. Astrophys.
Pages 95-98, (2015)

Neutral Particle Dynamics Around a Kerr and a Kiselev Black Hole

Mubasher Jamil [a,1]

[1]School of Natural Sciences (SNS), National University of Sciences and Technology (NUST), H-12, Islamabad, Pakistan

Abstract The dynamics of a neutral particle moving around a slowly rotating Kerr black hole and a Schwarzschild like black hole. We are interested to explore the conditions under which the charged particle can escape from the gravitational field of the black hole after colliding with another particle. The escape velocity of the particle in the innermost stable circular orbit is calculated.

Keywords Black hole · Escape velocity · Kerr geometry

1 Introduction

The dynamics of particles (wether massive or massless, charged or neutral) around compact objects such as a black hole is among the most important theoretical problems of black hole astrophysics. These studies not only help us to understand the geometrical structure of spacetimes but also shed light on the high energy phenomenon occurring near the black hole such as formation of jets (which involve particles to escape) and accretion disks (particles orbiting in circular orbits).

A rotating black hole (i.e. a Kerr black hole) may provide sufficient energy to the particle moving around it due to which the particle may escape to spatial infinity. This physical effect appears to play a crucial role in the ejection of high energy particles from accretion disks around black holes. In the process of ejection of high energy particles, besides the rotation of black hole, the magnetic field plays an important role [1,2].

In the present article, it is considered that a particle is orbiting in the innermost stable circular orbit (ISCO) of a black hole and is suddenly hit by a radially incoming neutral particle. The aftermath of collision will depend on the energy of the incoming particle which may result one of the three possible outcomes: charged particle may escape to infinity; being captured by the black hole or keep orbiting in ISCO. For simplicity we consider the motion in the equatorial plane only.

[a]e-mail: mjamil@sns.nust.edu.pk

2 Particle Dynamics Around a Slowly Rotating Kerr Black Hole

We consider the slowly rotating black hole and neglect the terms involving a^2. The line element is given by

$$ds^2 = (1-\frac{r_g}{r})dt^2 + \frac{4aM\sin^2\theta}{r}d\phi dt - \frac{1}{1-\frac{r_g}{r}}dr^2 - r^2d\theta^2 - r^2\sin^2\theta d\phi^2.$$

Here $r_g = 2M$, is the gravitational radius of the slowly rotating Kerr black hole just like Schwarzschild black hole. Note that for a slowly rotating Kerr and Schwarzschild black hole the horizon occurs at $r = r_g$.

In terms of Lagrangian mechanics ($\mathcal{L} = g_{\mu\nu}\dot{x}^\mu\dot{x}^\nu$), the t and ϕ coordinates are cyclic which lead to two conserved quantities namely energy and angular momentum with the corresponding Noether symmetry generators

$$\xi_{(t)} = \xi^\mu_{(t)}\partial_\mu = \frac{\partial}{\partial t}, \qquad \xi_{(\phi)} = \xi^\mu_{(\phi)}\partial_\mu = \frac{\partial}{\partial\phi}. \tag{1}$$

This shows that the black hole metric is invariant under time translation and rotation around symmetry axis. The corresponding conserved quantities are the energy $\mathcal{E}$ per unit mass and azimuthal angular momentum L_z per unit mass

$$\dot{t} = \frac{r^3\mathcal{E} + aL_zr_g}{r^2(r-r_g)},$$
$$\dot{\phi} = \frac{1}{r^2}\left(\frac{ar_g\mathcal{E}}{(r-r_g)} + \frac{L_z}{\sin^2\theta}\right). \tag{2}$$

From the astrophysical perspective, it is known that particle orbits a rotating black hole in the equatorial plane [3]. Therefore we choose $\theta = \frac{\pi}{2}$ to get

$$\dot{t} = \frac{r^3\mathcal{E} + aL_z r_g}{r^2(r-r_g)},$$
$$\dot{\phi} = \frac{1}{r^2}\left(\frac{ar_g\mathcal{E}}{(r-r_g)} + L_z\right). \tag{3}$$

Using the normalization condition, $u^\mu u_\mu = 1$, we get the equation of motion

$$\dot{r}^2 = \frac{(\mathcal{E}r^2 - aL_z)^2}{r^4} - \frac{r^2 - r_g r}{r^4}(r^2 + L_z^2 - 2a\mathcal{E}L_z). \tag{4}$$

At the turning points $\dot{r} = 0$, the equation of motion yields

$$\mathcal{E} = \frac{aL_z r_g \pm \sqrt{r^5(r-r_g) + L_z^2(r^4 - r^3 r_g + a^2 r_g^2)}}{r^3}, \tag{5}$$

which gives $\mathcal{E} = V_{\text{eff}}$, as the effective potential. The condition $\dot{r} = 0$ is termed as the turning point because it gives the location at which an incoming particle turns around from the neighborhood of the gravitating source [4].

The particle moving in the ISCO has the angular momentum and the energy as follows:

$$L_{zo} = \pm\frac{\sqrt{r_g}\left(r_o \pm a\sqrt{\frac{2r_g}{r_o}}\right)}{\sqrt{2r_o - 3r_g \mp 2a\sqrt{\frac{2r_g}{r_o}}}}, \tag{6}$$

$$\mathcal{E}_o = \frac{1 - \frac{r_g}{r} \mp \frac{a}{r}\sqrt{\frac{r_g}{2r}}}{\sqrt{1 - \frac{3r_g}{2r} \mp \frac{a}{r}\sqrt{\frac{2r_g}{r}}}}. \tag{7}$$

After the collision particle should have new values of energy and momentum $\mathcal{E}$, L_z and the total angular momentum L^2. We simplify the problem by applying the following conditions (i) the azimuthal angular momentum is fixed (ii) initial radial velocity remains same after the collision. Under these conditions only energy of the particle can determine its motion. After collision particle acquires an escape velocity $(v_\perp)$ in orthogonal direction of the equatorial plane [5]. The square of total angular momentum of the particle after collision is given by

$$L^2 = r^4\dot{\theta}^2 + r^4\sin^2\theta\dot{\phi}^2. \tag{8}$$

which turns out to be

$$L^2 = r^2 v_\perp^2 + \sin^2\theta\left(\frac{ar_g\mathcal{E}_o}{r-r_g} + \frac{L_{zo}}{\sin^2\theta}\right)^2. \tag{9}$$

Here we denote $v \equiv -r\dot{\theta}_o$. The angular momentum and the energy of the particle after the collision becomes

$$L^2 = r_o^2 v_\perp^2 + \left(\frac{ar_g\mathcal{E}_o}{r_o - r_g} + L_{zo}\right)^2, \tag{10}$$

$$\mathcal{E}_{\text{new}} = \frac{aLr_g + \sqrt{r_o^5(r_o - r_g) + L^2(r_o^4 - r_o^3 r_g + a^2 r_g^2)}}{r_o^3}. \tag{11}$$

These values of angular momentum and energy are greater than their values before the collision.

Therefore particle escapes to infinity if $\mathcal{E}_{\text{new}} \geq 1$, or

$$v_\perp \geq \pm\frac{r(r_g - r)(L_z(r-r_g) + ar_g(\mathcal{E}_o - 1))}{r^2(r-r_g)^2} + \frac{\sqrt{r^2 r_g(r-r_g)^2(r^3 + r_g(a^2 - r^2 - 2a^2\mathcal{E}_o))}}{r^2(r-r_g)^2}. \tag{12}$$

Particle escape condition is $|v| \geq v_\perp$ i.e. the magnitude of velocity should be greater than any orthogonal velocity.

3 Dynamics of a Neutral Particle Around Kiselev Black Hole

Quintessence is defined as a scalar field coupled to gravity with the potential [6]. The solution for a spherically symmetric black hole surrounded by quintessence matter was derived by Kiselev [7]. It has the state parameter in the range $-1 < w_q < \frac{-1}{3}$. We consider a Schwarzschild-like black hole surrounded by quintessence matter. We start with the simpler case of calculating the escape velocity of a neutral particle. The geometry of static spherically symmetric black hole surrounded by the quintessence matter is given by [7]

$$ds^2 = f(r)dt^2 - \frac{1}{f(r)}dr^2 - r^2 d\theta^2 - r^2\sin^2\theta d\phi^2,$$
$$f(r) = 1 - \frac{2M}{r} - \frac{c}{r^{3w_q+1}}. \tag{13}$$

Here M is the mass of black hole, c is the quintessence parameter and we focus on $w_q = \frac{-2}{3}$. The last metric diverges when $r = 0$ which is a curvature singularity. For $f(r) = 0$ we get two values of r:

$$r_+ = \frac{1 + \sqrt{1 - 8Mc}}{2c}, \quad r_- = \frac{1 - \sqrt{1 - 8Mc}}{2c}. \tag{14}$$

The region $r = r_-$ corresponds to black hole horizon while $r = r_+$ represents the cosmological horizon. Therefore, r_- and r_+ are the two coordinate singularities in the metric. If $8Mc = 1$ then we get the degenerate solution for the spacetime at $r_\pm = \frac{1}{2c}$ and if $8Mc > 1$ then horizons do not exist. For very small

value of c, $r_+ \approx \frac{1}{c}$. Further more, we can say that the restriction on c, is $c \leq \frac{1}{8M}$.

We discuss the dynamics of a neutral particle in the Schwarzschild-like background. There are three constants of motion corresponding in which two of them arise as a result of two Killing vectors

$$\xi_{(t)} = \xi^{\mu}_{(t)} = \partial_t, \qquad \xi_{(\phi)} = \xi^{\mu}_{(\phi)} = \partial_\phi. \tag{15}$$

where $\xi^{\mu}_{t} = (1,0,0,0)$ and $\xi^{\mu}_{\phi} = (0,0,0,1)$. The corresponding conserved quantities (conjugate momenta) are the energy per unit mass $\mathcal{E}$ and azimuthal angular momentum per unit mass L_z, respectively given by

$$\mathcal{E} \equiv f(r)\dot{t}, \tag{16}$$

$$-L_z \equiv \dot{\phi} r^2 \sin^2\theta. \tag{17}$$

Here over dot represents differentiation with respect to proper time τ. The third constant of motion is the total angular momentum of black hole comprising the black hole and particle's angular momentum, i.e.

$$L^2 = r^4\dot{\theta}^2 + \frac{L_z^2}{\sin^2\theta} = r^2 v_\perp^2 + \frac{L_z^2}{\sin^2\theta}. \tag{18}$$

Here we denote $v_\perp \equiv -r\dot{\theta}_o$. By using the normalization condition of 4-velocity $u^\mu u_\mu = 1$ and constants of motion, we get the equation of motion of neutral particle

$$\dot{r}^2 = \mathcal{E}^2 - (1 + \frac{L_z^2}{r^2\sin^2\theta}) f(r). \tag{19}$$

At the turning points of the moving particles from the trajectories $\dot{r} = 0$, hence we get

$$\mathcal{E}^2 = (1 + \frac{L_z}{r^2\sin^2\theta}) f(r) \equiv U_{\text{eff}}, \tag{20}$$

where U_{eff} is the effective potential.

Consider a particle in the circular orbit $r = r_o$, where r_o is the local minima of the effective potential. This orbit exists for $r_o \in (4M, \infty)$. Generally for non-degenerate case ($r_+ \neq r_-$) the energy and azimuthal angular momentum corresponding to local minima r_o are

$$L_{zo} = \frac{\sqrt{cr_o^2 - 2M}}{\sqrt{c + \frac{6M-2r_o}{r_o^2}}}, \tag{21}$$

$$\mathcal{E}_o = \frac{2\big(2M + r_o(cr_o - 1)\big)^2}{r_o\big(6M + r_o(cr_o - 2)\big)}. \tag{22}$$

For the degenerate case which is defined by $c = \frac{1}{8M}$ or $r_+ = r_-$. The energy and azimuthal angular momentum corresponding to r_o are

$$L_{zo} = \frac{\sqrt{\frac{r_o^2}{8M} - 2M}}{\sqrt{\frac{1}{8M} + \frac{6M-2r_o}{r_o^2}}}, \tag{23}$$

$$\mathcal{E}_o = \frac{2\big(2M + r_o(\frac{r_o}{8M} - 1)\big)^2}{r_o\big(6M + r_o(\frac{r_o}{8M} - 2)\big)}. \tag{24}$$

The ISCO is defined by $r_o = 4M$ which is the convolution point of the effective potential.

After collision the total angular momentum and energy of the particle become (at $\theta = \frac{\pi}{2}$)

$$L^2 = r_o^2 v_\perp^2 + L_z^2, \tag{25}$$

$$\mathcal{E} = \left[f(r)\left(1 + \frac{(L_z + r v_\perp)^2}{r^2}\right)\right]^{\frac{1}{2}}. \tag{26}$$

These new values of angular momentum and energy are greater from their values before collision because during collision colliding particle may impart some of its energy to the orbiting particle. The last equation yields the condition on the escape velocity for the particle from the vicinity of the black hole:

$$v_\perp^{\text{esc}} \geq \frac{L_z r(r - 2M - cr^2)}{r^2(2M + r(cr-1))} + \frac{\sqrt{r^4(r(1-cr) - 2M)(2M + r(cr + \mathcal{E}^2 - 1))}}{r^2(2M + r(cr-1))}, \tag{27}$$

particle would escape if $|v_\perp^{\text{esc}}| \geq v_\perp$.

4 Conclusion

We have briefly discussed the dynamics of neutral particles in two different gravitational backgrounds namely, a slowly rotating Kerr spacetime and the Kiselev spacetime. The analysis was performed using the symmetries of the spacetime, conserved quantities and then analyzing equations of motion. The later yields the conditions on the escape velocity of the particle from the vicinity of the black hole. Although studies dealing with single particle dynamics around black holes have some benefits, however it can not be used to predict the dynamics of particles in more complicated situations such as an accretion disk or an astrophysical jet. There one needs to employ relativistic magnetohydrodynamical equations to obtain realistic model for particle or fluid motion. Further details related to presented study can be seen in [9,10]

Acknowledgment

I would like to thank the warm hospitality of Department of Mathematics, University of the Punjab, Lahore where this work was presented during the conference entitled "International Conference on Relativistic Astrophysics".

References

1. S. Koide, K. Shibata, T. Kudoh, D. l. Meier, Science **295**, 1688(2002).
2. S. Kide, Phys. Rev. D **67**, 104010 (2003).
3. S. Chakrabarti, *The Sun, The Stars, The Universe and General Relativity* edited by R. Ruffini and G. Vereshchagin (AIP 2010).
4. A. Qadir, A.A. Siddiqui, Int. J. Mod. Phys. D 16, 25 (2007).
5. B. Punsly, Black Hole Gravitohydrodynamics (Springer-Verlag, Berlin, 2001).
6. E. J. Copeland, M. Sami and S. Tsujikawa, Int. J. Mod. Phys. **D 15** 1753 (2006).
7. V. V. Kiselev, Class. Quan. Grav. **20** 1187 (2003).
8. C. V. Borm, M. Spaans, Astron, Astrophy, **553**, L9 (2013).
9. M. Jamil, S. Hussain, B. Majeed, Eur. Phys. J. C **75**, 24 (2015).
10. S. Hussain, I. Hussain, M. Jamil, Eur. Phys. J. C **74**, 3210 (2014).

Proc. Int. Conf. Relativ. Astrophys.
Pages 99-103, (2015)

Gravitational Wave Detection from Space with eLISA

Philippe Jetzer [a,1]

[1]Department of Physics, University of Zürich,
Winterthurerstrasse 190, CH-8057 Zürich, Switzerland

Abstract eLISA (evolved Laser Interferometer Space Antenna) is a space-based mission designed to measure gravitational waves over a broad band of frequencies ranging from $\sim$ 0.1 mHz to $\sim$ 1 Hz. Possible sources are a variety of systems and events throughout the Universe, including the coalescences of massive black holes brought together by galaxy mergers; the inspirals of stellar-mass black holes and compact stars into central galactic black holes; several millions of ultracompact binaries, both detached and mass transferring, in the Galaxy; and possibly unforeseen sources such as the relic gravitational-wave radiation from the early Universe. eLISA's high signal-to-noise measurements will provide new insight into the structure and history of the Universe, and it will test general relativity in its strong-field dynamical regime.

Keywords Gravitational waves · Black holes · eLISA

1 Introduction

The proposal "The gravitational Universe" for a space mission dedicated to the detection of gravitational waves based on the eLISA concept has been selected in November 2013 as a science theme of the European Space Agency (ESA), which is foreseen to be implemented as the L3 mission in the framework of ESA's Cosmic Vision Programme [1]. eLISA will survey the low-frequency gravitational-wave sky (from 0.1 mHz to 1 Hz). The basic principle of gravitational wave detection for eLISA is based on a laser interferometer designed to detect the passage of a gravitational wave by measuring the time varying changes of optical path length between free-falling test masses. The two measurement arms are defined by three spacecraft orbiting the Sun in a triangular configuration (see Figs. 1 and 2). A key feature of the eLISA concept is that the test masses are protected from disturbances as much as possible by a careful design and the "drag-free" operation. Several of the needed technologies, in particular the drag-free operation will be tested in space with the satellite LISA-Pathfinder (Fig. 3), which is scheduled to be launched in fall 2015. LISA-Pathfinder is a ESA mission with a contribution from NASA [2,3]. For more details on eLISA and LISA Pathfinder we refer to the homepage: https://www.elisascience.org as well as to [4,5].

According to General Relativity, black holes and compact binaries are expected to be powerful sources of gravitational waves. Rather than seeing electromagnetic radiation, as all of astronomy has done until present, eLISA will hear the vibrations of the fabric of spacetime itself, emitted coherently by macroscopic bodies. Studying these signals will convey rich new information about the behaviour, the structure and the history of the Universe, and it will clarify several issues in fundamental physics.

Gravitational waves travel undisturbed through spacetime, and when observed they will be a new and uniquely powerful way to probe the very distant Universe, from the extremely early Big Bang to the early epoch of galaxy and black hole seed formation. This may allow us to address deep questions such as: what powered the Big Bang; how did galaxies and their black holes form and evolve; what is the structure of spacetime around the massive objects we believe to be black holes; what is the nature of the mysterious dark matter and dark energy accelerating the expansion of the Universe. In the frequency band covered by eLISA the Universe is richly populated by strong sources of gravitational waves. For binary systems the characteristic gravitational-wave frequency f is twice the Keplerian

[a]e-mail: jetzer@physik.uzh.ch

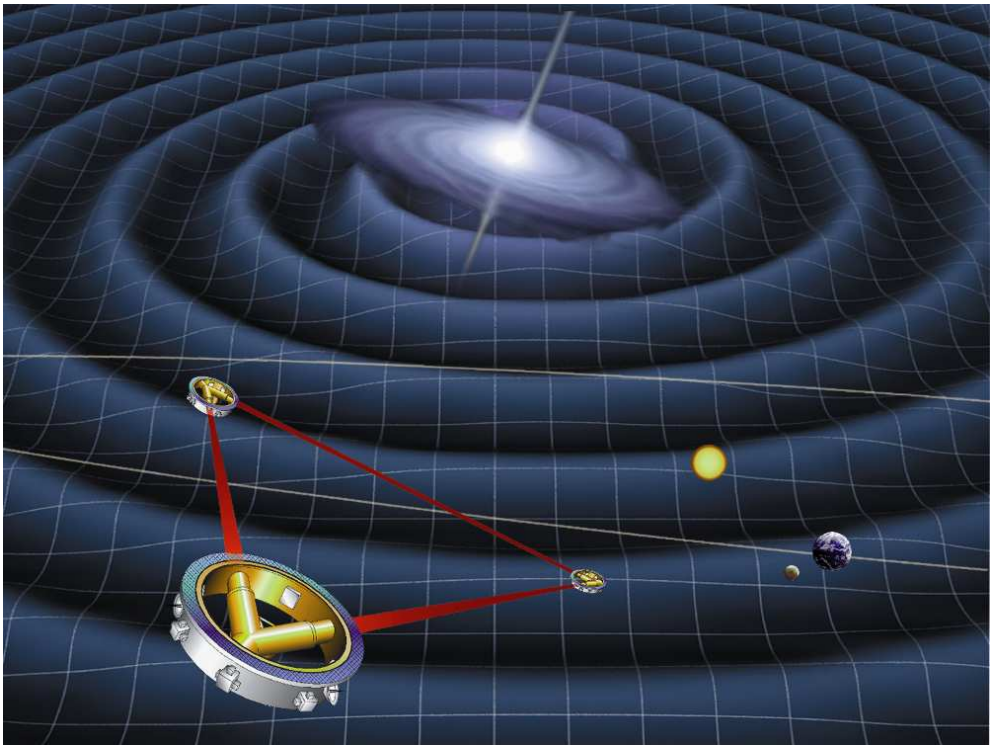

Fig. 1 The eLISA orbit: The constellation is shown trailing the Earth by about 20 degrees and is inclined by 60 degrees with respect to the ecliptic. The trailing angle will vary over the course of the mission duration from 10 to about 25 degrees. The separation between the spacecrafts is $L = 10^9$ m (from [5]).

orbital frequency, which in turn is proportional to $(M/a^3)^{1/2}$, where M is the total mass of the binary and a its semi-major axis. In the eLISA frequency band, gravitational waves are produced by close binaries of stellar-mass objects with orbital periods of a few to several minutes. Massive black hole binaries with $M \sim 10^4 M_\odot - 10^7 M_\odot$ and mass ratio $0.01 \leq q \leq 1$ on the verge of coalescing have orbital frequencies sweeping to higher and higher values, until the binary separation a becomes as small as the scale of the event horizon GM/c^2. Finally, eLISA could observe binaries comprising a massive black hole and a stellar-mass compact object (e.g., a stellar-mass black hole) skimming the horizon of the larger black hole before being captured: these systems are commonly referred to as extreme mass ratio inspirals (EMRIs). Furthermore, a stochastic background in the eLISA frequency band can be generated by less conventional sources, such as phase transition in the very early Universe.

2 Description of the mission

eLISA is based on a laser interferometer designed to detect the passage of a gravitational wave by measuring the time-varying changes of optical pathlength between free-falling masses. The measurement arms are defined by three spacecraft orbiting the Sun in a triangular configuration (Figs. 1 and 2). A key feature of the eLISA concept is a set of three orbits that maintain a near-equilateral triangular formation with an armlength of about $L = 10^9$ m, which is achieved by putting the different spacecrafts on orbits whose orbital plane is tilted with respect to the ecliptic. Depending on the initial conditions of the spacecraft, the formation can be kept in an almost constant distance to the Earth or be allowed to slowly drift away to about 70×10^9 m, the outer limit for communication purposes.

The centre of the formation is in the ecliptic plane 1AU from the Sun and 20 degrees behind the Earth. The plane of the triangle is inclined by 60 degrees with respect to the ecliptic. These particular heliocentric orbits for the three spacecraft were chosen such that the triangular formation is maintained throughout the year, with the triangle appearing to rotate about the centre of the formation.

A very attractive feature of the eLISA orbits is the almost constant Sun-angle of 30 degrees with respect to the normal to the top of the spacecraft, thereby resulting in an extremely stable thermal environment, minimizing the thermal disturbances on the spacecraft.

The three satellites, separated by a distance of 1 million km, will form a high precision interferometer that

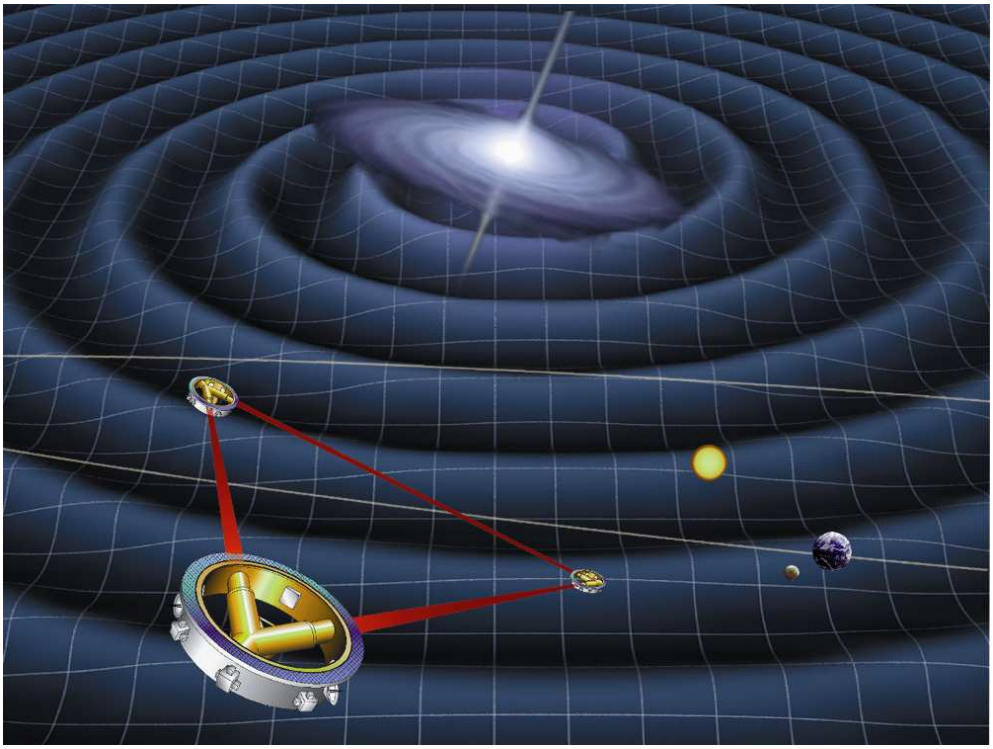

Fig. 2 Artistic view of eLISA triangular formation and its orbit around the Sun.

senses gravitational waves by monitoring the changes in distance between free falling test masses inside the spacecraft. The laser interferometer has thus an arm length of 1 million km. eLISA will coherently measure the stretching and squeezing of spacetime, including frequency, phase, and polarisation. Hence it will shed light on the origin of gravitational waves large-scale violent cosmic events and trace the motions of distant matter directly. Compared to the Earth-bound gravitational wave observatories like LIGO and VIRGO, eLISA addresses the much richer frequency range between 0.1 mHz and 1 Hz (Fig. 4), which is inaccessible on Earth due to armlength limitations and terrestrial gravity gradient noise.

3 Scientific goals of the mission

eLISA observations will probe massive black holes over a very wide range of redshift, covering essentially all important epochs in their evolutionary history. eLISA will offer a unique new way to address a number of unanswered questions: When did the first black holes form in pre-galactic haloes? What is their initial mass and spin? What is the mechanism of black hole formation in galactic nuclei? How do black holes evolve over cosmic time due to accretion and mergers? What can we learn about galaxy hierarchical assembly?

To answer these questions eLISA will discover the first black hole seeds out to redshifts of order 20, in the cosmic dark ages before reionisation, and determine their masses and spins, using gravity alone. eLISA will also study the evolution of massive black holes by tracking their merger history during cosmic dawn and high noon. To this end, it is important to precisely measure their mass, spin and redshift over a wide, yet unexplored range [6,7].

Intermediate massive black holes with masses in the interval between 10^4 $M_\odot$ and 10^7 $M_\odot$ will be detected by eLISA, to explore for the first time the low-mass end of the massive black hole population, at cosmic times as early as $z \sim 10$.

eLISA will make it possible to survey the vast majority of all coalescing massive black hole binaries throughout the whole universe. This will expose an unseen population of objects which will potentially carry precious information about the black hole population as a whole. It will provide both the widest and deepest survey of the sky ever, since gravitational wave detectors are non-directional in nature, and operate as non-pointed and weakly directional full-sky monitors. The range of black hole redshifts and masses that will be explored is complementary to the space explored by electromagnetic observations.

eLISA will detect all binary black hole mergers even when the black holes are not active. With this unbi-

Fig. 3 LISA-Pathfinder at the top of the propulsion module which will bring it at the L1 point (first Sun-Earth Lagrange point).

ased and complete survey, it will be possible to investigate the link between the growing seed population with the rich population of active supermassive black holes evolving during cosmic dawn and high noon, probing the light end of the mass function at the largest redshifts. Black hole coalescence events will illuminate the physical processes of black hole formation and feeding. While the mass distribution carries information about the seeds, the spin distribution charts the properties of the accretion flows, whether they are chaotic or coherent. Gravitational wave observations alone will be able to distinguish between the different massive black hole formation and evolution scenarios.

By probing the dynamics of intrinsically dark, relic stars in the nearest environs of a massive black hole, eLISA will allow the deepest view of galactic nuclei. The

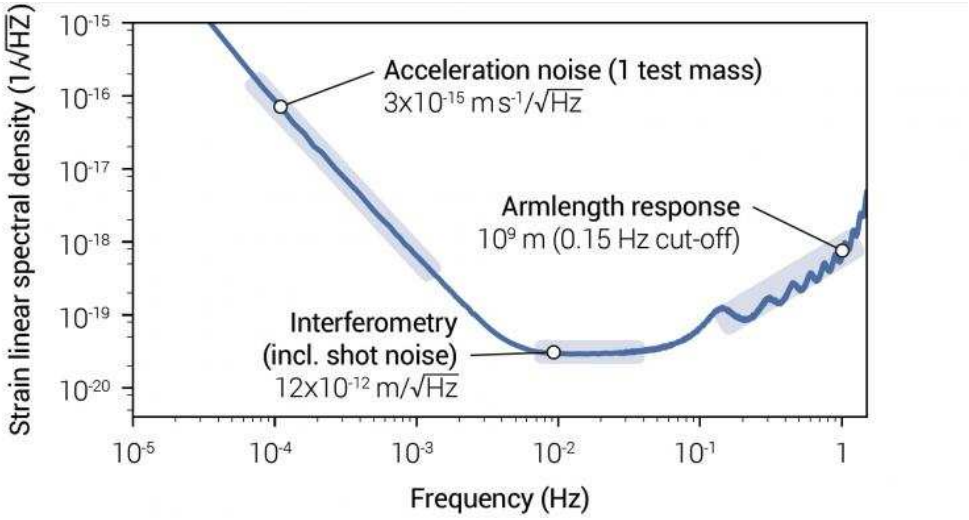

Fig. 4 Time, sky and polarisation averaged eLISA sensitivity (from [1]).

probes used are the so-called Extreme Mass Ratio Inspirals EMRIs: a compact star (either a neutron star or a stellar-mass black hole) captured into a highly relativistic orbit around the massive black hole and spiraling through the strongest field regions a few Schwarzschild radii from the event horizon before plunging into the massive black hole. As the compact star weighs much less than the massive black hole, the mass ratio is extreme, and as the star-black hole pair is a binary, the inspiral phase is governed by the emission of gravitational waves. eLISA will discover EMRI events, exploring the deepest regions of galactic nuclei, those near the horizons of black holes with masses close to the mass of the black hole at our Galactic Centre, out to redshifts as large as $z \sim 0.7$.

EMRIs are exquisite probes for testing stellar black hole populations in galactic nuclei. With eLISA we will learn about the mass spectrum of stellar-mass black holes, which is largely unconstrained both theoretically and observationally. The measurement of even a few EMRIs will give astrophysicists a totally new and different way of probing dense stellar systems, determining the mechanisms that govern stellar dynamics in the galactic nuclei.

4 Conclusions

General Relativity has passed all current tests in the weak field regime. eLISA will explore relativistic gravity in the strong field, non-linear regime, in a unique way not feasible by other methods [8,9]. Unlike the ground-based instruments, eLISA will have sufficient sensitivity to notice even small corrections to Einstein gravity. eLISA will map the spacetime around astrophysical black holes, yielding a battery of precision tests of General Relativity in an entirely new regime. These have the potential to uncover hints about the nature of quantum gravity, as well as enabling measurements of properties of the universe on the largest scales.

References

1. The eLISA Consortium: P. Amaro-Seoane et al., arXiv 1305.5720 (2013)
2. P. McNamara et al., ASP Conf. Ser **467** (2013) 5
3. F. Antonucci et al., Class. Quant. Grav. **29** (2012) 124014
4. P. Amaro-Seoane et al., Class. Quant. Grav. **29** (2012) 124016
5. P. Amaro-Seoane et al., GW Notes **6** (2013) 4-110
6. A. Klein, Ph. Jetzer and M. Sereno, Phys. Rev. **D80** (2009) 064027
7. L. De Vittori, A. Gopakumar, A. Gupta and Ph. Jetzer, Phys. Rev. **D90** (2014) 12, 124066
8. C. Huwyler, A. Klein and Ph. Jetzer, Phys. Rev. **D86** (2012) 0840028
9. C. Huwyler, E. Porter and Ph. Jetzer, Phys. Rev. **D91** (2015) 2, 024037

Proc. Int. Conf. Relativ. Astrophys.
Pages 110-121, (2015)

Developing Theoretical Relativistic Framework for Research in Open and Flexible Learning: A New Trend in Educational Research

Yousaf Khan[a,1]

[1]Department of Secondary Teacher Education, AIOU, Islamabad, Pakistan.

Abstract The purpose of research study was to develop a theoretical relativistic framework for research in open and flexible learning environment because it is a new dimension in the field of education. Developing a theoretical relativistic framework for any research study is first and prime step in walking on the track to reach the distinction set by the researcher. Open and flexible learning is a new trend in education, enriched with ICT-use as a basic demand of the 21st century generation in all parts of the globe. So, it requires a theoretical framework for its initiation, implementation, development and evaluation which is relatively developed and advanced from the existing framework. In any research study the literature review is carried out in order to develop, build or construct a theoretical framework. The researcher of the study has observed while attending the international conference on ODL (AAOU, 2013) that most of the studies require theoretical underpinning for ICT-use in education. The researcher assume that being a new trend in education to use ICT for teaching learning purposes; it requires conceptual clarity and theoretical background of the user and researcher, because, without theory the practice is wastage of money, time and energy and it becomes ineffective and requires relatively new conceptual development. So, the problem stated by the researcher for the study was: Developing theoretical relativistic framework for research in open and flexible learning: A new trend in educational research. The objective of the study was to integrate the interrelated concepts in order to build a pnemonological network for identifying the constructs in ICT-rich open and flexible learning environment. The study was significant because it provided theoretical background for conducting research in ICT-use in teaching and learning through open and flexible systems; whether it is blended or online learning and training. The methodology used by the researcher was qualitative and interpretive because there were reviewing of literature and meta-analysis for building the framework. The data were analyzed and interpreted by the researcher for the findings and drawing conclusions. On the basis of conclusions the researcher has made suggestions and recommendations for conducting further research in open and flexible learning environment by using this theoretical relativistic framework. The framework was named as Virtual Learning Environment Framework (VLEF).

Keywords Open and flexible learning, Research in ICT, Research in open and flexible learning and Pnemonological network in ODL and ICT.

1 Introduction: Virtual Learning Environment Framework (VLEF)

The framework developed by the researcher for the conference ICRA (2015) was based on the review of models, frameworks, theories, strategies and tools (interdisciplinary and cross disciplinary). The literature for reviewing was made available by ICT tools in open and flexible learning environment at the researcher life space (integrated study). The approach of the researcher was pragmatic and interdisciplinary as well as cross disciplinary in order to find a discipline that best suit to explain all the relevant and related concepts (pnomenalogical network) in the motion of a person towards the knowledge peak (wisdom) against the gravitational potential and to find competence in a discipline with the availability of scientific and psychological tools and vehicles or resources to reach to the peak of global knowledge (wisdom); so that his/her knowledge become virtual and global but at the same time measurable

[a]e-mail: uswat@hotmail.com

in the field of education (Figure:11). Knowledge development is relativistic in nature and it is develop iteratively. The researcher has found that the universe is material and a person (as a mass) is a part of it; and when the knowledge globe is iteratively developed, he/she also develops to move to the new step with incremental increase (change) in knowledge use through the help of tools (or resources) in a spiral manner (spiral framework of software development), using interaction in an instantaneous activity (small time) to provide experience for adaptation and development in a life space (Figure: 5). The researcher found that the person has both body and mind. The body is physical but the mind is psychological and dependent on thinking process. So, it requires measurement and evaluation of both qualitative and quantitative characteristics or variables of his knowledge in the globe for assessment and evaluation in the framework. The researcher found that the disciplines of physics and psychology has the capacity to explain these phenomena; because there is motion in developmental process towards wisdom (Figure:4 http://learning.pknursery.com/) and can be explained by the laws, theories and principles of physical sciences and personality development theories of psychology when we take the person as an energy system (Sigmund Freud theory of personally development). In this system, person (mass) is having a potential energy (P.E) and can be converted into kinetic energy (K.E) to make this system dynamically integrated but measurable and observable
(Figure:1 http://learning.pknursery.com/). So, the framework is used to develop the person's knowledge through the concepts of energy and motion to such an extent that the Einstein's theory of relatively ($E = mc^2$) and Quantum theory of mechanics (small energy) can be applied for incremental increase in his knowledge and comprehension (scaled agile framework of software development) and causes evolution (biological and psychological) frameworks. In this evolution the theory base is that of Charles Darwin, survival of the fittest and natural selection. Knowledge getting is a life-long and continuous process and ends when the life space is made fixed in grave (Islamic perspective and religious belief) while the spirit (soul) remains alive. It means that the person is moving from real knowledge (in a place) to virtual knowledge (in space) to make it global knowledge (Figures: 1 - 11 http://learning.pknursery.com/). This traveling is made possible by modern technological tools and social networking technologies and the progress is continuous and life-long which is the quest of Virtual Learning Environment Framework (VLEF) developed by the researcher in this study using interdisciplinary and cross disciplinary Critical Discourse Analysis (CDA) and vision in the field of education for open and flexible learning.

2 Basic Assumptions of VLEF:

The researcher has developed the following assumptions for the theoretical relativistic framework of open and flexible learning:
a) The person is in the knowledge globe and can be developed to the peak of this globe (wisdom) by using tools and technologies (toolkit) in open and flexible learning environment.
b) The person approaches and moves towards his/her destination with the help of tools (resources) and gadgets (devices) available due to scientific inventions and technological developments.
c) The person motion towards the knowledge field in the globe is interdisciplinary or contextualized (cross disciplinary).
d) The person motion towards the peak of knowledge (wisdom) is personalized (interpretive).
e) The person progress in the fields of knowledge is measurable and evaluated by using research tools of Critical Discourse Analysis (CDA) in a discursive practice (community of practice). Such as the conference ICRA (2015).
f) It requires incrementally developed software to evaluate researchers and their researches in open and flexible learning environment or education. (Relativistic knowledge).
g) The unit of analysis can be iteratively developed from real to virtual knowledge in a field to become philosophical and spiritual. (Knowledge in disciplines and discursive practice).
h) The person's knowledge can be measured by using scaled agile framework for software development in Pnemonological network. (To find the knowledge gap filled by the person).
i) A multi-dimensional framework is also needed for evaluating the total quality of open and flexible learning and education. (Interdisciplinary and cross disciplinary).

3 Objectives of using VLEF for Research:

a) In educational research the new approach is to evaluate the researcher when there is integration of ICT and education (interdisciplinary and cross disciplinary). The researcher must use an integrative framework developed through the modern scientific inventions for the development of education for all in a democratic, Open and Flexible Virtual Learning Environment (OFVLE)

a) Globalization of knowledge: Real and Virtual Framework (Fig. 1)

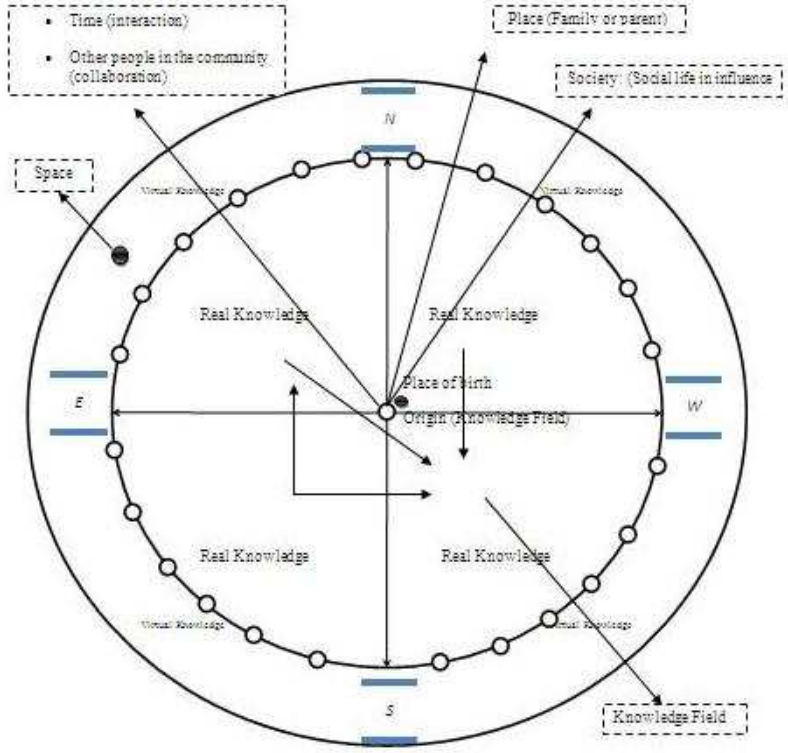

Fig.1: Globalization of Knowledge: Real and Virtual Knowledge

b) Physical science framework: (Fig. 2)

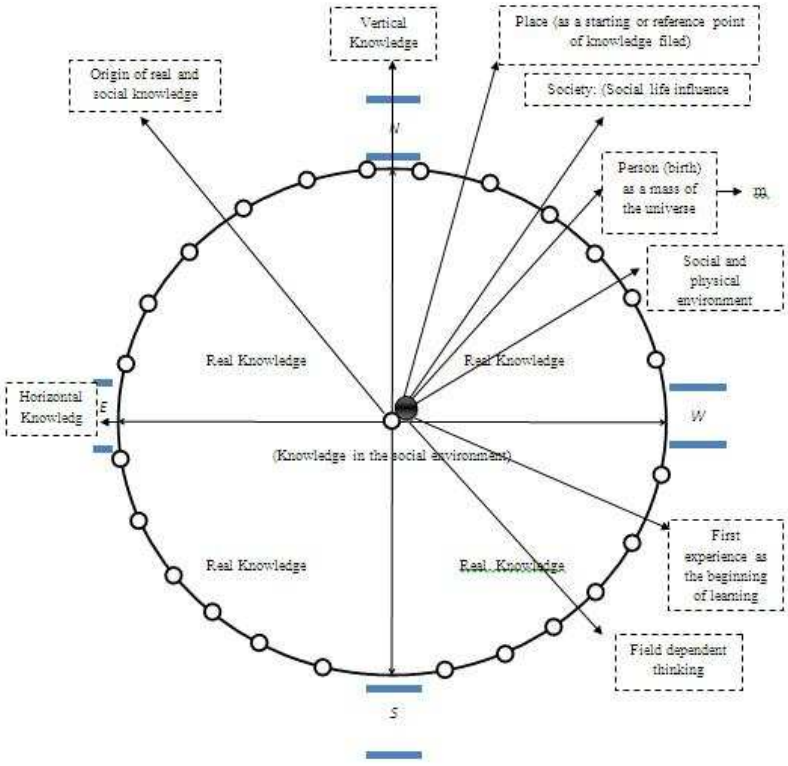

Fig.2: Physical science framework (Person or Mass) born in a place with potential to move in the Real knowledge field due to the influence of environmental forces: Push & Pull)

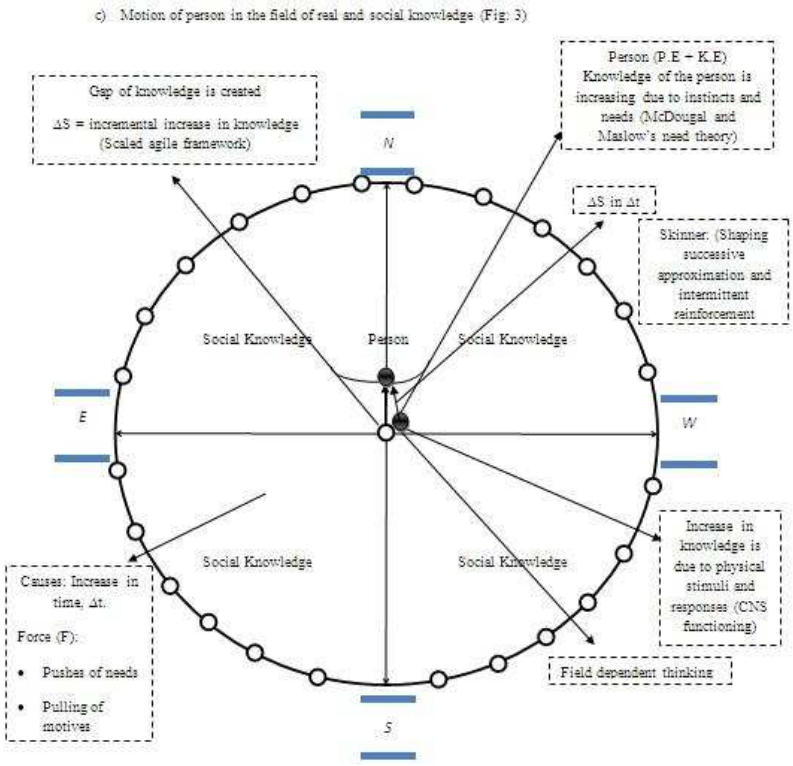

Fig.3: Motion of the person (as mass) in the field of knowledge from reference point or origin

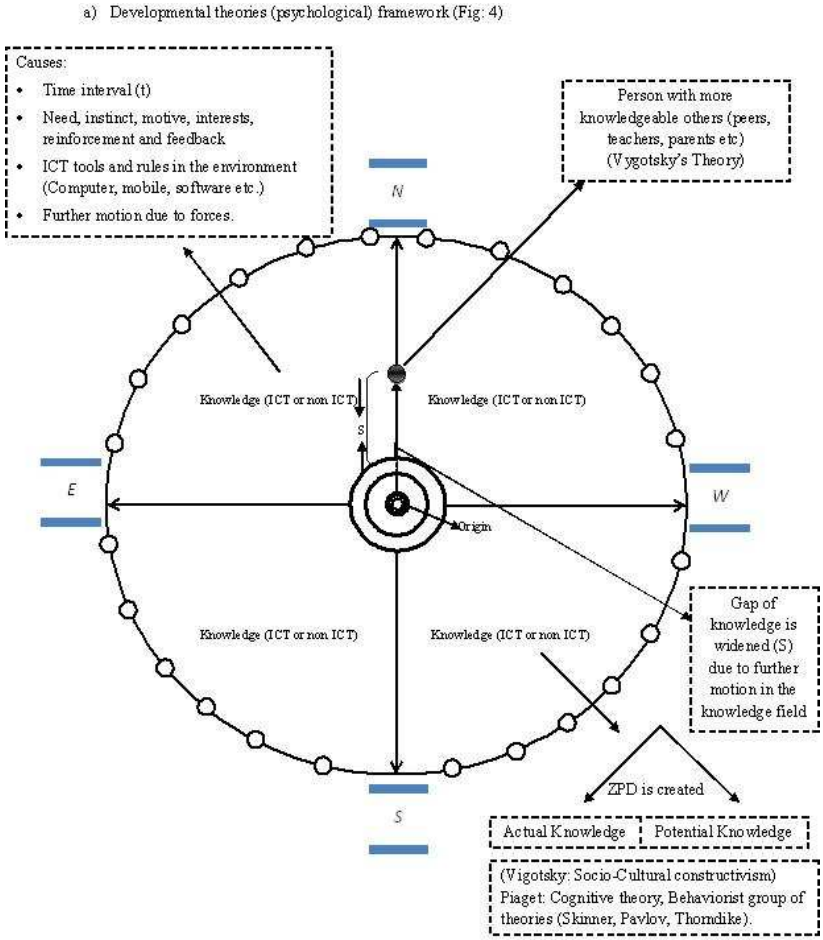

Fig.4: Developmental theories framework for physical development and learning

e) Activity system (Constructivist learning) framework (Fig: 5)

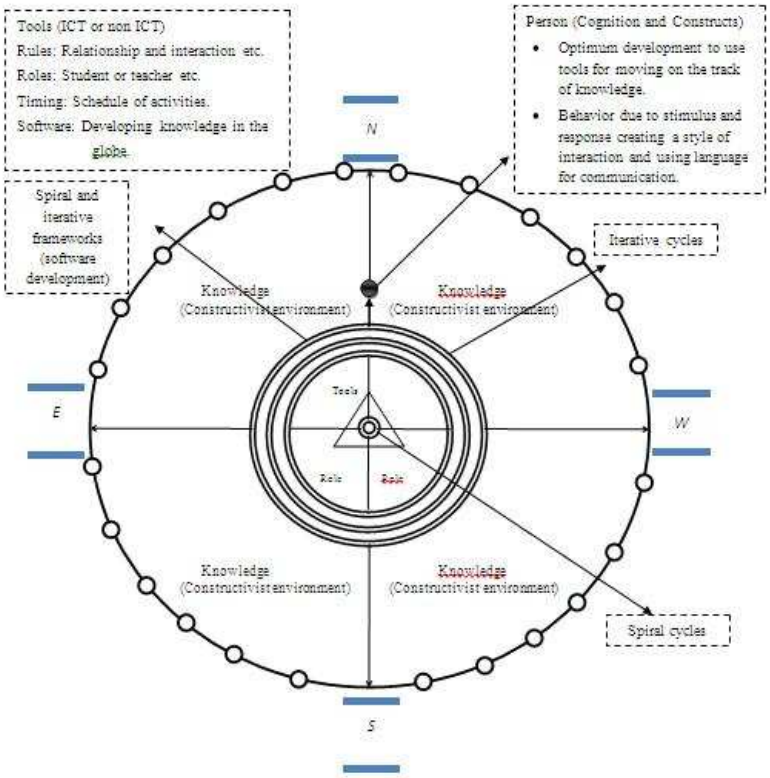

Fig.5: Activity system (constructivist learning) framework: Person utilizing tools (ICT or non ICT) for getting knowledge due to needs and motive with different styles (Open and flexible knowledge)..

f) Person-situation theory of construction of knowledge framework (Fig: 6)

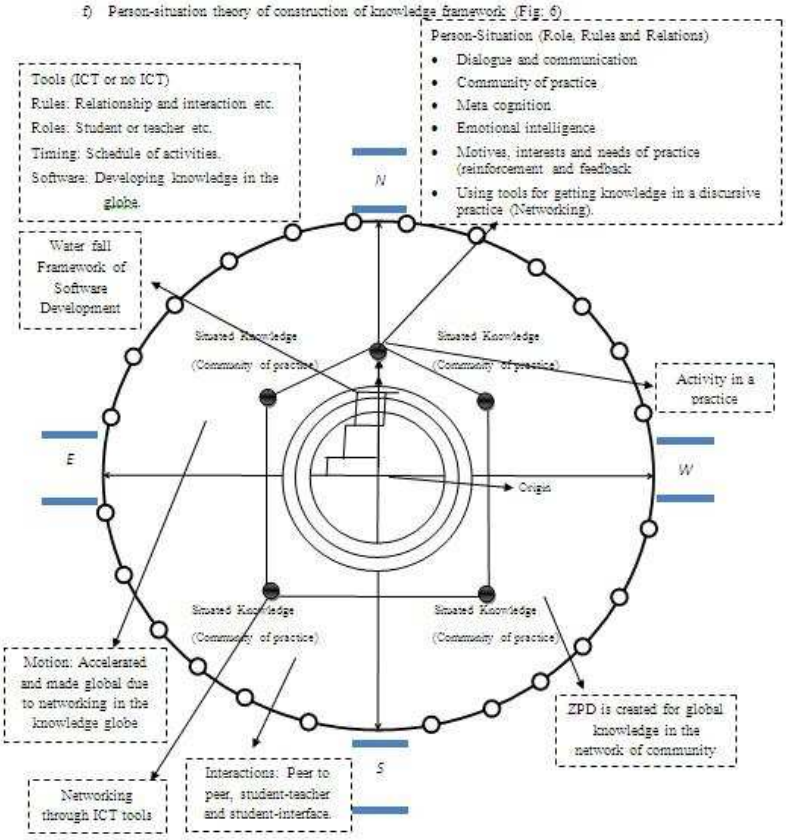

Fig.6: Person-situation theory of construction of knowledge:

- Person in discursive practices.
- Knowledge is directed in a practice
- Networking in community (social network for collaboration)

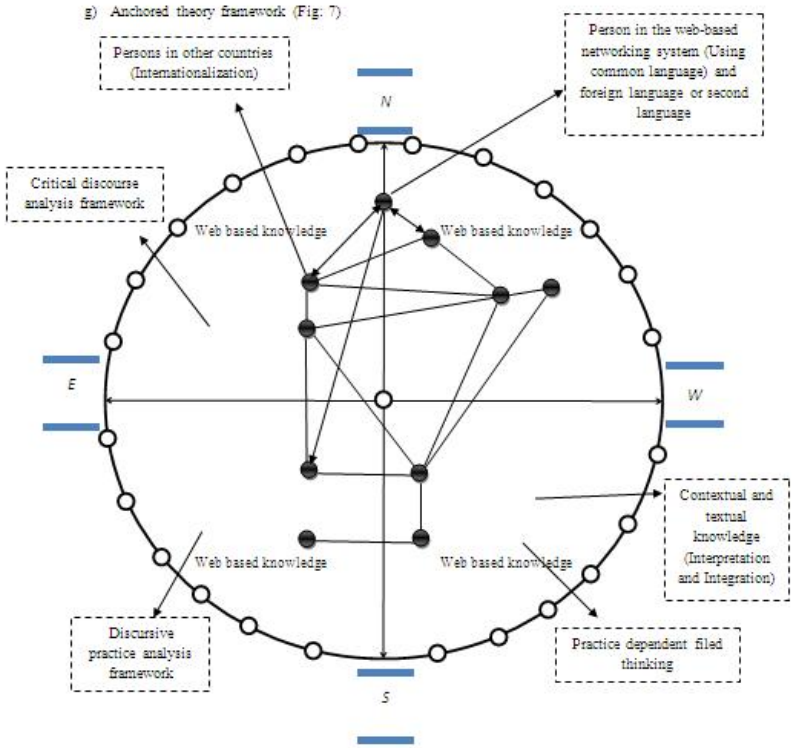

Fig.7: Anchored theory of person is creating networks with related practices in the globe (Web is created)

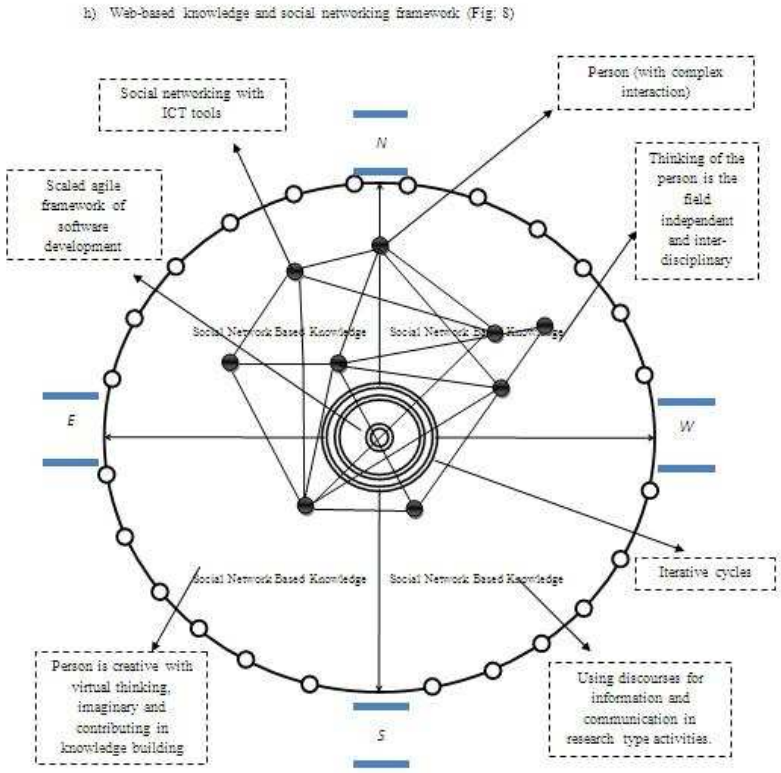

Fig.8: Web-based knowledge and social networking (Community of practice)

i) Stepping in the virtual space: Global knowledge framework (Fig: 9)

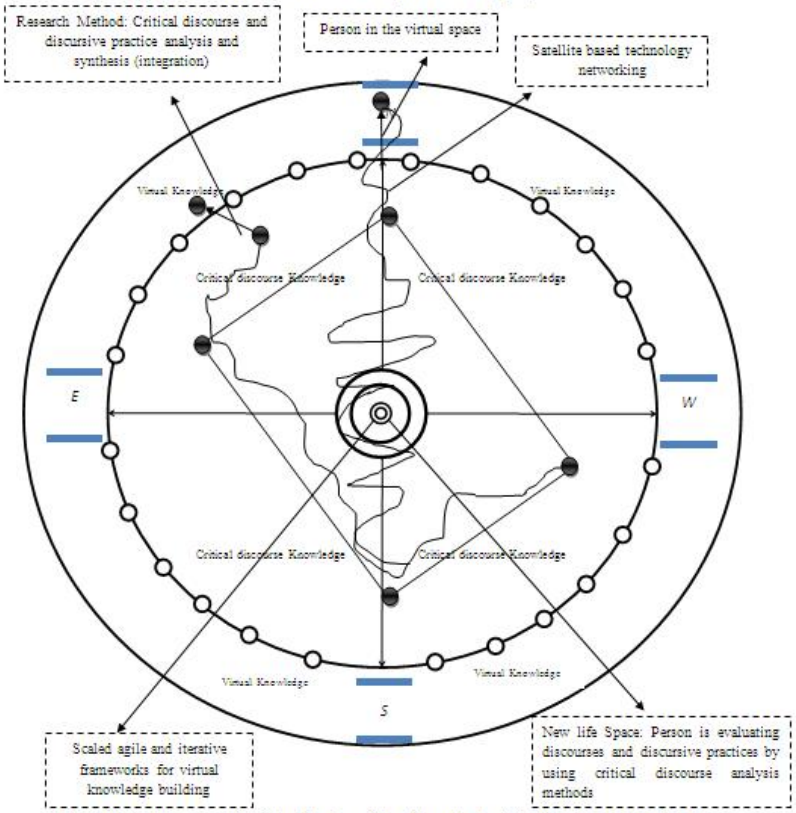

Fig.9: Web of the person is widened to four sides of knowledge globe: Stepping in the virtual space (Critical discourse knowledge)

- Community of practice is reduced
- Time for networking is reduced
- Social networking are used for peer-to-peer interaction

j) Virtual web-based interaction (community framework of practice) (Fig: 10)

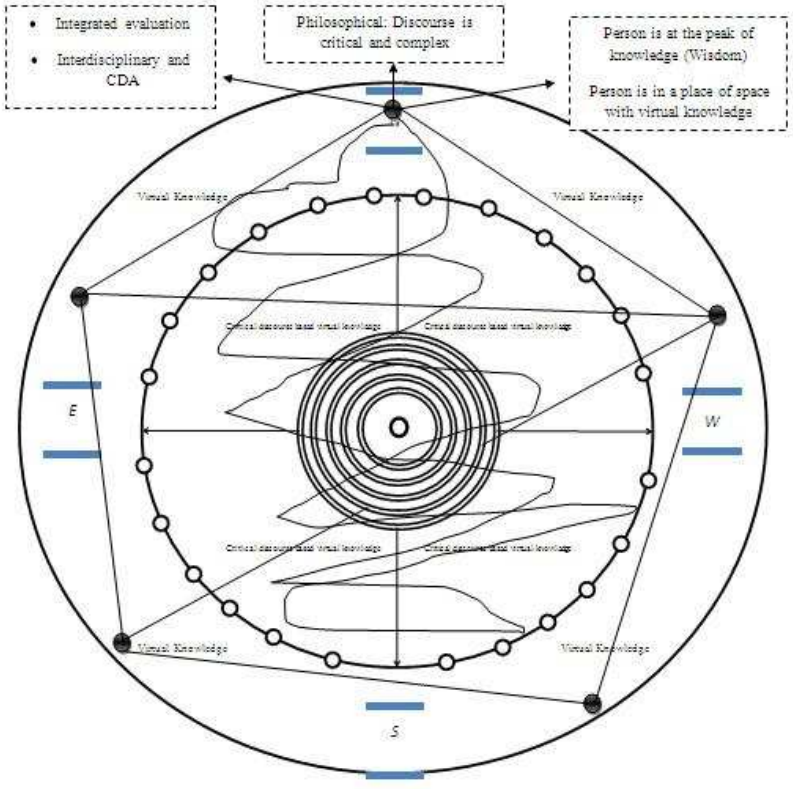

Fig.10: Virtual web-based interaction: Smaller community of practice network in the virtual space (knowledge sharing or collaboration)

k) Unit of analysis framework for global virtual knowledge (Fig: 11)

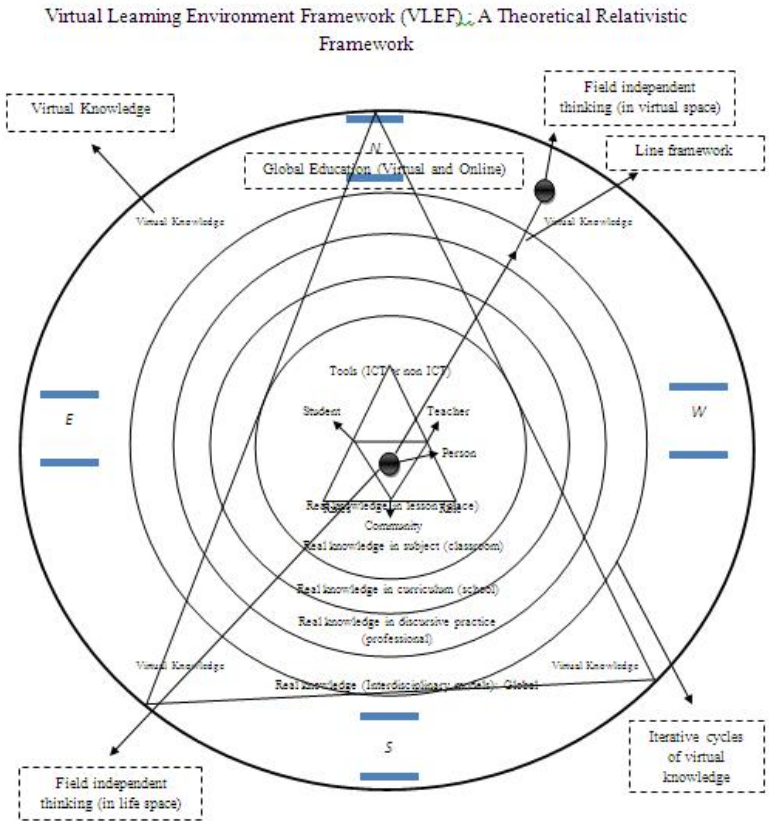

Fig.11: Unit of analysis, iteration and line framework for activity system

l) Multi-Dimensional framework for evaluating total quality in open and flexible learning system (Fig: 12)

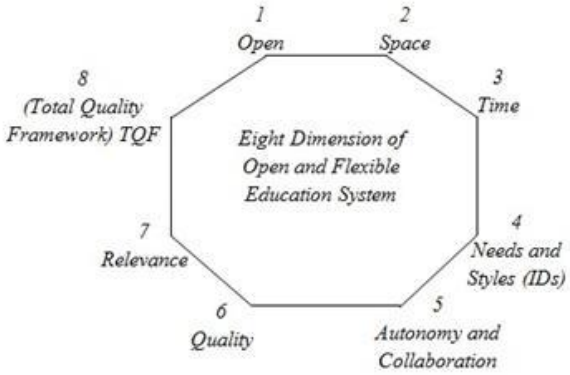

Figure: 12 Octagon of open and flexible education

by using the tools of social networking and mobile technology for autonomy, collaboration, interaction, communication and information exchange known as software of Learning Management System (LMS) used in virtually open, distance and flexible environments.
b) The best methodology for evaluation is analysis of the discursive practice and discourses for dialogue (interaction), structure (program) and practice (learner's autonomy and collaboration in a community).
c) The evaluation is not possible without using a software for discriminating disciplines in the field and developing the person's intelligence and knowledge to an artificial level known as artificial intelligence or virtual knowledge (scaled agile framework).
d) The knowledge development or incremental unit is very small and instantaneous (scaled agile framework) but its impact is wide in scope (Spiral framework and iterative framework).
e) The motion is relative and interpretive (potential dependent) in a constructivist learning environment (optimum iterative framework).
f) Developing Critical Discourse Analysis (CDA) is an authentic methodology for research in education to find gap and ambiguity in existing research (waterfall framework) and filling that gap to form a new whole (integrated) form or structure (meaningful learning) to convert it into new research (Scaled agile framework).

4 Discussion and Diagrammatical presentation of VLEF (Pnemonological Network):

The VLEF has been diagrammatically presented in (Figures: 1 - 12 http://learning.pknursery.com/). The VLEF has twelve stages of development in its Pnemonological network.
a) Globalization of knowledge: Real and Virtual Framework (Fig: 1)
b) Physical science framework (Fig: 2)
c) Motion of person in the field of real and social knowledge (Fig: 3)
d) Developmental theories (psychological) framework (Fig: 4)
e) Activity system (Constructivist learning) framework (Fig: 5)
f) Person-situation theory of construction of knowledge framework (Fig: 6)
g) Anchored theory framework (Fig: 7)
h) Web-based knowledge and social networking framework (Fig: 8)
i) Stepping in the virtual space: Global knowledge framework (Fig: 9)
j) Virtual web-based interaction (community framework of practice) (Fig: 10)
k) Unit of analysis framework for global virtual knowledge (Fig: 11)
l) Dimensional framework for evaluating total quality (Fig: 12)

5 Background of the Study (Methodology):

The study was aimed at developing a "framework" for research in open and flexible education in the context of ICT-rich environment to make provision of open and flexible education; evaluation and qualitative interpretation for ICOFE (2014) in the Open University of Hong Kong. The study was modified for making it relatively developed for ICRA (2015) at the University of The Punjab, Lahore on the eve of 100th anniversary of Einstein. The researcher found that Critical Discourse Analysis (CDA) framework was leading towards Virtual Learning Environment Framework (figure 1 - 11) and was best suited for this purpose.
The requirements of critical discourse analysis (CDA) and VLEF (Virtual Learning Environment Framework) were enlisted as:

- Activity analysis (process of learning in constructivist
- Interaction analysis (social and cultural aspects)
- Communication analysis (dialogue, discussion and communication)
- Conversation and dialogue analysis (Discursive practices and structure)
- Discursive practice analysis (Evaluation of practice)
- Focus group discourse analysis (Developing the practice)
- Analysis for integration in discursive practices (Interdisciplinary and cross disciplinary integration and analysis)
- Analysis of globalization in discourse (Whole integration for filling the gap in virtual environment) through scaled agile framework by using Pnemonological network for various constructs.

Analysis of learning by doing and interaction through mediating tools, (ICT and non ICT) in a virtual learning environment in the globe (synchronous and asynchronous) are important aspects in CDA and VLEF.

6 Need Analysis of Researchers in Virtual Learning Environments (VLEs):

In globalization due to technological advancements, there are needs of the researcher for Critical Discourse Analysis (CDA) of dissertations, theses, research papers, posters, practices, theories, articles, artifacts and tools:

- Unit of analysis for activity in virtual leaning environment is needed to evaluate holistic approach for integration.
- Common language is needed to analyze the dialogue in a discourse (situated in community).
- Unit of analysis in a discourse is needed (for common language analysis).
- Unit of analysis in a practice is needed (for competence or life skill knowledge)
- Unit of analysis in a structure for cognitive tools and strategies or toolkit is needed (for knowledge utilization)
- Unit of analysis for integration is needed (for interdisciplinary and cross disciplinary approach determination and evaluation)

7 Need Analysis of Researches in Education (Open and flexible learning):

Education is a field consisting of various disciplines and is dependent on educational activity starting from simple task in which there is S - R or S - O - R interaction in an environment or surrounding. So, it can be analyzed from biological, psychological, ecological, temporal, spatial, political and religious (cultural) perspectives in a place or life space. His/her knowledge is directed toward the educational field in a multiple meaningful layers of knowledge development (Iterative cycles). So, knowledge is multiphasic.

The knowledge development is open (for all) and flexible (time independent) due to relative motion of person in a knowledge discipline towards the peak of the field (wisdom). It means that flexibility is created due to schedule and time for motion in life space. So, motion is relative and not absolute.

The motion towards the peak of the field (wisdom)is accelerated by modern technologies and tools due to the application of theories in the field; to develop methodologies, techniques, strategies, tools, models, theories and frameworks and also to create artifacts in a practice; hence making the process of getting knowledge mechanical and automated (theory into practice). Hence, acceleration is made possible by tools and technologies.

Due to these technologies the person is able to move in all directions in the field of knowledge. The recent invention of social networking has converted the field of knowledge into knowledge globe by using a unit activity of the constructivist learning environment system (theory of construction) and is iteratively and spirally developed to form the globe of knowledge (wisdom) as an integrated whole. So, knowledge is integrated (interdisciplinary and cross disciplinary).

Hence, the globalization has created a gap in the already existing frameworks of learning due to open and flexible learning opportunities of getting knowledge through artifacts and tools using different learning theories and pedagogies (review of learning theories and pedagogical mapping). Globalization has created gap in knowledge by making the knowledge virtual and abstract.

So, this research in open and flexible learning in ICT-rich environment has made the existing research methodologies integrated into linear framework and models for making it more realistic, objectives and scientific. But due to social interaction it cannot be made fully realistic and remains always interpretive, context dependent and qualitative. Therefore, both qualitative and quantitative research is needed in open and flexible education.

Moreover, when the knowledge in the field of education is global, virtual and interpretive due to the person situation or position in the field at a point on the globe (life space situation theory). There are eight dimensions of open and flexible learning in the knowledge globe to develop an octagon structure Fig: 12 (Geometrical perspective):

1. Open (for all): Democratization of education all over the world is needed (Internationalization).
2. Space (place): location with reference to a point (position): Transactional theory of Distance Education (DE) is needed. Jung (2001).
3. Time: to cover distance in the filed with a pace (schedule): Flexible timing is needed (Scaled agile framework of software development).
4. Individuals needs and styles (force of motion): Diversity of structure, media and dialogue is needed.
5. Autonomy as well as collaboration: Diversity in modes of delivery and Instructional Designs (IDs) is needed.
6. Quality: authentic, efficient and effective learning environments are needed.
7. Relevance: market oriented, society-related, futuristic and individual based-learning is needed.
8. Total quality-based-framework: covering the quality of all the aspects of education system including research is needed.

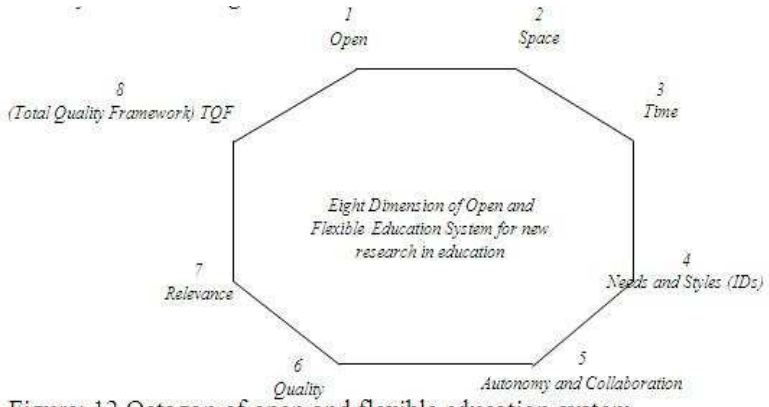

Figure: 12 Octagon of open and flexible education system

When it becomes flexible in all the eight dimensions: open, space, time, pace, need and style flexible, autonomy and collaboration, relevance, quality and total quality framework; it becomes fully flexible and open education system (Octo-Dimensional framework).

So, the open dimension brings democratization and internationalization in education while the dimension of time is to brings flexibility in task performance schedule and is more critical and discriminative dimension for flexibility and rigidity, because, other dimensions are dependent on time(schedule).

Time is needed and required to move (slow or fast) referring to the pace (autonomy). Hence, we can conclude that if time (schedule) of learning is flexible and according to the persons' need it will make learning flexible in a real sense.

Time is core component of flexibility in open system of education.

Flexibility can also be determined by its integration of traditional forms of education (multimedia and hypermedia). The other characteristics of open and flexible learning are anytime, anywhere i.e. synchronous and asynchronous (ubiquitous) this is also made possible by mobiles (m-learning), and ICT technologies in virtual learning environment (VLEs).

So, in an ICT-rich environment the knowledge is integrated (interdisciplinary) and the learner is in the globe of knowledge (Real and Virtual) with his own community of practice, and having virtual and real social interactions (collaboration) and discourses; moving on in an autonomous ladder for knowledge development to have self-actualization and contributions in the knowledge globe (utilizing wisdom) .

8 Findings:

The framework developed by the researcher in this study was based on the interdisciplinary and cross disciplinary review of literature and experience in the field of education and can be used as an epistemological, ontological and methodological guide for research evaluation in open and flexible education phenomenon. The approach is based on Critical Discourse Analysis (CDA) framework and is named as VLEF (Virtual Learning Environment Framework) and its nature is relativistic and virtually synonymous with Einstein theory of relativity in the conversion of real knowledge (mass) into virtual knowledge (energy). Here energy refers to wisdom.

9 Conclusion:

Keeping in view, the above discussion, a framework was developed by using activity system framework construction with mapping of scaled agile framework for software development to be used by a researcher to situate or position a discourse, theory, practice, artifact and tool developed by another researcher in education through critically analyzing the discourse for filling the gap in knowledge and development in education.
So, the best method to reach to the peak of all knowledge (ontology of wisdom) in open and flexible learning is Critical Discourse Analysis (CDA) framework and Virtual Learning Environment Framework (VLEF) is based on Critical Discourse Analysis (CDA) in a field.

10 Suggestions/Recommendations:

The following suggestions are proposed and recommended:

1. The (VLEF) framework is to be made a prototype (software) used in educational research evaluation related to the fields of education and ICT.
2. It can also be used as a developed model framework for evaluation of researchers in open and flexible learning environment and education.
3. It is proposed that the researchers may use Critical Discourse Analysis and VLEF as best and suitable methods for the evaluation of researches grounded in ICT or e-learning or virtual learning environments (a software is needed for it).
4. A further research is suggested for its theoretical underpinning, more grounded in theories of learning and software development and applications.
5. The name suggested for the framework is Virtual Learning Environment Framework (VLEF) for open and flexible learning and education.
6. It is also proposed that VLEF require Critical review by other researcher in the field of education and e-learning.
7. The new knowledge developed in educational research is to be evaluated on the basis of relativity and not on absolute scale. (Knowledge development is relativistic in nature).

11 Significance of the Study:

The study was significant because it had provided a framework for research in education taking place in open and flexible environment; where there are variety of ICT tools, approaches and social networking technologies to provide virtual learning opportunities across the globe and throughout life.
The study would be helpful in all disciplines in the field of education because of its interdisciplinary and cross disciplinary approach in educational research.

References

1. AAOU Annual Conference Abstracts (2013): Leveraging the power of open and distance learning for building diverging Asia: today's solutions and tomorrow's vision. 27th AAOU Annual Conference 2013; AIOU, Islamabad. www.aaou2013.com
2. M. Amin & Y. Khan (2004): Millennium 2000 Educational Psychology, Guidance and Counseling for B.Ed University of Peshawar. Radiant Publisher, Mardan.
3. HEA position paper (2009): Open and flexible learning: Higher Education authority: Retrieved 22-11-2013 www.deekin.edu.au
4. I. Jung (2001): Building a Theoretical Framework of Web-based Instruction in the Context of distance education. British Journal of Education Technology www.onlinelibrary.wiley.com
5. K.C. Li (2013): Flexible learning: Dimensions and Learner Preferences: 27th , AAOU Annual Conference, AIOU, Islamabad. Retrieved: 29/10/2013 www.aaou2013.com
6. T. Mayes & S. De Freitas (2013) JISC e-learning model review of e-learning framework and models. Program Book (2013): Desk study www.jis.ac.uk/
7. I. Sommerville (2011): Software Engineering, Ninth edition, publishing as Addison-Wesley www.pearsoned.couk/sommerville
8. Y. Khan (2000): Millennium 2000 Educational Psychology, Guidance and Counseling for B.Ed. Shaheen Book Agency, Nishat Chowk, Mingora Swat.
9. Y. Khan (2008): A research monograph on Advanced Educational Psychology. Higher Education Commission, Islamabad (Unpublished project).
10. Y. Khan (2010): Critical Analysis of Newly introduced science curriculum Vs old science curriculum at SSC level in NWFP. M.Phil thesis (unpublished). Institute of Education and Research, University of Peshawar.
11. Y. Khan (2013): Analysis of Teacher Training and Education Program of Pakistan for ICT Integration in Pakistan. A case study: 27th AAOU Annual Conference, AIOU, Islamabad.
12. Y. Khan (2014): Developing Theoretical Framework for Research in Open and Flexible Learning Environment in ICT-rich Environment: A New Trend in Educational Research. Program proceeding ICOFE (2014), Open University of Hong Kong. www.ouhk.edu.hk
13. Wikipedia, free encyclopedia: (2013). Scaled agile framework. Retrieved: 27/10/2013 www.google.com.pk

Proc. Int. Conf. Relativ. Astrophys.
Pages 104-109, (2015)

Zero Age Main Sequence Star Modeling by Using Statstar Code

Anam Khalid [a,1], **Saif Uddin Jilani** [2], **Mudassar Hassan Arsalan**[1], **Hira Fatima**[1] **and Rabia Tabassum**[1]

[1]Institute of Space and Planetary Astrophysics, University of Karachi, Karachi, Pakistan-75270
[2]Department of Physics, University of Karachi, Karachi, Pakistan-75270

Abstract Stars are formed following the gravitational collapse of cold molecular clouds found in the Universe. As the cloud or portions of it collapses, approximately half of the gravitational energy gained is used to increase the internal temperature of the cloud and the remaining energy is irradiated as electromagnetic radiation in space.

Zero Age Main Sequence (ZAMS) is the time when a star first joins the main sequence on the Hertzsprung-Russell diagram (HR diagram) by burning hydrogen in its core through fusion reactions. After this time, the star enters into a phase of stellar evolution that is quite stable, and steadily processes Hydrogen into higher elements. As a result, the main sequence is a broadband that is displaced slightly from this zero-age strip.

Stars are comparatively easier to analyze than some other astronomical objects because they have simple shapes and structure i.e. spherically symmetric. The stellar model contains four basic first-order differential equations; two represent the variability of the matter and pressure with the radius; and other two represent how temperature and luminosity vary with radius.

In our paper, the Statstar code has been used to model ZAMS star of mass $M = 10M_{\odot}$. The star is in hydrostatic equilibrium i.e. its size is fixed and the atmosphere, rotation and magnetic field of the star are exempted in this model. We have solved some basic stellar structure equations by assuming star into spherically symmetric mass shells with specified boundary conditions and calculated associated properties of the star such as temperature, pressure, density and opacity in each zone.

The study shows that the temperature and the pressure of the star is higher in the core while the luminosity and opacity of the star is higher at the surface.

Keywords HR Diagram, ZAMS, Stellar Evolution, Statstar Code.

1 Introduction

Stars are formed following the gravitational collapse of cold molecular clouds found in the Universe. As the cloud or portions of it collapses, approximately half of the gravitational energy gained is used to increase the internal temperature of the cloud and the remaining energy is irradiated as electromagnetic radiation in space. If the mass of the collapsed cloud is sufficient (i.e. more than approximately 8% of the mass of the Sun), the central temperatures will attain a value superior to the threshold temperature for sustained hydrogen fusion, which leads to star birth. The gravitational collapse will continue until equilibrium is reached, where the nuclear energy generated per unit time (or its power) at the center of the star equals the power output at its surface due to radiation emitted. A star at this stage of its life is commonly called a main - sequence star. Since gravity has radial symmetry, a star will have a spherical shape (unless it has a high rotational speed). The luminosity of a star depends on both its radius and effective temperature. Hertzsprung - Russell diagram (HRD), shows the relation between the luminosity and the effective temperature of stars. The HRD is extremely useful when studying the evolution of stars, since there are well - determined paths along which stars should travel as they evolve. These paths depend mostly on stellar mass [1 - 2].

Stars are comparatively easier to analyze than some other astronomical objects because they have simple

[a]e-mail: pisces221988@hotmail.com

shapes and structure i.e.spherically symmetric. The stellar model contains four basic first-order differential equations; two represent the variability of the matter and pressure with the radius; and other two represent how temperature and luminosity vary with radius. The diagonal line in the HRD where stars of various masses first reach the main sequence and begin equilibrium hydrogen burning is known as the zero-age main sequence (ZAMS)[1 - 2].

In this paper, basic stellar equations are verified for the zero age main sequence (ZAMS) star with a mass of $10_{\odot}$ M using StatStar code. Stellar models allow us to predict stellar evolution and also be able to tell us how changes in composition lead to changes in the structure.

2 Materials and Methods:

Inspection of the classical results given in Table 1 shows that the amount of time required for stars to collapse onto the ZAMS is inversely related to mass. For instance, a $0.8M_{\odot}$ star takes over 68 Myr to reach the ZAMS, where as a $60M_{\odot}$ star makes it to the ZAMS in only 28,000 years.

Figure 1: Classical pre-main-sequence evolutionary tracks computed for stars of various masses with the composition X=0.68, Y=0.30 and Z=0.02. The direction of evolution on each track is generally from low effective temperature to high effective temperature (right to left). The mass of each model is indicated beside its evolutionary track. The square on each track indicates the onset of deuterium burning in these calculations. The long-dash line represents the point on each track where convection in the envelope stops and the envelope becomes purely radiative. The short-dash line marks the onset of convection in the core of the star[1 - 2].

Contraction times for each track are given in Table 1 below:

Table 1: Pre-main-sequence contraction times for the classical models presented in Fig. 1 (Data from Bernasconi and Maeder, Astron. Astrophys., 307,829, 1996.)

Initial Mass($M_{\odot}$)	**Contraction Time (Myr)**
60	0.0282
25	0.0708
15	0.117
9	0.288
5	1.16
3	7.24
2	23.4
1.5	35.4
1	38.9
0.8	68.4

Stars on the zero-age main sequence are nearly homogeneous in composition and are in complete hydrostatic and thermal equilibrium. Detailed models of ZAMS stars are computed by solving the four differential equations for stellar structure numerically. From the homology relations, we expect a homogeneous, radiative star in hydrostatic and thermal equilibrium with constant opacity and an ideal-gas equation of state to follow a mass-luminosity and mass-radius relation: [2]

$$L\alpha\mu^4 M^3, R\alpha\frac{v-4}{\mu v-3}\ \frac{v-1}{Mv-3} \tag{1}$$

The StatStar code is based on the equations of stellar structure equations. It is designed to illustrate as clearly as possible, many of the most important aspects of numerical stellar astrophysics. To accomplish this goal, StatStar models are restricted to a fixed composition throughout as they are homogeneous zero-age main-sequence models (ZAMS). The four basic stellar structure equations are computed in the functions are: [1-3]

$$\frac{dP}{dr} = -G\frac{M_r}{r^2}\rho = \rho g \tag{2}$$

$$\frac{dM_r}{dr} = 4\pi r^2\rho \tag{3}$$

$$\frac{dL_r}{dr} = 4\pi r^2\rho\epsilon \tag{4}$$

$$\frac{dT}{dr} = -\frac{3}{4ac}\ \frac{\overline{k\epsilon}}{T^3}\ \frac{L_r}{4\pi r^2} \tag{5}$$

$$\left|\frac{dT}{dr}\right| = -\left(1-\frac{1}{r}\right)\frac{\mu mH}{k}\ \frac{GM_r}{r^2} \tag{6}$$

The density [$\rho(r) = rho$] is calculated directly from the ideal gas law and the radiation pressure equation in FUNCTION Opacity, given local values of the pressure [P(r) = P], temperature [T (r) = T], and mean molecular weight (μ = mu, assumed here to be for a completely ionized gas only). Once the density is determined, both the opacity [$\bar{k}(r) = kappa$] and the nuclear

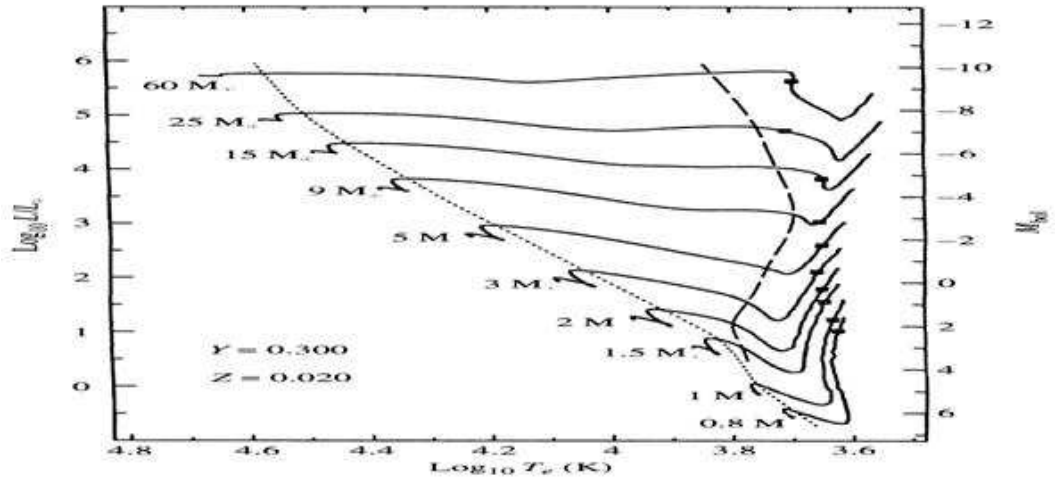

energy generation rate [ϵ(r) = epsilon] are calculated. The opacity is determined in FUNCTION Opacity using the bound-bound and bound-free opacity formulae:

$$\overline{K_{bf}} = 4.34x10^{21}\frac{gbf}{t}Z(+X)\frac{\rho}{T^{3.5}}m^2kg^{-1} \quad (7)$$

$$\overline{K_{ff}} = 3.68x10^{18}gff(1-Z)(1+X)\frac{\rho}{T^{3.2}}m^2kg^{-1} \quad (8)$$

Together with electron scattering

$$\overline{K_{es}} = 0.02(1+X)m^2kg^{-1} \quad (9)$$

and H-ion:

$$\overline{K_{H^-}} \approx 7.9\times10^{-34}(Z/0.02)\rho^{1/2}T^9m^2kg^{-1}... \quad (10)$$

The energy generation rate is calculated in Function Nuclear from the equations for the total pp chain:

$$\square_p p = 0.241\rho X^2 f_{pp}\Psi_{pp}C_{pp}T_6^{-2/3}e^{-33.80T_6^{-1/3}}Wkg^{-1}... \quad (11)$$

$$\square CNO = 8.67x10^{20}\rho X X_{CNO}C_{CNO}T_6^{-2/3}e^{-152.28T_6^{-1/3}}Wkg^{-1}... \quad (12)$$

2.1 Modeling of $M = 10_\odot$ Zero Age Main Sequence Star:

We used the central boundary conditions for modeling of ZAMS stars asthe interior mass and luminosity approach to zero, or

$$M_r \to 0$$

$$L_r \to 0$$

It reveals that the star is physically realistic and does not contain a hole, a core of negative luminosity, or central points of infinite ρ or ε. A second set of boundary conditions is required at the surface of the star. The simplest set of assumptions is that the temperature, pressure, and density all approach to zero at the surface for the star's radius(R_*), or

$$T \to 0$$

$$P \to 0$$

$$\rho \to 0$$

However, the conditions of the above equationsare difficult to obtain in a real star (especially, in the case of the temperature)[2].

2.2 Visualization:

By using StatStar we observed that how temperature, luminosity, density, pressure, opacity and optical depth vary from the surface to the core of ZAMS star of mass $10M_\odot$. All results have been obtained by using StatStar and for the graphical representation, weused Matlab R2012a Software.

2.3 Results and Discussion:

Temperature and Zones (Graph 1)show that temperature rapidly increasing as we approached to the center of a star. One of the facts of thermonuclear fusion reaction is due to such high temperature in the core of the star. In graph 2, we can see that the luminosity of the star is higher at the surface than at the core and this is due to the reason that the rate of fusion reaction is much higher in the core and the increased fusion rate causes the star's luminosity and radius to go up. As the

star fuses hydrogen the core begins to become "clogged up" with helium ash, which would tend to damp out the fusion reaction. The result is that the pressure goes up in the core and goes down on the surface which can be seen in the graph 3 i.e. between the pressure and zones of the star. In the process of nucleo-synthesis, the hydrogen in the core is converted into helium ash. This helium ash increases the density of the core which can be seen in graph 4. The opacity of a star is inversely proportional to its density. At the core, the fusion process is greater than at the surface and hence the density of the star is higher. Due to this reason, the opacity of the star is less at the core and high at the surface as shown in the graph 5 of opacity and zones [2-4, 7-10].

The scattering of photons is very low at the surface and very high at the core because of high density at the core of the star. As shown in the graph 6, the optical depth is directly proportional to the density that is why it is very high at the core as compared to the surface so that the outermost layer of the star is taken at τ=0 [2-6].

3 Conclusion:

It is concluded that the StatStar code is a handy tool to model the ZAMS. It can produce the physical characteristics of the evolutionary star. The molding in StatStar reveals that due to thermonuclear fusion reaction, the temperature, pressure, and density of the ZAMS star are rapidly increasing as we approached to the center of a star. The opacity of a star is the absorption of photons in the star and is inversely proportional to its density, therefore, the luminosity and opacity of the star is less at the core and high at the surface. Due to low scattering of photons at the surface, the optical depth of the star is high at the core where the outermost layer of the star is taken at $\tau = 0$.

Acknowledgements I would like to thank Mr. Ghulam Mustafa Laghari and Mr. Zain Rahim, Asst. Managers at Pakistan Space and Upper Atmosphere Commission (SUPARCO) for their guidance and never ending supportfor the accomplishment of this work.

References

1. An Introduction to Stellar Astrophysics, First Edition, Francis Leblanc, John Wiley and Sons, Ltd. The Atrium, Southern Gate, Chichester, West Sussex, PO19 8SQ, United Kingdom.
2. An Introduction To Modern Astrophysics, Second Edition, Bradley W. Carroll and Dale A. Ostlie, Addison-Wesley, 1301 Sansome St., San Francisco.
3. Astronomy: A Physical Perspective, First Edition, Marc L. Kutner, Cambridge University Press, New York, 2003.
4. Astrophysics: A New Approach, Second Edition, Professor Dr. WolfgangKundt, Springer, Berlin Heidelberg, NewYork, 2005.
5. An Introduction To The Theory Of Stellar Structure And Evolution, Fifth Edition, Dina Prialnik, Cambridge University Press, The United States Of America, 2007.
6. An Invitation To Astrophysics, World Scientific Series In Astronomy And Astrophysics - Volume 8, ThanuPadmanabhan, World Scientific Publishing Co. Pte. Ltd.5 Toh Tuck Link, Singapore 596224.
7. Galaxy Formation, Astronomy And Astrophysics Library, Second Edition, Malcolm S. Longair, Springer-Verlag Berlin Heidelberg 1998, 2008.
8. Astronomy: Understanding The Universe, First Edition, Edited By Sherman Hollar, Britannica Educational Publishing In Association With Rosen Educational Services, LLC 29 East 21st Street, New York, NY 10010.
9. Introduction to stellar astrophysics - Basic stellar observations and data, Volume 1, Erika Bohm-Vitense, the Press Syndicate of the University of Cambridge , The Pitt Building, Trumpington Street, Cambridge CB2 1RP, 1989.
10. Galaxy Formation And Evolution, First Edition, Houjon Mo, Frank Van Den Bosch And Simon White, the United States of America by Cambridge University Press, New York, 2010.

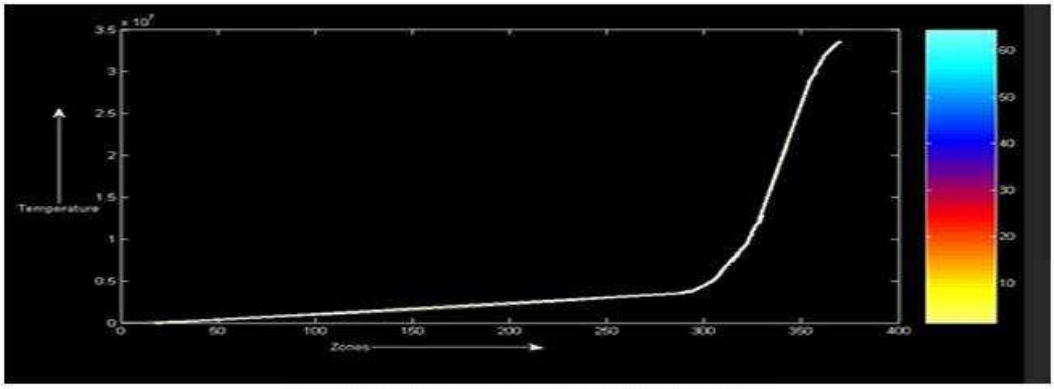

Graph 1: Temperature of ZAMS Star

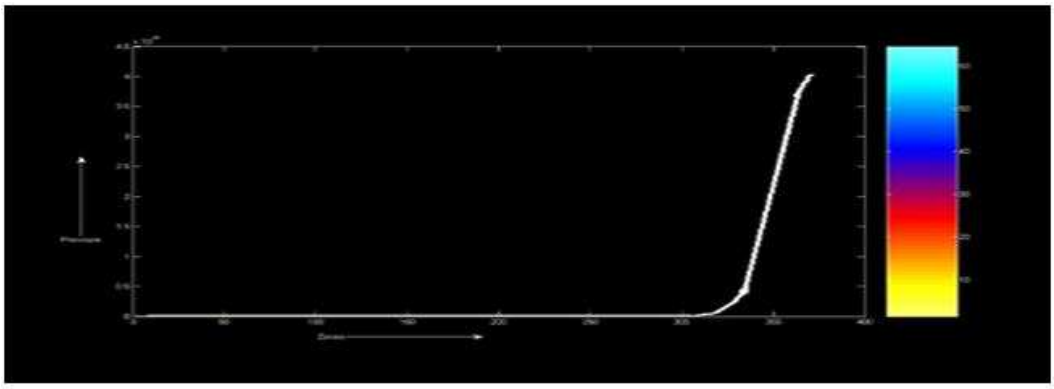

Graph 3: Pressure of a ZAMS Star

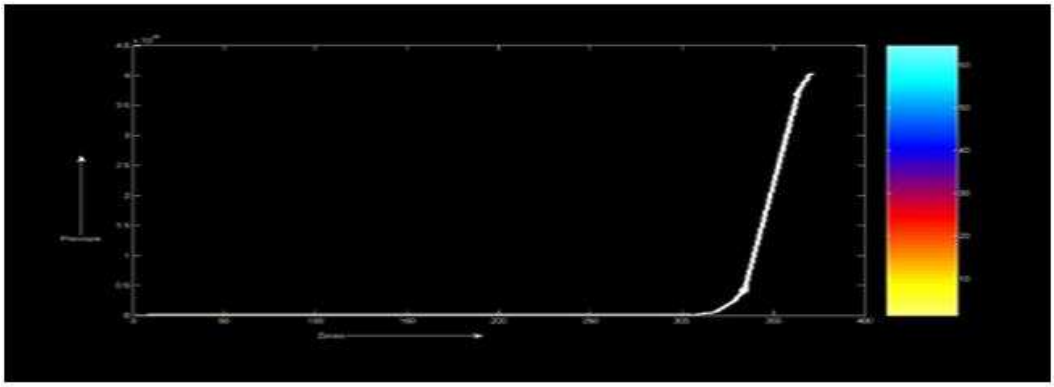

Graph 3: Pressure of a ZAMS Star

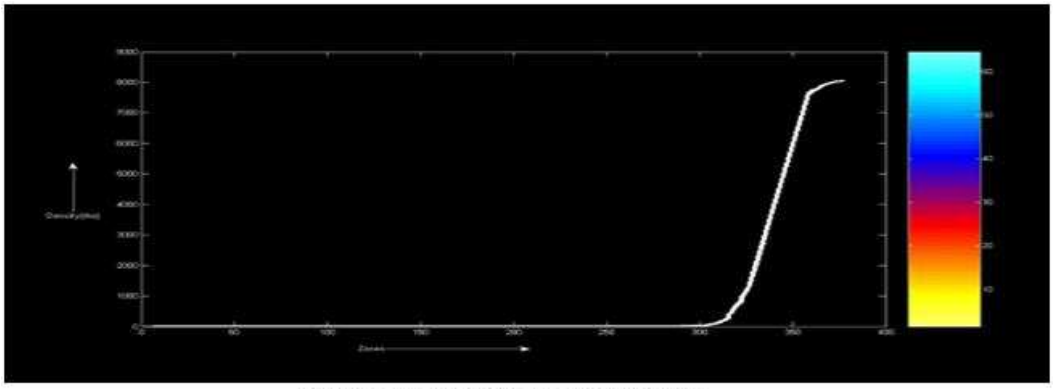

Graph 4: Density of a ZAMS Star

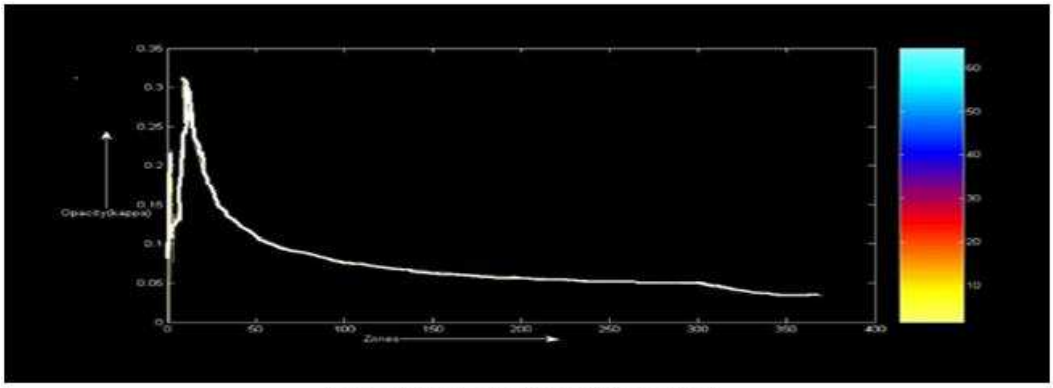

Graph 5: Opacity of a ZAMS Star

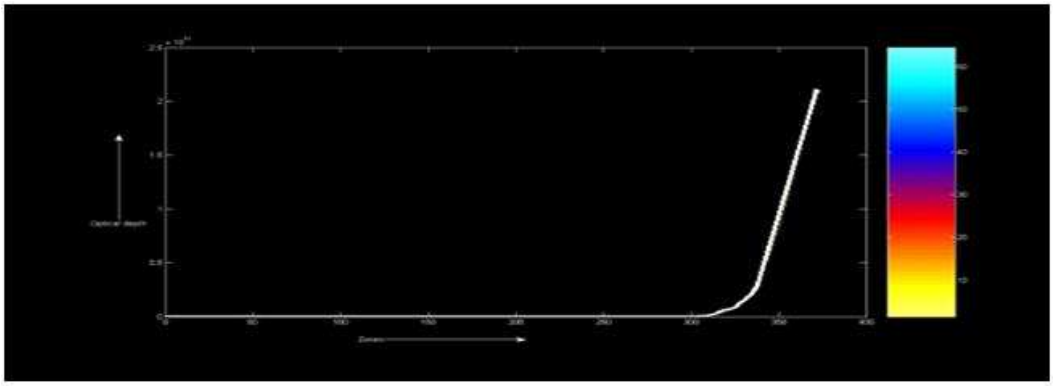

Graph 6: Optical Depth of a ZAMS Star

Proc. Int. Conf. Relativ. Astrophys.
Pages 122-128, (2015)

Spacetime invariants and their uses

Malcolm A.H. MacCallum[a,1]

[1]School of Mathematical Sciences, Queen Mary University of London

Abstract There are various types of global and local spacetime invariant in general relativity. Here I focus on the local invariants obtainable from the curvature tensor and its derivatives. The number of such invariants at each order of differentiation that are algebraically independent will be discussed. There is no universally valid choice of a minimal set. The number in a complete set will also be discussed. The invariants can then be used to characterize solutions of the Einstein equations (locally), to test apparently distinct solutions for equivalence, and to construct solutions. Other applications concern limits of families of spacetimes, and the characterization of horizons and singularities. Further uses are briefly mentioned.

Keywords Invariants · horizons · singularities · exact solutions

PACS 02.40.Ky · 04.20.-q · 04.20.Cv · 04.20.Dw · 04.20.Jb

1 Introduction and motivation

This lecture developed from one given some years ago at the retirement party of my friend, colleague and co-author Dr. Eduard ("Eddie") Herlt. At the Lahore meeting, time did not permit a complete exposition of all aspects of the subject. This text follows what was said rather than what might have been said in an expanded version. I intend to write up the expanded version as a review article in due course.

I could have been more precise in my title, at the cost of being rather lengthy. There are many occurrences of the word 'invariant' in our field, e.g.:
gauge-invariant (in gauge theory)
gauge-invariant (in perturbation theory)
invariant under a symmetry
Lorentz-invariant
scale-invariant.
And I could be talking about some global conserved quantity, without a well-defined local density, e.g. Bondi mass.

What I actually meant was local, geometric, invariants of spacetime: essentially curvature invariants.

I started to be seriously interested in this area when we were writing the first edition of the exact solutions book [1] in the late 1970s. One of the big problems we faced was that of identifying the same solution when found with different assumptions or for different reasons, and presented in different coordinate systems. I realised at the time that the work of the Stockholm group on invariant classification, which I will mention later, and which I first heard about in the late 70s, held the key.

This first application, as far as I was concerned, the "equivalence problem", was what got me started.

2 Mathematics

2.1 Definitions of invariants

Christoffel proved in 1869 that scalars constructed from the metric and its derivatives must be functions of the metric itself and the Riemann tensor and its covariant derivatives.

The first examples to spring to mind are **scalar polynomial (s.p.) invariants**, such as $R_{ab}R^{ab}$ or $C_{abcd}C^{cdef}C_{ef}{}^{ab}$. Often when people just say "invariant" they mean "s.p. invariant".

However, these are not adequate in all circumstances, as one can see by noting that *pp* waves and flat space

[a]e-mail: m.a.h.maccallum@qmul.ac.uk

both have all scalar polynomial invariants, of all orders, equal to zero [2].

Fortunately they are not the only choice. An important alternative is to use ideas due to Cartan, as follows. As a side benefit, in my view an important one, Cartan invariants require less calculation, in general.

Let $F(\mathcal{M})$ denote a "suitable" frame bundle over a spacetime $\mathcal{M}$ (i.e. take the set of all frames at each point) and $\mathcal{R}^q$ be the set $\{R_{abcd},\, R_{abcd;f},\, \ldots,\, R_{abcd;f_1 f_2 \cdots f_q}\}$ of the components of the Riemann tensor and its derivatives up to the qth in a frame.

Choose from $F(\mathcal{M})$ in a canonical and invariant way, e.g. use the principal null directions of the Weyl tensor, when they are distinct, as the basis vectors. The resulting $\mathcal{R}^q$ are called the **Cartan invariants**. They are scalars, because the frames are invariantly defined, e.g. if **a**, **b**, **c** and **d** are basis vectors (not necessarily all distinct) of the chosen frame, one of the Cartan invariants is $R_{ijkl}a^i b^j c^k d^l$. The idea is like characterizing a symmetric bilinear map (matrix) by its eigenvalues.

2.2 Independence of (s.p.) invariants

In a manifold $\mathcal{M}$ of n dimensions, at most n scalar invariants can be **functionally independent**, i.e. independent functions on $\mathcal{M}$.

The number of **algebraically independent** scalar polynomial invariants, i.e. s.p. invariants not satisfying any polynomial relation (called a *syzygy*), is rather larger, as we shall see next. (A set of algebraically independent Cartan invariants in a general spacetime, written using the Newman-Penrose spinor formalism, is given in [3]: it takes fully into account the Ricci and Bianchi identities.)

Larger still is the size of a complete set of s.p. invariants (a finite Hilbert basis): such a set $\{I_1,\, I_2, \ldots,\, I_k\}$ is **complete** if any other s.p. invariant can be written as a *polynomial* in the I_j but no invariant in the set can be so expressed in terms of the others.

One way to find the number of algebraically independent scalar invariants is to consider Taylor expansions of the metric and of the possible coordinate transformations [4]; another way follows Hilbert [5].

The result [6] is that in a general V_n the number of algebraically independent scalars constructible from the metric and its derivatives up to the pth order (the Riemann tensor and its derivatives up to the $(p-2)$th) is 0 for $p = 0$ or $p = 1$ and

$$N(n,p) = \frac{n[n+1][(n+p)!]}{2n!\,p!} - \frac{(n+p+1)!}{(n-1)!\,(p+1)!} + n,$$

for $p \geq 2$, except for $N(2,2) = 1$. Thus in a general space-time the Riemann tensor has $N(4,2) = 14$ algebraically independent scalar invariants. In particular cases the number is reduced.

The origin of many syzygies can be understood in terms of the vanishing of any object skewed over $(n+1)$ indices in n dimensions [7–9]. In a series of papers [10–12] Carminati and Lim have given a detailed discussion of the syzygies for scalar polynomial (s.p.) invariants of the Riemann tensor, using graph-theoretic techniques.

A given invariant may be written in more than one way, due to symmetries, and other relations between components, of the Riemann tensor and its derivatives. This is essentially a problem in representations of the permutation group. The issue is to select a canonical representative of each equivalence class in the orbit under permutations.

One wants to select a canonical set of invariants and then express any other invariant in terms of canonized members of the algebraically independent set.

Several methods have been used to do this for s.p. invariants, e.g. by Hörnfeldt, by Fulling et al., by Ilyin and Kryukov, and by Dresse. The method most readily available is due to Portugal [13]. It has been implemented in Maple™ and *Mathematica*® by Martin-Garcia *et al,* and is distributed in xAct, a package for use with *Mathematica*®. It has (e.g.) been applied to all objects with up to 12 derivatives of the metric [14].

Any complete set of s.p. invariants of the Riemann tensor, and any set which *always* contains a maximal set of independent scalars, contains redundant elements. Hence all the old papers giving specific sets of 14, in 4 dimensions, are inadequate.

The smallest known set of s.p. invariants for a general Riemann tensor that always contains a maximal set of algebraically independent scalars consists of 17 polynomials [15], though 16 suffice for perfect fluids and Einstein-Maxwell fields. There is a special subclass of spacetimes [16] which require 18.

The smallest set of s.p. invariants known to be complete contains 38 scalars [17], and Lim and Carminati [12] proved that it is minimal.

2.3 Computation of invariants

The s.p. invariants are expressions whose contractions hide very large numbers of individual terms, and are therefore hard to calculate. It is thus very useful to adopt a method that reduces the number of terms. One can use a bivector formalism (see e.g. [15]). Another way, in 4 dimensions, is to use the Newman-Penrose complex spinor (or null tetrad) formalism, the GHP

formalism, or related ideas: this has analogues in other dimensions (e.g. in three dimensions one can use real two-component spinors: see [18]).

For higher dimensions it may be efficient to use parallel computing, i.e. to split the calculation into subproblems e.g. by fixing some of the dummy indices, and then sending the subproblems to separate processors [19].

A simple practical way in many cases is to use Cartan invariants instead. They are quite cheap to calculate **provided** the frame choice is easy to calculate with, in particular because one never has to multiply curvature components, or their derivatives, together. In a general case, either s.p. or Cartan invariants would characterize the spacetime, as we shall see below. so the choice is really a question of convenience or purpose. There is an open research problem about which is actually more computationally efficient (or for which cases).

In four dimensions we can always choose a frame, for example by the principal null directions of the Weyl tensor, and thus compute Cartan invariants, but in general this may entail using the unpleasant algebraic expressions which arise from the general formulae for solutions of quartics. However, in practice many solutions give way easily. Note that in 5 dimensions or more there is no guarantee we can calculate frames of a specified type even if we can show they must exist, as there is no general algebraic formula for solutions of quintics.

2.4 Do scalar polynomial invariants suffice?

Until 2009, I would have said definitely not. I mentioned earlier that *pp* waves and flat space both have all scalar polynomial invariants, of all orders, equal to zero. In fact all vacuum type N and III metrics with $\rho = 0$ have this property [20]. There are also metrics which have equal non-zero s.p. invariants e.g. [21–23].

These ambiguities are associated with the indefiniteness of the metric and the non-compactness of the Lorentz group [24].

Coley *et al.* [25] gave an argument that spacetimes are completely characterized by their s.p. invariants, except for spacetimes in the Kundt class. Although their proof seems to me to have a gap, and I have not yet been able to see if it has been filled, the result seems correct.

In particular Coley and collaborators have followed up by a substantial number of papers, which I did not have time to review comprehensively in my Lahore talk. These consider not only 4D spacetimes, but higher dimensional spaces and various signatures. I just mentioned a few to give the flavour. In the initial paper [25], they also discuss what properties a given set of invariants characterize.

- Hervik and Coley [26] show that any metric with an analytic continuation to the pure Riemannian case is completely characterized by its s.p. invariants
- Coley *et al.* [27] give a detailed analysis of the generic 5D spacetimes.
- Hervik [28] gave arguments that spacetimes not characterized by s.p. invariants are limits of families that are so characterized.

It may be worth noting that since it is obvious that the algebraically independent set of Cartan invariants given in [3] completely and uniquely specify the s.p. invariants, the result of [25] amounts to saying that in general the converse is true, i.e. that the s.p. invariants uniquely determine the Cartan invariants (given the procedure for the choice of frame).

The work just described picked out the Kundt class as the exceptions. These are spacetimes which have a null vector field which is geodesic, and expansion-, shear- and twist- free. In a paper [29] which appeared just before [25] this class was discussed in detail. For it, one has to use the Cartan approach or some equivalent.

In [29] Coley *et al.* discussed the Petrov D examples in the Kundt class. Podolsky and Svarc [30] gave a classification of Kundt metrics in arbitrary dimension, and later discussed their physical interpretation. A subclass of "universal spacetimes" was discussed by Hervik *et al.* [31]: universal in that they solve vacuum equations of all gravitational theories with Lagrangian constructed from the metric, the Riemann tensor and its derivatives of arbitrary order. Hervik *et al.* [32] found all cases where there exists a continuous family of metrics having identical [scalar] polynomial invariants.

3 Uses of spacetime invariants

3.1 The Equivalence Problem

Now let me return to my original motivation, i.e. identifying the same solution when found with different motivations and assumptions and presented in different coordinate systems. It could be considered either a mathematical or a physical problem. It is essentially resolved by the following theorem (in terms of Cartan invariants).

Theorem 1 (Sternberg [33], Ehlers [34]) *Given two spacetimes, $\mathcal{M}$ and $\overline{\mathcal{M}}$, each expressed using some frames E and $\overline{E}$, then there is an isometry which maps (x, E) to $(\overline{x}, \overline{E})$ if and only if $\mathcal{R}^{p+1}$ for $\mathcal{M}$ is such that the independent quantities and the functional relations are*

the same for $\mathcal{R}^{p+1}$ and $\overline{\mathcal{R}}^{p+1}$, where p is the last derivative at which a new functionally independent entry in $\mathcal{R}^p$ arises.

See [35] for a more careful statement.

One could therefore calculate everything on a suitable frame bundle.

- Christoffel used coordinate frames. This works but the dimension of $F(\mathcal{M})$ is large.
- Cartan proposed using frames with constant scalar products, e.g. null frames or orthonormal frames, which is better (hence the credit for Cartan invariants).
- In 1965 Brans [36] proposed practical use of this method via lexicographic indexing of components.
- Later Brans and, more fully, Karlhede [37,38] realised that a more efficient way to implement the idea was to restrict the frames wherever possible by only allowing canonical forms of the curvature and its derivatives (i.e. go to Cartan invariants).
- This makes the whole thing manageable (with a computer) and it was first implemented by Åman in 1979 [39].

Given the Coley et al. results, we now know we could in general work only with s.p. invariants, but the present software [40,41] uses the Cartan method. In an algebraically general spacetime, one can choose the principal null directions of the Weyl tensor to fix the frame, or in a conformally flat spacetime one can begin with eigenvectors of the Ricci tensor. In the actual implementation we use the Weyl PNDs, where they exist, as the first choice.

Many details have been considered (by Åman, myself, Skea, d'Inverno, McLenaghan, Pollney and others) in specifying frames and in making the computations more efficient. The main aspects are the enumeration of canonical forms, the tests of which canonical form applies, and the transformation of the non-canonical to the canonical. The literature cited in the exact solutions book gives more information.

A first extension is to maps more general than isometries, e.g. homotheties [42] or conformal equivalence [43]. One can of course tackle Euclidean metrics and metrics in any dimension, though the details of making the method work efficiently are different (e.g. [44]).

The above ideas are in fact a special case of Cartan's general procedures (see e.g. [45]), which apply to other situations which can be expressed in differential forms and a connection or similar structures. In particular it applies to the equivalence of (systems of) differential equations, under coordinate transformations (see the books of Gardner [46] and Olver [47]).

Another context is that of gauge theories of physics, the gauge potential being just a connection [48].

One interesting issue for spacetimes is how large p in the theorem has to be. Karlhede [38] showed $p \leq 7$. For a long time examples suggested $p \leq 3$. At the time of the second edition of the exact solutions book [35] an example with $p = 5$ was known, as were a number of bounds for subclasses. We quoted results suggesting that $p \leq 5$ was generally true.

In 2009 (the result was actually first announced in 2007), Milson and Pelavas [49] showed that the original bound of 7 is sharp, by giving a (unique) example. This is still small enough for calculation to be practical. The example is of course in Kundt's class, as are those further examples they found where $p = 6$.

As well as giving a way to compare two spacetimes, the theorem above also implies that the Cartan invariants uniquely classify and determine the local geometry. This implies that all local properties are encoded in this information. I will rather briefly discuss some of the possible resulting applications. Aspects I was not able to cover in Lahore included: applications to three-dimensional spaces, including the use in checking junction conditions; applications in numerical relativity; applications to cosmology and to perturbations; use in constructing alternative theories of gravity; and applications to internal state spaces of thermodynamics. I think there must be more we have not yet explored.

Note that global topology is of course not determined by the invariants we have been considering (local invariants cannot distinguish a plane and a flat torus) and nor are continuations which do not respect the required differentiability for the theorem above.

My original motivation can now be carried out for many cases. I used these methods, for example, to disentangle the known exact solutions for inhomogeneous cosmologies with a symmetry group G_2. It would be good to have a complete online catalogue of (at least) the solutions in [35]. Skea and Lake have independently implemented systems to facilitate this. Properties such as the isometry group can also be found [50–52]: for examples see e.g. [53,54]. Similar results apply for homotheties [42].

3.2 Finding solutions

The same ideas can be used to *find* solutions, by working out consistent sets of Cartan invariants and then integrating to get a metric. Examples are mentioned in the exact solutions book. Machado Ramos and Edgar [55,56] used these ideas, implemented in their invariant operator formalism, to find pure radiation solutions of types N and O with a cosmological constant.

Coley and collaborators looked for all spacetimes in which all s.p. invariants vanish (which they called VSI spacetimes although not all Cartan scalar invariants vanish). In the 4-d Lorentzian case these give all spacetimes indistinguishable from flat space by s.p. invariants [57]. The higher dimensional cases give examples in supergravity and string theory. A closely related series of papers has studied the spacetimes with constant s.p. invariants (CSI spacetimes). For a review of this work see [58].

3.3 Limits of families of spacetimes

Another aspect, described first by Paiva *et al.* [59], is the use of invariants to work out the limits of families described by parameters. This enables one to find all possible limits in a coordinate-free way, whereas previous treatments were in effect trial and error. This is another area where further work would be useful.

I did not give more detail in my Lahore lecture, but passed quickly on to limiting points within spacetimes.

3.4 Black hole and other horizons

Karlhede *et al* [60] first noted that $R_{abcd;e}R^{abcd;e} = 0$ at the Schwarzschild horizon (so a prudent space traveller might monitor that). Skea in his thesis [61] noted that this is not true for other horizons (a point rediscussed by Saa [62] for higher-dimensional static cases: Saa also found points where $R_{abcd;e}R^{abcd;e} = 0$ but which are not horizons). Lake [63] continued the work on Kerr by considering first derivative invariants, and found their vanishing characterized the horizons.

Related to my arguments against the claims of Antoci and others that the Schwarzschild horizon was singular, I proposed in 2006 [64] a new test for occurrence of a horizon using ratios of Cartan invariants which works in all cases of Petrov type D. I believe it works more generally, but this needs further study. Maybe it could also be useful to numerical relativists (and space travellers).

More recently Abdelqader and Lake [65,66] have given an invariant characterization of the Kerr horizon, and, prompted by that, Page and Shoom [67] have given another for stationary black holes. I have not yet had the opportunity to check how these relate to earlier characterizations.

Moffat and Toth [68] considered the relation of the "Karlhede invariant" (i.e. $R_{abcd;e}R^{abcd;e}$) to discussions of a "firewall" at the horizon.

3.5 Singularities

Singularities in general relativity are defined to occur when a causal geodesic cannot be continued to infinite affine parameter values even when the spacetime is maximally extended – "geodesic incompleteness" (for the reasons for this definition see [69]).

It is well-known that this happens if an s.p. invariant of the Riemann tensor itself (not its derivatives) blows up along the geodesic. This does not however mean that:
(i) an "infinite" Riemann tensor implies a singularity, or
(ii) if an invariant blows up, there is a singularity, or
(iii) at all singularities, an s.p. invariant of the Riemann tensor blows up.

1. An "infinite" Riemann tensor does not imply a singularity. Geodesics can be continued across a delta function curvature modelling a thin shell or an impulsive gravitational wave.
2. The blowing up of an invariant does not imply a singularity. For example [64] the invariant $1/R_{abcd;e}R^{abcd;e}$ blows up at the Schwarzschild horizon, but the horizon is not singular.
3. There are singularities at which no s.p. invariant of the Riemann tensor blows up. At "whimper" singularities an invariant involving first derivatives does, though [70]. An example was studied by Podolsky and Belan [71].

Question: when does blow up of higher derivative invariants imply a singularity?

Another application is to "directional" singularities, where a singular point apparently has directionally dependent limits. Scott and Szekeres [72,73] showed that the directional singularity of the Curzon metric hid more extended regions at whose boundary the original coordinates broke down. My student Taylor [74] showed that such cases could be appropriately "unravelled" by using level surfaces of Cartan invariants to define new coordinates. Lake [63] used the Weyl tensor s.p. invariants to show that the Kerr singularity was not directional.

With Coley and others [75], I considered "kinematic singularities" (where fluid expansion blows up), giving examples in which, given an integer p, the Cartan (and hence s.p.) scalars can be finite up to the p-th derivative, but not the $(p+1)$-th.

Geodesic continuation needs a C^{2-} metric. In invariantly defined frames the connection coefficients (which would be C^{1-}) are typically expressible as ratios of first derivative Cartan invariants to zeroth derivative ones. We know that there are "intermediate" or "whimper"

singularities where s.p. invariants of the Riemann tensor do not blow up, while s.p. invariants of the first derivatives of the Riemann tensor do. Hence I conjecture that under some suitable differentiability conditions:

Conjecture: Spacetime singularities are either locally extendible or at least one Cartan invariant in $\mathcal{R}^1$ has an infinite limit along any curve approaching the singularity.

References

1. D. Kramer, H. Stephani, M.A.H. MacCallum, E. Herlt, *Exact solutions of Einstein's field equations* (Cambridge University Press, Cambridge, 1980)
2. P. Jordan, J. Ehlers, W. Kundt, Akademie der Wissenschaften und der Literatur, Abhandlungen der Mathematisch-naturwissenschaftliche Klasse (2), 21 (1960). Translated by Anita Ehlers and Manfred Trümper with ample help from Wolfgang Kundt and reprinted in *Gen. Rel. Grav.* **4**1, 2191 (2009)
3. M.A.H. MacCallum, J. Åman, Class. Quant. Grav. **3**, 1133 (1986)
4. S.T.C. Siklos, Singularities, invariants and cosmology. Ph.D. thesis, Cambridge (1976)
5. S.T.C. Siklos, Gen. Rel. Grav. **38**, 1083 (2006)
6. T.Y. Thomas, *Differential invariants of generalised spaces* (Cambridge University Press, Cambridge, 1934)
7. A. Harvey, J. Math. Phys. **36**, 356 (1995)
8. S. Bonanos, Gen. Rel. Grav. **30**, 653 (1998)
9. S.B. Edgar, Gen. Rel. Grav. **31**, 405 (1999)
10. A.E.K. Lim, J. Carminati, J. Math. Phys. **45**, 1673 (2004)
11. J. Carminati, A.E.K. Lim, J. Math. Phys. **47**, 052504 (2006)
12. A.E.K. Lim, J. Carminati, J. Math. Phys. **48**, 083503 (2007)
13. R. Portugal, Comp. Phys. Commun. **115**, 215 (1998)
14. J.M. Martin-Garcia, D. Yllanes, R. Portugal, Comp. Phys. Commun. **179**, 586 (2008)
15. E. Zakhary, C.B.G. McIntosh, Gen. Rel. Grav. **29**, 539 (1997). Errata: *Gen. Rel. Grav.* **29**, 1619-1620 (1997) and **30**, 341-341 (1998)
16. E. Zakhary, J. Carminati, J. Math. Phys. **42**, 1474 (2001)
17. G.E. Sneddon, J. Math. Phys. **40**, 5905 (1999)
18. F.C. Sousa, J.B. Fonseca, C. Romero, Class. Quantum Grav. **25**, 035007 (2008)
19. K.R. Koehler. Parallel symbolic computation of curvature invariants in general relativity. arXiv:cs/0602068 (2006). Submitted to Journal of Computational Physics
20. V. Pravda, J. Bičák. Curvature invariants in algebraically special spacetimes. arXiv:gr-qc/0101085 (2001). Contribution to the 9th Marcel Grossmann meeting (MG9), Rome, July 2000
21. S.T.C. Siklos, Class. Quant. Grav. **13**, 1931 (1996)
22. V. Pravda, Class. Quant. Grav. **16**, 3315 (1999)
23. S. Hervik, Class. Quantum Grav. **21**, 4273 (2004)
24. H.J. Schmidt, Int. J. Theor. Phys. **37**, 691 (1998)
25. A. Coley, S. Hervik, N. Pelavas, Class. Quantum Grav. **26**, 025013 (2009)
26. S. Hervik, A. Coley, Class. Quantum Grav. **27**, 095014 (2010)
27. A.A. Coley, S. Hervik, M.N. Durkee, M. Godazgar, Class. Quantum Grav. **28**, 155016 (2011)
28. S. Hervik, Class. Quantum Grav. **28**, 157001 (2011)
29. A. Coley, S. Hervik, G. Papadopoulos, N. Pelavas, Class. Quantum Grav. **26**, 105016 (2009)
30. J. Podolsky, R. Svarc, Class. Quantum Grav. **30**, 125007 (2013)
31. S. Hervik, V. Pravda, A. Pravdova, CQG **31**, 215005 (2014)
32. S. Hervik, A. Haarr, K. Yamamoto. Degenerate pseudo-Riemannian metrics. arXiv:1410.4347 (2014)
33. S. Sternberg, *Lectures on Differential Geometry* (Prentice-Hall, Englewood Cliffs, N.J., 1964)
34. J. Ehlers, in *E.B. Christoffel*, ed. by P. Butzer, F. Fehér (Birkhäuser Verlag, Basel, 1981), pp. 526-542
35. H. Stephani, D. Kramer, M.A.H. MacCallum, C.A. Hoenselaers, E. Herlt, *Exact solutions of Einstein's field equations, 2nd edition* (Cambridge University Press, Cambridge, 2003). Corrected Paperback edition, 2009
36. C.H. Brans, J. Math. Phys. **6**, 94 (1965)
37. C.H. Brans, J. Math. Phys. **18**, 1378 (1977)
38. A. Karlhede, Gen. Rel. Grav. **12**, 693 (1980)
39. A. Karlhede, J.E. Åman, in *EUROSAM '79: Symbolic and Algebraic Computation*, *Lecture notes in Computer Science*, vol. 72, ed. by E. Ng (Springer, Berlin, 1979), pp. 42–44
40. M.A.H. MacCallum, J.E.F. Skea, in *Algebraic computing in general relativity (Proceedings of the first Brazilian school on computer algebra, vol 2)*, ed. by M. Rebouças, W. Roque (Oxford University Press, Oxford, 1994)
41. D. Pollney, J.E.F. Skea, R.A. D'Inverno, Class. Quant. Grav. **17**, 643 (2000)
42. A. Koutras, Mathematical properties of homothetic space-times. Ph.D. thesis, Queen Mary and Westfield College (1992)
43. J.M. Lang, Contributions to the study of general relativistic shear-free perfect fluids: an approach involving Cartan's equivalence method, differential foms and symbolic computation. Ph.D. thesis, University of Waterloo (1993)
44. A. Karlhede, Class. Quant. Grav. **3**, L1 (1986)
45. É. Cartan, *Leçons sur la géométrie des espaces de Riemann* (Gauthier-Villars, Paris, 1946)
46. R.B. Gardner, *The method of equivalence and its applications* (SIAM, Philadelphia, 1989)
47. P.J. Olver, *Equivalence, invariants, and symmetry* (Cambridge University Press, Cambridge, 1995)
48. A. Karlhede, Class. Quant. Grav. **3**, L27 (1986)
49. R. Milson, N. Pelavas, Int. J. Geom. Meth in Mod. Phys. **06**, 99 (2009)
50. A. Karlhede, M.A.H. MacCallum, Gen. Rel. Grav. **14**, 673 (1982)
51. M.E. Araujo, T. Dray, J.E.F. Skea, Gen. Rel. Grav. **24**, 477 (1992)
52. C. Bona, B. Coll, J. Math. Phys. **33**, 267 (1992)
53. W. Seixas, Class. Quant. Grav. **9**, 225 (1992)
54. M.A.H. MacCallum, S.T.C. Siklos, J. Geom. Phys. **8**, 221 (1992)
55. M.P. Machado Ramos, S.B. Edgar, Class. Quantum Grav. **22**, 791 (2005)
56. S.B. Edgar, M.P. Machado Ramos, Gen. Relativ. Gravit. **39**, 539 (2007)
57. V. Pravda, A. Pravdova, A.A. Coley, R. Milson, Class. Quantum Grav. **19**, 6213 (2002)
58. A. Coley, Class. Quantum Grav. **25**, 033001 (2008). Topical Review
59. F.M. Paiva, M.J. Rebouças, M.A.H. MacCallum, Class. Quant. Grav. **10**, 1165 (1993)
60. A. Karlhede, U. Lindström, J.E. Åman, Gen. Rel. Grav. **14**, 569 (1982)

61. J.E.F. Skea, Anisotropic cosmologies and curvature invariants. Ph.D. thesis, University of Sussex (1986)
62. A. Saa, Class. Quantum Grav. **24**, 2929 (2007)
63. K. Lake, Gen. Relativ. Gravit. **35**, 2271 (2003)
64. M.A.H. MacCallum, Gen. Rel. Grav. **38**, 1887 (2006)
65. M. Abdelqader, K. Lake, Phys. Rev. D **88**, 064042 (2013)
66. M. Abdelqader, K. Lake. An invariant characterization of the Kerr spacetime: Locating the horizon and measuring the mass and spin of rotating black holes using curvature invariants. arXiv:1412.8757 (2014)
67. D.N. Page, A.A. Shoom. Local invariants vanishing on stationary horizons. arXiv:1510.03510 (2015)
68. J.W. Moffat, V.T. Toth. Karlhede's invariant and the black hole firewall proposal. arXiv:1404.1845 (2014)
69. R. Geroch, Annals of Physics **48**, 526 (1968)
70. S.T.C. Siklos, Commun. Math. Phys. **58**, 255 (1978)
71. J. Podolsky, M. Belan, Class. Quantum Grav. **21**, 2811 (2004)
72. S.M. Scott, P. Szekeres, Gen. Rel. Grav. **18**, 557 (1986)
73. S.M. Scott, P. Szekeres, Gen. Rel. Grav. **18**, 571 (1986)
74. J.P.W. Taylor, Class. Quant. Grav. **22**, 4961 (2005)
75. A.A. Coley, S. Hervik, W.C. Lim, M.A.H. MacCallum, Class. Quantum Grav. **26**, 215008 (2009)

Proc. Int. Conf. Relativ. Astrophys.
Pages 129-131, (2015)

Non-Singular Co-ordinates for Reissner Nordström Black Hole Surrounded by Quintessence

Bushra Majeed[a,1], **Azad A. Siddiqui**[b,1]

[1]School of Natural Sciences (SNS), National University of Sciences and Technology (NUST), H-12, Islamabad, Pakistan

Abstract Non-singular coordinates (T, R) for Reissner Nordström black hole surrounded by quintessence are obtained in this paper. We also find the geodesics equations of a test particle moving around the black hole, in these coordinates. In particular, it is observed that the value of dT/dR, is regular on the event horizon of the black hole in contrast with the derivative $dt/dr = \infty$, at the event horizon.

1 Introduction

Accelerated expansion of the universe is a well known observational phenomena in this era. Many candidates for dark energy have been proposed to explain this expansion behavior [1]. Quintessence field is a scalar field coupled to gravity, a candidate for dark energy, with state parameter in the range , $-1 < w_q < \frac{-1}{3}$ [2, 3]. Many aspects of quintessence field have been studied in literature (for details see [4]). Kiselev derived the solution for a spherically symmetric black hole surrounded by quintessence field [12]. In this paper we consider the Reissner Nordström black hole surrounded by quintessence (RN-Quintessence) and obtain its metric in non-singular coordinates.

In (t, r) coordinates, Schwarzschild spacetime has a singularity at $r = 2M$, where M is the black hole mass, which could be removed by using Kruskal coordinates and the maximal singularity free extension of Schwarzschild geometry is obtained [5]. Eddington Finkelstein (EF) and Kruskal Szekeres (KS) [6–8] coordinates are the most popular coordinate systems in which schwarzschild metric is regular at event horizon $r = 2M$. Extending this approach to other black hole metrics with an event horizon, the coordinate singularities could be avoided and the interior and exterior regions of the black hole could be described by the same metric [10, 11].

Kinematics of a test particle around a black hole could be better understood in KS coordinates (T, R) because working in these coordinates there is no barrier on the geodesics of the particle due to event horizon [9–11].

Constructing the KS-like coordinates for the RN-Quintessence black hole we derive the expression for the KS derivative dT/dR. We shall show that in accordance with the singularity free nature of the KS coordinates, geodesics are regular on the horizon in these coordinates. Plan of the paper is as follows: In section II coordinate singularities of the RN-Quintessence are discussed. In section III we present non singular KS-like coordinates for the RN-Quintessence black hole. In section IV geodesics of a test particle in KS-like coordinates are given. Conclusion is given in the last section.

2 Reissner Nordström Black Hole Surrounded by Quintessence

The spherically symmetric and static solution for Einstein's field equations, in the presence of energy-matter, was investigated by Kiselev [12], known as quintessence and black holes. Metric of the RN-Quintessence black hole is defined as [13]

$$ds^2 = -f(r)dt^2 + \frac{1}{f(r)}dr^2 + r^2(d\theta^2 + \sin^2\theta d\phi^2), \quad (1)$$

where $f(r)$ is

$$f(r) = 1 - \frac{2M}{r} + \frac{Q^2}{r^2} - \frac{\sigma}{r^{1+3\omega_q}}, \quad (2)$$

[a]Email Address: bushra.majeed@sns.nust.edu.pk
[b]Email Address: azad@sns.nust.edu.pk

here Q is charge of the black hole, and σ is normalization parameter and ω_q is state parameter of the quintessence field [12]. Choosing $\omega_q = \frac{-2}{3}$ we have

$$f(r) = \frac{-\sigma r^3 + r^2 - 2Mr + Q^2}{r^2}. \quad (3)$$

Solving $f(r) = 0$, horizons of black hole are obtained. Depending on the nature of the discriminant, Δ,

$$\Delta = 4(M^2 - Q^2) + \sigma(-32M^3 + 36MQ^2) - 27\sigma^2 Q^4, \quad (4)$$

of the cubic equation $\sigma r^3 - r^2 + 2Mr - Q^2 = 0$, there are following possible cases for the roots:

- All real roots,
- One real root and two complex roots.

We consider the later case, i.e. when $f(r)$ has one real root, $r = r_3$ (say), and two complex roots, in this case the RN- Quintessence spacetime has one horizon at $r = r_3$. We can write $f(r)$ as

$$f(r) = \frac{(r - r_3)(-\sigma r^2 + r(1 - \sigma r_3) + r_3 - \sigma r_3^2 - 2M)}{r^2}, \quad (5)$$

here $r = r_3$ is a coordinate singularity, we can remove it by an appropriate change of coordinates.

3 Non-singular coordinates for RN-Quintessence Black Hole

The in-going and out-going null geodesics of a particle moving around black hole satisfy

$$t = \pm r^* + constant, \quad (6)$$

where

$$r^* = \int \frac{dr}{f(r)}. \quad (7)$$

Define new coordinates u and v having directions of null geodesics as [6,7]

$$u = t - r^*, \quad v = t + r^*. \quad (8)$$

Kruskal and Szekeres developed a coordinate system [8], which changes (t, r) to (T, R), while θ and ϕ are left unchanged, given as

$$U = -\alpha \exp(\frac{-u}{\beta}), \quad V = \alpha \exp(\frac{v}{\beta}), \quad (9)$$

where α and β are arbitrary constants. Using Eqs. (8) and (9) the metric given in Eq. (1) becomes

$$ds^2 = -f(r) e^{\frac{-2r^*}{\beta}} \frac{\beta^2}{\alpha^2} dU dV + r^2(d\theta^2 + \sin^2\theta d\phi^2). \quad (10)$$

Or metric could be better understood with the help of coordinates T and R which correspond to mutually perpendicular axis, defined as

$$T = \frac{V + U}{2}, \quad R = \frac{V - U}{2}. \quad (11)$$

Using Eq. (11) in Eq. (10) we get

$$ds^2 = -F(r)(dT^2 - dR^2) + r^2(d\theta^2 + \sin^2\theta d\phi^2), \quad (12)$$

where $F(r) = \frac{f(r)\beta^2}{\alpha^2} e^{-2r^*/\beta}$.
Using Eq. (7) with Eq. (5) we have

$$r^* = \frac{-2(M + r_3 M\sigma + r_3(-1 + \sigma r_3)) \tan^{-1}(\frac{-1 + 2\sigma r + \sigma r_3}{K})}{K\lambda}$$
$$- \frac{r_3^2 \ln|r - r_3|}{\lambda} - \frac{M + r_3(-1 + \sigma r_3) \ln(X)}{\sigma\lambda}, \quad (13)$$

where

$$\lambda = 2M + r_3(-2 + 3\sigma r_3)$$
$$K = \sqrt{-1 + 8M\sigma - 2\sigma r_3 + 3r_3^2\sigma^2}$$
$$X = 2M + r^2\sigma + r(-1 + \sigma r_3) + r_3(-1 + \sigma r_3).$$

If we chose

$$\beta = \frac{(-2r_3^2)}{\lambda}, \quad \alpha = 1, \quad (14)$$

the metric given in Eq. (12) transforms to

$$ds^2 = -\frac{(-\sigma r^2 + r(1 - \sigma r_3) + r_3 - \sigma r_3^2 - 2M)}{r^2} \frac{(-2r_3^2)^2}{\lambda^2}$$
$$\left(\exp\left(\frac{-4(M + r_3 M\sigma + r_3(-1 + \sigma r_3)) \tan^{-1}(\frac{-1 + 2\sigma r + \sigma r_3}{K})}{2r_3^2 K\lambda}\right)\right)$$
$$(X)^{-\frac{M + r_3(-1 + \sigma r_3)}{\sigma r_3^2}} dU dV + r^2(d\theta^2 + \sin^2\theta d\phi^2). \quad (15)$$

Notice that the metric given is Eq. (15) is regular at $r = r_3$ so the coordinate singularity is removed in new coordinates (T, R). Relation between new and old coordinates is

$$R^2 - T^2 = \exp(2r^*/\beta), \quad (16)$$

using Eq. (3) we get

$$R^2 - T^2 = \exp$$
$$\left(\frac{4(M + r_2 M\sigma + r_3(-1 + \sigma r_3)) \tan^{-1}\left(\frac{-1 + 2\sigma r + \sigma r_3}{K}\right)}{2r\frac{2}{3} K\lambda}\right)$$
$$(r - r3)(2M + r^2\sigma + rX)^{\frac{M + r_3(-1 + \sigma r_3)}{\sigma r_3^2}}, \quad (17)$$

clearly at $r = r_3$

$$R^2 - T^2 = 0. \quad (18)$$

4 Geodesics of a Test particle Moving around RN-Quintessence Black Hole

Since the RN-Quintessence black hole metric is invariant under time translation and rotation around symmetry axis so the Killing vectors

$$\xi^{\mu}_{(t)}\partial_{\mu} = \partial_t, \qquad \xi^{\mu}_{(\phi)}\partial_{\mu} = \partial_{\phi}, \tag{19}$$

will give the constants of motion, where $\xi^{\mu}_{(t)} = (1,\ 0,\ 0,\ 0)$ and $\xi^{\mu}_{(\phi)} = (0,\ 0,\ 0,\ 1)$. The corresponding conserved quantities are the energy per unit mass $\mathcal{E}$ and angular momentum L of the moving particle, given by

$$\mathcal{E} = -f\dot{t}, \tag{20}$$

$$L = r^2\dot{\phi}. \tag{21}$$

The dot denotes the differentiation with respect to proper time τ and $f := f(r)$ throughout the calculations. Considering the planar motion of the particle i.e. for $\theta = \pi/2$ the normalization condition $u^{\mu}u_{\mu} = -1$, gives

$$\dot{r}^2 = \mathcal{E}^2 - V_{eff}, \tag{22}$$

where V_{eff} is the effective potential given as

$$V_{eff} = (1 - \frac{2M}{r} + \frac{Q^2}{r^2} - \sigma r)(1 + \frac{L^2}{r^2}). \tag{23}$$

Geodesics of a particle moving around a black hole are given by

$$\frac{dt}{dr} = \pm\frac{\mathcal{E}}{f(r)\sqrt{\mathcal{E}^2 - V_{eff}}}. \tag{24}$$

Since $f(r_3) = 0$ so the geodesics equation diverges at $r = r_3$, we can say that the geodesics are not complete in usual (t, r) coordinates. We need to write geodesics equation in modified (non-singular) coordinates.

Using Eqs. (7) and (8) along with Eq. (24) we get geodesic equation in KS coordinates as

$$\frac{dv}{du} = \frac{1 + A}{1 - A}, \tag{25}$$

where

$$A = \frac{\pm(\sqrt{\mathcal{E}^2 - V_{eff}})}{\mathcal{E}}. \tag{26}$$

Further using Eq. (26) with Eq. (9) we obtain

$$\frac{dV}{dU} = \frac{-V}{U}\Big(\frac{1 + A}{1 - A}\Big). \tag{27}$$

Using Eq. (27) with Eq. (11) we have

$$\frac{dR}{dT} = \frac{(T + R)(\mathcal{E} + A) + (T - R)(\mathcal{E} - A)}{(T + R)(\mathcal{E} + A) - (T - R)(\mathcal{E} - A)}. \tag{28}$$

This is clear from Eq. (28) that the geodesics equations are well behaved at singularity $r = r_3$.

5 Conclusion

Using the similar transformations, as introduced by Kruskal Szekeres, to obtain well known Kruskal Szekeres coordinates for the Schwarzschild black hole, we have obtained non-singular Kruskal Szekeres like coordinates for the Reissner Nordström black hole surrounded by quintessence, for the case when it has one horizon only. Further we find the expression for the geodesics equations in these coordinates. It is observed that the singularity appearing in the geodesics equations in usual (t, r) coordinates is removed in the new constructed Kruskal Szekeres (T, R) coordinates.

References

1. A.G. Riess et. al., Astron. J. 116 1009 (1998).
2. E. J. Copeland, M. Sami and S. Tsujikawa, Int. Jour. Modern. Phys. D15 (2006) 1753.
3. S. M. Carroll, Phys. Rev. Lett. 81 (1998) 3067.
4. S. Tsujikawa, Class. Quant. Grav., 30 (2013) 214003.
5. M. D. Kruskal, Phys. Rev. 119 (1960) 5.
6. A. S. Eddington, Nature 113 (1924) 192.
7. D. Finkelstein, Phys. Rev. 110 (1958) 965.
8. M. D. Kruskal, Phys. Rev. 119 (1960) 1743; G. Szekres, Publ. Mat. Debrecen, 7 (1960) 285.
9. A. Mitra, Astron. Astrophys. 2 (2012) 174.
10. A. Qadir, and A. A. Siddiqui, Int. J. Mod. Phys. D 16 (2007) 25.
11. S. J. Riaz A. A. Siddiqui, Gen. Relativ. Gravit. 43 (2011) 1167.
12. V.V. Kiselev, Class. Quant. Grav. 20 (2003) 1187.
13. S. Fernando, Gen. Relativ. Gravit. 45 (2013) 2053. 1

Proc. Int. Conf. Relativ. Astrophys.
Pages 132-139, (2015)

Dynamical Stability of Stars in Brans-Dicke Gravity:

M. Sharif [1], **Rubab Manzoor** [2]

[1]Department of Mathematics, University of the Punjab, Quaid-e-Azam Campus, Lahore-54590, Pakistan
[2]Department of Mathematics, University of Management and Technology, Johar Town Campus, Lahore-54782, Pakistan

Abstract Stability analysis can be used to describe gravitational collapse phenomenon in modified theories of gravity. It can explains collapse in different configurations (spherically, cylindrically and axially symmetries etc) as well as in different dynamical conditions, i.e., effects of dissipation and electromagnetism etc. In this manuscript, we explain instability of spherically symmetric star in Brans- Dicke gravity. For this purpose, we use contracted bianchi identities and perturbation approach to construct collapse equation (hydrostatic equilibrium). We obtain instability ranges in Newtonian regimes by incorporating equation of state involving adiabatic index (Γ).

PACS 04.50.Kd, 04.40.Dg, 04.25.Nx

Keywords Brans-Dicke theory, Instability, Newtonian Regimes

1 Introduction

Brans-Dicke (BD) theory, one of the most fascinated examples of scalar-tensor theories, is a generalized form of general relativity. It has the following main features: relation of scalar field ϕ with dynamical gravitational constant ($G = \frac{G_0}{\phi}$), a tuneable constant coupling parameter ω_{BD}, non-minimal coupling of geometry (R) with scalar field, compatibility with Mach's principle, Dirac's large number hypothesis and weak equivalence principle. This theory satisfies all weak field regimes test (solar system experiments and observation) for $|\omega| \geq 40,000$. It is the most dominant and prevailing case of modified theories which provides convenient evidences of many cosmic problems such as early and late behavior of the universe, inflation, coincidence problem and cosmic acceleration [1,2].

In relativistic physics, the phenomenon of dynamical instability of self-gravitating objects (stellar collapse) has been an interesting issue. Stellar collapse is a process in which a massive body collapses due to its own gravitational pull or it is a phenomenon in which stable celestial bodies turn into unstable objects due to their own gravity. It is well-known that different ranges of stability for celestial objects lead to different structures of collapsing objects as well as different evolution approaches of astronomical bodies during the collapse.

Chandrasekhar [3] was the first who described the instability ranges of isotropic fluid in general relativity (GR) with the help of adiabatic index Γ and found that the fluid becomes unstable for $\Gamma < \frac{4}{3}$. Later, many people [4]-[7] explored dynamical stability for anisotropic, shearing viscous, adiabatic as well as non adiabatic fluid and concluded that instability ranges depend on different physical characteristics of the fluid.

There has been a large body of literature which indicates keen interest on the stability analysis in modified theories of gravity. Nutku [8] investigated dynamical instability of isotropic fluid in BD gravity and found that the fluid remains unstable for $\Gamma > \frac{4}{3}$. Kwon et al. [9] described different stability ranges for the Schwarzschild black hole in BD gravity. Sharif and Kauser [10, 11] studied stability analysis for spherical as well as cylindrical collapsing system in $f(R)$ gravity. Sharif and Yousaf [12]-[15] explored the effects of matter variables as well as electromagnetic field on stability analysis for different cases in $f(R)$ theory of gravity. Sharif and Rani [16] investigated dynamical instability of spherical collapse in $f(T)$ gravity.

In this paper, we explore dynamical instability of spherically symmetric anisotropic collapsing model in BD gravity. The paper is designed in the following for-

[1]msharif.math@pu.edu.pk
[2]rubab.manzoor@umt.edu.pk

mat. The next section deals with BD equations, junction conditions and two dynamical equations describing the evolution of collapse. In section **3**, we apply perturbation scheme to BD as well as dynamical equations and obtain collapse equation from static and non-static configurations of dynamical equations. Section **4** explores dynamical instability ranges at Newtonian approximation. Finally, we summarize our results in the last section.

2 Brans-Dicke Gravity and Dynamical Equations

Brans-Dicke theory is the natural extension of GR in which gravity is mediated by the tensor field of GR and a massless scalar field. The action of self-interacting BD gravity with $8\pi G_0 = c = 1$ is [1]

$$S = \int d^4x\sqrt{-g}[\phi R - \frac{\omega_{BD}}{\phi}\nabla^\alpha\phi\nabla_\alpha\phi - U(\phi) + L_m], \quad (1)$$

where $U(\phi)$ and L_m represent the self-interacting potential and matter contribution, respectively. By varying Eq.(1) with respect to $g_{\mu\nu}$ and ϕ, we obtain BD equations as

$$G_{\mu\nu} = \frac{1}{\phi}(T^m_{\mu\nu} + T^\phi_{\mu\nu}), \quad (2)$$

$$\phi^{;\mu}_{;\mu} = \frac{T^m}{3+2\omega_{BD}} + \frac{1}{3+2\omega_{BD}}[\phi\frac{dU(\phi)}{d\phi} - 2U(\phi)], \quad (3)$$

where $G_{\mu\nu}$ $(\mu,\ \nu = 0,1,2,3)$ represents the Einstein tensor, $T^m_{\mu\nu}$ is a stress energy tensor of matter fluid, T^m is the trace of $T^m_{\mu\nu}$.

$$T^\phi_{\mu\nu} = [\phi_{,\mu;\nu} - g_{\mu\nu}\phi^{;\mu}_{;\mu}] + \frac{\omega_{BD}}{\phi}[\phi_{,\mu}\phi_{,\nu} - \frac{1}{2}g_{\mu\nu}\phi_{,\alpha}\phi^{;\alpha}] - \frac{U(\phi)}{2}g_{\mu\nu}, \quad (4)$$

defines the energy part of scalar field. Equation (2) describes the respective BD field equations and Eq.(3) being a wave equation describes the evolution of scalar field.

In order to discuss spherically symmetric collapse, we take 3-dimensional hypersurface $\Sigma^{(e)}$ as an external boundary of collapsing star. In this way, the 4-dimensional geometry splits into two regions named as exterior and interior spacetimes. The line element of interior spacetime is described by the most general spherically symmetric metric as

$$ds^2_- = A^2(t,r)dt^2 - B^2(t,r)dr^2 - C^2(t,r)d\theta^2 - C^2(t,r)\sin^2\theta d\phi^2). \quad (5)$$

In BD gravity, the only physically valid vacuum static spherical solution is the Schwarzschild solution which is taken as the exterior metric to $\Sigma^{(e)}$, having the line element of the form

$$ds^2_+ = \left(1 - \frac{2M}{r}\right)d\nu^2 + 2drd\nu - r^2(d\theta^2 + \sin^2\theta d\phi^2). \quad (6)$$

Here M is the total mass of the system and ν represents the retarded time, respectively. We assume that the interior region is filled with a non-dissipative anisotropic fluid described by the energy-momentum tensor as

$$T^m_{\mu\nu} = (\rho + p_\perp)u_\mu u_\nu - p_\perp g_{\mu\nu} + (p_r - p_\perp)\chi_\mu\chi_\nu, \quad (7)$$

where ρ is the energy density, $p_\perp$ represents the tangential pressure and p_r is the radial pressure. The four velocity, u^μ and a unit four-vector (along the radial direction), χ^μ, are evaluated by the relations $u^\mu = A^{-1}\delta^\mu_0$ and $\chi^\mu = B^{-1}\delta^\mu_1$, which satisfy $u^\mu u_\mu = 1,\ \chi^\mu\chi_\mu = -1,\ \chi^\mu u_\mu = 0$.

For the interior metric, the field equations (2) become

$$\left(\frac{2\dot{B}}{B} + \frac{\dot{C}}{C}\right)\frac{\dot{C}}{C} - \left(\frac{A}{B}\right)^2\left[\frac{2C''}{C} + \left(\frac{C'}{C}\right)^2 - \frac{2B'C'}{BC} - \left(\frac{B}{C}\right)^2\right] = \frac{1}{\phi}\left(\rho A^2 + \frac{\omega_{BD}}{2\phi}(\dot{\phi}^2 + \frac{A^2\phi'^2}{B^2})\right) - \frac{\dot{\phi}}{\phi}\left(\frac{\dot{A}}{A} + \frac{\dot{B}}{B} + \frac{2\dot{C}}{C}\right) + \frac{\phi'}{\phi CB^2}\left(\frac{A^2B'C}{B} + 2AA'C + 2A^2C'\right) + \frac{A^2\phi''}{B^2\phi} - \frac{A^2U(\phi)}{2\phi}, \quad (8)$$

$$2\left(-\frac{\dot{C}'}{C} + \frac{\dot{C}A'}{CA} + \frac{\dot{B}C'}{BC}\right) = \frac{\omega_{BD}}{\phi^2}(\dot{\phi}\phi') + \frac{1}{\phi}\left(\dot{\phi}' - \frac{\dot{A}\dot{\phi}}{A} - \frac{\dot{B}\phi'}{B}\right), \quad (9)$$

$$-\left(\frac{B}{A}\right)^2\left[\frac{2\ddot{C}}{C} - \left(\frac{2\dot{A}}{A} - \frac{\dot{C}}{C}\right)\frac{\dot{C}}{C}\right] + \left(\frac{2A'}{A} + \frac{C'}{C}\right)\frac{C'}{C} - \left(\frac{B}{C}\right)^2 = \frac{1}{\phi}\left(p_rB^2 + \frac{\omega_{BD}}{2\phi}(\phi'^2 + \frac{B^2\dot{\phi}^2}{A^2})\right) + \frac{\dot{\phi}}{\phi A^2C}\left(\frac{\dot{A}}{A}CB^2 + 2B\dot{B}C + \frac{2\dot{C}B^2}{C}\right) + \frac{\phi'}{\phi}\left(\frac{B'}{B} + \frac{A'}{A} + \frac{2C'}{C} + \frac{\dot{B}}{B}\right) + \frac{B^2U(\phi)}{2\phi}, \quad (10)$$

$$-\left(\frac{C}{A}\right)^2\left[\frac{\ddot{B}}{B} + \frac{\ddot{C}}{C} - \frac{\dot{A}}{A}\left(\frac{\dot{B}}{B} + \frac{\dot{C}}{C}\right) + \frac{\dot{B}\dot{C}}{BC}\right] + \left(\frac{C}{B}\right)^2 \times \left[\frac{A''}{A} + \frac{C''}{C} + \frac{A'B'}{AB} + \left(\frac{A'}{A} - \frac{B'}{B}\right)\frac{C'}{C}\right] = \frac{1}{\phi} \times \left(p_\perp C^2 + \frac{\omega_{BD}}{2\phi}(\frac{\dot{C}^2\dot{\phi}^2}{A^2} - \frac{C^2\phi'^2}{B^2})\right)$$

$$+\frac{\dot{\phi}}{A^2B\phi}\left(\dot{A}ABC^2+\dot{B}C^2+C\dot{C}B\right)-\frac{\phi'}{AB^2\phi}$$
$$\times\left(\frac{B'AC^2}{B}+A'C^2+3CC'A\right)+\frac{\ddot{\phi}C^2}{A^2\phi}+\frac{C^2U(\phi)}{2\phi}, \quad (11)$$

and the corresponding wave equation (5) takes the form

$$\dot{\phi}\left(-\frac{\dot{A}}{A}+\frac{\dot{B}}{A^2B}+\frac{2\dot{C}}{A^2B}\right)+\frac{\ddot{\phi}}{A^2}+\phi'\left(-\frac{A'}{AB^2}\right.$$
$$\left.+\frac{B'}{B^3}-\frac{2C'}{CB^2}\right)-\frac{\phi''}{B^2}=\frac{1}{2\omega_{BD}+3}\left[(\rho-p_r\right.$$
$$\left.-p_\perp)+\left(\phi\frac{dU}{d\phi}-2U\right)\right]. \quad (12)$$

Here prime and dot describe differentiation with respect to r and t, respectively.

Junction conditions represent the correct behavior of an exterior spacetime by smoothly connecting the exterior region to the interior region over a hypersurface $\Sigma^{(e)}$. Darmois junction conditions are assumed to be more appropriate to discuss gravitational collapse. For this purpose, we use Misner-Sharp mass function, $m(t,r)=\frac{C}{2}(1+g^{\mu\nu}C_{,\mu}C_{,\nu})$, which describes the total energy of spherical object of radius C. For Eq.(5), it becomes

$$m(t,r)=\frac{C}{2}\left(1+\frac{\dot{C}^2}{A^2}-\frac{C'^2}{B^2}\right). \quad (13)$$

Since in BD theory, the metric tensor as well as scalar field are the gravitational field variables (source of gravity), therefore, the matching of the exterior and interior regions require $\phi=\phi_{\Sigma^{(e)}}=$ constant along with continuity of first and second fundamental forms (Darmois conditions) [17]. The above consideration yields the following results on the boundary surface

$$r=r_{\Sigma^{(e)}}=\text{constant}, \quad M=^{\Sigma^{(e)}} m(t,r), \quad (14)$$

and

$$2\left(\frac{\dot{C}'}{C}-\frac{\dot{C}A'}{CA}-\frac{\dot{B}C'}{BC}\right)=\Sigma^{(e)}-\frac{B}{A}\left[\frac{2\ddot{C}}{C}-\left(\frac{2\dot{A}}{A}-\right.\right.$$
$$\left.\left.+\frac{\dot{C}}{C}\right)\frac{\dot{C}}{C}\right]+\frac{A}{B}\left[\left(\frac{2A'}{A}+\frac{C'}{C}\right)\frac{C'}{C}-\left(\frac{B}{C}\right)^2\right]. \quad (15)$$

Substituting the field equations (9) and (10) in the above equation, we get

$$\frac{-p_r}{\phi}=^{\Sigma^{(e)}}\frac{T^\phi_{11}}{B^2}-\frac{T^\phi_{01}}{AB}=\frac{U(\phi)}{2\phi}, \quad (16)$$

which represents the conservation of momentum flux across $\Sigma^{(e)}$. Dynamical equations of the collapsing star are obtained from the non-trivial contracted Bianchi identities, which provide conservation of total energy of the collapsing system. These identities are given as follows

$$\left(\frac{T^{\mu\nu}_m}{\phi}+\frac{T^{\mu\nu}_\phi}{\phi}\right)_{;\nu}u_\mu=0, \quad \left(\frac{T^{\mu\nu}_m}{\phi}+\frac{T^{\mu\nu}_\phi}{\phi}\right)_{;\nu}\chi_\mu=0, \quad (17)$$

yielding

$$\left[\frac{\dot{\rho}}{A}-\frac{\rho\dot{\phi}}{\phi^2A}+(\rho+p_r)\frac{\dot{B}}{AB}+2(\rho+p_\perp)\frac{\dot{C}}{AC}\right]$$
$$+H_1=0, \quad (18)$$
$$\left[\frac{p'_r}{B}+\frac{\phi'p_r}{\phi^2B}+(\rho+p_r)\frac{A'}{AB}+2(p_r-p_\perp)\frac{C'}{BC}\right]$$
$$+H_2=0, \quad (19)$$

where H_1 and H_2 are mentioned in Appendix **A**.

3 Perturbation Scheme

In this section, we develop collapse equation with the help of perturbation scheme. We assume that initially the system is in static equilibrium, i.e., material as well as metric parts have radial dependence only. After that all the metric functions and other dynamical quantities are perturbed and become time dependent. The metric functions and scalar field have the same time dependence, while the pressure, density and scalar potential have the same time dependence in their perturbations. We define

$$A(t,r)=A_0(r)+\varepsilon T(t)a(r), \quad (20)$$
$$B(t,r)=B_0(r)+\varepsilon T(t)b(r), \quad (21)$$
$$C(t,r)=C_0(r)+\varepsilon T(t)c(r), \quad (22)$$
$$\phi(r,t)=\phi_o(r)+\varepsilon T(t)\Phi(r), \quad (23)$$
$$p_r(t,r)=p_{r0}(r)+\varepsilon\bar{p}_r(t,r), \quad (24)$$
$$p_\perp(t,r)=p_{\perp0}(r)+\varepsilon\bar{p}_\perp(t,r), \quad (25)$$
$$\rho(t,r)=\rho_0(r)+\varepsilon\bar{\rho}(t,r), \quad (26)$$
$$U(\phi)=U_0(r)+\varepsilon\bar{U}(t,r), \quad (27)$$

where $0<\varepsilon\ll1$ and the static background is described by subscript zero. In order to obtain static and perturbed distribution of the field and dynamical equations, we choose $C_0=r$ as a radial coordinate. The static configuration of Eqs.(8)-(11) becomes

$$\frac{\rho_0}{\phi_0}+\frac{\omega_{BD}\phi_0'^2}{2B_0^2\phi_0^2}+\frac{B_0'\phi_0'}{B_0^3\phi_0}+\frac{2A_0'\phi_0'}{A_0B_0^2\phi_0}+\frac{2\phi_0'}{B_0^2r\phi_0}$$
$$+\frac{\phi_0''}{B_0^2\phi_0}+\frac{U_0}{2\phi_0}=\frac{1}{(B_0r)^2}\left(2r\frac{B_0'}{B_0}+B_0^2-1\right), \quad (28)$$
$$\frac{p_{r0}}{\phi_0}+\frac{\omega_{BD}\phi_0'^2}{2B_0^2\phi_0^2}-\frac{B_0'\phi_0'}{B_0^3\phi_0}-\frac{A_0'\phi_0'}{A_0B_0^2\phi_0}-\frac{2\phi_0'}{B_0^2r\phi_0}+\frac{U_0}{2\phi_0}$$

$$= \frac{1}{(B_0 r)^2}\left(2r\frac{A_0'}{A_0} - B_0^2 + 1\right), \tag{29}$$

$$\frac{p_{\perp 0}}{\phi_0} + \frac{\omega_{BD}\phi_0'^2}{2B_0^2\phi_0^2} - \frac{B_0'\phi_0'}{B_0^3\phi_0} - \frac{A_0'\phi_0'}{A_0 B_0^2\phi_0} - \frac{3\phi_0'}{B_0^2 r\phi_0} + \frac{\phi_0''}{B_0^2\phi_0} + \frac{U_0}{2\phi_0} = \frac{1}{B_0^2}\left[\frac{A_0''}{A_0} - \frac{A_0'}{A_0}\frac{B_0'}{B_0} + \frac{1}{r}\left(\frac{A_0'}{A_0} - \frac{B_0'}{B_0}\right)\right] . \tag{30}$$

The corresponding static distribution of wave equation is

$$\frac{\phi_0' A_0'}{A_0 B_0^2} - \frac{\phi_0' B_0'}{B_0^3} + \frac{2\phi_0'}{r B_0^2} = \frac{-1}{2\omega_{BD}+3}\left[(\rho_0 - p_{r0} - p_{\perp 0}) + (\phi_0 U_0 - 2U_0)\right].$$

The first dynamical equation (18) is identically satisfied in the static background while (19) turns out as

$$p_{r0}' + \frac{\phi_0' p_{r0}}{\phi_0} + (\rho_0 + p_{r0})\frac{A_0'}{A_0} + \frac{2}{r}(p_{r0} - p_{\perp 0}) - \frac{H_2'}{B_0\phi_0} = 0, \tag{31}$$

where H_2' is given in Appendix **A**. The junction condition (16) for static configuration is

$$\frac{p_{r0}}{\phi_0} =^{\Sigma^{(e)}} \frac{-U_0}{2\phi_0}, \tag{32}$$

and the perturbed form of the field Eqs.(8)-(11) takes the form

$$-\frac{2T}{B_0^2}\left[\left(\frac{c}{r}\right)'' - \frac{1}{r}\left(\frac{b}{B_0}\right)' - \left(\frac{B_0'}{B_0} - \frac{3}{r}\right)\left(\frac{c}{r}\right)' - \left(\frac{b}{B_0} - \frac{c}{r}\right)\left(\frac{B_0}{r}\right)^2\right] = -\frac{\bar{\rho}}{\phi_0} - \frac{T\rho_0\Phi}{\phi_0^2} + \frac{T\omega_{BD}\phi_0'^2 b}{\phi_0^2 B_0^3} + \frac{T\phi_0'}{\phi_0 B_0^2}\left[2\left(\frac{a}{A_0}\right)' + 2\left(\frac{c}{r}\right)' + \left(\frac{b}{B_0}\right)'\right] + \frac{2Tb\phi_0'}{\phi B_0^3} \times \left[\frac{A_0'}{A_0} - \frac{1}{r}\right] + \left[\frac{T}{B_0^2 r} + \frac{TA_0'}{B_0^2 A_0} + \frac{TB_0'}{B_0^3}\right]\left[\frac{\Phi}{\phi_0}\right]' + \frac{T\Phi''}{\phi_0 B_0^2} - \frac{2Tb\phi_0''}{B_0^3\phi_0} - \frac{T\phi_0'\Phi}{B_0^2\phi_0^2} - \frac{TU_0\Phi}{2\phi_0^2} - \frac{T\bar{U}}{2\phi_0}, \tag{33}$$

$$-\frac{c'}{c} + \frac{A_0'}{A_0} + \frac{b}{cB_0} = \frac{\omega_{BD}\dot{T}\Phi'}{\phi_0^2} - \frac{\dot{T}\Phi'}{\phi_0}, \tag{34}$$

$$-\frac{2\ddot{T}B_0^2 c}{rA_0^2} + \frac{2T}{r}\left[\left(\frac{a}{A_0}\right)' + \left(r\frac{A_0'}{A_0} + 1\right)\left(\frac{c}{r}\right)' + \frac{B_0^2}{r} \times \left(\frac{c}{r} - \frac{b}{B_0}\right)\right] = \frac{\bar{p}_r}{\phi_0} - \frac{Tp_{r0}\Phi}{\phi_0^2} - \frac{T\omega_{BD}\phi_0'^2 b}{\phi_0^2 B_0^3} - \frac{T\phi_0'}{\phi_0 B_0^2} \times \left[\left(\frac{a}{A_0}\right)' + 2\left(\frac{c}{r}\right)' + \left(\frac{b}{B_0}\right)'\right] + \frac{2Tb\phi_0'}{\phi B_0^3}\left[\frac{A_0'}{A_0} - \frac{1}{r}\right] - \left[\frac{T}{B_0^2 r} + \frac{TA_0'}{B_0^2 A_0} - \frac{TB_0'}{B_0^3}\right]\left[\frac{\Phi}{\phi_0}\right]' - \frac{\dot{T}b\phi_0'}{\phi_0 B_0^2} + \frac{\ddot{T}\Phi}{A_0^2\phi_0} - \frac{TU_0\Phi}{2\phi_0^2} + \frac{T\bar{U}}{2\phi_0}, \tag{35}$$

$$-\frac{\ddot{T}}{A_0^2}\left(\frac{b}{B_0} + \frac{c}{r}\right) + \frac{T}{B_0^2}\left[\left(\frac{a}{A_0}\right)'' + \left(\frac{c}{r}\right)'' + \left(\frac{2A_0'}{A_0} - \frac{B_0'}{B_0} + \frac{1}{r}\right)\left(\frac{a}{A_0}\right)' - \left(\frac{A_0'}{A_0} + \frac{1}{r}\right)\left(\frac{b}{B_0}\right)' + \left(\frac{A_0'}{A_0} - \frac{B_0'}{B_0} + \frac{2}{r}\right)\left(\frac{c}{r}\right)'\right] = -\frac{\bar{p}_\perp}{\phi_0} - \frac{Tp_{\perp 0}\Phi}{\phi_0^2} - \frac{T\omega_{BD}\phi_0'^2 b}{\phi_0^2 B_0^3} + \frac{T\omega_{BD}b\phi_0'\Phi'}{B_0^3\phi_0^2} - \frac{T\omega_{BD}\Phi\phi_0'^2}{\phi_0^3 B_0^2} - \frac{T\phi_0'}{\phi_0 B_0^2} \times \left[\left(\frac{a}{A_0}\right)' + 2\left(\frac{c}{r}\right)' + \left(\frac{b}{B_0}\right)'\right] + \frac{2Tb\phi_0'}{\phi B_0^3}\left[\frac{A_0'}{A_0} - \frac{1}{r}\right] - \left[\frac{T}{B_0^2 r} + \frac{TA_0'}{B_0^2 A_0} - \frac{TB_0'}{B_0^3}\right]\left[\frac{\Phi}{\phi_0}\right]' + \frac{\ddot{T}\Phi}{A_0^2\phi_0} - \frac{T\Phi''}{\phi_0 B_0^2} + \frac{2Tb\phi_0''}{B_0^3\phi_0} + \frac{T\phi_0'\Phi}{B_0^2\phi_0^2} + \frac{TU_0\Phi}{2\phi_0^2} + \frac{T\bar{U}}{2\phi_0}. \tag{36}$$

The perturbed wave equation becomes

$$\bar{H}_3 = \frac{1}{2\omega_{BD}+3}\left[\bar{\rho} + \bar{p}_r + 2\bar{p}_\perp + T\Phi U_0 - 2\bar{U}\right], \tag{37}$$

where

$$\bar{H}_3 = \frac{\ddot{T}\Phi}{A_0^2} - \frac{T\phi_0'}{B_0'^2}\left(\frac{a}{A_0}\right)' + T\phi_0'\left(\frac{b}{B_0^3}\right)' + \frac{T}{B_0}\left(\frac{\Phi}{B_0}\right)' - \frac{2T\phi_0'}{B_0^2}\left(\frac{c}{r}\right)' - \frac{2TbA_0'\phi_0'}{B_0^3 A_0} - \frac{T\Phi A_0'}{B_0^3 A_0} + \frac{4Tb\phi_0'}{B_0^3 r} - \frac{2T\Phi'}{rB_0^2} - \frac{2Tb\phi_0''}{B_0^3}.$$

The perturbed form of Eq.(18) takes the form

$$\dot{\bar{\rho}} + \left[(\rho_0 + p_{r0})\frac{b}{B_0} + 2(\rho_0 + p_{\perp 0})\frac{c}{r} + \frac{\Phi\rho_0}{\phi_0} + A_0\phi_0\bar{H}_1\right]\dot{T} = 0, \tag{38}$$

which on integration yields

$$\bar{\rho} = -\left[(\rho_0 + p_{r0})\frac{b}{B_0} + 2(\rho_0 + p_{\perp 0})\frac{c}{r} + \frac{\Phi\rho_0}{\phi_0} + A_0\phi_0\bar{H}_1\right]T. \tag{39}$$

The perturbed configuration of the second Bianchi identity provides

$$p_{r0}' - (\rho_0 + p_{r0})\left[\left(\frac{a}{A_0}\right)'\frac{B_0}{b} - \frac{A_0'}{A_0} - \frac{\Phi B_0}{A_0 b}\right] - (\bar{\rho} + \bar{p}_r)\frac{A_0' B_0}{\phi_0 A_0 T b} - 2(p_{r0} - p_{\perp 0})\left(\frac{B_0}{b}\left(\frac{c}{r}\right)' - \frac{1}{r}\right.$$

$$-\frac{B_0\Phi}{b\phi_0 r}\Big)-(\bar{p}_r-\bar{p}_\perp)\frac{2B_0}{Tbr\phi_0}-\frac{\Phi B_0}{Tb}\bar{p}'_r-\frac{p'_{r0}\Phi B_0}{\phi_0}$$
$$+\frac{\bar{p}_r\phi'_0B_0}{Tb\phi_0}-\frac{\phi_0\bar{H}_2}{Tb}=0, \quad (40)$$

where $\bar{H}_1$ and $\bar{H}_2$ are given in appendix **A**. The perturbed form of Eq.(16) is

$$-\bar{p}_r=^{\Sigma^{(e)}}-\frac{T\Phi p_{r0}}{\phi_0}-\frac{T\Phi U_0}{2\phi_0}+\frac{\bar{U}}{2\phi_0}. \quad (41)$$

Using junction conditions with this equation, Eq.(35) can be written as

$$a(r)\ddot{T}+b(r)T=^{\Sigma^{(e)}}0, \quad (42)$$

where

$$a(r)=^{\Sigma^{(e)}}\frac{\Phi}{\phi_0A_0^2}-\frac{2C}{rA_0^2},$$
$$b(r)=^{\Sigma^{(e)}}\frac{2}{r}\left[-\frac{1}{r}\left(\frac{b}{B_0}-\frac{c}{r}\right)\right].$$

The general solution of Eq.(42) is

$$T(t)=c_1\exp(w_{\Sigma^{(e)}}t)+c_2\exp(v_{\Sigma^{(e)}}t), \quad (43)$$

where $w_{\Sigma^{(e)}}=+\sqrt{\frac{b(r)}{a(r)}}$, $v_{\Sigma^{(e)}}=-\sqrt{\frac{b(r)}{a(r)}}$ and c_1, c_2 are arbitrary constants. The solution of the above equation represents static as well as non-static configurations which lead to stable and unstable phases of collapse. In order to discuss instability analysis for collapsing system, we consider only static solution. For this purpose, we assume that at $t=-\infty$, $T(-\infty)=0$, i.e., when the collapse process begins, the system is in complete hydrostatic equilibrium. Using these assumptions in Eq.(43), we obtain $c_2=0$ whereas $c_1=-1$ is taken arbitrarily. The corresponding solution is given by

$$T(t)=-\exp(w_{\Sigma^{(e)}}t). \quad (44)$$

For the instability regions to be in a real static distribution, we consider only positive values of $\frac{b(r)}{a(r)}$.

4 Dynamical Instability

In order to explore instability ranges of collapsing fluid, we use adiabatic index Γ by assuming Harison-Wheeler equation of state as

$$\bar{p}_r=\Gamma\frac{p_{r0}}{\rho_0+p_{r0}}\bar{\rho}. \quad (45)$$

The adiabatic index determines the variation of pressure with respect to density which describes the rigidity of the fluid. We assume this index to be constant throughout instability analysis of fluid. Using the value of $\bar{\rho}$ in the above relation, we obtain

$$\bar{p}_r=-\Gamma\left[\frac{b}{B_0}p_{r0}+\frac{2c}{r}\frac{\rho_0+p_{\perp0}}{\rho_0+p_{r0}}p_{r0}+\frac{p_{r0}}{\rho_0+p_{r0}}\frac{\Phi\rho_0}{\phi_0}\right.$$
$$\left.+\frac{p_{r0}}{\rho_0+p_{r0}}A_0\phi_0\bar{H}_1\right]T. \quad (46)$$

Using Eqs.(31), (37), (39) and (46) in (40), we have

$$p'_{r0}\left(1-\frac{\Phi B_0}{\phi_0}\right)-(\rho_0+p_{r0})\left[\frac{B_0}{b}\left(\frac{a}{A_0}\right)'\right.$$
$$\left.-\frac{A'_0}{A_0}-\frac{\Phi B_0}{bA_0}\right]-2(p_{r0}-p_{\perp0})\left[\frac{B_0}{b}\left(\frac{c}{r}\right)'-\frac{1}{r}-\frac{B_0\Phi}{br\phi_0}\right]$$
$$+\frac{\Gamma B_0}{b}\left[\frac{b}{B_0}p_{r0}+\frac{2c}{r}\frac{\rho_0+p_{\perp0}}{\rho_0+p_{r0}}p_{r0}+\frac{p_{r0}}{\rho_0+p_{r0}}\frac{\Phi\rho_0}{\phi_0}\right.$$
$$\left.+\frac{p_{r0}}{\rho_0+p_{r0}}A_0\phi_0\bar{H}_1\right],_1-\frac{\Gamma B_0}{b}\left[-\frac{\phi'_0}{\phi_0}+\frac{A'_0}{A_0}+\frac{3}{r\phi_0}\right]$$
$$\times\left[\frac{b}{B_0}p_{r0}+\frac{2c}{r}\frac{\rho_0+p_{\perp0}}{\rho_0+p_{r0}}p_{r0}+\frac{p_{r0}}{\rho_0+p_{r0}}\frac{\Phi\rho_0}{\phi_0}\right.$$
$$\left.+\frac{p_{r0}}{\rho_0+p_{r0}}A_0\phi_0\bar{H}_1\right]-\frac{B_0}{b}\left[\frac{A'_0}{A_0}-\frac{1}{r\phi_0}\right]$$
$$\times\left[\frac{b}{B_0}(\rho_0+p_{r0})-\frac{2c}{r}(\rho_0+p_{\perp0})-\frac{\Phi\rho_0}{\phi_0}+A_0\phi_0\bar{H}_1\right]$$
$$-\frac{B_0}{br\phi_0}\left[\bar{H}_3(2\omega_{BD}+3)+\bar{U}\right]-\frac{\phi_0\bar{H}_2}{Tb}=0, \quad (47)$$

where

$$p'_{r0}=-\frac{\phi'_0p_{r0}}{\phi_0}-(\rho_0-p_{r0})\frac{A'_0}{A_0}-\frac{2}{r}(p_{r0}-p_{\perp0})+\frac{H'_2}{B_0\phi_0}.$$

Equation (47) is the required general form of collapse equation which describes the instability ranges of an evolving celestial object in Newtonian and post-Newtonian limits.

4.1 Newtonian limit

The Newtonian approximation in BD gravity obeys the following conditions

$$\rho_0\gg p_{r0},\quad \rho_0\gg p_{\perp0},\quad p_{r0}\gg p_{\perp0},\quad B_0=1,$$
$$A_0=1-\frac{m_0}{rc^2},\quad \phi_0=\text{constant},\quad U_0=\bar{U}=0.$$

Using these conditions along with (43), the collapse equation with at most $O(c^{-2})$ turns out to be

$$\Gamma\left[\frac{1}{b}X_{N},_1-\left(\frac{m_0}{r^2c^2b}+\frac{3}{r\phi_0b}\right)X_N\right]-\rho_0Y_N$$
$$-2p_{r0}Z_N+H_{BD}=0, \quad (48)$$

where

$$X_N=\left(p_{r0}b(\frac{2c}{br}+1)\right),$$
$$Y_N=\left[\left(\frac{m_0}{r^2c^2}+\frac{2}{r}\right)\left(1-\frac{\Phi}{\phi_0}\right)+\left[\frac{a'}{bc}\left(1+\frac{m_0}{rc^2}\right)\right.\right.$$
$$+\left.+\frac{am_0}{brc^2}+\frac{\Phi}{b}\left(1+\frac{m_0}{rc^2}\right)\left(\frac{m_0}{r^2c^2b}-\frac{1}{br\phi_0}\right)\left(\frac{b}{B_0}\right.\right.$$
$$\left.\left.-\left.\frac{2c}{r}-\frac{\Phi}{\phi_0}\right)\right)\right],$$

$$Z_N = \left[\frac{1}{b}\left(\frac{c}{r}\right)' - \frac{1}{r} - \frac{\Phi}{\phi_0 rb}\right],$$

$$H_{BD} = \left(\frac{m_0}{r^2c^2} - \frac{1}{br\phi_0}\right)\bar{H}_{1N}\phi_0 - \frac{\phi_0\bar{H}_{2N}}{b} - \frac{\phi_0(2\omega_{BD}+3)\bar{H}_{3N}}{b}.$$

Here $\bar{H}_{1(N)}$ and $\bar{H}_{2(N)}$ are Newtonian approximations of $\bar{H}_1$ and $\bar{H}_2$ given in Appendix **A**. It is mentioned here that the dynamical instability of isotropic fluid depends upon the numerical value of the adiabatic index in GR. Here, Eq.(48) shows that adiabatic index (for an anisotropic fluid in BD gravity) depends on dynamical variables similar to the case of $f(T)$ and $f(R)$ gravity.

The above equation gives the instability ranges as

$$\Gamma < \frac{\rho_0 Y_N + 2p_{r0}Z_N - H_{BD}}{\left[\frac{1}{b}X_{N,1} - \left(\frac{m_0}{r^2c^2b} + \frac{3}{r\phi_0 b}\right)X_N\right]}, \tag{49}$$

which indicates that the adiabatic index depends on structural properties, such as energy density, anisotropic pressure and scalar field. Thus at Newtonian approximation, the collapsing system remains unstable until Eq.(49) is satisfied. In order to satisfy the dynamical instability condition, we consider

$$\frac{\rho_0 Y_N + 2p_{r0}Z_N - H_{BD}}{\left[\frac{1}{b}X_{N,1} - \left(\frac{m_0}{r^2c^2b} + \frac{3}{r\phi_0 b}\right)X_N\right]} > 0, \tag{50}$$

which means that both expressions (numerator and denominator) are either positive or negative. Moreover, the fraction

$$\frac{\rho_0 Y_N + 2p_{r0}Z_N - H_{BD}}{\left[\frac{1}{b}X_{N,1} - \left(\frac{m_0}{r^2c^2b} + \frac{3}{r\phi_0 b}\right)X_N\right]}, \tag{51}$$

leads to the following possibilities:

1. $\rho_0 Y_N + 2p_{r0}Z_N - H_{BD} = \frac{1}{b}X_{N,1} - (\frac{m_0}{r^2c^2b} + \frac{3}{r\phi_0 b}X_N,$
2. $\rho_0 Y_N + 2p_{r0}Z_N - H_{BD} < \frac{1}{b}X_{N,1} - (\frac{m_0}{r^2c^2b} + \frac{3}{r\phi_0 b})X_N,$
3. $\rho_0 Y_N + 2p_{r0}Z_N - H_{BD} > \frac{1}{b}X_{N,1} - (\frac{m_0}{r^2c^2b} + \frac{3}{r\phi_0 b})X_N.$

The first case together with (49) indicates that the system becomes unstable for $0 < \Gamma < 1$. In the second case, there will be different exact numerical value depending upon the values of dynamical variables but it is clear from the second inequality that it must be less than 1. Hence in this case the predicted value for instability will be $0 < \Gamma < 1$. Similarly, in the third case, different ranges of dynamical variables give different numerical values which show that these values are greater than 1. In this way, from Eqs.(49) and third possibility, we can conclude that the system remains unstable for $\Gamma > 1$. Thus, all the above cases indicate that $0 < \Gamma < 1$ always provides dynamical instability for the collapsing system under consideration.

5 Conclusion

In this paper, we have explored dynamical instability of a spherically symmetric collapsing body in the context of BD gravity. We have used general spherical symmetric metric filled with anisotropic fluid as an interior metric whereas the Schwarzschild metric as an exterior to $\Sigma^{(e)}$ and have derived two dynamical equations of collapsing model through contracted Bianchi identities. We have applied perturbation approach on BD as well as dynamical equations to describe both static and non-static (perturbed) configurations of metric functions as well as mater distribution. The collapse equation has been constructed through perturbed second dynamical equation.

The adiabatic index plays a key role in exploring the ranges of instability for a collapsing body. We have used Harison-Wheeler equation of state along with collapse equation to analyze the ranges of dynamical instability at Newtonian approximation. It is found that in this regime the adiabatic index depends upon structural properties (like pressure anisotropy, energy density and some constraints for the validity of instability condition). We conclude that $0 < \Gamma < 1$ provides dynamical instability in all cases while $\Gamma > 1$ is the instability range for only one special case. In the following, we give comparison of our results with GR and some modified theories.

- In GR, the dynamical instability of spherical and cylindrical configurations depends upon numerical values $\Gamma < \frac{4}{3}$ and $\Gamma < 1$. Here this depends on physical characteristics (density, pressure and scalar filed) that indicate that 1 is the critical value for the instability ranges, i.e., $0 < \Gamma < 1$ and $\Gamma > 1$ are two different instability criteria according to different conditions.
- In $f(R)$ gravity as well as in $f(T)$ gravity, the dynamical instability depends on physical variables such as density, pressure and respective modified dark terms. Here the instability criteria depends on physical quantities as well as some numerical instability predictions ($0 < \Gamma < 1$ and $\Gamma > 1$) through these physical variables.
- It is remarked that the instability range of isotropic fluid in BD gravity is $\Gamma > \frac{4}{3}$ but we have found that in anisotropic case, the numerically predicted instability ranges are $0 < \Gamma < 1$ or $\Gamma > 1$ in different cases.

Appendix A

The scalar terms H_1 and H_2 of Eqs.(18) and (19) are

$$\begin{aligned}
H_1 &= \left(T^{\phi}_{00}A^{-4}\right)_{,0}A-\left(T^{\phi}_{01}A^{-2}B^{-2}\right)_{,1}A\\
&+\left[\frac{2\dot{A}}{A}+\frac{\dot{B}}{B}+\frac{2\dot{C}}{C}\right]T^{\phi}_{00}A^{-3}+\frac{\dot{B}B^{-3}}{A}T^{\phi}_{11}\\
&+\frac{2\dot{C}C^{-3}}{A}T^{\phi}_{22}-\left[A'+\frac{B'A}{B}+\frac{2C'A}{C}\right](T^{\phi}_{01}A^{-2}B^{-2}),\\
H_2 &= \left(T^{\phi}_{11}B^{-4}\right)_{,1}B-\left(T^{\phi}_{01}A^{-2}B^{-2}\right)_{,0}B\\
&-\frac{2A'A}{B}T^{\phi}_{00}A^{-4}+\left[\frac{2\dot{B}}{B}+\frac{\dot{A}}{A}+\frac{2\dot{C}}{C}\right]T^{\phi}_{01}B^{-1}A^{-2}\\
&+\left[\frac{A'}{A}+\frac{2B'}{B}+\frac{2C'}{C}\right](T^{\phi}_{11}B^{-3})+\frac{2C'C^{-3}}{B}T^{\phi}_{22}.
\end{aligned}$$

The term H_2' in (31) is the static configuration of H_2 and is given by

$$\begin{aligned}
H_2' &= (B_0^{-2}T^{\phi}_{11(unp)})_{,1}B_0-\frac{A_0'A_0^{-1}}{B_0}T^{\phi}_{00(unp)}\\
&-\left[-2B_0B_0^2-\frac{A_0'B_0^3}{A_0}-\frac{2}{r}\right]\left(T^{\phi}_{11(unp)}B_0^{-4}\right)\\
&+\frac{2r^3}{B_0}T^{\phi}_{22(unp)}B_0^{-4}.
\end{aligned}$$

The perturbed terms $\bar{H}_1$ and $\bar{H}_2$ in Eqs.(38) and (40) are described as

$$\begin{aligned}
\bar{H}_1 &= \dot{T}\left[A_0T^{\phi}_{00(p)}-\left(T^{\phi}_{01(p)}A^{-2}B^{-2}\right)_{,1}A_0\right.\\
&\left.-\left(T^{\phi}_{01(p)}A^{-2}B^{-2}\right)\left[A_0'+\frac{B_0'A_0}{B_0}+\frac{2A_0}{r}\right]\right],\\
\bar{H}_2 &= -B_0\left(T^{\phi}_{11(p)}B_0^{-2}\right)_{,1}-2TB_0\left(bB_0^{-3}T^{\phi}_{11(unp)}\right)_{,1}\\
&+Tb\left(B_0^{-2}T^{\phi}_{11(unp)}\right)_{,1}-\left[\frac{T}{B_0}\left(aA_0^3\right)'-Tb\frac{A_0^3A_0'}{B_0^2}\right]\\
&\times T^{\phi}_{00(unp)}-\left[2B_0'B_0^2+\frac{A_0'B_0^{-1}}{A_0}\right]T^{\phi}_{11(p)}\\
&+\left[4TbB_0B_0'+Tb'B_0^2+TB_0^3\left(\frac{a}{A_0}\right)'\right.\\
&\left.+Tb\frac{B_0^2A_0'}{A_0}-2T\left(\frac{c}{r}\right)'B_0^3\frac{6TcB_0^2}{r}\right]T^{\phi}_{11(unp)}B_0^{-4}\\
&+\left[6Tcr^2+Tc'r^3-\frac{Tbr^3}{B_0}\right]T^{\phi}_{22(unp)}.
\end{aligned}$$

Here $T^{\phi}_{\mu\nu(unp)}$ and $T^{\phi}_{\mu\nu(p)}$ are unperturbed as well as perturbed configurations of BD energy-momentum tensor, respectively and are given in respective configurations of the BD field equations.

The Newtonian approximation of scalar terms $\bar{H}_1$, $\bar{H}_2$ and $\bar{H}_3$ are given as follows

$$\begin{aligned}
\bar{H}_{(1N)} &= \dot{w}_{\Sigma^{(e)}}e^{w_{\Sigma^{(e)}}(t)}\left[\left(1-\frac{m_0}{rc^2}\right)\left(\frac{1}{r}\right)+\frac{m_0}{rc^2}\right]\frac{\Phi}{\phi_0}\\
&+\frac{m_0}{rc^2}\frac{\Phi''}{\phi_0}-\frac{5m_0}{r^2c^2}\frac{\Phi'}{\phi_0}+\frac{\Phi''}{\phi_0}+\frac{2}{r}\frac{\Phi'}{\phi_0},\\
\bar{H}_{(2N)} &= -\left[\frac{1}{r}+\frac{m_0}{r^2c^2}\right]\frac{\Phi'}{\phi_0}+\left(\ddot{w}_{\Sigma^{(e)}}+\dot{w}^2_{\Sigma^{(e)}}\right)\\
&\times\left(1+\frac{m_0}{rc^2}\right)\frac{\Phi}{\phi_0},\\
\bar{H}_{(3N)} &= e^{w_{\Sigma^{(e)}}(t)}\left[\Phi'+\Phi\frac{m}{r^2c^2}-\frac{2\Phi'}{r\phi_0}\right.\\
&\left.+\ddot{w}_{\Sigma^{(e)}}\Phi\left(1-\frac{2m_0}{rc^2}\right)\right],
\end{aligned}$$

References

1. A.D. Felice, Relaxing nucleosynthesis constraints on Brans-Dicke theories, Phys. Rev. D, **74**, 103005 (2006).
2. N. Banerjee and D. Pavon, Cosmic acceleration without quintessence, Phys. Rev. D, **63**, 043504 (2001).
3. S. Chandrasekhar, The dynamical iinstability of gases masses approaching the Schwarzschild limit in general relativity, Astrophys. J., **140**, 417 (1964).
4. R. Chan et al., Dynamical instability for radiating anisotropic collapse, Mon. Not. R. Astron. Soc., **265**, 533 (1993).
5. M. Sharif and M. Azam, Effects of electromagnetic field on the dynamical instability of expansion-free gravitational collapse, Gen. Relativ. Gravit., **44**, 1181 (2012).
6. M. Sharif and M. Azam, Effects of electromagnetic field on the dynamical instability of cylindrical collapse, J. Cosmol. Astropart. Phys., **02**, 043 (2012).
7. M. Sharif, M. Azam, Stability of anisotropic cylinder with zero expansion, Mon. Not. R. Astron. Soc., **430**, 3048 (2013).
8. Y. Nutku, The post-Newtonian equations of hydrodynamics in the Brans-Dicke theory, Astrophys. J., **155**, 999 (1969).
9. O.J. Kwon et al, Stability of the Schwarzschild black hole in Brans-Dicke theory, Phys. Rev. D, **34**, 333 (1986).
10. M. Sharif and H.R. Kausar, Gravitational perfect fluid collapse in f (R) gravity, Astrophys. Space Sci., **331**, 281 (2011).
11. M. Sharif and H.R. Kausar, Effects of $f(R)$ model on the dynamical instability of expansion-free gravitational collapse, J. Cosmol. Astropart. Phys., **07**, 022 (2011).
12. M. Sharif and Z. Yousaf, Dynamical instability of the charged expansion-free spherical collapse in $f(R)$ gravity, Phys. Rev. D, **88**, 024020 (2013).
13. M. Sharif and Z. Yousaf, Instability of a dissipative restricted non-static axial collapse with shear viscosity in $f(R)$ gravity, J. Cosmol. Astropart. Phys., **06**, 019 (2014).
14. M. Sharif and Z. Yousaf, Dynamical analysis of self-gravitating stars in $f(R,T)$ gravity, Astrophys. Space Sci., **354**, 471 (2014).
15. M. Sharif and Z. Yousaf, Stability analysis of cylindrically symmetric self-gravitating systems in $R+\epsilon R^2$ gravity, Mon. Not. R. Astron. Soc., **440**, 3479 (2014).

16. M. Sharif and S. Rani, Dynamical instability of spherical collapse in $f(T)$ gravity, Mon. Not. Roy. Astron. Soc., **440**, 2255 (2014).
17. S.W Hawking, Black holes in the Brans-Dicke theory of gravitation, Commun. Math. Phys., **25**, 167 (1972).

Proc. Int. Conf. Relativ. Astrophys.
Pages 140-159, (2015)

First-forbidden β-decay Rates on Zn and Ge Isotopes for Speeding up r-process Calculations

FF β-decay rates on Zn and Ge isotopes

Jameel-Un Nabi[a,1], Necla Cakmak[2], Sabin Stoica[3], Zafar Iftikhar[1]

[1]Faculty of Engineering Sciences, GIK Institute of Engineering Sciences and Technology, Topi 23640, Khyber Pakhtunkhwa, Pakistan
[2]Department of Physics, Karabuk University, Karabuk, Turkey
[3]Horia Hulubei Foundation, P. O. Box MG-12, 071225, Magurele, Romania

Abstract As the proton number increases the first-forbidden (FF) charge-changing transitions start gaining prominence for the nuclei. This is partly because the allowed Gamow-Teller (GT) transitions get smaller for larger Z and partly due to phase space amplification for FF decays under stellar conditions. Against those by the GT contributions alone the FF transitions plays a vital role in scaling down the half-lives. In this paper we calculate allowed GT as well as $0^+ \rightarrow 0^-$ and $0^+ \rightarrow 2^-$ transitions for neutron-rich Zn and Ge isotopes. Two distinct pn-QRPA models were utilized with a schematic separable interaction to calculate GT and FF transitions. After the incorporation of FF transitions half-lives are found to be in excellent concurrence with experimental data. Our results are also compared with previous calculations and showed better results. For astrophysical applications allowed GT and unique FF stellar β-decay rates are also calculated. In case of ^{86,88}Ge a significant contribution to the total β-decay rate comes from unique FF transitions.

1 Introduction

During presupernova evolution the stellar nucleosynthesis of nuclei beyond iron is usually attributed to the neutron capture process known as r-process (see e.g. [1–4]) and is accountable for the mass abundance of the nuclei in the neutron rich environment of solar system. The r-process is the most favored process for the production of about half of heavy elements beyond iron. The r-process occurs at relatively high temperature ($\sim 10^9$K) and very high neutron densities ($>10^{20}$cm^{-3}) (see e.g. [5,6]). The elemental distribution on the r-path and the resulting final distribution of stable nuclei are highly sensitive to the β-decay properties [7,8] of neutron-rich nuclei engaged in the process. The β-processes are responsible for the flow of the r-process material to the elements with higher charge numbers [9] and for setting the r-process time scale. The appearance of the r-peak at A=80 surely indicate the role of the neutron shell closure at N=50 in the nucleosynthesis process. The calculation of β-decay rates, specially for waiting point nuclei, is one of the key issues of the r-process nucleosynthesis.

Weak interaction rates are the hallmark of all the stellar processes: the hydrostatic burning of massive stars, late (presupernova) stage of their evolution and production of heavy elements in stellar nucleosynthesis (see e.g. [10]). The major contribution to β^- rate comes from the GT strength function, i.e. most of the strength associated with the β^--decay operators lies in the GT resonance, well above the decay threshold. The first-forbidden (FF) decays have a strong impact on the β-decay characteristics of the r-process of the relevant nuclei with Z$\approx$28, N$>$50; Z$\geq$50, N$>$82 and Z=60-70, N$\approx$126 owing to the shell configuration effects.

In case of neutron rich nuclei, FF β-decay takes vital importance due to the enlarged phase space for the transitions [11,12]. The FF β transitions process provides convenient data in checking the effectiveness of theories associated with the r-process [13–15]. The FF transitions become important in an environment where the allowed β-decay approximation is not sufficient to describe the isotopic dependence of the β-decay characteristics. Forbidden transitions give a prevailing part to the total half-life for nuclei crossing the closed N and Z shells, specially for N $<$ 50 in ^{78}Ni region. At the same time the FF transitions become relatively important for nuclei with larger Z as the contribution from the allowed GT transitions get smaller for such nuclei

[a]e-mail: jameel@giki.edu.pk

and bear consequences for nucleosynthesis calculations [16]. It was shown in this study that the third peak of the element abundance of the r-process shifted toward higher mass region by using calculated half-lives including FF contributions. Cooperstein and Wambach [17] found in their calculation that FF process, particularly the 2^- unique first-forbidden (U1F) transitions, contributed effectively to the calculated stellar weak rates (see also [18]). Authors in Ref. [17] concluded that forbidden transitions are small as compared to allowed GT transitions, but soon begin to compete as soon as the chemical potential of the electron approaches 20 MeV at high stellar densities $\sim 10^{11} gcm^{-3}$. The increment was mainly attributed to the U1F transitions whose strength gets enhanced at high electron energies due to momentum dependence of the corresponding transition operator. The factual studies of the r-process can be achieved with understanding of just few nuclear properties, namely, the nuclear mass (from which neutron separation energies and β-decay Q values can be trivially obtained), the β-decay half-lives and β-delayed neutron-emission probabilities.

In this work the β-decay rates have been calculated using a microscopic model based on the proton neutron quasi-particle random phase approximation (pn-QRPA). The pn-QRPA was developed by Halbleib and Sorensen [19] by generalizing the usual RPA which was formulated for excitations induced by a charge-changing transition operator. In pn-QRPA model quasi-particle basis construction is performed first with a pairing interaction and after that with GT residual interaction the solution to RPA equation is found. Möller and his coworkers combined the pn-QRPA model with the Gross Theory of the FF decay (pn-QRPA+ffGT)[20] and gave a hybrid genre of pn-QRPA model. The pn-QRPA model describes the charge changing transitions, $(Z,A) \rightarrow (Z \pm 1, N \mp 1)$. Halbleib and Sorensen took the particle-hole terms of the separable Gamow-Teller force into account to calculate the Gamow-Teller strength function. The particle-particle interaction, first considered by Cha [21] was neglected. It was taken into account by simply adding a schematic GT interaction to the QRPA Hamiltonian. An excellent agreement with experimental decay rates was also achieved when QRPA is applied to β^- decay half-lives of nuclei far from stability [22]. The pn-QRPA theory was also successfully employed in calculations of β^+ /electron capture half-live and a satisfactory comparison with experimental half-lives was again reported [23]. It was Nabi and Klapdor-Kleingrothaus who used the pn-QRPA model, for the first time, to calculate stellar weak rates [24]. A systematical study of the total β-decay half-lives and delayed neutron emission probabilities was done by Homma and his coworkers [25] . We discuss here the calculation of the FF β-decay rates for neutron-rich even-even zinc ($^{76-82}$Zn) and germanium isotopes ($^{84-88}$Ge) using the pn-QRPA model. Inspiration of the current work came from the work of Ref. [26] where the authors showed their interest to incorporate rank 0 contribution to first forbidden (FF) decay rates. The total β-decay half-lives and the U1F β-decay rates (rank 2) for a number of neutron-rich nickel isotopes, $^{72-78}$Ni, were calculated using the pn-QRPA theory in stellar environment. In addition allowed GT, FF and U1F transitions were calculated and a comparison of total half-lives was made with experimental and different theoretical calculations.

Section 2 of this paper discusses briefly the required formalism for allowed GT, FF and U1F transitions rates. Results and discussions follow in Section 3. Finally Section 4 states our conclusions.

2 Formalism

The theory of allowed and FF β-decay transitions is well-established [14, 27–29]. The allowed β-decay is simple to calculate but the FF decay shows a far wider spectrum both in lepton kinematics and in nuclear matrix elements.

All our calculations for allowed and FF β-decay rates were performed within the framework of pn-QRPA. Two different pn-QRPA models were used to calculate allowed and forbidden weak rates. The first pn-QRPA model considered only spherical nuclei and used the Woods-Saxon potential basis and is referred to as pn-QRPA(WS) in this work. The transition probabilities in this model were calculated within the ξ approximation (ξ is a dimensionless parameter representing the magnitude of the Coulomb energy and is approximated by $1.2ZA^{-1/3}$). Calculation of rank 0 FF transitions ($0^+ \rightarrow 0^-$) was done within the pnQRPA(WS) formalism. Details of this model can be seen from [30]. For the same model, allowed GT transitions were also calculated using the Pyatov method (PM) [31] to solve the RPA equation. The second pn-QRPA model employed a deformed Nilsson basis and in referred to as pn-QRPA(N) in this work. A separable interaction was used both in particle-particle and particle-hole channels which reduced the eigenvalue equation to solving an algebraic equation of fourth order (for further details see [32]). Deformation of nuclei was taken into account in the pn-QRPA(N) model. Allowed GT and U1F transitions were calculated within the pn-QRPA(N) formalism.

In order to compare our results with experimental data and prior calculations, we introduced a quenching

factor of 0.6 [33–35] in both pn-QRPA(WS) and pn-QRPA(N) models. The same quenching factor was also used later to calculate astrophysical reaction rates.

The ft values for charge-changing first-forbidden transitions in the pn-QRPA(WS) model are given by:

$$(ft)_{\beta^-} = \frac{D}{(g_A/g_V)^2 4\pi B^{FF(U1F)}(I_i \longrightarrow I_f, \beta^-)}, \qquad (1)$$

where

$$D = \frac{2\pi^3\hbar^2 ln2}{g_V^2 m_e^5 c^4} = 6250 sec, \quad \frac{g_A}{g_V} = -1.24.$$

In Eq. 1, $B^{FF(U1F)}$ are the transition probabilities and are calculated within the ξ approximation [36]. Details of evaluating these nuclear matrix elements can be seen from [37].

Allowed GT transitions within the pn-QRPA(WS) model was calculated using the Pyatov method [31]. The ft values for the allowed GT β transitions are calculated using

$$ft = \frac{D}{(\frac{g_A}{g_V})^2 4\pi B^{GT}(I_i \rightarrow I_f, \beta^-)}, \qquad (2)$$

details of calculation of reduced matrix elements of GT transitions B^{GT} can be seen in [38].

In the pn-QRPA(N) formalism [32], proton-neutron residual interactions occur as particle-hole and particle-particle interactions. We used a schematic separable interaction (as in the case of pn-QRPA(WS) model). Details of the separable potential and detailed formalism of calculation of ft values may be seen from [26] (and references therein). The U1F stellar β-decay rates from the ith state of the parent to the jth state of the daughter nucleus is given by

$$\lambda_{ij}^{\beta} = \frac{m_e^5 c^4}{2\pi^3\hbar^7} \sum_{\Delta J^\pi} g^2 f(\Delta J^\pi; ij) B(\Delta J^\pi; ij), \qquad (3)$$

where $f(\Delta J^\pi; ij)$ and $B(\Delta J^\pi; ij)$ are the integrated Fermi function and the reduced transition probability for β-decay, respectively, for the transition $i \rightarrow j$ which induces a spin-parity change ΔJ^π and g is the weak coupling constant which takes the value g_V or g_A according to whether the ΔJ^π transition is associated with the vector or axial-vector weak-interaction. Details of calculation of phase-space factors $f(\Delta J^\pi; ij)$ and nuclear matrix elements $B(\Delta J^\pi; ij)$ can be seen from [26]. Due to finite probability of occupation of parent excited states at stellar temperatures, contribution of partial decay rates from these states must be taken into account to ensure satisfactory convergence in the total decay rate calculation. The rate per unit time per nucleus for stellar β-decay process is finally given by

$$\lambda^{\beta} = \sum_{ij} P_i \lambda_{ij}^{\beta}. \qquad (4)$$

We note that due to the availability of a huge model space (up to 7 major oscillator shells in the pn-QRPA(N) model) convergence is easily achieved in our rate calculations for excitation energies well in excess of 10 MeV (for both parent and daughter states).

3 Results and Discussion

The calculated GT, U1F and FF transitions in our pn-QRPA(N) and pn-QRPA(WS) models are shown in Table 1 for Zn isotopes and in Table 2 for Ge isotopes. All these charge-changing transitions were quenched by a factor of 0.6 as indicated before. Plainly evident from these tables the pn-QRPA(WS) model calculates high-lying transitions, specially for the FF case. The claim of [39, 40], by performing experiments, that average energy of 0^- giant FF resonance exceeds 20 MeV is supported by our results. It can be seen from the tables that neglect of deformation of nuclei forces transitions to high excitation energies in daughter and do not yield much fragmentation. In this respect the pn-QRPA(N) model displays much better results. Wherever available, the experimental (XUNDL) data were incorporated in the calculation to improve the authenticity of calculated transitions in our model. Calculated excitation energies were replaced with measured levels when they were within 0.5 MeV of each other. Where appropriate inverse transitions (along with their logft values) were also taken into account and measured states missing in the model were inserted. No attempt was taken in order to replace the theoretical levels with experimental ones for which the experimental data had no definite spin and/or parity. Only low-lying strength distribution up to an excitation energy of 2 MeV in daughter nucleus have been shown in Table 1 and Table 2 for the pn-QRPA(N) model (it is to be noted that calculations were performed up to 15 MeV in daughter nucleus). In addition transition strengths less than 10^{-4} are not reported in these tables. In the pn-QRPA(N) model the GT strength of ^{76,78}Zn is also well fragmented. Whereas no U1F transition strengths were calculated in ^{76,78}Zn up to 2 MeV they do show up in the case of ^{80,82,84,86}Zn. Using the same pn-QRPA(N) model similar results for Ge isotopes were also calculated (see Table 2). The low-lying U1F transitions should be noted in daughter arsenic isotopes. As would be seen later, the U1F transitions contribute in lowering the calculated β-decay half-lives bringing them in better agreement with the experimental data.

As mentioned before, the amplification of phase space, due to U1F transitions in stellar conditions, results in significant increment in the calculated total β-decay rates. The phase space integrals for U1F transitions

compete well with those of allowed GT and under certain stellar conditions supersede the allowed phase space. For the neutron-rich Zn and Ge isotope the phase space calculation of allowed and U1F transitions, as a function of stellar temperature and density, is shown in Fig. 1 and Fig. 2, respectively. Calculation of phase space is done at selected densities of 10^2 g/cm^3, 10^6 g/cm^3 and 10^{10} g/cm^3 (corresponding to low, intermediate and high stellar densities, respectively) with associated stellar temperature ranging from $T_9 = 0.01$ - 30 (T_9 gives the stellar temperature in units of 10^9 K). At low and intermediate densities the calculated U1F phase space, for the case of ^{78}Zn, is roughly a factor of 3 bigger than GT phase space (see Fig. 1). However the phase space factors for GT transitions start increasing at a much faster rate than those of U1F transitions. At $T_9 = 30$, the GT phase space is roughly an order of magnitude bigger. At high stellar densities the phase space gets choked and becomes finite only as stellar temperature soars to $T_9 = 0.2$. For ^{78}Zn the GT phase space is orders of magnitude bigger than U1F phase space at high stellar densities. A similar trend is seen for the phase space calculation of remaining five isotopes of Zn, namely ^{76,80,82,84,86}Zn and is not shown here to save space. Our calculation shows that increasing the number of neutron amplifies the phase space factor for U1F transitions.

For the case of ^{86}Ge the U1F phase space is around a factor six bigger at low and intermediate densities and low temperatures (Fig. 2). With increasing stellar temperature the GT phase space increases at a higher rate and approaches the U1F phase space for low and intermediate densities. A similar behavior exists for ^{84,88}Ge at low and intermediate densities. The difference appears at high densities where the allowed phase space is a shade smaller than U1F phase space. With soaring stellar temperatures the allowed phase space is observed coming closer to the U1F phase space. At high density (lower panel), the GT phase space is orders of magnitude smaller at low temperatures and the U1F phase space is a factor 1.2 bigger at $T_9 = 30$. As with the case of zinc isotopes, the U1F phase space for germanium isotopes also gets enlarged with increasing neutron number. Next we discuss the contribution of enlarged U1F phase space to the forbidden β-decay rates.

Calculation for allowed and U1F stellar β-decay rates were done at temperature ranging from $0.01 \leq T_9 \leq 30$ with associated densities covering the range of (10 - 10^{11}) g/cm^3. Figs. 3 - 11 show the pn-QRPA(N) calculated allowed and U1F stellar β-decay rates for Zn and Ge isotopes as a function of stellar temperature and density. The first panel depicts the β-decay rates at low stellar densities i.e. 10 - 10^4 g/cm^3 (in this density range the β-decay rates are observed to hold out constant). The middle panel shows the rates at intermediate stellar density of 10^7 g/cm^3 and the last panel depicts β-decay rates at high stellar density of 10^{11} g/cm^3. Stellar β-decay rates for ^{76}Zn in units of s^{-1} are shown in Fig. 3. It is to be noticed that contribution from all excited states are included in the final calculation of all decay rates. The allowed β-decay rates, for low and intermediate densities, in Fig. 3 are seen to be one order of magnitude bigger at low temperatures and around two order of magnitude bigger at $T_9 = 30$. For ^{76}Zn we calculated the phase space of allowed GT to be greater than U1F phase space by an order of magnitude. At high densities when the temperature is low the allowed β-decay rates are orders of magnitude bigger and around two orders of magnitude bigger at $T_9 = 30$. A similar trend is witnessed for the calculated β-decay rates of ^{78,80}Zn (see Fig. 4 and Fig. 5, respectively). The U1F rates are relatively more augmented at high temperatures and only around an order of magnitude smaller at $T_9 = 30$ for ^{82}Zn which is shown in Fig. 6. The behavior of ^{84}Zn (Fig. 7) and ^{86}Zn (Fig. 8)is interesting. At low and intermediate densities the allowed β-decay rates for ^{84}Zn is roughly a factor 2.27 smaller than that of the U1F decay rate. On other hand for ^{86}Zn the allowed β-decay rates (at low and intermediate densities) are a factor of 1.17 bigger than U1F rates. At high stellar densities the behavior is same as that of Zn isotopes explained earlier.

In Fig. 9 (^{84}Ge) the calculated β-decay rates for allowed GT are about a factor six greater than U1F at low temperatures and densities. At high temperatures allowed rates are 50 times bigger. With increasing density the allowed β-decay rates become orders of magnitude bigger at low temperatures and more than an order of magnitude bigger at $T_9 = 30$. For the case of ^{86}Ge in Fig. 10, the U1F decay rates at low temperatures and densities are only a factor two smaller. This trend is also seen at high densities where U1F rates are a factor five smaller. The reason is linked to the calculation of much larger U1F phase space (see Fig. 2).

In Fig. 11 for the case of ^{88}Ge, at low and intermediate densities and low stellar temperatures, the U1F stellar β-decay rates are competing very well with the allowed rates. At $T_9 = 30$, the allowed rates are only double the U1F rates (for all densities). The reason for this large U1F contribution may be traced back to the much larger phase space available for U1F transitions at all temperatures and densities.

Comparison of our half-life calculations with experimental data and other model calculations is done for Zn and Ge isotopes in Fig. 12. The top panel in Fig. 12 shows results for Zn isotopes whereas the bottom panel

gives terrestrail half-lives for Ge isotopes. The recent atomic mass evaluation data of Ref. [41] have been used for experimental half-lives values. Results of our pn-QRPA(N) and pn-QRPA(WS) allowed GT calculations alone and those including the FF contribution have been shown. Results of self-consistent density functional + continuum quasiparticle random phase approximation (DF3 + CQRPA) calculation from Ref. [42] including the FF contribution can also be viewed. The work of Möller and collaborators [43] on QRPA calculation including deformation of nucleus and folded-Yukawa single-particle potential is also presented in Fig. 12. It must be noted that [43] did not calculate FF contribution. It is noted from Fig. 12 that FF contribution brings substantial improvement in our pn-QRPA calculations. The pn-QRPA(N) calculation including deformation has more sizeable contribution from FF decay. The pn-QRPA(WS) results are better for Zn isotopes (see Fig. 12) whereas the pn-QRPA(N) shows overall best agreement with experimental data. The DF3+CQRPA results for Zn and Ge isotopes are roughly a factor two bigger than measured data. GT calculation of [42] are even bigger for obvious reason though for ^{82}Zn the agreement is excellent. Likewise for ^{88}Ge in Fig. 12 a marked improvement with measured data is noted. It may be concluded that QRPA calculation of Möller et al. improves as the nucleus becomes more neutron-rich. For ^{88}Ge DF3+CQRPA did not perform calculation. It is noted that pn-QRPA(N) emerges as the best model and has overall excellent agreement with experimentally determined half-lives of Zn and Ge isotopes. It is also expected to give reliable results for nuclei close to neutron-drip line for which no experimental data is available.

4 Conclusion

As the nuclei become heavier, allowed GT transitions get smaller and with increasing neutron number the contribution of FF transitions becomes more and more significant. We used two versions of the pn-QRPA model, one for spherical cases and other incorporating nuclear deformation. The spherical pn-QRPA(WS) was used to calculate allowed GT (using the Pyatov method) U1F and FF transitions whereas the deformed pn-QRPA(N) was used to calculate the allowed and U1F transitions. The FF transitions to 0^- daughter states were calculated at rather high excitation energies. However the 2^- states using the pn-QRPA(N) were connected also to low-lying daughter states. Further the spectra was more fragmented which was attributed to the deformation parameter incorporated in the model.

It was also shown that the U1F phase space has a sizeable contribution to the total phase space at stellar temperatures and densities. It was shown that the U1F phase space gets amplified with increasing neutron number. Specially for the case of ^{86,88}Ge the U1F phase space is orders of magnitude bigger which resulted in significant lowering of the β-decay half-lives as compared to those calculated only with allowed GT contribution. For ^{86,88}Ge roughly half the contribution to the total decay rate comes from U1F transitions. This is a significant finding of the current work. The microscopic calculation of U1F β-decay rates, presented in this work, could lead to a better understanding of the nuclear composition and Y_e in the core prior to collapse and collapse phase.

The terrestrial half-life calculations were also compared with the recent atomic mass evaluation 2012 data and other theoretical calculations. The FF inclusion improved the overall comparison of calculated terrestrial β-decay half-lives in the pn-QRPA(WS) model. Likewise, and more significantly, the UIF contribution improved the pn-QRPA(N) calculated half-lives. The pn-QRPA(N) model reproduced the experimental half-lives very well for Zn and Ge isotopes and showed better results than the pn-QRPA(WS) model. The DF3+CQRPA calculation was around a factor two bigger than experiential data and allowed GT calculation by Möller and collaborators was up to a factor 18 bigger but were in excellent agreement as neutron number increased (^{82}Zn and ^{88}Ge).

The reduced β-decay half-lives bear consequences for nucleosynthesis problem and site-independent r-process calculations. Our findings might result in speeding-up of the r-matter flow relative to calculations based on half-lives calculated from only allowed GT transitions. We are in a process of including rank 1 operators in our FF calculation of terrestrial β-decay half-lives in near future for still better results. The allowed and U1F β-decay rates on Zn and Ge isotopes were calculated on a fine temperature-density grid, suitable for simulation codes, and may be requested as ASCII files from the corresponding author.

Acknowledgements N. Cakmak would like to thank C. Selam for very fruitful discussion on calculation of $0^+ \rightarrow 0^-$ transitions. S. Stoica and J.-U. Nabi would like to acknowledge the support of the Horia Hulubei Foundation and Romanian Ministry of National Education, CNCS UEFISCDI, project PCE-2011-3-0318, Contract no. 58/28.10/2011. J.-U. Nabi would like to acknowledge the support of the Higher Education Commission Pakistan through the HEC Project No. 20-3099.

References

1. D.D. Clayton, (University of Chicago Press,Chicago, 1983).
2. K.L. Kratz, J.P. Bitouzet, F.K. Thielemann, P. Möller, B. Pfeiffer, Astrophys. J. **403**, 216 (1993).
3. B.S. Meyer, G.J. Mathews, W.M. Howard, S.E. Woosley and R.D. Hoffman, Astrophys. J. **399**, 656 (1992); S.E. Woosley et al, ibid. **433**, 229 (1994).
4. J.J. Cowan and F.K. Thielemann, Phys. Today. Oct. **47**, (2004).
5. E.M. Burbidge, G.R. Burbidge, W.A. Fowler and F. Hoyle, Rev. Mod. Phys. **29**, 547 (1957).
6. J.J. Cowan, F.K. Thielemann, J.W. Truran, Phys. Rep. **208**, 267 (1991).
7. H.V. Klapdor, Prog. Part. Nucl. Phys. **10**, 131 (1983).
8. K. Grotz, H.V. Klapdor, *Particle and Astrophysics*, Adam Hilger, Bristol, Philadelphia, New York (1990).
9. G. McLaughlin, G. Fuller, Astrophys. J. **489**, 766 (1997).
10. K. Langanke and G. Martínez-Pinedo: *Nuclear weak-interaction process in stars.*, Rev. Mod. Phys. **75**, 819 (2003).
11. E.K. Warburton, J.A. Becker, D.J. Millener, B.A. Brown: *First-forbidden beta decay near A = 40.*, Ann. Phys. **187**, 471 (1988).
12. E.K. Warburton, I.S. Towner, B.A. Brown: *First-forbidden ęÂ decay: meson-exchange enhancement of the axial charge at A ąń 16.*, Phys. Rev. C **49**, 824 (1994).
13. I.N. Borzov, Nucl. Phys. **A718**, 635c (2003).
14. H.F. Schopper, *Weak interactions and nuclear beta decay* (North-Holland, Amsterdam, 1966).
15. O. Civitarese and J. Suhonen, Nucl. Phys. **A607**, 152 (1996).
16. T. Suzuki, M. Honma, T. Yoshida, H. Mao, T. Kajino and T. Otsuka T, Prog. Part. Nucl. Phys **66**, 385-389 (2011).
17. J. Cooperstein and J. Wambach, Nucl. Phys. **A420**, 591-620 (1984).
18. G.M. Fuller, W.A. Fowler and M.J. Newman, Astrophys. J. Suppl. Ser. **42**, 447-473 (1980); Astrophys. J. Suppl. Ser. **48**, 279-320 (1980); Astrophys. J. **252**,741-764 (1982); Astrophys. J. **293**, 1-16 (1985).
19. J.A. Halbleib, R.A. Sorensen, Nucl. Phys. **A98**, 542 (1967).
20. P. Möller, B. Pfeiffer, K.L. Kratz, Phys. Rev. C **67**, 055802 (2003).
21. D. Cha, Phys. Rev. C, vol. 27, p. 2269, (1983).
22. E. Bender, K. Muto, and H.V. Klapdor-Kleingrothaus, Phys. Lett. B, vol. 208, p. 53, (1988).
23. M. Hirsch, A. Staudt, K. Muto, and H.V. Klapdor-Kleingrothaus, At. Data Nucl. Data Tables **53**, 165 (1993).
24. J.Un- Nabi and H.V. Klapdor-Kleingrothaus, Eur. Phys. J. **A5**, 337-339 (1999).
25. H. Homma, E. Bender, M. Hirsch, K. Muto, H.V. Klapdor-Kleingrothaus, T. Oda, Phys. Rev. C **54** 6 (1996).
26. J.Un- Nabi, S. Stoica, Astrophysics and Space Science, **349**, 843-855 (2013).
27. E.W. Grewe et al, Phys. Rev. C **78**, 044301 (2008).
28. C.S. Wu, S.A. Moszkowski, Wiley, NewYork, (1966).
29. E.D. Commins, McGraw-Hill, NewYork, (1973).
30. N. Cakmak, K. Manisa, S. Unlu and C. Selam, Pranama J. Phys. **74**, 541 (2010).
31. N.I. Pyatov and D.I. Salamov, Nucleonica **22**, 1-127 (1977).
32. K. Muto, E. Bender, T. Oda, H.V. Klapdor-Kleingrothaus, Z. Phys. **A341**, 407 (1992).
33. M.C. Vetterli, O. Häusser, R. Abegg, w.P. Alford, A. Celler, D. Frekers, R. Helmer, R. Henderson, K.H. Hicks, K.P. Jackson, R.G. Jeppesen, C.A. Miller, K. Raywood and S. Yen, Phy. Rev. C **40**, 559-569 (1989).
34. S. Cakmak, J.Un- Nabi, T. Babacan and C. Selam, Astrophys. Space Sci. **352**, 645-663 (2014).
35. S. Cakmak, J.Un- Nabi, T. Babacan and I. Maras, Adv. Space Sci. DOI: 10.1016/j.asr.2014.10.015 (2014).
36. A. Bohr and B.R. Mottelson, Nuclear Structure, (Benjamin, W.A. Inc., New York) Vol. 1, (1969).
37. J.Un- Nabi, N. Cakmak, S. Stoica and Z. Iftikhar (2015) submitted to Phys. Scr.
38. N. Cakmak, S. Unlu, C. Selam, Phys. Atm. Nuc. **75**, 8 (2012).
39. D.J. Horen et al, Phys. Lett. **B95**, 27 (1980).
40. D.J. Horen et al, Phys. Lett. **B99**, 383 (1981).
41. G. Audi, M. Wang, A.H. Wapstra, F.G. Kondev, M. MacCormick, X. Xu and B. Pfeiffer, Chin. Phys. C **36** 1287 (2012); M. Wang, G. Audi, A.H. Wapstra, F.G. Kondev, M. MacCormick, X. Xu and B. Pfeiffer B, Chin. Phys. C **36** 1603 (2012).
42. I.N. Borzov, Phys. Rev. C **71** 065801 (2005).
43. P. Möller et al, At. Data Nucl. Data Tables **66**, 131 (1997).

Tables and Figures

Table 1 Calculated strength distributions for allowed GT, U1F transitions and FF transitions for ^{76,78,80,82,84,86}Zn.

A	Calculated strength distributions									
	E_j (MeV)	pn-QRPA(N) (GT)	E_j (MeV)	pn-QRPA(N) (U1F)	E_j (MeV)	pn-QRPA(WS) (GT)	E_j (MeV)	pn-QRPA(WS) (U1F)	E_j (MeV)	pn-QRPA(WS) (FF)
76	0.2	4.0×10^{-3}			4.9	0.2×10^{0}	7.6	2.0×10^{0}	20	2.14×10^{-2}
	0.2	1.0×10^{-3}			7.2	4.7×10^{0}	15.0	1.8×10^{0}	24	4.74×10^{-2}
	0.3	8.0×10^{-3}			11.0	11×10^{0}	19.0	2.5×10^{0}		
	0.6	3.0×10^{-2}			12.0	0.6×10^{0}	20.0	1.9×10^{0}		
	1.0	8.0×10^{-2}					23.0	4.4×10^{0}		
	1.6	1.2×10^{-1}								
	1.8	8.0×10^{-2}								
	1.8	3.8×10^{-1}								
78	0.3	2.0×10^{-4}			6.7	1.1×10^{0}	15.0	2.4×10^{0}	20.5	2.2×10^{-2}
	0.3	1.0×10^{-3}			7.5	7.3×10^{0}	17.0	1.1×10^{0}	24.1	9.4×10^{-3}
	0.6	5.7×10^{-3}			9.0	8.3×10^{0}	17.0	2.7×10^{0}	24.2	1.8×10^{-2}
	0.7	3.0×10^{-4}			11.0	5.2×10^{0}	19.0	1.9×10^{0}	24.5	1.9×10^{-2}
	0.9	7.6×10^{-3}					20.0	1.7×10^{0}		
	1.0	4.5×10^{-3}					23.0	2.2×10^{0}		
	1.9	5.7×10^{-2}								
80	0.7	6.9×10^{-4}	0.9	2.4×10^{-4}	7.9	3.0×10^{0}	9.0	3.0×10^{0}	22	1.8×10^{-2}
	1.1	9.0×10^{-4}	1.0	3.4×10^{-4}	8.0	7.2×10^{0}	15.0	1.1×10^{0}	25	6.8×10^{-2}
	1.4	9.0×10^{-3}	1.3	7.8×10^{-4}	9.5	6.5×10^{0}	17.0	3.2×10^{0}	26	9.4×10^{-2}
			1.5	9.0×10^{-4}	13.0	1.5×10^{0}	19.0	0.9×10^{0}		
							20.0	1.6×10^{0}		
							21.0	2.7×10^{0}		
							24.0	1.7×10^{0}		
							25.0	2.9×10^{0}		
82	0.4	3.4×10^{-4}	0.0	2.0×10^{-4}	8.6	2.6×10^{0}	5.6	1.6×10^{0}	23	1.2×10^{-2}
	1.1	7.0×10^{-3}	0.5	5.3×10^{-4}	8.9	3.9×10^{0}	11.0	2.2×10^{0}	25	9.9×10^{-3}
	1.8	1.0×10^{-3}	1.5	3.9×10^{-4}	11.0	5.6×10^{0}	17.0	1.1×10^{0}	26	5.8×10^{-2}
					12.0	1.3×10^{0}	19.0	1.6×10^{0}		
					13.0	2.7×10^{0}	21.0	1.1×10^{0}		
							23.0	4.6×10^{0}		
							27.0	4.3×10^{0}		
							29.0	1.5×10^{0}		
84	7.0	1.3×10^{-4}	1.0	4.7×10^{-4}	8.8	5.1×10^{0}	5.5	1.7×10^{0}	22	0.8×10^{0}
	1.2	9.9×10^{-3}	2.0	3.9×10^{-3}	9.5	2.6×10^{0}	10.0	2.2×10^{0}	26	3.4×10^{0}
	2.4	1.4×10^{-3}			11.0	6.6×10^{0}	18.0	1.8×10^{0}	29	4.7×10^{0}
					13.0	0.8×10^{0}	19.0	1.2×10^{0}		
							22.0	2.5×10^{0}		
							23.0	6.2×10^{0}		
							27.0	5.4×10^{0}		
							29.0	3.2×10^{0}		
86	0.1	1.1×10^{-1}	0.5	9.1×10^{-3}	6.7	4.5×10^{0}	6.0	1.7×10^{0}	23	0.9×10^{0}
	0.9	1.5×10^{-3}	1.3	2.9×10^{-3}	9.2	3.5×10^{0}	11.0	2.2×10^{0}	24	0.6×10^{0}
	1.2	6.4×10^{-2}	1.9	3.0×10^{-3}	12.0	7.1×10^{0}	17.0	1.8×10^{0}	27	5.4×10^{0}
	2.4	2.0×10^{-2}	2.1	8.1×10^{-3}			20.0	1.5×10^{0}		
							23.0	0.8×10^{0}		
							24.0	5.8×10^{0}		
							26.0	2.6×10^{0}		
							27.0	2.5×10^{0}		
							28.0	6.0×10^{0}		

Table 2 Same as Table 1 but for ^{84,86,88}Ge.

A	Calculated strength distributions									
	E_j (MeV)	pn-QRPA(N) (GT)	E_j (MeV)	pn-QRPA(N) (U1F)	E_j (MeV)	pn-QRPA(WS) (GT)	E_j (MeV)	pn-QRPA(WS) (U1F)	E_j (MeV)	pn-QRPA(WS) (FF)
84	0.6	9.2×10^{-3}	0.1	2.9×10^{-4}	8.3	4.5×10^{0}	11.0	2.2×10^{0}	22.0	1.0×10^{-2}
	1.2	9.2×10^{-4}	0.1	1.9×10^{-4}	9.1	5.6×10^{0}	16.0	1.3×10^{0}	25.0	3.6×10^{-2}
	1.6	2.9×10^{-3}	0.2	5.7×10^{-4}	10.0	8.2×10^{0}	18.0	1.7×10^{0}	28.0	4.8×10^{-2}
	1.8	7.3×10^{-4}	1.3	3.7×10^{-4}	12.0	3.4×10^{0}	19.0	1.3×10^{0}		
	1.9	3.4×10^{-2}	1.8	1.2×10^{-4}			21.0	1.4×10^{0}		
							23.0	4.1×10^{0}		
							25.0	1.6×10^{0}		
							27.0	3.0×10^{0}		
							28.0	1.7×10^{0}		
86	1.1	2.9×10^{-4}	0.1	2.2×10^{-4}	8.8	6.6×10^{0}	5.2	1.7×10^{0}	26.0	3.4×10^{-2}
	1.3	2.2×10^{-2}	0.7	1.8×10^{-3}	10.0	8.3×10^{0}	10.0	2.2×10^{0}	29.0	5.1×10^{-2}
	1.5	3.9×10^{-3}	1.2	4.4×10^{-4}	12.0	2.0×10^{0}	16.0	1.7×10^{0}		
							18.0	1.8×10^{0}		
							21.0	1.7×10^{0}		
							23.0	5.1×10^{0}		
							26.0	4.4×10^{0}		
							29.0	3.1×10^{0}		
88	0.9	2.8×10^{-2}	0.1	1.9×10^{-4}	8.4	3.0×10^{0}	5.9	1.7×10^{0}	23.0	2.2×10^{-2}
	1.1	3.8×10^{-4}	0.3	6.6×10^{-4}	9.3	3.8×10^{0}	11.0	2.2×10^{0}	26.0	1.7×10^{-2}
	1.3	1.7×10^{-2}	0.9	9.0×10^{-4}	11.0	4.5×10^{0}	17.0	1.4×10^{0}	28.0	5.3×10^{-2}
	1.5	5.2×10^{-3}	1.8	2.0×10^{-3}	12.0	6.0×10^{0}	19.0	1.4×10^{0}		
	1.9	4.9×10^{-3}					22.0	1.5×10^{0}		
							25.0	2.1×10^{0}		
							27.0	4.5×10^{0}		
							29.0	1.6×10^{0}		

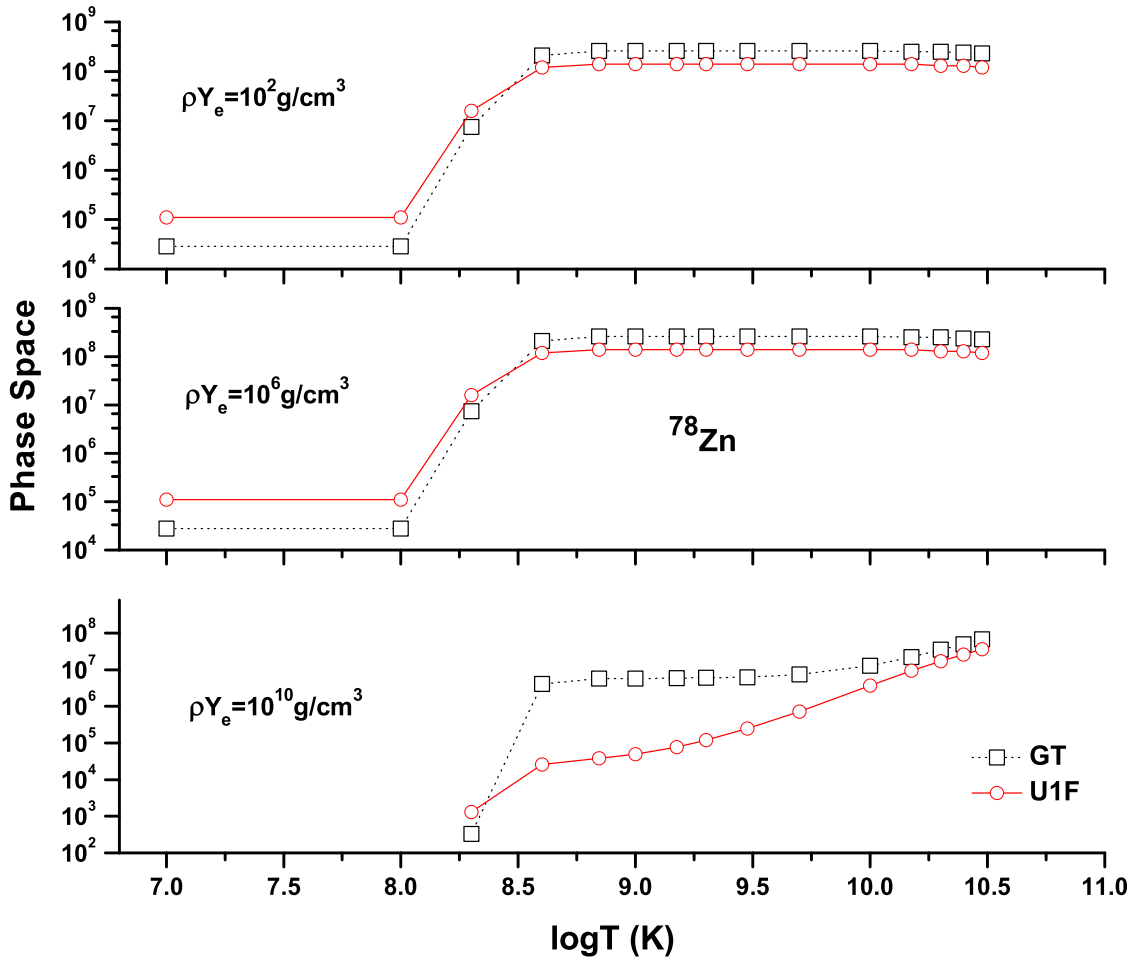

Fig. 1 Comparison of calculated phase space for allowed and U1F transitions for ^{78}Zn as a function of stellar temperatures and densities.

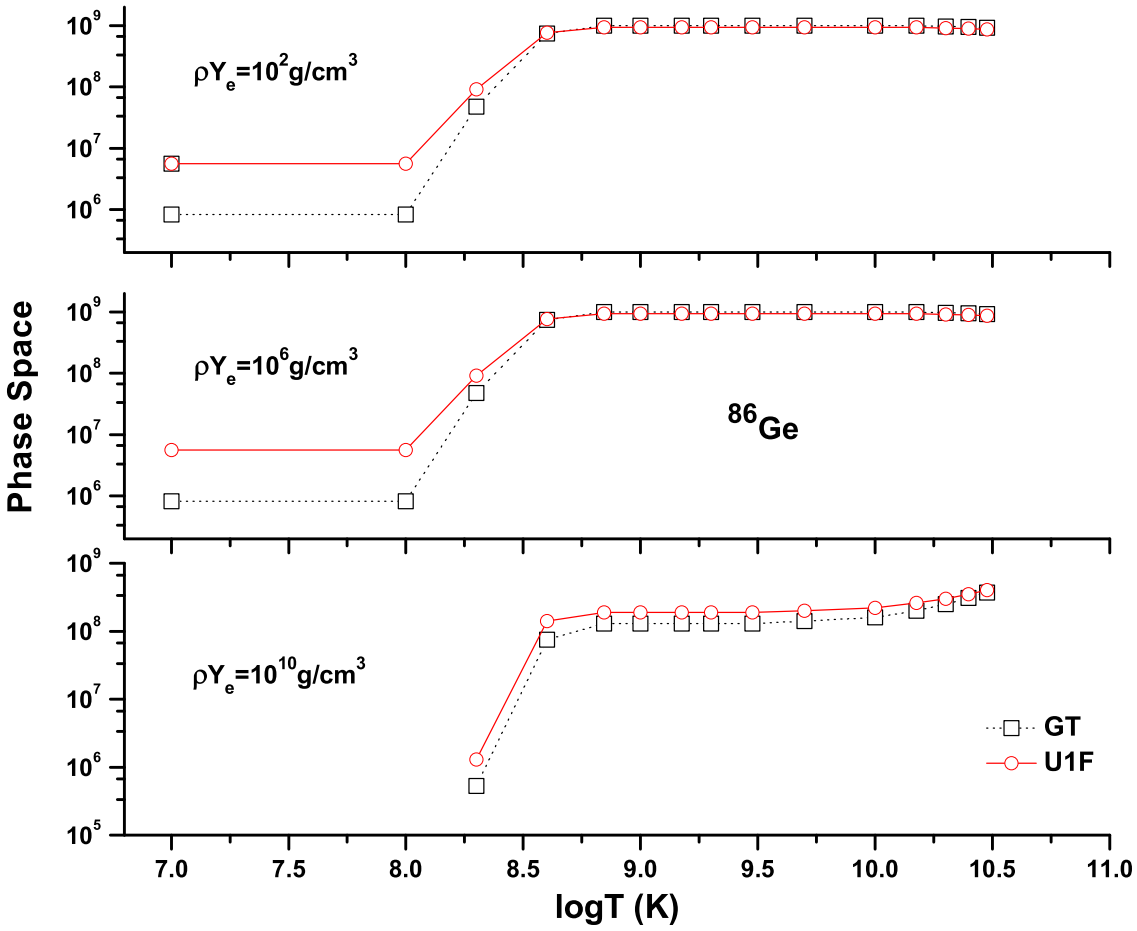

Fig. 2 Same as Fig. 1 but for ^{86}Ge.

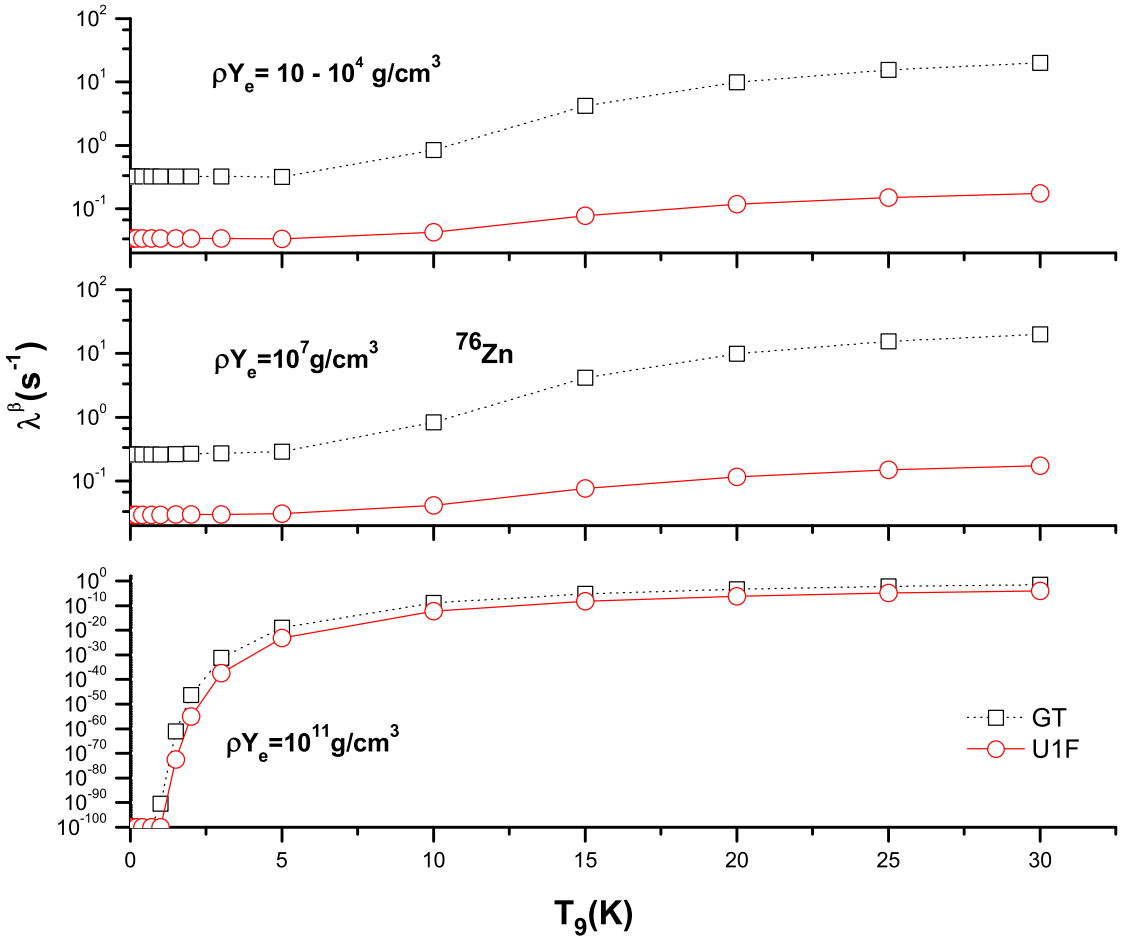

Fig. 3 Allowed (GT) and unique first-forbidden (U1F) β-decay rates on ^{76}Zn as a function of temperature for different selected densities. All β decay rates are given in units of sec^{-1}. Temperatures (T_9) are given in units of 10^9 K.

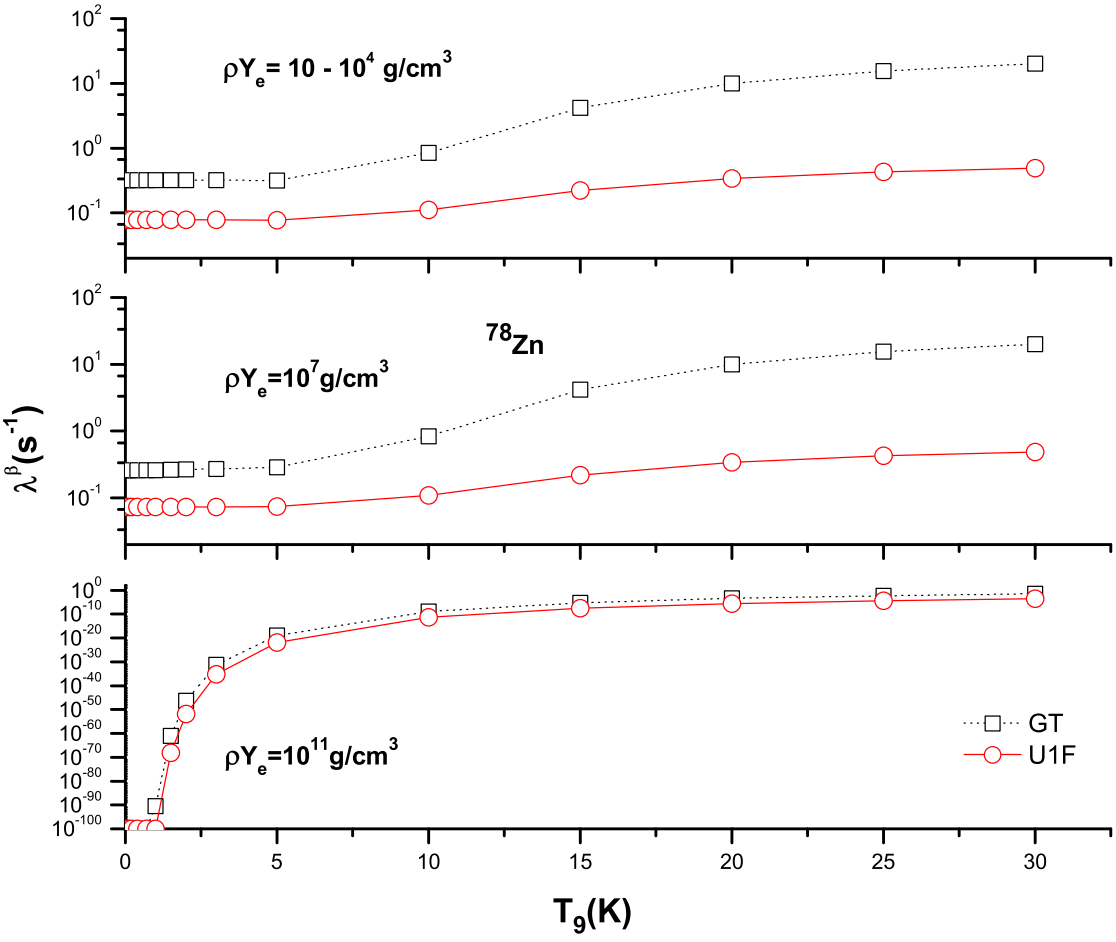

Fig. 4 Same as Fig. 3 but for ^{78}Zn.

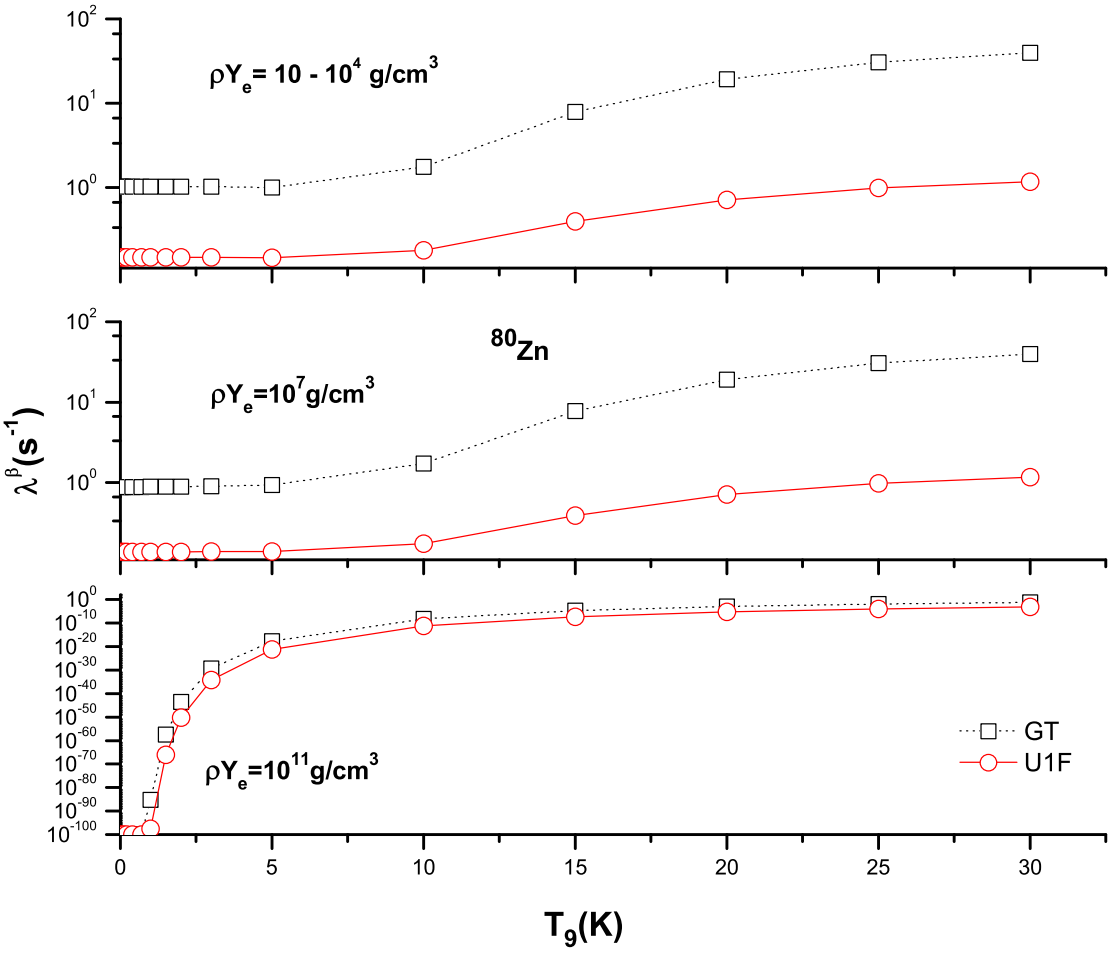

Fig. 5 Same as Fig. 3 but for ^{80}Zn.

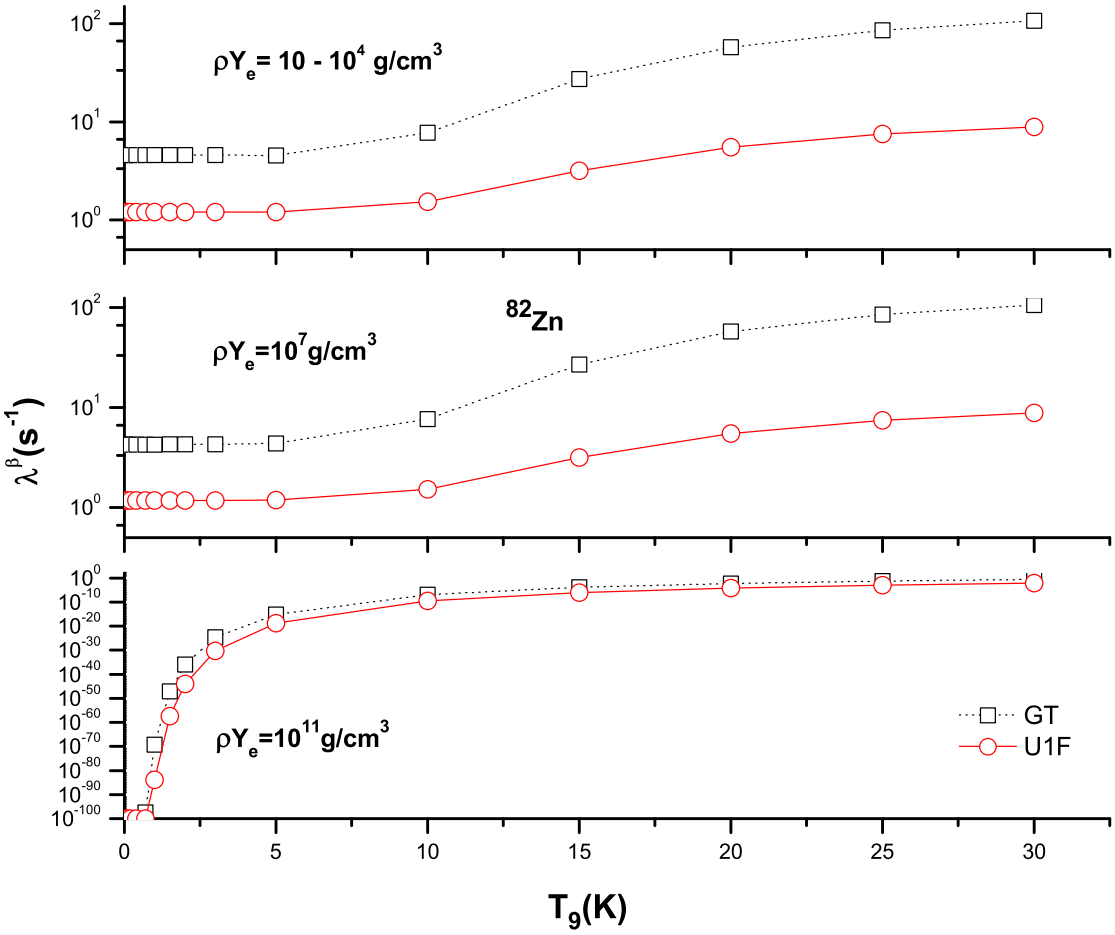

Fig. 6 Same as Fig. 3 but for ^{82}Zn.

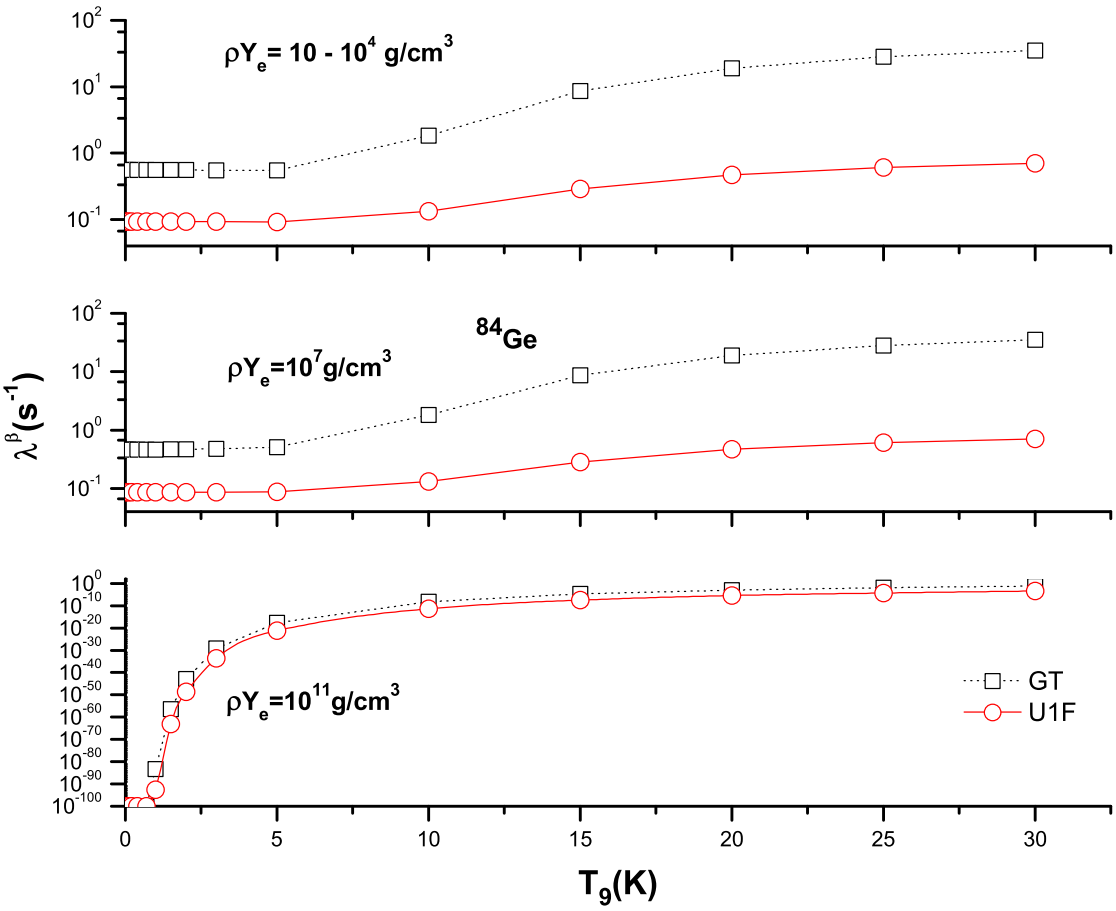

Fig. 7 Same as Fig. 3 but for ^{84}Zn.

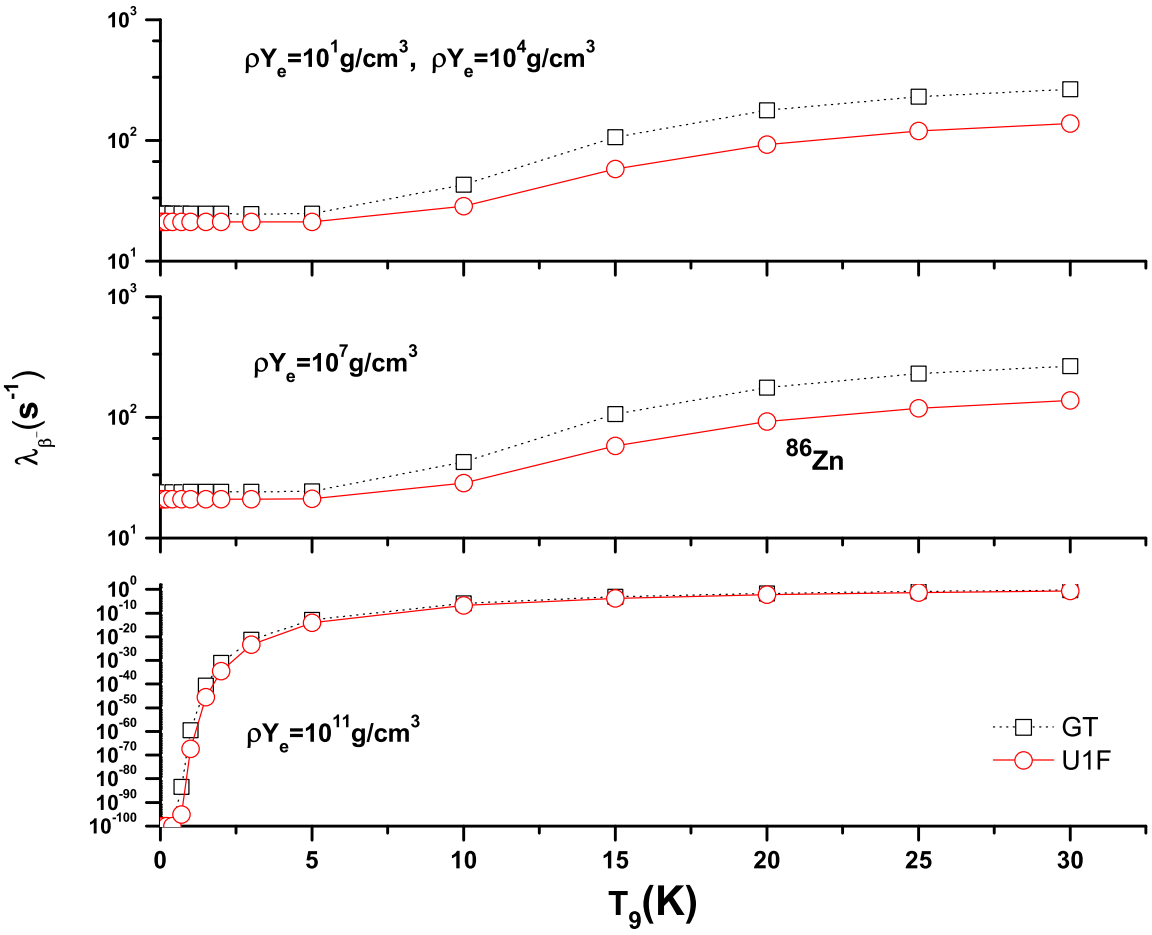

Fig. 8 Same as Fig. 3 but for ^{86}Zn.

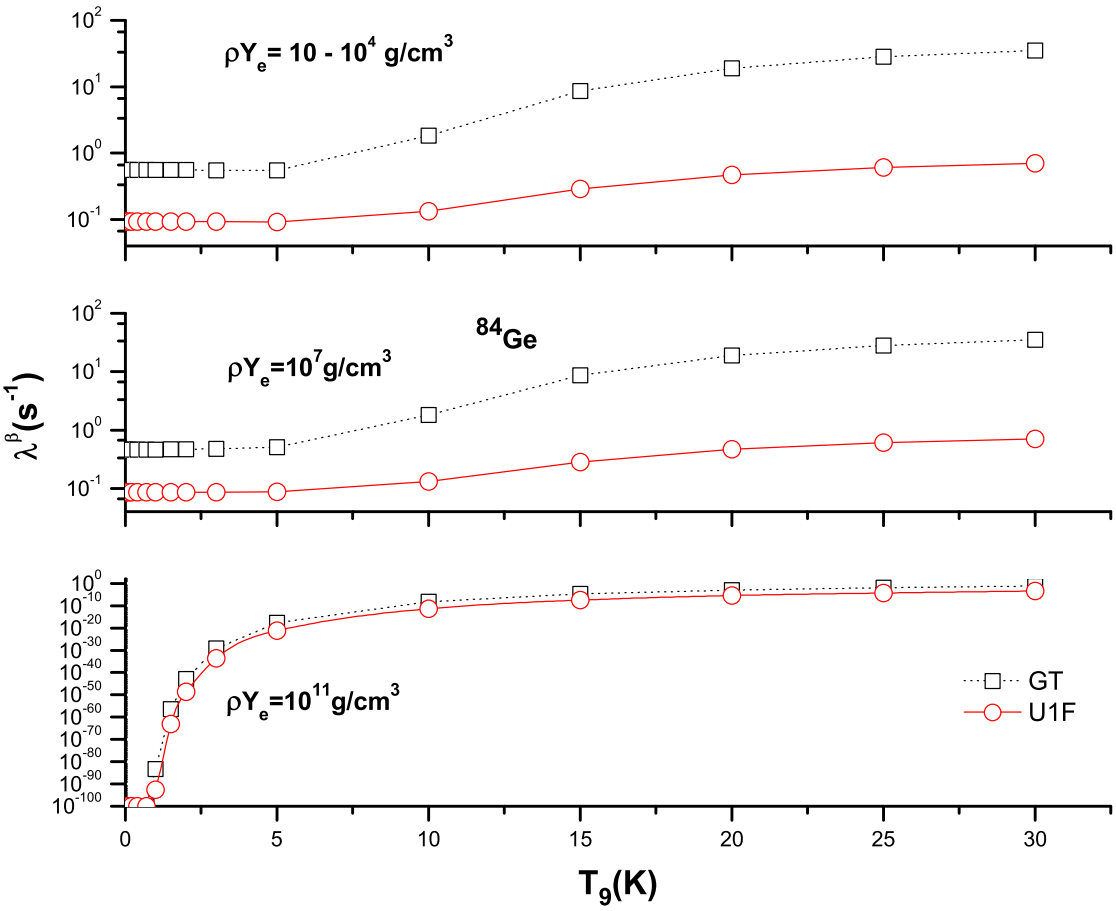

Fig. 9 Same as Fig. 3 but for ^{84}Ge.

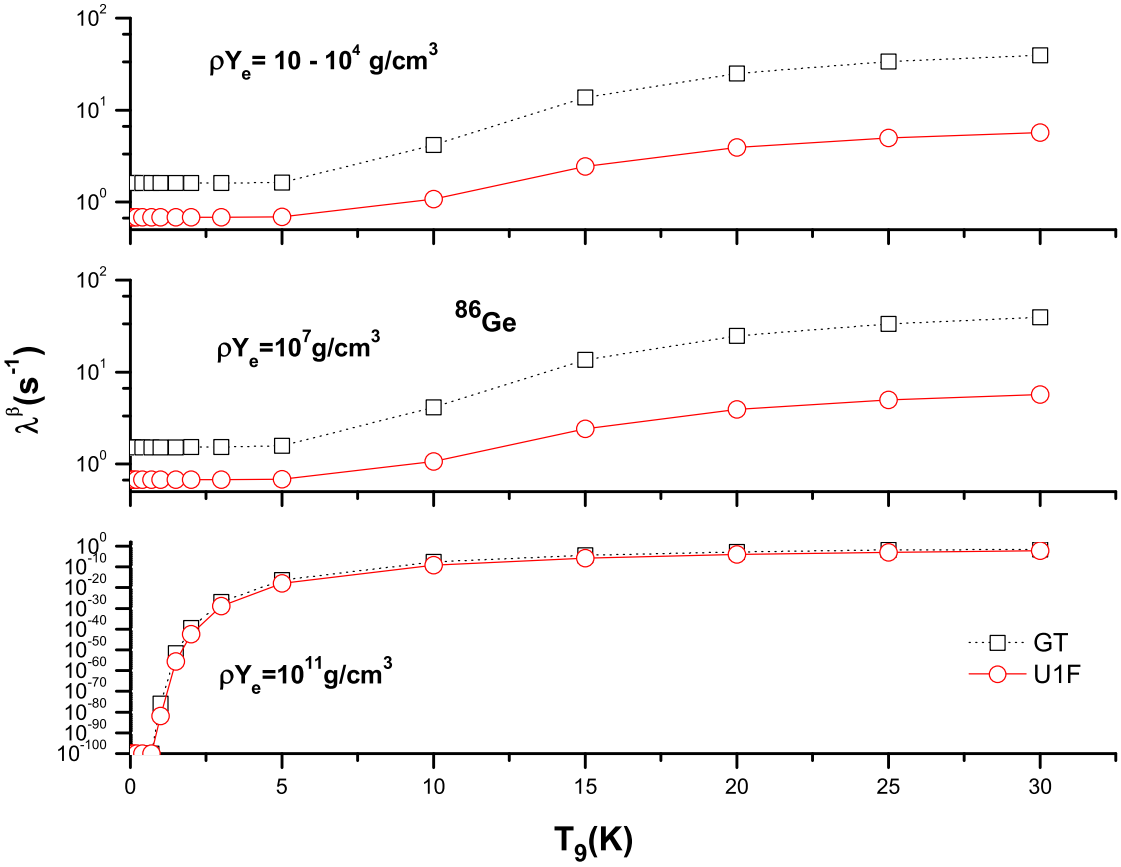

Fig. 10 Same as Fig. 3 but for ^{86}Ge.

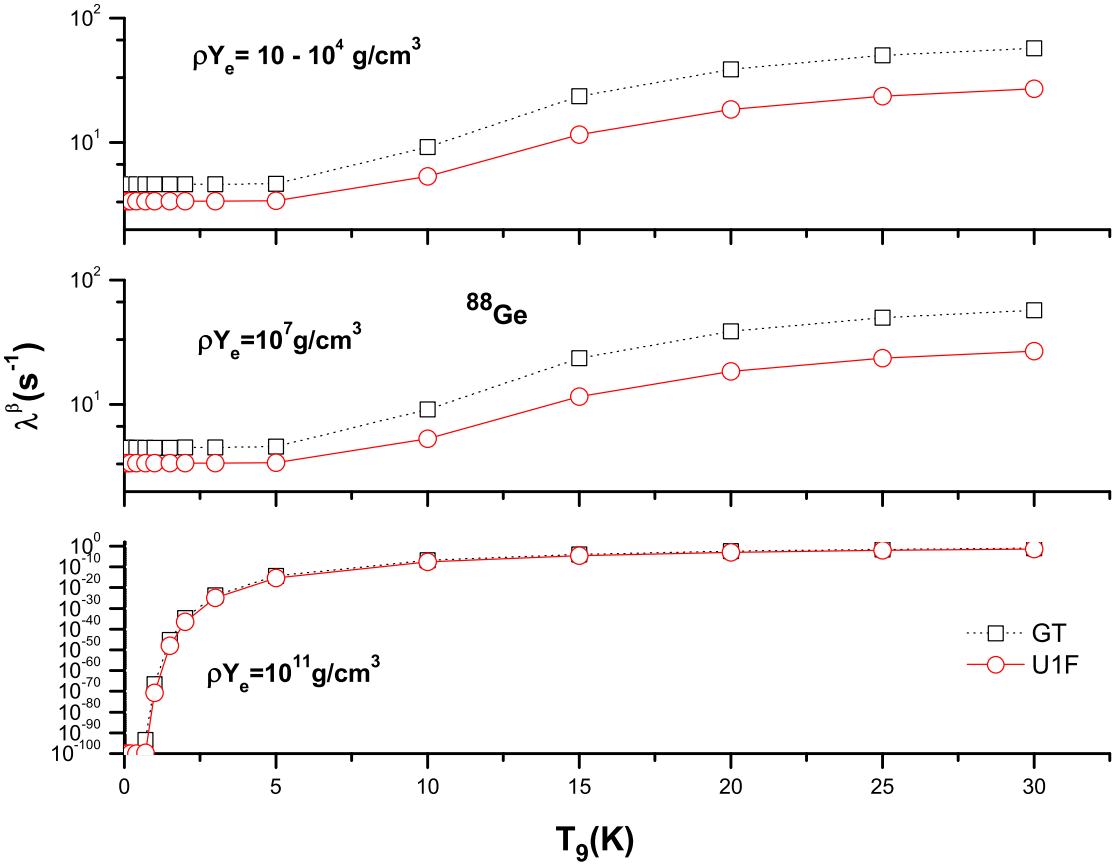

Fig. 11 Same as Fig. 3 but for ^{88}Ge.

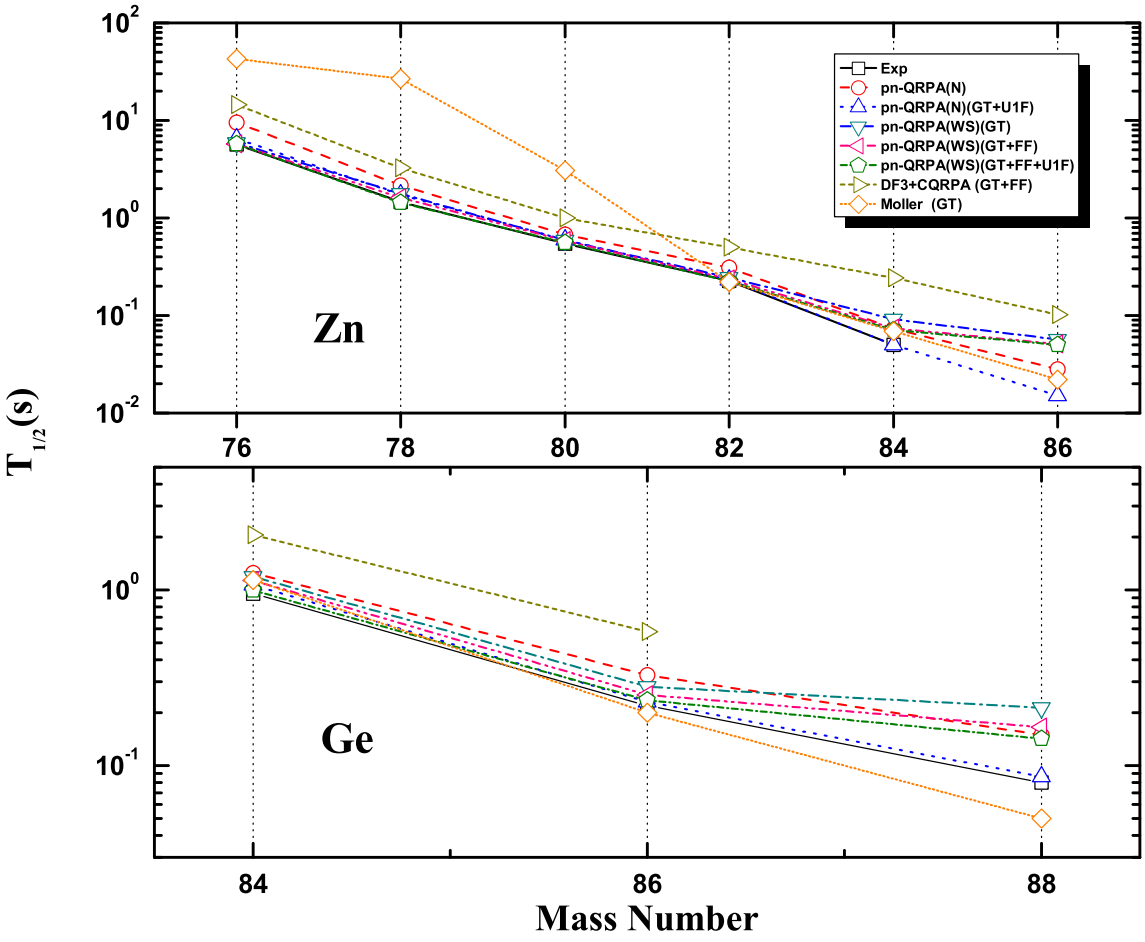

Fig. 12 Total β-decay half-lives for Zn and Ge isotopes calculated from the pn-QRPA(N) and pn-QRPA(WS) (this work) including only the allowed (GT), allowed plus unique first-forbidden (GT+U1F) and allowed plus first-forbidden (GT+FF) transitions, in comparison with experimental data [41], the DF3+CQRPA [42] calculation and those by [43].

Proc. Int. Conf. Relativ. Astrophys.
Pages 160-169, (2015)

Noether Gauge Symmetries of Bianchi I Space-time in Scalar-Coupled Gravity Theories

Işıl Basaran Oz [a,1], **Uğur Camci** [b,1] **and Aydın Yildirim** [c,1]

[1]Akdeniz University, Department of Physics 07058 Antalya, Turkey

Abstract In this study, we consider the induced theory of gravity in Bianchi I space-time. We found new exact solutions of those space-time via Noether gauge symmetries. We use the Noether gauge symmetries to calculate the first integrals which give rise the exact solutions of field equations for the induced theory of gravity.

Keywords Bianchi I space-time, Scalar-coupled theory of gravity, Noether gauge symmetry

1 Introduction

The existence of cosmological problems such as dark matter, dark energy, the flatness and horizon problems, in the Universe as well as the recent observational data [1–11] supporting the accelerated mode of expansion of the Universe constitutes a fundamental theoretical problems to the Einstein's "standard" theory of gravity and the standard model of particle physics [12]. The study of alternative theories of gravity that might be able to solve these problems and at the same time reduce to GR in the weak field regime [13]. Scalar tensor theories include non-minimal scalar field to gravity. They introduce naturally scalar fields which are capable of giving rise to inflationary behaviour [16, 14, 15] of the universe, and generate dark energy dynamics [17]. For these reasons, scalar tensor theories become one of those issues which are of interest in cosmology.

All cosmological models, except the Friedmann-Lemaitre-Robertson-Walker (FLRW) model, contain more arbitrary functions. Then this function can be determined by the field equations. Alternative theories of gravity may bring arbitrary functions from their Lagrangian and thus increases arbitrariness. One suitable way to restrict this arbitrariness is to use Noether symmetries which are directly related to the presence of conserved quantities, as selection rules. Symmetries are a fundamental tool to study physical systems since they allow to reduce dynamics and give insight into conserved quantities. They allow us to select the scalar field's self-interaction potential in a dynamical way, and might be able to reduce the number of dynamical variables of the system of differential equations due to possible cyclic variables.

A Lagrangian density $\mathcal{L}$ accept a strict Noether symmetry if there exists a vector field $\mathbf{X}$, for which the Lie derivative of the Lagrangian vanishes, i.e. $\pounds_{\mathbf{X}}\mathcal{L} = 0$. This approach in terms of space-times like FLRW and Bianchi type universe models has already been used with great success in the frameworks of $f(R)$, $f(T)$ and specific models of scalar-tensor gravity theories. Using this method, the determination of the dynamic conserved quantity and the exact solutions derived, studies are available [18–27].

The strict Noether symmetry approach can be generalized to include a gauge term, giving the *Noether gauge symmetry* (NGS) approach. This method can be a more suitable method to seek for physically motivated solutions of field equations; for some applications; see [28–34].

In this study, we apply the NGS to Bianchi I (BI) space-time, generalizing their earlier work [26]. In the next section, we introduce the Lagrangian, re-derive for completeness, both the equations of motion in scalar-coupled theory of gravity, and their specialized forms for BI space-time. In section 3, we discuss the NGS approach to the Lagrangian for BI space-time, and give solutions of the NGS equations for the scalar-coupled gravity theory motivated from induced gravity. In sec-

[a]e-mail: isilbasaran@akdeniz.edu.tr
[b]e-mail: ucamci@akdeniz.edu.tr
[c]e-mail: aydinyildirim@akdeniz.edu.tr

tion 4, we search for exact solutions of the field equations using the obtained NGS. Finally, in section 5, we offer a brief overview and discuss the obtained results.

2 The Equations of Motion

The general form of the Lagrangian density for the action $\mathcal{A} = \int \mathcal{L}dt$ involving gravity non-minimally coupled with a real scalar field Φ is given by [19]

$$\mathcal{L} = \int d^3x\sqrt{-g}\left[F(\Phi)R - \frac{1}{2}g^{ab}\Phi_a\Phi_b - U(\Phi)\right] \tag{1}$$

where R is the Ricci scalar, $F(\Phi)$ is the generic function describing the coupling, $U(\Phi)$ is the potential for the scalar field, $\Phi_a = \Phi_{,a}$ stand for the components of the gradient of Φ and the signature of metric is $(-+++)$, $(+2)$. We use Planck units. For $F(\Phi) = -1/2$, it reduces to the Einstein-Hilbert action minimally coupled with a scalar field. For $F(\Phi) = \Phi^2/6$, the conformally coupled theory can be obtained. For $F(\Phi) = F_0\Phi^2/12, (F_0 \neq -1)$ represents the theory motivated from induced gravity, and for $F(\Phi) = 1-\zeta\Phi^2$, $\mathcal{L}$ is of the form of the more standard non-minimally coupled scalar field theory.

The variation of the action $\mathcal{A}$ with respect to g_{ab} provides the field equations

$$F(\Phi)G_{ab} = +\frac{1}{2}T^{\Phi}_{ab} - g_{ab}F(\Phi) + F(\Phi)_{;ab} \tag{2}$$

where is the d'Alembert operator,

$$G_{ab} = R_{ab} - \frac{1}{2}Rg_{ab} \tag{3}$$

is the Einstein tensor, and

$$T^{\Phi}_{ab} = \Phi_a\Phi_b - \frac{1}{2}g_{ab}\Phi_c\Phi^c - g_{ab}U(\Phi) \tag{4}$$

is the energy-momentum tensor of the scalar field. The variation with respect to Φ gives rise to the Klein-Gordon equation governing the dynamics of the scalar field

$$\Box\Phi + RF'(\Phi) - U'(\Phi) = 0, \tag{5}$$

where the prime indicates the derivative with respect to Φ. The Bianchi identity $G^{ab}_{\ ;b} = 0$, which gives the conservation laws for the scalar field, also yields the Klein-Gordon equation (5) as a general result [21].

As discussed in the introduction, we will treat the BI space-time. The line element for this space-time can be written in the common form

$$ds^2 = -dt^2 + A^2dr^2 + B^2\left(d\theta^2 + \sin^2\theta d\Phi^2\right), \tag{6}$$

where A and B depend on t.

The Ricci scalar computed from the line element is

$$R = 2\left[\frac{\ddot{A}}{A} + 2\frac{\ddot{B}}{B} + \frac{\dot{B}^2}{B^2} + 2\frac{\dot{A}\dot{B}}{AB}\right], \tag{7}$$

where the dot represents the derivation with respect to time. Then, the Lagrangian of BI space-time become

$$L = -2FA\dot{B}^2 - 4FB\dot{A}\dot{B} - 2F'B^2\dot{A}\dot{\Phi} - 4F'AB\dot{B}\dot{\Phi} + AB^2\left[\frac{\dot{\Phi}^2}{2} - U(\Phi)\right]. \tag{8}$$

The field equations (2) and Klein-Gordon equation (5) for the metric (6) become

$$\frac{\dot{B}^2}{B^2} + 2\frac{\dot{A}\dot{B}}{AB} + \frac{F'}{F}\left(\frac{\dot{A}}{A} + 2\frac{\dot{B}}{B}\right)\dot{\Phi} - \frac{1}{2F}\left[\frac{\dot{\Phi}^2}{2} + U(\Phi)\right] = 0, \tag{9}$$

$$2\frac{\ddot{B}}{B} + \frac{\dot{B}^2}{B^2} + \frac{F'}{F}\left[\ddot{\Phi} + 2\frac{\dot{B}}{B}\dot{\Phi}\right] + \left(\frac{F''}{F} + \frac{1}{4F}\right)\dot{\Phi}^2 - \frac{1}{2F}U(\Phi) = 0, \tag{10}$$

$$\frac{\ddot{A}}{A} + \frac{\ddot{B}}{B} + \frac{\dot{A}\dot{B}}{AB} + \frac{F'}{F}\left[\ddot{\Phi} + \left(\frac{\dot{A}}{A} + \frac{\dot{B}}{B}\right)\dot{\Phi}\right] + \left(\frac{F''}{F} + \frac{1}{4F}\right)\dot{\Phi}^2 - \frac{1}{2F}U(\Phi) = 0, \tag{11}$$

$$\frac{\ddot{A}}{A} + 2\frac{\ddot{B}}{B} + \frac{\dot{B}^2}{B^2} + 2\frac{\dot{A}\dot{B}}{AB} + \frac{q}{B^2} - \frac{1}{2F'}\left[\ddot{\Phi} + \left(\frac{\dot{A}}{A} + 2\frac{\dot{B}}{B}\right)\dot{\Phi} + U'(\Phi)\right] = 0, \tag{12}$$

where $F' \neq 0$. Note that the equations (10)-(12) can also be obtained as the Euler-Lagrange equations using the Lagrangian (8), whereas eq.(9), the (0,0)-Einstein equation, can be obtained as the requirement for the energy function E_L associated with the Lagrangian (8)

$$E_L = \frac{\partial L}{\partial\dot{A}}\dot{A} + \frac{\partial L}{\partial\dot{B}}\dot{B} + \frac{\partial L}{\partial\dot{\Phi}}\dot{\Phi} - L = \frac{\dot{B}^2}{B^2} + 2\frac{\dot{A}\dot{B}}{AB} + \frac{F'}{F}\left(\frac{\dot{A}}{A} + 2\frac{\dot{B}}{B}\right)\dot{\Phi} - \frac{1}{2F}\left[\frac{\dot{\Phi}^2}{2} + U(\Phi)\right] \tag{13}$$

to vanish.

If $\ddot{A}$ and $\ddot{B}$ can be eliminated form the Eqs. (10)-(12) the continuity equation can be found as

$$2(3F'^2 + F)\left[\ddot{\Phi} + \frac{\dot{A}}{A}\dot{\Phi} + 2\frac{\dot{B}}{B}\dot{\Phi}\right] + F'(6F'' + 1)\dot{\Phi} - 2(2UF' - FU') = 0. \tag{14}$$

The unknown quantities of the field equations are $A, B, \Phi, U(\Phi)$ and $F(\Phi)$, but we have only four independent differential equations, namely, Eqs. (9)-(12). Then, in order to solve this system of nonlinear differential equations we need to assume a functional form of the scalar field potential energy $U(\Phi)$ or the function $F(\Phi)$.

3 Noether Gauge Symmetries

We search the condition for the Lagrangian (8) to accept NGS.

Let us consider a NGS generator

$$\mathbf{X} = \xi \frac{\partial}{\partial t} + X^i \frac{\partial}{\partial Q^i}, \tag{15}$$

where the configuration space of the Lagrangian is $Q^i = (A, B, \Phi)$ with tangent space $TQ = (A, B, \Phi, \dot{A}, \dot{B}, \dot{\Phi})$, $X^i = (\alpha, \beta, \gamma)$, $i = 1, 2, 3$; and the components ξ, α, β and γ are functions of t, A, B and Φ. The existence of a NGS implies the existence of a vector field $\mathbf{X}$ as given in (15), if the Lagrangian $L(t, Q^i, \dot{Q}^i)$ satisfies

$$\mathbf{X}^{[1]} L + L(D_t \xi) = D_t f, \tag{16}$$

where $\mathbf{X}^{[1]}$ is the first prolongation of the NGS generator (15) in the form

$$\mathbf{X}^{[1]} = \mathbf{X} + \dot{X}^i \frac{\partial}{\partial \dot{Q}^i}, \tag{17}$$

$f(t, A, B, \Phi)$ is a gauge function, D_t is the total derivative operator with respect to t

$$D_t = \frac{\partial}{\partial t} + \dot{Q}^i \frac{\partial}{\partial Q^i}, \tag{18}$$

and $\dot{X}^i$ is defined as $\dot{X}^i = D_t X^i - \dot{Q}^i D_t \xi$. It is important to give the following first integral to emphasize the significance of NGS: If $\mathbf{X}$ is the NGS generator corresponding to the Lagrangian $L(t, Q^i, \dot{Q}^i)$, then

$$I = -\xi E_L + X^i \frac{\partial L}{\partial \dot{Q}^i} - f, \tag{19}$$

is the Noether first integral, i.e. the Hamiltonian or a conserved quantity associated with the generator $\mathbf{X}$. Here, E_L is the energy function defined for any Lagrangian, $E_L = \dot{Q}^i \frac{\partial L}{\partial \dot{Q}^i} - L$.

Obviously, the gauge function f is arbitrary up to an additive constant, and this arbitrariness will be used to simplify expressions in the rest of the paper, whenever possible. Also, the trivial Noether gauge symmetry ∂_t is related to the conservation of energy, and gives rise to the Hamiltonian ($E_L = 0$) of the dynamical system.

From the Lagrangian (8) the NGS condition (16) yields the following set of over-determined system of equations

$$\xi_A = 0, \quad \xi_B = 0, \quad \xi_\Phi = 0, \tag{20}$$

$$-2B\left(2F\beta_t + F' B \gamma_t\right) - G_A = 0, \tag{21}$$

$$-4\left[F\left(B\alpha_t + A\beta_t\right) + F' AB\gamma_t\right] - G_B = 0, \tag{22}$$

$$-2F'\left(B^2\alpha_t + 2AB\beta_t\right) + AB^2\gamma_t - G_\Phi = 0, \tag{23}$$

$$2F\beta_A + BF'\gamma_A = 0, \tag{24}$$

$$\alpha + 2B\alpha_B + 2A\beta_B + A\frac{F'}{F}\left(\gamma + 2B\gamma_B\right) - A\xi_t = 0, \tag{25}$$

$$\alpha + 2\frac{A}{B}\beta + 2A\gamma_\Phi - 4F'\left(\alpha_\Phi + 2\frac{A}{B}\beta_\Phi\right) - A\xi_t = 0, \tag{26}$$

$$\beta + B\left[\alpha_A + \beta_B + \frac{F'}{F}\left(\gamma + A\gamma_A + \frac{B}{2}\gamma_B\right)\right] + A\beta_A - B\xi_t = 0, \tag{27}$$

$$\frac{F'}{F}\left(2\beta + B\alpha_A + B\gamma_\Phi + 2A\beta_A - B\xi_t\right) + \frac{F''}{F}B\gamma + 2\beta_\Phi - \frac{1}{2F}AB\gamma_A = 0, \tag{28}$$

$$\frac{F'}{F}\left(\alpha + \frac{A}{B}\beta + \frac{B}{2}\alpha_B + A\beta_B + A\gamma_\Phi - A\xi_t\right) + \frac{F''}{F}A\gamma + \alpha_\Phi + \frac{A}{B}\beta_\Phi - \frac{1}{4F}AB\gamma_B = 0, \tag{29}$$

$$-2qF\left(\alpha + \frac{F'}{F}A\gamma + A\xi_t\right) + B(B\alpha + 2A\beta + AB\xi_t)U(\Phi) + AB^2\gamma U'(\Phi) = 0. \tag{30}$$

Then, selecting the function F, the above NGS equations will give the solutions for $\xi, \alpha, \beta, \gamma, f$ and the potential $U(\Phi)$.

For BI space-time the Hessian determinant $W = \Sigma\left|\frac{\partial^2 L}{\partial \dot{Q}_i \partial \dot{Q}_j}\right|$ is given by

$$W = -16AB^4F(3F'^2 + F). \tag{31}$$

There exists two cases depending on the Hessian determinant W vanishes or not:

3.1 **Case (i):**

If the Lagrangian (8) is degenerate, then the Hessian determinant W vanishes, and therefore the function F is given by

$$F(\Phi) = -\frac{1}{12}\Phi^2. \tag{32}$$

In this case, the first two of the three main terms of eq.(14) vanish, enabling us to directly determine

$$U(\Phi) = \lambda\Phi^4 \tag{33}$$

whenever (14) applies.

We show some of the NGSs in Tables 1 and 2. In order to keep the tables compact, we explicitly present the simplest case **(i.1)** in the text, and then express some results of some other cases in terms of the explicitly presented ones. We also explicitly display some cases, **(i.3), (ii.a.1)** and **(ii.a.4)**, that are too long to fit in the tables.

Case (i.1): $U(\Phi) = 0$. For this case, the components of the NGS generator (15) are found as follows:

$$\begin{aligned}
\xi &= c_1\frac{t^2}{2} + c_2 t + c_3,\\
\alpha &= A(c_1 t + c_2) - 2c_4 A + 2c_5 A\ln(B\Phi)\\
&\quad + 2c_6\frac{(A/B)^{1/3}}{\Phi} - 2c_7\frac{A}{B\Phi} - 2c_8 A,\\
\beta &= c_1 tB - c_5 B\ln(A\Phi) - c_6\frac{(B/A)^{2/3}}{\Phi} + \frac{c_7}{\Phi} + c_8 B,\\
\gamma &= -c_1 t\Phi + \left[c_4 + c_5\ln\left(\frac{A}{B}\right)\right]\Phi\\
&\quad + c_6(A^2B)^{-1/3} + \frac{c_7}{B},
\end{aligned} \tag{34}$$

where c_i's are constants of integration. Then, the *eight* NGSs are given by

$$\begin{aligned}
&\mathbf{X}_1 = \partial_t, \qquad \mathbf{X}_2 = -2A\partial_A + B\partial_B,\\
&\mathbf{X}_3 = -2A\partial_A + \Phi\partial_\Phi, \qquad \mathbf{X}_4 = t\partial_t + A\partial_A,\\
&\mathbf{X}_5 = t^2\partial_t + 2t\left(A\partial_A + B\partial_B - \Phi\partial_\Phi\right),\\
&\mathbf{X}_6 = 2A\ln(B\Phi)\partial_A - B\ln(A\Phi)\partial_B + \Phi\ln\left(\frac{A}{B}\right)\partial_\Phi,\\
&\mathbf{X}_7 = -\frac{2A}{B\Phi}\partial_A + \frac{1}{\Phi}\partial_B + \frac{1}{B}\partial_\Phi,\\
&\mathbf{X}_8 = 2\frac{(A/B)^{\frac{1}{3}}}{\Phi}\partial_A - \frac{(B/A)^{\frac{2}{3}}}{\Phi}\partial_B + (A^2B)^{-\frac{1}{3}}\partial_\Phi.
\end{aligned} \tag{35}$$

with the non-vanishing Lie brackets

$$\begin{aligned}
&[\mathbf{X}_1,\mathbf{X}_4] = \mathbf{X}_1 \quad [\mathbf{X}_1,\mathbf{X}_5] = 2(\mathbf{X}_2 - \mathbf{X}_3 + \mathbf{X}_4),\\
&[\mathbf{X}_2,\mathbf{X}_6] = 2\mathbf{X}_2 - 3\mathbf{X}_3, \quad [\mathbf{X}_2,\mathbf{X}_7] = -\mathbf{X}_7,\\
&[\mathbf{X}_2,\mathbf{X}_8] = \mathbf{X}_8, \qquad [\mathbf{X}_3,\mathbf{X}_6] = \mathbf{X}_2 - 2\mathbf{X}_3,\\
&[\mathbf{X}_3,\mathbf{X}_7] = -\mathbf{X}_7, \quad [\mathbf{X}_3,\mathbf{X}_8] = \frac{1}{3}\mathbf{X}_8,\\
&[\mathbf{X}_4,\mathbf{X}_5] = \mathbf{X}_5, \qquad [\mathbf{X}_4,\mathbf{X}_6] = \mathbf{X}_3 - \mathbf{X}_2,\\
&[\mathbf{X}_4,\mathbf{X}_8] = -\frac{2}{3}\mathbf{X}_8,\\
&[\mathbf{X}_6,\mathbf{X}_7] = \frac{1}{B\Phi}(\mathbf{X}_2 - 3\mathbf{X}_3) + \ln(B\Phi)\mathbf{X}_7,\\
&[\mathbf{X}_6,\mathbf{X}_8] = \frac{3}{(A^2B)^{1/3}\Phi}(\mathbf{X}_2 - \mathbf{X}_3)\\
&\qquad + \ln\left(\frac{1}{(A^2B)^{1/3}\Phi}\right)\mathbf{X}_8.
\end{aligned} \tag{36}$$

Using (19), we find the first integrals for those of eight NGSs:

$$I_1 = -E_L, \quad I_2 = \frac{1}{3}AB^2\Phi^2\left(\frac{\dot{A}}{A} - \frac{\dot{B}}{B}\right), \tag{37}$$

$$I_3 = \frac{1}{3}AB^2\Phi^2\left(\frac{\dot{A}}{A} + \frac{\dot{\Phi}}{\Phi}\right), \tag{38}$$

$$I_4 = -tE_L + \frac{1}{3}AB^2\Phi^2\left(\frac{\dot{B}}{B} + \frac{\dot{\Phi}}{\Phi}\right), \tag{39}$$

$$I_5 = -t^2E_L, \tag{40}$$

$$\begin{aligned}
I_6 = \frac{1}{3}AB^2\Phi^2\Big[&-\ln(B\Phi)\frac{\dot{A}}{A} + \ln(A\Phi)\frac{\dot{B}}{B}\\
&+\ln\left(\frac{A}{B}\right)\frac{\dot{\Phi}}{\Phi}\Big],
\end{aligned} \tag{41}$$

$$I_7 = \frac{1}{3}AB\Phi\left(2\frac{\dot{A}}{A} + \frac{\dot{B}}{B} + 3\frac{\dot{\Phi}}{\Phi}\right), \tag{42}$$

$$I_8 = (AB^5)^{1/3}\Phi\left(\frac{\dot{B}}{B} + \frac{\dot{\Phi}}{\Phi}\right). \tag{43}$$

Case (i.3): $U(\Phi) = \lambda\Phi^m$, where $m(\neq 2)$ is a constant. In this case, it follows from the continuity equation (14) that $m = 4$. Then the NGS components are obtained by

$$\begin{aligned}
\xi &= g(t),\\
\alpha &= A\dot{g}(t) - \frac{2}{B\Phi^3}\left(c_1\frac{A}{3B^2} + \frac{c_2}{A}\right) - 2c_3 A,\\
\beta &= B\dot{g}(t) - \frac{5c_1}{3B^2\Phi^3} - \frac{c_2}{A^2\Phi^3} + c_3 B,\\
\gamma &= -\Phi\dot{g}(t) + \frac{1}{B\Phi^2}\left(\frac{c_1}{B^2} + \frac{c_2}{A^2}\right),
\end{aligned} \tag{44}$$

where $g(t)$ is an arbitrary function of t. This result is interesting because of that there exists an infinite family of NGSs due to the functional dependence of NGS components. Thus the *four* NGSs of this case are $\mathbf{X}_1^3 = \mathbf{X}_2$ given above and

$$\begin{aligned}
\mathbf{X}_2^3 &= -\frac{2}{AB\Phi^3}\partial_A - \frac{1}{A^2\Phi^3}\partial_B + \frac{1}{A^2B\Phi^2}\partial_\Phi,\\
\mathbf{X}_3^3 &= -\frac{2A}{3B^3\Phi^3}\partial_A - \frac{5}{3B^2\Phi^3}\partial_B + \frac{1}{B^3\Phi^2}\partial_\Phi,\\
\mathbf{X}_4^3 &= g(t)\partial_t + \dot{g}(t)\left(A\partial_A + B\partial_B - \Phi\partial_\Phi\right).
\end{aligned} \tag{45}$$

The non-zero Lie brackets due to the NGS generators $\mathbf{X}_3^3$ and $\mathbf{X}_4^3$ are

$$[\mathbf{X}_2,\mathbf{X}_3^3] = -3\mathbf{X}_3^3, \quad [\mathbf{X}_2,\mathbf{X}_2^3] = 3\mathbf{X}_2^3. \tag{46}$$

Table 1 The potential functions and lists of NGSs of cases (i) and (ii) for the BI space-time, where λ is a constant.

Potential Function	$Case(i)\, F=-\Phi^2/12$	$Case(ii.a)\, F=F_0\Phi^2/12$	$Case(ii.b)\, F=1-\zeta\Phi^2$
1. $U(\Phi)=0$	$\mathbf{X}_1,\mathbf{X}_2,\mathbf{X}_3,\mathbf{X}_4,\mathbf{X}_5,\mathbf{X}_6,\mathbf{X}_7,\mathbf{X}_8$	$\mathbf{X}_1,\mathbf{X}_2,\mathbf{X}_3,\mathbf{X}_4,\mathbf{X}_5^{a1},\mathbf{X}_6^{a1}$	$\mathbf{X}_1,\mathbf{X}_2,\mathbf{X}_4$
2. $U(\Phi)=\lambda$	$\mathbf{X}_1,\mathbf{X}_2,\mathbf{X}_3,\mathbf{X}_6,\mathbf{X}_5^2$	$\mathbf{X}_1,\mathbf{X}_2,\mathbf{X}_3^{a2}$	$\mathbf{X}_1,\mathbf{X}_2$
3. $U(\Phi)=\lambda\Phi^m, m\neq 2$	$\mathbf{X}_2,\mathbf{X}_2^3,\mathbf{X}_3^3,\mathbf{X}_4^3$	$\mathbf{X}_1,\mathbf{X}_2,\mathbf{X}_3^{a3}$	$\mathbf{X}_1,\mathbf{X}_2$
4. $U(\Phi)=\lambda\Phi^2$	$\mathbf{X}_1,\mathbf{X}_2,\mathbf{X}_3,\mathbf{X}_6,\mathbf{X}_5^4$	$\mathbf{X}_1,\mathbf{X}_2,\mathbf{X}_3,\mathbf{X}_4^{a4},\mathbf{X}_5^{a4},\mathbf{X}_6^{a4}$	$\mathbf{X}_1,\mathbf{X}_2$

Table 2 The NGSs and corresponding first integrals for the BI spacetime cases not covered in the text.

Case	NGS	First Integral
(i.2)	$\mathbf{X}_1^2=\mathbf{X}_1,\quad \mathbf{X}_2^2=\mathbf{X}_2,\quad \mathbf{X}_3^2=\mathbf{X}_3,\quad \mathbf{X}_4^2=\mathbf{X}_6$ $\mathbf{X}_5^2=t\partial_t-A\partial_A+\Phi\partial_\Phi$	$I_1^2=I_1,\quad I_2^2=I_2,\quad I_3^2=I_3,\quad I_4^2=I_6$ $I_5^2=\frac{1}{3}AB^2\Phi^2\ \ \frac{\dot A}{A}+\frac{\dot B}{B}+2\frac{\dot\Phi}{\Phi}$
(i.4)	$\mathbf{X}_1^4=\mathbf{X}_1,\quad \mathbf{X}_2^4=\mathbf{X}_2,\quad \mathbf{X}_3^4=\mathbf{X}_3,\quad \mathbf{X}_4^4=\mathbf{X}_6$ $\mathbf{X}_5^4=t\partial_t-A[4\ln(B\Phi)+1]\partial_A-B\ln(B\Phi)\partial_B$ $+3\Phi\ln(B\Phi)\partial_\Phi$	$I_1^4=I_1,\quad I_2^4=I_2,\quad I_3^4=I_3,\quad I_4^4=I_6$ $I_5^4=\frac{1}{3}A(B\Phi)^2\left[\ln(B\Phi)\ \ 2\frac{\dot A}{A}+\frac{\dot B}{B}+3\frac{\dot\Phi}{\Phi}\ -\ \frac{\dot B}{B}+\frac{\dot\Phi}{\Phi}\ \right]$
(ii.a.2)	$\mathbf{X}_1^{a2}=\mathbf{X}_1,\quad \mathbf{X}_2^{a2}=\mathbf{X}_2,\quad \mathbf{X}_3^{a2}=\mathbf{X}_5^2$	$I_1^{a2}=I_1,\quad I_2^{a2}=I_2,\quad I_3^{a2}=I_5^2$
(ii.a.3)	$\mathbf{X}_1^{a3}=\mathbf{X}_1,\quad \mathbf{X}_2^{a3}=\mathbf{X}_2$ $\mathbf{X}_3^{a3}=t\partial_t+\frac{(m+2)}{(m-2)}A\partial_A-\frac{2}{(m-2)}\Phi\partial_\Phi$	$I_1^{a3}=I_1,\quad I_2^{a3}=I_2$ $I_3^{a3}=\frac{k_3}{3(m-2)}A(B\Phi)^2\left[m\ \ \frac{\dot B}{B}+\frac{\dot\Phi}{\Phi}\ -2\ \ \frac{\dot A}{A}+\frac{\dot B}{B}-\frac{\dot\Phi}{\Phi}\ -\frac{6}{k_3}\frac{\dot\Phi}{\Phi}\right]$
(ii.b.1)	$\mathbf{X}_1^{b1}=\mathbf{X}_1,\quad \mathbf{X}_2^{b1}=\mathbf{X}_2,\quad \mathbf{X}_3^{b1}=\mathbf{X}_4$	$I_1^{b1}=I_1,\quad I_2^{b1}=I_2,\quad I_3^{b1}=I_4$
(ii.b.2)	$\mathbf{X}_1^{b2}=\mathbf{X}_1,\quad \mathbf{X}_2^{b2}=\mathbf{X}_2$	$I_1^{b2}=I_1,\quad I_2^{b2}=I_2$
(ii.b.3)	$\mathbf{X}_1^{b3}=\mathbf{X}_1,\quad \mathbf{X}_2^{b3}=\mathbf{X}_2$	$I_1^{b3}=I_1,\quad I_2^{b3}=I_2$
(ii.b.4)	$\mathbf{X}_1^{b4}=\mathbf{X}_1,\quad \mathbf{X}_2^{b4}=\mathbf{X}_2$	$I_1^{b4}=I_1,\quad I_2^{b4}=I_2$

The first integrals for the NGSs of this case are given by

$$
\begin{aligned}
I_1^3&=\frac{1}{3}AB^2\Phi^2\left(\frac{\dot A}{A}-\frac{\dot B}{B}\right),\\
I_2^3&=-\frac{B}{3A\Phi}\left(\frac{\dot B}{B}+\frac{\dot\Phi}{\Phi}\right),\\
I_3^3&=-\frac{A}{9B\Phi}\left(2\frac{\dot A}{A}+\frac{\dot B}{B}+3\frac{\dot\Phi}{\Phi}\right),\\
I_4^3&=-g(t)E_L.
\end{aligned}
\tag{47}
$$

3.2 **Case (ii):**

If the Lagrangian (8) is non-degenerate, then the Hessian determinant W does not vanish. For the form of F, we will consider **(ii.a)** $F=F_0\Phi^2/12$, where $F_0\neq -1$, the form motivated by induced gravity; or **(ii.b)** $F(\Phi)=1-\zeta\Phi^2$, which is a more standard form of non-minimally coupled scalar field theory, where ζ is a constant.

We now present solutions of the NGS equations in the BI space-time for the coupling functions $F(\Phi)$ listed above. The NGS equations also allow determination of $U(\Phi)$ via eq.(30), but we will classify the solutions according to the $U(\Phi)$ functions from the beginning, in addition to the classification according to the $F(\Phi)$ functions outlined just above. We will show the results in tables, elaborating on only some of them in the text.

Case (ii.a.1): $U(\Phi)=0$. For this case, the components of NGS generators, and the gauge function are found as

$$
\begin{aligned}
\xi&=c_1\frac{t^2}{2}+c_2t+c_3,\\
\alpha&=A\left(c_1\frac{k_4}{k_1}t+c_2-2c_4\right)+2c_5A\ln(B\Phi^{\frac{k_4}{k_3}})-2c_6,\\
\beta&=c_1\frac{5}{k_1}Bt+c_5B\ln(\frac{\Phi^{\frac{k_4}{k_3}}}{A})+c_6B,\\
\gamma&=c_1\frac{k_3}{k_1}t\Phi+c_4\Phi+c_5\Phi\ln(A/B),\\
f&=c_1\frac{k_2k_3}{k_1}AB^2\Phi^2,
\end{aligned}
\tag{48}
$$

where $k_1=-8F_0-9, k_2=-F_0-1, k_3=-F_0$ and $k_4=-2F_0-3$. It is easily seen that k_2 and k_3 are non-zero in this case, but k_1 or k_4 could be. Hence, we need to consider subcases where they are both nonzero, vs. where one or the other vanishes. The latter singular ones cannot be obtained as special cases of the above solutions, they have to be trated from scratch.

Subcase ii.a.1.1. $k_1\neq 0$, $k_4\neq 0$. In this subcase, the number of NGSs is *six* which are $\mathbf{X}_1^{a1}=\mathbf{X}_1, \mathbf{X}_2^{a1}=$

$\mathbf{X}_2, \mathbf{X}_3^{a1} = \mathbf{X}_3, \mathbf{X}_4^{a1} = \mathbf{X}_4$ and

$$\mathbf{X}_5^{a1} = t^2\partial_t + \frac{2t}{k_1}\left[k_4(A\partial_A + B\partial_B) + k_3\Phi\partial_\Phi\right], \tag{49}$$

$$\mathbf{X}_6^{a1} = 2A\ln\left(B\Phi^{\frac{k_4}{k_3}}\right)\partial_A + B\ln\left(\frac{\Phi^{\frac{k_4}{k_3}}}{A}\right)\partial_B + \Phi\ln(A/B)\partial_\Phi. \tag{50}$$

The non-vanishing Lie brackets due to $\mathbf{X}_5^{a1}$ and $\mathbf{X}_6^{a1}$ are

$$\begin{aligned}
&[\mathbf{X}_1, \mathbf{X}_5^{a1}] = \frac{k_4}{k_1}\mathbf{X}_2 + \frac{k_3}{k_1}\mathbf{X}_3 + \mathbf{X}_4,\\
&[\mathbf{X}_2, \mathbf{X}_6^{a1}] = 2\mathbf{X}_2 - 3\mathbf{X}_3,\\
&[\mathbf{X}_3, \mathbf{X}_6^{a1}] = -2\mathbf{X}_3 - c\mathbf{X}_2,\\
&[\mathbf{X}_4, \mathbf{X}_5^{a1}] = \mathbf{X}_5^{a1},\\
&[\mathbf{X}_4, \mathbf{X}_6^{a1}] = \mathbf{X}_4 - \mathbf{X}_6^{a1}.
\end{aligned} \tag{51}$$

where $c = -(3 + 4F_0)/F_0$. The first integrals of the generators $\mathbf{X}_5^{a1}$ and $\mathbf{X}_6^{a1}$ are

$$I_5 = \frac{2k_2k_3}{k_1}AB^2\Phi^2\Big[t\Big(\frac{\dot{A}}{A} + 2\frac{\dot{B}}{B} + 2\frac{\dot{\Phi}}{\Phi}\Big) - 1\Big], \tag{52}$$

$$I_6 = \frac{2k_3}{3}tAB^2\Phi^2\Big[\frac{1}{2}\ln(B^{-1}\Phi^\ell)\frac{\dot{A}}{A} + \ln(\Phi^{\frac{3\ell}{2}})\frac{\dot{B}}{B} + \ln(B\Phi^4/A)^{\ell/2}\frac{\dot{\Phi}}{\Phi}\Big], \tag{53}$$

where $\ell = k_4/k_3$.

Subcase ii.a.1.2. $F_0 = -9/8$, i.e. $k_1 = 0$. There are *seven* NGSs for this subcase, which are $\mathbf{Y}_1 = \mathbf{X}_1, \mathbf{Y}_2 = \mathbf{X}_2, \mathbf{Y}_3 = \mathbf{X}_3, \mathbf{Y}_4 = \mathbf{X}_4$ and

$$\mathbf{Y}_5 = -8t\left[\frac{2}{3}(A\partial_A + B\partial_B) - \Phi\partial_\Phi\right], \tag{54}$$

$$\mathbf{Y}_6 = -\frac{2A}{3}[\ln(B\Phi)^2 + 1]\partial_A - \frac{B}{3}[\ln(B\Phi^2)]\partial_B + \Phi\ln(B\Phi^{\frac{4}{3}})\partial_\Phi, \tag{55}$$

$$\mathbf{Y}_7 = \frac{2A}{3}[\ln(B) - 1]\partial_A - \frac{B}{3}[\ln(BA^3\Phi^4)]\partial_B + \Phi\ln(A\Phi^{\frac{4}{3}})\partial_\Phi, \tag{56}$$

where we have a nonzero gauge function for $\mathbf{Y}_5$ as $f = AB^2\Phi^2$. The non-zero Lie brackets for this subcase are

$$\begin{aligned}
&[\mathbf{Y}_1, \mathbf{Y}_5] = -\frac{16}{3}\mathbf{Y}_2 + 8\mathbf{Y}_3,\\
&[\mathbf{Y}_2, \mathbf{Y}_6] = -\frac{1}{3}\mathbf{Y}_2 + \mathbf{Y}_3, \quad [\mathbf{Y}_2, \mathbf{Y}_7] = \frac{5}{3}\mathbf{Y}_2 - 2\mathbf{Y}_3,\\
&[\mathbf{Y}_3, \mathbf{Y}_6] = -\frac{2}{3}(\mathbf{Y}_2 - 2\mathbf{Y}_3),\\
&[\mathbf{Y}_3, \mathbf{Y}_7] = \frac{2}{3}(\mathbf{Y}_2 - \mathbf{Y}_3), \quad [\mathbf{Y}_4, \mathbf{Y}_5] = \mathbf{Y}_5,\\
&[\mathbf{Y}_4, \mathbf{Y}_7] = -\mathbf{Y}_2 + \mathbf{Y}_3,\\
&[\mathbf{Y}_5, \mathbf{Y}_6] = \frac{2}{3}\mathbf{Y}_5, \qquad [\mathbf{Y}_5, \mathbf{Y}_7] = \frac{2}{3}\mathbf{Y}_5,\\
&[\mathbf{Y}_6, \mathbf{Y}_7] = \frac{2}{3}(\mathbf{Y}_2 - \mathbf{Y}_3) + \frac{1}{3}(\mathbf{Y}_6 - \mathbf{Y}_7).
\end{aligned} \tag{57}$$

The first integrals related to $\mathbf{Y}_5, \mathbf{Y}_5$ and $\mathbf{Y}_7$ are

$$I_5 = AB^2\Phi^2\left[t\Big(\frac{\dot{A}}{A} + 2\frac{\dot{B}}{B} + 2\frac{\dot{\Phi}}{\Phi}\Big) - 1\right], \tag{58}$$

$$I_6 = \frac{1}{4}AB^2\Phi^2\Big[\ln(B\Phi)\frac{\dot{A}}{A} + \Big(\ln(B^{\frac{1}{2}}\Phi) - 1\Big)\frac{\dot{B}}{B} + \Big(\ln(B\Phi^{\frac{4}{3}}) - 1\Big)\frac{\dot{\Phi}}{\Phi}\Big], \tag{59}$$

$$I_7 = \frac{1}{8}\Big[-\ln(B)\frac{\dot{A}}{A} + (\ln(A^3B\Phi^4) - 2)\frac{\dot{B}}{B} + (\ln(A^3\Phi^{-4}) - 2)\frac{\dot{\Phi}}{\Phi}\Big]. \tag{60}$$

Subcase ii.a.1.3. $F_0 = -3/2$, i.e. $k_4 = 0$. There are *six* NGSs for this subcase: $\mathbf{Y}_1 = \mathbf{X}_1, \mathbf{Y}_2 = \mathbf{X}_2, \mathbf{Y}_3 = \mathbf{X}_3, \mathbf{Y}_4 = \mathbf{X}_4$ and

$$\mathbf{Y}_5 = \frac{t^2}{2}\partial_t + \frac{t}{2}\Phi\partial_\Phi, \tag{61}$$

$$\mathbf{Y}_6 = 2A\ln(B)\partial_A - B\ln(A)\partial_B - \Phi\ln(\frac{A}{B})\partial_\Phi, \tag{62}$$

with a nonzero gauge function $f = \frac{1}{4}AB^2\Phi^2$ for $\mathbf{Y}_5$. The non-zero Lie brackets of the above vector fields yield

$$\begin{aligned}
&[\mathbf{Y}_1, \mathbf{Y}_5] = \frac{1}{2}\mathbf{Y}_3 + \mathbf{Y}_4,\ [\mathbf{Y}_2, \mathbf{Y}_6] = 2\mathbf{Y}_2 - 3\mathbf{Y}_3,\\
&[\mathbf{Y}_3, \mathbf{Y}_6] = 2(\mathbf{Y}_2 - \mathbf{Y}_3),\ [\mathbf{Y}_4, \mathbf{Y}_5] = \mathbf{Y}_5,\\
&[\mathbf{Y}_4, \mathbf{Y}_6] = -\mathbf{Y}_2 + \mathbf{Y}_3.
\end{aligned} \tag{63}$$

The first integrals of $\mathbf{Y}_5$ and $\mathbf{Y}_6$ are

$$I_5 = \frac{1}{4}AB^2\Phi^2\left[t\Big(\frac{\dot{A}}{A} + 2\frac{\dot{B}}{B} + 2\frac{\dot{\Phi}}{\Phi}\Big) - 1\right], \tag{64}$$

$$I_6 = AB^2\Phi^2\Big[\ln(\frac{B^{1/2}}{A})\frac{\dot{A}}{A} + \ln(\frac{B^2}{A^{3/2}})\frac{\dot{B}}{B} + 2\ln(B/A)\frac{\dot{\Phi}}{\Phi}\Big]. \tag{65}$$

Case (ii.a.4): $U(\Phi) = \lambda\Phi^2$. For this case, we find the following NGS components and gauge function:

$$\begin{aligned}
\xi &= c_1 + c_2\sin(at) + c_3\cos(at),\\
\alpha &= \frac{ak_4}{k_1}A\left[c_2\cos(at) - c_3\sin(at)\right] - c_5\frac{2A}{k_2k_3}\ln(B\phi) - 2(c_4 + c_6)A,\\
\beta &= \frac{ak_4}{k_1}B\left[c_2\cos(at) - c_3\sin(at)\right] - c_5B\ln(A\phi^{-k_4/F_0}) + c_6B,\\
\gamma &= \frac{ak_3}{k_1}\Phi\left[c_2\cos(at) - c_3\sin(at)\right] + c_4\Phi + c_5\Phi\ln(A/B),\\
f &= -2\lambda AB\Phi^2\left[c_2\sin(at) + c_3\cos(at)\right].
\end{aligned} \tag{66}$$

where $a=\sqrt{2\lambda k_1/k_2k_3}, k_1=-8F_0-9, k_2=-F_0-1, k_3=-F_0$ and $k_4=-2F_0-3$. Here we observe that k_2 is different from zero because $F_0\neq -1$, and it is clear that $k_3\neq 0$. Therefore, again we need to consider subcases analogous to the Case (ii.a.1).

Subcase ii.a.4.1. $k_1\neq 0$, $k_4\neq 0$. The NGSs are obtained as $\mathbf{X}_1^{a4}=\mathbf{X}_1, \mathbf{X}_2^{a4}=\mathbf{X}_2, \mathbf{X}_3^{a4}=\mathbf{X}_3$ and

$$\begin{aligned}\mathbf{X}_4^{a4}&=2A\ln(B\phi^{-k_4/F_0})\partial_A-B\ln(A\phi^{-k_4/F_0})\partial_B\\&\quad+\Phi\ln(A/B)\partial_\Phi,\\ \mathbf{X}_5^{a4}&=\frac{a}{k_1}\cos(at)\Big[k_4(A\partial_A+B\partial_B)+k_3\Phi\partial_\Phi\Big]\\&\quad+\sin(at)\partial_t,\\ \mathbf{X}_6^{a4}&=-\frac{a}{k_1}\sin(at)\Big[k_4(A\partial_A+B\partial_B)+k_3\Phi\partial_\Phi\Big]\\&\quad+\cos(at)\partial_t,\end{aligned}\tag{67}$$

where $f=-2\lambda AB\Phi^2\sin(at)$ and $f=-2\lambda AB\Phi^2\cos(at)$ for $\mathbf{X}_5^{a4}$ and $\mathbf{X}_6^{a4}$, respectively. The non-zero Lie brackets for this case are

$$[\mathbf{X}_1,\mathbf{X}_5^{a4}]=a\mathbf{X}_6^{a4},\qquad [\mathbf{X}_1,\mathbf{X}_6^{a4}]=-a\mathbf{X}_5^{a4},\tag{68}$$

$$[\mathbf{X}_2,\mathbf{X}_4^{a4}]=-3\mathbf{X}_4+2\mathbf{X}_2,\tag{69}$$

$$[\mathbf{X}_3,\mathbf{X}_4^{a4}]=2\mathbf{X}_3+b\mathbf{X}_2,\ [\mathbf{X}_5^{a4},\mathbf{X}_6^{a4}]=-a\mathbf{X}_1.\tag{70}$$

where $b=-(3+4F_0)/F_0$. Then, the first integrals read

$$I_4=\frac{k_3}{3}AB\Phi^2\Big[\ln(\Phi^{\frac{k_4}{F_0}}/B)\frac{\dot A}{A}+\ln(B\Phi^{-\frac{k_4}{F_0}})\frac{\dot B}{B}+\frac{k_4}{k_3}\ln(B/A)\frac{\dot\Phi}{\Phi}\Big],\tag{71}$$

$$I_5=\frac{3ak_2k_3}{k_1}\cos(at)AB^2\Phi^2\Big[\frac{\dot A}{A}+2\frac{\dot B}{B}+2\frac{\dot\Phi}{\Phi}+\frac{a\tan(at)}{B}\Big],\tag{72}$$

$$I_6=-\frac{3ak_2k_3}{k_1}\sin(at)AB^2\Phi^2\Big[\frac{\dot A}{A}+2\frac{\dot B}{B}+2\frac{\dot\Phi}{\Phi}-\frac{a\cot(at)}{B}\Big].\tag{73}$$

Subcase ii.a.4.2. $F_0=-9/8$, i.e. $k_1=0$. The *six* NGSs are found as $\mathbf{Y}_1=\mathbf{X}_1, \mathbf{Y}_2=\mathbf{X}_2, \mathbf{Y}_3=\mathbf{X}_3$ and

$$\mathbf{Y}_4=t\partial_t+\frac{1}{3}(16\lambda t^2+3)A\partial_A+8\lambda t^2(\frac{2}{3}B\partial_B-\Phi\partial_\Phi),\tag{74}$$

$$\mathbf{Y}_5=-\frac{2}{3}t(A\partial_A+B\partial_B)+\phi\partial_\phi\tag{75}$$

$$\mathbf{Y}_6=-2A\ln(B\phi^{2/3})\partial_A-B\ln(A\phi^{2/3})\partial_B+\phi\ln(\frac{A}{B})\partial_\phi,\tag{76}$$

$$\begin{aligned}\mathbf{Y}_7&=\frac{1}{6}\Big[-8\lambda t^2+3\ln(B)-3\Big]A\partial_A\\&\quad-\frac{1}{12}\Big[16\lambda t^2+3\ln(A^3B\Phi^4)\Big]B\partial_B\\&\quad+\frac{1}{4}\Big[8\lambda t^2+\ln(A^3\Phi^4)\Big]\Phi\partial_\Phi,\end{aligned}\tag{77}$$

where the corresponding non-zero Lie brackets for this subcase are

$$\begin{aligned}&[\mathbf{Y}_1,\mathbf{Y}_4]=\mathbf{Y}_1-16\lambda\mathbf{Y}_5,\ \ [\mathbf{Y}_1,\mathbf{Y}_5]=-\frac{2}{3}\mathbf{Y}_2+\mathbf{Y}_3,\\&[\mathbf{Y}_1,\mathbf{Y}_7]=4\lambda\mathbf{Y}_5,\ \ [\mathbf{Y}_2,\mathbf{Y}_6]=-2\mathbf{Y}_2+3\mathbf{Y}_3,\\&[\mathbf{Y}_2,\mathbf{Y}_7]=\frac{5}{4}\mathbf{Y}_2-\frac{3}{2}\mathbf{Y}_3,\ \ [\mathbf{Y}_3,\mathbf{Y}_6]=-\frac{4}{3}\mathbf{Y}_2+2\mathbf{Y}_2,\\&[\mathbf{Y}_3,\mathbf{Y}_7]=-\frac{1}{2}(\mathbf{Y}_2-\mathbf{Y}_3),\ \ [\mathbf{Y}_4,\mathbf{Y}_5]=\mathbf{Y}_5,\\&[\mathbf{Y}_4,\mathbf{Y}_6]=\mathbf{Y}_2-\mathbf{Y}_3,\ \ [\mathbf{Y}_4,\mathbf{Y}_7]=-\frac{3}{4}(\mathbf{Y}_2-\mathbf{Y}_3),\\&[\mathbf{Y}_5,\mathbf{Y}_7]=\frac{1}{2}\mathbf{Y}_5,\ \ [\mathbf{Y}_6,\mathbf{Y}_7]=\frac{1}{2}(\mathbf{Y}_2-\mathbf{Y}_3)+\frac{1}{4}\mathbf{Y}_6.\end{aligned}\tag{78}$$

The first integrals of the six NGSs are given by

$$I_4=\frac{1}{8}AB\Phi^2\Big[-8\lambda t^2\frac{\dot A}{A}+(3-16\lambda t^2)\frac{\dot B}{B}+(40\lambda t^2+3)\frac{\dot\Phi}{\Phi}+\frac{4}{3}\lambda t\Big],\tag{79}$$

$$I_5=\frac{1}{8}AB\Phi^2\Big[(3-2t)\frac{\dot A}{A}+(6-4t)\frac{\dot B}{B}+(8-6t)\frac{\dot\Phi}{\Phi}+1\Big],\tag{80}$$

$$I_6=\frac{3}{8}AB\Phi^2\Big[-\ln\Big(B\Phi^{2/3}\Big)\frac{\dot A}{A}+\ln\Big(\frac{A}{(B\Phi)^2}\Big)\frac{\dot B}{B}+\ln\Big(\frac{A^{2/3}}{B^{14/3}\Phi^{8/3}}\Big)\frac{\dot\Phi}{\Phi}\Big],\tag{81}$$

$$\begin{aligned}I_7&=\frac{1}{32}AB\Phi^2\Big[(8\lambda t^2-3\ln B)\frac{\dot A}{A}\\&\quad+(16\lambda t^2+3\ln(A^3B\Phi^4-6))\frac{\dot B}{B}\\&\quad+2(8\lambda t^2+\ln(A^3\Phi^4-3))\frac{\dot\Phi}{\Phi}+16\lambda t\Big].\end{aligned}\tag{82}$$

Subcase ii.a.4.3. $k_4=0$, i.e. $F_0=-3/2$. There are *six* NGSs which are $\mathbf{Y}_1=\mathbf{X}_1, \mathbf{Y}_2=\mathbf{X}_2, \mathbf{Y}_3=\mathbf{X}_3$ and

$$\begin{aligned}\mathbf{Y}_4&=2A\ln(B)\partial_A-B\ln(A)\partial_B-\Phi\ln(\frac{A}{B})\partial_\Phi,\\ \mathbf{Y}_5&=sin2\sqrt{2\lambda}t\partial_t+\Phi\sqrt{2\lambda}\cos2\sqrt{2\lambda}t\partial_\Phi,\\ \mathbf{Y}_6&=\cos2\sqrt{2\lambda}t\partial_t-\Phi\sqrt{2\lambda}\sin2\sqrt{2\lambda}t\partial_\Phi,\end{aligned}\tag{83}$$

with the non-zero Lie brackets

$$\begin{aligned}&[\mathbf{Y}_1,\mathbf{Y}_5]=2\sqrt{2\lambda}\mathbf{Y}_6,\quad [\mathbf{Y}_1,\mathbf{Y}_6]=-2\sqrt{2\lambda}\mathbf{Y}_5,\\&[\mathbf{Y}_2,\mathbf{Y}_4]=2\mathbf{Y}_2-3\mathbf{Y}_3,[\mathbf{Y}_3,\mathbf{Y}_4]=2\mathbf{Y}_2-2\mathbf{Y}_3,\\&[\mathbf{Y}_5,\mathbf{Y}_6]=-2\sqrt{2\lambda}\mathbf{Y}_1.\end{aligned}\tag{84}$$

The first integrals are

$$I_4 = \frac{1}{2}AB\Phi^2\Big[\ln(\frac{1}{B})\frac{\dot{A}}{A} + \ln(A)\frac{\dot{B}}{B}\Big], \tag{85}$$

$$I_5 = \frac{1}{2}AB\Phi^2\Big[\sqrt{2\lambda}\cos(2\sqrt{2\lambda}t)\Big(\frac{\dot{A}}{A} + 2\frac{\dot{B}}{B} + 2\frac{\dot{\Phi}}{\Phi}\Big) + 4\sin(2\sqrt{2\lambda}t)\Big], \tag{86}$$

$$I_6 = -\frac{1}{2}AB\Phi^2\Big[\sqrt{2\lambda}\sin(2\sqrt{2\lambda}t)\Big(\frac{\dot{A}}{A} + 2\frac{\dot{B}}{B} + 2\frac{\dot{\Phi}}{\Phi}\Big) - 4\cos(2\sqrt{2\lambda}t)\Big]. \tag{87}$$

4 Exact Solutions

In order to find new exact solutions of the field equations in the cases of the above section, the algebra of the NGS generators has to be closed, and the first integrals need to be utilized. Now, we proceed in this manner.

For case (i), in the view of relation (32), the field equations (9)-(12) of BI space-time reduce to

$$\frac{\dot{B}^2}{B^2} + 3\frac{\dot{\Phi}^2}{\Phi^2} + 2\frac{\dot{A}\dot{B}}{AB} + 2\frac{\dot{A}\dot{\Phi}}{A\Phi} + 4\frac{\dot{B}\dot{\Phi}}{B\Phi} + 6\frac{U(\Phi)}{\Phi^2} = 0, \tag{88}$$

$$2\frac{\ddot{B}}{B} + 2\frac{\ddot{\Phi}}{\Phi} + \frac{\dot{B}^2}{B^2} - \frac{\dot{\Phi}^2}{\Phi^2} + 4\frac{\dot{B}\dot{\Phi}}{B\Phi} + 6\frac{U(\Phi)}{\Phi^2} = 0, \tag{89}$$

$$\frac{\ddot{A}}{A} + \frac{\ddot{B}}{B} + 2\frac{\ddot{\Phi}}{\Phi} - \frac{\dot{\Phi}^2}{\Phi^2} + \frac{\dot{A}\dot{B}}{AB} + 2\left(\frac{\dot{A}}{A} + \frac{\dot{B}}{B}\right)\frac{\dot{\Phi}}{\Phi} + 6\frac{U(\Phi)}{\Phi^2} = 0, \tag{90}$$

$$\frac{\ddot{A}}{A} + 2\frac{\ddot{B}}{B} + 3\frac{\ddot{\Phi}}{\Phi} + \frac{\dot{B}^2}{B^2} + 2\frac{\dot{A}\dot{B}}{AB} + 3\left(\frac{\dot{A}}{A} + 2\frac{\dot{B}}{B}\right)\frac{\dot{\Phi}}{\Phi} + 3\frac{U'(\Phi)}{\Phi} = 0. \tag{91}$$

We consider only case (i) here, because unfortunately in case (ii) it has proven difficult, if sometimes impossible, to find any solutions of the field equations satisfying NGSs.

For this space-time, we find from the above field equations that λ vanishes in cases (i.2), (i.4), (ii.a); and the scalar field Φ is constant in case (ii.b.1). Therefore, we drop these cases and only consider cases (i.1) and (i.3).

Case (i.1): To get a closed algebra of the NGS generators $\mathbf{X}_6, \mathbf{X}_7$ and $\mathbf{X}_8$ in this case of vanishing potential, the commutator relations (36) of Lie brackets require that

$$B\Phi = k, \qquad A = (k\ell)^{-3/2}B, \tag{92}$$

where k and ℓ are non-zero constants. Note that we have not explicitly obtained the scalar field Φ, but the metric functions A and B are stated in terms of the field.

The non-zero Lie brackets of $\mathbf{X}_6, \mathbf{X}_7$ and $\mathbf{X}_8$ become

$$[\mathbf{X}_6, \mathbf{X}_7] = \frac{1}{k}(\mathbf{X}_2 - 3\mathbf{X}_3) + \ln(k)\,\mathbf{X}_7,$$
$$[\mathbf{X}_6, \mathbf{X}_8] = 3\ell(\mathbf{X}_2 - \mathbf{X}_3) + \ln(\ell)\mathbf{X}_8,$$

which give indeed a closed algebra. Then, using the fact that $E_L = 0$ because of (9), eqs. (37)-(43) yield that all the first integrals $I_1, \ldots, I_8$ vanish. Eq. (92) gives also

$$\frac{\dot{A}}{A} = \frac{\dot{B}}{B} = -\frac{\dot{\Phi}}{\Phi}. \tag{93}$$

Putting these relations in the field equations (9)-(12) we find that the field equations are identically satisfied.

Case (i.3): Recall that for this case the potential is $U(\Phi) = \lambda\Phi^4$, and the coupling function $F(\Phi)$ is given by (32). For simplicity of writing, we will rename the constants of motion found in (47) as $I_1^3 \equiv J_1$, $I_2^3 \equiv J_2$, $I_3^3 \equiv J_3$ and $I_4^3 \equiv J_4$. The last one vanishes by (88) and for the others we get

$$\frac{\dot{A}}{A} - \frac{\dot{B}}{B} = \frac{3J_1}{AB^2\Phi^2}, \tag{94}$$

$$\frac{\dot{B}}{B} + \frac{\dot{\Phi}}{\Phi} = -3J_2\frac{A\Phi}{B}, \tag{95}$$

$$2\frac{\dot{A}}{A} + \frac{\dot{B}}{B} + 3\frac{\dot{\Phi}}{\Phi} = -9J_3\frac{B\Phi}{A}, \tag{96}$$

which are actually the constraints that have to be satisfied by the field equations (88)-(91). Substitution of (95) into the field equations (90) and (91) gives

$$\frac{\ddot{A}}{A} + \frac{\ddot{\Phi}}{\Phi} - \frac{\dot{\Phi}^2}{\Phi^2} + \frac{\dot{A}\dot{\Phi}}{A\Phi} - 6J_2\frac{A\Phi}{B}\left(\frac{\dot{A}}{A} + \frac{\dot{\Phi}}{\Phi}\right) + 6\lambda\Phi^2 = 0, \tag{97}$$

$$\frac{\ddot{A}}{A} + \frac{\ddot{\Phi}}{\Phi} - \frac{\dot{\Phi}^2}{\Phi^2} + \frac{\dot{A}\dot{\Phi}}{A\Phi} - 12J_2\frac{A\Phi}{B}\left(\frac{\dot{A}}{A} + \frac{\dot{\Phi}}{\Phi}\right) + 9(J_2)^2\left(\frac{A\Phi}{B}\right)^2 + 12\lambda\Phi^2 = 0. \tag{98}$$

Then, subtracting Eq. (97) from Eq. (98)), one gets

$$-6J_2\frac{A\Phi}{B}\left(\frac{\dot{A}}{A} + \frac{\dot{\Phi}}{\Phi}\right) + 9(J_2)^2\left(\frac{A\Phi}{B}\right)^2 + 6\lambda\Phi^2 = 0, \tag{99}$$

which yields the constraint equation

$$(A\Phi)^{\cdot} = 3J_2\frac{A^2\Phi^2}{2B} + \frac{\lambda}{J_2}B\Phi^2, \tag{100}$$

where $J_2 \neq 0$. Here we need to correct a mistake in our previous study [26], where we have used c_0 instead of the constant of motion J_2; and they are related by $c_0 = -3J_2$. Also, it can be seen that the Eq. (42) of that reference is erroneously calculated, the correct one

is Eq.(98). Thus, the Eqs. (43) and (47) of Ref. [26] do not apply and the solution (49) does not exist.

Using the Eqs. (94) and (95) in (96) we find another constraint relation

$$2J_1 - 3J_2A^2B\Phi^3 + 3J_3(B\Phi)^3 = 0. \tag{101}$$

Considering (94)-(96) in the field equations (88) and (89) gives the third constraint relation

$$-6J_1I_2 + 9J_2A^2B\Phi^3 + 2\lambda(B\Phi)^3 = 0. \tag{102}$$

The remaining field equations (90) and (91) are identically satisfied using the obtained relations (101) and (102). Now, we use the transformation of the time coordinate by $dt = (B/A\Phi)d\tau$ in the above Eqs. (95) and (100). Further, after integration with respect to the new time coordinate we find

$$A^2 = \frac{2}{9a(J_2)^3\Phi^2}\left(3J_1J_2e^{3J_2\tau} - \lambda a^3e^{-6J_2\tau}\right), \tag{103}$$

$$B = a\,\frac{e^{-3J_2\tau}}{\Phi}, \tag{104}$$

where a is a constant of integration. Again, we have given the metric functions in terms of the scalar field.

5 Concluding remarks

In this paper, we have considered the induced theory of gravity and studied the Noether gauge symmetry approach to search the Noether symmetries of Lagrangian (8) for BI space-time. We have shown that a number of Noether gauge symmetries for BI space-time exist and each of them are related to a constant of motion. Using the two coupling functions $F(\Phi)$ and the choices given in Tables 1 for the potential $U(\Phi)$, we used the first integrals obtained through the NGSs to solve the field equations for BI space-time. In some cases, the NGSs and the first integrals are explicitly elaborated in the paper, for other cases, the NGS vector fields and corresponding first integrals are collected in Tables 2.

The maximum number of NGS generators is found to vary from two to eight in the cases considered. Here we also correct a mistake in our previous study [26], namely we find that NGSs for BI space-time *do* exist, contrary to the claim of that work.

In both of the cases (i) and (ii), it is possible to find particular exact solutions for the system of field equations (9)-(12), obtaining the explicit behaviour of the scale factors $A(t)$ and $B(t)$. For BI space-time, we have found the exact solutions (92) in case (i.1) and (103)-(104) in case (i.3). As it is clearly seen in the solutions (92), (103)-(104) in terms of the conformal time τ, both of the scale factors $A(\tau)$ and $B(\tau)$ are proportional to the inverse of the scalar field Φ. We do not have the explicit form of the scalar field Φ in the cases (i.1) and (i.3) for BI space-time.

Acknowledgements This work was supported by The Scientific Research Projects Coordination Unit of Akdeniz University (BAP). We would like to thank The University of Punjab for the financial grant of the successful meeting "International Conference on Relativistic Astrophysics (ICRA)", The University of Punjab, Department of Mathematics, Lahore-Pakistan held in February 10-14, 2015.

References

1. S. Perlmutter et al., *Astrophys. J.* 483, 565 (1997)
2. S. Perlmutter et al., *Nature* 391, 51 (1998).
3. S. Perlmutter et al.,*Astrophys. J.* 517, 565 (1999).
4. S. Perlmutter et al.,*Astrophys. J.* 598, 102 (2003).
5. A.G. Riess et al., *Astron. J.* 116, 1009 (1998).
6. A.G. Riess et al., *Astrophys. J.* 607, 665 (2004).
7. J.L. Tonry et al., *Astrophys. J.* 594, 1 (2003).
8. C.L. Bennett et al., *Astrophys. J. Suppl. Ser.* 148, 1 (2003)
9. D.N. Spergel et al., *Astrophys. J. Suppl. Ser.* 148, 175 (2003)
10. M. Tegmark et al., *Phys. Rev. D* 69, 03501 (2004)
11. A. Clocchiatti et al., *Astrophys. J.* 642, 1 (2006).
12. A. Stabile and S. Capozziello, *Galaxies* **2**, 520 (2014).
13. Y. Fujii and K. Maeda, *The Scalar-Tensor Theory of Gravitation*, Cambridge University Press, Cambridge, 2003.
14. A. A. Starobinsky, *Zh. Eksp. Teor. Fiz.* **30**, 719 (1979) [*JETP Lett.* **30**, 682 (1979)].
15. A. A. Starobinsky, *Phys. Lett. B* **91**, 99 (1981).
16. A. Guth, *Phys. Rev. D* **23**, 347 (1981).
17. S. Carloni, J. A. Leach, S. Capozziello and P. K. S. Dunsby, *Class. Quantum Grav.***25**, 035008 (2008).
18. M. Demianski, R. de Ritis, C. Rubano, and P. Scudellaro, *Phys. Rev. D* **46**, 1391 (1992).
19. S. Capozziello and R. de Ritis, *Phys. Lett. A* **177**, 1 (1993).
20. S. Capozziello, R. de Ritis, and P. Scudellaro, *Phys. Lett. A* **188**, 130 (1994).
21. S. Capozziello and R. de Ritis, *Class. Quantum Grav.***11**, 107 (1994).
22. S. Capozziello and G. Lambiase, *Gen. Relativ. Gravit.***32**, 673 (2000).
23. S. Capozziello and R. de Ritis, *Class. Quant. Grav.***24**, 2153 (2007).
24. S. Capozziello and A. de Felice, *JCAP* **08**, 016 (2008).
25. S. Capozziello, E. Piedipalumbo, C. Rubano and P. Scudellaro, *Phys. Rev. D* **80**, 104030 (2009).
26. U. Camci and Y. Kucukakca, *Phys. Rev. D***76**, 084023 (2007).
27. Y. Kucukakca, U. Camci and I. Semiz, *Gen. Relativ. Gravit.* **44**, 1893 (2012).
28. Y. Kucukakca and U. Camci, *Astrophys. Space Sci.***338**, 211 (2012).
29. M. Jamil, D. Momeni and R. Myrzakulov, Eur. Phys. J. C **72**, 2137 (2012).
30. M. Jamil, S. Ali, D. Momeni and R. Myrzakulov, Eur. Phys. J. C **72**, 1998 (2012).
31. M. Sharif and S. Waheed, *JCAP* **02**, 043 (2013).
32. Y. Kucukakca, *Eur. Phys. J. C* **73**, 2327 (2013).

33. A. Aslam, M. Jamil, D. Momeni and R. Myrzakulov, Can. J. Phys. **91**, 93 (2013).
34. M. Jamil, F. M. Mahomed and D. Momeni, Phys. Lett. B **702**, 315 (2011).

Proc. Int. Conf. Relativ. Astrophys.
Pages 170-177, (2015)

Generating Magnetic Fields in Plasmas by Spacetime Curvature

Asghar Qadir[a,1,2], **Rhameez S. Herbst**[b,2]

[1]School of Natural Sciences, National University of Sciences and Technology, H-12, Islamabad, Pakistan
[2]Centre for Differential Equations, Continuum Mechanics and Applications, School of Computational and Applied Mathematics University of the Witwatersrand, Wits 2050, South Africa

Abstract There is a question that arises of the generation of magnetic fields primordially. Following up on a suggestion of Mahajan and Yoshida that special relativistic effects in plasmas could provide the desired magnetic field, Asenjo, Mahajan and Qadir suggested the generation by a strong gravitational field through its curvature. The first attempt, using a plasma in an accretion disc about a simple black hole provided the seed but the fields so obtained were extremely low. Later a rotating black hole was considered and it not only gave large enough fields but in fact the field appeared to diverge. The expectation is that this divergence would be eliminated by the back-reaction of the radiation from the plasma surrounding the black hole. This work is reviewed here.

1 Introduction

Cosmic rays were originally the source of particles with the highest energies. Even now, despite the tevatrons, the highest energy photon recorded $\sim TeV$, came from cosmic rays. The recent discovery of a neutron star emitting particles with energies $\sim 10^1 - 10^2 TeV$ means that there are such particles produced in astrophysical processes. To produce the particles in the laboratory, we use particle accelerators. They are normally (roughly) circular and several kilometers in diameter and use extremely high magnetic fields. To get a comparable linear accelerator we would need even larger dimensions and even higher (electric) fields. The question is, how do the cosmic accelerators that produce cosmic rays work? It should be borne in mind that the cosmic rays come from very far away, outside our galaxy, outside our local cluster and quite probably from a whole lot further away. As such, they come from the very far past, i.e. the early Universe.

We know that astronomical bodies have magnetic fields. The Earth and the planets have relatively small fields and stars have larger fields. This is related to the rotation and composition of the bodies. White dwarfs have considerably higher magnetic fields as they are more compact and hence spin faster. Neutron stars have very much higher magnetic fields. We need giant structures like enormous dust clouds or whole galaxies to produce the observed cosmic rays. Gas clouds, being irregular, are not good sources and normal galaxies are probably too diffuse. Only neutron stars, gamma ray bursters and quasars could be the sources but how do they get their magnetic fields? There have been various proposals for spontaneous magnetic field generation. One of them is that special relativistic effects could lead to a plasma acquiring a magnetic field. Since high accelerations often give results similar to high speeds, one could also look for spacetime curvature generating magnetic fields.

The essential problem is that in the early Universe there was no preferred direction. The net spin of the Universe is measured to be zero to a very high accuracy and there *were* no magnetic fields. Also, the interstellar medium is an undifferentiated gas which cannot have any preferred directions. To generate the fields one may look to a plasma. A plasma is an electrically neutral gas of charged particles. Though overall neutrality is assured, the fact that it consists of charges means that there will be electromagnetic interactions between the charges. As they are moving charges, there will be magnetic fields. However, due to lack of a preferred direction, the fields will be random and evanescent, arising and disappearing, with a zero net field over any significant time period. In other words, they would just be thermal fluctuations in the plasma. Once a magnetic

[a]Email Address: asgharqadir46@gmail.com
[b]Email Address: rhameez.herbst@gmail.com

field is started, we can rely on nonlinear effects in the plasma to make it grow, but how can we have a net significant field started?

2 The Special Relativistic Mechanism

Mahajan and Yoshida [1] suggested that one could provide the preferred direction, which they called a "generalized vorticity" and denoted by $\mathbf{\Omega}$, by special relativistic effects in a plasma. Using Classical Mechanics the corresponding generalized helicity for a non-relativistic plasma is $K = \int \mathbf{P} \cdot \mathbf{\Omega} dx$, where $\mathbf{P} = m\mathbf{V} + (q/c)\mathbf{A}$ is the canonical momentum, m the mass, $\mathbf{V}$ the fluid velocity, q the generalized charge, c the speed of light and $\mathbf{A}$ a vector potential. There will then be a generalized magnetic field, $\mathbf{B} = \nabla \times \mathbf{A}$.

The circulation $\oint_L \delta Q$, associated with a physical quantity Q, calculated along the loop L, may be zero or finite depending on whether Q is an exact differential $d\phi$ or not, ϕ being a state variable. For example, if $\delta Q = TdS$, where T is the temperature and S the entropy; the circulation is generally finite and measures the heat gained in a quasi-static thermodynamic cycle.

For a moving loop, $L(t)$, in an ideal fluid flow,

$$\oint_L \mathbf{P} \cdot d\mathbf{x} = \oint_L \mathbf{P_{fluid}} \cdot d\mathbf{x}, \tag{1}$$

where $\mathbf{V}$ is the flow velocity. Since the integrand is minus the derivative of the energy, $\epsilon = \frac{1}{2}mV^2\phi + h$, where ϕ is the potential energy and h the enthalpy density, the left side of equation (1) is zero and hence the circulation is conserved. However, relativistically an exact differential would be re-scaled by a factor $\gamma^{-1} = \sqrt{1 - V^2/c^2}$, and hence the circulation would no longer be conserved.

This can be seen more rigorously by taking the inner product of the momentum and position 4-vectors in the integral. The right side integrand will now be the line integral of the inner product of the velocity 4-vector and the generalized curl of the momentum. The generalized curl is the angular momentum tensor. Since the canonical momentum is,

$$P^\mu = mcfV^\mu + (q/c)A^\mu, \tag{2}$$

where f is a factor corresponding to the thermal increase of mass, the angular momentum tensor is

$$M^{\mu\nu} = 2\partial^{[\mu}P^{\nu]} = mcS^{\mu\nu} + (q/c)F^{\mu\nu}, \tag{3}$$

where $S^{\mu\nu}$ and $F^{\mu\nu}$ are the spin (angular momentum per unit mass) tensor and Maxwell tensor respectively.

The equation of motion now becomes

$$cM_{\mu\nu}V^\nu = TS_{,\mu}, \tag{4}$$

where T is the temperature and "$,\mu$" stands for the derivative with respect to the position 4-vector. Taking the space part of this equation one can write it in terms of the generalized electric and magnetic fields as

$$q\gamma[\mathbf{E} + \mathbf{V} \times \mathbf{B}/c] = cT\nabla S. \tag{5}$$

Hence the source for the magnetic field generation is

$$\mathbf{G} = -\frac{cT}{q\gamma}\nabla S = -\nabla \times \left(\frac{cT}{q\gamma}\nabla S\right), \tag{6}$$

which may be broken into the familiar baroclinic term

$$\mathbf{G}_b = -(c/q\gamma)\nabla T \times \nabla S, \tag{7}$$

and the relativistically induced correction

$$\mathbf{G}_r = -(c\gamma T/2q)\nabla(\frac{V}{c})^2 \times \nabla S. \tag{8}$$

. Writing $(V/c) = \beta$, the ratio of the magnitudes of the forces is $\beta^2\gamma^2$.

Now, for a stable plasma $\nabla T \times \nabla S = 0$. Hence the baroclinic term averages to zero, meaning that there is no long term significant seed magnetic field in that term. However, the relativistically induced term *is* significant. The resistive dissipation, is

$$\mathbf{D} = \nabla \times (\eta\mathbf{J}) = (c/4\pi)\nabla \times (\eta\nabla \times \mathbf{B}). \tag{9}$$

Then the relative strengths are:

$$\frac{|\mathbf{G}_r|}{|\mathbf{D}|} = \frac{(\gamma V/c)^2(T/mc^2)}{(V_A/c)(\nu/\omega_p)}, \tag{10}$$

where V_A is the Alfven speed, ν is the collision frequency and ω_p is the plasma frequency. The relativistic term generates $\sim 1G$ at $T = 20eV \sim 2 \times 10^4\ ^oK$.

3 Re-interpretation of special relativistic effect

Einstein had early on noted that with accelerated motion one must modify the geometry as Euclidean geometry could not hold. Though he never published the argument till much later, he claimed that he had already come to it in 1908. The argument is beautifully simple and telling (see for example [2]). Consider an observer at the edge of a circular disc of radius a rotating with an angular speed ω. A rod placed along the direction of rotation will appear contracted by a factor $\sqrt{1 - a^2\omega^2/c^2}$, while a rod of the same size placed along the radial direction will be unchanged (as it lies perpendicular to the direction of motion). Consequently, the observer will measure the ratio of the circumference to the diameter as shrunk by the same factor. *Since, in Euclidean geometry this ratio defines π, and the measured value will be less than pi, the geometry cannot be Euclidean.* Notice that even though the speed does not change and only the direction does, it is enough to warp the geometry. This warping of the geometry will play a crucial role in understanding how the special relativistic

drive, discussed above, can work, when the effect seems to be only frame dependent.

The conservation laws of Physics may be seen as arising from Noether's theorem, that for every dynamical symmetry there is a conserved quantity [3]. Thus, for the gauge symmetry of classical electrodynamics, that $A_\mu \to \tilde{A}_\mu = A_\mu + \partial f(x^\nu)\partial x^\mu$ leaves the Maxwell field $F_{\mu\nu}$ invariant, the conserved quantity is the charge [2]. Thus in classical mechanics spatial translational invariance, R^3, yields momentum conservation, temporal translational invariance, R, yields energy conservation and rotational invariance, $SO(3)$ yields angular momentum conservation. Thus we could characterize free-particle classical mechanics by the invariance group $R \bigotimes [R^3 \bigotimes_s SO(3)]$, where $\bigotimes_s$ is the "semi-direct product" (signifying that the two subgroups do not commute), the spatial part (in the square bracket) is the 3-dimensional Euclidean group. For special relativity the group has to be the 4-dimensional symmetry group for Minkowski space, called the Poincaré group, $R^4 \bigotimes_s SO(1,3)$. Instead of separate energy and momentum conservation the R^4 gives conservation of energy-momentum, allowing a 'mixing' of the two. The $SO(1,3)$ contains the rotational group as a proper subgroup, but also contains spin-angular momentum in it. thus the conservation is of the two together and they can mix as well; $\mathbf{J} = \mathbf{L} + \mathbf{S}$.

Since this special relativistic effect is frame dependent for a homogeneous stress-energy tensor the Lorentz rotation can be undone over the entire spacelike hypersurface in a homogeneous spacetime. However, it persists in an *inhomogeneous* system as undoing it at one place will simply push the twist elsewhere. In other words, there would still be no "seed" without charges to introduce the non-homogeneity required in the spacetime. Thus a plasma is needed to provide the effect. The distortion is purely in the spacelike section (as the spacetime remains flat). This could now be undone locally, but not globally, by a change of frame because of inhomogeneity.

4 Plasma dynamics in a curved space

We now come to plasmas in the general theory of curved spacetimes, where the energy content of the spacetime is responsible for the curvature. In principle this will be no different from the case where it is the motion that is responsible for the effective curvature of the 3-space. We can take the local rest-frame at one point as given by the tangent space, using Riemann normal coordinates, and compare it with the local rest-frame at another point. There will be a definable local Lorentz factor there, giving the above special relativistic effect produced by gravity. The frame chosen by us is a special Fermi-Walker frame, which gives the geodesics *as if* they were straight lines bent due to an (appropriately modified) force of gravity. The GR effects open up the exciting possibility of spontaneous generation of magnetic fields near gravitating sources.

Consider a plasma with the ideal fluid stress-energy tensor density, $T^{\mu\nu} = hV^\mu V^\nu + pg^{\mu\nu}$, where h is the enthalpy density, V^μ is the velocity 4-vector and p is the pressure. Since we have total energy-momentum conservation, and there is also the electromagnetic energy density of the plasma, the conservation equation is ${T^{\mu\nu}}_{;\nu} = qnF^{\mu\nu}V_\nu$, where q is the charge and n is the number density of the charged particles. The continuity equation for the plasma particles is $(nV^\mu)_{;\mu} = 0$. Then the conservation of energy becomes $mnV^\nu(fV^\mu)_{;\nu} = qnF^{\mu\nu}V_\nu + p, \nu g^{\mu\nu}$, where $f = h/mn$ and m is the particle mass.

Equation (4) still holds with the angular momentum tensor of the plasma field, using the flow velocity 4-vector, V_μ, to give the spin tensor $S_{\mu\nu}$,

$$M_{\mu\nu} = (q/c)F_{\mu\nu} + 2(fV_{[\nu)_{,\mu]}}. \tag{11}$$

The entropy density S is related to the pressure p by

$$S_{,\mu} = \frac{p_{,\mu} - mnf_{,\mu}}{nT}. \tag{12}$$

This along with the Maxwell equations gives the complete description of the system.

We will use the canonical formalism [4] to compute the general relativistic effect in the plasma. Though one would ideally like to use the charged Kerr metric for the background spacetime and then include back-reactions, in this first step we will use the simpler case of the Schwarzschild metric and a more naive way of seeing the effects. The approach used for the purpose is the "pseudo-Newtonian", or "ψN formalism". (It was invented by Mahajan, Valanju and me [5], and later developed formally by my students and I, starting with Jawaid Quamar [7,8] for static metrics, applying it to pulsars with Rafique [9,10] and Sharif [11–13] for time-varying metrics.)

This formalism takes a preferred frame, which corresponds to an observer falling freely in the gravitational field from rest at infinity, or given a velocity corresponding to that from any place in the spacetime. The special feature of this frame is that the observer sees the special relativistic, Minkowski, space. In geometric terms the spatial sections turn out to be flat (at least this is explicitly proved for spherically symmetric static spacetimes). In terms of the usual canonical formalism, this frame is a special Fermi-Walker frame [14]. The advantage of using this formalism is that it allows one to

use ones usual intuition based on forces in Newtonian mechanics.

Working out the tidal force from the geodesic deviation formula for the tidal force:

$$A^\mu = R^\mu{}_{\nu\rho\pi} t^\nu l^\rho t^\pi, \tag{13}$$

where $\mathbf{R}$ is the curvature tensor, $\mathbf{t}$ the unit timelike 4-vector tangent to the geodesic and $\mathbf{l}$ the spacelike separation 4-vector, one can define the $\psi N-$force as the quantity whose directional derivative along the separation vector. We can now choose the time axis along $\mathbf{t}$ and the space section orthogonal to it. This leads to a $\psi N-$potential, whose gradient is the negative of this force. This potential turns out to be $\frac{1}{2}\ln(g_{00})$ in this frame.

The general metric written in the canonical formalism is:

$$ds^2 = \alpha^2 dt^2 + 2\beta_i dt dx^i + \Gamma_{ij} dx^i dx^j, \tag{14}$$

where α^2 is g_{00}, giving the gravitational potential, β_i is the shift vector, giving the momentum, and Γ_{ij} is the 3-space metric tensor, having chosen units in which the speed of light is unity. We can choose a gauge (by performing an appropriate gauge transformation, i.e. choosing a frame) in which the shift vector is zero. The ψN-frame corresponds to this very choice. We now write the unit timelike vector in the chosen coordinates as

$$t^\mu = (\alpha, 0, 0, 0)\ ,\ t_\mu = (1/\alpha, 0, 0, 0), \tag{15}$$

so that we can write the 3-d metric tensor with the full 4×4 matrix form as

$$\Gamma_{\mu\nu} = t_\mu t_\nu - g_{\mu\nu}. \tag{16}$$

Then $V^\mu = (\gamma, \gamma\mathbf{v})$ and we can write

$$V^\mu = \gamma\left(\alpha t^\mu - \Gamma^\mu_\nu v^\nu\right), \tag{17}$$

where the index of the 3-d metric tensor is raised by the 4-d metric tensor and v^ν is the local fluid 3-velocity. This allows us to write the generalization of the usual Lorentz factor,

$$\gamma = 1/\sqrt{\alpha^2 - \Gamma_{\mu\nu} t^\mu t^\nu}. \tag{18}$$

Whereas the fluid particle velocity is defined by $v = dx/dt$ the velocity according to the fiducial observer is defined as $v_f = dx/d\tau$ giving $\gamma_f = \alpha\gamma$. Then $t_\mu = V^\mu = \gamma f$.

5 The general relativistic effect

In the chosen frame we can write the electric and magnetic fields as

$$E_\nu = F_{\mu\nu} t^\mu\ ,\ B^\mu = \frac{1}{2}\epsilon^{\mu\nu\rho\pi} t_\nu F_{\rho\pi}, \tag{19}$$

so that both fields are spacelike, i.e. $\mathbf{t}.\mathbf{E} = \mathbf{t}.\mathbf{B} = 0$, where these are taken to be 4-vectors. Using the Maxwell equations we get $\nabla.\mathbf{E} = 4\pi qn\alpha\gamma$, where the ∇ is defined by the requirement that $\nabla\Gamma = 0$. Direct manipulation of the other Maxwell equations yields

$$\nabla \times (\alpha\mathbf{B}) = 4\pi qn\alpha\gamma\mathbf{v} + \mathbf{E}_t, \tag{20}$$

and the continuity equation gives

$$(qn\alpha\gamma)_t + \nabla.(qn\alpha\gamma\mathbf{v}) = 0, \tag{21}$$

where the suffix t stands for the derivative with respect to the coordinate time. The other two Maxwell equations come from the identity $\mathbf{d} \times \mathbf{F} = 0$ as $\mathbf{F} = \mathbf{d} \times \mathbf{A}$ and hence remain unaltered by the breaking of the metric tensor into the time and space parts, except that in the Faraday law the electric field picks up a factor of α.

Now defining the generalized electric and magnetic fields

$$\xi^\mu = M^{\mu\nu} t_\nu\ ,\ \Omega^\mu = \frac{1}{2}\epsilon^{\mu\nu\rho\pi} t_\nu M_{\rho\pi}, \tag{22}$$

where

$$M_{\mu\nu} = F_{\mu\nu} + \frac{m}{q} S_{\mu\nu}\ . \tag{23}$$

Since from (22)

$$M_{\mu\nu} = \xi_\mu t_\nu - \xi_\nu t_\mu - \epsilon_{\mu\nu\rho\pi}\Omega^\rho t^\pi, \tag{24}$$

using the spacelike condition for the fields

$$\alpha q\underline{\xi} = \alpha q\mathbf{E} - \nabla(f\alpha^2\gamma) - m(f\gamma\mathbf{v})_t\ ,$$
$$\underline{\Omega} = \mathbf{B} + m\nabla \times (f\gamma\mathbf{v}). \tag{25}$$

The $\underline{\Omega}$ corresponds to the generalized vorticity vector mentioned earlier. Thus the GR effect comes from the local Lorentz factor. Using the above generalized electric and magnetic fields in the earlier equations, we get

$$q\alpha\gamma\mathbf{v} \cdot \underline{\xi} T S_t\ ,$$
$$q\alpha\gamma\underline{\xi} + q\gamma\mathbf{v} \times \underline{\mathbf{\Omega}} = T\nabla S. \tag{26}$$

The generalized Maxwell equations yield

$$\underline{\Omega}_t = -\nabla \times \underline{\xi}. \tag{27}$$

Using the earlier constraints and equations one arrives at

$$\underline{\Omega}_t - \nabla \times \mathbf{v} \times \underline{\Omega} = \underline{\Xi}_b + \underline{\Xi}_r, \tag{28}$$

where $\underline{\Xi}_b$ is the baroclinic term given by (7) and $\underline{\Xi}_r$ is the relativistic term given by (8). Here the latter becomes

$$2q\underline{\Xi}_r = \gamma T[-\nabla\alpha^2 + \nabla v^2] \times \nabla S. \tag{29}$$

This provides a drive for the generation of the magnetic field, even without high speeds. Of course, the high speeds can either add in or subtract out from the curvature effect depending on their direction. The net

result for a non-zero baroclinic term is that the ratio of the strengths of the curvature and baroclinic terms is

$$\frac{|\underline{\Xi}_r|}{|\underline{\Xi}_b|} = \frac{\gamma^2 \Gamma}{2} |\nabla \alpha^2 + \nabla v^2|. \tag{30}$$

Notice that the gradient of the metric coefficient is directly related to the ψNforce and the second term is the directional derivative of the fluid velocity vector, while the Lorentz factor square $\sim$ inverse of the difference of the metric coefficient and fluid speed square. As such, if these two are close together but directions are different, the ratio can be arbitrarily large. Striking result is that the gravitational potential, through g_{00} (or α), can produce a magnetic field in any region populated by charged particles even if their local velocities are negligible. Despite the confusion of terminology, where "gravitomagnetic" is used for the particular components of the curvature tensor, we feel that this should be called a gravito-magnetic battery!

6 Relativistic drives for different spacetimes

The GR drive will obviously require very high gravitational fields such as are found in the vicinity of a black hole. As such, we will consider three black hole spacetimes: (a) Schwarzschild [15]; (b) Reissner-Nordstrom [16]; (c) Kerr [16]. The first, being the simplest and a good approximation to a simple gravitational source is an obvious initial choice. What may seem strange is to use the Reissner-Nordstrom spacetime for this purpose. After all, astrophysical bodies are charge neutral and it does not seem possible to generate a significantly charged black hole that will retain its charge for any length of time. The reason to take it is just as an exercise, to guide us to the calculations for the more complicated spinning black hole given by the Kerr metric.

(a) The Schwarzschild black hole spacetime

The Schwarzschild metric is

$$ds^2 = e^{\nu} dt^2 + e^{-\nu} dr^2 + r^2 d\theta^2 + r^2 sin2\theta d\phi^2, \tag{31}$$

where, $e^{\nu} = (1 - r_o/r)$. Consider a particle in the plasma following a Keplerian orbit. Choose the plane of the orbit to be the equatorial plane. Clearly, the azimuthal speed must be much greater than the radial speed for the orbit to be stable. The drive, $\underline{\Xi}_r$, depends on the gradient of the entropy variations. The usual definition of the entropy density is valid as the GR nonlinearity is only significant close to the surface of a black hole, say $5r_o$. Since $S = F(T)$, $(T/c)\nabla S \propto \nabla T$ and hence the baroclinic term, $\underline{\Xi}_b$, is zero and the only drive is the GR drive,

$$|\underline{\Xi}_r| = \frac{3c\zeta r_0 e^{\nu/2}}{4qr^3} (1 - \frac{3r_o}{2r})^{-1/2} \frac{\partial}{\partial \phi}, \tag{32}$$

where q is now the electric charge for the plasma particle, ϕ is the azimuthal angle and $\zeta = F'(T)T/c$. This drive acts in the z-direction. For a thin disc the poloidal temperature gradients would be negligible compared with the azimuthal gradients, so the entire plasma would contribute to the drive.

At $5r_o$ and taking the average temperature of the plasma as coming from a black body at $5 \times 10^7 (M_{\odot}/-M)^{1/4} K$ [17], the total GR drive (obtained by integrating over all ϕ) will be $|\underline{\Xi}_{r,t}| = 3 \times 10^{-2} \zeta (M_{\odot}/M)^{9/4}$. Note that the plasma is at a non-relativistic temperature as the rest energy of the particles is much greater than the thermal energy for even solar mass stars. The total seed magnetic field will be proportional to the time for generating it. Putting in estimates we find the field to be $\sim 10^{-9} (M_{\odot}/M)^{1/4} G$. It should be noted that though the seed is very small, even for very high mass objects, it is not expected to provide a large field directly. It only sets the process of magnetic field generation in motion, where there was none. Also, closer to the surface of the object, the factor goes as $\zeta T/e^{\nu} q r_o$, and hence as $e^{-\nu}$, which blows up at the black hole surface. As such, if objects are nearly black holes they can produce fairly large fields. For an effective drive we would need a black hole. Of course, we are depending on a plasma in the form of an accretion disc about the object.

The Reissner-Nordström black hole

To go beyond the simple black hole for simplicity of visualization and calculation, we need to use the ψN-formalism. Here we only need the time component of the metric to obtain the gravitational potential. As the simplest extension we take the Reissner-Nordström metric, for which we replace the factor e^{ν} in (31) by $(1 - 2m/r + Q^2/r^2)$, where m is the mass and Q the charge in gravitational units $c = G = 4\pi\epsilon_o = 1$. (The earlier, $r_o = 2m$.) The ψN-potential is the natural logarithm of this quantity. Since the relativistic drive is related to its gradient, the ψN-force comes in (with a scale factor due to the ψN term). We only need to see how its modification changes the strength of the drive. The $|\nabla e^{\nu}| = |2M/r^2 + 2Q^2/r^3|$, and the change comes from the ratio of the second term to the first. At $5r_o$ it is $Q^2/10M^2$. As such, the strength is decreased by this amount. This is not expected to be a serious model for the seed generation as there *are* no significantly charged astrophysical bodies. As such, it does

not matter that we have here neglected the interaction between the charges in the plasma and the charge of the black hole, which could be sizable for an extreme (or near-extreme) black hole.

The Kerr black hole

A spinning black hole changes the discussion in a different way. The approximations used for estimates depended crucially on neglecting polar angle derivatives. This would be badly off for an axially symmetric source. Further, reduction from staticity to stationarity could also make a significant difference. (Recall that a metric is *stationary* if it admits a global timelike Killing vector and *static* if the Killing vector is globally hypersurface orthogonal). For this purpose a more detailed analysis would be needed. At present we just look at the changes in the ψN-potential and the ψN-force.

Here we have ,

$$g_{oo} = 1 - \frac{2GMr/c^2}{r^2 + a^2\cos^2\theta} \;:=\; 1 - \frac{2Rr}{\rho^2}, \tag{33}$$

where a is the "spin", i.e. the angular momentum per unit mass. The ψN-potential is $\ln\sqrt{g_{oo}}$ and so the ψN-force is θ-dependent:

$$\nabla \ln\sqrt{g_{oo}} = \frac{R}{\rho^2\chi^2}(r^2 - a^2\cos^2\theta, -2ra^2\cos\theta\sin\theta, 0), \tag{34}$$

where $\chi^2 = r^2 - 2Rr + a^2\cos^2\theta/c^2$. The squared magnitude of the force then becomes

$$F^2_{\psi N} \;=\; \frac{R^2}{\rho^6\chi^4}[(r^2 - 2rR + a^2)(r^2 - a^2\cos^2\theta)^2$$

$$+a^4r^2\sin^2 2\theta\ . \tag{35}$$

This is too complicated to convey much wisdom, so we need to look at special cases to make sense of what it means. At the poles we get

$$F^2_{\psi N} \;=\; \frac{R^2(r^2 - a^2)^2}{(r^2 + a^2)^3(r^2 - 2Rr + a^2)}. \tag{36}$$

which is slightly less than for the Schwarzschild black hole. At the equator we get

$$F^2_{\psi N} \;=\; \frac{R^2(r^2 - 2Rr + a^2)}{r^4(r - 2R)^2}. \tag{37}$$

which is more, and can be much more, than for the Schwarzschild. Since the plasma will lie in an equatorial orbit and the drive is stronger there than for the Schwarzschild case, there will anyhow be an enhancement. Further, since the expression blows up at $r = 2R$, which is accessible, it will be much more! The behavior of the ψN-force is shown in the graphs in Figures 1(a) and (b).

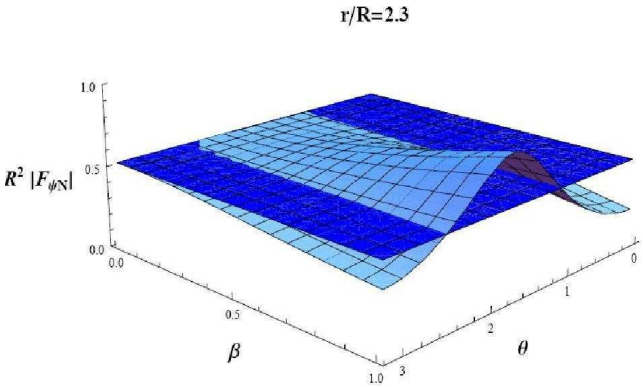

Fig. 1 The normalized magnitude of the ψN-force for a given distance $r/R = 2.3$ in terms of θ and $\beta = a/Rc$. The dark blue plane is the Schwarzschild drive and the light blue curve is the Kerr drive. The Kerr drive could be smaller or greater than the Schwarzschild drive depending of the value of β. For $a \neq 0$, the Kerr drive at the poles is always smaller than the Schwarzschild drive, while on the equator the Kerr drive is always greater than the Schwarzschild drive. Notice how the maximum of the Kerr drive is around $\pi/2$.

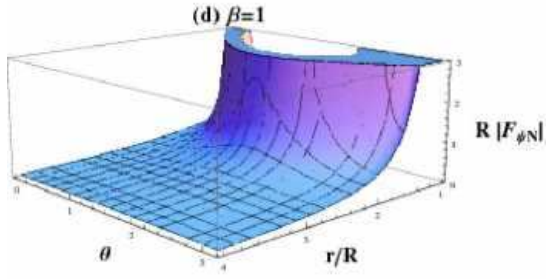

Fig. 2 The normalized magnitude of the ψN-force is plotted in terms of the normalized distance r/R and θ, for the extreme Kerr black hole, $\beta = 1$.

7 Radiation reaction in the Kerr spacetime

Our problem now is that we have "too much of a good thing". We had wanted to get a large enough seed generated, but not an *infinite* seed. To avoid this outcome we need to incorporate the damping of the field due to radiation reaction. For this purpose we use the $\psi N-$formalism once again. We consider the Kerr equivalent of radially inward falling particles, starting at infinity coming radially in and then spiraling in along a cone of constant polar angle θ_o [18]. These particles will be in a ψN-frame and so one can look for the change in the force due to the radiation. (This approach is Wheeler's "poor man's" way of getting results without having to work through complicated calculations that may lose sight of the underlying Physics. As he used to say, "I never start a calculation unless I already know the answer", quoted in [19].)

We first calculate the change in the metric, which we write as $h_{\mu\nu}$. Since the radiation should be emitted radially outward, we take the ansatz that the only non-zero components are h_{tt} and h_{tr}. The equation for h_{tr} yields the solution $h_{tr} \sim \rho^2/\chi^2$. For the h_{tt} the first non-zero term to appear is at the 8^{th} order (the term is independent of θ) and yields

$$h_{tt} = \frac{c_1}{4\omega}\left[e^{-\xi^3}\left(1-3\xi^3\right)+3\xi^6 E_{1/3}\left(\xi^3\right)\right], \tag{38}$$

where c_1 is an arbitrary constant, E is the exponential integral function [21] defined as

$$E_n(x) = \int_1^\infty e^{-xt}t^{-n}dt,$$

$\xi = \left(\frac{\omega^2}{3R}\right)^{1/3} r$ and ω is the wave frequency. The presence of c_1 is important in that it can be determined in such a way that the singularity found at $r = 2R$ in the Kerr case is eliminated. This results in a value for c_1 which is given by

$$c_1 = \frac{3e^{\frac{8\omega 2}{3}}}{8\omega\left[32\omega^4 E_{-2/3}\left(\frac{8\omega^2}{3}\right)-3(1+4\omega^2)\right]}.$$

To the same order, the expression for h_{tr} is given by

$$h_{tr} = -\frac{c_1 e^{i\omega t}r}{3\xi}\Gamma_{1/3}\left(\xi^3\right) \tag{39}$$

where Γ is the incomplete gamma function [20].

To this end the reaction-corrected version of the g_{00} component of the metric is given by

$$g_{00} = 1 - \frac{2}{r^2+a^2\cos^2\theta} + \frac{e^{-\xi^3}\left(1-3\xi^3\right)+3\xi^6 E_{1/3}\left(\xi^3\right)}{32\omega^2\left[32\omega^4 E_{-2/3}\left(\frac{8\omega^2}{3}\right)-3e^{-\frac{8\omega^3}{3}}\left(1+4\omega^2\right)\right]}, \tag{40}$$

ξ has is defined as it was above. From this the square of the ψN-force may by found to be

$$F^2_{\psi N} = \frac{A+B^2}{C^2}, \tag{41}$$

where A, B and C are defined by

$$A = \frac{9\xi_0^2}{16\chi}\left[8e^{\xi^3}\left(3e^{\xi_0^3}\xi_0^6 E_{-2/3}\left(\xi_0^3\right)-3\xi_0^3-2\right)\left(8\xi^2-\xi_0^2\rho^2\right) - 2\xi^2 e^{\xi_0^3}\rho^4\left(3e^{\xi^3}\xi^6 E_{-2/3}(\xi^3)-3\xi^3-2\right)\right],$$

$$B = 12e^{\xi^3}\xi\xi_0^2\sin 2\theta\left(2+3\xi_0^3-3e^{\xi_0^3}\xi_0^6 E_{-2/3}(\xi_0^3)\right) \tag{42}$$

and

$$C = 6e^{3\xi}\xi_0^2\rho(\xi_0\rho^2-4\xi)(2+3\xi_0^3-3e^{\xi_0^3}\xi_0^6 E_{-2/3}(\xi_0^3)) + \rho^3 e^{\xi_0^3}3e^{\xi^3}\xi^6 E_{1/3}-3\xi^3+1). \tag{43}$$

The variables χ, ρ and ξ have their usual meanings and $\xi_0 = \xi|_{r=2}$. Once again the equation for the force squared is too complicated to perform any meaningful analysis. We therefore consider the force along the pole and equator particularly at $r = 2R$, the force increases toward $r = 0$ and rapidly decreasing as r are increases. In both cases we see that there are no singularities in the limit as $\xi \to \xi_0$.

Acknowledgements

We are grateful to Usman Qadir for some help with preparation of the manuscript. AQ is grateful to the DECMA Centre and the School of Computational and Applied Mathematics for hosting him when this work was completed.

References

1. S.M. Mahajan and J. Yoshida, *Phys. Rev. Lett.* **105** (2010) 095005; *Phys. Plasmas* **18** (2011) 055701.
2. A. Qadir, *Relativity: An Introduction to the Special Theory*, World Scientific 1989.
3. H. Goldstein, C.P. Poole Jr. and J.L. Safko, *Classical Mechanics* 3^{rd} Edition), Addison-Wesley 2001.
4. C.W. Misner, K.S. Thorne and J.A. Wheeler, *Gravitation*, W.H. Freeman and Company 1973.
5. S.M. Mahajan, A. Qadir and P.M. Valanju, *Nuovo Cimento B* **65** (1981) 404.
6. A. Qadir and J. Quamar, *Proc. Third Marcel Grossman Meeting*, ed. Hu Ning, North Holland Publishing Company (1983) 189; *Europhys. Lett.* **2** (1986) 423.
7. A. Qadir and J. Quamar, *Proc. Third Marcel Grossmann Meeting*, ed. Hu Ning, North Holland Publishing Company (1983)189-220.
8. J. Quamar, "Relativistic gravitodynamics and forces", PhD Thesis, Quaid-i-Azam University 1984.
9. A. Qadir and M. Rafique, *Proc. Fourth Marcel Grossmann Meeting*, ed. R. Ruffini (Elsevier Science Publishers 1986) 1597; *Chinese Physics Letters* **3** (1986) 189.
10. M. Rafique, "Some implications of the ψN-formalism", PhD Thesis, Quaid-i-Azam University 1985.
11. A. Qadir and M. Sharif, *Nuovo Cimento B* **107** (1992) 1071.
12. A. Qadir and M. Sharif, *Phys. Lett. A* **167** (1992) 331.
13. M. Sharif, "Forces in non-static spacetimes", PhD Thesis, Quaid-i-Azam University 1991.
14. A. Qadir and I. Zafarullah, *Nuovo Cimento B* **111** (1996) 79.
15. F.A. Asenjo, S.M. Mahajan and A. Qadir, *Phys. Plasmas* **20** (2013) 22901.
16. A. Qadir, F.A. Asenjo and S.M. Mahajan, *Physica Scripta* **89** (2014) 084002.
17. M. Vietri, *Foundations of High-Energy Astrophysics*, University of Chicago 2008.
18. A. Qadir J. Quamar and M. Rafique, *Physics Letters A* **109** (1985) 90.
19. F. Depaolis, A. Qadir and R. Ruffini, "Preface", *Gen. Rel. & Grav.* **43** (2011).

20. M.A. Chaudhry and S.M Zubair, *On a Class of Incomplete Gamma Functions with Applications*, Chapman and Hall 2001.
21. G. Arfken, *Mathematical Methods for Physicists,* 3rd ed. Orlando, FL: Academic Press, pp. 566-568, 1985.

Proc. Int. Conf. Relativ. Astrophys.
Pages 178-182, (2015)

Dynamics of Logamediate Anisotropic Warm Inflation

M. Sharif [1], **Rabia Saleem** [2]

[1]Department of Mathematics, University of the Punjab, Quaid-e-Azam Campus, Lahore-54590, Pakistan.

Abstract In this paper, we analyze the effects of generalized dissipative coefficient on the dynamics of warm logamediate inflationary universe models during strong dissipative regime. We explore these models within the framework of locally rotationally symmetric Bianchi type I universe. We evaluate inflaton, scalar potential, dissipative coefficient, slow-roll parameters, scalar (tensor) power spectra, scalar spectral index and tensor-scalar ratio under slow-roll approximation. The inflationary model as well as perturbed parameters are constrained using recent data. We conclude that $n = 1$ is the only consistent case during logamediate era.

Keywords Warm inflation · Slow-roll approximation

PACS 98.80.Cq · 05.40.+j.

1 Introduction

The standard hot big-bang cosmology successfully explains the observations of CMBR. The issues including horizon problem, flatness, magnetic monopole and origin of fluctuations still remain unresolved. Inflation is very successful paradigm in addressing the shortcomings of standard model providing an elegant mechanism to resolve these issues. The simplest primary ingredient of inflation is that of scalar field which provides a seed for causal interpretation of the origin of LSS distribution and observed temperature anisotropies in CMBR [1]. The standard inflationary models are classified into slow-roll and reheating epochs. During slow-roll inflationary period, the scalar potential must have a very flat region as potential energy dominates kinetic energy and all the interactions among scalar fields as well as other fields become negligible, hence the universe inflates [2]. The universe then enters into reheating period where both types of energy (potential and kinetic) are comparable and the inflaton starts an oscillation about minimum of its potential losing their energy to other fields present in the theory [3].

A more general class of models where fluctuation-dissipation effects are significant is known as warm inflation. It has an appealing feature of joining the end stage of inflation with the present structure of the universe. During this regime, density thermal fluctuations arise rather than quantum fluctuations [4]. Warm inflationary era ends when the universe stops inflating, finally enters into the radiation dominated phase smoothly. The remaining inflatons or dominant radiation fields create matter components of the universe [5]. Dissipation is a natural outcome of the interactions between the inflaton field and other degrees of freedom which are required to ensure a graceful exit into radiation dominant era. Bastero-Gil et al. [6] made considerable explicit calculations using quantum field theory method that compute all the relevant decay and scattering rates in the warm inflationary models.

Exact solutions of the inflationary cosmology can also be obtained for intermediate and logamediate scenarios with specific growth of the scale factor [7,8]. This intermediate type of expansion is slower than de Sitter inflation but faster than power-law inflation, so dubbed as "intermediate". These models were originally developed as exact solutions of inflationary cosmology but were best formulated using slow-roll approximation which may lead to give a spectral index $n_s = 1$. In particular, intermediate inflation leads to $n_s = 1$ for special value of $f^* = 2/3$ that corresponds to the Harrizon-Zel'dovich spectrum [9,10]. In both models, an important observational quantity is the tensor-scalar ratio (r), which is significantly non-zero [11]. Recently, the ef-

[1]msharif.math@pu.edu.pk
[2]rabiasaleem1988@yahoo.com

fects from BICEP2 experiment of gravitational waves in B-mode have been analyzed which predict $r = 0.2^{+0.07}_{-0.05}$ (68% C.L.) and take out the value $r = 0$ at a significance of 7.0σ [12].

Setare and Kamali [13,14] studied characteristic of "warm inflation" with vector and non-abelian gauge fields during intermediate and logamediate scenarios using flat FRW background taking constant and variable dissipative coefficients. We have proved that locally rotationally symmetric (LRS) Bianchi I (BI) universe model remains compatible with WMAP7 observations with both types of field [15,16]. Inflationary dynamics of generalized cosmic Chaplygin gas using standard and tachyon scalar fields (with and with out viscous pressure) during intermediate and logamediate scenarios is discussed in [17,18]. We have investigated dynamics of warm viscous inflation in LRS BI universe model with constant and variable dissipative as well as bulk viscosity coefficients [19]. Herrera et al. [20] analyzed the possible realization of an expanding intermediate and logamediate scale factors within the framework of FRW as well as loop quantum cosmology models.

In this paper, we check the compatibility of LRS BI model with recent data during strong dissipative regime. The paper is organized as follows. The basic formalism of warm LRS BI inflationary universe is given in section **2**. Section **3** deals with strong dissipative regime developing the model during logamediate inflation. We evaluate explicit expressions for inflaton, scalar potential, rate of decay and perturbed parameters. These parameters are analyzed through graphical trajectories by constraining the model parameters with recent observations. Finally, the results are concluded in the last section.

2 Anisotropic Inflationary Model

The line element of LRS BI universe model is given as

$$ds^2 = -dt^2 + X^2(t)dx^2 + Y^2(t)(dy^2 + dz^2). \tag{1}$$

A proportionality relationship between expansion and shear scalar leads to a linear relationship, $X = Y^{\mu}$ ($\mu \neq 1$ stands for anisotropic parameter). Under this relation, the above metric is reduced to

$$ds^2 = -dt^2 + Y^{2\mu}(t)dx^2 + Y^2(t)(dy^2 + dz^2). \tag{2}$$

The basic ingredients of the universe are assumed to be self-interacting scalar field (ψ) and radiation field (γ). The inflaton possesses the following energy density (ρ_ψ) and pressure (P_ψ)

$$\rho_\psi = \frac{\dot{\psi}^2}{2} + V(\psi), \quad P_\psi = \frac{\dot{\psi}^2}{2} - V(\psi), \tag{3}$$

where $V(\psi)$ is the effective potential and dot represents derivative with respect to cosmic time t. The dynamics of anisotropic warm inflation is described by the evolution equation as well as conservation equations of inflaton and radiation given by

$$\begin{aligned} H_2^2 &= \frac{\kappa}{1+2\mu}(\rho_\psi + \rho_\gamma) = \frac{\kappa}{1+2\mu}\left(\frac{\dot{\psi}^2}{2} + V(\psi) + \rho_\gamma\right), \\ \dot{\rho_\psi} &+ (\mu+2)H_2(\rho_\psi + P_\psi) = -\Gamma\dot{\psi}^2, \\ \dot{\rho}_\gamma &+ \frac{4}{3}(\mu+2)H_2\rho_\gamma = \Gamma\dot{\psi}^2, \end{aligned} \tag{4}$$

where ρ_γ is the radiation density and H_2 is the Hubble parameter in y direction. The second law of thermodynamics suggests $\Gamma > 0$ implying that ρ_ψ dissipates into ρ_γ. This factor has specific forms as it may be a constant, function of inflaton ($\Gamma(\psi)$), function of temperature ($\Gamma(T)$), function of both ($\Gamma(\psi, T)$) and equivalent to $V(\psi)$ in some papers [4].

We have considered a more general form of the dissipative coefficient as

$$\Gamma = C_\psi \frac{T^n}{\psi^{n-1}}, \tag{5}$$

where n be any arbitrary integer and C_ψ is associated to the dissipative microscopic dynamics [21]. In this reference, Zhang and Basero-Gil et al. analyzed different choices of n that correspond to different expressions for dissipative coefficient. In particular, for $n = 3$, $C_\psi = 0.64h^4\mathcal{N}$, where $\mathcal{N} = \mathcal{N}_\chi \mathcal{N}^2_{decay}$ ($\mathcal{N}_\chi$ is the multiplicity of $\mathcal{X}$ superfield and $\mathcal{N}$ is the number of decay channels available in $\mathcal{X}$'s decay) [21–23]. The value $n = 1$ leads to $\Gamma \propto T$ (represents the high-temperature SUSY case), $n = 0$ generates $\Gamma \propto \psi$ (corresponds to an exponentially decaying propagator in the SUSY case) and $n = -1$ leads to the decay rate $\Gamma \propto \frac{\psi^2}{T}$ (corresponds to the non-SUSY case). The case $n = 3$ implies the most common form $\Gamma \sim T^3$ considered for the warm intermediate and logamediate models [24,25].

During inflation, stable regime can be obtained by applying an approximation, i.e., $\rho_\psi \approx V(\psi)$, $\rho_\psi > \rho_\gamma$. Under this limit, the evolution equation is reduced to

$$H_2^2 = \frac{\kappa}{1+2\mu}\rho_\psi = \frac{\kappa}{1+2\mu}V(\psi). \tag{6}$$

Using this equation along with conservation equation of inflaton, we have

$$\dot{\psi}^2 = \frac{2(1+2\mu)(-\dot{H}_2)}{(\mu+2)\kappa(1+R)}, \tag{7}$$

where decay rate between Γ and H_2 is given by $R = \frac{\Gamma}{(\mu+2)H_2}$. In warm inflation, the radiation production is assumed to be quasi-stable where $\dot{\rho_\gamma} \ll \frac{4}{3}(\mu+2)H_2\rho_\gamma$,

$\dot{\rho}_\gamma \ll \Gamma\dot{\psi}^2$. Using Eq.(7) and quasi-stable condition in the last equation of Eq.(4), it follows that

$$\rho_\gamma = \frac{3(1+2\mu)\Gamma(-\dot{H}_2)}{2\kappa C_\gamma(\mu+2)^2(1+R)H_2} = C_\gamma T^4, \tag{8}$$

where $C_\gamma = \frac{\pi^2 g_*}{30}$ in which g_* is known as the number of relativistic degrees of freedom. The temperature of thermal bath can be extracted from second equality of the above equation as

$$T = \left[\frac{3(1+2\mu)\Gamma(-\dot{H}_2)}{2\kappa(\mu+2)^2(1+R)H_2}\right]^{\frac{1}{4}}. \tag{9}$$

Substituting the value of T in Eq.(5), we have

$$\Gamma^{\frac{4-n}{4}} = \alpha_n(1+R)^{-\frac{n}{4}}\left(\frac{-\dot{H}_2}{H_2}\right)^{\frac{n}{4}}\psi^{1-n}, \tag{10}$$

where $\alpha_n = C_\psi\left[\frac{3(1+2\mu)}{2\kappa C_\gamma(\mu+2)^2}\right]^{\frac{n}{4}}$. The effective potential can be obtained from the first evolution equation with the help of Eqs.(7) and (8) as

$$V(\psi) = \left(\frac{1+2\mu}{\kappa}\right)H_2^2 + \frac{(1+2\mu)\dot{H}_2}{(\mu+2)\kappa(1+R)}\left[1+\frac{3}{2}R\right]. \tag{11}$$

Next, we check the compatibility of the desired model with recent observations in the context of logamediate regime.

2.1 Warm Logamediate Strong Regime

The logamediate scale factor evolutes as [8]

$$Y(t) = Y_0\exp[A^*(\ln t)^{\lambda^*}]. \tag{12}$$

The solution $\psi(t)$ can be found using the above equation as

$$\psi(t) - \psi(t_0) = \xi_6\gamma_n[t], \tag{13}$$

where ξ_6 and the incomplete gamma function $\gamma_n[t]$ are defined as

$$\xi_6 = \left[\frac{(1+2\mu)(3-n)^2(A^*\lambda^*)^{\frac{8-n}{4}}}{2\kappa(\mu+2)^{\frac{n}{4}}\alpha_n}\right]^{\frac{1}{3-n}} \times\left(\frac{n-2}{4}\right)^{\frac{(n-8)(\lambda^*-1)-1}{4(3-n)}},$$

$$\gamma_n[t] = \left[\Gamma\left(1+\frac{(8-n)(\lambda^*-1)}{8}, \left(\frac{2-n}{4}\right)\ln t\right)\right]^{\frac{2}{3-n}}.$$

In this case, $H_2(\psi)$ and $V(\psi)$ have the following form

$$H_2(\psi) = (A^*\lambda^*)\left(\ln\gamma_n^{-1}\left[\frac{\psi}{\xi_6}\right]\right)^{\lambda^*-1}\left(\gamma_n^{-1}\left[\frac{\psi}{\xi_6}\right]\right)^{-1},$$

$$V(\psi) = \left(\frac{1+2\mu}{\kappa}\right)(A^*\lambda^*)^2\left(\ln\gamma_n^{-1}\left[\frac{\psi}{\xi_6}\right]\right)^{2(\lambda^*-1)} \times\left(\gamma_n^{-1}\left[\frac{\psi}{\xi_6}\right]\right)^{-2}.$$

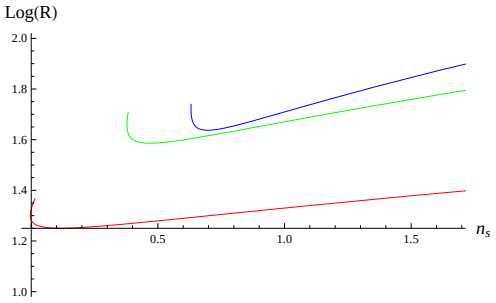

Fig. 1 Log(R) versus n_s for $\mu \approx 0.5$, $n = 1$, $C_\gamma = 70$, $A^* = 1\times10^{-3}$, $\lambda^* = 3.55$, $C_\psi = 3\times10^{-1}$ (red), $A^* = 1.2\times10^{-3}$, $\lambda^* = 3.65$, $C_\psi = 5\times10^{-1}$ (green) $A^* = 1.5\times10^{-3}$, $\lambda^* = 3.75$,$C_\psi = 7\times10^{-1}$ (blue) during logamediate regime.

The strong dissipation coefficient turns out to be

$$\Gamma(\psi) = \alpha_n\left[(\mu+2)(A^*\lambda^*)\right]^{\frac{n}{4}}\left(\ln\gamma_n^{-1}\left[\frac{\psi}{\xi_6}\right]\right)^{\frac{n(\lambda^*-1)}{4}}\left(\gamma_n^{-1} \times\left[\frac{\psi}{\xi_6}\right]\right)^{-\frac{n}{2}}\psi^{1-n}.$$

Figure **1** shows that for $n = 1$, R attains larger values with the increasing value of C_ψ. For $n = -1,\ 0$, the model remains incompatible with strong regime.

The slow-roll parameters in logamediate era are

$$\epsilon = \left(\frac{3}{\mu+2}\right)(A^*\lambda^*)^{-1}\left(\ln\gamma_n^{-1}\left[\frac{\psi}{\xi_6}\right]\right)^{(1-\lambda^*)},$$

$$\eta = \left(\frac{3}{\mu+2}\right)(A^*\lambda^*)^{-1}\left(\ln\gamma_n^{-1}\left[\frac{\psi}{\xi_6}\right]\right)^{-\lambda^*}\left[2\ln\gamma_n^{-1}\left[\frac{\psi}{\xi_6}\right] - (\lambda^*-1)\right].$$

In this case, the extent of inflation is

$$N = \left(\frac{\mu+2}{3}\right)A^*\left[\left(\ln\gamma_n^{-1}\left[\frac{\psi_2}{\xi_6}\right]\right)^{\lambda^*} - \left(\ln\gamma_n^{-1}\left[\frac{\psi_1}{\xi_6}\right]\right)^{\lambda^*}\right]. \tag{14}$$

The initial and final inflatons are calculated as

$$\psi_1 = \xi_6\gamma_n\left(\exp\left[\left(\frac{3}{\mu+2}\right)(A^*\lambda^*)^{-1}\right]^{\frac{1}{\lambda^*-1}}\right),$$

$$\psi_2 = \xi_6\gamma_n\exp\Xi.$$

where $\Xi = \left[\left(\frac{3}{\mu+2}\right)\left[\frac{N}{A^*} + \left(\left(\frac{3}{\mu+2}\right)(A^*\lambda^*)^{-1}\right)^{\frac{\lambda^*}{\lambda^*-1}}\right]\right]^{\frac{1}{\lambda^*}}$.

The number of e-folds dependent P_R turns out to be

$$P_R = \left(\frac{(\mu+2)^{\frac{3(6-n)}{8}}KC_\psi^{\frac{3}{2}}}{18\sqrt{3}\pi^2(3(1+2\mu))^{\frac{3(2-n)}{8}}}\right)\left(\frac{A^*\lambda^*}{2KC_\gamma}\right)^{\frac{3n+2}{8}} \times(\Xi)^{\frac{(\lambda^*-1)(3n+6)}{8}}\exp\left[-\frac{3n}{4}\Xi\left[\xi_6\gamma_n\left(\exp\Xi\right)\right]\right]^{\frac{3(1-n)}{2}}.$$

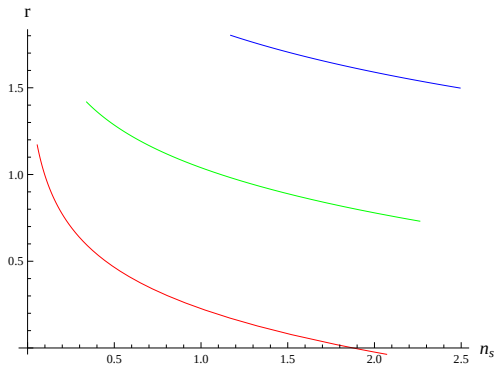

Fig. 2 Plot of r versus n_s for $\mu \approx 0.5,\ n = -1,\ C_\gamma = 70,\ A^* = 3 \times 10^{-1},\ \lambda^* = 3.00,\ C_\psi = 10^7$ (red), $A^* = 2.5 \times 10^{-1},\ \lambda^* = 3.05,\ C_\psi = 10^6$ (green), $A^* = 2 \times 10^{-1},\ \lambda^* = 3.15,\ C_\psi = 10^5$ (blue).

The spectral index becomes

$$n_s = 1 - \frac{9n}{4(A^*\lambda^*)(\mu+2)}\left(\Xi\right)^{1-\lambda^*} + \left(\frac{3(\lambda^*-1)(3n+6)}{8(A^*\lambda^*)(\mu+2)}\right) \times \Xi^{-1} + \Xi^{\lambda^*(-1+n(\frac{1-\lambda^*}{8\lambda^*}))} \exp \Xi^{(1-\lambda^*)(\frac{n+2}{4\lambda^*})} \times \left[\xi_6\gamma_n \left(\exp \Xi\right)\right]^{-1}.$$

Finally, the tensor-scalar ratio takes the form

$$r = \frac{2\kappa}{\pi^2}\left(\frac{\mu+2}{3}\right)^2 (A^*\lambda^*)^{\frac{10-3n}{8}} (2KC_\gamma)^{\frac{3n+2}{8}} \times \left(\frac{18\sqrt{3}\pi^2(3(1+2\mu))^{\frac{3(2-n)}{8}}}{(\mu+2)^{\frac{3(6-n)}{8}} KC_\psi^{\frac{3}{2}}}\right) \Xi^{\lambda^*\frac{(\lambda^*-1)(10-3n)}{8}} \times \exp\left(\frac{3n-8}{4}\Xi\right)\left[\xi_6\gamma_n\left(\exp\Xi\right)\right]^{\frac{3(n-1)}{2}}. \quad (15)$$

In order to constrain the physical parameters in warm logamediate model, we numerically solve equations only for $n = 1$. In this case, we are unable to find any specific range of C_ψ for three values of n. The only case $n = 1$ shows that two-dimensional marginalized constraints on the inflationary parameters r and n_s are compatible with recent observations for $\mu \approx 0.5,\ n = -1,\ C_\gamma = 70,\ A^* = 3 \times 10^{-1},\ \lambda^* = 3.00,\ C_\psi = 10^7$ represented by red curve (Figure **2**). This proves that our anisotropic warm logamediate inflationary model is compatible with recent observations in the range $10^5 < C_\psi < 10^7$. However, the model does not well fitted with recent observations for $n = -1,\ 0$.

3 Final Remarks

Recent observational data from the Planck satellite proves that the large angle anomalies represent real feature of the CMB map of the universe. This outcome has a key importance in this sense that the small temperature anisotropies and large angle anomalies may be caused by some unknown mechanism or anisotropic phase during the early evolution of the universe. This statement is particularly interesting as it helps to construct an alternative model of the universe to decode the effects of the early universe on the present structure of LSS without affecting the processes in the nucleosynthesis [**?**].

To study the warm inflation comprehensively on small scale structure of the universe, we have used the framework of homogeneous but anisotropic LRS BI universe model which is asymptotically equivalent to the standard FRW universe. It is assumed that the universe is composed of standard scalar field and radiation. We have analyzed possible realization of an expanding logamediate scale factor during strong dissipative regime and checked that how this type of inflation work with generalized form of the dissipation coefficient.

During warm logamediate inflationary era, the explicit expressions for inflaton (ψ), corresponding effective potential ($V(\psi)$) and rate of strong dissipation (R) are calculated by applying slow-roll approximation. We have also evaluated inflationary parameters in strong regime: slow-roll parameters ($\epsilon,\ \eta$) to find more general conditions on the starting and ending points for the occurrence of inflationary era, scalar and tensor power spectra ($P_R,\ P_T$), scalar spectral index (n_s) and finally observational parameter of interest, tensor-scalar ratio (r). We have constrained the model parameters ($A^*,\ f^*,\ \lambda^*,\ C_\psi$) by WMAP9, Planck and BICEP2 data for three particular values of $n = 1, 0, -1$. It is concluded that the logamediate model is not in good agreement with recent observations for $n = -1,\ 0$. The $r - n_s$ trajectories plotted in both regimes are the verifications of our results.

It is noted that compatibility of the model disturbs for too large values of the anisotropic parameter $\mu > 10^3$. The case $n = 3$ ($\Gamma \propto T^{-\frac{2}{3}}$) is discussed during logamediate regime [15]. It is worth mentioning here that all the results reduce to the isotropic universe for $\mu = 1$ [20] and $n = 3$ leads to [24].

References

1. D. Larson et al., *Seven-Year Wilkinson Microwave Anisotropy Probe (WMAP) Observations: Power Spectra and WMAP-Derived Parameters*, Astrophys. J. Suppl., **192**, 16 (2011).
2. E.W. Kolb and M.S. Turner, *The Early Universe* (Addison-Wesley, 1990).
3. B.A. Bassett, S. Tsujikawa and D. Wands, *Inflation Dynamics and Reheating*, Rev. Mod. Phys., **78**, 537 (2006).
4. A. Berera, *Warm Inflation*, Phys. Rev. Lett., **75**, 3218 (1995).

5. I.G. Moss, *Primordial Inflation with Spontaneous Symmetry Breaking*, Phys. Lett. B, **154**, 120 (1985).
6. M. Bastero-Gil, A. Berera, R.O. Ramos and J.G. Rosa, *General dissipation coefficient in low-temperature warm inflation*, J. Cosmol. Astropart. Phys., **1301**, 016 (2013).
7. J.D. Barrow, *Graduated inflationary universes*, Phys. Lett. B, **235**, 40 (1990).
8. J.D. Barrow and N.J. Nunes, *Dynamics of "logamediate" inflation*, Phys. Rev. D, **76**, 043501 (2007).
9. J.D. Barrow and A.R. Liddle, *Perturbation spectra from intermediate inflation*, Phys. Rev. D, **47**, R5219 (1993).
10. A.A. Starobinsky, *Inflaton field potential producing the exactly flat spectrum of adiabatic perturbations*, J. Exp. Theor. Phys. Lett., **82**, 169 (2005).
11. W.H. Kinney, E.W. Kolb, A. Melchiorri and A. Riotto, *Inflation model constraints from the Wilkinson Microwave Anisotropy Probe three-year data*, Phys. Rev. D, **74**, 023502 (2006).
12. P.A.R. Ade et al., *BICEP2 I: Detection Of B-mode Polarization at Degree Angular Scales*, arXiv:1403.3985.
13. M.R. Setare and V. Kamali, *Warm vector inflation*, Phys. Lett. B, **726**, 56 (2013).
14. M.R. Setare and V. Kamali, *Warm Gauge-Flation*, Gen. Relativ. Gravit., **46**, 1642 (2014).
15. M. Sharif and R. Saleem, *Warm Anisotropic Inflationary Universe Model*, Eur. Phys. J. C, **74** 2738 (2014).
16. M. Sharif and R. Saleem, *Dynamics of Warm Inflation with Gauge Fields in Bianchi Type I Universe Model*, Astropart. Phys., **62**, 100 (2015).
17. M. Sharif and R. Saleem, *Study of Inflationary Generalized Cosmic Chaplygin Gas for Standard and Tachyon Scalar Fields*, Eur. Phys. J. C, **74**, 2943 (2014).
18. M. Sharif and R. Saleem, *Effects of viscous pressure on warm inflationary generalized cosmic Chaplygin gas model*, J. Cosmol. Astropart. Phys., **12**, 038 (2014).
19. M. Sharif and R. Saleem, *Warm anisotropic inflation with bulk viscous pressure in intermediate era*, Astropart. Phys., **62**, 241 (2015).
20. R. Herrera, M. Olivares and N. Videla, *General dissipative coefficient in warm intermediate and logamediate inflation*, Phys. Rev. D, **88**, 063535 (2013).
21. Y. Zhang, *Warm Inflation with a General Form of the Dissipative Coefficient*, J. Cosmol. Astropart. Phys. **03**, 030 (2009).
22. A. Berera, I.G. Moss and R.O. Ramos, *Local Approximations for Effective Scalar Field Equations of Motion*, Rept. Prog. Phys. **72**, 026901 (2009).
23. M. Bastero-Gil, A. Berera and R.O. Ramos, *Dissipation coefficients from scalar and fermion quantum field interactions*, J. Cosmol. Astropart. Phys., **09**, 033 (2011).
24. S. del Campo and R. Herrera, *Intermediate inflation under the scrutiny of recent data*, J. Cosmol. Astropart. Phys., **04**, 005 (2009).
25. R. Herrera and M. Olivares, *Warm-Logamediate inflationary universe model*, Int. J. Mod. Phys. D, **21**, 1250047 (2012).
26. J.C. Hwang and H. Noh, *Cosmological Perturbations with Multiple Fluids and Fields*, Phys. Rev. D, **66**, 084009 (2002).

Int. Conf. Relativ. Astrophys.
Pages 183-187, (2015)

Black holes in Melvin universe

Muhammad Rizwan[a,1], **K. Saifullah**[b,1]

[1]Department of Mathematics, Quaid-i-Azam Univerity, Islamabad, Pakistan

Received: date / Accepted: date

Abstract A technique was developed by F. J. Ernst in 1976 for immersing black hole spacetimes in Melvin's magnetic universe. This method for magnetizing lack holes uses Harrison's transformations. In this paper we review the earlier work done on magnetizing the Schwarzschild, Reissner-Nordström and Kerr-Newman black holes.

1 Introduction

In 1952 W. B. Bonner gave the solution for empty space having cylindrical symmetry containing electromagnetic field and discussed its physical interpretation [1,2]. This was subsequently rediscovered by M. A. Melvin [3]. It is now usually referred to as the "Melvin universe". The metric that describes Melvin universe is [3, 4]

$$ds^2 = (1+\tfrac{1}{4}B^2\rho^2)^2(-dt^2+d\rho^2+dz^2) + (1+\frac{1}{4}B^2\rho^2)^{-2}\rho^2 d\phi^2, \quad (1)$$

with $t,\ z \in (-\infty,+\infty)$, $\rho \in [0,\infty)$, $\phi \in [0,2\pi)$. The electromagnetic field can be described by the Maxwell tensor

$$F = e^{-i\psi}B(dz\wedge dt), \quad (2)$$

where ψ is a real parameter of duality rotation. In particular, for $\psi = 0$, the Maxwell tensor is $F = Bdz\wedge dt$ which describes an electric field pointing along the z-direction, whereas for $\psi = \pi/2$ one obtains $F = B(1+1/4B^2\rho^2)^{-2}\rho d\rho\wedge d\phi$, which represents a purely magnetic field oriented along the z-direction. It is a spacetime which is static cylindrically symmetric and in which there exists an axial magnetic and/or electric field aligned with the z-axis, and the magnitude of the field is determined by the parameter B. This solution represents a universe which contains a parallel bundle of electric or magnetic flux held together by its own gravitational pull. Further, for $B = 0$, the metric is Minkowski metric in cylindrical coordinates. If $B \neq 0$, the metric is not asymptotically flat because $1+1/4B^2\rho^2$ does not go to 1 at any z.

The above Melvin magnetic solution has been considered as a useful model in, among others, the studies of astrophysical processes, quantum black hole pair creation and gravitational collapse. Its importance derives also from the fact that it appears as a limit in more complicated solutions and is therefore considered as a background for a number of interesting solutions. It was shown already by Melvin [5] and Thorne [6] that the spacetime is, somewhat surprisingly, stable against small radial perturbations, as well as arbitrarily large perturbations which are confined to a finite region about the axis of symmetry.

In 1976, F. J. Ernst using Harrison's transformation [7] presented a procedure for transforming asymptotically flat axially symmetric solutions of the coupled Einstein-Maxwell equations into solutions resembling Melvin's magnetic universe [8,9]. He used this technique for the removal of the nodal singularity of the C-metric [10], and studied the Schwarzschild, Reissner-Nordström and Kerr-Newman black holes in Melvin universe [8,9]. Recently, Ernst's solution generating technique is used by M. Astorino for embedding hairy black holes in Melvin universe [11] and by G. W. Gibbons et. al. for Kerr-Newman black holes [12]. In this paper we present a review of this work and discuss some examples that illustrate how Ernst used Harrison's transformation [7] to generate some electrovac solutions, which

[a]Electronic Address: rizvi_g@hotmail.com
[b]Electronic Address: saifullah@qau.edu.pk

are of physical interest. In Section 2 we shall discuss how Ernst obtained Melvin universe using Harrison's transformation. Sections 3 and 4 deal with Schwarzschild and Reissner-Nordström black holes in Melvin universe. In Section 5 we review the work [12] done on Kerr-Newman solution having electric as well as magnetic charge in Melvin universe. A brief conclusion is given at the end.

2 Melvin universe by Ernst's technique

The line element of Minkowski space in cylindrical coordination is given by

$$ds^2 = -dt^2 + dz^2 + d\rho^2 + \rho^2 d\phi^2, \tag{3}$$

and the general form of stationary axial symmetric line element can be written as [8]

$$ds^2 = f^{-1}[-2P^{-2}d\xi d\xi^* + \rho^2 dt^2] - f(d\phi - \omega dt)^2. \tag{4}$$

On comparing Eqs. (3) and (4) we have

$$f = -\rho^2, \quad \omega = 0, \quad P = \rho^{-1}, \quad d\xi = \frac{(dz + id\rho)}{\sqrt{2}}. \tag{5}$$

The complex gravitational potential ε associated with gravity is defined by

$$\varepsilon = f - |\Phi|^2 + i\varphi, \tag{6}$$

where Φ is the complex electromagnetic potential, whose real and imaginary parts are electrostatic and magnetostatic potentials, respectively and $|\Phi|$ is the magnitude of complex potential. If E_r, E_θ, H_r and H_θ are the radial and angular components of electric and magnetic fields, the complex electromagnetic potential may be evaluated by

$$H_r + iE_r = P\frac{\partial \Phi}{\partial \theta}, \quad H_\theta + iE_\theta = -P\frac{\partial \Phi}{\partial r}. \tag{7}$$

In Eq. (6) φ is the twist potential. If one defines the symbol

$$\nabla = r\frac{\partial}{\partial r} + i\frac{\partial}{\partial \theta}, \tag{8}$$

the twist potential may be determined by equation

$$-\rho^{-1} f^2 \nabla\omega = i\nabla\varphi + \Phi^*\nabla\Phi - \Phi\nabla\Phi^*. \tag{9}$$

Here Φ^* is the conjugate of Φ. Since initially there is no electromagnetic field, so complex gravitational, electromagnetic and twist potentials are given by

$$\varepsilon = f = -\rho^2, \Phi = 0, \quad \varphi = 0. \tag{10}$$

Now by Harrison's transformations new functions are defined as [8]

$$\Lambda = 1 + B\Phi - \tfrac{1}{4}B^2\varepsilon, \tag{11}$$

$$\varepsilon' = \Lambda^{-1}\varepsilon, \tag{12}$$

$$\Phi' = \Lambda^{-1}(\Phi - \tfrac{1}{2}B\varepsilon), \tag{13}$$

and under this transformation functions, f and ω are transformed into new functions f' and ω' as

$$f' = Re\varepsilon' + |\Phi'|^2 = |\Lambda|^{-2} f, \tag{14}$$

$$\nabla\omega' = |\Lambda|^2 \nabla\omega + \rho f^{-1}(\Lambda^*\nabla\Lambda - \Lambda\nabla\Lambda^*), \tag{15}$$

where the operator ∇ is different for different cases, while the function P and ρ are unmodified. From Eqs. (11) - (13)

$$\Lambda = 1 + \frac{1}{4}\rho^2 B^2, \tag{16}$$

$$\varepsilon' = \Lambda^{-1}\varepsilon = -\frac{\rho^2}{1 + \frac{1}{4}\rho^2 B^2}, \tag{17}$$

$$f' = |\Lambda|^{-2} f = -\frac{\rho^2}{(1 + \frac{1}{4}\rho^2 B^2)^2}. \tag{18}$$

As $\Lambda = 1 + \frac{1}{4}\rho^2 B^2$ is real so $\Lambda^*\nabla\Lambda - \Lambda\nabla\Lambda^* = 0$, and from Eq. (5) $\omega = 0$, so $\omega' = 0$. Using the new functions f' and ω' in Eq. (4) the transformed line element is [8]

$$ds^2 = (1 + \frac{1}{4}B^2\rho^2)^2[-dt^2 + dz^2 + d\rho^2] + (1 + \frac{1}{4}B^2\rho^2)^{-2}\rho^2 d\phi^2, \tag{19}$$

with the electromagnetic potential

$$\Phi' = \frac{1}{2}\Lambda^{-1}B\rho^2 = \frac{1}{2}\frac{B\rho^2}{(1 + \frac{1}{4}\rho^2 B^2)}. \tag{20}$$

From the above equation the components of magnetic field are

$$H_z = \Lambda^{-2}B, \quad H_\rho = 0 = H_\phi. \tag{21}$$

This solution is same as Melvin's magnetic universe (1).

3 Schwarzschild black hole in Melvin universe

The Harrison transformation can be used to magnetize the Schwarzschild black hole. The metric of the Schwarzschild black hole is given by

$$ds^2 = -(1 - \frac{2M}{r})dt^2 + \frac{dr^2}{(1 - \frac{2M}{r})} + r^2 d\theta^2 + r^2\sin^2\theta d\phi^2, \tag{22}$$

or

$$ds^2 = -\frac{1}{r^2}(r^2 - 2Mr)dt^2 + \frac{r^2 dr^2}{(r^2 - 2Mr)} + r^2 d\theta^2 + r^2\sin^2\theta d\phi^2. \tag{23}$$

Comparing the above equation with Eq.(4) we have

$$f = -r^2 \sin^2\theta, \quad \omega = 0, \quad \rho = (r^2 - 2Mr)^{1/2}\sin\theta, \tag{24}$$

$$P = (r^2 \sin\theta)^{-1}, \quad d\xi = \frac{1}{\sqrt{2}}\left(\frac{dr}{(r^2-2Mr)^{1/2}} + id\theta\right). \tag{25}$$

The radial and angular components of electric and magnetic fields satisfy the equation

$$H_r + iE_r = P\frac{\partial \Phi}{\partial \theta}, \quad H_\theta + iE_\theta = -P(r^2 - 2Mr)^{1/2}\frac{\partial \Phi}{\partial r}. \tag{26}$$

If one defines the symbol

$$\nabla = (r^2 - 2Mr)^{1/2}\frac{\partial}{\partial r} + i\frac{\partial}{\partial \theta}, \tag{27}$$

the twist potential may be determined by

$$-\rho^{-1} f^2 \nabla\omega = i\nabla\varphi + \Phi^*\nabla\Phi - \Phi\nabla\Phi^*. \tag{28}$$

Since initially there is no electromagnetic field, also $\omega = 0$, so the complex gravitational, electromagnetic and twist potentials are given by

$$\varepsilon = f = -r^2\sin^2\theta, \quad \Phi = 0, \quad \varphi = 0, \tag{29}$$

while Eqs. (11)-(13) yield

$$\Lambda = 1 + B\Phi - \frac{1}{4}B^2\varepsilon = 1 + \frac{1}{4}B^2 r^2 \sin^2\theta, \tag{30}$$

$$\varepsilon' = \Lambda^{-1}\varepsilon = -(1 + \frac{1}{4}B^2 r^2\sin^2\theta)^{-1} r^2 \sin^2\theta, \tag{31}$$

$$\Phi' = \Lambda^{-1}(\Phi - \frac{1}{2}B\varepsilon) = \frac{1}{2}(1 + \frac{1}{4}B^2 r^2\sin^2\theta)^{-1} B r^2 \sin^2\theta. \tag{32}$$

The transformed fields f' and ω' from Eqs. (14) and (15) are

$$f' = |\Lambda|^{-2} f = -\frac{r^2\sin^2\theta}{(1 + \frac{1}{4}B^2 r^2\sin^2\theta)^2}, \quad \omega' = 0. \tag{33}$$

Using f' from ω' from the above equations and unmodified functions P and ρ from Eq. (4) we obtain the transformed line element [8]

$$ds^2 = |\Lambda|^2\left[-(1 - \frac{2M}{r})dt^2 + \frac{dr^2}{(1 - \frac{2M}{r})} + r^2 d\theta^2\right] + |\Lambda|^{-2} r^2 \sin^2\theta d\phi^2. \tag{34}$$

In this case the magnetic field components are given by

$$H_r = \Lambda^{-2} B\cos\theta, \tag{35}$$

$$H_\theta = -\Lambda^{-2} B(1 - \frac{2M}{r})^{1/2}\sin\theta. \tag{36}$$

Note that if $M = 0$ the above metric becomes Melvin's magnetic universe, while for $M \neq 0$ there is an event horizon at $r = 2M$ and the angular component of magnetic field vanishes at the event horizon. Further, the metric has singularity at $r = 0$, as in the case of Schwarzschild metric. If we take $B = 0$, this reduces to the Schwarzschild solution.

4 Reissner-Nordström black hole in Melvin universe

The application of the procedure to the Reissner-Nordström black hole is not so simple. In this case $\mathbf{E} \times \mathbf{H}$ serves as a source for twist potential, and the transformed metric is not static as in the case of the Schwarzschild black hole, but stationary. The spacetime of Reissner-Nordstr öm black hole is

$$ds^2 = -(1 - \frac{2M}{r} + \frac{q^2}{r^2})dt^2 + (1 - \frac{2M}{r} + \frac{q^2}{r^2})^{-1}dr^2 + r^2 d\theta^2 + r^2\sin^2\theta d\phi^2, \tag{37}$$

or, we can write

$$ds^2 = -\frac{1}{r^2}(r^2 - 2Mr + q^2)dt^2 + r^2(r^2 - 2Mr + q^2)^{-1}dr^2 + r^2 d\theta^2 + r^2\sin^2\theta d\phi^2. \tag{38}$$

Comparing Eq. (38) with Eq. (4) we note that

$$f = -r^2\sin^2\theta, \ \omega = 0, \ \rho = (r^2 - 2Mr + q^2)^{1/2}\sin\theta, \tag{39}$$

$$P = (r^2\sin\theta)^{-1}, \ d\xi = \frac{1}{\sqrt{2}}\left(\frac{dr}{(r^2 - 2Mr + q^2)^{1/2}} + id\theta\right). \tag{40}$$

The complex electromagnetic potential Φ, whose real and imaginary parts are electrostatic and magnetostatic potentials, respectively, may be evaluated by the equations

$$H_r + iE_r = P\frac{\partial\Phi}{\partial\theta}, \tag{41}$$

$$H_\theta + iE_\theta = -P(r^2 - 2Mr + q^2)^{1/2}\frac{\partial\Phi}{\partial r}. \tag{42}$$

Solving the above equation we have $\Phi = -\imath q\cos\theta$. If one defines the symbol

$$\nabla = (r^2 - 2Mr + q^2)^{1/2}\frac{\partial}{\partial r} + i\frac{\partial}{\partial\theta}, \tag{43}$$

the twist potential φ can be determined from

$$-\rho^{-1} f^2 \nabla\omega = i\nabla\varphi + \Phi^*\nabla\Phi - \Phi\nabla\Phi^*. \tag{44}$$

Since Φ is pure imaginary so $\Phi^*\nabla\Phi - \Phi\nabla\Phi^* = 0$, also $\omega = 0$, so the twist potential is also equal to zero i.e. $\varphi = 0$. The complex gravitational potential ε associated with gravity is given by

$$\varepsilon = f - |\Phi|^2 + i\varphi = -r^2\sin^2\theta - q^2\cos^2\theta, \tag{45}$$

while Eqs. (11) - (14) take the form

$$\Lambda = 1 + B\Phi - \frac{1}{4}B^2\varepsilon = 1 + \frac{1}{4}B^2(r^2\sin^2\theta + q^2\cos^2\theta) - iBq\cos\theta, \tag{46}$$

$$\varepsilon^{'} = \Lambda^{-1}\varepsilon$$
$$= -\left(\frac{r^2\sin^2\theta + q^2\cos^2\theta}{1+\frac{1}{4}B^2(r^2\sin^2\theta+q^2\cos^2\theta) - iBq\cos\theta}\right) \quad (47)$$
$$f^{'} = |\Lambda|^{-2} f$$
$$= -\frac{r^2\sin^2\theta}{(1+\frac{1}{4}B^2(r^2\sin^2\theta+q^2\cos^2\theta))^2 + (Bq\cos\theta)^2} \quad (48)$$

and $\omega^{'}$ can be evaluated by the equation

$$\nabla\omega^{'} = \rho f^{-1}(\Lambda^*\nabla\Lambda - \Lambda\nabla\Lambda^*). \quad (49)$$

Integrating Eq. (49) yields the following expression for $\omega^{'}$

$$\omega^{'} = -2Bqr^{-1} + B^3qr + \frac{1}{2}B^3q^3r^{-1} - \frac{1}{2}B^3qr^{-1} \times (r^2 - 2Mr + q^2)\sin^2\theta + const. \quad (50)$$

Consequently, the transformed metric takes the form [8]

$$ds^2 = |\Lambda|^2\,[-(1-\frac{2M}{r}+\frac{q^2}{r^2})dt^2 + (1-\frac{2M}{r}+\frac{q^2}{r^2})^{-1}dr^2 + r^2d\theta^2] + |\Lambda|^{-2}\,r^2\sin^2\theta(d\phi-\omega^{'}dt)^2, \quad (51)$$

where Λ and $\omega^{'}$ are given by Eqs. (46) and (50). The above metric is known as the Reissner-Nordström black hole in Melvin universe which is the charged generalization of Schwarzschild black hole in Melvin universe. If $q = 0$ then this metric reduces to the Schwarzschild black hole in Melvin universe, and if $B = 0$, then the above metric reduces to Reissner-Nordström black hole.

Finally, the components of the electric and magnetic fields may be evaluated from electromagnetic potential $\Phi^{'}$. The results are

$$H_r + iE_r = \Lambda^{-2}[i(\frac{q}{r^2})\{1-\frac{1}{4}B^2(r^2\sin^2\theta+q^2\cos^2\theta)\} + B(1-\frac{1}{2}iBq\cos\theta)(1-\frac{q^2}{r^2})\cos\theta], \quad (52)$$

$$H_\theta + iE_\theta = -B\,|\Lambda|^2\,(1-\frac{1}{2}iq^2\cos\theta) \times (1-\frac{2M}{r}+\frac{q^2}{r^2})^{1/2}\sin\theta. \quad (53)$$

5 Kerr-Newman black hole in Melvin universe

The spacetime describing magnetized Kerr-Newman black hole of mass M, angular momentum per unit mass a, carrying electric charge q and magnetic charge p, embedded in a Melvin's universe of magnetic field B is [12]

$$ds^2 = H[-fdt^2 + R^2(\frac{dr^2}{\Delta}+d\theta^2)] + \frac{\Sigma\sin^2\theta}{HR^2}(d\phi-\omega dt)^2, \quad (54)$$

where

$$R^2 = r^2 + a^2\cos^2\theta, \quad (55)$$
$$\Delta = (r^2+a^2) - 2Mr + q^2 + p^2, \quad (56)$$
$$\Sigma = (r^2+a^2)^2 - a^2\Delta\sin^2\theta, \quad (57)$$
$$f = \frac{R^2\Delta}{\Sigma}, \quad (58)$$
$$H = 1 + \frac{H_{(1)}B + H_{(2)}B^2 + H_{(3)}B^3 + H_{(4)}B^4}{R^2}, \quad (59)$$

with

$$H_{(1)} = 2aqr\sin^2\theta - 2p(r^2+a^2)\cos\theta,$$
$$H_{(2)} = \frac{1}{2}[(r^2+a^2)^2 - a^2\Delta\sin^2\theta]\sin^2\theta + \frac{3}{2}\overline{q}^2(a^2+r^2\cos^2\theta),$$
$$H_{(3)} = -\frac{qa\Delta}{2r}[r^2(3-\cos^2\theta)\cos^2\theta + a^2(1+\cos^2\theta)] - \frac{1}{2}p(r^4-a^4)\sin^2\theta\cos\theta + \frac{q\overline{q}^2a[(2r^2+a^2)\cos^2\theta+a^2]}{2r} - pa^2\Delta\sin^2\theta\cos\theta - \frac{1}{2}p\overline{q}^2(r^2+a^2)\cos^3\theta + \frac{aq(r^2+a^2)^2(1+\cos^2\theta)}{2r},$$
$$H_{(4)} = \frac{1}{16}(r^2+a^2)^2R^2\sin^4\theta + \frac{1}{4}M^2a^2[r^2(\cos^2\theta-3)^2\cos^2\theta + a^2(1+\cos^2\theta)^2] + \frac{1}{16}\overline{q}^4[r^2\cos^2\theta + a^2(1+\sin^2\theta)]\cos^2\theta + \frac{1}{4}Ma^2r(r^2+a^2)\sin^6\theta + \frac{1}{4}Ma^2\overline{q}^2r(\cos^2\theta-5)\sin^2\theta\cos^2\theta + \frac{1}{8}\overline{q}^2(r^2+a^2)(r^2+a^2+a^2\sin^2\theta)\sin^2\theta\cos^2\theta.$$

Here $\overline{q}^2 = q^2 + p^2$, and

$$\omega = \frac{1}{\Sigma}[(2Mr-\overline{q}^2)a+\omega_{(1)}B+\omega_{(2)}B^2+\omega_{(3)}B^3+\omega_{(4)}B^4], \quad (60)$$

with

$$\omega_{(1)} = -2qr(r^2+a^2) + 2ap\Delta\cos\theta,$$
$$\omega_{(2)} = -\frac{3}{2}a\overline{q}^2(r^2+a^2+\Delta\cos^2\theta),$$
$$\omega_{(3)} = 4qM^2a^2r + \frac{1}{2}ap\overline{q}^4\cos^3\theta + \frac{1}{2}qr(r^2+a^2)[r^2-a^2 +(r^2+3a^2)\cos^2\theta] + \frac{1}{2}ap(r^2+a^2)[3r^2+a^2-(r^2 -a^2)\cos^2\theta]\cos\theta - aM\overline{q}^2(2aq+pr\cos^3\theta) - apMr \times[2R^2+(r^2+a^2)\sin^2\theta]\cos\theta + \frac{1}{2}ap\overline{q}^2[3r^2+a^2$$

$$+2a^2\cos^2\theta]\cos\theta+\frac{1}{2}q\overline{q}^2r[(r^2+3a^2)\cos^2\theta-2a^2]$$
$$+qM[r^4-a^4+r^2(r^2+3a^2)\sin^2\theta],$$
$$\omega_{(4)}=\frac{1}{2}a^3M^3r(3+\cos^4\theta)-\frac{1}{8}a\overline{q}^4[r^2(2+\sin^2\theta)\cos^2\theta$$
$$+a^2(1+\cos^4\theta)]+\frac{1}{16}a\overline{q}^2(r^2+a^2)[r^2(1-6\cos^2\theta$$
$$+3\cos^4\theta)-a^2(a+\cos^4\theta)]-\frac{1}{4}a^3M^2\overline{q}^2(3+\cos^4\theta)$$
$$-\frac{1}{16}a\overline{q}^6\cos^4\theta+\frac{1}{4}aM^2[r^4(3-6\cos^2\theta+3\cos^4\theta)$$
$$+2a^2r^2(3\sin^2\theta-2\cos^4\theta)-a^4(1+\cos^4\theta)]$$
$$+\frac{1}{8}aM\overline{q}^4r\cos^4\theta+\frac{1}{8}aM\overline{q}^2r[2r^2(3-\cos^2\theta)$$
$$\times\cos^2\theta-a^2(1-3\cos^2\theta-2\cos^4\theta)]+\frac{1}{8}aMr$$
$$\times(r^2+a^2)[r^2(3+6\cos^2\theta-\cos^4\theta)$$
$$-a^2(1-6\cos^2\theta-3\cos^4\theta)].$$

The electromagnetic vector potential is

$$A=(\Phi_0-\omega\Phi_3)dt+\Phi_3d\phi, \tag{61}$$

where

$$\Phi_0=\frac{\Phi_0^{(0)}+\Phi_0^{(1)}B+\Phi_0^{(2)}B^2+\Phi_0^{(3)}B^3}{4\Sigma}, \tag{62}$$

with

$$\Phi_0^{(0)}=4[-qr(r^2+a^2)+ap\Delta\cos\theta,$$
$$\Phi_0^{(1)}=-6a\overline{q}^2(r^2+a^2+\Delta\cos^2\theta),$$
$$\Phi_0^{(2)}=-3q[(r+2M)a^4-(r^2+4Mr+\Delta\cos^2\theta)r^3$$
$$+a^2(2\overline{q}^2(r+2M)-6Mr^2-8M^2r-3r\Delta\cos^2\theta)]$$
$$+3p\Delta[3ar^2+a^3+a(a^2+\overline{q}^2-r^2)\cos^2\theta]\cos\theta,$$
$$\Phi_0^{(3)}=-\frac{1}{2}a[4a^4M^2+12a^2M^2\overline{q}^2+2a^2\overline{q}^4+2a^4Mr$$
$$-24a^2M^3r+4a^2M\overline{q}^2r-24a^2M^2r^2-4a^2Mr^3$$
$$-\overline{q}^2r^4-6Mr^5-6r\Delta\{2M(r^2+a^2)-\overline{q}^2r\}\cos^2\theta$$
$$+a^4\overline{q}^2-12M^2r^4+\Delta(\overline{q}^4-3\overline{q}^2r^2+2Mr^3$$
$$+a^2(4M^2+\overline{q}^2-6Mr))\cos^4\theta],$$

and

$$\Phi_3=\frac{\Phi_3^{(0)}+\Phi_3^{(1)}B+\Phi_3^{(2)}B^2+\Phi_3^{(3)}B^3}{R^2H}, \tag{63}$$

with

$$\Phi_3^{(0)}=aqr\sin^2\theta-p(r^2+a^2)\cos\theta,$$
$$\Phi_3^{(1)}=\frac{1}{2}[\Sigma\sin^2\theta+3\overline{q}^2(a^2+r^2\cos^2\theta)],$$
$$\Phi_3^{(2)}=\frac{3}{4}aqr(r^2+a^2)\sin^4\theta-\frac{3}{4}p(r^2+a^2)^2\sin^2\theta\cos\theta$$
$$+3a^2pMr\sin^2\theta\cos\theta+\frac{3}{2}aqm[r^2(3-\cos^2\theta)$$
$$\times\cos^2\theta+a^2(1+\cos^2\theta)]-\frac{3}{4}aq\overline{q}^2r\sin^2\theta\cos^2\theta$$
$$-\frac{3}{4}p\overline{q}^2[(r^2-a^2)\cos^2\theta+2a^2]\cos\theta,$$
$$\Phi_3^{(3)}=\frac{1}{4}\overline{q}^2(r^2+a^2)[r^2+a^2+a^2\sin^2\theta\cos^2\theta]-\frac{1}{2}a^2\overline{q}^2$$
$$\times Mr(5-\cos^2\theta)\sin^2\theta\cos^2\theta+\frac{1}{2}a^2M^2[r^2(3$$
$$-\cos^2\theta)^2\cos^2\theta+a^2(1+\cos^2\theta)^2]+\frac{1}{2}a^2Mr(r^2$$
$$+a^2)\sin^6\theta+\frac{1}{8}R^2(r^2+a^2)^2\sin^4\theta+\frac{1}{8}\overline{q}^4[r^2\cos^2\theta$$
$$+a^2(2-\cos^2\theta)^2]\cos^2\theta.$$

6 Conclusion

We have described Ernst's solution generating technique [8–10] which uses Harrison's transformations for magnetizing black holes. We have reviewed the earlier work in this direction on Schwarzschild, Reissner-Nordström and Kerr-Newman black holes. Note that if we take electric charge e and magnetic charge p equal to zero the metric for Kerr-Newman black hole in Melvin universe reduces to Kerr black hole in Melvin universe. Further if we take the rotation parameter a equal to zero the metric reduces to the magnetized Schwarzschild black hole. If we put the magnetic field $B=0$ all the metrics reduce to their unmagnetized versions. Other properties of these magnetized black holes and further work in this direction [13] will be reported elsewhere.

Acknowledgements KS would like to thank the organizers of ICRA for hospitality provided in Lahore. A research grant from the Higher Education Commission of Pakistan under its Project No. 20-2087 is gratefully acknowledged.

References

1. W. B. Bonner, *Proc. Phys. Soc.* **A 66** (1953) 145.
2. W. B. Bonner, *Proc. Phys. Soc.* **A 67** (1954) 225.
3. M.A. Melvin, *Phys. Lett.* **8** (1965) 65.
4. J. B. Griffiths, J. Podolsky, *Exact Space-Times in Einstein's General Relativity*, Cambridge University Press, Cambridge (2009).
5. M. A. Melvin, *Phys. Rev.* **B 139** (1965) 225.
6. K. S. Thorne, *Phys. Rev.* **B 139** (1965) 244.
7. B. K. Harrison, *J. Math. Phys.* **9** (1968) 1744.
8. F. J. Ernst, *J. Math. Phys.* **17** (1976) 54.
9. F. J. Ernst, W. J. Wild, *J. Math. Phys.* **17** (1976) 182.
10. F. J. Ernst, *J. Math. Phys* **17** (1976) 515.
11. M. Astorino, *Phys. Rev.* **D 87** (2013) 084029.
12. G. W. Gibbons, A. H. Mujtaba and C. N. Pope, *Class. Quant Grav.* **30** (2013) 125008.
13. M. Rizwan, *M.Phil. Thesis*, Quaid-i-Azam University, Islamabad (2015).

Proc. Int. Conf. Relativ. Astrophys.
Pages 188-195, (2015)

Direction of Holy Kaaba, Diameter of The Sun, Horizontal and Equatorial Coordinates of the Sun with the Help of Potable Homemade Device

Muhammad Usman Saleem[a,1]

[1]Institute of Geology. University of the Punjab, Quaid-e-Azam Campus, Lahore-54590, Pakistan.

Abstract This paper mainly describes how to make a potable homemade tool to calculate the Horizontal coordinates of Celestial bodies like sun. The sun altitude and azimuth are the functions of the earth motion around the sun. They are functionally varied throughout the year. The conversion of these coordinates to equatorial coordinates has also described. Direction of Holy Kaaba with the help of this tool has been calculated for the study area Lahore Pakistan. Mathematical techniques of Concurrent and Similarity has used to calculate the diameter of the sun. With the assumption of the sun is a spherical in shape the volume of the sun disk has been calculated. The complete description to make this tool is also the part of this paper.

1 Introduction

In ancient times gnomon *(vertical stick casting shadow)* was used as sun dial and other observations. With the passage of time it starts to use as tool to navigations. Still it is reliable instrument for the basic astronomical as well as geographical calculations.

2 Study Area

Lahore (74.27985278E, 31.4421667N) is the capital city of Punjab province, Pakistan. It is the second most populated city of Pakistan. An estimate in the 2014, it has population of 7,566,000.By geography it is flat area. The hottest month is June, when average highs temperature routinely exceeds 40 C. The monsoon season starts in late June and the wettest month is July, with heavy rainfalls. The coolest month is January with dense fog. Elevation of the Lahore from mean sea level is 208 to 213m. (See fig 1).

[a]e-mail: osman.geomatics@gmail.com

3 Objectives

The primary purpose of this research was to build an instrument which can help us in calculating position of the observer in the survivor conditions. This instrument can calculate Geographic coordinates as well as Horizontal and Equatorial Coordinates of the Sun. Able us to calculate the direction of Holy Kaaba, Apparent solar noon time, Time of Sun set and Sun rise. Using the Techniques of Al Buruni, it helps us to calculate radius of the earth (not discuss here) and through the techniques of similarity and enlargement it help us to calculate diameter of the celestial bodies like sun, moon.

4 Data Set Use

Solar azimuth and altitude angles have been calculated for the January 2, 2015. Time of observation was different for azimuth and altitude. Observations are taken from 11:30am to 16:00pm (UTC+5h). Through these data sets objectives of this research are achieve and for the validation, output has been compared with the US Navy Observatory Data and NOAA Earth System Research Laboratory Data.

5 Research Methods and Methodology

5.1 Direction of Holy Kaaba

S.Abdali (1997)[1] mentioned as the direction of Qibla for a person is, a ray coming out of his eye in that direction of the plane of the great circle passing through

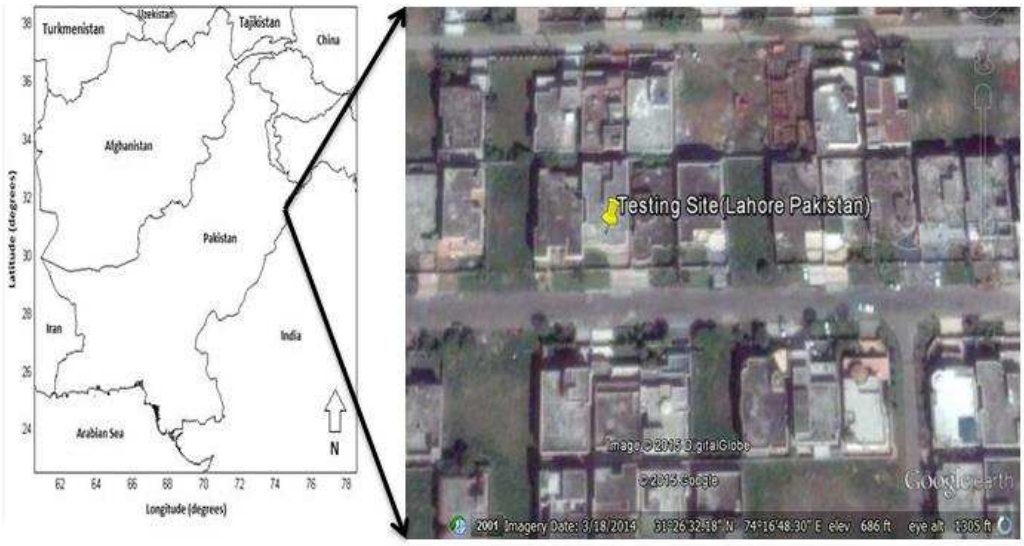

Fig.1. Geographic map of Pakistan with map of testing site(Lahore) at large scale .

the direction of his zenith and the point corresponding to (the zenith) of Mecca. The cube of Holy Kaaba has the central significance in the follower of world's second most religious Islam. This figure has the main direction for the five time prayers per day in Islam.

5.2 Direction of Holy Kaaba

It is not advisable to determine direction of Holy Kaaba using compass especially for orienting Mosque. The following method which uses the sun is more reliable. It has been observed for centuries and reported in many books by Muslims around the world that two times a year the sun comes overhead above Kaaba. This is observational fact for centuries, and is used to set the correct prayer direction in places far from Mecca by Muslims for last so many centuries. Those two dates and times are:
May 28 at 9:18UTC
July 16 at 9:27UTC

5.3 Basic Spherical Trigonometric Formula

Use the rule of spherical trigonometry (S.Abdali, 1997) [1]

$$\lambda = arc\tan\left[\frac{\text{sine}(\square\lambda)}{\text{cosine}(\phi_L)^*\text{tangent}(\phi_K) - \sin e(\phi_L)^* \cos ine(\square\lambda)}\right]. \quad (1)$$

To prove the formula we have to rely on Four Part formula: Cosine (inner side)*Cosine (inner angle) =Sine (inner angle)*Cot (other side)-Sine (inner angle)*cot (other angle). (See fig 2)

$$\cos(90^0 - \phi_L)^*\cos(\square\lambda) = \sin(90^0 - \phi_L)^*\cot(90^0 - \phi_K) - \sin(\square\lambda)^*\cot(\lambda)$$

$$\sin(\phi_L)^*\cos(\square\lambda) = \cos(\phi_L)^*\text{tangent}(\phi_K) - \sin(\square\lambda)^*\cot(\lambda)$$

Rearranging the terms

$$\sin(\square\lambda)^*\cot(\lambda) = \cos(\phi_L)^*\text{tangent}(\phi_K) - \sin(\phi_L)^*\cos(\square\lambda)$$

$$\therefore \cot(\lambda) = \frac{\text{cosine}(\phi_L)^*\text{tangent}(\phi_K) - \sin e(\phi_L)^* \cos ine(\square\lambda)}{\text{sine}(\square\lambda)}$$

$$\Rightarrow \lambda = \arctan\left[\frac{\sin(\square\lambda)}{\cos(\phi_L)^*\text{tangent}(\phi_K) - \sin e(\phi_L)^* \cos ine(\square\lambda)}\right]$$

Which is the prove of equation (1).

λ_L = Longtitude of Lahore (testing site)

λ_K = Longtitude of the Holy Kaaba

ϕ_L = Latitude of Lahore (testing site)

ϕ_K = Latitude of Holy Kaaba

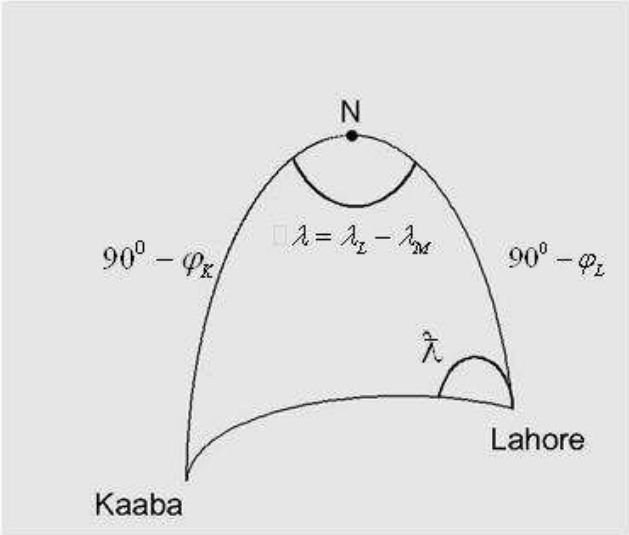

Fig.2. Spherical triangle can be solve to find the direction of Qibla.

Inner angle = $\square\lambda - \lambda_L - \lambda_M$ = 74.27985278-39.82624 =34.45361278

Inner side = $90^0 - \phi_L$ = 90-31.33066582=58.6693418

Other side = $90^0 - \phi_K$ = 90-21.42249444=68.5775.556

Other angel=λ= Direction of the Holy Kaaba from Lahore (testing site) with respect to magnetic north (fig.2). Putting the values from table 1 into equation (1)

$$= \text{arc tan}\left[\frac{0.5657387908}{-0.09358561315}\right]$$

Hence the direction of Holy Kaaba from the testing site (Lahore) is

λ = 180+(-80.60703027)=99.39296973 west of north

5.4 Horizontal Coordinates for Sun

The Pole star (Polaris) is lies very near to the direction of the North celestial pole. The north celestial pole is the angle above the horizon equal to your Latitude (ϕ).Halfway between the North celestial pole and south celestial pole is the Celestial equator. The number of the degrees that a celestial object is north or south of the celestial equator is its Declination (δ).A celestial object reaches its maximum elevation angle (Alt) above the horizon when it is on the celestial meridian. Hour angle is measured in the earth equatorial plane. It is the angle between the projection of the line draw from the location to the center of the earth and the projection of the line draw from the center of the Earth to the center of the Sun. At solar noon, the hour angle is 0^0 and the westward direction for the solar noon is taken positive (Kreith & West, 1996)[2].For the Azimuth and altitude angles of the sun, use an instrument having plane horizontal surface (remember wood changes its shapes with seasons).Cut this sheet of wood into a circle of convenient diameter. At the center of the sheet makes two small holes and adjust a meter rod and movable antenna (gnomon) in these holes. Put two bubble levelers on the wood sheet which will tell us about the level of the instrument in horizontal plane. To achieve the horizontal level, that instrument is mounted with net screws of around 3 inches length. Put a magnetic compass on the wooden plane so that we can calculate azimuth of the sun. Before a day or two the experiment, makes your quartz clocks as accurate as you can with your local time, also takes a look on the weather condition from the National Weather Forecasting Center. Select a site where the gnomon shadow throughout the day is easily measureable and obstacles are not present between the sun and gnomon. Use a plum line to ensure the verticality of the gnomon. Before one or two hours the experiment set your apparatus. Use millimeter to calculate the length of the shadow cast by gnomon and height of the gnomon. It is best to measure the length of the shadow, from 100 minutes before the time of the

Table 1 Inputs to spherical triangle.

	λ_L	ϕ_L	λ_M	ϕ_K
Calculated	74.27985E	31.33066583N	39.82624E	21.42249444N

Table 2 Errors in Qibla direction.

Uncertainty in magnetic declination	$\pm 0.29^0$
Error in Direction	0.1783641

local apparent noon until 100 minutes after the local apparent noon. To avoid the effect of Umbral and Penumbral shadow of the gnomon, use white paper to produce the contrast. Table 3 shows solar elevation angle with time of observations. Note that these time of observation is not uniform spaced due to clouds prominent. Sun altitude angle is the angle of the sun disk center to the plane of horizon of the observer.Altitude angle varies though out the year.Its depends on the earth position around the sun during its orbit.Solar altitude angle will be 0^0 at the time of sun rise and sun set. 90^0 solar altitudes indicate you are standing at the equator. Apparent solar noon occur when sun's altitude angle in the day is highest or when the shadow cast by the gnomon will be minimum. The only one time no shadow cast by the gnomon will be occur when the sun is directly overhead of the gnomon (solar declination varies though out the years from $+23.50^0$ N to -23.50^0 S). The sun rays coming parallel to the gnomon cast its shadow. By calculating the length or height of gnomon we can estimates the altitude angle (Alt) using trigonometry.(see equation 2)

$$Alt = \tan^{-}1\left(\frac{height}{lengthofshadow}\right) \tag{2}$$

In order to calculate the solar azimuth angles (angle from the earth geographic north pole to toward eastward) use the same apparatus with some magnetic compass. The value of the azimuth angle varying from 0^0 to 360^0. If the solar azimuth angle is 0^0 to 180^0, then sun is seting and if this angle is between 180^0 to 360^0 then sun is riseing. With the use of buble levelers ,we make the horizontal plane of the apparatus in level. Put a piece of the paper and fixed it on the wooden plane so that errors in taking reading will be minimize. When the gnomon cast shadow, takes a magnetic compass and draw the direction of the magnetic north pole on the paper. Now also draw a line which showing the direction of the shadow of the gnomon. Measure the angle you will get the solar azimuth angle. We know the earth magnetic poles are not aligne with the true geographic poles.There is some some angular shift between them.This angular shift is called *magnetic declination*. If this magnetic declination is 100^0W, then ture geographic north is 10^0 west of magnetic north pole. Compass gives the direction of magnetic North Pole. NOAA gives the magnetic field calculator based on these two magnetic field models, IGRF (1590-2019) & WMM (2014-2019)[3]. From the WMM (2014-2019) model, on the date 2 January 2015, we find the values of magnetic declinations which were 1.8033^0 E. It means that the magnetic North Pole on this date lies 1.8033^0 E from the true geographic north pole.(see table 4) It is advice to set the apparatus before the time of observations so that you can take correct solar azimuth angles.

5.5 Equatorial Coordinates of the Sun

As on the January 2, 2015 the sun has declination of southern hemisphere therefore using the spherical triangles

$$\delta = \phi - (90 - Alt) \tag{3}$$

Where ϕ = latitude of the observer and Alt = is the solar altitude angle at local apparent noon (when the show of the gnomon will be minimum). Taking the values from the table (1) and (3) and putting these values in equation (3).

$$\delta = 31.4421667 - (90 - 35.69) = -22.867833$$

Actual value taken from the US Navy data is = -22.89585 decimal degrees. Error in the declination is 0.01752^0. Negative singe indicate it is in southern hemisphere.

5.6 Hour Angle At Sun set And Sun rise

Hour angle is defined as the number of the hours between the solar noon and the time of interest multiplied by the constant 15^0 /hour. The value of this constant is known by the rate at which the sun appears to move

Table 3 Data for the Solar Elevation angles.

Time (UTC+5h)	Length of shadow (mm)	Height of gnomon (mm)	Solar elevation angel (decimal degree)
11:28am	281	199	35.305
11:45am	280	199	35.401
12:00am	277	199	35.69
12:24am	282	199	35.2
13:08am	307	199	32.95
11:47am	348	199	29.76
14:11am	361	199	28.86
14:40am	459	199	23.43
15:26am	679	200	16.41
15:59am	898	200	12.54

Table 4 Particular informantions and Magnetic decliantion taken from the NOAA NationaGeographic Data Center.[3]

Date	2-Jan-15
Latitude	31.4421667N
Longitude	74.279852778E
Elevation from the sea level	208.983m
Magnetic declination (+E/-W)	1.8283degree/year
Change/year	0.0587degree/year
Uncertainty	0.29degree
Model for magnetic field	WMM(2014-2019)

Table 5 Calculation of Solar Azimuth Angle with US Naval Observatory Data.

Time	Calculated Azimuth (with magnetic north)	Magnetic declination	Azimuth (with geographic north)	US Navy Data
(UTC+5h)	Azimuth(E of N)	(+E/-W)	True Azimuth(E of N)	Azimuth (E of N)
11:32am	162	1.8283	163.8283	170.2
11:48am	169	1.8283	170.8283	174.7
12:01pm	172	1.8283	173.8283	178.4
12:24pm	178	1.8283	179.8283	184.9
13:09pm	191	1.8283	192.8283	197.2
13:47pm	197	1.8283	198.8283	206.9
14:12pm	204.9	1.8283	206.7283	212.8
14:38pm	212	1.8283	213.8283	218.4
15:23pm	228	1.8283	229.8283	227.1
15:54pm	231.9	1.8283	233.7283	232.3

around the earth namely 360^0 in 24h or 15^0 per hour. In calculating the hour angle it is important to use solar time not clock time, Standard time rather than day light time must be used. Sun rise and sun set define as the time at which the solar altitude angle is zero.it means that center of the sun has passed below the local horizontal plane. Hourset is at the sunset hour angle which is calculated as

$$Hourset = \cos^{-1}[\tan(\delta)\tan(\phi)] \quad (4)$$

For the time of sunset occurs, Hourset, is expressed in degrees is divided by 15. The result is the number of hours after local solar noon at which the sun sets. To find the hour of sunrise, this same number of hours is subtracted from the noon (Kreider & Kreith, 1982)[4].

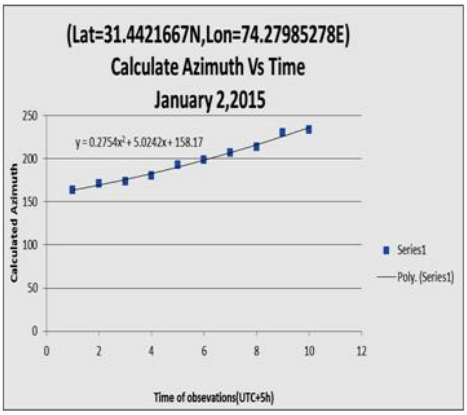

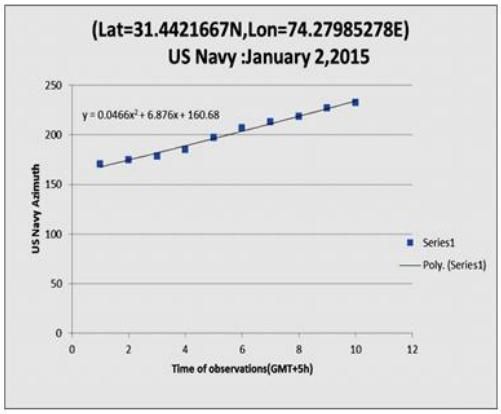

Fig.3. Calculated Solar Azimuth with time (UTC+5). Fig.4. US Naval Observatory Solar Azimuth with time.

Table 6 Calculations for Hour Angle (Calculated, US Navy observatory, NOAA Data)

(ϕ, δ)	Difference from US (Navy Data(decimal degrees)		Difference from NOAA data (decimal degrees)	
	Hourset	Hourrise	Hourset	Hourrise
Actual	0.180984	0.0356823	0.09765066	-0.047651
Calculated	0.191783	0.05234934	0.075115896	-0.06431736

Putting the values as we calculated from the gnomon Hourset= $\cos -1[-\tan(-22.867833)\tan(31.33067)] = 75.123261060$=5.008217404h. From table 3, we can see that apparent solar noon(when altitude angle is maximum) occur at 12pm. Therefore following the formula describe in literature (see equation (5))

$$Hourrise = LocalApparentNoon - Hourset \tag{5}$$

Hour rise $=12 - 5.008217404 - 699765066^0$

For the difference in values Hourrise and Hourset from the true values table 7 is given below

5.7 Size of the Sun

Aristarchus was the first to estimate the distance of the sun from the earth at the half moon using the trigonometrically techniques. He then calculates the radius of the sun on the lunar eclipses. We use the property of two similar side angle side (SAS).On the top of the gnomon, we have attached a shirt button which has diameter of 1.1cm (taken from the venial caliper). Hold this apparatus some good time in day when the sun disk is not very blurry. Use the solar glasses to avoid the harmful effect from the sun radiations. Now hold the apparatus such that disk of the button fully cover disk of the sun. Now calculate the distance from your eyes to the button (usually center of the button).There are two triangles will formed. One is formed between the eye of the observer and diameter of the button while other is formed by the diameter of the sun and observer eye. When the button fully covers the sun disk then the second triangle is just enlargement of the first triangle. Earth sun distance varies though out the year. As the earth orbit is elliptical, having mean eccentricity of 0.01671022. During the journey of the earth around sun, it comes close to the sun called Perihelion (distance=$147.09^*10^6 km$) and Aphelion when it is farthest from the sun ($152.10^*10^6 km$) (Williams, 2013)[5]. Use the simple formula to calculate the size of the sun.

$$\frac{\text{Diameter of the button}}{\text{Diameter of the sun}} = \frac{\text{Distance of button from eye}}{\text{Distance of the sun from eye}} \tag{6}$$

To calculate the volume of the sun disk, use the formula

$$V = \frac{4}{3} * 3.143^* r^3 \tag{7}$$

Volume of the sun disk is $2.356730366^*10^{18} km^3$

Table 7 Difference in the Hourset, Hourrise from the US Navy and NOAA Data.

	Coordinates Used	Hour Angles for Testing Site		US Navy Data (UTC+5h)		NOAA Data (UTC+5h)	
Observations	Latitude	Hourset	Hourrise	Hourset	Hourrise	Hourset	Hourrise
Calculated with gnomon	31.33067	5.008217	6.99765066	7.05	17.2	6.9333333	17.0833333

Table 8 Sun diameter calculations.

Earth sun distance(m)	diameter of the button(m)	distance from the eye(m)	Diameter of the sun(km)	Actual diameter (km)	Difference (km)
$1.47097^{*}10^{11}$	0.011	0.98	1651088.776	1391684	259404.8

6 Conclusion

Fewer errors in the each calculation suggest us; gnomon can be used in the basic calculations of Astromical, Astrophysical and remote navigations.

Acknowledgements The author would like to acknowledge the assistance of his student Muhammad Mohid for the acquisition of data for this research.

References

1. S.Abdali, K. (1997). The Correct Qibla.(p.,15) Retrieved 24 February 2015, from http://patriot.net/ abdali/ftp/qibla.pdf
2. Kreith, F., & West, R. (1996). Handbook of energy efficiency (p. 717). Boca Raton, Fla.: CRC.
3. Ngdc.noaa.gov,. (2015). Help: Magnetic Field Calculator ngdc.noaa.gov. Retrieved 30 January 2015, from http://www.ngdc.noaa.gov/geomag/help//igrfwmmHelp.html#interpretingresults
4. Kreider, J., & Kreith, F. (1982). Solar heating and cooling (p. 24). Washington: Hemisphere Pub. Corp.
5. Williams, D. (2013). Earth Fact Sheet. Nssdc.gsfc.nasa.gov. Retrieved 8 February 2015, from http://nssdc.gsfc.nasa.gov/planetary/factsheet/earthfact.html

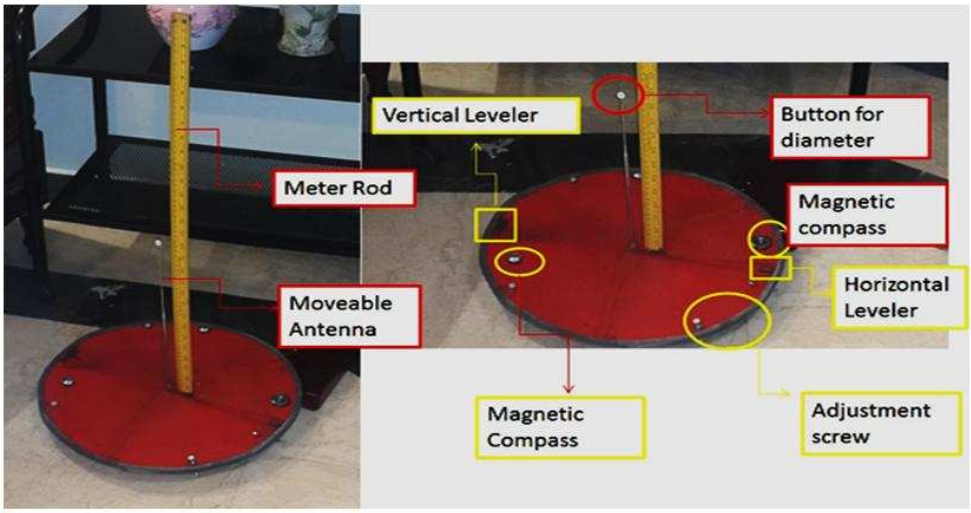

Fig.5. Gnomon used for research work.

Proc. Int. Conf. Relativ. Astrophys.
Pages 196-201, (2015)

Introduction to Teleparallel, and $f(T)$ Gravity and Cosmology

Emmanuel N. Saridakis [a,1,2]

[1]CASPER, Physics Department, Baylor University, Waco, TX 76798-7310, USA
[2]Instituto de Física, Pontificia Universidad de Católica de Valparaíso, Casilla 4950, Valparaíso, Chile

Abstract We investigate the cosmological implications of a class of modified gravity based on torsion. Starting from the Teleparallel Equivalent of General Relativity (TEGR), in which the gravitational field is described by the torsion tensor instead of the curvature one, we extend the Lagrangian to arbitrary functions of the torsion scalar. In such a scenario, one obtains an extra geometrodynamic sector, and thus the torsional modification can describe the dynamics of the universe without the need of introducing extra components by hand. We show that this scenario can describe inflationary and bouncing solutions, as well as late-time acceleration. The whole discussion can be enlightening as to what roads one could follow and what possibilities one has, in order to modify the gravitational interaction.

Keywords teleparallel gravity · $f(T)$ gravity · dark energy

1 Introduction

The standard paradigm of gravitational interactions is General Relativity. In this theory, and contrary to the rest of the fundamental interactions, gravity is described through geometry. In particular, the distribution of matter, namely its energy-momentum tensor, changes the curvature of space-time, and then the curved space-time determines the motion of matter in it [1]. However, the discovery of the accelerating nature of the universe expansion through various and different cosmological observations [2], clearly asks for a solution beyond the standard picture of physics. The simplest explanation is to consider a cosmological constant, however the data still allow the component that drives inflation to be of dynamical nature. This possibility led to a huge amount of research along two main directions.

The first is to maintain General Relativity but introduce the concept of "dark energy", that is introduce an exotic component alongside the standard-model particles [3]. The second possible direction is to modify the gravitational sector itself, that is to modify General Relativity in order to be able to trigger acceleration at large distances. In order to do so, one usually adds higher-order corrections to the Einstein-Hilbert action. The simplest model is to replace the Ricci scalar R by functions of it, giving rise to $f(R)$ gravity [4], which can lead to interesting cosmological behavior both in inflation [5] and late-time acceleration [6, 7]. Additionally, one could proceed to other higher-curvature corrections, such as the Gauss-Bonnet term G [8] the Lovelock terms [9], the Weyl term [10] etc (for reviews on modified gravity see [11]).

All the above gravitational modifications use as basis the standard formulation of gravity, i.e. General Relativity, that is they start from the curvature gravitational formulation. However, it is well known that Einstein had also constructed the so-called "Teleparallel Equivalent of General Relativity" (TEGR), in which the gravitational field is described by the torsion tensor instead of the curvature one [12, 13]. In particular, contracting the torsion tensor one constructs the torsion scalar T, and using it as a Lagrangian he obtains exactly the same equations with General Relativity. Hence, a question arises naturally, namely whether we can modify gravity starting from TEGR instead of GR. Indeed, the simplest such modification would be to extend T to $f(T)$ in the Lagrangian, obtaining $f(T)$ gravity [14]. The interesting feature is that although TEGR is completely equivalent with GR, their modifications $f(T)$ and $f(R)$ are different, corresponding to distinct classes of gravitational modifications. This

[a]e-mail: Emmanuel_Saridakis@baylor.edu

led to a huge amount of research on the cosmological applications of the theory [15–27].

In this talk we desire to explore some of the possibilities of $f(T)$ gravity, reviewing some of its basic properties and investigating some possible solutions relating to inflationary, bouncing and late-time accelerating solutions.

2 Teleparallel Equivalent of General Relativity

The dynamical variables in torsional formulation of gravity are the vielbein field $e_a(x^\mu)$, and the connection 1-form $\omega^a{}_b(x^\mu)$ which defines the parallel transportation.[1] In terms of coordinates, they can be expressed in components as $e_a = e_a{}^\mu \partial_\mu$ and $\omega^a{}_b = \omega^a{}_{b\mu} dx^\mu = \omega^a{}_{bc} e^c$. The dual vielbein is defined as $e^a = e^a{}_\mu dx^\mu$. One can express the commutation relations of the vielbein as

$$[e_a, e_b] = C^c{}_{ab} e_c \,, \tag{1}$$

where $C^c{}_{ab}$ are the structure coefficients functions given by $C^c{}_{ab} = e_a{}^\mu e_b{}^\nu (e^c{}_{\mu,\nu} - e^c{}_{\nu,\mu})$, and comma denotes differentiation.

One can now define the torsion tensor, expressed in tangent components as

$$T^a{}_{\mu\nu} = e^a{}_{\nu,\mu} - e^a{}_{\mu,\nu} + \omega^a{}_{b\mu} e^b{}_\nu - \omega^a{}_{b\nu} e^b{}_\mu \,. \tag{2}$$

Similarly, one can define the curvature tensor as

$$R^a{}_{b\mu\nu} = \omega^a{}_{b\nu,\mu} - \omega^a{}_{b\mu,\nu} + \omega^a{}_{c\mu}\omega^c{}_{b\nu} - \omega^a{}_{c\nu}\omega^c{}_{b\mu} \,. \tag{3}$$

Additionally, there is an independent object which is the metric tensor g. This allows us to make the vielbein orthonormal $g(e_a, e_b) = \eta_{ab}$, where $\eta_{ab} = \mathrm{diag}(-1, 1, ...1)$, and we have the relation

$$g_{\mu\nu} = \eta_{ab}\, e^a{}_\mu\, e^b{}_\nu. \tag{4}$$

As it is well known, amongst the infinite connection choices there is only one that gives vanishing torsion, namely the Christoffel or Levi-Civita one $\Gamma^a{}_b$, with $\Gamma_{abc} = \frac{1}{2}(C_{cab} - C_{bca} - C_{abc})$. For clarity, we denote the curvature tensor corresponding to the Levi-Civita connection as $\bar{R}^a{}_{bcd}$. The arbitrary connection ω_{abc} is then related to the Christoffel connection Γ_{abc} through the relation

$$\omega_{abc} = \Gamma_{abc} + \mathcal{K}_{abc} \,, \tag{5}$$

where $\mathcal{K}_{abc} = \frac{1}{2}(T_{cab} - T_{bca} - T_{abc}) = -\mathcal{K}_{bac}$ is the contorsion tensor.

As long as the vielbein $e^a{}_\mu$ and the connection $\omega^a{}_{b\mu}$ remain independent from each other, the Einstein-Hilbert Lagrangian density eR (with $R = e^{a\mu} e^{b\nu} R_{ab\mu\nu}$ the Ricci scalar and $e = \det(e^a{}_\mu) = \sqrt{|g|}$) is a function of $e^a{}_\mu, \omega^a{}_{b\mu}$, and thus a first-order formulation is needed. If we now calculate the Ricci scalar R corresponding to the arbitrary connection, and the Ricci scalar $\bar{R}$ corresponding to the Levi-Civita connection, they are found to be related through

$$R = \bar{R} + T - 2T_\nu{}^{\nu\mu}{}_{;\mu} \,. \tag{6}$$

where we have defined

$$T = \frac{1}{4} T^{\mu\nu\lambda} T_{\mu\nu\lambda} + \frac{1}{2} T^{\mu\nu\lambda} T_{\lambda\nu\mu} - T_\nu{}^{\nu\mu} T^\lambda{}_{\lambda\mu}. \tag{7}$$

We mention that the quadratic quantity T is diffeomorphism invariant since $T_{\mu\nu\lambda}$ is a tensor under coordinate transformations. Additionally, T is local Lorentz invariant, since T_{abc} is a Lorentz tensor.

One can now introduce the concept of teleparallelism by imposing the condition of vanishing Lorentz curvature

$$R^a{}_{bcd} = 0, \tag{8}$$

which holds in all frames. One way to realize this condition is by assuming the Weitzenböck connection $\tilde{\omega}^\lambda{}_{\mu\nu}$ which is defined in terms of the vielbein $e_a{}^\mu$ in all coordinate frames as

$$\tilde{\omega}^\lambda{}_{\mu\nu} = e_a{}^\lambda e^a{}_{\mu,\nu}. \tag{9}$$

The corresponding torsion tensor is related to the structure coefficients, the contorsion tensor or the Weitzenböck connection, through

$$\tilde{T}^\lambda{}_{\mu\nu} = \tilde{\omega}^\lambda{}_{\nu\mu} - \tilde{\omega}^\lambda{}_{\mu\nu} \,, \tag{10}$$

while (5) simplifies to $\Gamma_{abc} = -\tilde{\mathcal{K}}_{abc}$.

As we observe the Lagrangian density $e\bar{R}$ of General Relativity (that is the one calculated with the Levi-Civita connection) differs from the torsion density $-eT$ only by a total derivative. Therefore, one can immediately deduce that the General Relativity action

$$S_{EH} = \frac{1}{2\kappa_D^2} \int_M d^D x\, e\, \bar{R}, \tag{11}$$

is equivalent (up to boundary terms) to the action

$$S^{(1)}_{Tel}[e^a{}_\mu, \omega^a{}_{b\mu}] = -\frac{1}{2\kappa_D^2} \int_M d^D x\, e\, T \tag{12}$$

(κ_D^2 is the D-dimensional gravitational constant).

If the Weitzenböck connection (9) is adopted, then the teleparallel action (12) becomes a functional only of the vielbein, which is denoted for clarity as $S^{(1)}_{tel}[e^a{}_\mu]$ and has the same functional form as (12), but with tilde quantities. Varying $S^{(1)}_{tel}[e^a{}_\mu]$ with respect to the vielbein gives again the Einstein field equations. That is why the constructed theory in which one uses torsion

[1] Our notation is the following: Greek indices span the coordinates of the D-dimensional space-time, while Latin indices span the tangent space.

to describe the gravitational field, under the teleparallelism condition, was named by Einstein as Teleparallel Equivalent of General Relativity. In particular, variation of the action $S^{(1)}_{tel}+S_m$, with S_m the matter action, in terms of the vierbein $e^a{}_\mu$, gives rise to the equations of motion of the theory, namely

$$e^{-1}\partial_\mu(ee^\rho_A S_\rho{}^{\mu\nu}) - e^\lambda_A T^\rho{}_{\mu\lambda} S_\rho{}^{\nu\mu} + \frac{1}{4}e^\nu_A T = \frac{\kappa^2_D}{2} e^\rho_A \overset{\mathbf{em}}{T}{}_\rho{}^\nu, \tag{13}$$

where $S_\rho{}^{\mu\nu} \equiv \frac{1}{2}\Big(K^{\mu\nu}{}_\rho + \delta^\mu_\rho\, T^{\alpha\nu}{}_\alpha - \delta^\nu_\rho\, T^{\alpha\mu}{}_\alpha\Big)$, and with $\overset{\mathbf{em}}{T}{}_\rho{}^\nu$ the matter energy-momentum tensor. As we observe, the above equations indeed coincide with those of General Relativity.

3 $f(T)$ gravity and cosmology

Inspired by the $f(R)$ extension of GR, in [14] the author replaced T by $T+f(T)$ in the action of TEGR, namely

$$S = \frac{1}{2\kappa^2_D}\int d^D x e\,[T + f(T)]\,. \tag{14}$$

Hence, variation of $S+S_m$ gives the equations of motion

$$e^{-1}\partial_\mu(ee^\rho_A S_\rho{}^{\mu\nu})(1+f_T) - e^\lambda_A T^\rho{}_{\mu\lambda} S_\rho{}^{\nu\mu}(1+f_T)$$
$$+e^\rho_A S_\rho{}^{\mu\nu}\partial_\mu(T) f_{TT} + \frac{1}{4}e^\nu_A\,[T+f(T)] = \frac{\kappa^2_D}{2} e^\rho_A \overset{\mathbf{em}}{T}{}_\rho{}^\nu, \tag{15}$$

where f_T and f_{TT} denote the first and second derivatives of the function $f(T)$ with respect to T, respectively.

In order to apply the above theory to a cosmological framework, we first restrict to four dimensions, with $\kappa^2 = 8\pi G$ the four-dimensional Newton's constant. Additionally, we consider a spatially flat Friedmann-Robertson-Walker (FRW) geometry of the form

$$ds^2 = -dt^2 + a^2(t)\delta_{\hat{i}\hat{j}} dx^{\hat{i}} dx^{\hat{j}}\,, \tag{16}$$

where $a(t)$ is the scale factor (the hat indices run in the three spatial coordinates). This metric arises from the diagonal vierbein

$$e^a{}_\mu = \mathrm{diag}(1, a(t), a(t), a(t)) \tag{17}$$

through (4), while the dual vierbein is

$$e_a{}^\mu = \mathrm{diag}(1, a^{-1}(t), a^{-1}(t), a^{-1}(t)), \tag{18}$$

and its determinant $e = a(t)^3$.

Inserting the above vierbein ansantz into (15) we obtain the Friedmann equations of $f(T)$ cosmology, namely

$$6H^2 + f - 12H^2(1+f_T) = 2\kappa^2\rho_m, \tag{19}$$

$$6H^2 + f - 4(\dot{H}+3H^2)(1+f_T) - 48 f_{TT} H^2 \dot{H} = -2\kappa^2 p_m\,, \tag{20}$$

where $H = \frac{\dot{a}}{a}$ is the Hubble parameter and dots denote differentiation with respect to t. Additionally, note that inserting the vierbein (17) into (7) we find

$$T = 6\frac{\dot{a}^2}{a^2} = 6H^2, \tag{21}$$

which is a very useful relation connecting T and H^2.

The Friedmann equations (19), (20) can be rewritten in the usual form

$$H^2 = \frac{\kappa^2}{3}(\rho + \rho_{DE}) \tag{22}$$

$$\dot{H} = -\frac{\kappa^2}{2}(\rho + p + \rho_{DE} + p_{DE}), \tag{23}$$

that is the torsion gives rise to an effective dark energy sector with energy density and pressure given by

$$\rho_{DE} = -\frac{1}{2\kappa^2}(f - 12H^2 f_T) \tag{24}$$

$$p_{DE} = \frac{1}{2\kappa^2}\Big[f - 4(\dot{H}+3H^2)f_T - 48 f_{TT} H^2 \dot{H}\Big]\,. \tag{25}$$

Since the standard matter is conserved independently, i.e. $\dot{\rho}_m + 3H(\rho_m + p_m) = 0$, we obtain from (24), (25) that the effective dark energy density and pressure also satisfy the usual evolution equation $\dot{\rho}_{DE} + 3H(\rho_{DE} + p_{DE}) = 0$. Finally, we can define the dark energy equation-of-state parameter as $w_{DE} = p_{DE}/\rho_{DE}$.

4 Inflation and dark energy

As we saw, in $f(T)$ gravity the gravitational field is described through torsion. Hence, in the context of $f(T)$ cosmology, one can describe the dynamics of the expansion through the effects of torsion, obtaining a geometrodynamic effective dark energy sector. Indeed, torsional gravity can describe very efficiently the inflationary stage and of course the late-time universe acceleration.

4.1 Inflation

Let us first describe the inflationary regime. We consider a quadratic $f(T)$ ansantz of the form $f(T) = T^2$, and hence we consider the total action to be

$$S_{tot} = \frac{1}{2\kappa^2}\int d^4x\, e\,\left[T + \alpha T^2\right]. \tag{26}$$

Note that since we focus on inflation realization, we neglect the matter sector. In order to investigate the effects on the universe dynamics of the above scenario, we numerically evolve the system of cosmological equations and in Fig. 1 we present the evolution of the scale factor as a function of time. One can clearly observe the exponential expansion. Hence inflation can be easily realized in the context of $f(T)$ gravity.

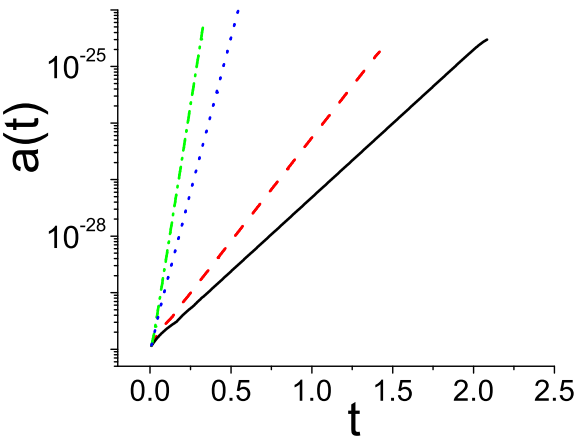

Fig. 1 Four inflationary solutions for the ansatz $T + \alpha T^2$, corresponding to a) $\alpha = -20$ (black-solid), b) $\alpha = -8$ (red-dashed), c) $\alpha = 2$ (blue-dotted), d) $\alpha = 2.8$ (green-dashed-dotted). All parameters are in units where $\kappa^2 = 1$.

4.2 Bounce

Although inflation is considered to be a crucial part of the cosmological history of the universe, it still faces the problem of the initial singularity. A potential solution to this problem may be provided by non-singular bouncing cosmologies [28]. Such scenarios have been constructed through various approaches to modified gravity, such as gravitational actions with higher order corrections [29–34], braneworld scenarios [35,36], non-relativistic gravity [37,38], nonlinear massive gravity [39], or in the frame of loop quantum cosmology [40]. Hence it would be interesting to see whether $f(T)$ cosmology can lead to bouncing behavior.

We start with a bouncing scale factor of the form [41]

$$a(t) = a_B \left(1 + \frac{3}{2}\sigma t^2\right)^{1/3}, \tag{27}$$

where a_B is the scale factor at the bouncing point, and σ is a positive parameter which describes how fast the bounce takes place. Such an ansatz presents the bouncing behavior, corresponding to matter-dominated contraction and expansion, and additionally it exhibits the advantage of allowing for semi-analytic solutions. In such a scenario t varies between $-\infty$ and $+\infty$, with $t = 0$ the bounce point. Finally, in the following we normalize the bounce scale factor a_B to unity.

Straightforwardly we find

$$H(t) = \frac{\sigma t}{(1 + 3\sigma t^2/2)}\ , \quad T(t) = \frac{6\sigma^2 t^2}{\left(1 + \frac{3}{2}\sigma t^2\right)^2}.$$

Therefore, provided $-\sqrt{\frac{2}{3\sigma}} \leqslant t \leqslant \sqrt{\frac{2}{3\sigma}}$, the inversion of this expression gives the $t(T)$ relation as

$$t(T) = \pm\left(-\frac{4}{3T} - \frac{2}{3\sigma} + \frac{4\sqrt{T\sigma^3 + \sigma^4}}{3T\sigma^2}\right)^{1/2}, \tag{28}$$

where we have kept the solution pair that gives the correct ($t = 0$ at $T = 0$) behavior. Notice that when $t > \sqrt{\frac{2}{3\sigma}}$ and $t < -\sqrt{\frac{2}{3\sigma}}$ we have assumed the usual Einstein gravity or the TEGR to be the prevailing framework, thus negating the need to pursue an $f(T)$ action in that region. Furthermore, we assume the matter content of the universe to be dust, namely $w_m \approx 0$. When inserted in the evolution-equation, this leads to the usual dust-evolution $\rho_m = \rho_{mB} a_B^3/a^3$, with ρ_{mB} its value at the bouncing point.

Inserting the above expressions into the Friedmann equations, we obtain a differential equation for $f(t)$, which can be easily solved analytically as

$$f(t) = \frac{4\kappa^2 t}{(2 + 3\sigma t^2)} \times \left[\frac{\rho_{mB}}{t} + \frac{6t\sigma^2}{\kappa^2\,(2 + 3t^2\sigma)} + \sqrt{6\sigma}\rho_{mB}\ \mathrm{ArcTan}\left(\sqrt{\frac{3\sigma}{2}}t\right)\right]. \tag{29}$$

Hence inserting (28) into (29) we finally obtain the $f(T)$ form that can produce the bouncing solution (27).

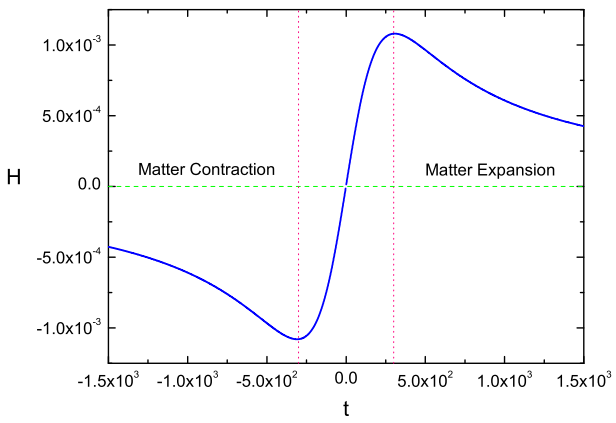

Fig. 2 Evolution of the Hubble parameter H as a function of t in the $f(T)$ scenario at hand, for $\sigma = 7 \times 10^{-6}$ and $\rho_{mB} = 1.41 \times 10^{-5}$, in units where $\kappa^2 = 1$.

In Fig. 2 we depict the evolution of the Hubble parameter for the scenario at hand. Clearly, one can observe the matter bounce realization in $f(T)$ gravity.

4.3 Dark Energy

Let us now describe dark energy, through the modified torsional geometry of $f(T)$ gravity. We consider an exponential $f(T)$ ansatz, and thus the total action takes the form [14]

$$S_{tot} = \frac{1}{2\kappa^2}\int d^4x\, e\, \left[T + \alpha T_0(1 - e^{-p\sqrt{T/T_0}})\right] + S_m, \tag{30}$$

with α and p the two model parameters. At $p \to +\infty$ this model reduces to ΛCDM cosmology, since as we can see $\lim_{p\to+\infty}[T + f(T)] = T - 2\Lambda$, with $\Lambda = -\alpha T_0/2$. Note that since we now focus on the late-time evolution, we consider also the matter sector S_m.

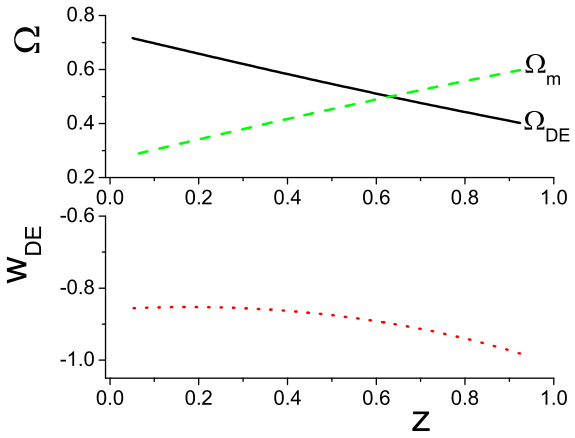

Fig. 3 Upper graph: The evolution of the dark energy density parameter Ω_{DE} (black-solid) and the matter density parameter Ω_m (green-dashed), as a function of the redshift z, for the exponential ansatz $T+\alpha T_0(1-e^{-p\sqrt{T/T_0}})$, with $\alpha = 0.82$ and $p = 2$. Lower graph: The evolution of the corresponding dark energy equation-of-state parameter w_{DE}. All parameters are in units where the present Hubble parameter is 1, and we have set the present values of the dark matter and dark energy density parameters to be $\Omega_{m0} \approx 0.3$ and $\Omega_{DE0} \approx 0.7$ respectively.

In the upper graph graph of Fig. 3 we depict the evolution of the matter and effective dark energy density parameters, while in the lower graph we show the corresponding behavior of the dark energy equation-of-state parameter, for a specific choice of the model parameters. As independent variable we use the redshift $z = a_0/a - 1$, with a_0 the present value of the scale factor. As we observe, the $f(T)$ scenario at hand can describe the thermal history of the universe, as well as the late-time acceleration, in agreement with the observed behavior.

5 Conclusions

In the present work we investigated the cosmological implications of a class of modified gravity based on torsion. In particular, starting from the Teleparallel Equivalent of General Relativity (TEGR), in which instead of using the torsionless Levi-Civita connection one uses the curvatureless Weitzenböck one, and thus the gravitational field is described by the torsion tensor instead of the curvature one, we extended the Lagrangian to arbitrary functions of the torsion scalar $f(T)$. In such a scenario, one obtains an extra geometrodynamic sector, and thus the torsional modification can describe the dynamics of the universe without the need of introducing a dark energy sector by hand.

As we saw, the scenario of $f(T)$ gravity can describe the inflationary stage of the universe, that is it can give rise to de Sitter solutions. Additionally, $f(T)$ cosmology can describe the late-time acceleration of the universe very efficiently, with the equation-of-state parameter of dark energy acquiring a dynamical nature due to torsion. In summary, the rich behavior of the above scenario of $f(T)$ gravity makes it a promising cosmological scenario. More importantly, the whole discussion can be enlightening as to what roads one could follow and what possibilities one has, in order to modify the gravitational interaction.

References

1. C. W. Misner, K. S. Throne and J. A. Wheeler, *Gravitation*, W. H. Freeman and Company, New York (1973).
2. A. G. Riess *et al.* [Supernova Search Team Collaboration], *Observational evidence from supernovae for an accelerating universe and a cosmological constant*, Astron. J. **116**, 1009 (1998).
3. E. J. Copeland, M. Sami and S. Tsujikawa, *Dynamics of dark energy*, Int. J. Mod. Phys. D **15**, 1753 (2006).
4. A. De Felice and S. Tsujikawa, *f(R) theories*, Living Rev. Rel. **13**, 3 (2010).
5. A. A. Starobinsky, *A New Type of Isotropic Cosmological Models Without Singularity*, Phys. Lett. B **91**, 99 (1980).
6. S. Capozziello, V. F. Cardone and A. Troisi, *Reconciling dark energy models with f(R) theories*, Phys. Rev. D **71**, 043503 (2005).
7. S. Nojiri and S. D. Odintsov, *Modified f(R) gravity consistent with realistic cosmology: From matter dominated epoch to dark energy universe*, Phys. Rev. D **74**, 086005 (2006).
8. J. T. Wheeler, *Symmetric Solutions to the Gauss-Bonnet Extended Einstein Equations*, Nucl. Phys. B **268**, 737 (1986).
9. D. Lovelock, *The Einstein tensor and its generalizations*, J. Math. Phys. **12**, 498 (1971).
10. P. D. Mannheim and D. Kazanas, *Exact Vacuum Solution to Conformal Weyl Gravity and Galactic Rotation Curves*, Astrophys. J. **342**, 635 (1989).
11. S. Capozziello and M. De Laurentis, *Extended Theories of Gravity*, Phys. Rept. **509**, 167 (2011).

12. A. Unzicker and T. Case, *Translation of Einstein's attempt of a unified field theory with teleparallelism*, [physics/0503046].
13. R. Aldrovandi and J. G. Pereira, *Teleparallel Gravity: An Introduction*, Springer, Dordrecht (2013).
14. E. V. Linder, *Einstein's Other Gravity and the Acceleration of the Universe*, Phys. Rev. D **81**, 127301 (2010).
15. S. H. Chen, J. B. Dent, S. Dutta and E. N. Saridakis, *Cosmological perturbations in f(T) gravity*, Phys. Rev. D **83**, 023508 (2011).
16. J. B. Dent, S. Dutta, E. N. Saridakis, *f(T) gravity mimicking dynamical dark energy. Background and perturbation analysis*, JCAP **1101**, 009 (2011).
17. P. Wu, H. W. Yu, *Observational constraints on $f(T)$ theory*, Phys. Lett. **B693**, 415 (2010).
18. R. Zheng and Q. G. Huang, *Growth factor in f(T) gravity*, JCAP **1103**, 002 (2011).
19. K. Bamba, C. Q. Geng, C. C. Lee and L. W. Luo, *Equation of state for dark energy in $f(T)$ gravity*, JCAP **1101**, 021 (2011).
20. M. Sharif, S. Rani, *F(T) Models within Bianchi Type I Universe*, Mod. Phys. Lett. **A26**, 1657 (2011).
21. S. Capozziello, V. F. Cardone, H. Farajollahi and A. Ravanpak, *Cosmography in f(T)-gravity*, Phys. Rev. D **84**, 043527 (2011).
22. L. Iorio and E. N. Saridakis, *Solar system constraints on f(T) gravity*, Mon.Not.Roy.Astron.Soc. 427 (2012) 1555.
23. S. Capozziello, P. A. Gonzalez, E. N. Saridakis and Y. Vasquez, *Exact charged black-hole solutions in D-dimensional f(T) gravity: torsion vs curvature analysis*, JHEP **1302** (2013) 039.
24. S. Nesseris, S. Basilakos, E. N. Saridakis and L. Perivolaropoulos, *Viable f(T) models are practically indistinguishable from LCDM*, Phys. Rev. D **88**, 103010 (2013).
25. M. Sharif and S. Azeem, *Cosmological Evolution for Dark Energy Models in f(T) Gravity*, Astrophys. Space Sci. **342**, 521 (2012).
26. S. Capozziello, O. Luongo and E. N. Saridakis, *Transition redshift in $f(T)$ cosmology and observational constraints*, arXiv:1503.02832 [gr-qc].
27. M. Sharif and S. Jabbar, *Phase Space Analysis and Anisotropic Universe Model in f(T) Gravity*, Commun. Theor. Phys. **63**, no. 2, 168 (2015).
28. V. F. Mukhanov and R. H. Brandenberger, *A Nonsingular universe*, Phys. Rev. Lett. **68**, 1969 (1992).
29. R. Brustein and R. Madden, *A model of graceful exit in string cosmology*, Phys. Rev. D **57**, 712 (1998).
30. T. Biswas, A. Mazumdar and W. Siegel, *Bouncing universes in string-inspired gravity*, JCAP **0603**, 009 (2006).
31. T. Biswas, R. Brandenberger, A. Mazumdar and W. Siegel, *Non-perturbative gravity, Hagedorn bounce and CMB*, JCAP **0712**, 011 (2007).
32. Y. F. Cai and E. N. Saridakis, *Cyclic cosmology from Lagrange-multiplier modified gravity*, Class. Quant. Grav. **28** (2011) 035010.
33. Y. F. Cai and E. N. Saridakis, *Non-singular Cyclic Cosmology without Phantom Menace*, J. Cosmol. **17**, 7238 (2011).
34. Y. F. Cai, J. Quintin, E. N. Saridakis and E. Wilson-Ewing, *Nonsingular bouncing cosmologies in light of BICEP2*, JCAP **1407**, 033 (2014).
35. Y. Shtanov and V. Sahni, *Bouncing braneworlds*, Phys. Lett. B **557**, 1 (2003).
36. E. N. Saridakis, *Cyclic Universes from General Collisionless Braneworld Models*, Nucl. Phys. B **808**, 224 (2009).
37. R. Brandenberger, *Matter Bounce in Horava-Lifshitz Cosmology*, Phys. Rev. D **80**, 043516 (2009).
38. Y. F. Cai and E. N. Saridakis, *Non-singular cosmology in a model of non-relativistic gravity*, JCAP **0910**, 020 (2009).
39. Y. F. Cai, C. Gao and E. N. Saridakis, *Bounce and cyclic cosmology in extended nonlinear massive gravity*, JCAP **1210**, 048 (2012).
40. M. Bojowald, *Absence of singularity in loop quantum cosmology*, Phys. Rev. Lett. **86**, 5227 (2001).
41. Y. -F. Cai, S. -H. Chen, J. B. Dent, S. Dutta, E. N. Saridakis, *Matter Bounce Cosmology with the f(T) Gravity*, Class. Quant. Grav. **28**, 2150011 (2011).

Int. Conf. Relativ. Astrophys.
Pages 202-207, (2015)

Dynamical Instability of Relativistic Fluids in $f(R)$ Gravity

M. Sharif[a,1] **and Z. Yousaf** [b,1]

[1]Department of Mathematics, University of the Punjab, Quaid-e-Azam Campus, Lahore-54590, Pakistan.

Abstract In this paper, we discuss the role of $f(R)$ model on dynamical instability of self-gravitating system. For this purpose, we consider such a system a system which begins collapse under some constraints. We evaluate dynamical equations and consider perturbation scheme which linearize field equations and help to construct collapse equation to study the role of stiffness parameter.

Keywords: $f(R)$ gravity; Instability; Electromagnetic field.
PACS: 04.50.Kd; 04.25.Nx.

1 Introduction

Gravitational collapse and dark energy (DE) are considered to be the most fundamental and fascinating issues of gravitational physics and cosmology. The gravitational repulsion in the universe causes the accelerating expansion. Astronomical data obtained from high redshift type Supernova Ia experiments as well as the cosmic microwave background radiation show that the universe is expanding as well as accelerating [1]. General Relativity (GR), despite of many favorable outcomes in the astronomical study, unable to describe the expanding behavior of the universe. Consequently, many alternative mechanisms are introduced out of them alternative theories of gravity, for example, scalar tensor theory, Brans-Dick theory, $f(T)$ theory, Gauss-Bonnet theory and $f(R)$ theory, have been suggested to handle these issues. The theory of $f(R)$ gravity [2] has gained a lot of interest due to its possible explanation of DE in a simplest manner.

[a]e-mail: msharif.math@pu.edu.pk
[b]e-mail: zeeshan.math@pu.edu.pk

Gravitational collapse is basically a process in which a massive body falls inward due to its own gravity. Stable celestial objects turn out to unstable objects when they suffer gravitational collapse. The most energetic explosions from the self-gravitating fluid distributions occur frequently in the universe. The analysis of stellar stability against fluctuations plays a significant role to study its existence. It is remarkable that different instability ranges of the astronomical bodies lead to different patterns of the evolution and structure formation. The stability of such systems can be discussed through dynamical equations. Misner and Sharp [3] presented dynamical equations of self-gravitating sphere of ideal fluid which are used to explain relativistic gravitational collapse.

Herrera and Santos [4] extended this work for dissipation case including both streaming out and diffusion approximations. By coupling the dynamical and transport equations, they showed that the effective inertial mass density of fluid decreases by a factor which depends on dissipative variables. Di Prisco *et al.* [5] generalized it by considering anisotropic fluid undergoing dissipation in the form of shear viscosity as well as the electromagnetic field. Sharif and Bhatti [6] found that the increase of gravitational mass through coupled dynamical transport equations causes rapid collapse in the presence of electromagnetic field.

It is argued that the range of dynamical instability is discoursed with the aid of an adiabatic index Γ. Chandrasekhar [7] investigated the stability of isotropic relativistic spherical body. Later, it was found that various physical variables like shearing viscosity, dissipation, radiation, anisotropy, etc affect the dynamical instability of the relativistic stars. Herrera *et al.* [8] examined the instability range for non-adiabatic spherical system with locally isotropic fluid dissipating in the form of heat flow at both Newtonian (N) and post

Newtonian (pN) regimes. Chan *et al.* [9] explored the results of anisotropic and shearing viscous collapsing relativistic fluids at both N and pN eras. Sharif and his collbaorators [10], [11] described subsequent evolution of compact relativistic matter distributions under various kinematical variables in GR as well as modified theories of gravity.

Recent literature demonstrates some interesting consequences through the inclusion of an electromagnetic field to discuss stability and gravitational collapse. Ghezzi [12] discussed the stabiliy, relativistic structure as well as gravitational collapse of charged neutron star and showed that stars undergo a direct collapse in unstable state to form a BH. Di Prisco *et al.* [13] studied gravitational collapse of the non-rotating anisotropic cylindrical fluid distribution under certain conditions. Joshi and Malafarina [14] investigated the stability of Oppenheimer, Snyder and Datt BHs under small tangential pressure and found that this BH is unstable inside the collapsing cloud.

In this paper, we discuss dynamical instability of spherically symmetric non-viscous and adiabatic collapsing body filled with isotropic charged fluid with Carrol-Duvvuri-Trodden-Turner (CDTT) $f(R)$ model. The paper is organized as follows. In section **2**, we formulate the field equations and present a viable extended $f(R)$ model. Section **3** provides dynamical equations and also the collapse equation through perturbation scheme. In section **4**, we discuss instability ranges of the fluid configuration along with their asymptotic behavior at N and pN regimes. Finally, we summarize and conclude the results.

2 Matter Configuration and CDTT $f(R)$ Model

The $f(R)$ generalization of Einstein-Hilbert action with Maxwell source takes the form

$$S_{f(R)+M}=\frac{1}{2}\int d^4x\sqrt{-g}\left(\frac{f(R)}{\kappa}-\frac{\mathcal{F}}{2\pi}\right),$$

where $f(R)$ is an arbitrary function of scalar curvature, $\mathcal{F}=\frac{1}{4}F_{\mu\nu}F^{\mu\nu}$ is the Maxwell invariant and κ is the coupling constant. The metric $f(R)$ field equations, by keeping the first variation zero, are obtained as

$$f_R R_{\alpha\beta}-\frac{1}{2}fg_{\alpha\beta}-\nabla_\alpha\nabla_\beta f_R+g_{\alpha\beta}\Box f_R=\kappa(T_{\alpha\beta}+E_{\alpha\beta}), \tag{1}$$

where ∇_α is the covariant derivative, $f_R=\frac{df}{dR}$ and $\Box=\nabla^\alpha\nabla_\alpha$. We can write in the configuration of the field equations of GR as

$$G_{\alpha\beta}=\frac{\kappa}{f_R}(X_{\alpha\beta}), \tag{2}$$

where $X_{\alpha\beta}=T_{\alpha\beta}+\overset{(D)}{T}_{\alpha\beta}+E_{\alpha\beta}$ with

$$\overset{(D)}{T}_{\alpha\beta}=\frac{1}{\kappa}\left\{\frac{f-Rf_R}{2}g_{\alpha\beta}+\nabla_\alpha\nabla_\beta f_R-\Box f_R g_{\alpha\beta}\right\},$$

as the effective stress energy tensor. The $f(R)$ gravity may be associated to explain the nature of DE and expanding behavior of the universe in the gravitational phenomenon.

We take a timelike $3D$ spherical boundary surface that demarcates the $4D$ line elements into two regions, i.e., interior and exterior. The line element of the interior region is [15]

$$ds_-^2=A^2(t,r)dt^2-B^2(t,r)dr^2-C^2(t,r)(d\theta^2+\sin^2\theta d\phi^2), \tag{3}$$

while for the exterior region, we take

$$ds_+^2=\left(1-\frac{2M}{r}+\frac{Q^2}{r^2}\right)d\nu^2+2d\nu dr-r^2(d\theta^2+\sin^2\theta d\phi^2), \tag{4}$$

where M, ν and Q indicate the total mass, retarded time and total charge of the fluid. Since gravitational collapse is an extremely dissipative mechanism, so it would be interesting to examine the effects of dissipation in the study of collapse. The energy-momentum tensor of dissipative nature with pressure isotropy is [15]

$$T_{\alpha\beta}=(\mu+P)V_\alpha V_\beta-Pg_{\alpha\beta}+q_\alpha V_\beta+q_\beta V_\alpha, \tag{5}$$

where μ, q_α, P and V_α are the energy density, heat flux, pressure and four velocity of the matter, respectively. The vectors $V^\alpha=A^{-1}\delta_0^\alpha$ and $q^\alpha=qB^{-1}\delta_1^\alpha$ in comoving coordinates yield

$$V^\alpha V_\alpha=1,\quad q_\alpha V^\alpha=0.$$

The electromagnetic energy-momentum tensor is given as

$$E_{\alpha\beta}=\frac{1}{4\pi}\left(-F_\alpha^\gamma F_{\beta\gamma}+\frac{1}{4}F^{\gamma\delta}F_{\gamma\delta}g_{\alpha\beta}\right), \tag{6}$$

where $F_{\alpha\beta}=\phi_{\beta,\alpha}-\phi_{\alpha,\beta}$ represents the electromagnetic field tensor, ϕ_α is the four potential. The electromagnetic field equations are

$$F^{\alpha\beta}_{\ \ ;\beta}=\mu_0 J^\alpha,\quad F_{[\alpha\beta;\gamma]}=0, \tag{7}$$

where J^α and μ_0 are the four current and magnetic permeability. In order to solve the Maxwell equations, we assume that in comoving coordinates, the magnetic field in the the interior will be zero. Thus we choose

$$\phi_\alpha=\phi(t,r)\delta_\alpha^0,\quad J^\alpha=\rho(t,r)V^\alpha,$$

where ϕ and ρ indicate the scalar potential and the charge density, respectively.

The Maxwell field equations yield

$$\frac{\partial^2\phi}{\partial r^2}-\left(\frac{B'}{B}+\frac{A'}{A}-\frac{2C'}{C}\right)\frac{\partial\phi}{\partial r}=4\pi\rho B^2A, \tag{8}$$

$$\frac{\partial}{\partial t}\left(\frac{\partial\phi}{\partial r}\right)-\left(\frac{\dot{B}}{B}+\frac{\dot{A}}{A}-\frac{2\dot{C}}{C}\right)\frac{\partial\phi}{\partial r}=0, \tag{9}$$

where dot and prime mean differentiation with respect to t and r, respectively. Integration of Eq.(8) yields $\phi'=qBAC^{-2}$, where

$$q(r)=2\pi\int_0^r\rho BC^2dr, \tag{10}$$

is the total amount of charge interior to radius r. The corresponding electric field intensity is

$$E(t,r)=\frac{q}{4\pi C^2}. \tag{11}$$

The field equations (2) for the interior metric (3) become

$$\frac{\kappa A^2}{f_R}\left[\mu+2\pi E^2+\frac{1}{\kappa}\left\{\frac{f-Rf_R}{2}+\frac{f''_R}{B^2}-\left(\frac{\dot{B}}{B}-\frac{2\dot{C}}{C}\right)\times\frac{\dot{f}_R}{A^2}-\left(\frac{B'}{B}-\frac{2C'}{C}\right)\frac{f'_R}{B^2}\right\}\right]=\left(\frac{2\dot{B}}{B}+\frac{\dot{C}}{C}\right)\frac{\dot{C}}{C}-\left(\frac{A}{B}\right)^2\times\left[\frac{2}{C}\left\{C''-\frac{B'C'}{C}\right\}+\left(\frac{C'}{C}\right)^2-\left(\frac{B}{C}\right)^2\right], \tag{12}$$

$$\frac{\kappa}{f_R}\left[qAB-\frac{1}{\kappa}\left(\dot{f}'_R-\frac{\dot{f}_RA'}{A}-\frac{\dot{B}f'_R}{B}\right)\right]=\frac{2}{C}\left(\dot{C}'-\frac{A'\dot{C}}{A}-\frac{\dot{B}C'}{B}\right), \tag{13}$$

$$\frac{\kappa B^2}{f_R}\left[P+2\pi E^2-\frac{1}{\kappa}\left\{\frac{f-Rf_R}{2}-\frac{\ddot{f}_R}{A^2}+\left(\frac{2\dot{C}}{C}+\frac{\dot{A}}{A}\right)\times\frac{\dot{f}_R}{A^2}+\left(\frac{2C'}{C}+\frac{A'}{A}\right)\frac{f'_R}{B^2}\right\}\right]=-\left(\frac{B}{A}\right)^2\left[\frac{2\ddot{C}}{C}+\left(\frac{\dot{C}}{C}-\frac{2\dot{A}}{A}\right)\frac{\dot{C}}{C}\right]-\left(\frac{B}{C}\right)^2+\left(\frac{2A'}{A}+\frac{C'}{C}\right)\frac{C'}{C}, \tag{14}$$

$$\frac{\kappa C^2}{f_R}\left[P+2\pi E^2-\frac{1}{\kappa}\left\{\frac{f-Rf_R}{2}+\frac{f''_R}{B^2}-\frac{\ddot{f}_R}{A^2}-\left(\frac{\dot{B}}{B}-\frac{\dot{C}}{C}-\frac{\dot{A}}{A}\right)\frac{\dot{f}_R}{A^2}-\left(\frac{B'}{B}-\frac{C'}{C}-\frac{A'}{A}\right)\frac{f'_R}{B^2}\right\}\right]=-\left(\frac{C}{A}\right)^2\times\left[\frac{\ddot{B}}{B}+\frac{\dot{B}\dot{C}}{BC}-\frac{\dot{A}}{A}\left(\frac{\dot{B}}{B}+\frac{\dot{C}}{C}\right)-\frac{\ddot{C}}{C}\right]+\left(\frac{C}{B}\right)^2\times\left[\frac{A''}{A}+\frac{C''}{C}+\frac{A'}{A}\left(\frac{C'}{C}-\frac{B'}{B}\right)-\frac{B'C'}{BC}\right]. \tag{15}$$

The CDTT $f(R)$ model is given by

$$f(R)=R+\rho\frac{\delta^4}{R}, \tag{16}$$

which describes the accelerating behavior of the universe in the late-time era. Here $\delta>0$ is a parameter with the same units as that of mass and $\delta^{-1}\sim(10^{33}eV)^{-1}\sim10^{18}$sec. However, there are controversion in defining ρ which was initially taken to be -1 [16]. The stability condition for this model is $1/(3\sqrt{3}\delta^2-1)>0$. For the viable $f(R)$ model, it must give $f_{RR}>0$ as well as $f_R>0$. The former inequality is required to prevent tachyonic instability while the later is introduced to give up the state of ghost. However, this model with $\rho=-1$ does not work as a reasonable $f(R)$ model since it gives $f_{RR}<0$ which leads to instability of tachyons. Moreover, it suffers several issues such as failure in satisfying the local gravity constraints [17], the instability of cosmological perturbations [18], matter instability [19] etc. Sawicki and Hu [20] suggested that this model with $\rho=+1$ resolves various problems of instability and meets the stability requirement $f_{RR}>0$ all over in and around the polytrope. This model can be used to obtain matter domination epoch and consistent results [21]. We shall take $\rho=+1$ for this model.

3 Dynamical Equations and Perturbation Scheme

In this section, we first formulate dynamical equations and then develop collapse equation through perturbation scheme. The dynamical equations are very important to understand the behavior of the dynamical system. These equations have the following form

$$|X^{\alpha\beta}|_{;\beta}V_\alpha=0,\quad |X^{\alpha\beta}|_{;\beta}q_\alpha=0, \tag{17}$$

yielding

$$\dot{\mu}+\frac{A}{B}q'+\left(\frac{2\dot{C}}{C}+\frac{\dot{B}}{B}\right)(P+\mu)+2q\left(\frac{C'}{C}+\frac{A'}{A}\right)\frac{A}{B}+H_0(t,r)=0, \tag{18}$$

$$P'+\frac{B}{A}\dot{q}+\frac{A'}{A}(P+\mu)+2q\left(\frac{\dot{C}}{C}+\frac{\dot{B}}{B}\right)\frac{B}{A}-\frac{4\pi E}{C}(CE'+2EC')+H_1(t,r)=0, \tag{19}$$

where the components of the dark source, i.e., H_0 and H_1 are given in Appendix **A** of [15].

The perturbative expansion refines the expressions with the help of correction terms which become smaller

and smaller controlled by the perturbation parameter, α. We use here the perturbation technique which leads to the collapse equation. In this scenario, we assume initially that the metric coefficients and fluid variables are enforced to have r dependence, i.e., the system is in complete static equilibrium. After perturbation, all these quantities will become time dependent. Taking $0 < \alpha \ll 1$, it follows that

$$A(t,r) = A_0(r) + \alpha T(t)a(r), \tag{20}$$
$$B(t,r) = B_0(r) + \alpha T(t)b(r), \tag{21}$$
$$C(t,r) = C_0(r) + \alpha T(t)c(r), \tag{22}$$
$$E(t,r) = E_0(r) + \alpha T(t)s(r), \tag{23}$$
$$\mu(t,r) = \mu_0(r) + \alpha\bar{\mu}(t,r), \tag{24}$$
$$P(t,r) = P_0(r) + \alpha\bar{P}(t,r), \tag{25}$$
$$q(t,r) = \alpha\bar{q}, (t,r), \tag{26}$$
$$R(t,r) = R_0(r) + \alpha T(t)e(r), \tag{27}$$
$$f(t,r) = \left[R_0(r) + \delta^4 R_0^{-1})\right] + \alpha T(t)e(r)\left[1 - \delta^4 R_0^{-2}\right], \tag{28}$$
$$f_R(t,r) = 1 - \delta^4 R_0^{-2} + 2\alpha T(t)e(r)\delta^4 R_0^{-3}. \tag{29}$$

Taking $C_0(r) = r$ as the Schwarzschild coordinate (by the degree allowed in the r coordinate), Eq.(18) is trivially satisfied for the static configuration, while Eq.(19) turns out to be

$$P_0' + (P_0 + \mu_0)\frac{A_0'}{A_0} - \frac{4\pi}{r}(2E_0^2 + rE_0E_0') + \frac{H_2(r)}{\kappa} = 0, \tag{30}$$

where $H_2(r)$ is mentioned in Appendix **A** of [15]. Under the perturbation scheme, Eqs.(18) and (19) give

$$\dot{\bar{\mu}} + \frac{A_0}{B_0}\bar{q}' - 2\bar{q}\left(\frac{1}{r} - \frac{A_0'}{A_0}\right)\frac{A_0}{B_0} + \left[(\mu_0 + P_0)\left(\frac{c}{r} + \frac{b}{B_0}\right) + \frac{H_3(r)}{\kappa}\right]\dot{T} = 0, \tag{31}$$

$$\bar{P}' + \dot{\bar{q}}\frac{B_0}{A_0} + (\bar{P} + \bar{\mu})\frac{A_0'}{A_0} + T(P_0 + \mu_0)\left(\frac{a}{A_0}\right)' - \frac{4\pi E_0 T}{r} \times \left[4s + 2rE_0\left(\frac{c}{r}\right)' + rs' + rs\frac{E_0'}{E_0}\right] + T\frac{H_4(t,r)}{\kappa} = 0, \tag{32}$$

where $H_3(r)$ and $H_4(r)$ are given in Appendix **A** of [15]. Using Eqs.(20)-(29), we obtain $\bar{q}$

$$\bar{q} = \frac{2(R_0^2 - \delta^4)}{\kappa R_0^2 A_0 B_0}\left[\frac{cA_0'}{rA_0} + \frac{b}{rB_0} - \frac{c'}{r} + \frac{R_0^2}{R_0^2 - \delta^4}\left\{\frac{\delta^4}{R_0^3} \times \left(\frac{e'}{R_0} + \frac{eA_0'}{R_0A_0} - 4e\frac{R_0'}{R_0^2} + R_0'\frac{b}{B_0}\right)\right\}\right]\dot{T} = 0. \tag{33}$$

Using the above relation in Eq.(31) and integrating, it follows that

$$\bar{\mu} = -\left[(P_0 + \mu_0)\left(\frac{c}{r} - \frac{b}{B_0}\right) - H_5(r)\right] = 0, \tag{34}$$

where H_5 is mentioned in Appendix **A** of [15].

Now, we formulate the collapse equation which has a crucial importance for the stellar stability investigation. To have a link between $\bar{\mu}$ and $\bar{P}$, we choose an equation of state of Harrison-Wheeler type in the framework of second law of thermodynamics. This equation of state is the ratio of specific heat [22]

$$\bar{P} = \Gamma\frac{P_0}{P_0 + \mu_0}\bar{\mu}, \tag{35}$$

where Γ is an adiabatic index that determines the change of pressure relative to the given change in density. We treat it as a constant term in the evolution of matter distribution taken under consideration. Substituting the value of $\bar{\mu}$ in the above equation, we have

$$\bar{P} = -\Gamma P_0\left(\frac{c}{r} + \frac{b}{B_0}\right)T + \Gamma\frac{P_0}{P_0 + \mu_0}H_5T = 0. \tag{36}$$

Using Eqs.(33), (34) and (36) in Eq.(32), it follows that

$$\left[\Gamma\left\{P_0\left(\frac{c}{r} + \frac{b}{B_0}\right) + \frac{P_0}{P_0 + \mu_0}D_5\right\}' + (\mu_0 + P_0)\left(\frac{a}{A_0}\right)' - \frac{A_0'}{A_0}\left\{(\mu_0 + \Gamma P_0 + P_0)\left(\frac{c}{r} + \frac{b}{B_0}\right) - \left(\Gamma\frac{P_0}{P_0 + \mu_0} + 1\right) \times H_5\right\} - \frac{4\pi E_0}{r}\left\{4s + 2rE_0\left(\frac{c}{r}\right)' + rs' + rs\frac{E_0'}{E_0}\right\} + \frac{H_4}{\kappa}\right] \times T - \frac{2(R_0^2 - \delta^4)}{(R_0A_0)^2\kappa}\left[\frac{cA_0'}{rA_0}. + \frac{b}{rB_0} - \frac{c'}{r} + \frac{R_0^2}{R_0^2 - \delta^4}\left\{\frac{\delta^4}{R_0^3} \times \left(\frac{e'}{R_0} + \frac{eA_0'}{R_0A_0} - 4e\frac{R_0'}{R_0^2} + R_0'\frac{b}{B_0}\right)\right\}\right]\ddot{T} = 0. \tag{37}$$

The perturbed configuration of the Ricci scalar yields

$$\ddot{T}(t) - \omega(r)T(t) = 0, \tag{38}$$

where $\omega(r)$ is mentioned in Appendix **A** of [15]. All terms in $\omega(r)$ are supposed to be positive just for the sake of stellar instability range. The solution obtained from the above equation is given as

$$T(t) = -\exp\left(\sqrt{\omega}t\right). \tag{39}$$

4 Instability Regions in the Newtonian and post-Newtonian Limits

Here, we discuss the instability ranges of the relativistic star at both N and pN order as well as the role of Γ in this context. In order to compare our solutions to GR, we also calculate the asymptotic behavior of the corresponding results.

4.1 Newtonian Limit

We analyze the contribution of matter variables of the evolving star by assuming

$$\mu_0 \gg P_0, \quad A_0 = 1, \quad B_0 = 1,$$

for which Eq.(37) gives

$$\left[\Gamma\left\{-P_0\left(\frac{c}{r}+b\right)\right\}' + \mu_0 a' - \frac{4\pi E_0}{r}\left\{4s + 2rE_0\left(\frac{c}{r}\right)' + rs' + rs\frac{E_0'}{E_0}\right\} + \frac{H_{4(N)}}{\kappa}\right] T - 2\frac{(R_0^2-\delta^4)}{R_0^2\kappa}\left[\frac{b}{r} - \frac{c'}{r} + \frac{(R_0^2-\delta^4)}{R_0^2}\left\{\frac{\delta^4}{R_0^3}\left(\frac{e'}{R_0'} + bR_0' - 4e\frac{R_0'}{R_0^2}\right)\right\}\right]\ddot{T} = 0, \quad (40)$$

where $H_{4(N)}$ are the terms of N approximation of Eq.(32). Using Eq.(39) in the above equation, the required constraint for the dissipative and isotropic spherically symmetric collapsing matter distribution is given as

$$\Gamma < \frac{1}{\left\{-P_0\left(\frac{c}{r}+b\right)\right\}'}\left(\mu_0 a' - \frac{4\pi E_0}{r}\left\{4s + 2rE_0\left(\frac{c}{r}\right)' + rs' + rs\frac{E_0'}{E_0}\right\} + \frac{H_{4(N)}}{\kappa} + H_6(r)\right), \quad (41)$$

where H_6 is the dark source component. We see that the adiabatic index Γ plays a central role to investigate dynamical instability of the relativistic system. Thus, at N approximation, the matter distribution will be unstable until (41) is satisfied. We also note that the dependence of inequality on Γ implies that instability of the system relies on the stiffness of the fluid. However, there is no contribution of heat flux in defining the dynamical instability conditions, while this range of instability decreases in the presence of electromagnetic field in spherical symmetric background. When δ approaches to zero, (41) reduces to

$$\Gamma < \frac{1}{\left\{-P_0\left(\frac{c}{r}+b\right)\right\}'}\left(\mu_0 a' - \frac{4\pi E_0}{r}\left\{4s + 2rE_0\left(\frac{c}{r}\right)' + rs' + rs\frac{E_0'}{E_0}\right\} + 2\frac{\omega}{\kappa}\left(\frac{b}{r} - \frac{c'}{r}\right)\right), \quad (42)$$

which provides the solution of GR.

4.2 Post Newtonian Limit

Here we study the conditions for the dynamical instability in the scenario of pN approximations. For this purpose, we consider effects upto $O\left(\frac{m_0}{r} + \frac{Q^2}{2r^2}\right)$ and assume

$$A_0 = 1 - \frac{m_0}{r} + \frac{Q^2}{2r^2}, \quad B_0 = 1 + \frac{m_0}{r} - \frac{Q^2}{2r^2}. \quad (43)$$

Using Eqs.(43), Eq.(37) reduces to

$$\Gamma < \frac{\eta + \lambda + H_7(r)}{\beta\varphi' + \varphi}, \quad (44)$$

where

$$\eta = \left(\frac{m_0 r - Q^2}{r^3}\right)\left(1 + \frac{m_0}{r} - \frac{Q^2}{2r^2}\right)\left[(P_0+\mu_0)\left\{b\left(1 + \frac{m_0}{r} - \frac{Q^2}{2r^2}\right) + \frac{c'}{r}\right\} - H_{5(PN)}\right] + (P_0+\mu_0)\left[a \times \left(1 + \frac{m_0}{r} - \frac{Q^2}{2r^2}\right)\right]', \quad \lambda = -\frac{4\pi E_0}{r}\left(1 - \frac{m_0}{r} + \frac{Q^2}{2r^2}\right) \times \left[4s + 2rE_0\left(\frac{c}{r}\right)' + rs' + rs\frac{E_0'}{E_0}\right],$$

$$\beta = \left(\frac{m_0 r - Q^2}{r^3}\right)\left(1 + \frac{m_0}{r} - \frac{Q^2}{2r^2}\right),$$

$$\varphi = \left[P_0\left\{b\left(1 + \frac{m_0}{r} - \frac{Q^2}{2r^2}\right) + \frac{c'}{r}\right\} - \frac{P_0}{P_0+\mu_0}H_{5(PN)}\right],$$

and H_7 is mentioned in [15]. For the onset of the dynamical instability, the expression (44) must be satisfied. In addition, it is argued that instability will develop as long as all the terms in the above expression are positive. Thus we require that all terms in (44) should be positive. For this purpose, the following inequalities must hold

$$(P_0+\mu_0)\left\{b\left(1 + \frac{m_0}{r} - \frac{Q^2}{2r^2}\right) + \frac{c'}{r}\right\} > H_{5(PN)}, \quad (45)$$

$$P_0\left\{b\left(1 + \frac{m_0}{r} - \frac{Q^2}{2r^2}\right) + \frac{c'}{r}\right\} > \frac{P_0}{P_0+\mu_0}H_{5(PN)}, \quad (46)$$

$$\frac{m_0}{r} + \frac{Q^2}{2r^2} < 1. \quad (47)$$

It is observed that in the phenomenon of gravitational collapse, the energy density may increase or decrease which is controlled by the electromagnetic field, pressure and higher curvature terms of CDTT $f(R)$ model. The system remains unstable at pN order under the above inequalities. Taking δ to be zero, we get the same constraint for dynamical instability of the relativistic fluid configuration with spherical symmetry as mentioned in (44) with the difference that $H_7(r)$ goes to zero. This shows that the system becomes more stable in the presence of electric charge.

5 Summary and Discussion

This work investigates dynamical instability of the charged spherical dissipative collapse in $f(R)$ gravity. For this purpose, we have assumed non-adiabatic collapsing sphere with inhomogeneous energy density and locally isotropic charged fluid in CDTT $f(R)$ model. Here dark source $f(R)$ curvature terms suffer the collapse rate and the

passive gravitational mass. In order to study the effects of electromagnetic field and the $f(R)$ model, we have applied the perturbation scheme on the field equations and on the dynamical equations, which leads to the collapse equation.

In general, the adiabatic index determines the dynamical instability of relativistic stars. It is worth mentioning here that for $\Gamma < \frac{4}{3}$ and $\Gamma < 1$, the spherical [7] and cylindrical [24] relativistic body becomes unstable thereby enforces the importance of index Γ. We have also established the relevance of such index in the discussion as seen from expressions (41) and (44) at both N and pN eras. We conclude that the stability of the fluid is affected by the local pressure isotropy, electromagnetic field, energy density and higher curvature terms of $f(R)$ CDTT model.

For the onset of self-gravitating dynamical instability, we require that the system meets the requirements (41) and (44)-(47). The violation of these constraints leads the system to decrease instability. These results indicate that the physical variables of the relativistic star has a central role for stellar stability which is well consistent with [8]-[10] and [23]-[25]. It is also seen that the invoking of electromagnetic field in the star decreases the range of instability thus making it more stable. This behavior agrees with the results obtained in [25]. The relevance of dynamical instability analysis in astrophysical study stems from the fact that this may be fruitful in the evolution and structure formation of the relativistic bodies.

References

1. S. Perlmutter, et al.: Astrphys. J. **517**(1999)565; A.G. Riess et al.: Astron. J. **116**(1998)1009.
2. S. Capozziello: Int. J. Mod. Phys. D **11**(2002)483.
3. C.W. Misner and D.H. Sharp: Phys. Rev. **136**(1964)B571.
4. L. Herrera and N.O. Santos: Phys. Rev. D **70**(2004)084004.
5. A. Di Prisco, L. Herrera, G. Le Denmat, M.A.H. MacCallum and N.O. Santos: Phys. Rev. D **76**(2007)064017.
6. M. Sharif and M.Z. Bhatti: Gen. Relativ. Gravit. **44**(2012)2811.
7. S. Chandrasekhar: Astrophys. J **140**(1964)417.
8. L. Herrera, G. Le Denmat and N.O. Santos: Mon. Not. R. Astron. Soc. **237**(1989)257.
9. R. Chan, L. Herrera and N.O. Santos: Mon. Not. R. Astron. Soc. **265**(1993)533; ibid. **267**(1994)637.
10. M. Sharif and M.Z. Bhatti: Mod. Phys. Lett. A **27**(2012)1250141; ibid. **29**(2014)1450094; ibid. 27(2012)1450129; ibid. **29**(2014)1450165; Can. J. Phys. **90**(2012)1233; Int. J. Mod. Phys. D **23**(2014)1450085; ibid. **24**(2015)1550014; Phys. Lett. A **378**(2014)469; Phys. Scr. **89**(2014)084004; Astrophys. Space Sci. **347**(2013)337; ibid. **349**(2014)995; **352**(2014)883; ibid. **355**(2014)389; J. Exp. Theor. Phys. **147**(2015)942.
11. M. Sharif and Z. Yousaf: Phys. Rev. D **88**(2013)024020; Mon. Not. R. Astron. Soc. **440**(2014)3479; Astropart. Phys. **56**(2014)19; Astrophys. Space Sci. **351**(2014)351; **352**(2015)321; **357**(2015)49; Eur. Phys. J. C **75**(2015)58; ibid. **75**(2015)194; Gen. Relativ. Gravi. **47**(2015)48.
12. C. Ghezzi: Phys. Rev. D **72**(2005)104017.
13. A. Di Prisco, L. Herrera, M.A.H. MacCallum and N.O. Santos: Phys. Rev. D **80**(2009)064031.
14. P.S. Joshi and D. Malafarina: Phys. Rev. D **83**(2011)024009.
15. M. Sharif and Z. Yousaf: Mon. Not. R. Astron. Soc. **434**(2013)2529.
16. S.M. Carroll, V. Duvvuri, M. Trodden and M.S. Turner: Phys. Rev. D **70**(2004)043528.
17. I. Navarro and K. Van Acoleyen: J. Cosmol. Astropart. Phys. **02**(2007)022.
18. Y.S. Song, W. Hu and I. Sawicki: Phys. Rev. D **75**(2007)044004.
19. V. Faraoni: Phys. Rev. D **74**(2006)104017.
20. I. Sawicki and W. Hu: Phys. Rev. D **75**(2007)127502.
21. J.D. Evans, L.M.H. Hall and P. Caillol: Phys. Rev. D **77**(2008)083514.
22. B.K. Harrison, K.S. Thorne, M. Wakano and J.A. Wheeler: *Gravitation Theory and Gravitational Collapse* (University of Chicago Press, 1965).
23. M. Sharif and Z. Yousaf: Mon. Not. R. Astron. Soc. **432**(2013)264; Astrophys. Space Sci. **352**(2014)943; **354**(2014)431; **354**(2014)471; **354**(2014)481; **355**(2014)317; J. Cosmol. Astropart. Phys. **06**(2014)019.
24. M. Sharif and M.Z. Bhatti: J. Cosmol. Astropart. Phys. **10**(2013)056.
25. M. Sharif and M.Z. Bhatti: M.Z.: J. Cosmol. Astropart. Phys. **11**(2013)014; Astropart. Phys. **56**(2014)35.